for Kodiak

Environmental Assessment of the Alaskan Continental Shelf

Volume 14. Ice

Principal Investigators' Reports
for the Year Ending March 1976

U. S. DEPARTMENT OF COMMERCE
National Oceanic and Atmospheric Administration

U. S. DEPARTMENT OF INTERIOR
Bureau of Land Management

April 1976

Annual Reports from Principal Investigators

Volume:
1. Marine Mammals
2. Marine Birds
3. Marine Birds
4. Marine Birds
5. Fish, Plankton, Benthos, Littoral
6. Fish, Plankton, Benthos, Littoral
7. Fish, Plankton, Benthos, Littoral
8. Effects of Contaminants
9. Chemistry and Microbiology
10. Chemistry and Microbiology
11. Physical Oceanography and Meteorology
12. Geology
13. Geology
14. Ice

Environmental Assessment of the Alaskan Continental Shelf

Volume 14. Ice

Fourth quarter and annual reports for the reporting period ending March 1976, from Principal Investigators participating in a multi-year program of environmental assessment related to petroleum development on the Alaskan Continental Shelf. The program is directed by the National Oceanic and Atmospheric Administration under the sponsorship of the Bureau of Land Management.

ENVIRONMENTAL RESEARCH LABORATORIES / Boulder, Colorado / 1976

CONTENTS

Annual Report

Contract #03-5-022-67
Research Unit #87
Reporting Period:
1 July 1975 - 1 April 1976
Number of Pages: 6

The Interaction of Oil with Sea Ice in the Arctic Ocean

Seelye Martin
Department of Oceanography
University of Washington
Seattle, WA 98195

24 March 1976

ANNUAL REPORT

I. Summary of objectives, conclusions, and implications with respect to OCS oil and gas development.

A. Objective: The objective of our sub-program is to understand the small-scale interaction of oil and sea ice. This involves answering the following question: How do the microscale salinity, temperature, and crystal structure properties of sea ice affect the way in which the ice absorbs petroleum?

B. Preliminary conclusions: Because the properties of young sea ice differ between the Bering and Beaufort Sea, an oil spill in either area will behave in different ways. In the Beaufort, the oil is likely to remain under the ice until late spring, at which time it will rise to the surface through brine channels and thermal cracks. In the Bering Sea, oil will reach the surface immediately through either porous grease ice or the spaces separating pancake ice.

C. Implications: The design of clean-up procedures and the analysis of the impact of the spilled oil on birds, wildlife, and marine life will be very different for the two seas.

II. Introduction

A. General nature and scope of study: The purpose of the present study is to outline the various ways in which the sea ice of the Alaskan coast will entrain and interact with an oil spill or blow-out under the ice. The study concentrates on the small-scale properties of sea ice; namely, its salinity, temperature, and crystal structure, and is only indirectly concerned with the large scale transport and deformation of sea ice. The study divides into two parts: a laboratory experiment on ice growth in a wave field, which simulates parts of the Bering Sea, and a field survey which consists of taking ice cores from the Beaufort Sea at different times of the year. In the laboratory experiment, we inject oil under the growing ice to study the entrainment; in the field survey, we analyze the cores to see how oil might be entrained within them.

B. Specific objectives:

1. Describe from the laboratory experiments how oil is entrained within grease and pancake ice.

2. From the field observations, describe the kinds of ice which grow within the Beaufort Sea.

3. Relate the observed small-scale properties to the entrainment and diffusion of petroleum within sea ice.

C. Relevance to problems of petroleum development: The work will do the following:

1. help predict the under-ice extent of an off-shore oil spill or blowout;

2. aid in the design of clean-up strategies;

3. contribute to discussions of the impact of oil spills upon biological systems.

III. Current state of knowledge. This is best summarized in two reports from the Canadian Beaufort Sea Project (Environment Canada, Pacific Region, 512 Federal Building, Victoria, B. C. V8W 1Y4); namely Report #27, The Interaction of Crude Oil with Sea Ice, and Report M5, Oil in Sea Ice, which are available upon request.

This contract has also submitted one report to OCSEAP titled "Data Report on the October-November 1975 field traverse of BLM-NOAA Task Order Contract No. 03-5-022-67, Task Order No. 6", which gives the results of our ice coring in the Beaufort Sea. This report is available from the OCSEAP office.

IV. Study area

A. Field experiment: The sea ice on the continental shelf north of Alaska.

B. Laboratory experiment: The grease and pancake ice grown in a wave tank in a cold room.

V. Sources, methods and rationale of data collection

A. Sources: Ice cores and samples taken from a laboratory test tank and the sea ice of the Beaufort Sea.

B. Methods: We take the ice cores with a SIPRE corer. The means of determination of temperature, salinity, and crystal structure are described in detail in our data report cited in III.

C. Rationale: The rationale for taking ice cores is that it is the best way to study the small-scale properties of sea ice.

VI. Results:

A. Field observations:

1. The results of our October-November 1975 field traverse are contained in our data report cited in III.

2. The results of our February-March 1976 field traverse are being analyzed.

B. Laboratory:

1. Oil absorption by grease and slush ice: Our laboratory experiments show that grease and slush ice are made up of approximately 40% ice and 60% sea water. Any oil released under this ice, which may grow to a thickness of 100 mm, comes rapidly to the surface.

2. Oil absorption by pancake ice: Our preliminary laboratory experiments suggest that most of the oil released under a field of pancake ice comes to the sea water surface through the spaces between the cakes, where the oscillatory motion of the pancakes pumps the oil away from the spill site.

VII. Discussion

A. Beaufort Sea: Our field observations suggest that there are a large number of ways by which oil spilled under the mobile pack ice during October-November will be trapped and contained with the ice field by absorption, ice rafting, or ridging. This will have two effects:

1. This oil containment will limit the spatial extent of a spill;

2. The trapping or oil within pressure ridges, rafted ice, and rubble fields will make any clean-up extremely difficult, as well as store the oil for future release during the biologically very important late spring-early summer period.

B. Bering Sea: Overflights of the Bering Sea during February-March 1973 suggest that much of the new ice is grease and pancake ice. Figure 1, which comes from the BESEX report (Results of the U. S. Contribution to the Joint U.S./U.S.S.R. Bering Sea Experiment, NASA document X-910-74-141, available from Technical Information Division, Code 250, Goddard Space Flight Center, Greenbelt, Maryland 20771), shows for one day those areas which are very likely grease and pancake ice. Our experiments suggest that any oil released under this ice will immediately appear on the surface and for the case of pancake ice be pumped away from the spill site.

VIII. Conclusions

Because of the differences between the ways in which sea ice forms in the Beaufort and Bering Seas, oil discharges within these regions will behave very differently. Also, clean-up techniques for such spills must be tailored to the way in which the oil interacts with the ice. Before the granting of oil drilling permits in the mobile pack ice of either the Bering or Beaufort Sea, we should determine the trajectories of any possible spills, and both design and test oil spill clean-up procedures for the different areas.

IX. Needs for further study:

A. Field: We need data on the kinds of ice which exist in the Bering Sea in the fall and winter.

B. Laboratory: We need experiments which should be run with different Arctic crude oils, on both the freezing in and the melting out of oil in different kinds of sea ice.

C. Combined: An extremely important oil absorption site will be pressure ridges. We need experiments on the fate of oil which was originally entrained in flat young sea ice, then crushed into a pressure ridge.

X. Summary of 4th quarter operations:

A. Laboratory activities: none

B. Field Activities:

1. Field trip schedule
   a. Dates: 17 February - 2 March 1976
   b. Aircraft: Helicopter, Bell 205 (chartered)

2. Scientific Party:
   a. Peter Kauffman, University of Washington, Chief Scientist
   b. Edward Josberger, University of Washington, assistant
   c. Terren Niedrauer, University of Washington, assistant

3. Methods: The techniques used in this field traverse were the same as those used in the October-November 1975 field traverse, which are described in the data report cited in III.

4. Sample localities: Figure 2 shows the locations at which we pulled ice cores. We occupied 8 stations off Lonely, 7 off Deadhorse, and 7 off Barter Island. Because of the importance of the lagoon between the barrier islands and Prudhoe Bay, we pulled one additional core 3 nautical miles inshore of Narwhal Island.

5. Data collected or analyzed:
   a. Numbers and types of samples/observations: A total of 29 ice cores were taken from locations off Lonely, Deadhorse, and Barter Island.
   b. Number and types of analyses:
      i. Number: three (temperature, salinity and crystal structure).
      ii. Types:
         a. Temperature: thermistor measurement of temperature profile.
         b. Salinity: Measurement of index-of-refraction of water samples.
         c. Crystal Structure: Visual appearance of core.
   c. Miles of trackline: Approximately 180 nautical miles.

Figure 1.

Grease and Pancake Ice in the Bering Sea

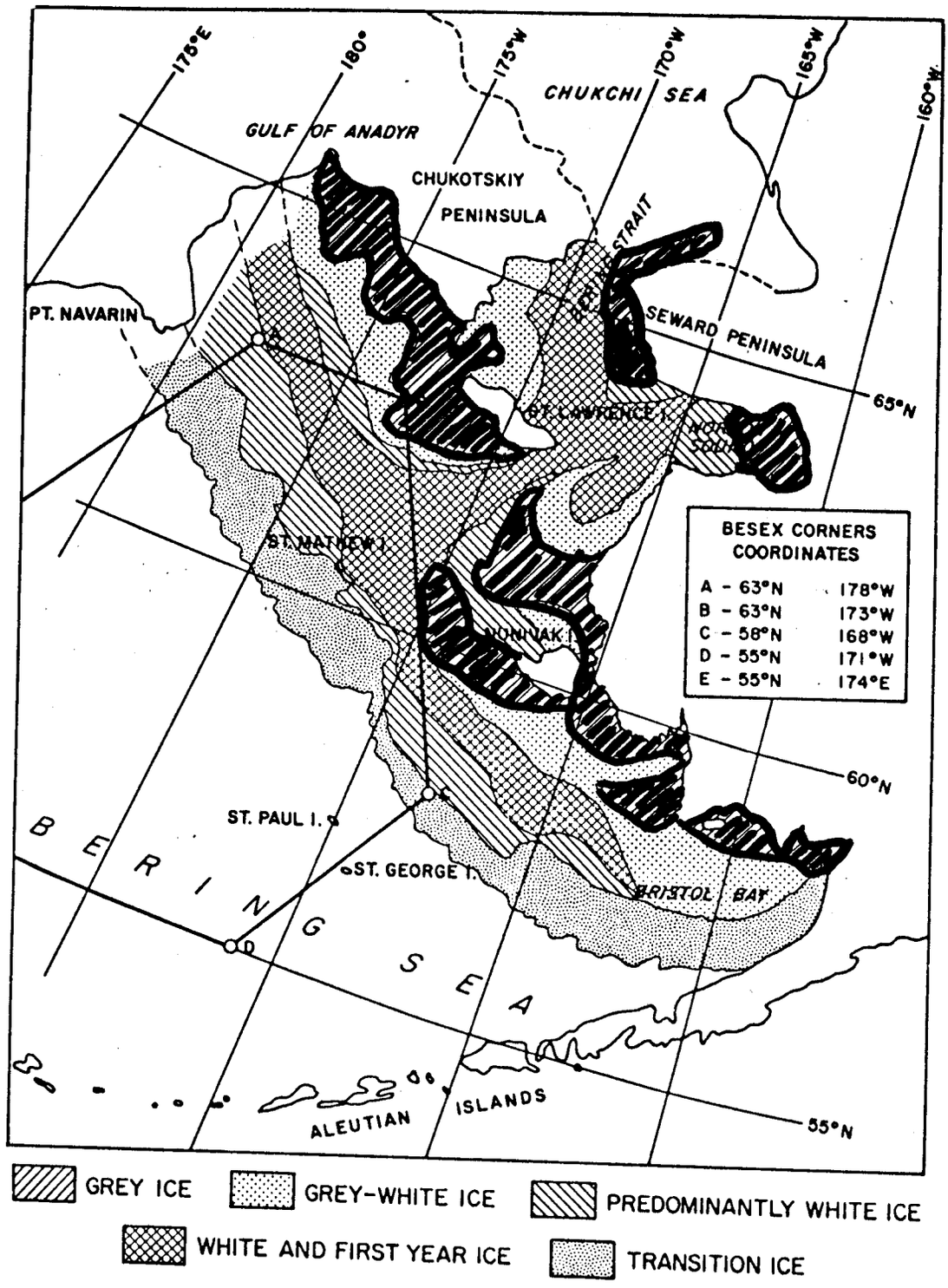

Location of Ice Cores taken in February - March 1976

• ice core locations

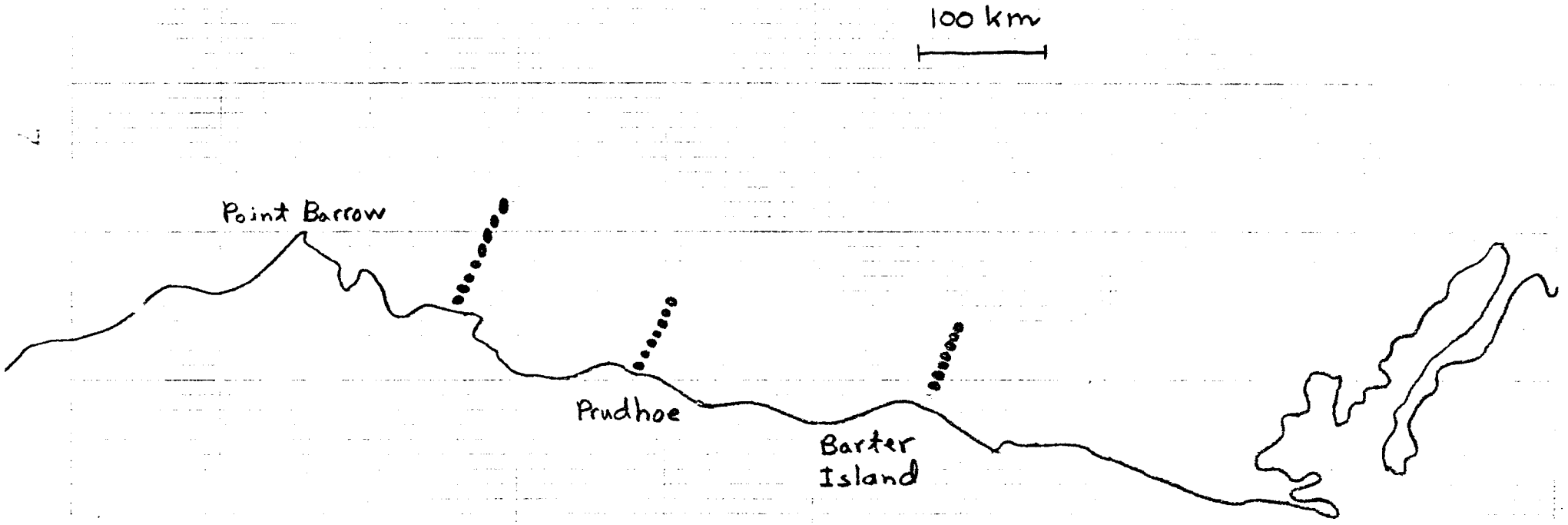

Figure 2.

ANNUAL REPORT

RU #88: Dynamics of
Near-shore Ice
P.O.: 01-3-022-2313
Reporting Period:
Apr 1975 - Apr 1976
Number of Pages: 11

Dynamics of Near-Shore Ice

W. F. Weeks and A. Kovacs

Cold Regions Research and Engineering Laboratory

Hanover, NH 03755

28 March 1976

I. SUMMARY OF OBJECTIVES, CONCLUSIONS AND IMPLICATIONS WITH RESPECT TO OCS OIL AND GAS DEVELOPMENT

The purpose of this project is to measure the motions of both the fast ice and the near shore pack ice to see if the motions of the latter can be understood and used to predict the motions of the former. While these measurements are being made a number of other studies will be undertaken on the nature of near shore sea ice (ice structure, ice thickness, bottom scoring, ridge characteristics, grounded ice features). Work is also underway to characterize the variations in near shore pressure ridging by the use of laser profilometry and SLAR imagery.

We are, as yet, not far enough into the data analysis phase of this program to be able to draw representative conclusions. However, even now it is clear that significant and systematic decreases occur in the amount of pressure ridging as one moves toward the west from Barter Island along the coast of the Northslope.

II. INTRODUCTION

A. General nature and scope of the study

The funding that CRREL has received under PO: 01-3-022-2313 has been used on two rather different but related projects. These can be described as the

1. Narwhal Island Ice Motion Study (Near Shore Radar Transponder and Fast Ice Studies), and
2. Remote Sensing Studies of Coastal Sea Ice in the Chukchi and Beaufort Seas.

The purpose of the Narwhal Island Program is to obtain detailed quantitative information on the movement and deformation of both the near shore pack ice and the fast ice along the coast of the Beaufort Sea (with particular emphasis on the region north of Prudhoe Bay). Studies will also be made of ridges and ridge systems within the vicinity of Narwhal Island and of the bottom scoring associated with specific ice features. Some limited work is also planned on the internal structure of sea ice and on lateral variations in ice thickness.

The Remote Sensing Studies are designed to extract as much information as possible from the SLAR images obtained by the USGS aircraft based remote sensing program during the summer and all of 1975 and to obtain and analyze sequential laser profilometer tracks made at several locations along the coast of the Beaufort and Chukchi Seas.

B. Specific objectives

The Narwhal Island Program uses a radar ranging system that is based from Cross and Narwhal Islands to obtain quantitative information on the movements (rates, directions, accelerations) and deformation rates (i.e. spatial variations in the ice velocity field) of both the offshore pack ice and the fast ice in the vicinity of the offshore islands that are located approximately 20 km north of Prudhoe Bay, Alaska. This set of information will be supplemented by precise strain measurements by a laser ranging system of a number of corner reflectors sited at locations around Narwhal Island. Observations

will also be made of the geometry and internal structure of pressure ridges and pressure ridge systems that occur in the vicinity of the field site as well as at other sites of opportunity. Measurements of ice thickness variations are also planned by using the GSSI pulsed radar system as are studies of the internal structure of undeformed fast ice located just south of Narwhal Island.

In the Remote Sensing Studies we intend to use the SLAR transects obtained north from Lonely to study variations in ridging intensity and the distribution of floe sizes. The SLAR images also clearly reveal that a very large floeberg (welded set of pressure ridges) was drifting along the coast north of Oliktok in October. Good photographic coverage of this impressive ice feature was obtained. We also plan to a) visit fragments of this feature that have been incorporated in the fast ice north of Cross Island in order to provide some detailed observations on this type of phenomenon and to b) profile it during the laser flights.

In the laser profilometer study we intend to study temporal and spatial changes in the degree of ridging and deformation present in the ice within 200 km of the coast. An attempt will also be made to develop an ice type classification based on surface roughness. Also if there are sufficient numbers of areas showing open water, we may be able to use the laser data to estimate the total volume of ice present in the Alaskan coastal zone.

C. Relevance to problems of petroleum development

A knowledge of the motion deformation and physical characteristics of both the near-shore pack ice and the fast ice is essential to adequately designing and estimating the hazards associated with a variety of engineering options that may be considered for offshore operations in the near coastal areas of the Beaufort and Chukchi Seas (e.g. construction of gravel islands, structural platforms, causeways, reinforced ice platforms, buried pipelines, or the utilization of the ice sheet itself to carry large, long-term loads). The present program contributes directly to the solution of this general class of engineering problem in that it will provide much of the geophysical and engineering data upon which sound engineering and regulatory decisions can be made. The general geographical area that is being studied is under intense present study by the petroleum companies because it possesses favorable geologic structures and is a natural extension of the known Prudhoe Bay field. Of all the Alaskan OCS areas it is one that will undoubtedly be developed in the very near future inasmuch as a transportation system is nearing completion (the Alyeska Pipeline) that will enable the operating companies to move the oil and gas south to existing markets.

III. CURRENT STATE OF KNOWLEDGE

There has never been a comparable detailed study of pack ice-fast ice motion and deformation in near coastal waters. What data exists for pack Ice (Hibler et al., 1974 a, b) was either obtained far from

shore or based on a very short time (3 days) series of satellite observations. In both cases these other studies will only be useful in a comparative sense. Perhaps the study most closely related to the present one is R.U. #250 Mechanics of the Origin of Pressure Ridges, Shear Ridges, and Hummock Fields in Landfast Ice, which is currently underway. Its focus is however quite different in that it primarily investigates ridge mechanics as opposed to ice motion and the coupling between the fast ice and the pack which is the purpose of the present study. There have also been several studies that were focused purely on the motion of the fast ice. Much of this work was undertaken in the vicinity of the Mackenzie Delta by oil companies and is not fully available (Wetzel, et al., 1974). The work that has just been completed under the auspices of the Beaufort Sea Project (Cooper, 1975) indicates that fast ice movements of several tens of meters can occur during a winter. The only work along this line that has been undertaken off the Northslope of Alaska is currently underway under the auspices of AOGA (Alaskan Oil and Gas Association). The majority of its ice movement sites are on the fast ice to the south and west of Narwhal and Cross Island. However, there is one station located outside of the barrier islands (northeast of Narwhal Island). We currently are operating a radar transponder at the same location.

IV. STUDY AREA

We selected the Narwhal/Cross Island area of the barrier islands northeast of Prudhoe Bay because it was believed to be representative

of the large number of barrier islands located north of the Northslope. It was also an area of intense interest to the oil companies which would make our data both generally applicable to a type of environmental setting as well as site specific for certain leasing questions. It also had a number of logistic advantages because of the nearness of the Deadhorse/Prudhoe Bay complex.

In the laser profilometer studies we decided to fly replicate sample tracks oriented roughly normal to the coast starting from a number of clearly identifiable features (Point Lay, Wainwright, Barrow, Lonely, Cross Island, Barter Island). The length of the sample tracks was 200 km which was a compromise between our desire to penetrate well away from the coast into the main polar pack and the time required for each flight. The locations of the ridging studies are primarily controlled by where certain representative or interesting ice conditions occur. This is especially true of our studies on the island of grounded sea ice in the Chukchi Sea.

V. SOURCES, METHODS AND RATIONALE OF DATA COLLECTION

There was no source of pre-existing data on the ice behavior in the vicinity of the barrier islands north of Prudhoe Bay. Therefore we had to guess the scale of the ice movements we would be studying from scattered bits of unpublished information. We chose the Del Norte radar transponder system because it offered high accuracy positioning (±1m) and a reasonably long life of the remote stations. Its range

was also suitable (the limiting factor on range is actually the earth's curvature plus the height of the ridges along the transmission path). The laser selected for use should be adequate for the line lengths that will be surveyed. The other techniques that will be used are reasonably conventional in sea ice studies. The exact location of transponder and corner reflector sites will be influenced by our estimate of the location of the fast-pack ice boundary (this boundary is not always obvious). At least one transponder should be in the pack ice. The 3 hour spacing of the measurements is a compromise between defining diurnal effects and excessive battery drain.

VI. RESULTS

In April 1975 a short trip was made to Narwhal and Cross Islands by a two-man field party in order to obtain a feeling of the typical ice conditions at these sites. During this visit a study was made of the characteristics of and the bottom scoring associated with a large floeberg located to the WNW of Cross Island (Kovacs and Gow, 1976). This report is inclosed as Appendix 1. During the same time period a short visit was made to the grounded sea ice island northwest of Barrow in the Chukchi Sea (Kovacs, Gow and Dehn, 1975). A copy of this report is included as Appendix 2.

In October 1976 a four-man field party revisited Narwhal and Cross Islands, installed a permanent three-building camp and two 50 m high towers on which the radar masters were to be installed later (in March).

In early March 1976 the Narwhal Island camp was reoccupied and the main field project started. At the present time (30 March 1976) the radar system is operational with eight transponders installed. The main problems, so far, have been with polar bears destroying the remote stations.

In the remote sensing area the analysis of the SLAR data has been postponed until the University of Alaska can make suitable strip prints of the negatives. The laser profilometer studies have, however, progressed quite satisfactorily. In February 1976 a complete set of the six transects were obtained (approximately 2500 km of laser track). The parameters recorded were laser range (40 ft. full scale), reflectometer intensity, phase lock, and time plus comments. We were completely satisfied with the performance of the system. At the present time we are starting data analysis procedures. We have also arranged for a camera system which will be used in conjunction with the laser on future flights. The next set of laser flights is scheduled for late April-early May 1976.

VII. DISCUSSION

The two completed reports (Appendices 1 and 2) are self-explanatory. We cannot adequately discuss the results of the Narwhal Island program until the field phase is completed (mid-June 1976) but the program is currently going well. The laser profilometer program has also been very successful. The only problem area has been in getting prints of

the SLAR images. This is, however, more a nuisance than a serious problem. If this is not resolved by early summer, the prints can be prepared by a commercial contractor.

VIII. CONCLUSIONS

Again it is too early to adequately prepare such a section.

IX. NEEDS FOR FURTHER RESEARCH

We can only address this subject when we get further into the analysis phase of our program.

X. SUMMARY OF 4TH QUARTER OPERATIONS (January-February-March 1976)

1. Field Activities

   a. 1 January - 15 February 1976

      Testing of the radar transponder system in Hanover, N.H.

      A number of technical problems were located and eliminated. In addition valuable experience was gained on the operation of the system (Kovacs, Hibler, Tucker, Mock).

   b. 12 - 27 February 1976

      Completion of the 1st set of laser profilometer flights from Barrow, Alaska. Transects into the Chukchi Sea from Point Lay, Wainwright and Barrow (headings 315° true) and into the Beaufort Sea from Lonely, Cross Island and Barter Island (headings 025° true) were completed. Each transect

consisted of a 200 km leg both out and back. Striking differences in ridging intensity were noted both along and normal to the coast with the most intense deformation occurring in the vicinity of Barter Island (Weeks and Frank).

c. 1 March - present

Initiation of Narwhal Island field program

Installation of the radar transponder array has now been completed with eight transponders currently in operation. Work is underway to activate the other components of this program (Kovacs, Hibler, Tucker).

REFERENCES

Cooper, P.F. Jr. (1975) Movement and deformation of the landfast ice of the southern Beaufort Sea. Beaufort Sea Project Technical Report No. 37, 16 pp.

Hibler, W.D., W.F. Weeks, A. Kovacs, and S.F. Ackley (1974a) Differential sea ice drift. I. Spatial and temporal variations in sea ice deformation. Journal of Glaciology 13 (69), 437-55.

Hibler, W.D., S.F. Ackley, W.K. Crowder, H.L. McKim and D.M. Anderson (1974b). Analysis of shear zone deformation in the Beaufort Sea using satellite imagery. In "The Coast and Shelf of the Beaufort Sea" (J.C. Reed and J.E. Sater, eds.) p. 285-296. Arctic Institute of North America, Arlington, Virginia.

Kovacs, A., A. Gow and W.F. Dehn (1975) Islands of grounded sea ice. POAC Conference, Fairbanks, in press. (inclosed Appendix 2).

Kovacs, A. and A. Gow (1976) Some characteristics of grounded floebergs near Prudhoe Bay, Alaska. Arctic, in press. (inclosed Appendix 1).

Wetzel, V.F., R.K. Atwater and T.E. Huta (1974) Arctic ice movement and environmental data stations. In "The Coast and Shelf of the Beaufort Sea" (J.C. Reed and J.E. Sater, eds.) p. 269-284 Arctic Institute of North America, Arlington, Virginia.

Appendix 1 RU#88

Submitted to Arctic
on 4 March 1976

SOME CHARACTERISTICS OF GROUNDED FLOEBERGS NEAR PRUDHOE BAY, ALASKA

by

Austin Kovacs and Anthony J. [redacted]

U. S. Army Cold Regions Research and Engineering Laboratory
Hanover, N.H., USA

ABSTRACT

Some physical characteristics of two grounded floebergs near Prudhoe Bay, Alaska, are described. Cross-sectional profiles of the sails and keels of both floebergs were obtained by levelling and from drilling and sonar measurements respectively. Additional studies included investigations of the internal structure of the floebergs, surveys of the sea floor for evidence of scoring induced during grounding of the floebergs and a brief examination of the organic and sedimentary debris found entrained within the floebergs.

INTRODUCTION

During the winter of 1974-75 a large number of floebergs were found incorporated in the fast ice northwest of Prudhoe Bay between Bodfish and Cross Islands. Many of the floebergs had been driven up onto the sea floor and become stranded, as indicated by their high freeboard. The grounding of ice on the continental shelves of the Arctic is of considerable interest today, not only within the oil industry which is moving to develop the oil and gas reserves located offshore, but also within environmental groups which are concerned with the safety of offshore producing platforms and bottom-founded structures. Much of this interest concerns the forces which develop when large, deep-drafted ice becomes grounded and is then pushed by the pack across the sea floor. During this process the sea bed may become gouged and scored or otherwise extensively modified by the

plowing action of the ice. Thus, for both economic and environmental reasons, sea floor production systems must be designed to resist these forces or be buried below the deepest contemporary ice scoring.

In order to gather information on the geometry of floebergs and their effect upon the sea bed during grounding, a short field trip was made to the area of stranded floebergs in April 1975. Field studies included the determination of the surface relief of two floebergs and snow thickness measurements using standard surveying techniques, the profiling of the floeberg keel using a sonar technique developed by Kovacs (1970), and examination of the internal structure, void and impurity content in the floebergs, as observed in fracture faces on the floeberg sail and of that portion of the keel uplifted upon grounding.

STUDY AREA

The area of study was located approximately 12 km north of Long Island (Figure 1). The fast ice surface in the immediate area of the floebergs was highly irregular, due largely to the incorporation of ice fragments into the ice sheet. The surface was covered with a layer of snow that varied in thickness from 10 to 40 cm depending on the extent of the local ice relief.

RESULTS AND DISCUSSIONS

Two floebers, A and B, were investigated in detail. An aerial view of Floeberg A is shown in Figure 2. This view shows the floeberg ice surface to be substantially free of voids, that is, all space between the original ice blocks is now thoroughly cemented with refrozen melt or rain water. The fracture faces on the east and west sides of the floeberg also lacked voids. Thus, for all intents and purposes, this fragment of a multi-year pressure ridge now consisted entirely of solid ice.

The north face of the floeberg was found to have an accumulation of broken first-year ice piled upon it. This indicates that the floeberg was driven aground during a storm which pushed the ice from the north toward the coast. Upon grounding, Floeberg A became immobile. The pressure on the first-year ice to the north of the formation continued to force the ice sheet southward. Unable to resist the stresses developed, the ice sheet failed against the floeberg, causing the broken ice to accumulate in a pile on its north side and leaving a wake of ice fragments trailing to the south.

A closer view of the east side of the floeberg (Figure 3) shows a distinctive ice shelf or ledge at about the same level as the man's head. This ledge encircled the floeberg completely and marks the position of the water line when the ice formation was free-floating. The ledge was elevated approximately 1.85 m above the surrounding ice surface, indicating that the floeberg had been driven upward onto the sea floor by this amount during grounding.

The cross-section of Floeberg A is presented in Figure 4a. No voids were encountered at the site of the exploratory hole, indicating that this part of Floeberg A was composed of thoroughly cemented blocks of ice. The maximum sail height of Floeberg A was 6.06 m; the keel depth measured approximately 12.4 m. If we now adjust these dimensions for the uplift of 1.85 m associated with grounding, then the sail height reduces to 4.21 m and the keel depth increases to 14.25 m. This yields a sail height to keel depth ratio of 1 to 3.38, which is in good agreement with the 1 to 3.3 sail height to keel depth ratio found by Kovacs et al. (1973) and Kovacs and Mellor (1974) for multi-year pressure ridges.

To determine if the ice keel had scored the sea floor during grounding, a series of holes (marked A-L in Figure 2) were drilled through the ice cover along a line parallel to the north side of the floeberg. The depth to the sea floor was then measured by lowering a weighted tape through the holes. Results of these measurements, presented graphically in Figure 4b, reveal some micro-relief between stations A and C, where depths were measured every meter, but no major depression was observed which would indicate the keel had significantly scored the sea floor. Soundings made along the east and west side of the floeberg also failed to reveal any definite trace of scoring of the sea bed. This lack of scoring behind Floeberg A might be attributed to a flat-bottomed keel that "slid" along, rather than "plowed" through the sea floor which, at this location, was composed mainly of coarse sand.

An aerial view of Floeberg B is shown in Figure 5. The floeberg is roughly triangular in shape, and as with Floeberg A, a large accumulation of fragmented first-year ice was piled along its north side. Trailing to the south was a wake of broken ice. These observations imply that Floeberg B had also gone aground during a storm which had driven the ice cover southward toward the coast. This grounding was accompanied by uplift of the floeberg into its present position. Eventually the floeberg became so firmly grounded that the thin first-year sea ice failed and began to pile up on its northern face. In this particular instance, the weight of additional ice caused the floeberg to tip to one side. This tilting of the floeberg prevented us from making any accurate assessment of the total uplift associated with grounding.

The cross-section of the floeberg is given in Figure 6a. The highest elevation on the surface profile was 6.65 m and the keel is shown to be grounded in approximately 12.5 m of water. The extent to which first-year ice has piled up on the north side of the floeberg is also indicated.

The profile of the sea floor immediately behind the floeberg is shown in Figure 6b. The sea floor has a deep depression near the center of the north face of the floeberg at Station E. On each side of this depression the sea bed has an undulating relief with a mean depth of approximately 12.5 m. The depressior is believed to have been created by the keel of the floeberg as it plowed into the sea

floor during grounding. The maximum depth of the score below the mean sea floor depth is 1.1 m. The score is approximately 15 m wide and has an average depth of 32 cm.

Large numbers of ice keels, coming aground on the arctic shelf, have caused widespread scoring of the sea floor. The effect of this scoring on biological activity of the sea floor is significant for, as Geikie (1882), Wright and Priestley (1922), Rex (1955), Kovacs and Mellor (1971), Kovacs (1972), Reimnitz and Barnes (1974), Barnes and Reimnitz (1974) and others have reported, contemporary ice scoring does cause mixing of sea bed deposits, destroying stratification and allowing for oxygenation of the sediments. Such interaction of ice with the sea floor not only disrupts bottom conditions sufficiently to hinder the growth of plants, it also inhibits the occupation of the sea bed by many marine species which might otherwise inhabit the area.

Visual examination of some 50 additional floebergs in the general area of Floebergs A and B showed that all were composed of tabular blocks and assorted fragments of ice, ranging in size from a few centimeters to several meters across, and firmly cemented together with no trace of interblock voids. Internal structure was best revealed in the exposed faces of floebergs that had split apart and a typical example of such structure is presented in Figure 7.

All floebergs contained variable quantities of debris inclosed within and between the blocks of ice. Most of this debris was organic in nature, composed principally of brown algae that had

obviously been trapped in the ice during freezing. Sedimentary material was identified mainly as of silt-clay composition, though coarse sandy debris was occasionally observed. The finer sedimentary particles are probably of eolian origin but the exact source and manner of entrapment of the coarser particles has not been firmly established.

ACKNOWLEDGEMENTS:

This work was supported by the U. S. Department of Commerce National Oceanic and Atmospheric Administration under Purchase Order No. 01-5-022-1651. We wish to acknowledge the review of this paper by Dr. W. F. Weeks and Mr. S. F. Ackley.

LIST OF REFERENCES

Barnes, P.W. and E. Reimnitz (1974) Sedimentary processes on arctic shelves off the northern coast of Alaska, In the Coast and Shelf of the Beaufort Sea. Proceedings of the Arctic Institute of North America Symposium on Beaufort Sea Coast and Shelf Research.

Geikie, J. (1882) The great ice age, and its relation to the antiquity of man, New York, Appleton.

Kovacs, A. (1970) On the structure of pressured sea ice, USA CRREL Contract Report to the U. S. Coast Guard.

Kovacs, A. (1972) Ice scoring marks floor of the Arctic shelf, The Oil and Gas Journal, Oct. 23.

Kovacs, A. and M. Mellor (1971) Sea ice pressure ridges and ice islands, Creare Technical Note 122, Creare, Inc., Hanover, N.H.

Kovacs, A. and M. Mellor (1974) Sea ice morphology and ice as a geological agent in the southern Beaufort Sea, In the Coast and Shelf of the Beaufort Sea. Proceedings of the Arctic Institute of North America Symposium on Beaufort Sea Coast and Shelf Research.

Kovacs, A., W. F. Weeks, S. F. Ackley and W. D. Hibler III (1973). The structure of a multi-year pressure ridge, Arctic, Vol. 26, No. 1.

Reimnitz, E. and P. W. Barnes (1974) Sea ice as a geologic agent on the Beaufort Sea shelf of Alaska, In the Coast and Shelf of the Beaufort Sea. Proceedings of the Arctic Institute of North America Symposium on Beaufort Sea Coast and Shelf Research.

Rex, R. W. (1955) Microrelief produced by sea ice grounding in the Chukchi Sea near Barrow, Alaska, Arctic, Vol. 8, No. 3.

Wright, C. S. and R. E. Priestley (1922) Glaciology: British Terra Nova Antarctica Expedition 1910-1913, London, Harrison.

LIST OF FIGURES

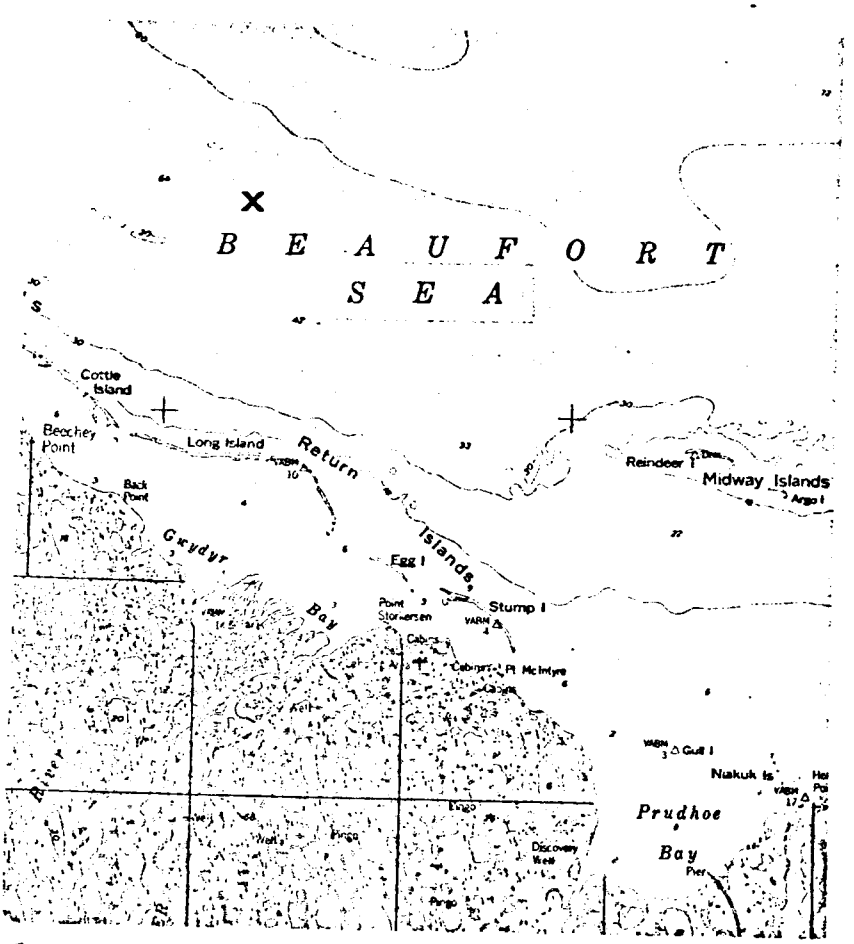

Figure 1. Map of Prudhoe Bay area showing location of floeberg study site (marked with X). Water depths are in feet.

Figure 2. Aerial view of Floeberg A. The line of drill holes marked A-L measures approximately 44 m; arrows indicate the position and direction of the cross-section profile.

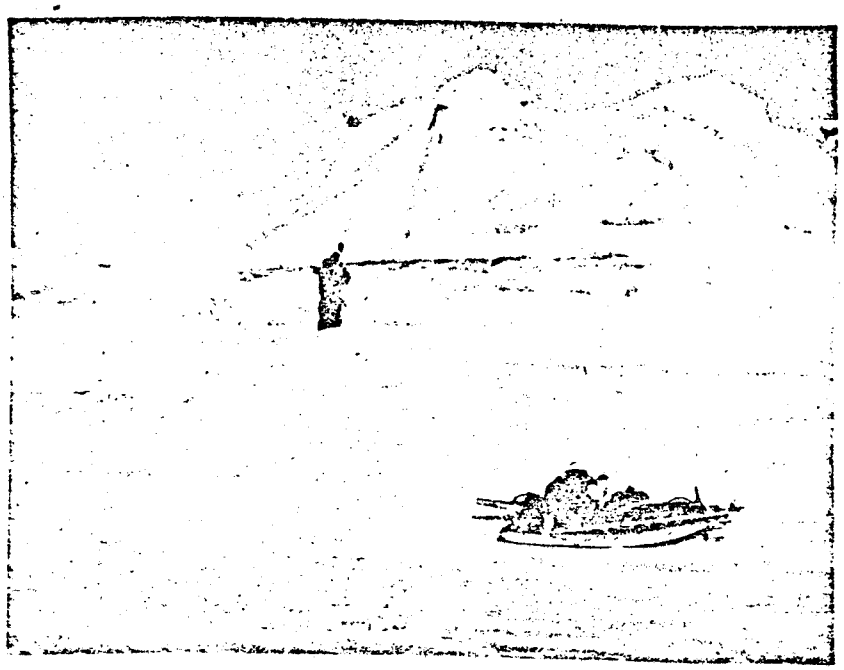

Figure 3. Close-up of grounded Floeberg A. Note original wave-cut ledge now elevated at level of man's head.

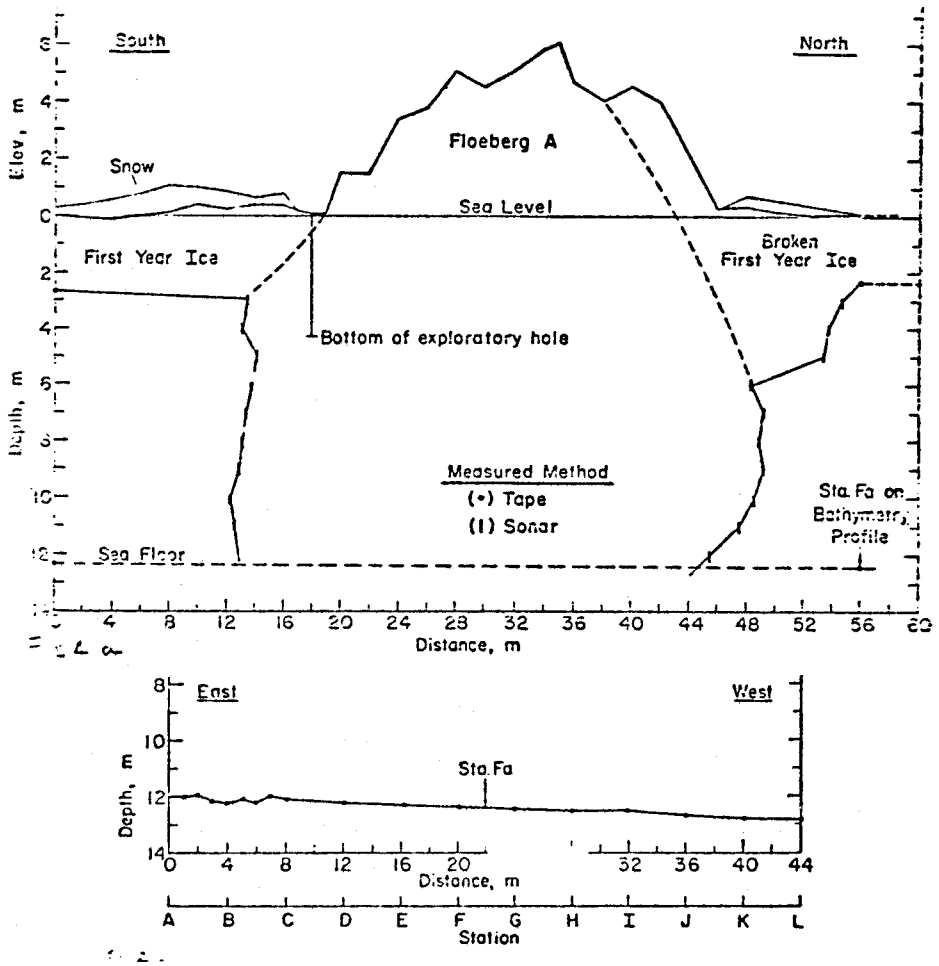

Figure 4. (a) Cross-section of Floeberg A together with (b) profile of sea floor from directly behind the floeberg.

Figure 5. Aerial view of Floeberg B. The line of drill holes marked A-M measures approximately 40 m; arrows indicate the position and direction of the cross-section profile.

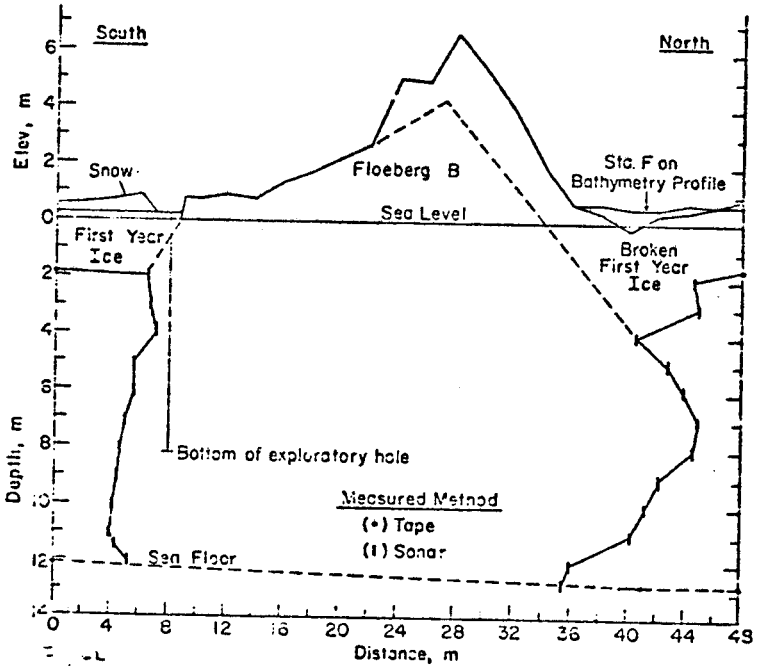

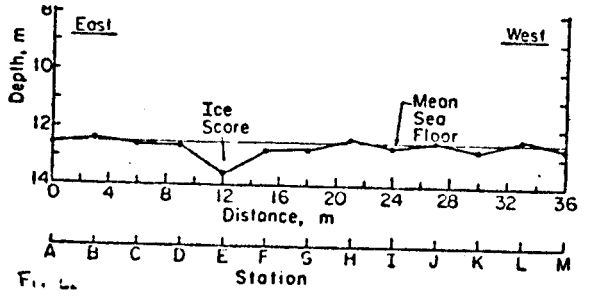

Figure 6(a) Cross-section of Floeberg B
(b) Profile of sea floor from directly behind the floeberg.

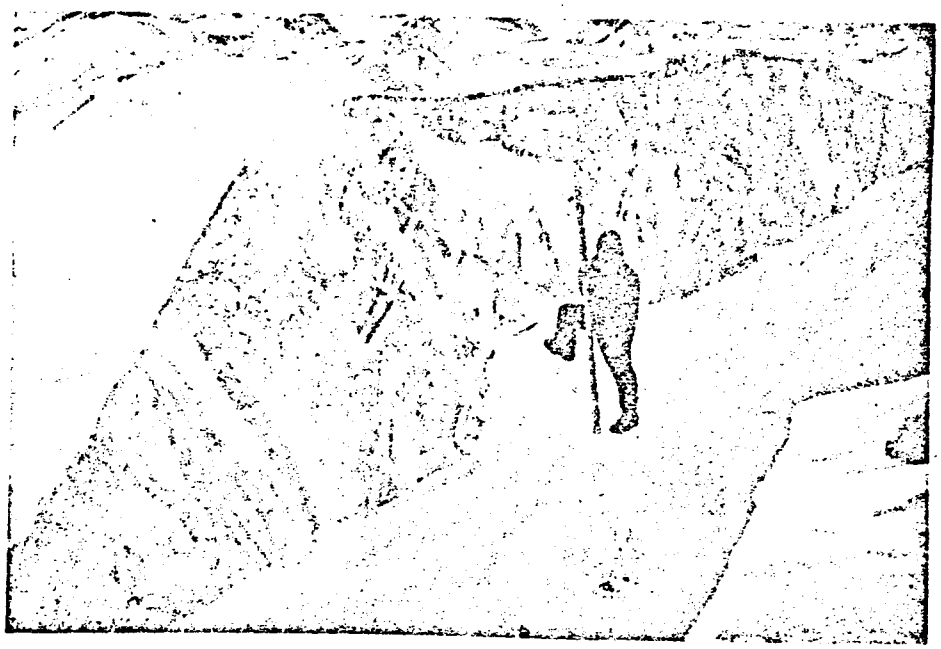

Figure 7. Exposed section through center of floeberg showing structural arrangement of ice blocks. Ice contains abundant algal remains and some sedimentary material (dark patches).

Appendix 2 RU#88
Preprint 1975
POAC
Conference

ISLANDS OF GROUNDED SEA ICE

Austin Kovacs and Anthony Gow

U.S. Army Cold Regions Research and Engineering Laboratory
Hanover, New Hampshire
United States

W. F. Dehn

6701 Belfast Place,
Oxon Hill, Maryland
United States

ABSTRACT

Large areas of grounded sea ice have been reported by early arctic explorers and more recently by the U.S. Coast Guard. The ESSA, ERTS, NOAA, and DMSP satellites now provide multi-spectral imagery with sufficiently high resolution to allow detailed sequential observations to be made of the movement and spatial extent of arctic sea ice. This report discusses the location, formation, and decay of five large (>30 km^2) islands of grounded sea ice in the southern Chukchi Sea as observed for an extended period of time using satellite imagery. Measurements of the bathymetry around one grounded sea ice feature are presented along with observations made and photos taken from the ice surface. The potential use of these sea ice islands as research stations is also discussed.

INTRODUCTION

From the earliest voyages to polar seas in small sailing vessels to more recent trips over arctic seas in aircraft, travelers have reported discovering new islands which have defied the attempts of all subsequent travelers to relocate. Mysterious disappearing northern islands of the past include the famous Gunnbjorn Skerries found by a Norwegian in 877 while sailing between Iceland and Greenland (Zukriegel, 1935; Nansen, 1911). While never seen again, Gunnbjorn's discovery remained on the maps and in the minds of men for centuries. Perhaps the most famous island discovered was sighted off the southern coast of east Greenland by Frobisher in 1578 (Best, 1578) and referred to as the Isle of Buss, the Land of Buss and, finally, when it could not be relocated, the Sunken Land of Buss. This land too remained on the maps for centuries and as late as 1818 Edward Parry is known to have made a special search for it (Parry, 1821). Then there were the lands and islands known as Arctic Land, hypothesized by Harris (1904) to be west of Prince Patrick Island; Keenan Land, searched for by Mikkelson (1909) in the Beaufort Sea; Presidents Land, reported in 1876 to be in the Lincoln Sea; Bradley Land, sighted by Cook (1911) at 85°N, north of Axel Heiberg Island; Sannikov Land; Crocker Land, sighted by Peary (1907) northwest of Ellesmere Island; the sandy island located in the Beaufort Sea at 76°N 150°W by Gracianski in 1937 while looking for the lost crew of a Russian polar flight (Brower, 1960); and Takpuk's Island, found in the early 1930's at about 71°N, 145°W in the Beaufort Sea. This last island was reported by Takpuk to have small ponds, grass and moss on it and a scattering of boulders up to the size of a man's head (Stefansson, 1934).

Several of these "islands" are now believed to have been large tabular icebergs, the so-called ice islands, which have been seen in considerable numbers in the Arctic Ocean during the last thirty years (Kovacs and Mellor, 1971 and 1974). These are undoubtedly what Gracianski and Takpuk saw and reported as islands. New "islands" have now been found and are discussed in this paper.

THE DISCOVERY

The first indication of an anomalous condition existing in the sea ice approximately 160 km northwest of Pt. Barrow, Alaska, occurred during a routine inspection of NOAA-1 satellite imagery in the spring of 1971. The site of the anomaly was indicated by the existence of a large polynya which persisted in one general location. This area of open water appeared as a dark spot in a field of gray sea ice on the NOAA imagery (Fig. 1, position 1). Soon after this discovery, contact was made with the Naval Arctic Research Laboratory (NARL) at Pt. Barrow and the director was informed of the discovery. It was requested that a mission be flown to the site to determine if the polynya was associated with the grounding of a large ice island or was due to an extensive accumulation of grounded sea ice on a shoal shown to be 22 meters below sea level at 71°54'N, 161°8'W on the 6th edition of the U.S.C. and G.S. Arctic Coast of Alaska Map No. 9400. However, this mission was not flown.

Information of the find was also given to the U.S. Coast Guard and a request was made for the icebreaker *Burton Island*, which was scheduled for summer operation in the Chukchi Sea in 1972, to investigate ice conditions in the area of the polynya, which continued to appear on NOAA satellite imagery through the winter and spring of 1972. In August 1972, the *Burton Island* visited the area. A large ice formation was observed with highly irregular relief that appeared to rise as much as 9 m above the sea. Although the description given was of a large hummock field of pressured sea ice, news quickly spread that the formation was a large piece of shelf ice, i.e., an ice island, 8 by 20 km in size (Untersteiner, 1972a and b).

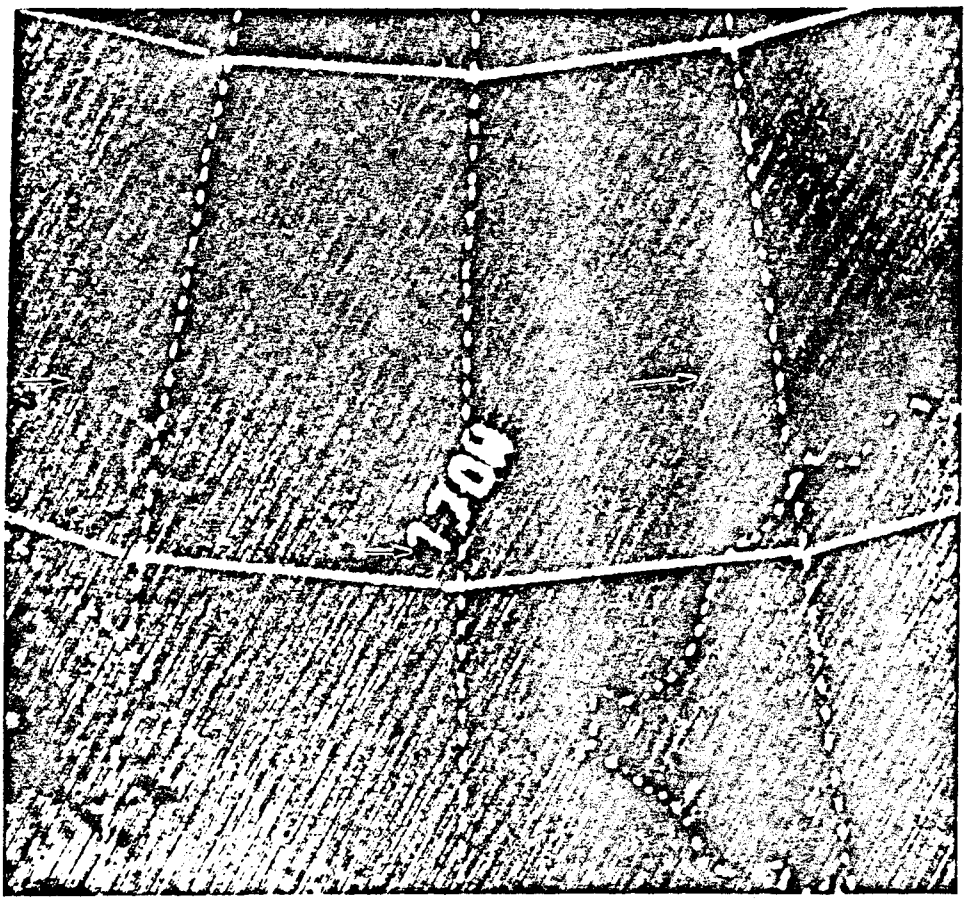

Figure 1. NOAA-1 satellite image of 13 May 1971. Orbit No. 1922, showing polynya associated with the grounded sea ice feature (1) and polynyas associated with grounded ice on Herald Shoal (2) and on a shoal west of Wrangel Island (3).

Photographs taken by Captain Robert G. Moore during the *Burton Island* visit did not become available to us until the spring of 1975 (courtesy of Dr. A. Grantz). Three of the twenty-one photos received are shown as Figures 2, 3, and 4. Figure 2 shows approximately three quarters of the grounded island of ice as it appeared at a distance from the air. The contrast between the sunlit pressure ridges incorporated in the island and the rarefied summer pack is quite apparent. The extreme southwestern tip of the island, here designated Dehn Point, is shown in Figure 3 to consist of belts of shear ridges, hummocked ice and floes of multi-year ice. A close-up of the summer melt features on the island is shown in Figure 4.

None of the Coast Guard photos of the island showed any fragments of shelf ice, i.e., ice islands. In September 1972, W. Dehn flew over the site to assess and photograph the surface structure of the grounded ice. Several photographs taken on this trip revealed the existence of a cluster of twenty-seven ice island fragments with abnormally high freeboards (Fig. 5). This latter situation was presumed to be the result of uplift associated with grounding. This discovery led to the speculation that an ice island had drifted onto the shoal and was then pushed higher up on the shoal by the moving pack until the ice island had become firmly grounded. Stresses associated with grounding are believed to have resulted in fragmentation of the island. It was assumed that the grounded ice island fragments were the anchor point against which the moving pack failed, eventually to form the large area of grounded ice shown in Figure 2. Detection of the island of grounded ice on satellite imagery

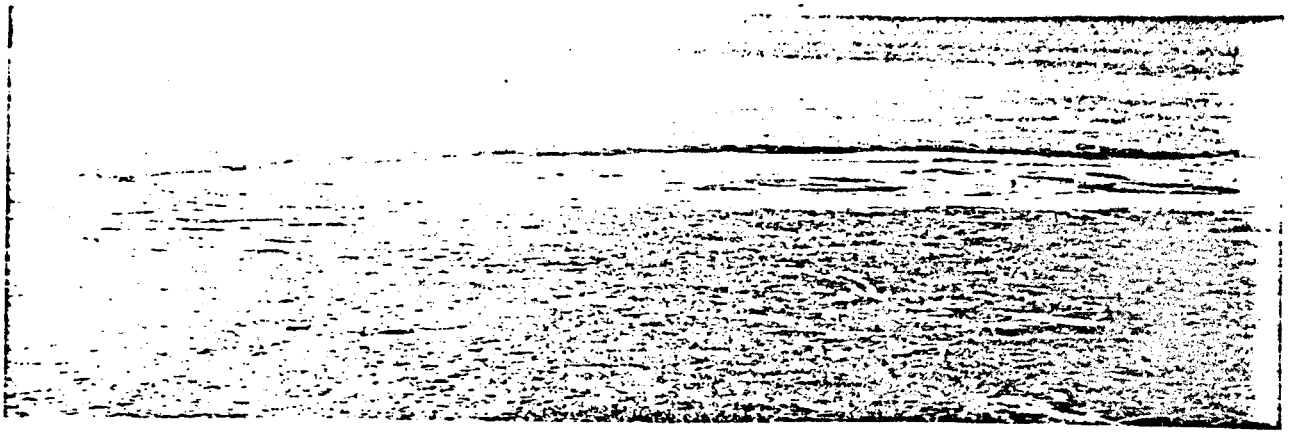

Figure 2. Oblique view of grounded sea ice feature showing approximately 75% of its linear dimension. Dehn Point is at left end (southwestern tip) of island.

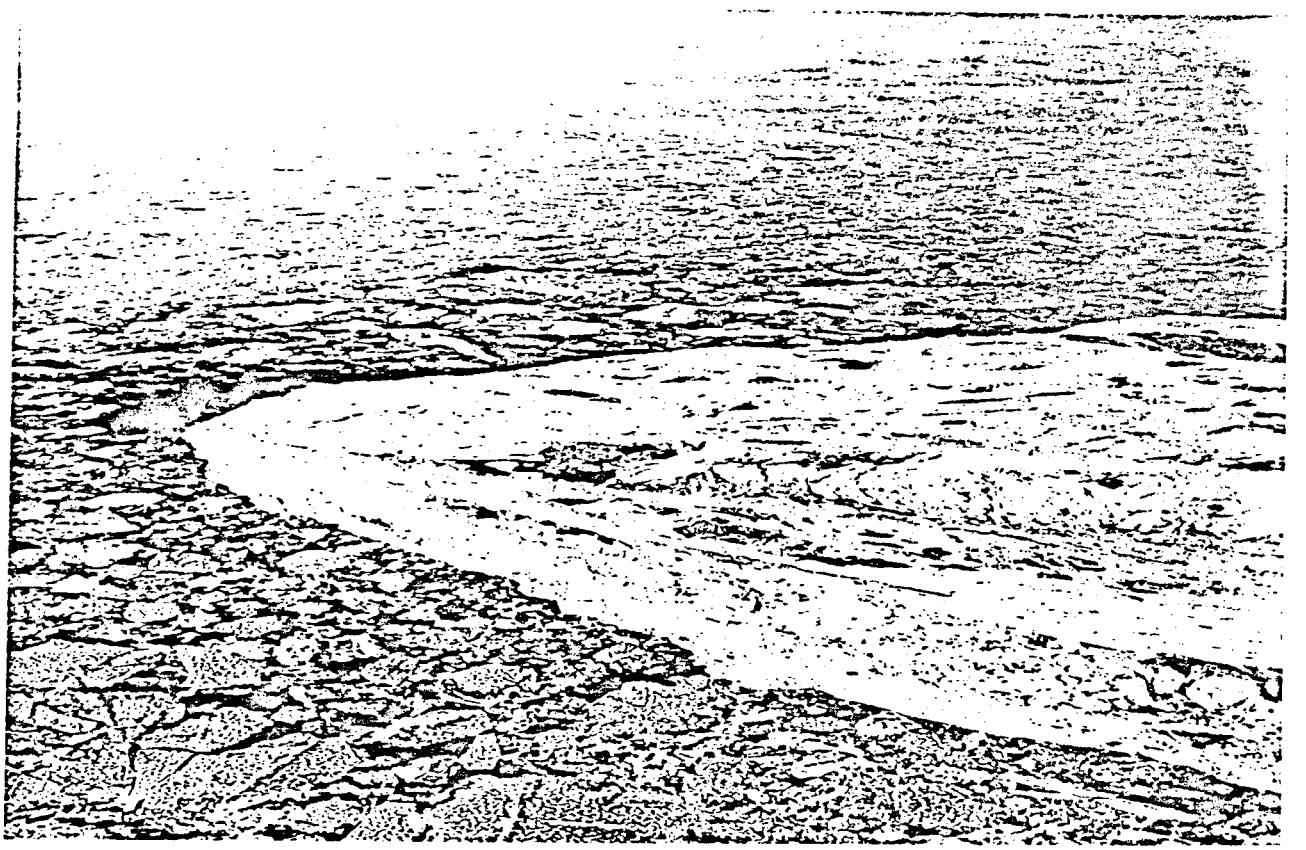

Figure 3. Aerial view showing structural characteristics of ice incorporated into the grounded sea ice feature at Dehn Point.

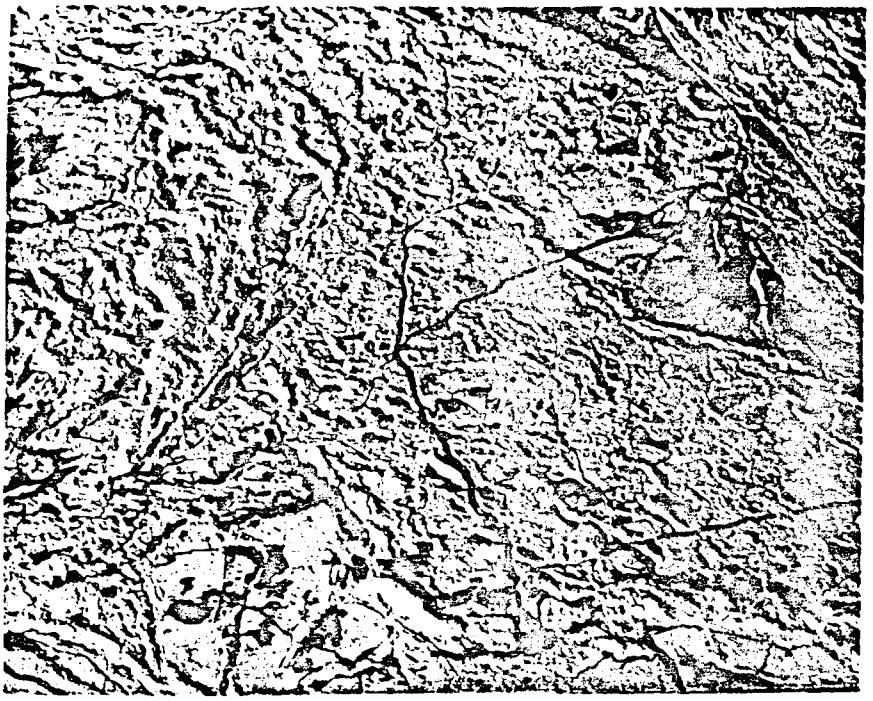

Figure 4. Aerial view of summer melt features near the edge of the island of grounded sea ice.

Figure 5. Cluster of ice island fragments incorporated into grounded sea ice feature. Photograph was taken in September 1972.

was therefore made possible by the large polynya which forms on the side of the island opposite the direction in which the pack ice is moving.

AGE OF THE ISLAND

To determine how long the island of grounded ice had been in existence, hundreds of NOAA, ESSA and Nimbus satellite images of the area were inspected. The earliest imagery available to us was that of 1966 from the Nimbus satellite. Although of very low resolution, this imagery revealed the polynya associated with the island (14 June 1966 Nimbus orbit 408, frame 30). For the years 1967 through 1972 the polynya may be seen on the following selected imagery: 16 May 67 ESSA-3 orbit 2844; 7 May 68 ESSA-3 orbit 7328; 11 May 69 ESSA-9 orbit 932; 5 May 70 ESSA-9 orbit 5416 ; 13 May 71 NOAA-1 orbit 1922 (see Fig. 1); and 3 May 72 NOAA-1 orbit 4522. Satellite imagery thus establishes the fact that the island is not new but has indeed been in existence for many years.

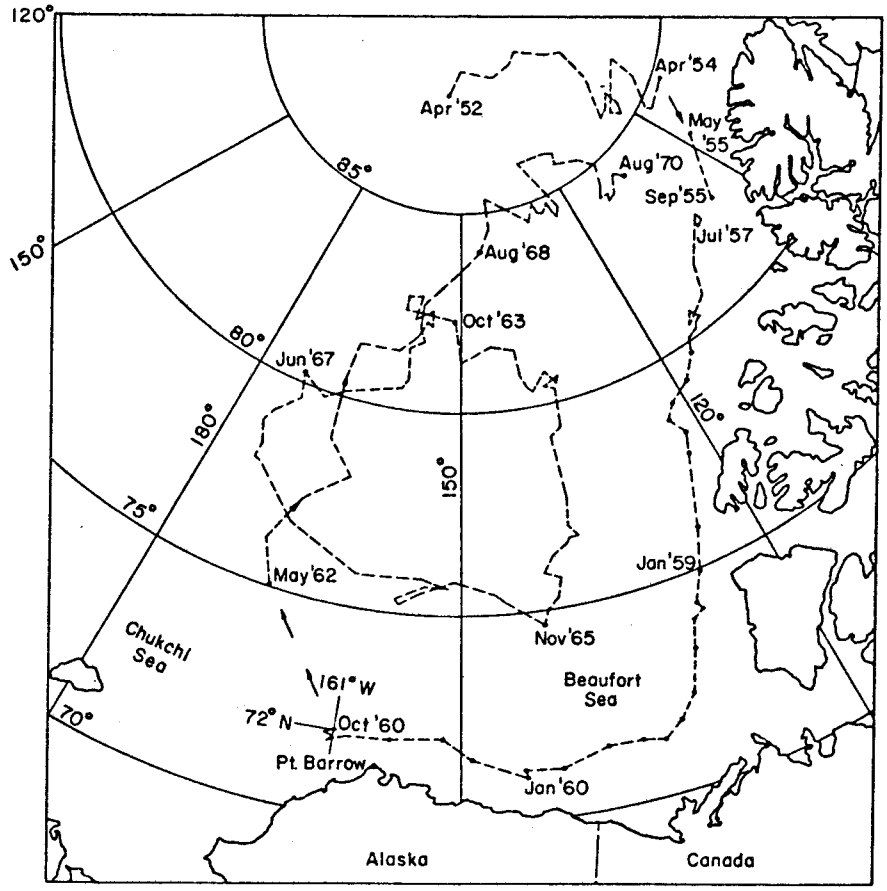

Figure 6. Drift track of ice island T-3 from April 1952 to August 1970. The approximate position of the island when it came aground in October 1960 is shown as 72°N, 161°W.

It is interesting to note that in 1960 the United States drifting ice island research station T-3 came aground on a shoal at 71°43'N, 161°14'W (Schindler, 1968) (Fig. 6). T-3 was 16.5 by 8 km in size just before it grounded but split into at least two pieces soon after. The research station was abandoned in October 1960 but was re-occupied in 1961 when the fragment on which it was located was found to be drifting northward away from the shoal. The size of T-3 was only 6.4 by 3.2 km when it was remanned (Smith, 1971). What happened to the larger portion of the T-3 ice island is not known. Could it be that the ice island fragments seen in Figure 6 are from T-3? If so then the island of grounded ice has existed since 1960.

A recent study has been made using higher resolution 1973 and 1974 ERTS-1 satellite imagery to determine the position of the island of grounded ice and to observe its enlargement and decay with time (Kovacs *et al.*, 1975). This 1973 imagery revealed for the first time the existence of two grounded ice formations in the area of the polynya seen in the NOAA imagery; one was located at 72°N, 162°W and the second at 72°07'W, 162°10'W (Fig. 7). The ice formations were observed to increase and decrease in size as the direction and compactness of the moving pack changed. It is interesting to note that the smaller ice formation seen in the 1973 imagery at 72°07'N, 162°10'W could not be found in the 1974 ERTS-1 imagery of the area that Kovacs *et al.* (1975) reviewed. The 4 September 1974 NOAA-3 image shows only the larger ice formation surrounded by an extensive area of open water (Fig. 8, position 1). At this time the ice

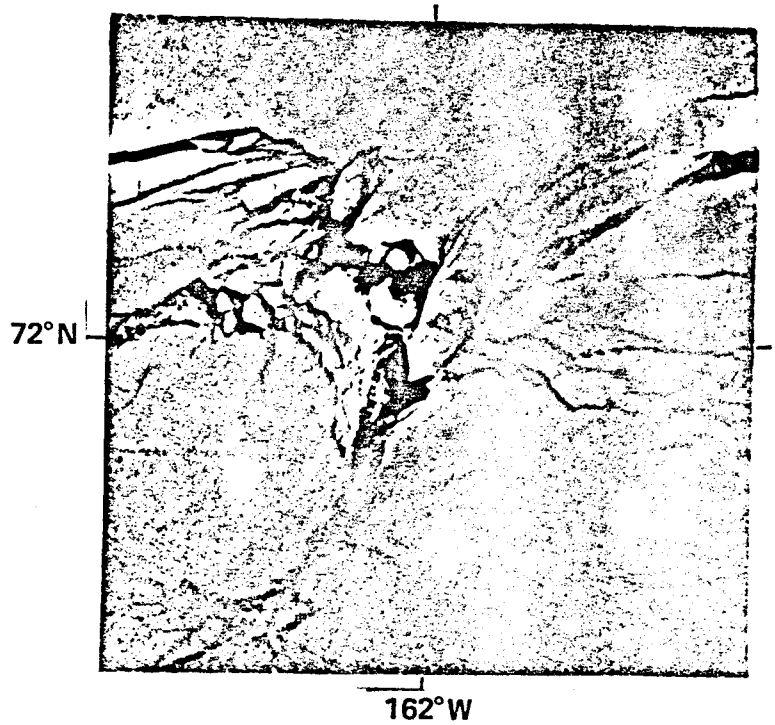

Figure 7. ERTS-1 satellite image (ID No. 1282-22261) of 1 May 1973 showing two grounded ice features near the polynya seen in the NOAA-1 image presented in Figure 1.

Figure 8. NOAA-3 satellite image No. 3807 V2F2276 of 4 September 1974 showing grounded sea ice island (1) surrounded by large area of open water. Note the size of the island of grounded ice relative to that of Big Diomede Island (2).

Figure 9. View of landing site and surrounding features on grounded island of sea ice.

formation was somewhat larger than Big Diomede Island which is approximately 9.3 km in length and clearly visible in the NOAA-3 image at position 2. The 1975 ERTS (Landsat) imagery also reveals that the smaller ice formation had not re-formed. This finding indicates that islands of grounded ice are not necessarily permanent features and may even be seasonal formations.

Neither of the two islands of grounded ice was located near the shoal shown at 71°54'N, 161°8'W on the 6th edition of U.S.C. and G.S. Arctic Coast of Alaska Map No. 9400. The most recent edition of this map, published in 1973, shows not one but two shoals near the area of the grounded ice formations, one 18 meters below the ocean surface at 71°50'N, 161°10'W and the other approximately 22 meters below the surface at 71°50'N, 161°7'W. Kovacs *et al.* (1975) found that "these shoals are approximately 35 km east-southeast of the site of the two grounded ice formations found in the 1973 ERTS-1 imagery" and speculated "that the two grounded ice formations are resting upon these shoals." They reasoned that since corrected "ERTS-1 imagery can be used to position surface features to within 300 meters of their true geographic positions, the location of the shoals in the bathymetric chart may be in error."

ISLAND VISIT

A field trip was made to the island of grounded ice to obtain bathymetric measurements around it, to investigate its surface morphology and compositional structure, and to ascertain if it could be safely used for a manned research base. On 13 April 1975, a flight was made to the island. An extensive search was made for a place to land, but without success. On 15 April another flight was made to the island and a small area of first-year ice was found on its central western edge which was large enough to land on. The landing area and the formidable hummock field surrounding it are shown in Figure 9.

The search for a landing site revealed an ice surface of highly varying relief. Incorporated in the island were small areas of first- year ice which had formed in the numerous summer melt pools (see Fig. 4), many multi-year floes which either developed on site or had become a part of the island during the yearly winter accretion process, and endless belts of shear ridges and fields of brecciated ice averaging 5 to 6 meters high with many peaks on the order of 15 meters high (Fig. 10). A number of large floebergs were seen (Fig. 11), but nothing that could be identified as a fragment of shelf ice. This feature would thus appear to be a true island of grounded sea ice.

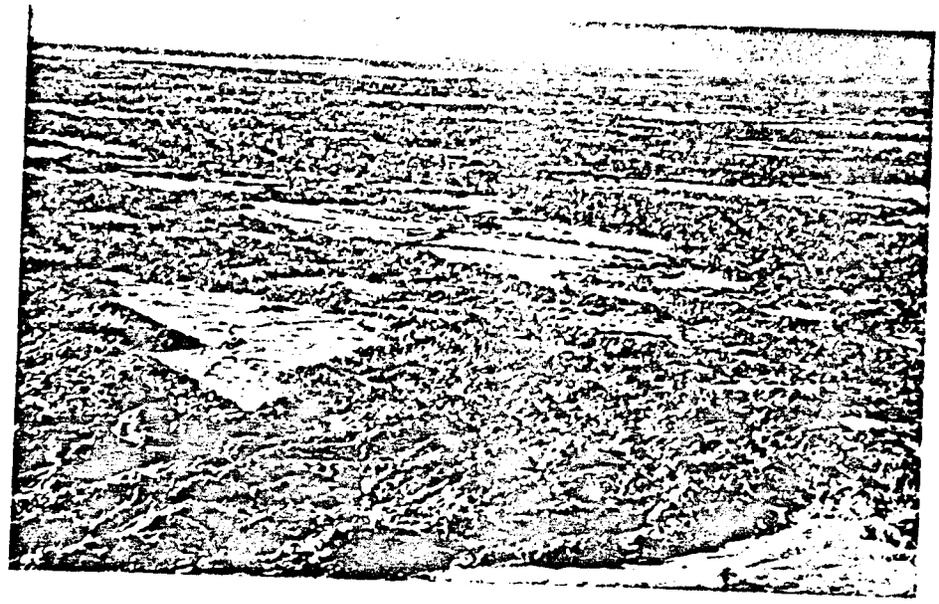

Figure 10. View of hummock field in grounded sea ice with ridge peaks up to 15 m high.

Figure 11. View showing floebergs incorporated into the grounded sea ice island.

Accompanying us to the island in a helicopter was Mr. Jack Lentfer of the U.S. Fish and Wildlife Service. Mr. Lentfer, internationally known for his research on polar bears, was at the time engaged in his annual spring polar bear tagging program. His interest in the island in general, and in the polar bears which might be found there, allowed us to prevail upon him to assist in the field deployment of our camp and to make a low level inspection by helicopter.

The field camp was established on a thick multi-year floe incorporated into the western side of Dehn Point. This site was selected because it provided access to a long refrozen lead which meandered northwest toward the interior of the island. On this lead we planned to walk toward the interior, taking water depth and ridge height measurements en route. This route was denied to us the following morning when at approximately 9 o'clock the ice to the west began to pressure. Within two hours the ice in the lead was transformed into a hummock field of first-year and multi-year ice. The field began within 15 meters of our camp and extended as far as one could see to the west from the top of a 7-meter-high pressure ridge. Ice conditions around the island of grounded ice on 15 and 16 April 1975 are shown in Figures 12 and 13.

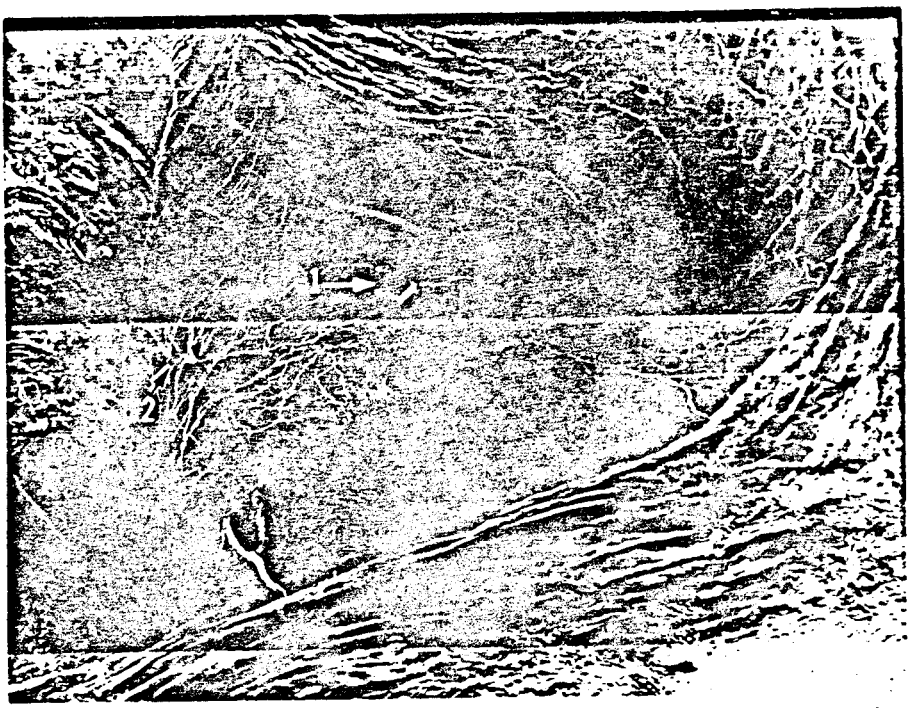

Figure 12. Defense Meteorological Satellite Program (DMSP) image of 15 April 1975 showing ice conditions around the island of grounded sea ice (1) and the existence of two islands of grounded ice on Herald Shoal (2).

There was a large polynya on the southeast side of the island and a tongue of pressured ice nearly 50 km long extended outward from the northwest side. It was the ice movement and the resulting pressuring associated with the formation of this tongue that caused the crushing of the lead next to our camp. In the Landsat image of 29 April (Fig. 14) this ice tongue is no longer apparent.

Our convenient route into the interior of the island now gone, we attempted to move directly over the ice surface. This effort was soon terminated when it became apparent that both we and the equipment would suffer considerably and there was not sufficient time to make a long trek over the snow-slickened rubble extending toward the interior. The relief which was before us is shown in Figure 15.

Our stay lasted two days. This short visit revealed that the surface relief was a chaotic jumble of pressured sea ice covered by a surprisingly deep layer of snow. Walking over this terrain was exceedingly difficult and treacherous when snow bridges between the ice blocks gave way under foot.

Bathymetric measurements made at six sites around the periphery of the island varied from 28 to 31 meters, averaging 30 meters. During the spring of 1976 we plan a helicopter trip to the island for the purpose of making additional bathymetric measurements throughout its interior. These measurements will allow us to determine the depth of the shoal upon which the island of sea ice is grounded.

OTHER ISLANDS OF GROUNDED ICE

Besides the two islands of grounded sea ice discussed, we have found similar formations on Herald Shoal (70°30'N, 171°30'W), and on a shoal off the northwest coast of Wrangel Island. Unlike the island of grounded sea ice northwest of Pt. Barrow, which remains year round, these other islands do not survive the summer and in some locations

Figure 13. NOAA-4 satellite image No. 1906 V2F1492 of 16 April 1975 showing ice conditions around the island of grounded sea ice at 72°N 162°W (1), two grounded ice features on Herald Shoal (2), and a grounded ice feature west of Wrangel Island (3).

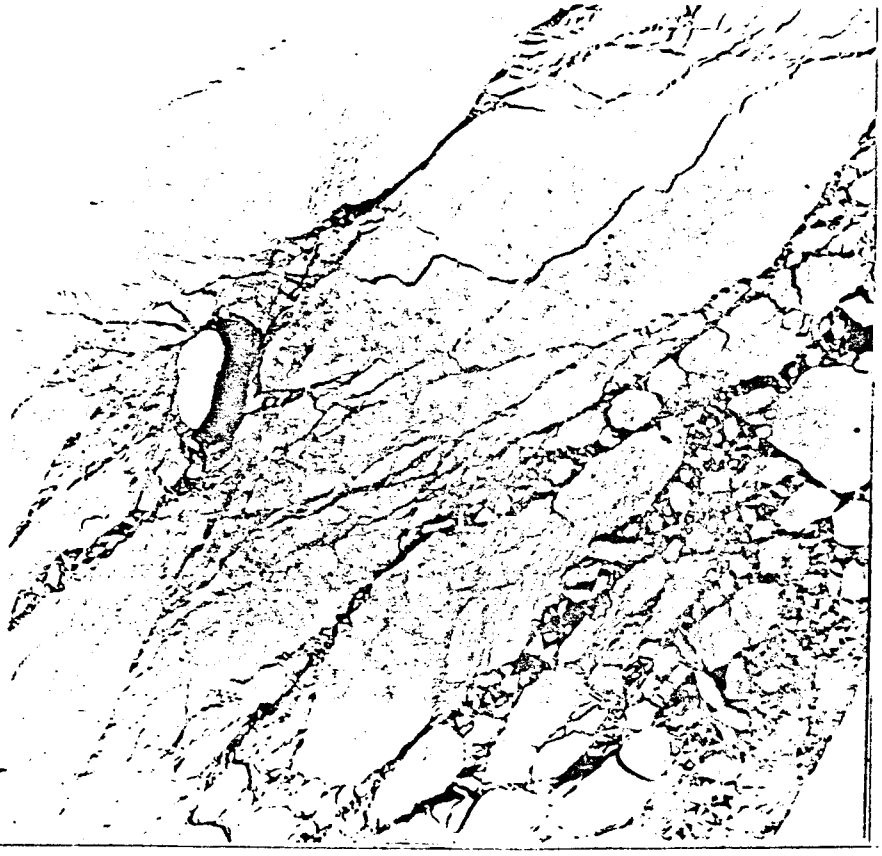

Figure 14. LANDSAT satellite image (ID No. 2097-22081) showing ice condition around the island of grounded sea ice on 29 April 1975.

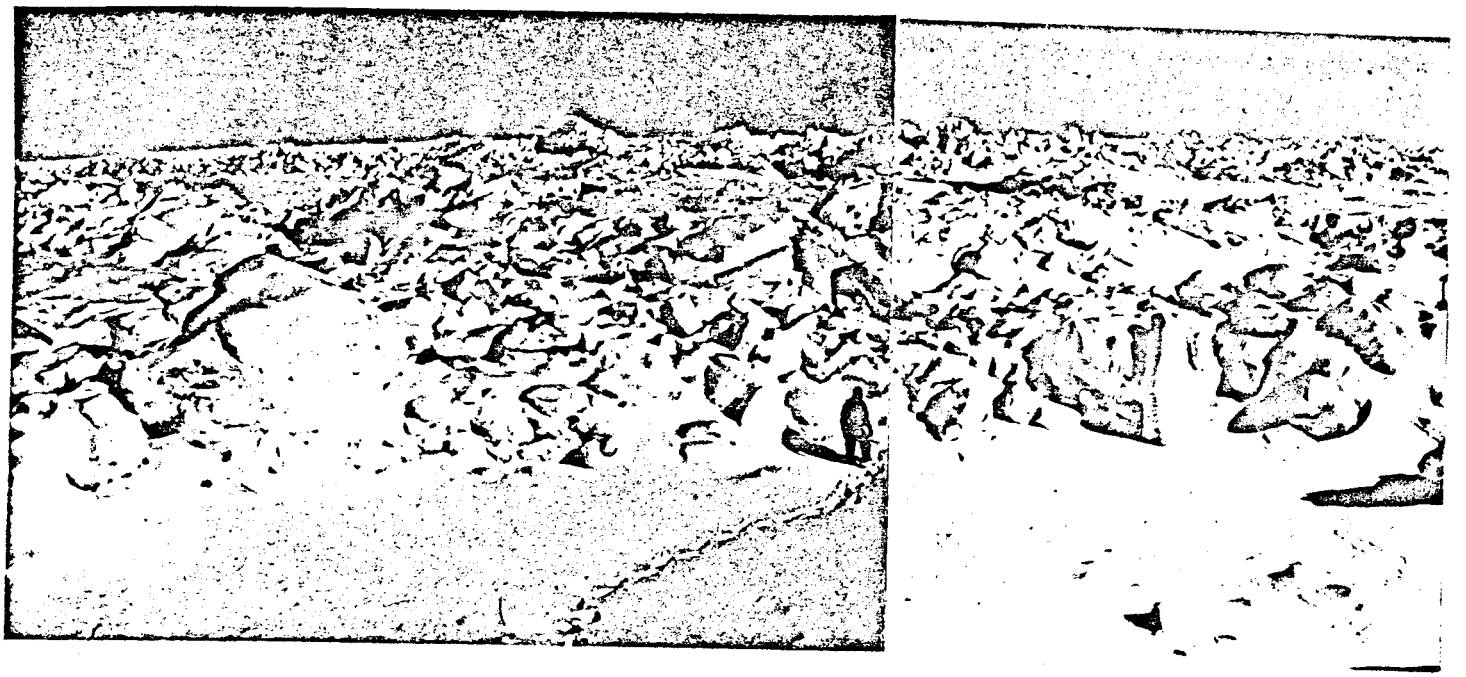

Figure 15. View showing characteristic surface relief (snow-covered) in vicinity of camp site located near edge of grounded sea ice feature. The peak at the left center is 11 meters high.

islands do not form each year. An example of the latter is the grounding of ice on Herald Shoal. The 1973-74 NOAA-3 imagery did not reveal any grounded ice formation on this shoal. However, the low resolution spring imagery from the ESSA-3 satellite in 1968, the ESSA-9 satellite in 1969, and the NOAA-1 satellite in 1971 (see Fig. 1, position 2) shows a polynya associated with an island of grounded ice on this shoal. In the winter of 1974-75 two islands of grounded ice formed on this shoal. Both are easily detected in the higher resolution NOAA-4 and DMSP satellite imagery shown in Figures 12 and 13 at position 2. Another area where an island of grounded sea ice has been observed to form each year is approximately 50 km off the northwest coast of Wrangel Island (see position 3 in Fig. 1 and 13).

DISCUSSION

Satellite imagery has revealed the existence of islands of grounded ice on shoals in the Arctic Ocean. One has been found to be a "permanent" feature, at another location an islands re-forms each winter, while at a third location such formations do not appear to occur each year. Recent calculations of pressure ridge keel depth distribution in the Arctic Ocean indicate that several hundred ice keels 20 meters or more in depth can be expected to pass a given location during the course of a year (Weeks *et al.*, 1971). Therefore, the potential impact frequency of pressured ridge keels and the occasion for them to become firmly grounded can be great in the shoal area of the grounded ice formations. In addition, in recent years several hundred ice island fragments have been found both adrift and grounded off the Beaufort Sea coast of Alaska and Canada (Kovacs, 1972, Kovacs and Mellor, 1974). These fragments typically have keels 15 to 30 meters in depth. While their numbers are few in relation to the numerous ridge keels that can be expected to drift over a given location in a year, the grounded ice formation at 72°N, 162°W has been shown (Fig. 5) to have had fragments of grounded shelf ice incorporated into it.

Ridge grounding on shoals has been found to create a barrier against which the floes of the pack are pushed. Unable to resist the stresses developed, the floes eventually

Figure 16. View of shear ridge field north of Cross Island as observed in April 1975.

fail. The resulting sea ice blocks are pushed to considerable height and the area of the grounded sea ice is enlarged (Kovacs, 1972). In this way the ice formation at 72°N, 162°W increased in size from 2 x 5 km on 8 March 1973 to 6 x 20 km on 1 May 1973 (Kovacs *et al.*, 1975). Under the rarefied conditions of the summer pack, this ice formation has been shown to decrease in size, presumably as a result of collisions with passing floes and flexure associated with summer storm waves (Kovacs *et al.*, 1975), while all the other islands of grounded sea ice were found to disappear entirely during the summer.

The overall size and extreme surface roughness of the island of grounded sea ice at 72°N, 162°W places it in company with such well-known ice formations as the winter shear ridge field which develops north of Cross Island, first reported by Stockton (1890) to be 16 km long and grounded in 24 m of water (Fig. 16), and the massive fields of grounded ridges which are found off the Beaufort Sea Coast of the Canadian Archipelago (McClure, 1857; Armstrong, 1858; Sverdrup, 1904; and Stefansson, 1921). The basic difference between an island of grounded sea ice and these coastal formations is that the ice island is completely surrounded by the massive floes of the polar pack and must be sufficiently anchored to the bottom to resist the tremendous forces exerted by the pack from whichever direction it happens to be moving. The grounded sea ice formations which develop along the coast generally do so at the outer edge of the fast ice and thus are only exposed to the pressures of the moving pack from the seaward side. These formations remain immobile, not only because their keels are grounded, but because the fast ice helps to anchor them in place.

If the "core" of this grounded sea ice feature is as stable as it appears from our observations then it could prove most useful as a platform for conducting a variety of research activities. However, any coordinated program of research would require the establishment of a semi-permanent camp or station. This camp would preferably be located on multi-year ice in the center of the island and should be of "hard" construction to provide adequate protection against the elements and possible visits by bears. Because of the widespread occurrence of ice ridges and rubble fields, which renders surface movement virtually impossible, it would probably be necessary to rely on helicopters to support the field operations.

The establishment of a research station on the island of grounded sea ice would allow for a variety of scientific investigations, including those of a 1) biological, 2) glaciological, 3) oceanographic, 4) meteorological and 5) geological and/or geophysical nature.

1) Bears, walruses and seals are known to exist in some numbers on and around the grounded sea ice feature (Underwood, 1974, and this paper). This fixed platform situated some distance out on the arctic shelf is a most convenient location for examining the distribution and life habits of marine mammals and bears.

2) This grounded sea ice feature is, in a sense, a glaciological oddity, and a thorough examination of its surface morphology and compositional and internal structure seems warranted at this time. The relationship of the grounded sea ice to the surrounding pack should be investigated. In addition to being used to monitor the dynamic motions of the pack ice, this fixed ice platform would also facilitate direct examination of the mechanics of formation of pressure ridges and rubble fields. Our own brief experience of observing rubble field formation at the edge of this grounded sea ice feature indicates that time-lapse photography could prove a most useful tool for examining the mechanics of ice ridge and rubble field formation.

3) Oceanographic investigations should include a thorough survey of water depths in the immediate vicinity of the island, and studies of the compositional and flow characteristics of the water.

4) This island would seem to be an excellent place for an unmanned weather station at a fixed site within the pack ice. This would provide useful information on meteorological conditions within the general area of the grounded ice. Such a station could be readily serviced from Barrow.

5) The existence of a fixed platform some distance out from the North Slope of Alaska offers unique opportunities for exploratory drilling of the marine sediments underlying the grounded ice. Apart from the obvious geological value of assessing the petrographic, lithologic and geophysical properties of the sedimentary columns, the drill holes themselves would also allow measurement of temperature profiles and determinations of geothermal flux.

Additional studies might also include acoustical research projects aimed at determining the propagation, scattering and reverberation of sound waves in and adjacent to the grounded ice feature. Overall, it would seem that this island of grounded sea ice offers a unique opportunity for profitable scientific investigation. This opportunity should not be overlooked, especially in light of the fact that this island of grounded sea ice is located within easy reach of existing research and logistical facilities at NARL, Barrow.

It is relevant to note that recently the term *floeberg* has been used to describe the island of grounded ice at 72°N, 162°W (Stringer and Barrett, 1975). This is an incorrect usage. *Floeberg* was coined during the Nares expedition of 1875-76 (Nares, 1878). Sir Clements R. Markham, who accompanied this expedition, gave the following definition for *floeberg* in the 1887 Encyclopedia Britannica: "In the palaeocrystic sea, there are floes from 80 to 100 ft thick --- and the smaller pieces broken from them have been very appropriately named floebergs." By this description, it is apparent that a floeberg is a large piece of ice which has separated from an even larger accumulation of pressured sea ice. Once separated, a floeberg will drift with the pack or may come aground, whereupon it is called a grounded floeberg. A large number of individual floebergs, such as those shown in Figure 11, may come aground together. Nares coined the term "floeberg beach" to describe this formation because it was a line of grounded floebergs which protected his ship, the *Alert*, from the

moving pack while the ship was in winter quarters. A similar definition for floeberg is given in the WMO Sea-Ice Nomenclature (Anon, 1970) under the heading "Forms of *Floating* Ice." The two photos given in the WMO publication clearly show that a floeberg is not a large area of hummocked ice but only a drifting fragment thereof. *Islands of grounded sea ice* seems the appropriate term to describe the new island discoveries reported in this paper. This term is technically correct because the formations are islands in the sea which in this instance are composed of grounded sea ice, though they may, on occasion, consist in part of shelf ice. The term *grounded ice island* was not used because this would tend to imply that such features were pieces of grounded shelf ice.

ACKNOWLEDGMENTS

This work was supported by the Office of Naval Research under MIPR No. N0001475MP50013. The logistic support of the Naval Arctic Research Laboratory, Barrow, and the helicopter support provided by the U.S. Fish and Wildlife Service, through Mr. Jack Lentfer, are gratefully appreciated.

REFERENCES

Anon. 1970. WMO sea-ice nomenclature. World Meteorological Organizationreport WMO/OMM/BMO-No. 259. TP. 145, Geneva, Switzerland.

Armstrong, Sir A. 1858. *A personal narrative of the discovery of the north-west passage*. Hurst and Blackett, London.

Best, G. 1578. *True discourse*. London.

Brower, C.D. 1960. *Fifty years below zero*. Dodd, Mead and Company, N.J.

Cook, F.A. 1911. My attainment of the Pole, Mitchel Kennerly, New York.

Harris, R.A. 1904. Indications of land in the vicinity of the North Pole. Nat. Geog. Mag. 15.

Kovacs, A. 1972. Ice scoring marks the floor of the Arctic Shelf. The Oil and Gas Journal 70 (43).

Kovacs, A. and M. Mellor 1971. Investigation of the ice islands in Babbage Bight. Creare Inc. Technical Note N-118, Hanover, N.H.

Kovacs, A. and M. Mellor 1974. Sea ice morphology and ice as a geological agent in the southern Beaufort Sea. *In* The Coast and Shelf of the Beaufort Sea. Proceedings of the Arctic Institute of North America Symposium on Beaufort Sea Coast and Shelf Research.

Kovacs, A., H. L. McKim and C.L. Merry 1975. Islands of grounded ice. Arctic 28(3).

McClure, R. 1857. *Discovery of the northwest passage*. Sherard Osborn, Editor, London.

Mikkelson, E. 1909. *Conquering the arctic ice*. London and Philadelphia.

Nansen, F. 1911. *In northern mists*. William Heinemann, London, Vol. 1.

Nares, Sir G.S. 1878. *Narrative of a voyage to the polar sea during 1875-76 in H.M. ships* Alert *and* Discovery. Second ed., New York.

Parry, W.F. 1821. *Journal of a voyage for the discovery of the northwest passage.* London.

Peary, R.E. 1907. *Nearest the pole, a narrative of the expedition of the Peary Arctic Club in the* S.S. Roosevelt, *1905-1906.* London.

Schindler, J.F. 1968. The impact of ice islands-the story of Arlis II and Fletcher Ice Island, T-3, since 1962. *In* J. E. Sater, ed. Arctic Drifting Stations. The Arctic Institute of North America.

Smith, C.L. 1971. A comparison of Soviet and American drifting ice stations. The Polar Record 15(99).

Stefansson, V. 1921. *The friendly Arctic.* Macmillan, New York.

Stefansson, V. 1934. An Eskimo discovery of an island north of Alaska. Geographic Review, January.

Stockton, C.H. 1890. Arctic cruise of the *USS Thelis.* Nat. Geog. Mag. 2.

Stringer, W.J., and Barrett, S.A. 1975. Ice motion in the vicinity of a grounded floeberg. *In* Abstracts of papers presented at Third International Conference on Port and Ocean Engineering Under Arctic Conditions, University of Alaska, August 11-15, 1975.

Sverdrup, O. 1904. *New land.* London, Vol. 1.

Underwood, D. 1974. This week at NARL. NARL Newsletter, 30 September to 6 October.

Untersteiner, N. 1972a. Letter of 14 August to LCDR W.F. Dehn, Fleet Weather Facility, Washington, D.C.

Untersteiner, N. 1972b. Letter of 14 August to Dr. A.F. Treshnikov, Arctic and Antarctic Research Institute, Leningrad, USSR.

Weeks, W.F., A. Kovacs and W.D. Hibler, III 1971. Pressure ridge characteristics in the Arctic coastal environment. Proceedings of the First International Conference on Port and Ocean Engineering Under Arctic Conditions, Vol. 1. The Technical University of Norway, Trondheim, Norway.

Zukriegel, J. 1935. Cryologia maris (Study of sea ice). Geographic Institute Charles IV, Praha.

Annual Report

Contract: 03-5-022-67, Task Order No. 5
Research Unit: 98
Reporting Period: 1 April 1975 - 30 March 1976
Number of pages: 6

Dynamics of Near-Shore Ice
(Data Buoys)

Nobert Untersteiner
Professor Atmospheric Sciences and Geophysics
AIDJEX Project Director
University of Washington
Seattle, Washington 98195

23 March 1976

I. Task Objective

The University of Washington under Task Order No. 5 of NOAA Contract 03-5-022-67 agreed to deploy 20 ice buoys to gather data on ice movement and oceanographic and atmospheric conditions in the near-shore areas of the Beaufort and Chukchi Seas of the Arctic Ocean. The buoy deployments were to be accomplished in conjunction with field work being conducted by the Arctic Ice Dynamics Joint Experiment (AIDJEX). Three types of buoys were developed and produced for the task under contracts from the NOAA Environmental Research Laboratory monitored by the NOAA Data Buoy Office (NDBO). Fourteen of the buoys are designed to be dropped by parachute from aircraft and report position only through a Random Access Measuring System (RAMS) platform and the NIMBUS-6 satellite. Two additional buoys of this type have been modified to include a pressure sensor. All 16 of these buoys were produced by Polar Research Laboratory, Inc., (PRL) of Santa Barbara, California. The other four buoys are of a more complex design and are instrumented with atmospheric pressure and temperature sensors, current meters at 3 and 30 meters under the ice, and a RAMS platform to provide position. Again, all data are transmitted through the NIMBUS-6 satellite. These buoys were developed and produced by the Applied Physics Laboratory, University of Washington. Data from the buoys are placed in the AIDJEX Data Bank after receipt from NASA.

II. Field Activities

A. Field Schedule

As planned, four buoys with oceanographic and meteorological sensors were deployed along the continental shelf break in November, 1975, by NOAA chartered helicopter from Deadhorse, Alaska, and the AIDJEX main ice station

in the Beaufort Sea, and eight tracking-only buoys were parachuted from NOAA chartered aircraft (R4D and Twin Otter) in December.

Deployment dates and initial location of the meteorological/oceanographic buoys, identified by RAMS platform number, were as follows:

RAMS platform	1451,	2 Nov.	71°21'N	149°00'W
	1416,	2 Nov.	71°32'N	147°00'W
	1245,	3 Nov.	71°00'N	135°00'W
	1143,	5 Nov.	73°44'N	130°00'W

Deployment dates and initial locations of the air-dropped buoys, by RAMS platform number, were as follows:

12 Dec.	10	72°08'N	129°25'W
15 Dec.	57	73°04'N	131°30'W
15 Dec.	26	74°54'N	128°59'W
20 Dec.	502	70°48'N	139°30'W
20 Dec.	320	70°48'N	143°45'W
20 Dec.	61	70°30'N	146°00'W
23 Dec.	316	70°15'N	147°00'W
23 Dec.	534	71°23'N	154°00'W

The initial positions of both types of buoys were determined by the navigation system on the aircraft used in the deployment. At the time of this writing (23 March), eight additional air-droppable buoys, two of which were instrumented with pressure sensors, were undergoing predeployment testing at Barrow by personnel from PRL. It is planned to deploy these buoys in the next few weeks.

B. Scientific Party

Mr. Patrick C. Martin, AIDJEX Technical Coordinator, worked closely with NDBO and the contractors during the design and production phases to

insure that the buoys would meet the program requirement. In addition, Mr. Martin was responsible for installing, in the field, the meteorological/ oceanographic buoys, with the assistance of two people from the Applied Physics Laboratory, Mr. Fred Karig and Mr. M. Dozier. Deployment of the airdropped buoys was under the direction of Mr. Andy Heiberg, AIDJEX Base Manager of Field Operations, at Barrow, Alaska. Mr. Heiberg was assisted by two employees from PRL under a subcontract from the University.

C. Methods

As mentioned above, the program relies on deployment of three types of buoys in the OCS area of the Beaufort and Chukchi Seas.

The meteorological/oceanographic buoy is basically a short (18 ft.) spar buoy which is inserted into the ocean through a 10-inch hole drilled through the ice. Current sensors are suspended from the bottom of the buoy. After installation, the buoys become frozen into the ice but become free-floating in summer. The hulls are 9-inch diameter polyethylene tubing. The designed operating life is in excess of one year.

Data transmission and buoy tracking utilizes the Random Access Measurement System (RAMS) aboard the NIMBUS-6 satellite. Air pressure, air temperature, buoy heading, and ocean current speed and direction at two depths are sampled every 3 hours. Ten minute averages are computed for all data. Twenty-four hours of data are contained in memory and transmitted to the satellite. Power is provided by air-cell primary batteries. The communications system is a specifically modified Buoy Transmit Terminal (BTT) developed by the NDBO for buoy application.

The air droppable buoy (ADRAMS) consists of a 22" diameter "lexan" sphere mounted on a 15" diameter, 12" high foam crash pad. The electronics and battery pack form a single unit inside the sphere, which is free to

rotate in any direction on its teflon bearings. The electronics module contains a pendulous weight so that regardless of the final resting position of the sphere after deployment, the antenna will be properly oriented.

The system is powered by newly developed inorganic lithium batteries. These batteries allow operation down to the low temperature limit of the system, -50°C.

A special ruggedized BTT (Buoy Transmit Terminal) was developed to survive the shock of an air drop as well as the low temperature extremes of the Arctic ice pack.

The third type of buoy is an ADRAMS buoy to which a pressure sensor has been added. None of these buoys have been deployed at this time, though two are in Barrow undergoing field testing.

D. Sample Tracklines

Original deployment positions are plotted on the enclosed chart. Only three of the buoys have drifted appreciably since deployment. One, 534, has moved from north of Pt. Barrow to a position off Icy Cape, a distance of about 350 kilometers. Two others, 1451 and 1416, have drifted about 100 kilometers northwest from Prudhoe Bay.

E. Data Collected

1. ADRAMS report location fixes 6 to 8 times a day.
2. Meteorological/Oceanographic buoys report location fixes 10 to 12 times a day and take synoptic environmental data (temperature, atmospheric pressure, azimuth, and current speed and direction at 3 and 30 meters) eight times a day.

III. Results

All eight of the ADRAMS buoys are functioning, though two of them

have given indications of minor difficulties. Position accuracy is about 2 kilometers for both ADRAMS and meteorological/oceanographic buoys. Two of the meteorological/oceanographic buoys, 1245 and 1416 are functioning except that the upper current meter has a high threshold and the barometric pressure sensor resolution is 1.4 millibars, about 1 mb higher than desirable. One of the meteorological/oceanographic buoys, 1451, is providing fixes only and no environmental data. The fourth buoy, 1143, was damaged during installation operations. Repairs were made at the installation site, but the buoy ceased to function, except for occasional transmission within a few hours. An attempt to repair the buoys is planned if weather and time permit.

Data from the buoys are being received and placed in the AIDJEX Data Bank.

IV. Preliminary interpretation of results

None, yet. This task order did not provide for analysis beyond processing and verification. Some interpretation will be made during development of the AIDJEX numerical model.

V. Problems encountered

None, except for those normal to the environment. The time constraints were tighter than one could wish.

VI. Estimate of funds expended

Funds expended or obligated under this task order as of 29 February 1976 totaled $53,744.31. The $18,696.69 remaining under the task order will be sufficient to complete the work.

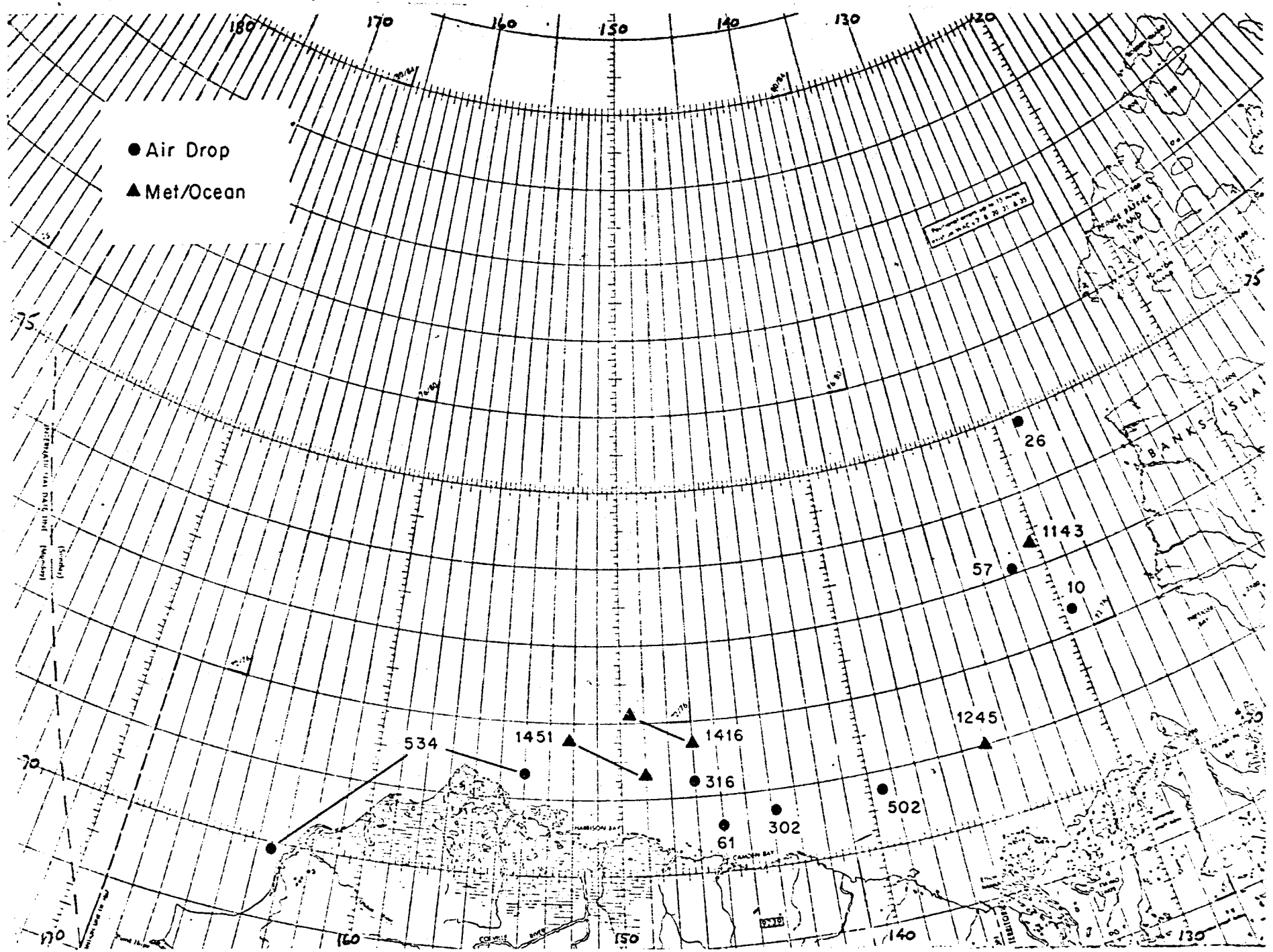
● Air Drop
▲ Met/Ocean
180
170
160
150
140
130
120
75
70
26
1143
57
10
1245
1416
1451
534
316
61
302
502

Annual Report

Contract #03-5-022-91
Research Unit #244
Reporting Period 1 April 1975 -
15 March 1976
Number of Pages 11 + Appendixes

STUDY OF CLIMATIC EFFECTS ON FAST ICE EXTENT AND ITS SEASONAL DECAY ALONG THE BEAUFORT SEA COAST

Roger G. Barry

Institute of Arctic and Alpine Research

University of Colorado

Boulder, Colorado 80309

15 March 1976

I. TASK OBJECTIVES

The primary objective of this study is to assess the role of climatic factors in determining the extent and seasonal decay of fast ice along the Beaufort Sea coast. Particular attention is being given to synoptic meteorological events during critical phases of the seasonal cycle.

II.1 FIELD ACTIVITIES

A. Field schedule:
Ice reconnaissance and measurements on the fast ice near Barrow, 17 May - 1 June, 1975.

B. Party:
R. E. Moritz, Research Assistant

C. Methods:
1) Familiarization with the fast ice environment, comparison with eastern Baffin Island.

2) Measurements of undisturbed first-year ice thickness and salinity (see Quarterly Report, September 1975) and condition of snowpack.

3) Flight of opportunity, 20 May.

D. Localities:
1) Barrow - Elson Lagoon and Chukchi coast
2) Barrow - Pt. McIntyre

E. Data:
Tabulated in Quarterly Report, September 1975.

II.2 OFFICE ACTIVITIES

A. Period:
1 April 1975 - 31 March 1975

B. Personnel:
R. G. Barry, P. I.
J. Rogers, Research Associate (from 15 January 1976)
R. Moritz, Graduate Research Assistant
R. L. Weaver, Graduate Research Assistant (from 1 September 1976)

C. Methods:
1) Remote Sensing Data
(a) LANDSAT imagery (bands 4 and 7) was obtained for selected dates from spring 1973 to fall 1974. The selection was based on cloud cover estimates in EROS listings and files at the Geophysical Institute, University of Alaska, Color IR imagery was also obtained from the U-2 flight on 21 June 1974.

(b) Morphological categories of ice surface features were determined based on (1) previous work with fast ice along the eastern coast of Baffin Island; and (2) analysis of the U-2 photography and synchronous LANDSAT images.

The initial plan was to develop a system to combine relative greyscale, uniformity of greyscale, and ice morphology in a single map product. However, it was determined that the grey scale and morphology map units did not always conform to each other. Therefore, a two step process has been adopted whereby the greyscale changes are mapped separately from the surface morphology.

The classification system (presented in Table 1) was developed under the following guidelines:

1. All categories must be visible and detectable in the LANDSAT imagery on a scale of 1:1,000,000 and meaningful to the synoptic climatological analysis.

2. All classification criteria must be easily understood by a second party so that mapping may be done by several individuals without variation in the final maps.

3. All classes must be reasonably stable so that differing cartographers and variable LANDSAT image quality, due primarily to fluctuations in photographic processing by EROS, do not alter the interpretation.

4. The "ground truth" photography represents actual surface conditions and possible subresolution features are ignored. (Note: this may in some cases lead to incorrect classification. This problem cannot be resolved with the present data set.)

A mapping procedure has been worked out as follows:

1) map the extent of shorefast ice using acetate overlays on each LANDSAT transparency.

   The limits will then be compiled into a seasonal map for the entire coast on a 1:1M scale. The first significant puddling (darker) areas will be noted as to date.

2) Based on defined characteristics (surface reflectance, ridging, separation of pressure ridges/hummock fields, open water areas) 1:500,000 sector maps will be prepared. The U-2 photography is being compared with nearly synchronous ERTS imagery.

   Both categories of map, plus W. Stringer's mapped information, are being used as input to the climatic analysis.

(c) A LANDSAT frame (1702-21093, 25 June, 1974) was selected for digital processing and classification by computer aided mapping programs. This analysis will be carried out by the Laboratory for the Application of Remote Sensing, Purdue University (under subcontract).

2) Meteorological Data

(a) Daily weather information was obtained from the National Climatic Center for Barrow, Barter Island, Prudhoe Bay, Lonely and Oliktock Point. Basic climatic parameters (freezing, thawing indices) of significance to ice growth/decay have been derived.

(b) An objective procedure using NMC grid-point data was developed for classifying the daily pressure pattern over the sector 58°-79°N, 125°-170°W (Figures 1A and 1B). On this basis a daily catalog of pressure-pattern types has been prepared (see Appendix 1). Climate-ice interrelationships are being examined within this framework. This approach is designed to relate the climatic controls on fast ice behaviour to the atmospheric circulation by providing:

(1) A meaningful basis with which to assess the annual formation, decay and evolution of the fast ice as they relate to the seasonal course of the climatic regime.

(2) A useful tool for identifying and classifying short-term meteorological events and anomalies which show important influence on the fast ice.

(3) A descriptive basis for examining interannual differences in the fast ice environment over a longer period than that for which good observational data are available.

(4) A rational link with (possible) large-scale shifts in climate and circulation which may influence the ice.

(5) Insight into the predictability of fast ice and methods of approach for predictive models based on atmospheric data.

(c) An analysis of variance (ANOVA) study of the temperature and wind characteristics of the pressure-pattern types was carried out as a basis for assessing the distinctiveness of the type categories (see Appendix 2).

(d) Mean monthly MSL pressure patterns were computed using the NMC data.

(e) Geostrophic surface winds have been determined from the NMC grid-point pressure data for along-shore and offshore components (see Appendix 3) and zonal (west-east) and meridional (north-south) indexes have been derived for the classification sector.

3) Ice Data
In view of the virtual absence of detailed records of fast ice thickness, Billelo's 1964-75 data on lake ice thickness in northern Alaska since winter 1961-62 have been used as a surrogate with respect to analysis of some climatic parameters. The year-to-year differences in maximum thickness should indicate gross differences in climatic factors that also affect fast ice; the thicknesses are comparable.

D. Sample Localities

Not applicable

E. Data collected/analyzed

1) Remote sensing data
(a) LANDSAT imagery and Color IR photography obtained from the EROS data center are summarized in the Quarterly Report for September 1975. The digital tape for LANDSAT frame 1702-21093 has been forwarded to LARS.

(b) The ice morphology classification system is based on two "ground truth" data sets. The first is a series of hand held oblique 35 mm black and white photographs taken on the ground simultaneously with a LANDSAT overpass over the east coast of Baffin Island (16 June 1974). The second data set for the Beaufort coast includes U-2 CIR photography on 21 June 1974 on a scale of 1:130,000 and a series of four LANDSAT frames from 21 to 26 June.

2) Meteorological data
(a) Meteorological data obtained from NCC are summarized in Appendix 2. Climatic parameters of significance to ice growth/decay have been determined for Barrow, Prudhoe Bay and Barter Island for 1971-1974.

(b) The MSL daily pressure-pattern catalog for the sector 58^{o}-79^{o}N, 125^{o}-170^{o}W (see Figure 1) was prepared for the period of October 1969 to August 1974.

(c) Mean monthly MSL pressure maps have been prepared for the sector shown in Figure 1 for January 1946 to August 1974.

(d) Daily temperature departures from average and resultant wind magnitudes at Barrow and Barter Island have been analyzed by analysis of variance with respect to the pressure-pattern types for the period January 1969-August 1974.

(e) Daily 1200 Z surface geostrophic wind components in the I and J directions (NMC coordinate axes) have been computed at three points along the Beaufort Coast for the period October, 1968 through September, 1974.

(f) Daily 1200 Z surface zonal and meridional wind indices for the sector 65^{o}-75^{o}N, 125^{o}-170^{o}W have been computed for the period October, 1968 through September, 1974, and averaged by month.

III. RESULTS

A. Field Measurements:

The results have been presented in Quarterly Report, September 1975. They are discussed below.

B. Ice Features:

1) Surface morphological categories have been classified in a system shown in Table 1. The categories are more restricted than some traditional systems, such as those employed by the Canadian Ice Reconnaissance Patrol or those given in the WMO sea ice nomenclature, but this is due to the broader scale on which we are obliged to work. It must be emphasized that this scheme is preliminary and may be revised as more ground truth information and aerial photography are acquired. The scheme is intended as the basis for linking satellite-observed surface changes to climatic (and other) factors.

2) Working maps of ice features in the Prudhoe Bay sector during summer 1974 have been compiled. Figure 4 shows the map for 26 June based on LANDSAT frame 1703-21151. Comparison with the U-2 color IR photography for 21 June shows that major groups were correctly determined with 96% accuracy. However, the "surface descriptor" (see Table 1) was only 73% correct. This is attributed to the problem of puddled versus flooded ice, or the presence of thaw holes and possibly the time change between the two dates. The map for 21 June (Figure 5), based on LANDSAT frame 1698-20470, is correct for all six categories. However, this frame is considerably less complex than that for 26 June.

3) Maps of grey scale information from 1975 LANDSAT frames between 145° and 151°W longitude have been prepared. Figure 6 is an example of one such map which was derived from the 26 June 1974 frame. Areas in each image with approximately uniform density have been mapped into single units. The density for each contiguous area was then compared to the greyscale step wedge which is attached to each image. The step position was assigned to the map unit as well as a variability designation (see Table 1).

Fifteen representative sample areas of approximately 16 km^2 each across the mapped area were chosen in an attempt to evaluate the progression of surface reflected radiance through the melt season (see Figure 7). The step wedge relative density of each point was determined from the maps discussed above. Figure 8 illustrates the progression of the fifteen points through the 1974 season. Early spring data were excluded due to low stratus cloud obstruction of the surface in the LANDSAT frames. The actual data values are listed in Table 2.

The error bars in Figure 8 represent a $\pm$ one standard deviation envelope about the mean and are an indication of the inhomogeneous nature of the surface reflected radiance at this time of the year. The error envelope for the early September frame is much less and is due to the high dominance of open water. In fact the variability in this frame is due entirely to presence of pack ice at some of the data points.

In addition to the overall mean trend, the two points (9, 10, Figure 7) over smooth ice in Prudhoe Bay and two points over a hummocky area of the Jones Islands (6, 7, Figure 7) were separately graphed. The graphs are presented in Figure 9 and actual data values are listed in Table 3. Both of these data sets show variations quite different from the mean data. The 14-15 July jump to higher values is most likely associated with the presence of ridged pack ice in the bay area after the initial phase of fast ice breakup. The pack ice, in a highly compressed and overthrusted state would present a more highly reflective surface than does the rotten smooth fast ice found in the 12 July frame. The Jones Island area of ridged ice follows a rather uniform decrease in reflected radiance right through to open water which is present in the September frame.

Certain LANDSAT MSS system uncertainties must be discussed before acceptance of the results presented above. The radiometric accuracy of the final bulk-processed LANDSAT image depends on several uncertainties in the data processing chain. The chief areas of concern include the following:

1. MSS sensor absolute radiometric calibration and calibration stability.

2. Noise introduction in the digital telemetry and processing system.

3. Errors in linearity of the step wedge generator.

4. Photographic processing of intermediate and final imagery products.

5. Atmospheric contribution to total reflected radiance recorded by the sensor system in space.

If relative radiometric measurements are substituted for absolute measurements, then the root mean square (RMS) error for problems 1-3 is estimated to be 6% of full scale radiance, (ERTS Data Users Handbook, p F-14). Errors introduced in the enlargement and photographic processing of second generation imagery may be as much as 8% (Ibid., p. F-16). Thus, the total system density uncertainty for a 9.5 inch transparency is approximately 15% RMS. The errors are generally greater for the denser portions of the positive transparency.

In addition to the above system errors, the variation of atmospheric turbidity (Problem 5) decreases the system accuracy even more. Here, it is assumed that the atmospheric variation acts evenly across a given frame (excluding cloud effects) and that detectable variation has a longer response time than a few days. Therefore, it is estimated that the combined effect of all errors leads to an uncertainty of 15-20% RMS in the reflected radiance from the surface. The above analysis does not consider these errors but they are discussed in the conclusions which follow.

C. Synoptic Climatology

1) Objective MSL pressure-pattern types
The 21 key days generated by the synoptic typing routine are shown in Appendix 4, together with the daily catalog. These maps are normalized grid value isopleths at MSL with a contour interval of 0.5 (½ standard deviation for the given maps). They indicate the spatial pattern of highs, lows, troughs, ridges and relative pressure-gradient magnitudes that individual days must have to be grouped with the respective key day. The actual MSL pressures for the seven most frequent types are presented in Figures 10-16. These types account for about 78% of the days in the six-year period, September 1969-August 1974.

2) Climatic characteristics
The characteristics of the pressure pattern types have been examined in terms of temperature and wind conditions for the mid-season months January, April, July, and October. Tabulated results will be provided in the next report. The analysis of variance is in progress.

3) Wind indices
The winds indices have been determined for both along-shore and offshore components at Barrow and Barter Island for all months from 1969 to August 1974, but preliminary analysis has concentrated on the winter months. The direction of the geostrophic wind will be determined for the major pressure-pattern types and presented in the form of a wind rose or histogram. The direction of airmass advection associated with each type should then explain the temperature anomalies associated with each type.

D. Specific Ice-Related Climatic Parameters
In addition to the synoptic types and wind indices other specific ice-related climatic parameters such as air temperature, surface wind speed and direction, snow and cloud cover are being analyzed with respect to their characteristics within each synoptic type. Tabulations of freezing and thawing degree days (FDD's and TDD's) have been made for the period of air temperature records at Barrow and Barter Island (1952 onward and 1957 onward respectively) (see Table 5).

IV. PRELIMINARY INTERPRETATION OF RESULTS

A. Field Measurements
1) Undisturbed first-year fast ice thicknesses were 2m ±20 cm in the Elson Lagoon and inshore Chuckchi Sea areas near NARL. These may be slightly less than the maximum winter thicknesses.

2) Mean (for a particular core sample) salinities of undisturbed first year fast ice were 6 $^{o}/_{oo}$ ± 2 $^{o}/_{oo}$. However, the salinity variation within any given core varied from 4 to 24 $^{o}/_{oo}$, as one would expect (higher salinity at the bottom of the core).

3) The snowpack was heated strongly (approaching 0^{o} C in late May when the winds were low, due to the continuous solar radiation. The snow was essentially gone on the smooth ice immediately west of NARL on June 1, but this is likely to be a local effect. Elson lagoon still had a variable snow cover of 0-25 cm at this time.

4) On May 31 the fast ice west of NARL still had some 'cold content', but was very near thawing in the top 7 cm.

5) General observations on foot and from the air indicate that the Beaufort Sea Coast is, as we expected, subject to much stronger ridging than the ice in western Davis Strait. The shallower waters on the Beaufort Sea shelf cause the ice features (ridges, hummocks, smooth ice, leads) to conform much more closely to the bathymetry than in western Davis Strait, for example. While the offshore extent of stationary "attached" ice (see Stringer, 1974) may depend on the temperature conditions at certain times in the year, the seaward extent of well-grounded fast ice is controlled more by the bathymetry, the magnitude of ridge-forming processes during the establishment of immobile ice, and the motions of the polar pack ice offshore.

6) Inshore of the barrier islands (e.g. Elson Lagoon) and in some embayments, thermodynamic modelling of ice formation or ice-melt processes may provide useful insights into the interannual differences in ice thickness and breakup patterns. However, it is likely that the breakup of the ridged (and often grounded) fast ice further seaward can be best approached by looking at wind-stress, presence/absence of offshore pack ice, motion of pack ice at the fast-ice edge, and intensity of storms during the ridge-forming season (if such a season can be defined - see e.g. Stringer (1975) regarding the date when the late winter ice appears to become immobile).

B. Ice Features

The results of the trial mapping show that it is feasible to map the general ice characteristics and at least separate the rougher areas due to ridging and hummocks from the smoother areas. This distinction between the two general ice classes should be of use to interpretation of climate-ice response links. Although the presence of surface water is readily detected, it is not possible to determine if an area is puddled, flooded, or has a high percentage of thawholes.

The close agreement between the LANDSAT imagery interpretation and the larger scale U-2 photography must be accepted with some qualification. First, the greyscale dynamic range in these frames is probably at the seasonal peak, making classification much easier. Second, the frames were cloud free which again permitted greater definition in the images. Mapping of lesser quality frames will determine if this classification is useful for the greater part of the year.

The error analysis of the greyscale data shows a 15-20% RMS uncertainty in the radiance, but despite this it is still possible to interpret some of the grey scale information. It is possible, for example, to detect the date of first puddling in the imagery. It

may also be feasible to use an estimate of the homogeneity of the reflected radiance to assess surface water concentration and hence ice morphological types. It is uncertain that unique reflected radiance decay curves can be derived for specific ice morphological types. However, the Prudhoe Bay and Jones Island examples suggest that this may be the case.

C. Synoptic Climatology

1) Objective MSL pressure-pattern types

Preliminary inspection of the type maps shows that type I, with a low center near Cook Inlet and higher pressure over the Beaufort Sea, strongly resembles the mean pressure field in the region for the winter months. This correspondence is not surprising, since type I occurs on some 50% of winter days and 34% of days overall, in the six-year sample analyzed. It is also worth noting that type one is essentially identical to type "A" of the subjective classification by Putnins (1966), for the Alaska region. Preliminary analysis shows that Putnin's types correspond fairly well to one or another of our types. The analysis of type characteristics and intertype differences by the ANOVA model (see Appendix 2) will provide a fuller picture of the weather associated with particular circulation patterns. Contingency analysis of transition frequences for each type is in progress. Occurrences of strong patterns (high standard deviations) and seasonally-anomalous type sequences are being identified for analysis in conjunction with the fast ice characteristics.

2) Climatic characteristics

It has been determined that, of the seven major types which account for 78% of the days (Section III. S. 1) in the five year period (1969-74), types I, III, VII are often associated with below normal temperatures while types II, IV, V, and VI are often associated with above normal temperatures as well as lessened rates of lake ice thickness increase and early (April vs. May) decrease in lake ice thickness (see IV. D). The characteristics of the geostrophic wind conditions for the winter months of January reveal only a few exceptions to the rule that the warmer months are associated with southerly surface geostrophic flow and the colder months with northerly flow and the cold types. The months which are exceptions may be related to the inversion intensity during the winter or to some features of the upper level flow. This will be checked by analysis of summertime data when the inversion is less predominant.

3) Wind indices

Examination of the geostrophic wind indices shows that for the ten warmest July's at Barrow the geostrophic wind direction was in the sector 130-220^{o} (approx. SE to SW) in eight of them (i.e. over land). Of the twelve cold months only one had a direction in that range, all others were from directions over ice and cold near shore water.

At Barter Island, all five warmest July's had a direction in the range 100° to 285° (southerly directions) and only one of the five coldest July's had a similar direction of transport.

Thus the direction of transport is closely related to the relative anomaly of temperature at these stations. In turn this air flow is expected to be identifiable in terms of distinctive pressure patterns.

D. Specific Ice-Related Climatic Parameters

The FDD and TDD tabulations have been analyzed with respect to ice thickness conditions on inland lakes (Billello, 1964-75) since the winter of 1961-62. It was found that the difference in maximum ice thickness between the coldest (1970-71) and warmest (1966-67) winters was 216-156=60 cm and at the same time this was associated with a difference of 10051-7720=2331 FDD's (Table 5) accumulated to final date of freezing temperatures. Five-year running means of the frequency of occurrence of the cold synoptic types (I, III, VII) and warm types (II, IV, V, VI) reveals that the daily occurrences of warm types peaked during the 1966-67 winter while their frequency has been at a minimum during the 1970's. The frequency of cold types was at a minimum in 1966-67 and had peaked once again by 1971.

V. PROBLEMS/RECOMMENDATIONS

A. Problems

Major problems encountered during the period have been mainly organizational ones beyond our control. The prime one is the very limited provision of aircraft underflight data, originally scheduled by the USGS, to meet our requests in the work statement. A subsidiary one is in the flow of ice maps being prepared under RU 441 by W. Stringer. The problem here arises from the fact that his analysis is proceeding by season rather than by year. The 1973-74 summer season maps will not be available until about August 1976, largely excluding our use of them during this contract. We are coordinating closely with Dr. Stringer to ensure maximum interchange of information and still anticipate analysis of the demarcated coastal sections for 1973-75 data.

A slightly revised schedule has also had to be arranged with our subcontractor for digital mapping at LARS due to the time delay in obtaining the digital LANDSAT tape from EROS after selection of an appropriate scene. However, this presents no serious difficulties.

B. Recommendations

Underflight data at about two weekly intervals from 1 May - 31 July (at least) are vital to this project for reliable interpreattion of LANDSAT imagery. In addition, field determinations of selected ice parameters, especially state of surface, must be collected during June 1976 via the requested helicopter support along areas of both the Chukchi and Beaufort coasts. Our work during spring-summer 1976 will be coordinated with flights on which SLAR imagery will be collected by JPL (M.L. Bryan). Preliminary arrangements to this effect have been made.

VI. ESTIMATE OF FUNDS EXPENDED

$25,000. Expenditure during the coming six months will be proportionately greater as a result of the timing of staff appointments and 100% input of assistants in the summer months.

REFERENCES

Billello, M. A. 1964. Ice thickness observations, U. S. Army CRREL Special Report, 43 (1, 2).

Billello, M. A., and Bates, R. E. 1966, 1969, 1971, 1972, 1975. Ice thickness observations, U. S. Army CRREL Special Report, 43 (3, 4, 5, 6, 7).

Kirchhofer, W. 1973. Classification of European 500 mb patterns. Swiss Met. Inst., Arbeits No. 3, 16 pp.

Putnins, P. 1966. Studies on the meteorology of Alaska: the sequences of baric weather patterns over Alaska. ESSA, Silver Springs, Md., 81 pp.

Stringer, W. J. 1974. The morphology of Beaufort Sea shorefast ice. Beaufort Sea Symposium, AINA.

Stringer, W. J. 1975. Morphology of Beaufort nearshore ice conditions. September Quarterly Report (OCS), RU 244, Mimeo.

Weaver, R. L., Jacobs, J. D. and Barry, R. G. 1975. Fast ice studies in western Davis Strait. 3rd International POAC Conference, Fairbanks, in press.

TABLE 1

FAST ICE CLASSIFICATION CATEGORIES FOR LANDSAT IMAGERY

A. Greyscale information consisting of two characteristics

1) Greyscale density from 1 to 15 corresponding to the greyscale stepwedge on the border of each LANDSAT frame, band 4 (0.5-0.6 m). Low numbers correspond to low density or high reflectance.

2) a subjective uniformity index

A = highly uniform within mapped unit
B = slight variation within mapped unit
C = high variation within mapped unit

B. Surface Morphologic Classification consisting of two numerals separated by a decimal point. The general ice category is to the left of the decimal point. The general ice category is to the left of the decimal and the specific surface descriptor is to the right.

Numeral	General Category	Surface Descriptor
1	Open water	Undifferentiated
1.1		With silt
2	Heavily ridged hummocked zone	Undifferentiated
2.1		Grounded system
2.2		Ungrounded system
3	Pans or floes smaller than 2 km in maximum dimension	Undifferentiated
3.1		No surface water detected
3.2		Puddled
3.3		Flooded (puddles greater than 90%)
4	Pans or floes greater than 2 km in maximum dimension and separated by ridge systems	Undifferentiated
4.1		No surface water detected
4.2		Puddled
4.3		Flooded (puddles greater than 90%)
5	Smooth ice, pans larger than 2 km with no significant imbedded pressure ridges. Tidal and thermal cracks allowed	Undifferentiated
5.1		No surface water detected
5.2		Puddled
5.3		Flooded (puddles greater than 90%)
6	Surface morphology undetermined	N/A

Note: "t" after the numeric code indicates thawholes are present

Table 2

Progression of Grey Scale Values for Entire Fifteen Point Set

(Note: All fifteen points may not be visible on any given day)

Date	1	2	3	4	5	6	7	8	9	10	11	12	13	14	15	$\bar{X}$	N	s.d.
3-11	no data, cloud covered																	
3-31	no data, cloud covered																	
5-2	no data, cloud covered																	
5-3	no data, cloud covered																	
5-4	no data, cloud covered																	
5-21	no data, cloud covered																	
6-26	1a	11c	10c	8c	11c	5b	5b	5b	1a	7b	10c	5b	3a	1a	-	5.9	14	3.7
7-12	-	-	-	-	-	-	-	2b	11c	11c	9c	8a	7b	3b	-	6.8	8	3.6
7-14	6c	12c	11c	11c	1a	9c	7c	3b	4b	4b	11c	3b	8b	3b	-	6.6	14	3.8
7-15	3a	12b	12b	11c	1a	9c	7c	3b	8b	8b	10c	-	-	-	-	7.6	11	3.8
7-16	3b	11c	11c	10c	1a	9c	9c	-	-	-	-	-	-	-	-	7.7	7	4.0
8-2	4b	14a	14a	10c	4b	13c	13c	14a	14a	14a	-	-	-	-	-	11.6	11	4.0
9-6	7c	14a	14a	14a	14a	14a	14a	14a	14a	14a	14a	14a	14a	14a	14a	14.0	14	1.9

The codes refer to categories in Table 1.

Table 3

Progression of Grey Scale Values for Two Selected Areas

Date	Prudhoe Bay			Jones Island		
	9	10	Mean	6	7	Mean
6-26	1	7	4	5	5	5
7-12	11	11	11	-	-	-
7-14	4	4	4	9	7	8
7-15	8	8	8	9	7	8
7-16	-	-	-	9	9	9
8-2	14	14	14	13	13	13
9-6	14	14	14	14	14	14

MONTH	J1	J2	J3	I1	I2	I3	# days with data
1	.25	-1.09	-2.54	-.54	1.03	1.18	176
2	4.01	3.86	3.37	-1.32	-.61	.23	161
3	4.05	4.62	5.01	-2.00	-1.60	-.89	182
4	6.34	6.84	6.83	-2.58	-2.63	-1.38	176
5	5.08	5.95	5.65	-1.58	-2.25	-1.13	180
6	3.42	4.31	4.33	-1.48	-2.50	-1.42	170
7	.18	.61	.94	-.05	-.81	-.35	185
8	.29	.42	.33	-.33	-.65	-.37	185
9	.94	1.18	1.59	-.42	-.70	-.14	179
10	3.10	1.87	1.00	.24	-.56	.50	186
11	5.52	4.01	2.71	-.98	-.23	1.43	179
12	3.57	2.69	1.27	-.34	.60	1.75	185

DATA ARE IN METERS PER SECOND

TABLE 4

Mean Surface Geostrophic Winds Components Computed by Month for the Period 9/1969-8/1974 at the six points Labelled in Figure 3.
(Note: the positive J-direction is alongshore from East to West)

TABLE 5. Freezing-Degree Days (°F) at Barter Island (Sept. 1961 - Jan. 1976)

	1961	1962	1963	1964	1965	1966	1967	1968	1969	1970	1971	1972	1973	1974	1975	1976	Norma
n.		4431	3613	4314	5037	4450	3798	4314	4441	4201	5210	4503	3873	3926	5959	5446	4511
b.		5464	4887	5952	6829	6032	5274	5958	6031	5579	6952	6005	5231	5642	7376		5939
r.		6884	6381	7645	8050	7718	6604	7254	7426	7169	8539	7598	6992	7276	8610		7445
r.		7859	7149	8905	8875	8882	7450	8334	8173	8144	9688	8696	8009	8467	9669		8471
y		8309	7304	9272	9256	9276	7720	8603	8433	8516	10051	9105	8304	8923	10001		8803
ne		8312	7318		9331	9280			8496	8537				8979	10008		8823
ly																	
g.							5				6				2		1
pt.	7	36	26	67	51	0	101	40	72	180	51	79	28	78	179		67
t.	621	392	559	691	761	418	761	490	401	1082	687	429	530	906	870		620
v.	1728	1157	1750	1633	1496	1156	1772	1543	1550	2063	1626	1362	1415	2211	2178		1638
c.	3315	2292	2758	3344	2897	2480	3031	2941	2722	3514	2999	2500	2596	4105	3818		3012

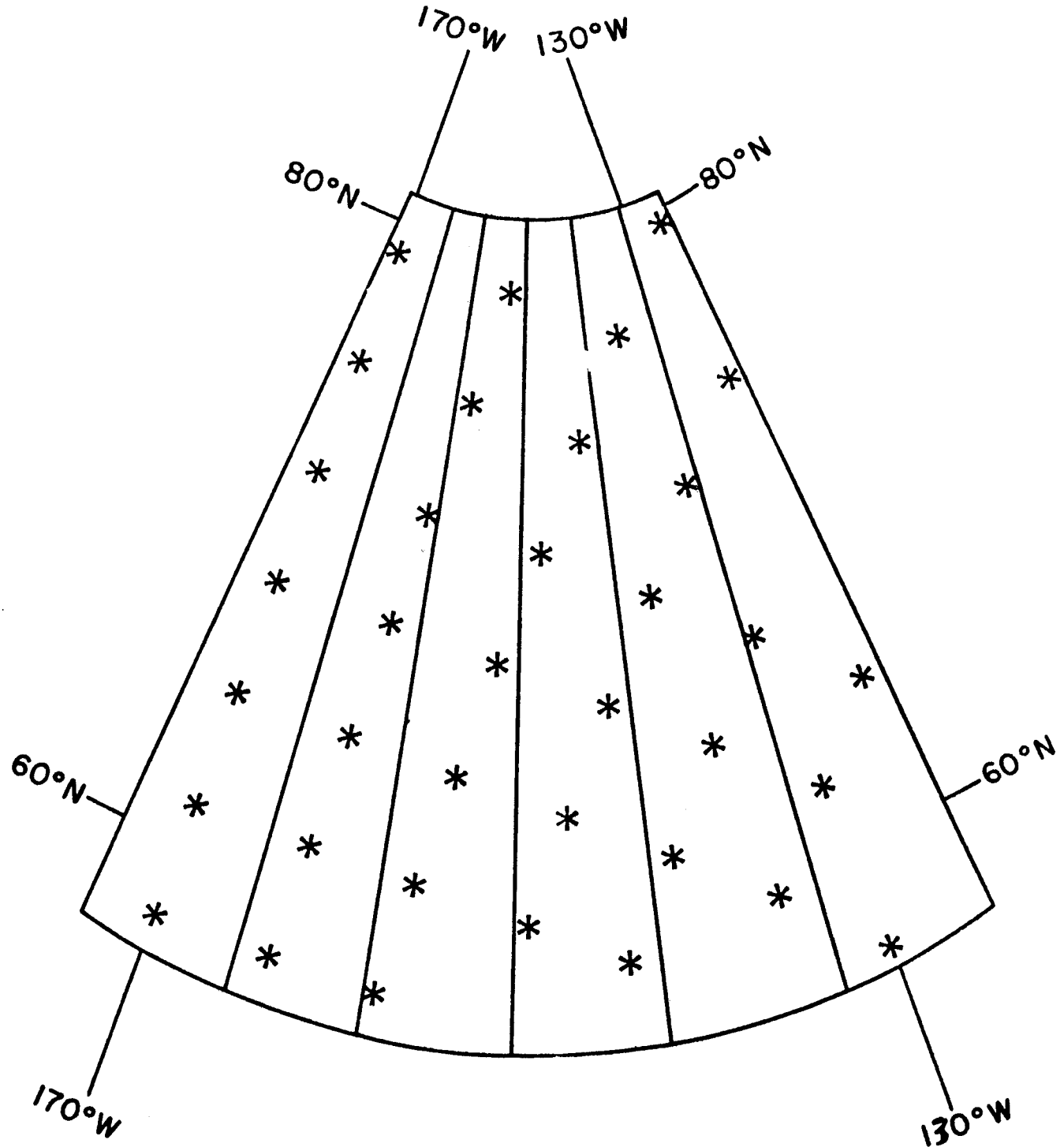

FIGURE 1A
Column Grouping for Pressure Pattern Similarity Tests
(NMC points shown)

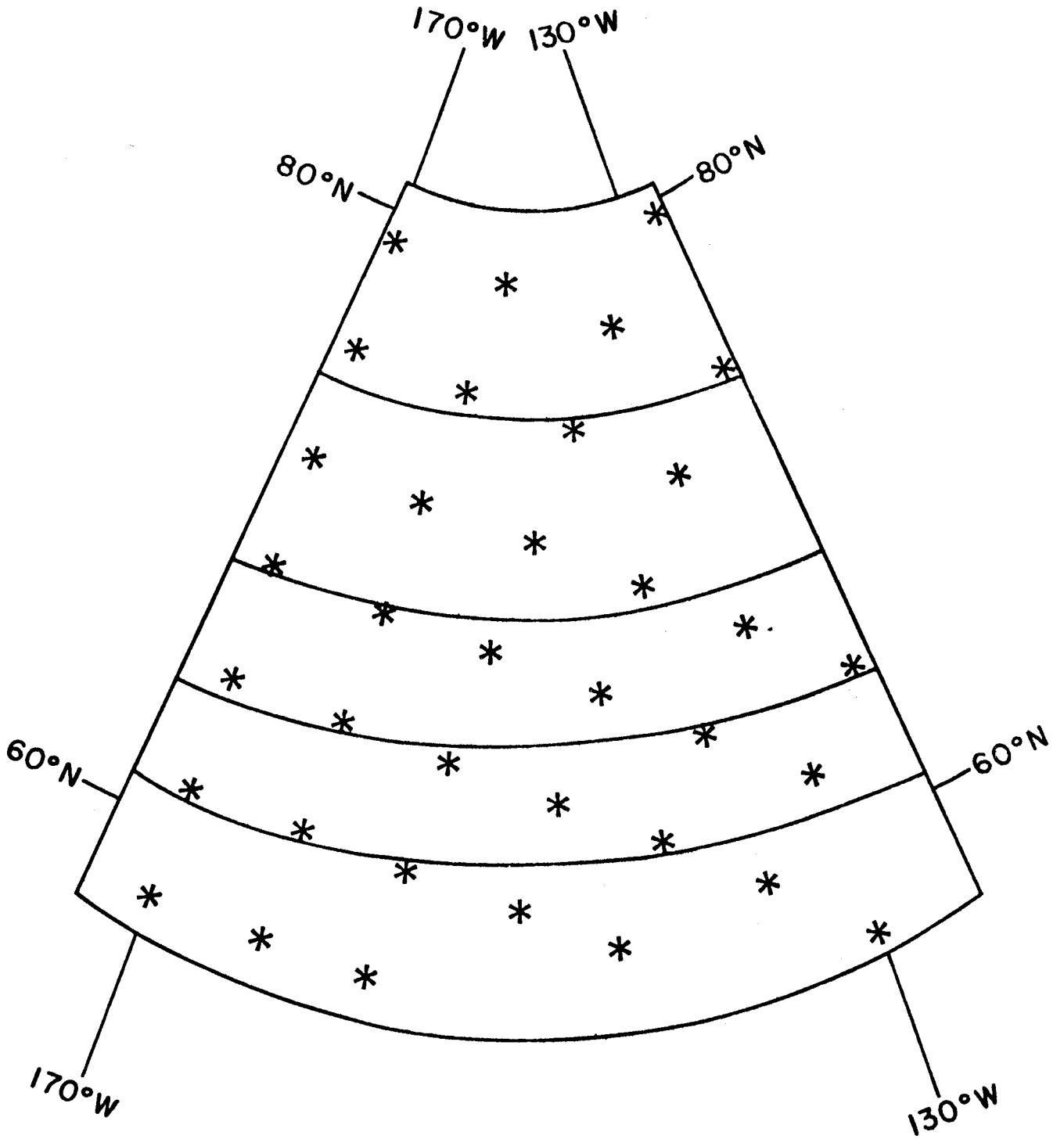

FIGURE 11B
Row Grouping for Pressure Pattern Similarity Tests
(NMC points shown)

FIGURE 3

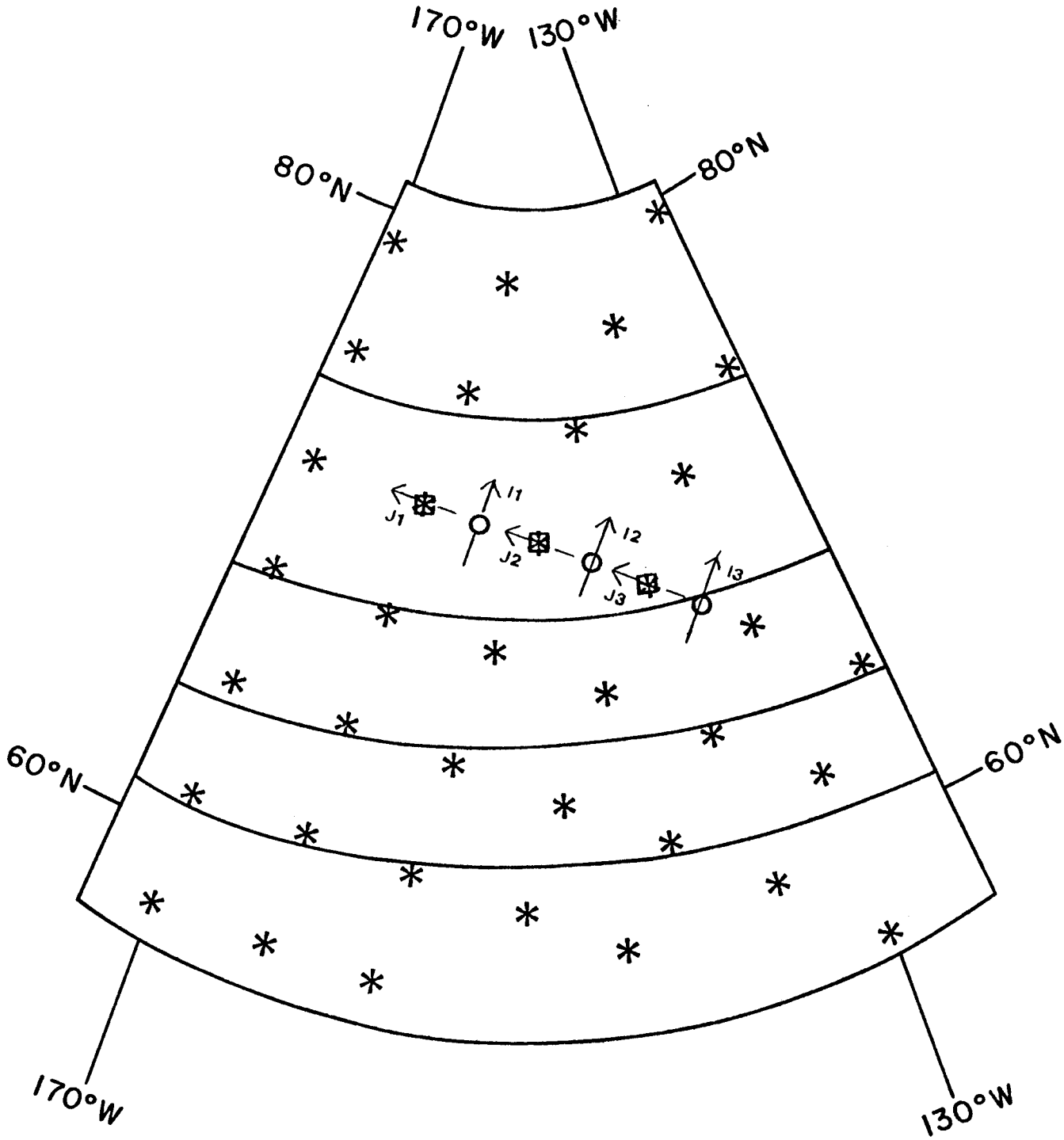

Location of NMC points for computing I and J surface geostrophic wind components.

FIGURE 4

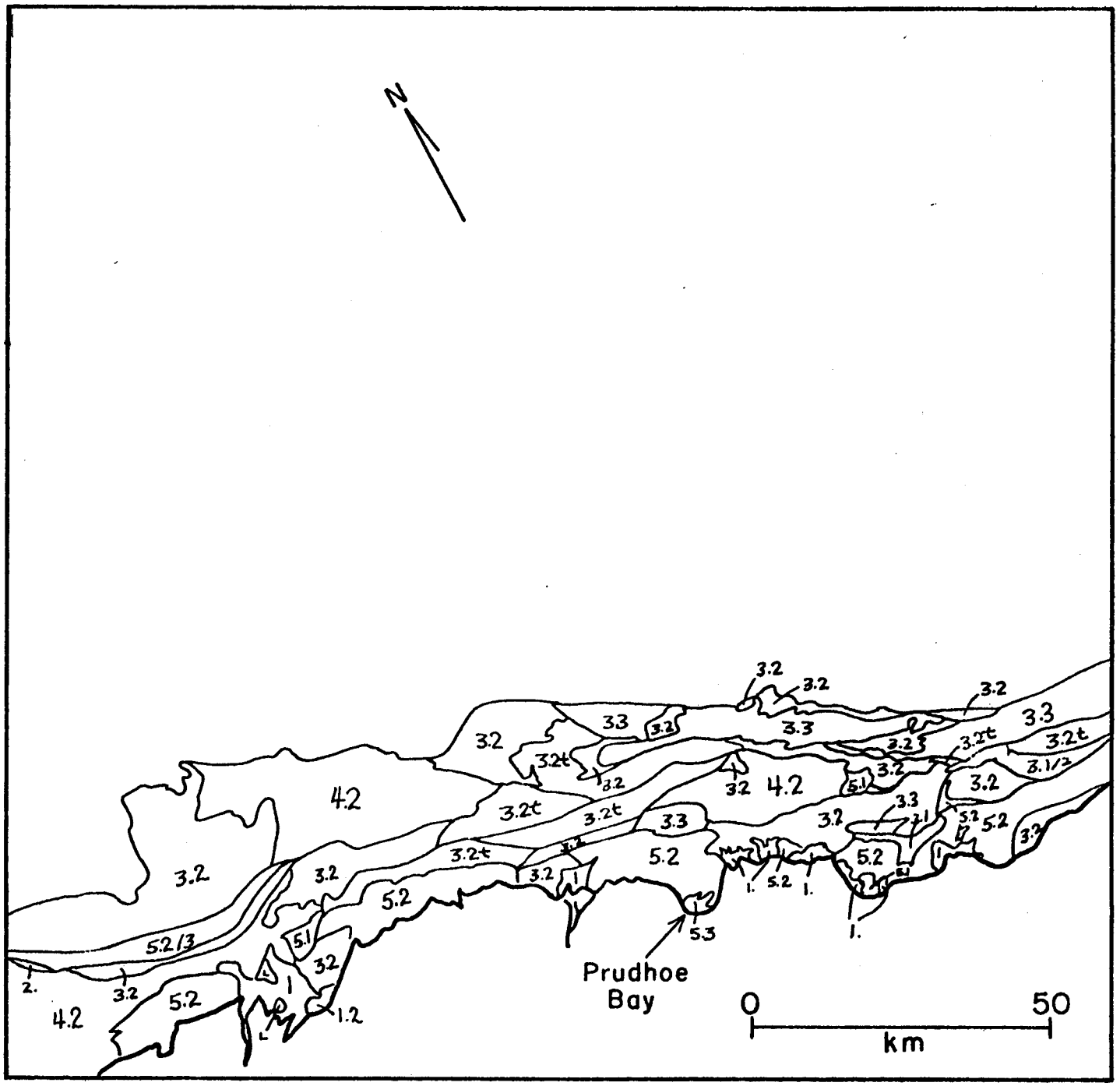

Near shore ice morphologic map for 26 June 1974 from LANDSAT frame 1703-21151.

Figure 5

Morphologic Map from Landsat Frame 1698-20470, 21 June, 1974

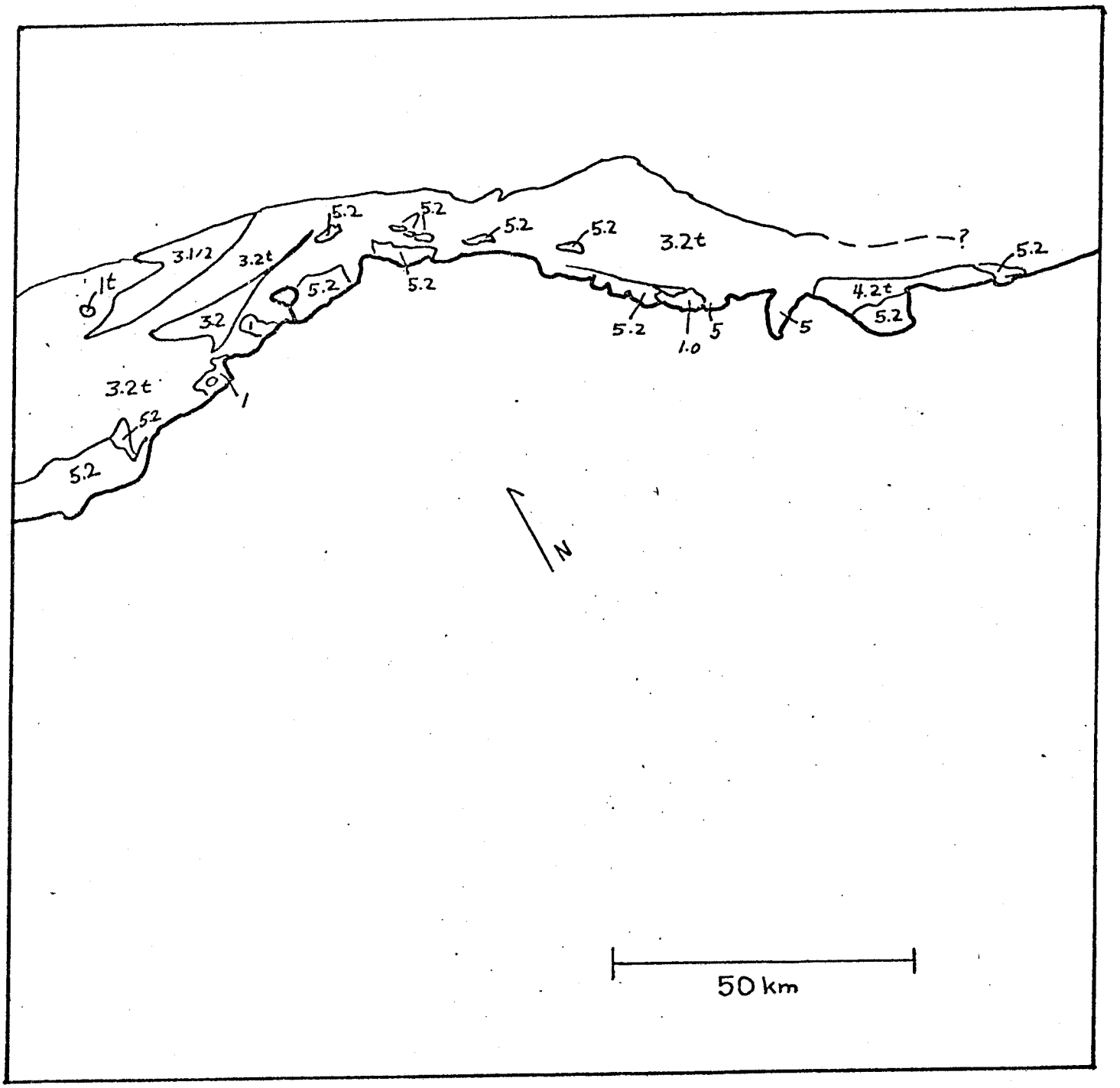

FIGURE 6

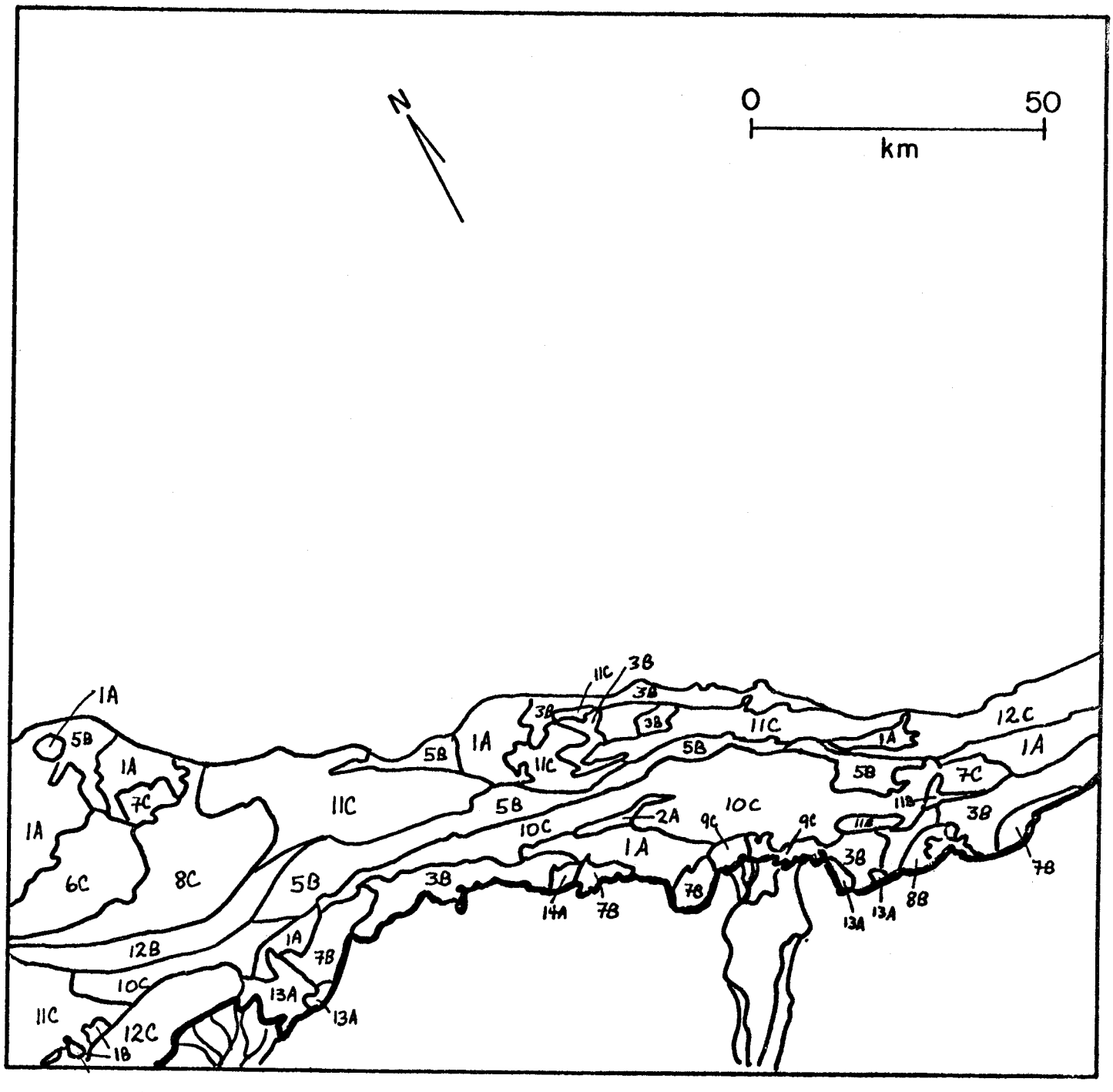

Near shore ice relative greyscale map for 26 June 1974 from LANDSAT frame 1703-21151.

FIGURE 7

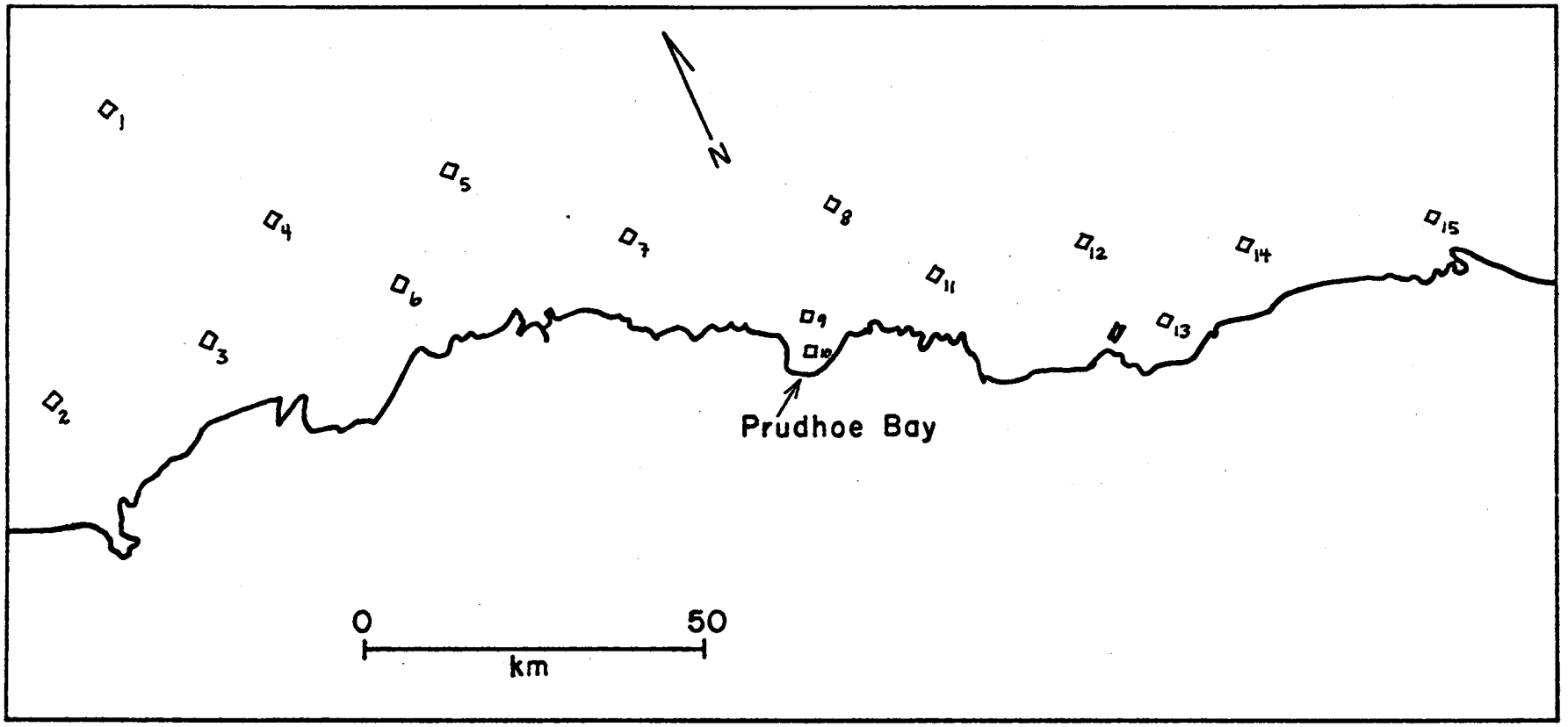

Greyscale site location map, Prudhoe Bay Region.

FIGURE 8

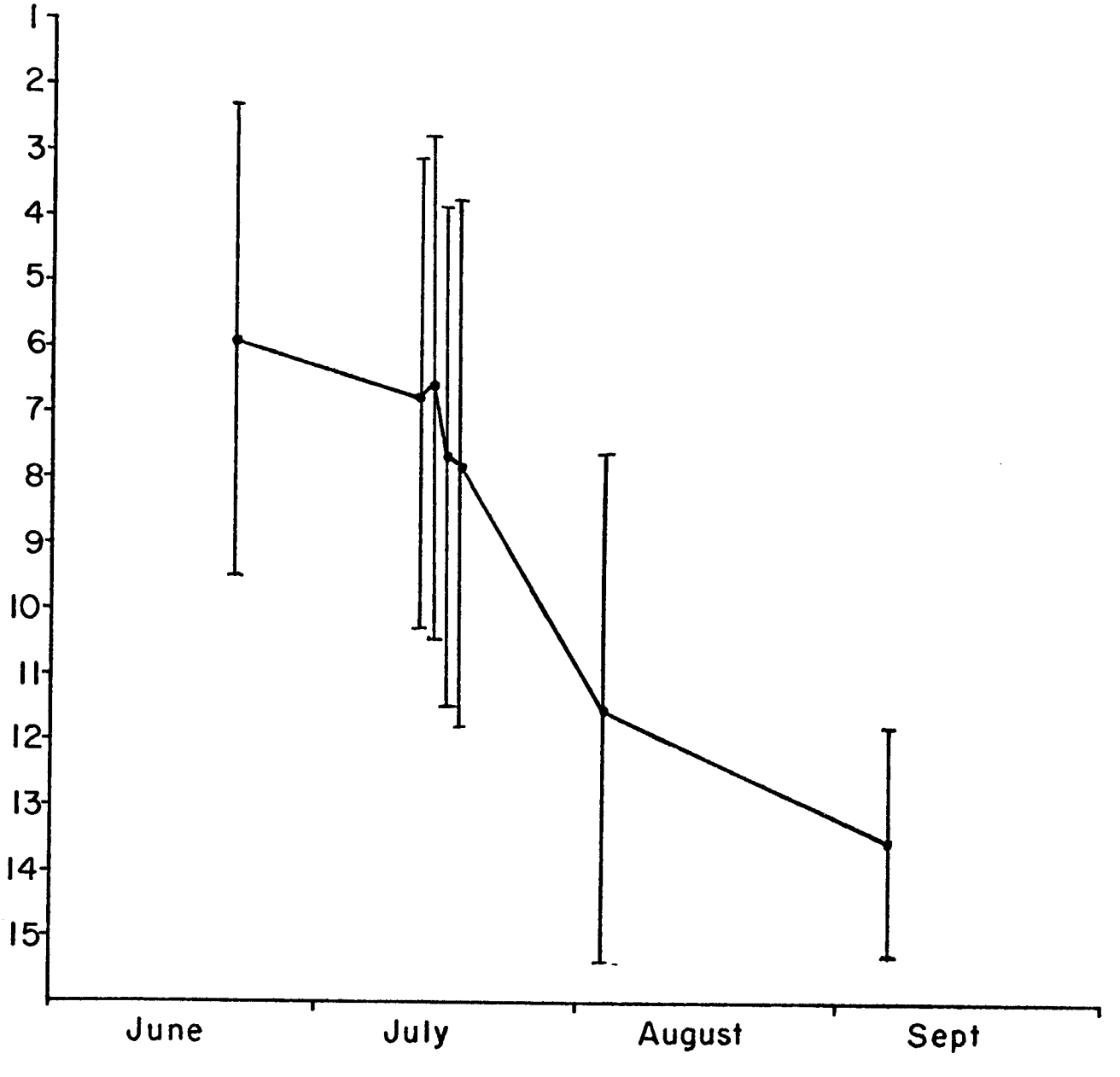

Greyscale progression for all fifteen sample areas.

FIGURE 9

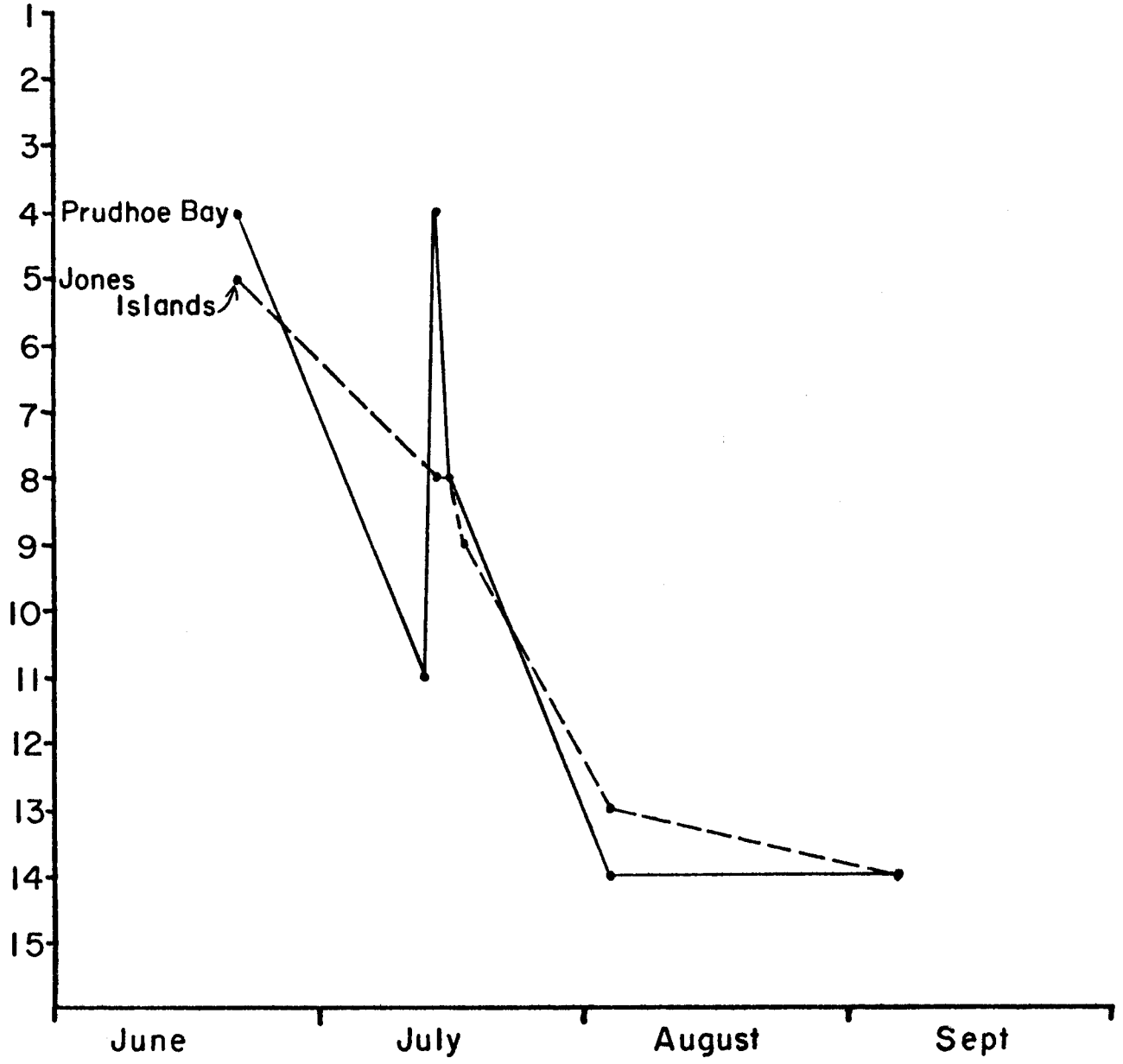

Trend of greyscale values for two selected study sites

The objective classification is a modified version of the method used by Kirchoffer (1973) to classify European 500mb height patterns. The data used in the present analysis are selected from the daily (1200Z) MSL pressures on the NMC magnetic tape archives. A 36-point grid (Figures 1A and 1B) is used as the classification field. In order to maximize the applicability of the classification to current ice problems, the sample was chosen from the most recent data on hand: October, 1969 through August, 1974 (1795 days with 36 points per day is the maximum sample size compatible with the extended core storage (ECS) limits in the CDC 6400 computer). This choice also reduces errors associated with the increasingly unreliable synoptic pressure analyses in the Arctic as one goes back in time.

The first step in the process is to normalize the 36-point grid for each individual day. The mean ($\bar{P}_j$) and standard deviation (s_j) of the 36 pressures are calculated for each ("jth") day individually. Each day's grid is then normalized individually so that the actual pressure at the "ith" point on the "jth" map (P_{ij}) is replaced by:

$$(1) \qquad Z_{ij} = \frac{P_{ij} - \bar{P}_j}{s_j}$$

i.e. the number of standard deviations by which it differs from the map mean. Z_{ij} will be referred to as the normalized grid value of the "ith" point on the "jth" map. The effects of this procedure are twofold:

1) All reference to the absolute magnitudes of the pressures are removed. e.g. a closed circular low with a uniform pressure gradient will have the same normalized pattern no matter what the central pressure is.

2) Weak actual pressure patterns can become stronger normalized patterns. That this is so can be seen by considering two maps with identical isobar pattern shapes and identical mean pressures, but with different standard deviations. The differences in pressure $P_{ij} - \bar{P}_j$ for the weak pattern (low standard deviation) will be less in each case than the corresponding differences in the strong pattern. However, the weak pattern's standard deviation s_j will be even more-strongly reduced, because it is calculated from a sum of squared deviations from the mean. The net effect is to cause grid patterns of normalized values to become stronger (more isopleths) than their corresponding (weak) actual pressure patterns.

The second step in the procedure is to determine for each day in the sample the number of other days classified as having a similar normalized pattern to that of the given day. Similarity is tested by computing the quantity:

$$(2) \qquad (\Delta_i)_{jk} = (Z_{ij} - Z_{ik})$$

where the subscripts indicate that we take the difference between normalized grid values at the "ith" point of the "jth" and "kth" daily maps. We then square and sum over the 36 points:

$$(3) \qquad SUM\Delta^2 = (\Sigma\Delta_i^2)_{jk}$$

which yields the total sum of squared differences between corresponding normalized grid point values between the two (j & k) maps. The magnitude of $SUM\Delta^2$ is then a measure of the dissimilarity of the two maps in question. Previous work with this technique in the Western U.S. suggests that two patterns can be satisfactorily grouped as similar if $SUM\Delta^2$ is less than or equal to N,

the number of grid points (36 in this case). It should be emphasized that the selection of such a "threshold" is a subjective process, involving visual inspection of similiar maps and testing of the program with various thresholds. The total sum of squared grid-point differences over the map gives a measure of similarity for the entire field, but it might still be possible to have similar maps with rather undesirable pattern differences concentrated in a small portion of the field. Therefore, the maps were divided into five (roughly) zonal rows and six meridional columns. The $SUM\Delta^2$'s for the points in each of these subdivisions are then calculated for each pair of maps and must be less than or equal to 1.8NN, where NN is the number of points in the subdivision, in order to be classified as similar. This threshold was also determined subjectively, based on test cases in the Alaska region as well as previous work elsewhere. The rows and columns are shown in Figures 1 and 2. After repeating this procedure for all pairs of maps in the 1795-day sample, we have a "table" (within the computer) listing against each day, all days passing both similarity tests.

The third step in the classification is to find the key days which serve as pattern-types or representatives for the rest of the sample. The day having the largest number of similar days is designated as key day number one. All days listed as similar to key day number one are then removed from the lists of similar days in the rest of the "table". After these days are cleared from the matrix, the day having the greatest number of remaining similar days in its list is designated as key day number two. This process is repeated until there are no days with greater than or equal to five similar days in their lists. Any residual days are listed as "unclassified".

The final step in the typing procedure is to assign all non-key days in the sample to the key day with which it had the lowest $SUM\Delta^2$. The need for this step arises when we clear each successive key day's list of similar days from the remaining table. This latter procedure removes from the remaining lists all days which passed with the key day presently under consideration. However, some of the days so removed may have a lower $SUM\Delta^2$ with respect to a key day generated later in the typing program. (i.e. it was "similar" to more than one key day, and had a lower score with the key day which occurred later in the program).

Having completed the steps above, then, we have a small set of key days, each with a list of all days having the lowest score with itself. The rationale for this typing procedure is that each key day is a good representative of a group of pressure patterns which reappear in the sector through time. The synoptic-scale atmospheric history is thus composed of these several types plus a small group of unclassified patterns.

In order to assess the distinctiveness and characteristics of the synoptic types in terms of surface weather, the daily resultant wind speeds and mean daily temperature departures at Barrow and Barter Island are assessed by analysis of variance (ANOVA) for the period 1969-1974. The initial goal of the analysis is to find out which patterns contribute which types of weather (and whether or not the patterns differ in this respect), so that measures of central tendency and scatter for the meteorological elements known to affect fast ice can be derived for each type. Wind direction is a circular variable and must be treated separately. Cloudiness and precipitation have distinctly non-Gaussian distributions and must likewise be assessed separately. Problems in applying statistics of variance to the data arise from four different sources:

1) Meteorological data are usually serially correlated whereas these statistical measures require independent data for validity.
2) The data series possess regular periodicities of various frequencies and amplitudes (e.g. secular, annual and diurnal cycles).
3) Type characteristics may differ from one location to the next.
4) A (stochastic for our model) error exists for each measurement on a meteorological variable, deriving from factors not accounted for by the synoptic pressure pattern typing scheme (e.g. upper air variations, air mass trajectories, local surface conditions, measurement errors).

In order to apply ANOVA, the data should comprise an independent sample from a normally-distributed population with mean μ and standard deviation σ. To achieve conformity to these conditions, the conceptual model of Godske (1959) is used. Here V_t will represent a particular measurement on a meteorological variable t, say, the mean daily temperature. The independent variables upon which the particular value of t depends are then:

1) g: for geographical location
2) s: for secular time (unit 1 year)
3) a: for annual time (unit 1 day)
4) d: for diurnal time (unit 1 hour)
5) w: for weather type (synoptic pattern in our case).

Following Godske, then, we may write the equation for a particular measurement V_t as follows:

$$V_t = \Phi_t(g_o,s,a_o,d_o,w_o) + \Psi_t(g_o,s,a,d_o,w_o) + \chi_t(g_o,s,a,d,w_o) + \Theta_t(g_o,s,a,d,w) + \varepsilon_t(g_o,s,a,d,w) \quad (1)$$

where the subscript "o" indicates that the variable is held constant in the particular term. The functions Φ, Ψ, χ, represent the variation of t on secular, annual, and diurnal time scales, while Θ and ε are the systematic variation of t with weather type and the random error, respectively. We shall examine the stations separately, so that g is held constant in all terms, as in (1). In order to evaluate the type characteristics, we would like to stratify the data by type (w) and evaluate the central tendency and scatter associated with the variable t for each type. We must first remove the dep-

endence of V_t on the first three terms in (1). For the six-year period from 1969-1974 it is assumed that secular trends are negligible, so that term one drops out of (1). In order to reduce the obvious dependence of temperature on the annual course of the seasons, we consider t as a departure from the long-term mean for each day. However, the statistical parameters of the departures may also vary systematicly with season (although with a much smaller amplitude than the temperature itself) so we must also group the data by seasons:

1) winter = December through March
2) Spring = April through June
3) Summer = July through September
4) Fall = October through November

We have effectively removed the diurnal term by considering departures from the daily mean temperature. After we stratify the data into categories according to synoptic pattern and season, then, we have:

$$(2) \qquad (V_t)_{\hat{s},w} = \Theta_t(g_o,\hat{s},w) + \varepsilon_t(g_o,\hat{s},w)$$

where $(V_t)_{\hat{s},w}$ is a particular measurement on t for weather type w and season $\hat{s}$. Θ is the function for the systematic variation in V_t due to occurrence of type w and season $\hat{s}$. This systematic variation can be modeled as a set of mean values, one for each type and season. ε is the error function, describing the scatter for each type and season about its respective mean. This term does not yet, however, represent an independent measure of error taken at random from a normal population, as required by ANOVA, because it is serially correlated with values from previous and subsequent days. In order to remove this dependence, the linear correlation coefficient for serial data:

$$(3) \qquad \frac{\Sigma t_i t_{i+L} - \frac{\Sigma t_i \Sigma t_{i+L}}{n}}{\sqrt{\left\{\Sigma t_i^2 - \frac{(\Sigma t_i)^2}{n}\right\}\left\{\Sigma t_{i+L}^2 - \frac{(\Sigma t_{i+L})^2}{n}\right\}}}$$

was computed for lags 1 through 60 days to ascertain the minimum time separation allowable for independence of data.

The final problem involves assessing the number of degrees of freedom associated with each occurrence of a synoptic type. A run of N consecutive days, all having pressure pattern type K, may have similar characteristics (upper air pattern, air mass trajectory, surface conditions, etc.) which are not accounted for by the typing scheme and will vary less within such a run than between cases from different runs of type K. The variation that we wish to assess, on the other hand, is the random scatter ε which allows all these factors to vary. Therefore, only one degree of freedom can be assigned for days in a run of consecutive types (K). So we must take only one case from each run of consecutive types for analysis or compute some average of the meteorological variable in question as a representative of the run, assigning only one degree of freedom in either case.

The data set selected by the above processes comprises the ANOVA sample. In order to test the data for normality, the mean and standard deviation of each stratified sample are computed. The frequencies of variates in each sample are then divided into class intervals, and the observed class frequencies are tested against the expected frequencies for a normal curve with the same mean and standard deviation in a chi-square contingency table. If the hypothesis that the data come from a non-normal distribution is rejected at the 95% level in the chi-square test, then the ANOVA model is assumed valid for the data.

Appendix 3

Daily Surface geostrophic wind components in the I and J directions were computed from 10 points on the NMC grid (Figure 3). The equations used for the calculations are:

$$(1) \qquad V_J = \frac{R\overline{T}}{\Delta I \Omega \sin\overline{\phi}} \left(\frac{P1 - P2}{P1 + P2}\right)$$

$$(2) \qquad V_I = \frac{R\overline{T}}{\Delta J \Omega \sin\overline{\phi}} \left(\frac{P1 - P2}{P1 + P2}\right)$$

where:

R = gas const. for dry air

$\overline{T}$ = average of the mean monthly temperatures at Barrow and Barter Island for the given month

ΔI = Distance between points (m)

ΔJ = Distance between points (m)

Ω = Angular velocity of earth

$\overline{\phi}$ = Mean of latitudes at points 1 and 2

P_1 = Pressure at point 1

P_2 = Pressure at point 2

The points on the coast corresponding to the V_1 calculations are circled in Figure 3. The V_J points have a square enclosure. On the Beaufort coast, the I-direction is very nearly perpendicular to the coastline (offshore) while the J-direction is alongshore (to the west). Thus we can derive rough indicators onshore and alongshore windspeed, wind direction and wind stress on the fast-ice.

In order to analyze the seasonal course of geostrophic surface winds and their variability, the monthly means and SD's of V_I and V_J for the six points were calculated for the period 9/68 → 8/74. It should be noted that the actual surface winds (and hence the wind stress) are turned roughly 15°-30° to the left of the geostrophic winds due to frictional backing (see e.g. Sater, et al., 1974), and will be slowed by ∿ 30%. Calculations of approximate sfc winds and wind stresses from these data will incorporate these (rule of thumb) corrections in the analyses of ice-related meteorological events and mean conditions to appear in later reports. Table 4 is a listing of mean monthly I and J surface geostrophic wind components and their standard deviations for the 6 years: 9/1969-8/1974.

APPENDIX 4 (ND = No NMC data that day)

LISTING OF SYNOPTIC TYPES BY MONTH FOR 1969 ALASKA

OCT	3	1	1	6	2	4	1	1	6	2	4	13	4	4	1	1	1	1	1	3	9	9	10	2	2	5	7	1	1	1	1
NOV	1	1	8	10	1	8	1	1	8	19	19	4	1	3	3	9	4	4	1	1	1	1	1	4	13	1	13	1	1	1	.
DEC	4	1	1	1	1	1	1	1	1	1	1	1	1	3	1	13	4	1	13	1	1	1	1	1	1	1	1	1	13	6	13

LISTING OF SYNOPTIC TYPES BY MONTH FOR 1970 ALASKA

	1	2	3	4	5	6	7	8	9	10	11	12	13	14	15	16	17	18	19	20	21	22	23	24	25	26	27	28	29	30	31
JAN	6	5	13	4	4	9	1	1	1	1	7	3	1	7	7	7	7	1	1	1	1	3	3	3	3	3	3	7	7	1	1
FEB	1	1	1	1	1	1	1	17	1	1	1	4	1	1	1	1	1	1	1	1	1	1	1	6	6	4	10		.	.	.
MAR	7	7	1	1	1	1	1	8	1	1	1	1	1	1	1	1	7	1	1	4	1	1	1	4	1	1	6	1	4	1	6
APR	8	3	3	3	3	3	1	1	1	3	1	4	13	13	4	1	6	6	1	1	6	1	1	8	3	1	1	1	1	1	.
MAY	8	8	1	1	1	1	1	1	3	10	1	1	1	1	1	1	1	17	1	1	1	1	6	1	8	17	17	11	11	15	15
JUN	14	16	3	6	11	9	7	8	1	1	11	11	13	11	2	5	4	4	6	2	2	2	2	11	5	5	5	2	11	1	.
JUL	8	14	14	11	2	14	18	6	2	2	4	4	6	6	6	21	1	6	6	17	17	1	1	17	16	20	4	6	6	6	15
AUG	6	17	3	10	6	6	6	8	17	1	1	1	1	1	6	6	17	1	6	6	2	2	2	2	15	2	2	2	14	11	14
SEP	1	1	1	1	8	5	5	5	5	2	2	2	2	14	14	13	12	8	8	5	5	19	5	4	1	13	3	7	7	7	.
OCT	14	5	3	7	4	4	4	2	13	8	17	16	20	18	18	5	9	3	3	1	1	3	3	3	4	1	1	6	6		1
NOV	13	4	4	1	10	4	4	4	4	12	1	3	13	1	1	10	2	2	5	2	5	2	9	9		9	10	5	5	5	.
DEC	9	9	7	9		1	1	1	1	1	1	1	1	1	1	10	4	10	10	2	10	10	4	6	13	3	3	3	1	3	1

LISTING OF SYNOPTIC TYPES BY MONTH FOR 1971 ALASKA

	1	2	3	4	5	6	7	8	9	10	11	12	13	14	15	16	17	18	19	20	21	22	23	24	25	26	27	28	29	30	31
JAN	13	4	1	1	1	3	5	9	9	2	2	4	4	9	9	9	9	1	1		12	19	19	3	3	3	9	9	9	1	1
FEB	1	1	9	4	4	1	1	1	1	1	7	7	7	3	1	1	1	1	1	1	1	8	3	19	5	10	10	13	.	.	.
MAR	3	3	19	3	3	3	1	1	1	1	3	3	3	1	1	4	4	4	4	9	1	1	1	1	1	1	1	1	1	1	1
APR	1	7	1	1	1	1	1	3	3	1	1	1	1	1	1	1	1	1	8	1	1	1	1	13	4	11	3	8	3	1	.
MAY	1	1	1	17	1	1	18	11	14	1	1	1	1	1	17	17	13	1	1	13	6	6	17	1	1	1	6	1	11	4	13
JUN	1	6	2	4	4	1	1	1	1	1	1	8	8	1	6	4	17	8	8	21	1	1	1	1	1	1	1	1	1	1	.
JUL	1	1	11	19	16	10	10	10	19		14			8	8	14	2	4	4	1	6	17	4	4	4	2	2	2	2	2	2
AUG	2	8	8	5	14	2	14	14	2	14	7	7	3	3	4	4	4	12	1	8	3	1	1	18	18	14	4	4	7	7	1
SEP	3	1	1	8	8	1	3	1	1	1	1	3	21	2	2	4	2	4	4	2	2	15	10	15	5	5	5	4	4	7	.
OCT	7	7	3	3	9	21	12	1	13	1	8		18	4	4	6	8	8		7	20	10	10	19	19	2	2	12		13	8
NOV	19	3	9	4	4	1	1	3	1	1	1	1	1	1	4	4	4	1	1	13	3		10	10	9	9	3	3	3	3	.
DEC	3	1	1	1	1	4	1	1	3	4	9	4	1	4	4	8	4	2	5	5	9	4	4	ND	2	6	4	6	6	1	

LISTING OF SYNOPTIC TYPES BY MONTH FOR 1972 ALASKA

	1	2	3	4	5	6	7	8	9	10	11	12	13	14	15	16	17	18	19	20	21	22	23	24	25	26	27	28	29	30	31
JAN	5	4	4	1	1	1	1	1	3	5	5	5	7	7	3	3	9	9	4	4	7	7	4	4	4	4	6	2	2	2	2
FEB	7	1	4	4	1	1	1	1	1	1	1	1	1	1	3	3	5	5	9	9	9	2	5	3	9	3	3	1	9	.	.
MAR	7	3	5	5	3	3	7	7	9	3	3	3	3	1	1	1	1	1	1	1	3	3	1	1	6	16	1	18	3	3	9
APR	20	20	10	8	3	3	3	19	10	1	1	1	8	8	19	1	1	1	8	3	1	1	4	1	1	3	3	1	1	6	.
MAY	6	4	1	1	1	6	17	13	7	1	1		8	8	3	10	1	1	1	16	16	17	17	1	1	1	4	10	19	10	8
JUN	10	6	6	6	1	8	19	6	4	17	1	1	1	16	16	1	1	6	6	17	8	16	17	21	17	1	1	8	18	15	.
JUL	2	2		9	1	7	4	9	7	4	20	1	1	2	2	2	2	2	2	5	19	3	1	1	1	1	1	6	6	6	4
AUG	17	1	1	12	2	15	2	5	5	5	2	2	11	6	6	14	16	6	10	6	4	1	1	6	8	8	15	1	1	13	2
SEP	2	15	12	6	1	1	1	1	16	16	7	1	16	6	8	8	3	3	9	3	9	9	4	14	2	2	5	13	1	8	.
OCT	8	3	5	4	12	18	15		10	2	2	2	2	2	4	6	6	2	2	4	4	1	12	21	10	15	10	6	6	14	4
NOV	5	5	9	4	1	1	1	1	1	1	1	1	1	1	1	1	1	1	1	1	1	1	1	1	1	16	4	1	6	3	.
DEC	5	20	2	4	4	2	2	2	2	15	15	5	5	3	3	1	1	7	7	7	7	4	1	1	1	1	1	13	1	3	3

LISTING OF SYNOPTIC TYPES BY MONTH FOR 1973 ALASKA

	1	2	3	4	5	6	7	8	9	10	11	12	13	14	15	16	17	18	19	20	21	22	23	24	25	26	27	28	29	30	31
JAN	5	4	4	1	1	1	1	1	3	5	5	5	7	7	9	3	3	3	3	3	7	ND	ND	5	5	2	4	2	2	5	9
FEB	10	6	2	2	2	4	4	4	7	7	7	9	4	4	7	ND	ND	ND	ND	ND	ND	ND	ND	1	9	1	1	1	.	.	.
MAR	1	1	1	1	1	13	1	1	1	3	1	1	1	ND	3	3	1	3	1	1	1	1	1	1	4	1	4	1	1	1	12
APR	12	12	3	1	1	4	1	1	1	1	17	4	1	1	1	1	1	ND	1	1	3	3	3	1	1	3	1	1	1	1	.
MAY	1	1	1	1	1	1	1	1	1	12	12	12	10	4	1	17	7	1	17	1	1	1	ND	1	1	6	1	6	2		17
JUN	1	1	17	1	1	12	18	8	18	15	21	3	1	1	1	ND	8	8	8	2	4	14	8	3	8	6	21	10	17	17	.
JUL	1	8	ND	8	8	8	8	5	2	2	14	14	11	2	2	2	2	5	5	5	5	2	2	2	2	2	2	12	6	2	2
AUG	15	2	9		6	6	8	18	15	2	2	5	5	3	5	10	2	2	2	2	2	15	5	6	ND	8	5	5	2	2	4
SEP	12		4	1	1	1	13	1		6	4	4	6	2	4	4	6	6	10	19	8	5	5	ND	2	12	8	15	10	6	.
OCT	6	8	8	6	1	1	1	4	12	13	8	3	3	3	9	10	6	12	3	3	3	4	4	4	4	12	12	6	12	3	3
NOV	9	4	4	2	9	9	2	5	2	2	5	5	9	9	1	1	1	1	1	1	1	6	1	1	8	3	3	3	3	4	.
DEC	4	4	1	1	1	1	1	4	4	1	1	3	3	1	1	3	13	1	1	1	1	13	7	7	4	4	4	1	10	2	2

LISTING OF SYNOPTIC TYPES BY MONTH FOR 1974 ALASKA

	1	2	3	4	5	6	7	8	9	10	11	12	13	14	15	16	17	18	19	20	21	22	23	24	25	26	27	28	29	30	31
JAN	2	2	2	2	2	14	7	7	7	7	7	9	9	5	3	3	1	1	1	7	7	4	4	7	5	7	3	3	3	7	13
FEB	1	1	1	4	4	13	1	1	1	1	3	1	3	3	3	8	3	3	3	3	3	3	3	9	9	2	5	.	.	.	
MAR	9	4	8	ND	19	5	3	ND	9	9	ND	9	1	1	1	1	1	4	4	7	4	1	1	1	1	1	1	1	1	1	1
APR	1	1	ND	1	1	1	1	1	1	1	1	7	7	1	1	1	1	1	7	7	3	7	1	ND	4	4	1	16	1	ND	.
MAY	1	1	1	1	1	ND	1	1	1	1	1	1	1	1	8	19	1	16	1	1	5	3	3	3	3	1	4	16	16	1	1
JUN	8	8	8	17	12	15	15	5	5	ND	8	15	15	2	13	1	21	21	21	1	16	3	1	1	1	21	8	18	5	5	.
JUL	5	5	7	16	8	8	16	8	8	8	21	1	11	4	9	11	2	2	2	14	14	7	1	15	15	2	2	2	2	2	
AUG	2	5	11		11	17	4	2	14	2	2	2	2	2	2	15	5	5	8	3	1	1	4	6	6	6	6	6	4	4	2

DATES OF KEY DAYS

KEY DAY NUMBER	DATE
I	12/03/1969
II	09/20/1971
III	01/15/1972
IV	01/24/1972
V	01/24/1973
VI	08/06/1973
VII	09/29/1970
VIII	06/02/1974
IX	02/25/1974
X	10/25/1972
XI	06/14/1970
XII	09/01/1973
XIII	02/28/1971
XIV	07/02/1970
XV	06/12/1974
XVI	06/22/1972
XVII	08/17/1970
XVIII	07/07/1970
XIX	10/25/1971
XX	04/02/1972
XXI	06/18/1974

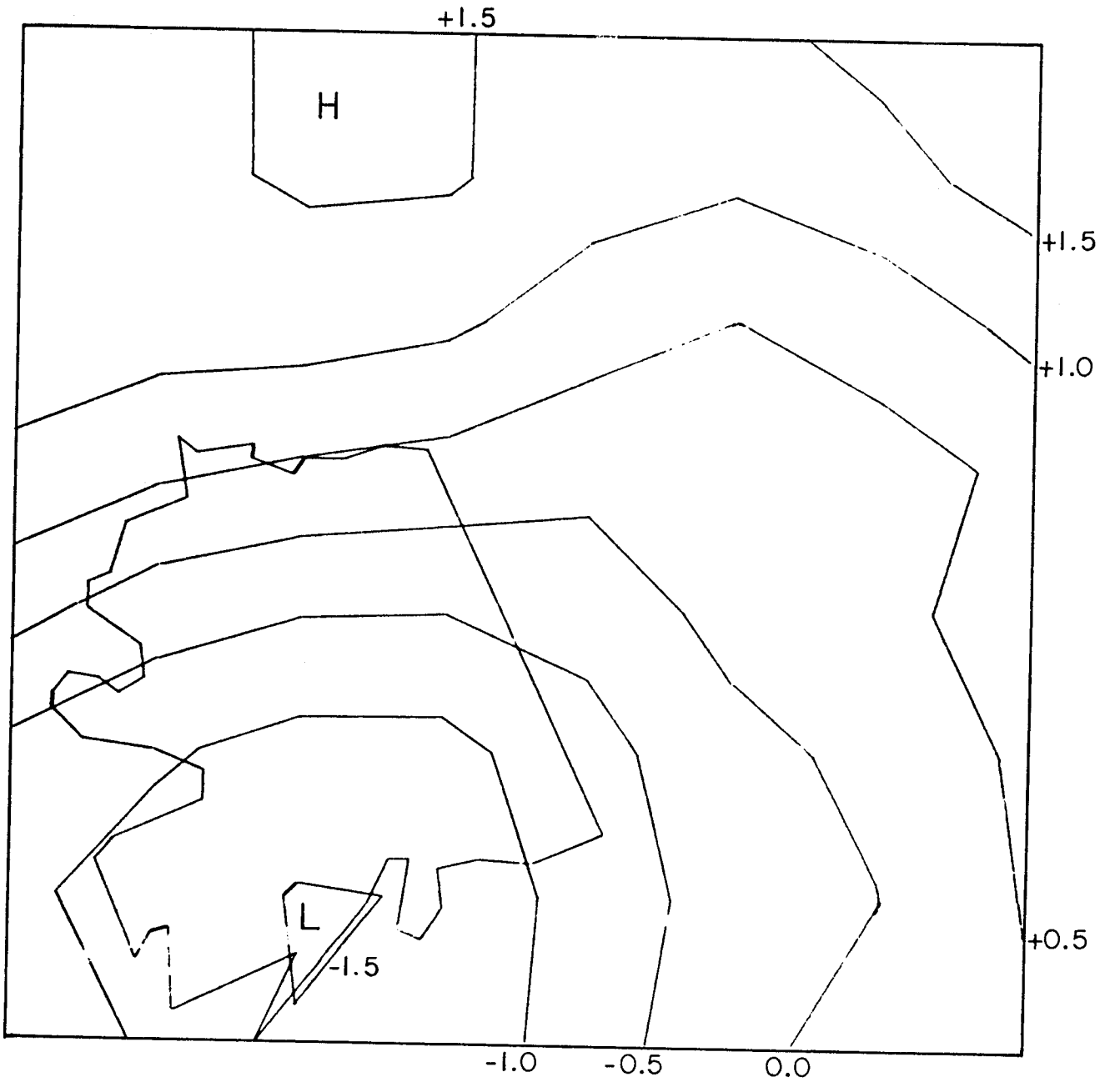

KEY DAY :

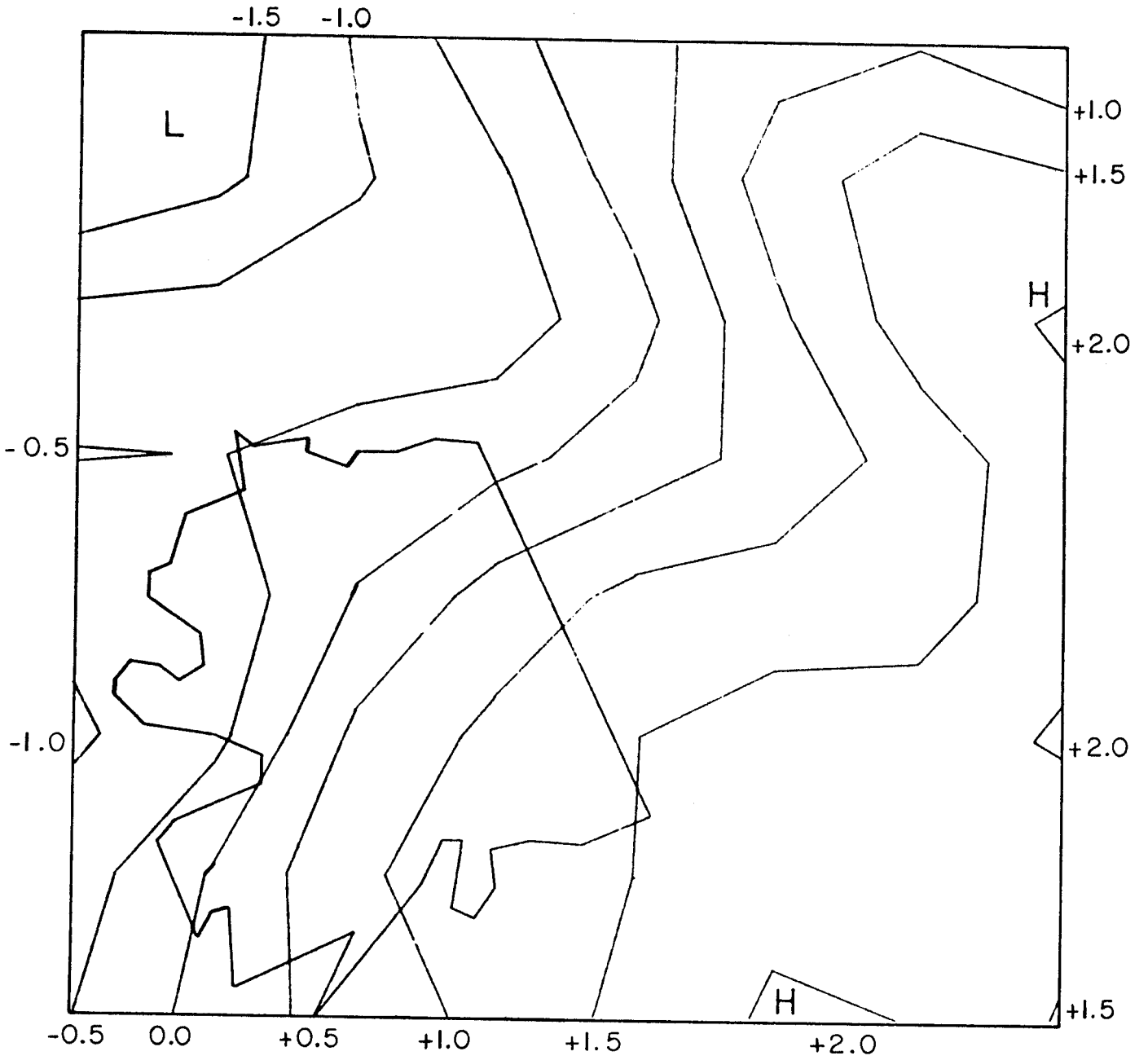

KEY DAY 2

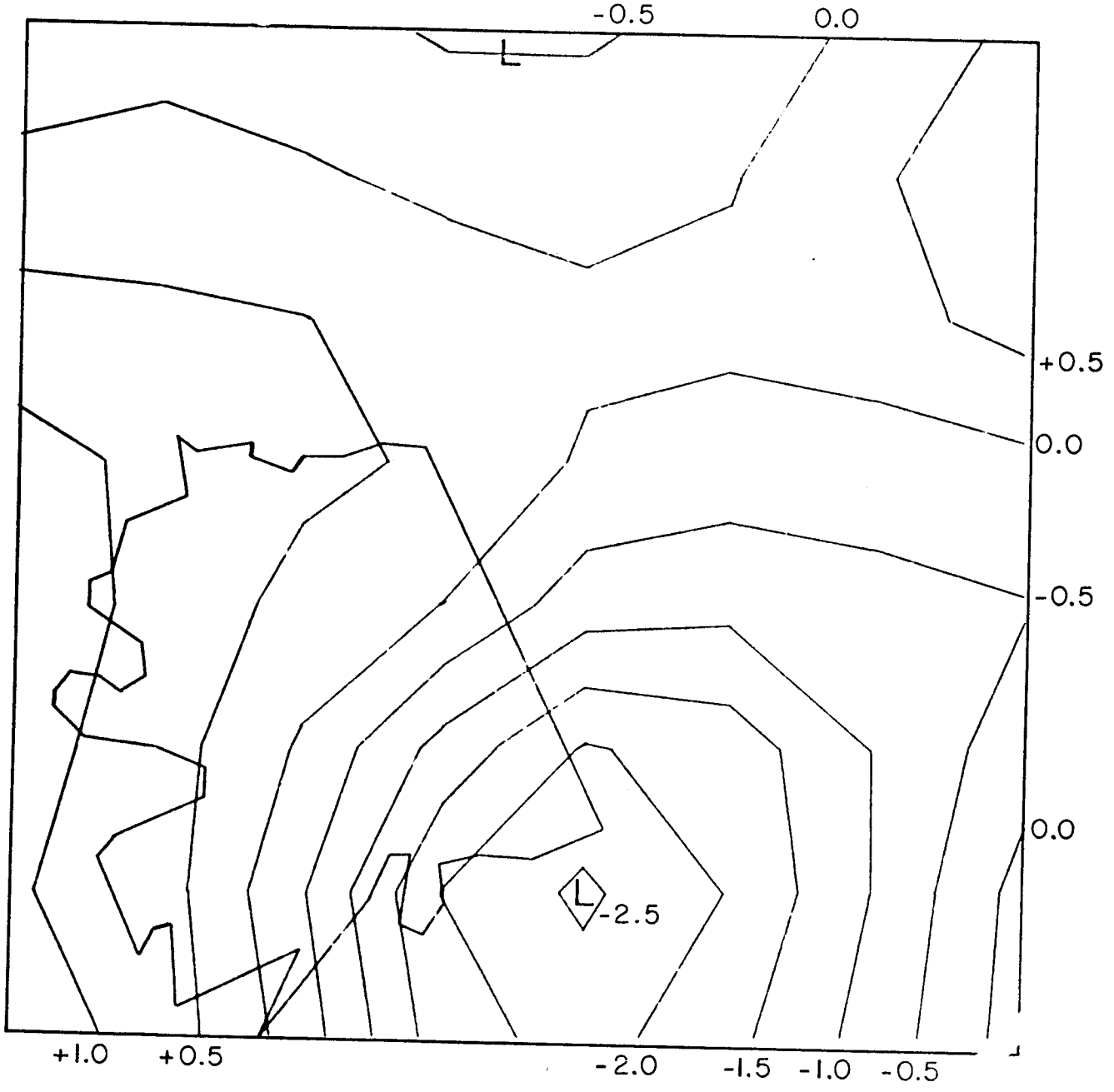

KEY DAY 3

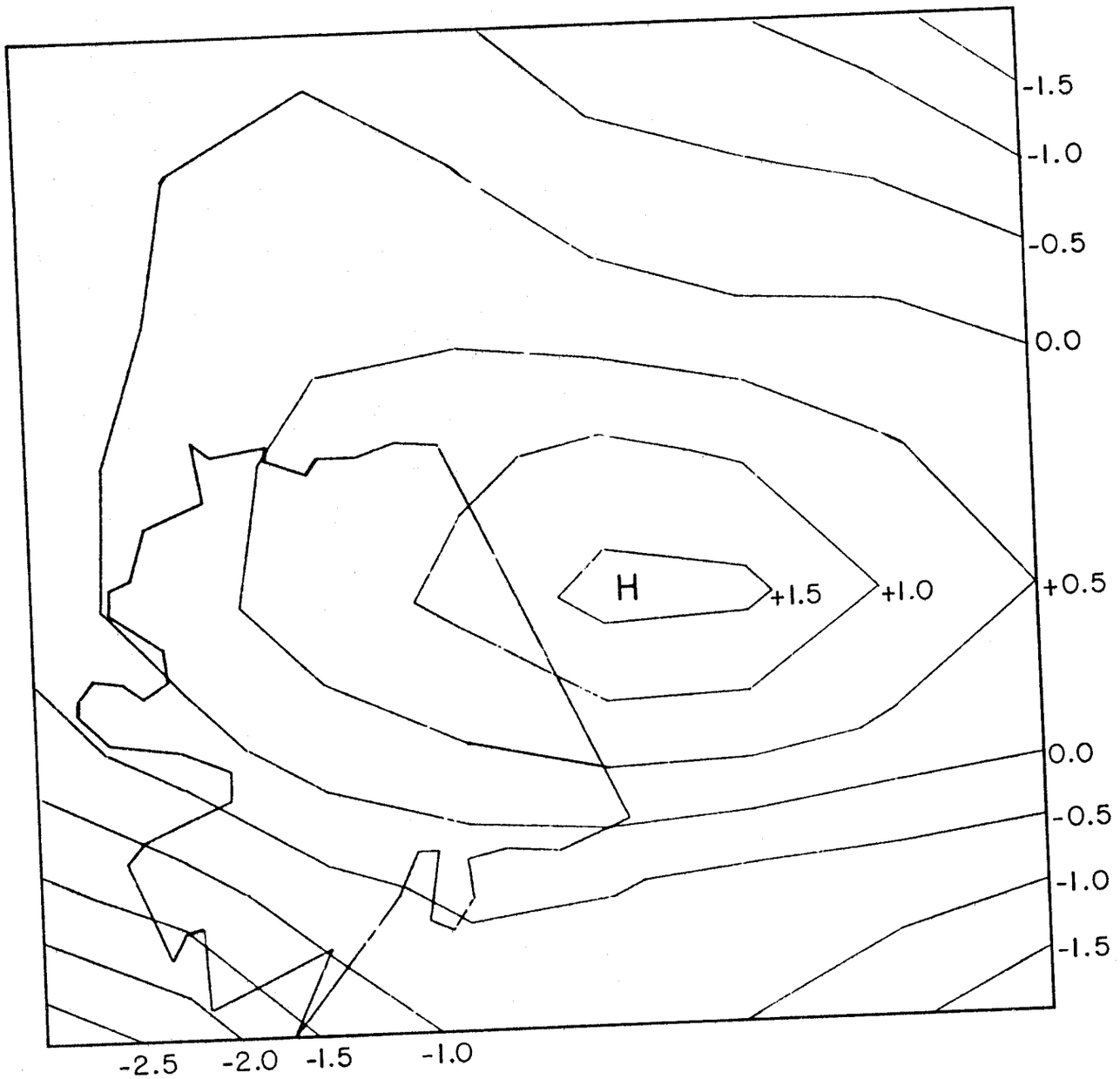

KEY DAY 4

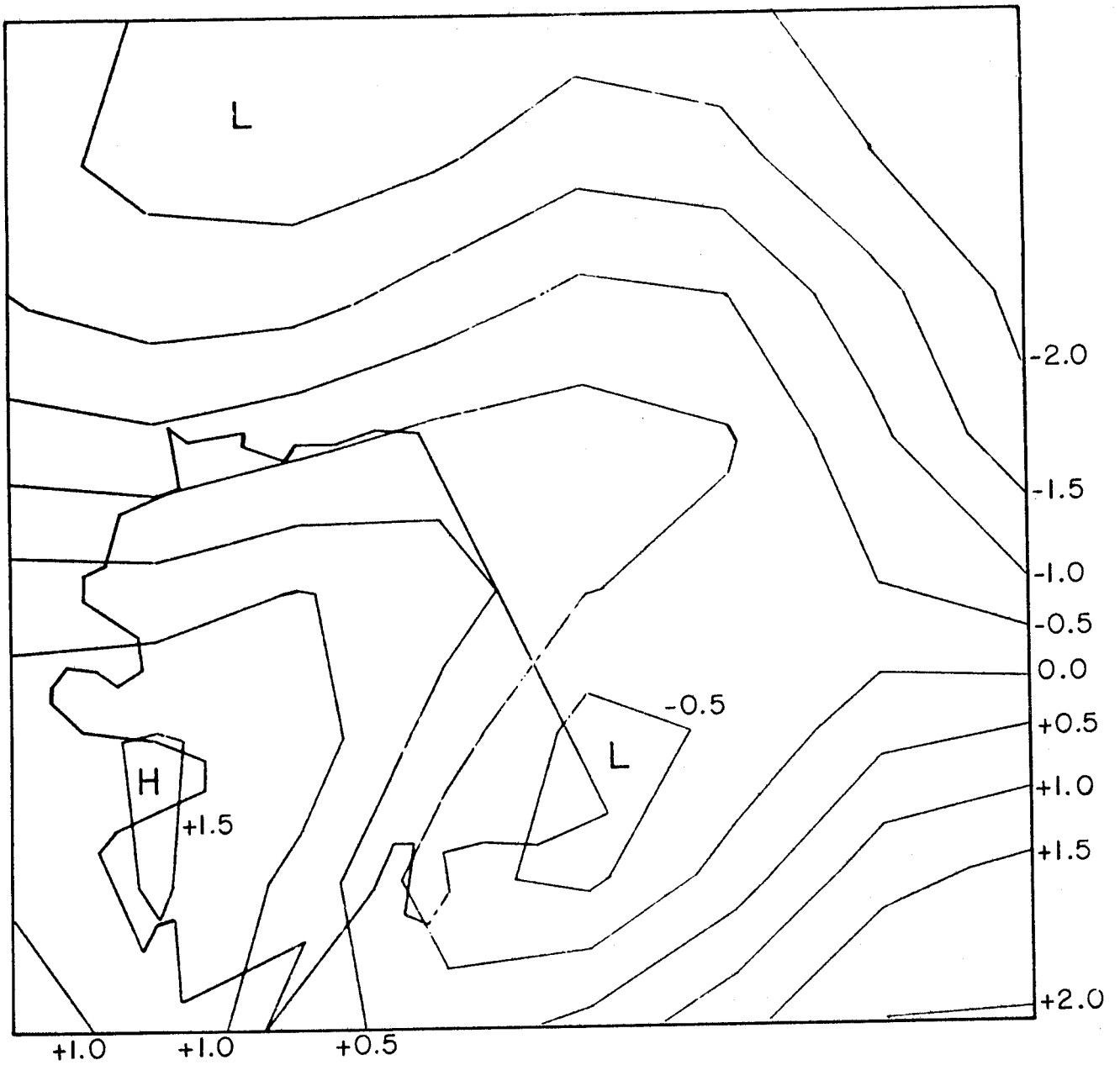

KEY DAY 5

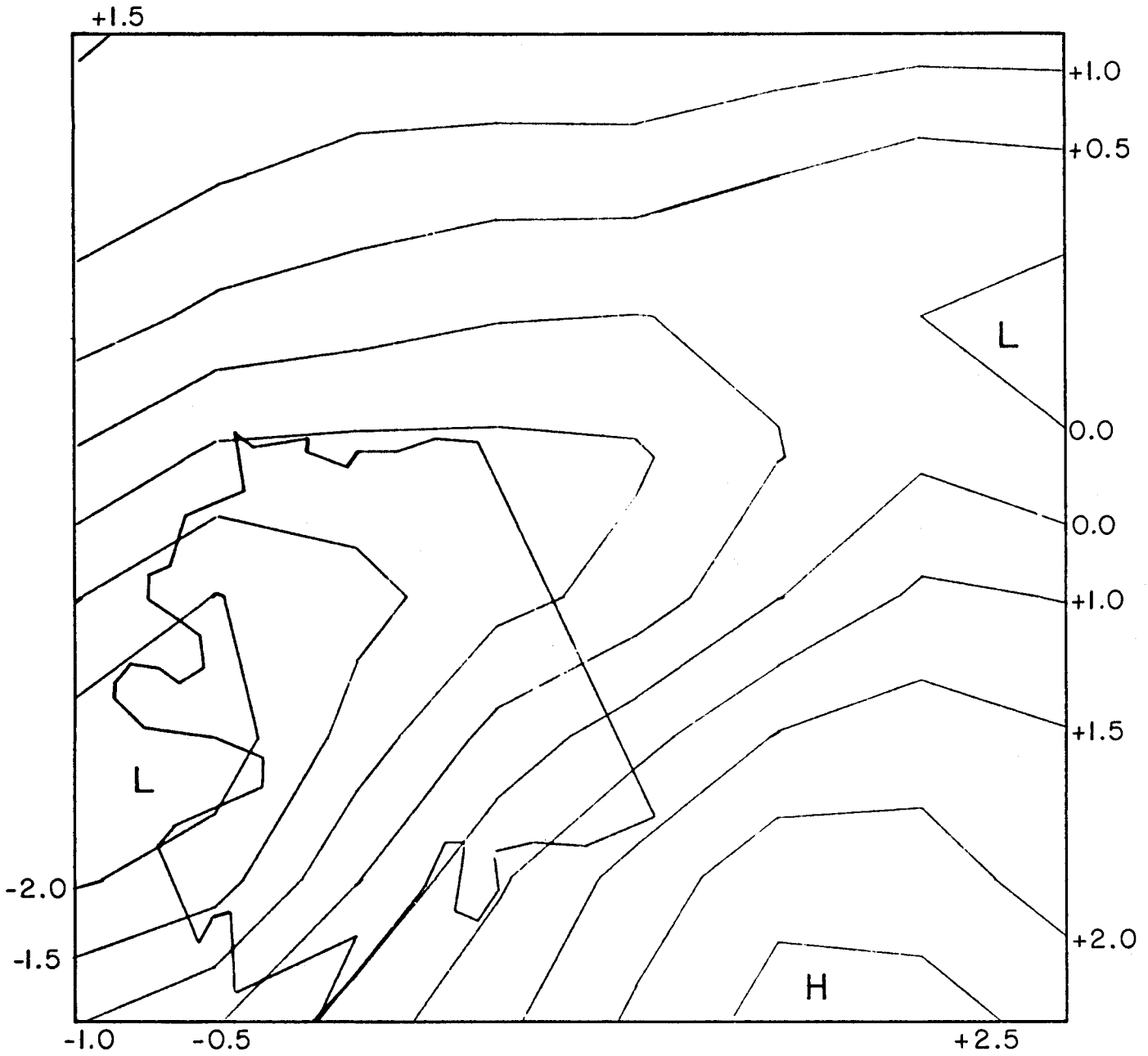

KEY DAY 6

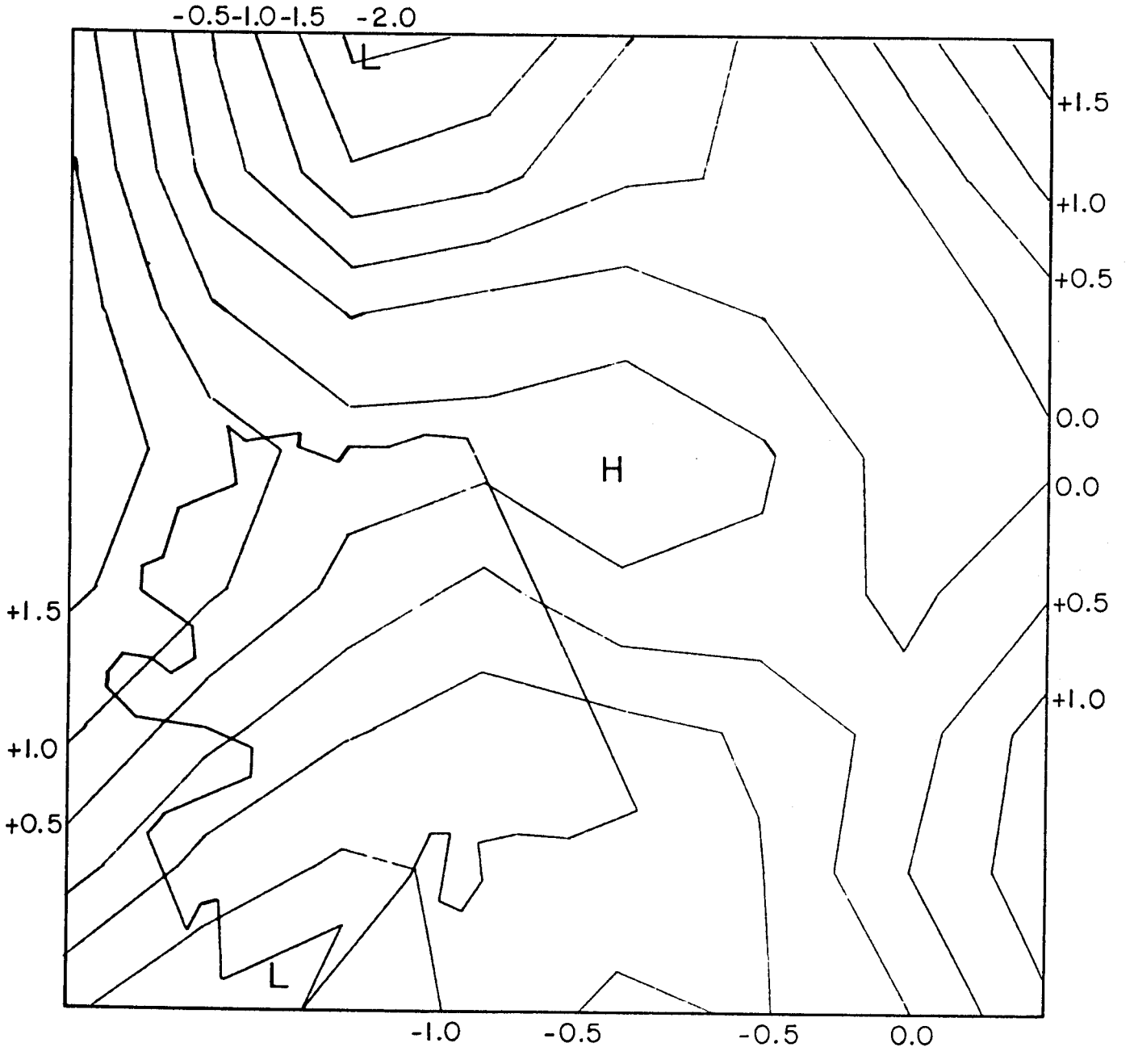

KEY DAY 7

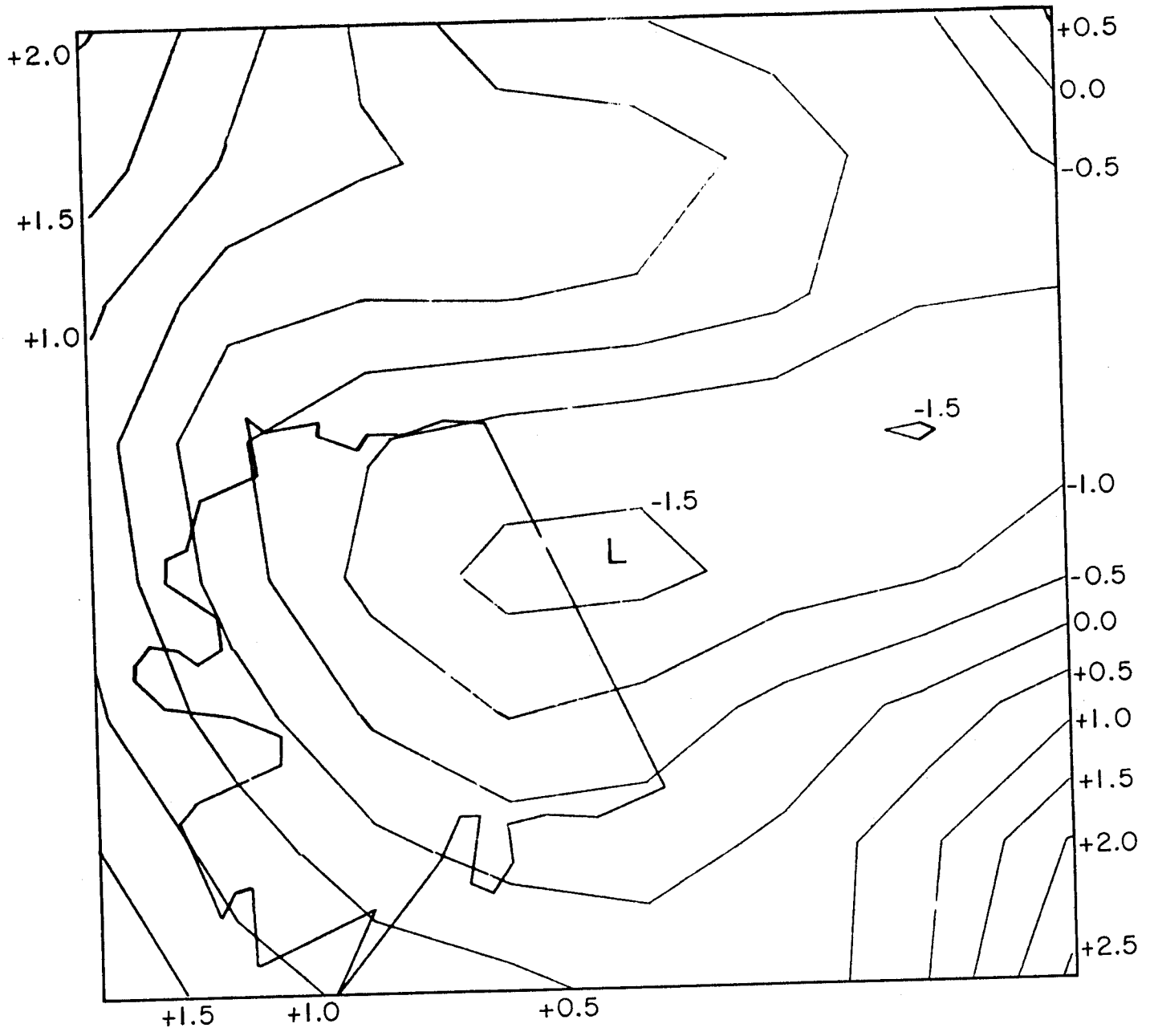

KEY DAY 8

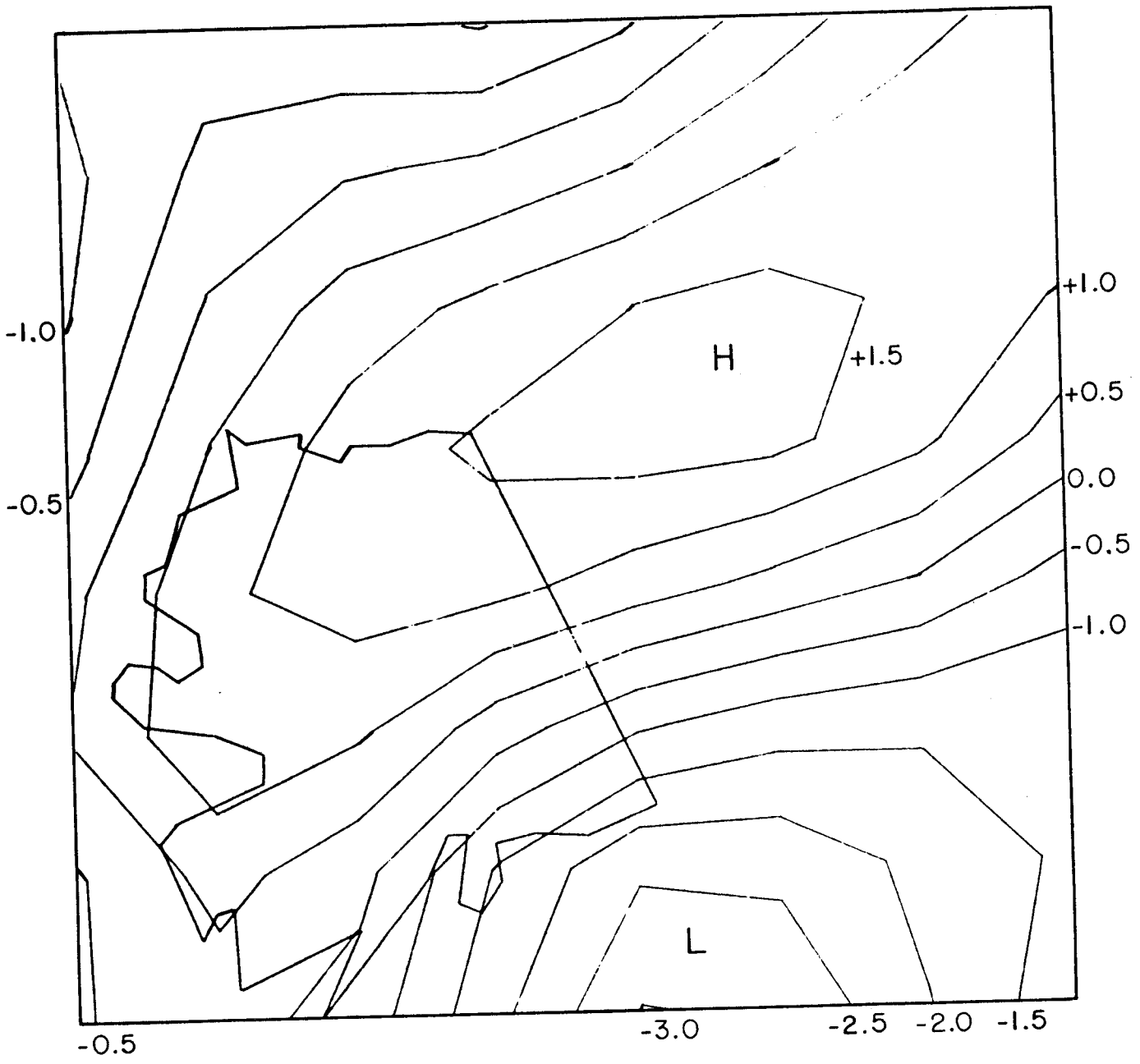

KEY DAY 9

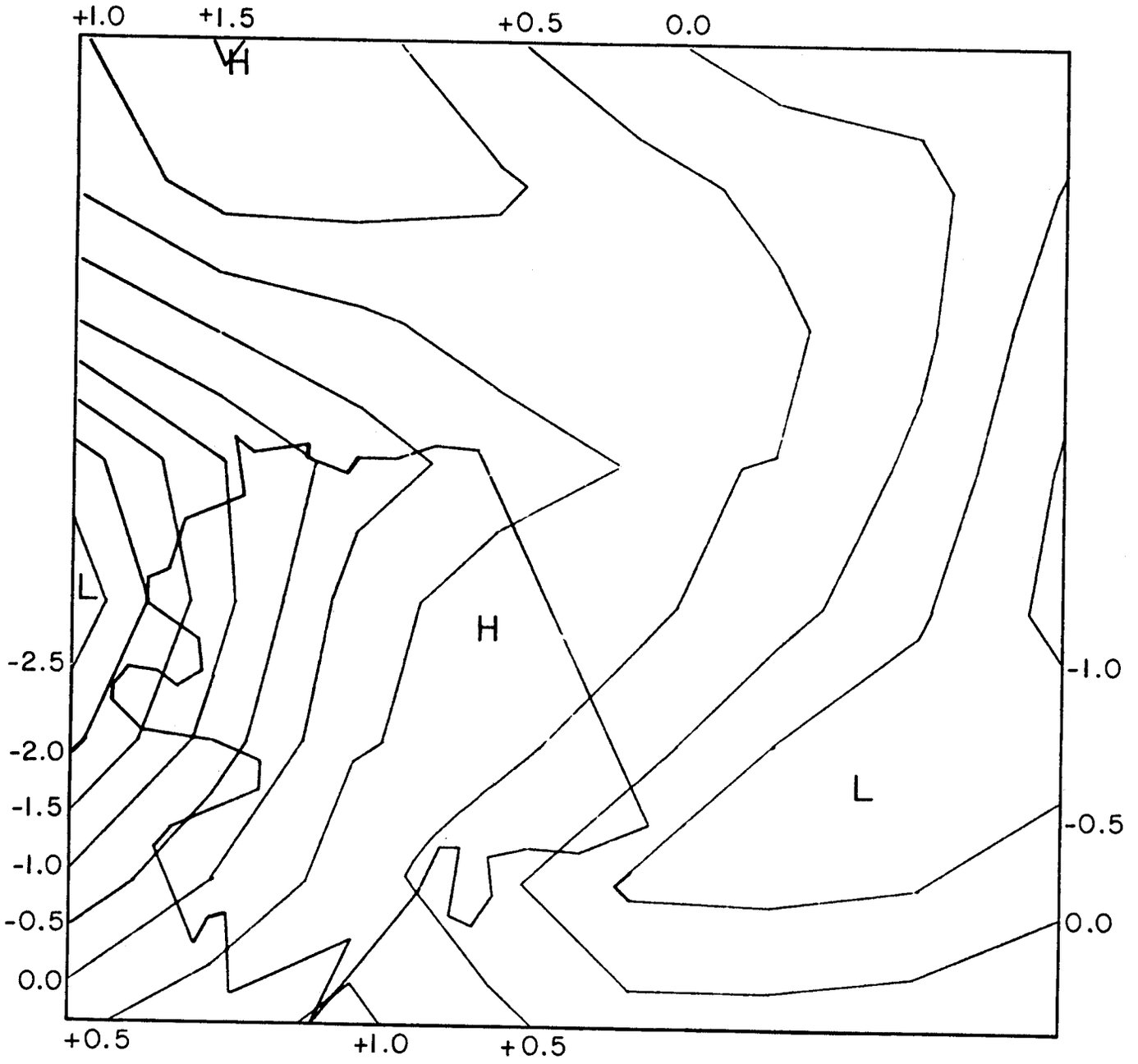

KEY DAY 10

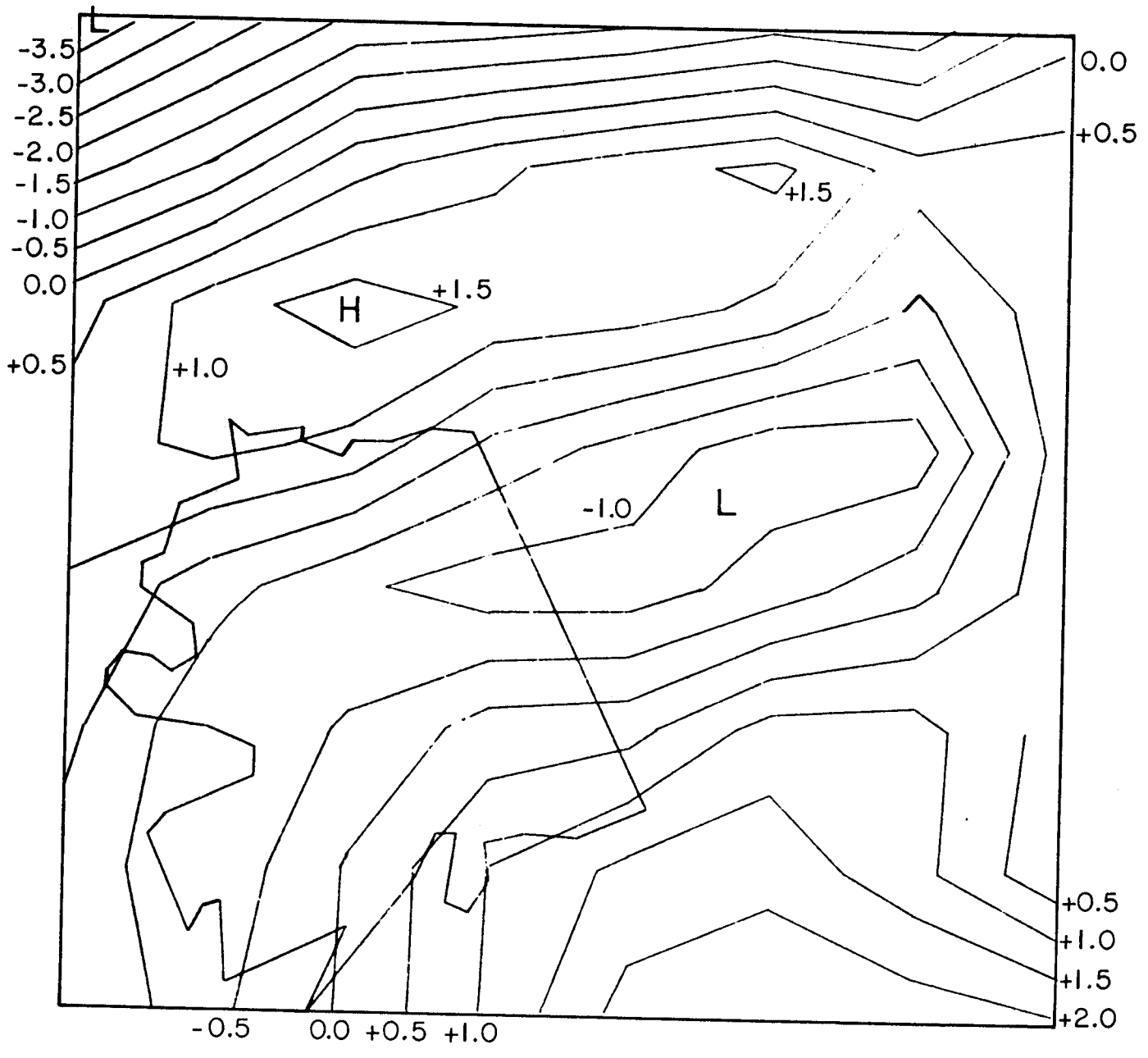

KEY DAY 11

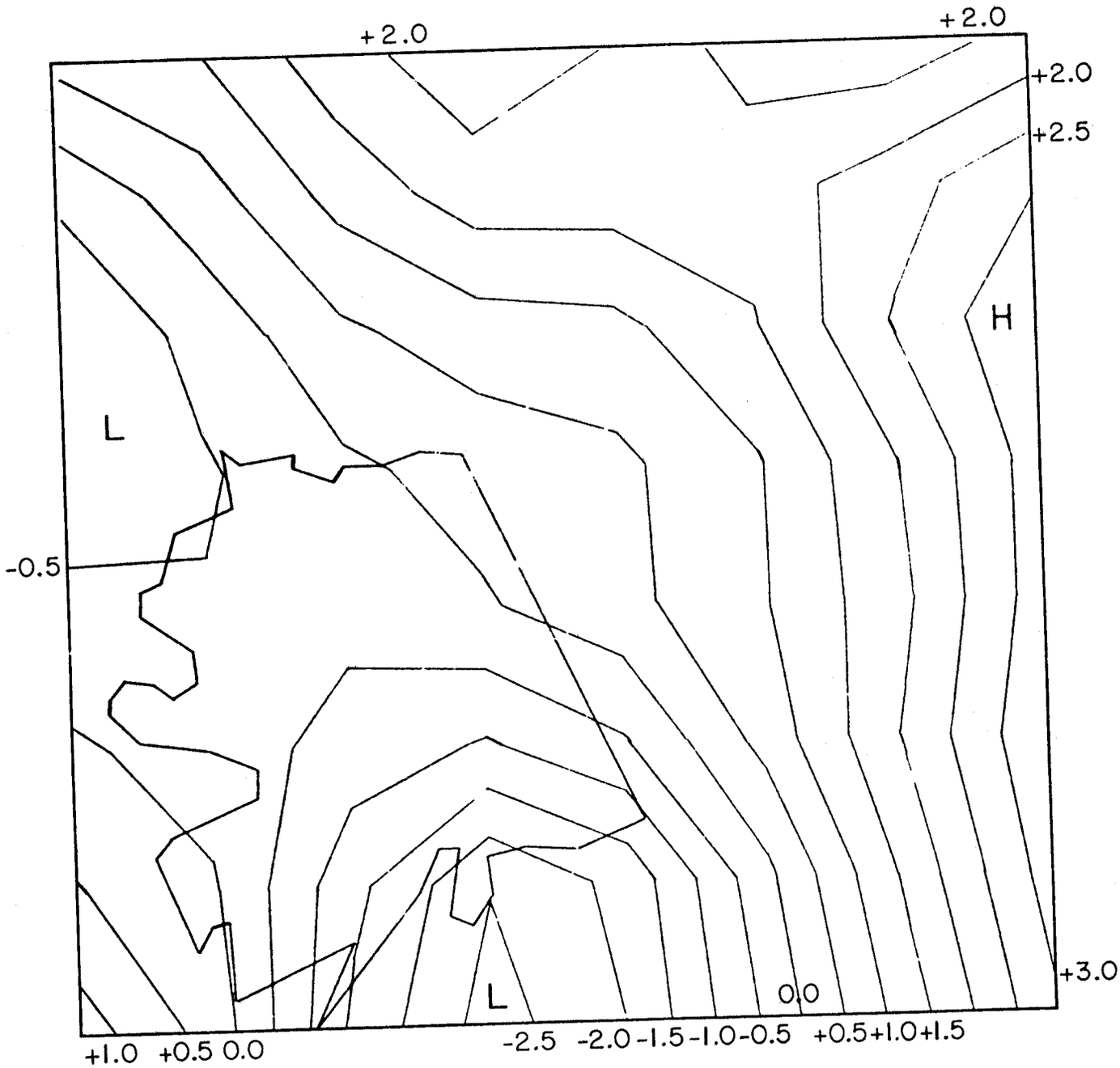

KEY DAY 12

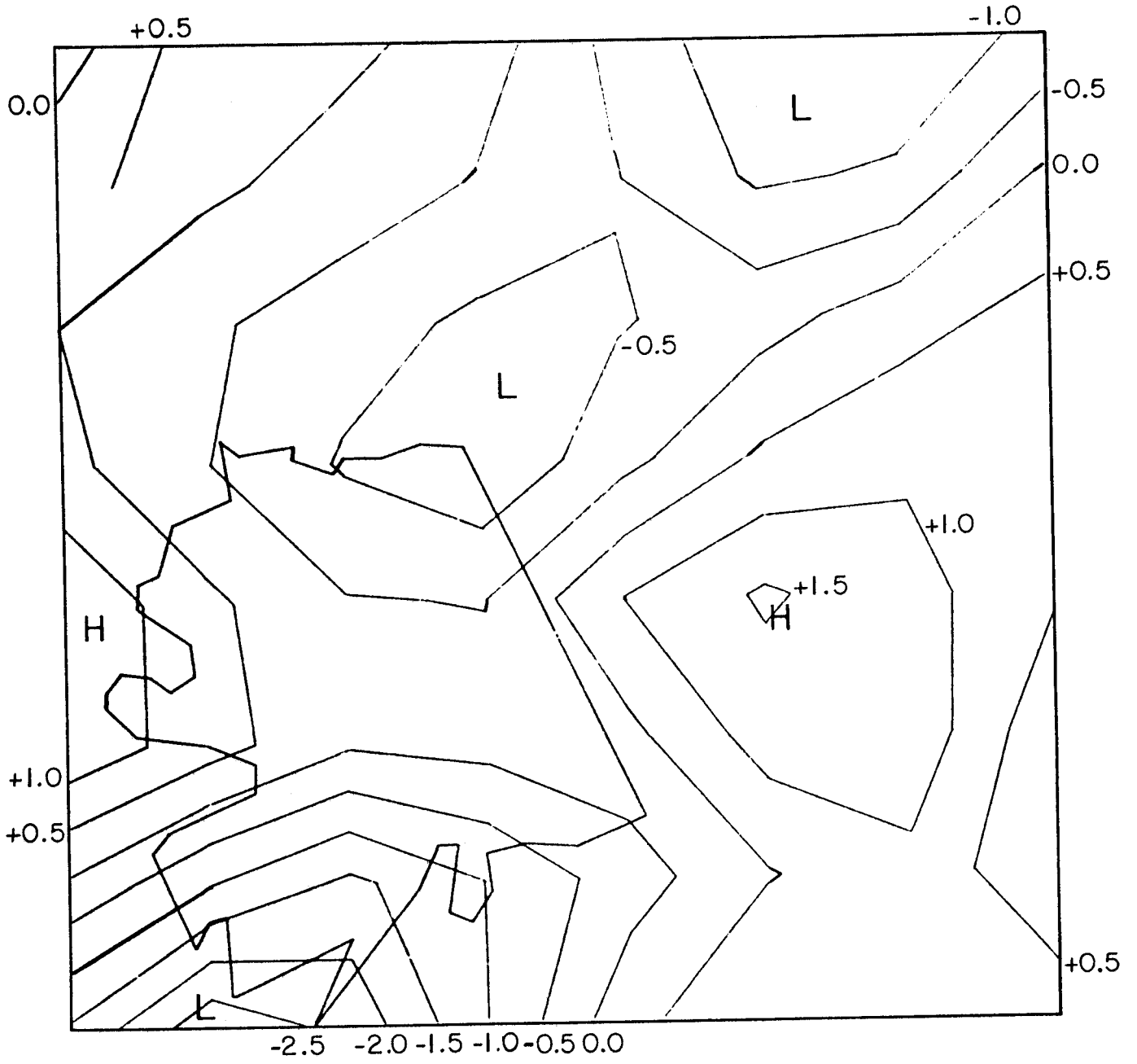

KEY DAY 13

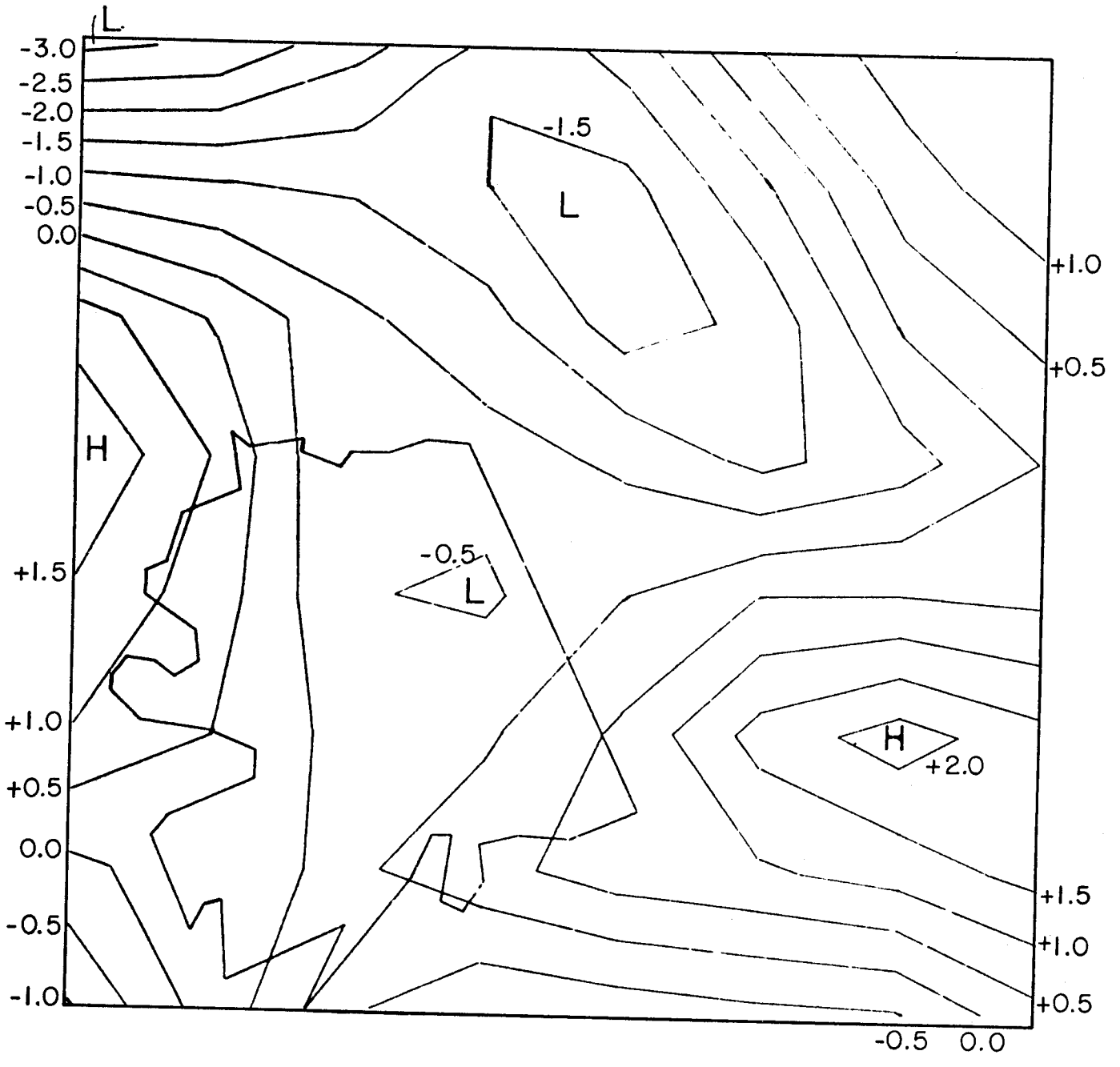
L
-3.0
-2.5
-2.0
-1.5
-1.0
-0.5
0.0
-1.5
L
+1.0
+0.5
H
+1.5
-0.5
L
+1.0
H
+2.0
+0.5
0.0
-0.5
-1.0
+1.5
+1.0
+0.5
-0.5
0.0

KEY DAY 14

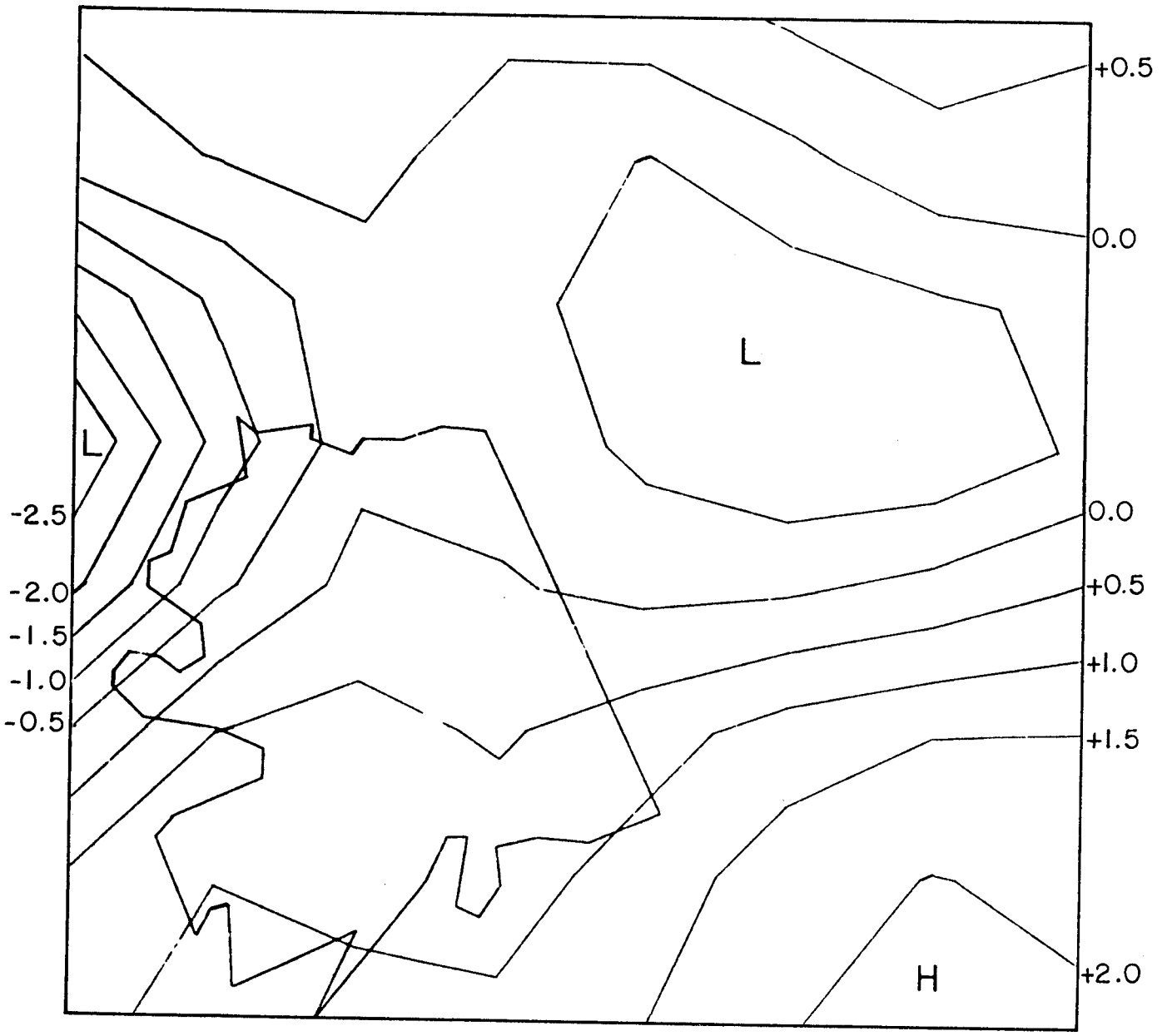

KEY DAY 15

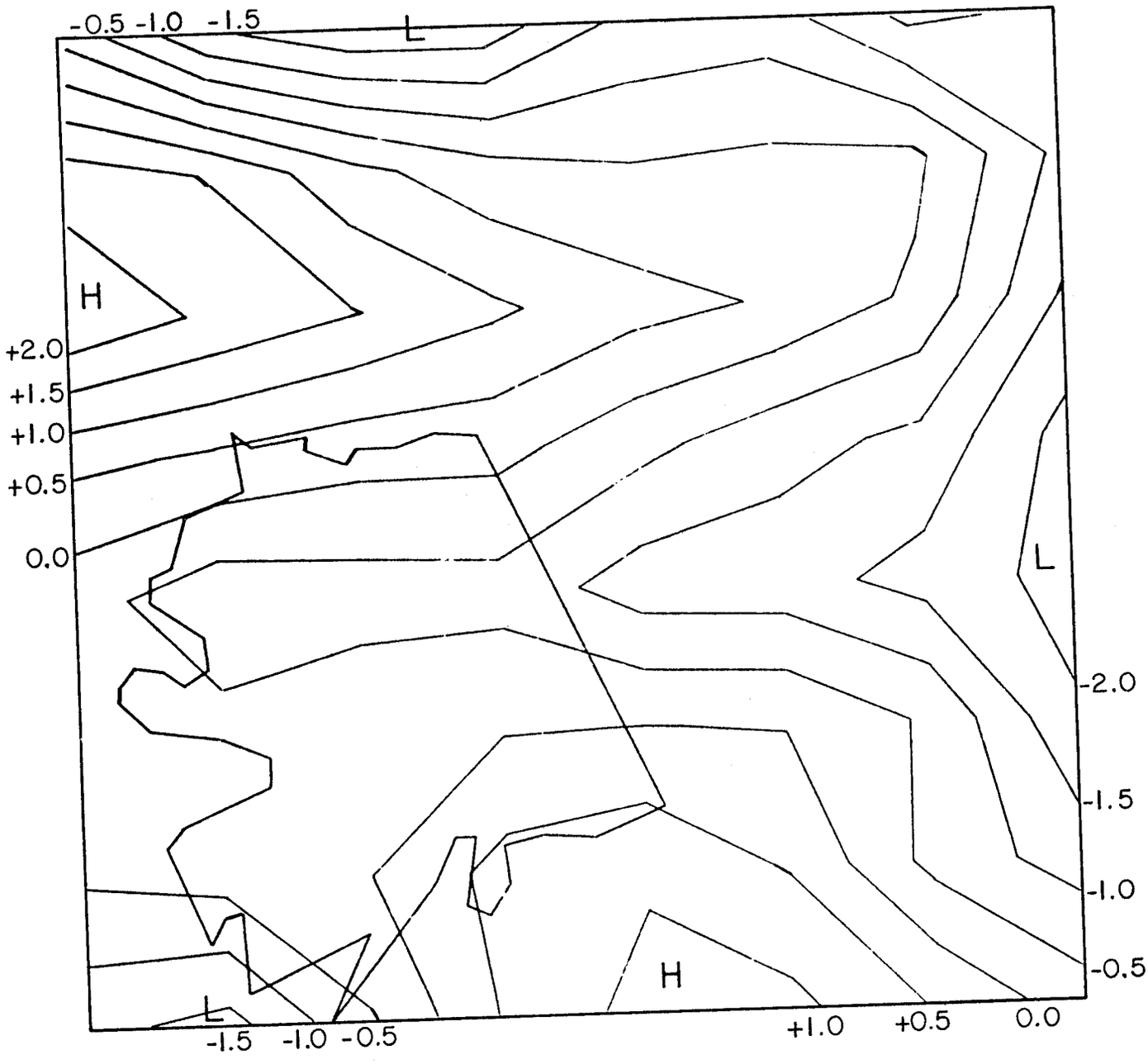

KEY DAY 16

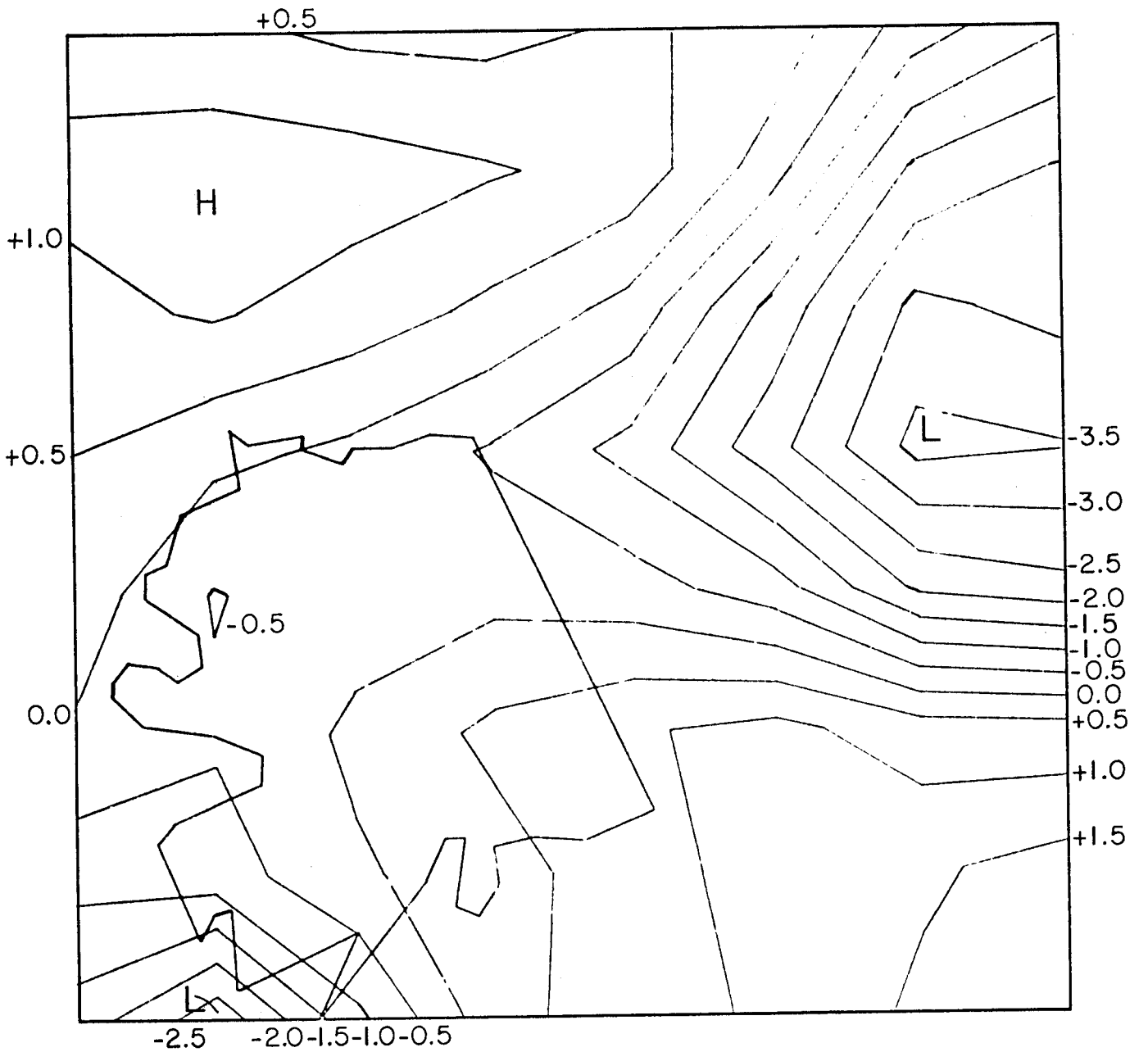

KEY DAY 17

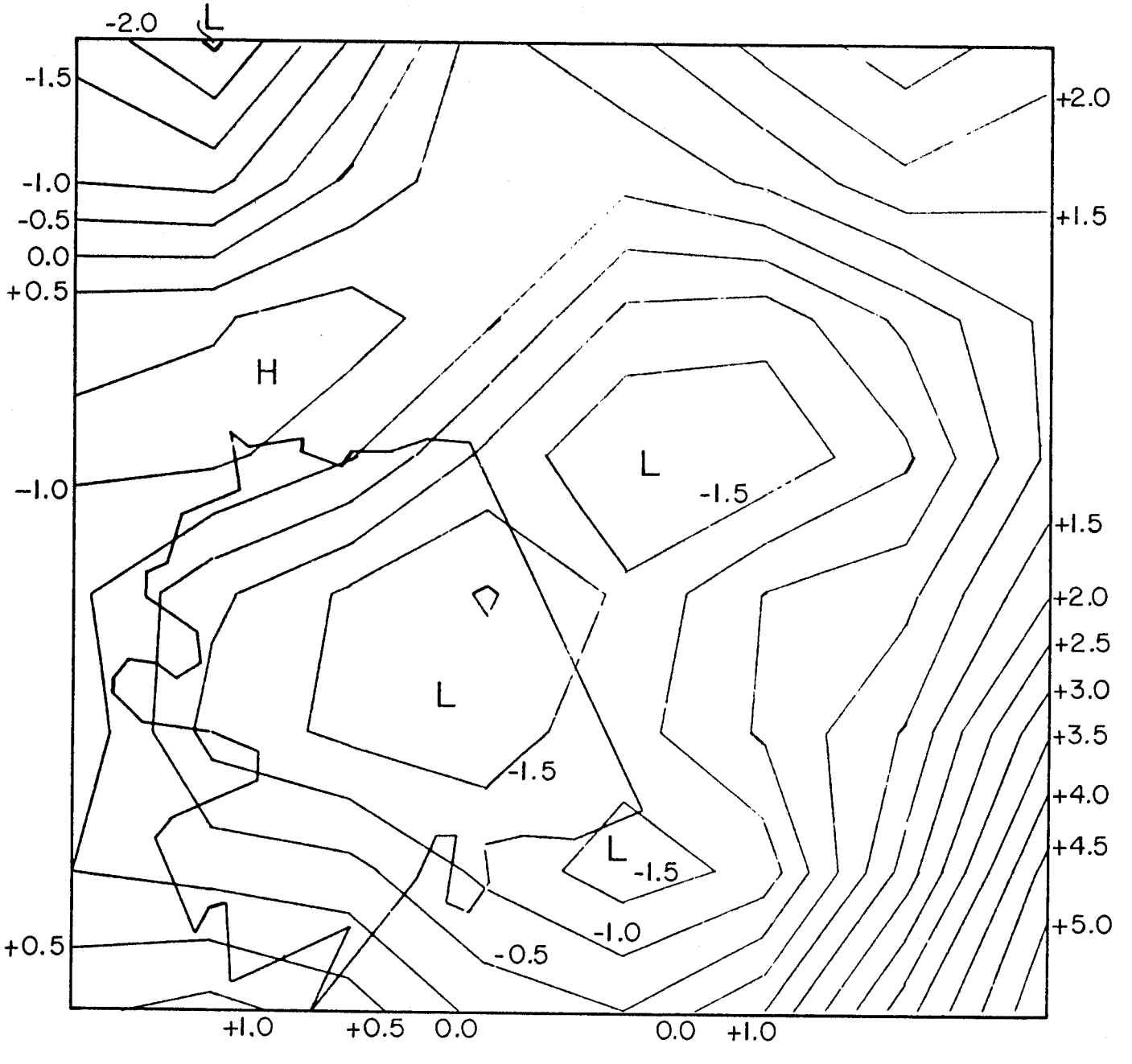
-2.0
L
-1.5
-1.0
-0.5
0.0
+0.5
H
-1.0
+0.5
+1.0
+0.5
0.0
0.0
+1.0
L
-1.5
L
-1.5
L
-1.5
-1.0
-0.5
+2.0
+1.5
+1.5
+2.0
+2.5
+3.0
+3.5
+4.0
+4.5
+5.0

KEY DAY 18

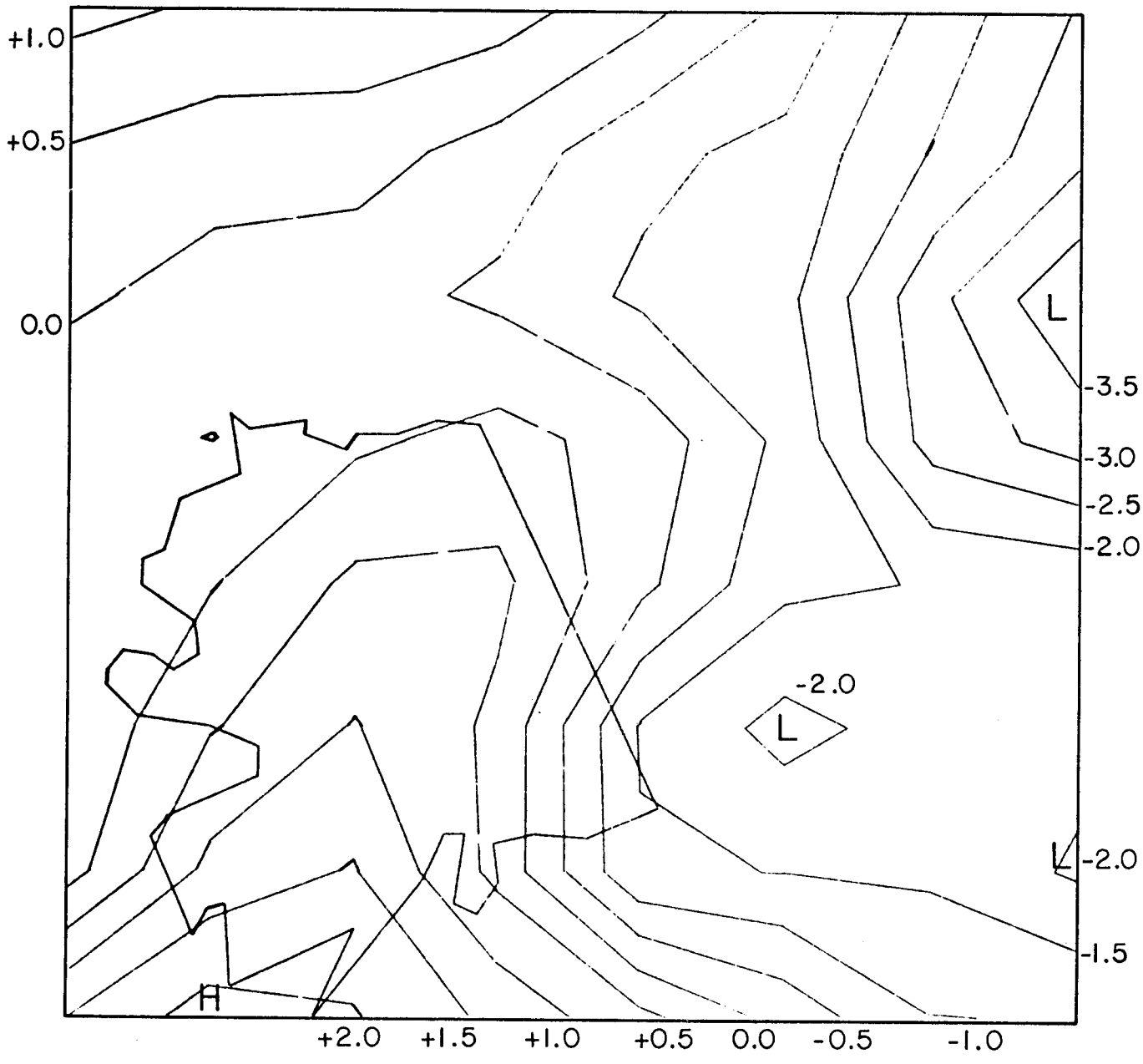

KEY DAY 19

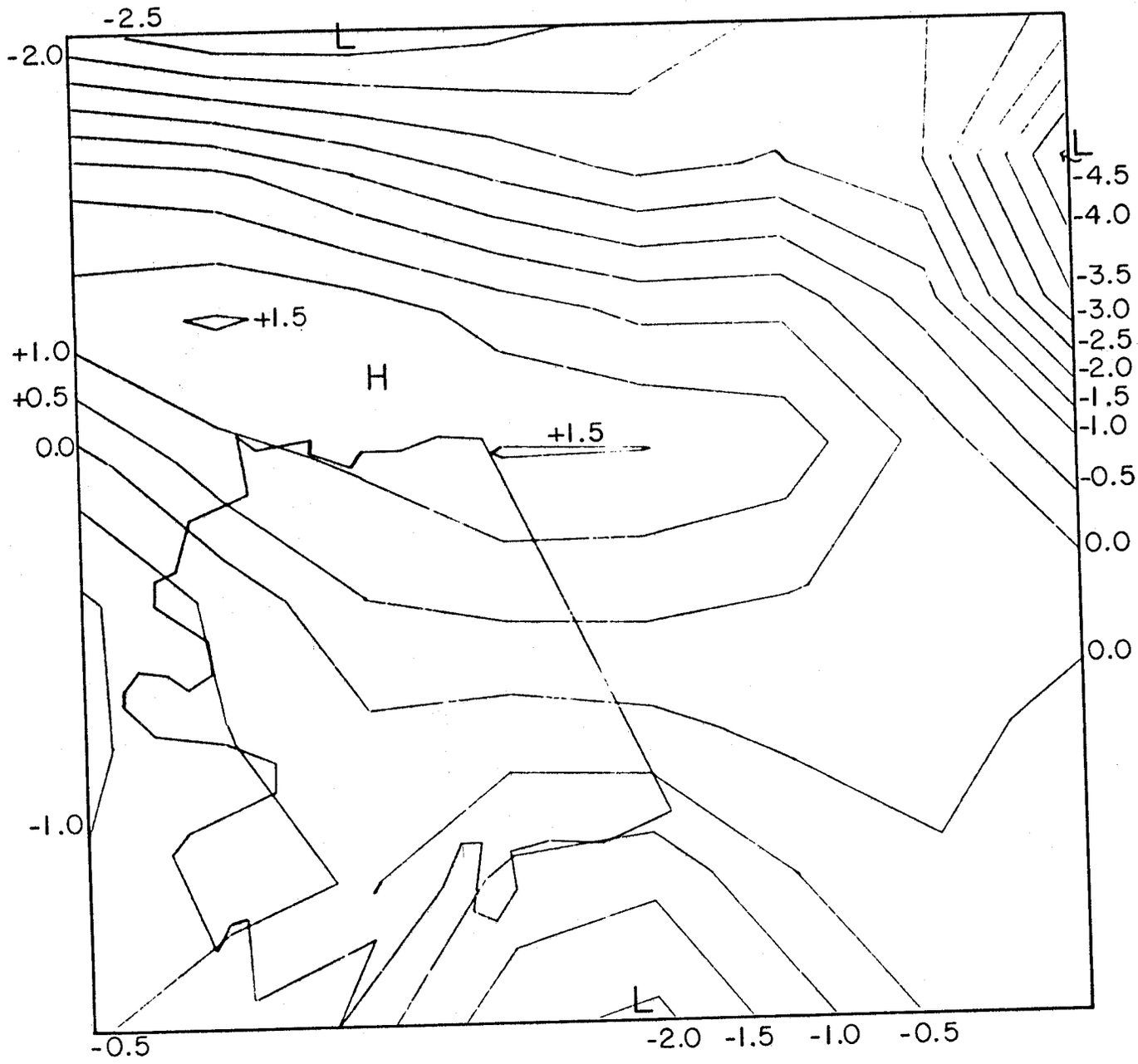
-2.5
L
-2.0
L
-4.5
-4.0
-3.5
-3.0
-2.5
-2.0
-1.5
-1.0
-0.5
0.0
0.0
+1.5
H
+1.0
+0.5
0.0
+1.5
-1.0
L
-0.5
-2.0 -1.5 -1.0 -0.5

KEY DAY 20

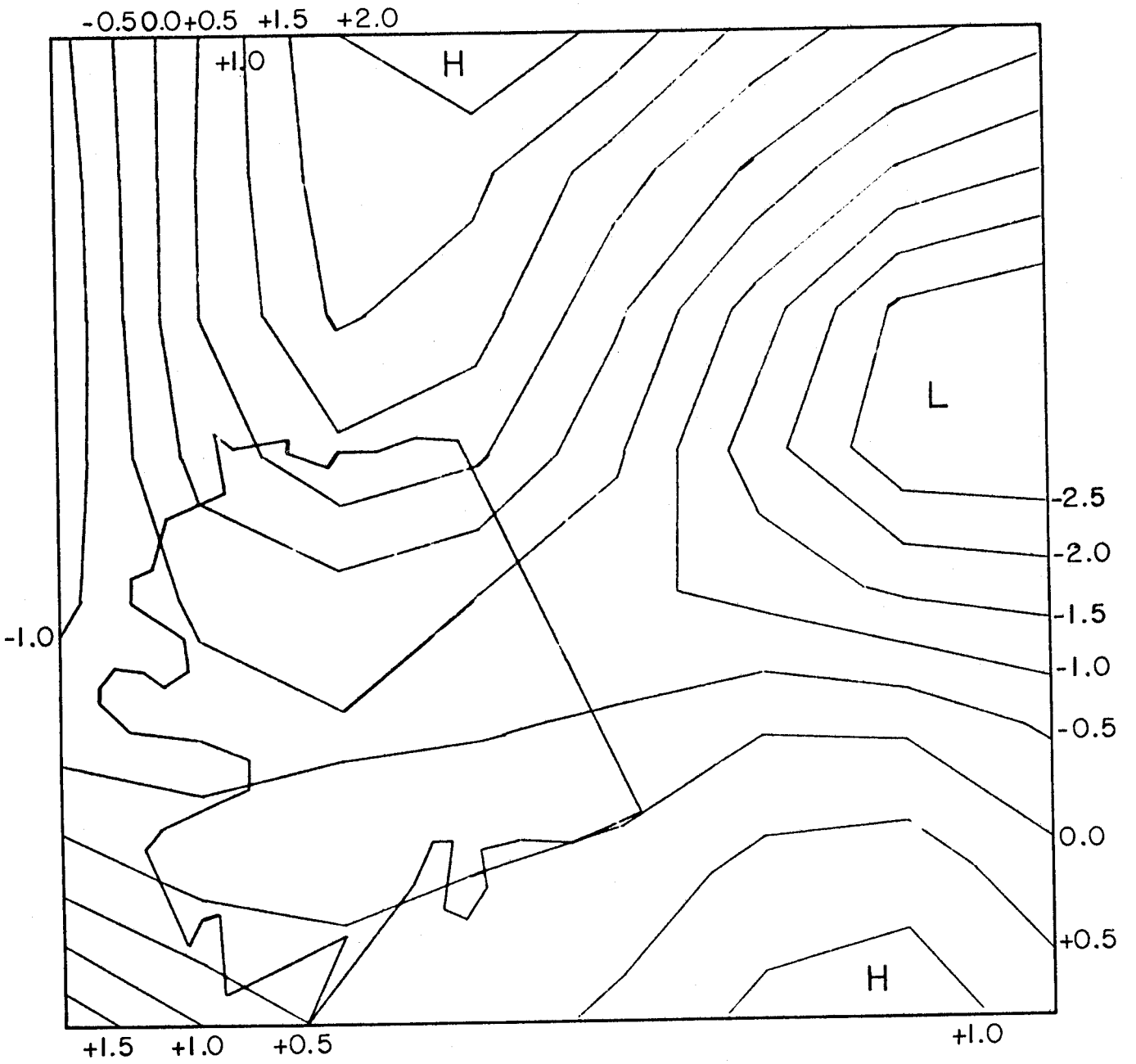

KEY DAY 21

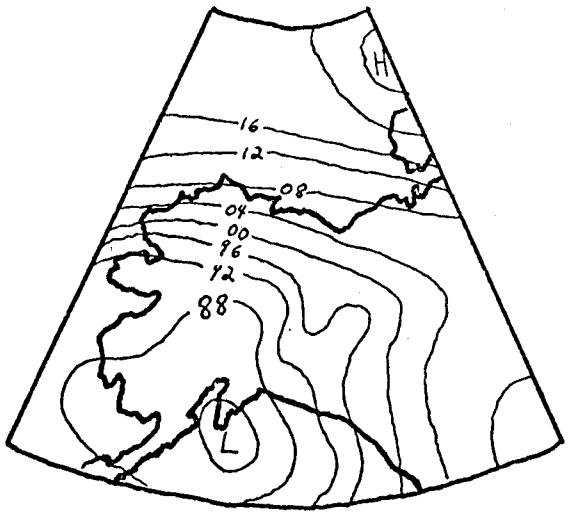

KEY DAY NUMBER I: 12/3/1969

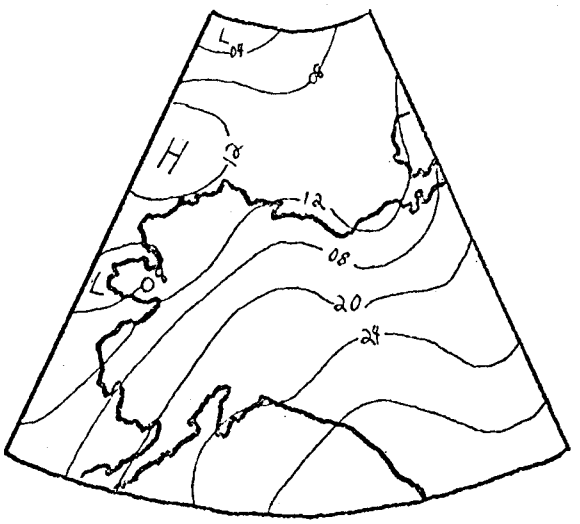

KEY DAY NUMBER II: 9/20/71

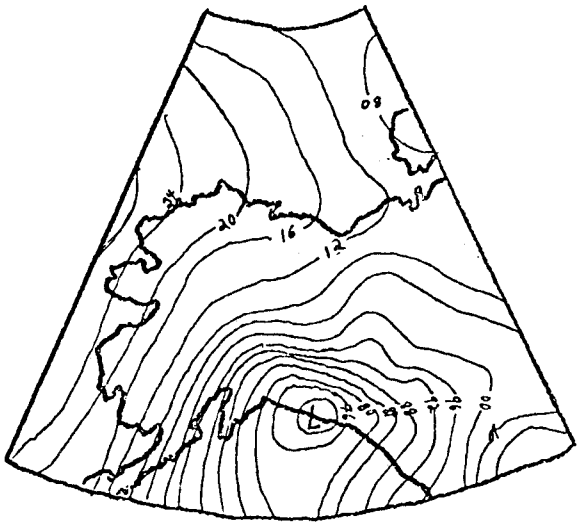

KEY DAY NUMBER III: 1/15/1972

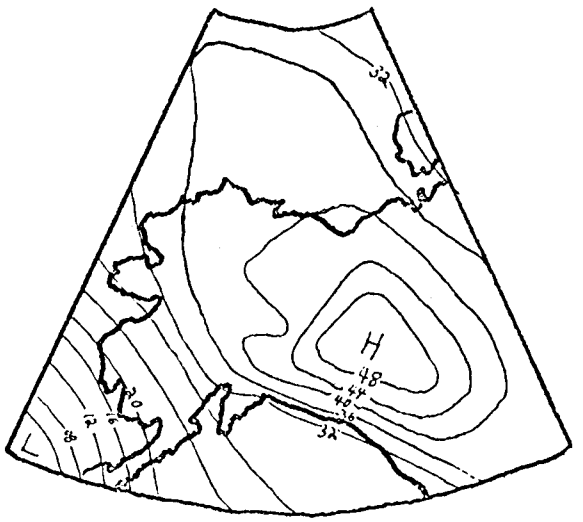

KEY DAY NUMBER IV: 1/24/1972

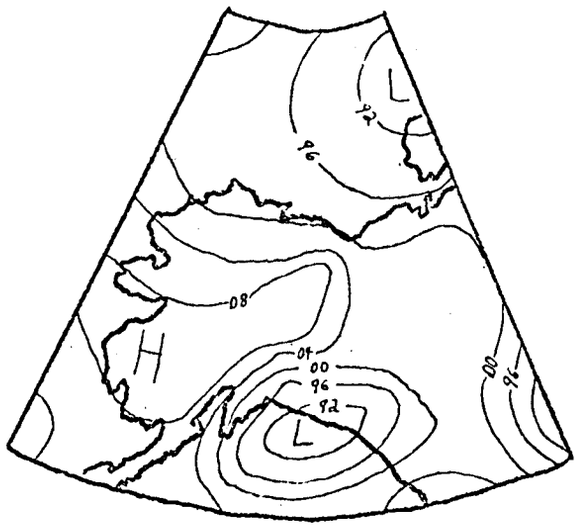

KEY DAY NUMBER V: 1/24/1973

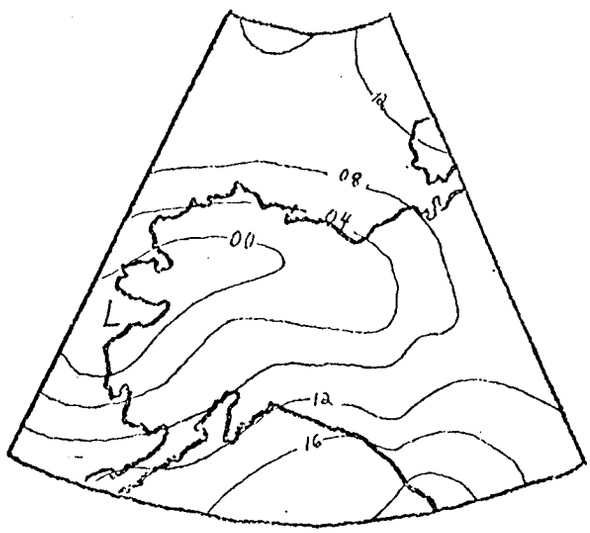

KEY DAY NUMBER VI: 8/6/1973

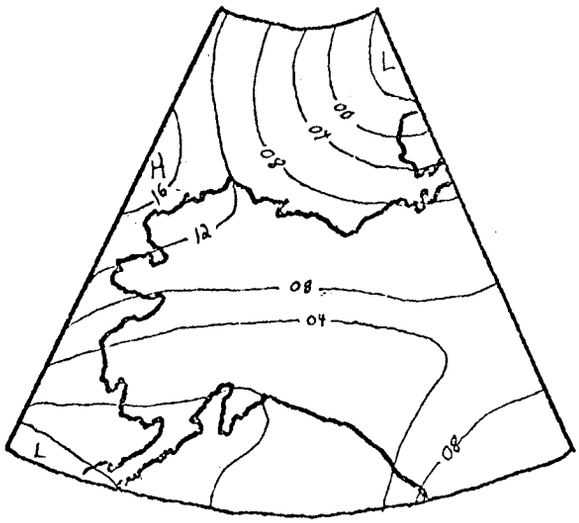

KEY DAY NUMBER VII: 9/29/1970

ANNUAL REPORT

Contract Number: 03-5-022-55

Research Unit Number: 250

Reporting Period: June 1975 to March 31, 1976

Number of Pages: 31 plus figures

MECHANICS OF ORIGIN OF PRESSURE RIDGES, SHEAR RIDGES AND HUMMOCK FIELDS IN LANDFAST ICE

Lewis H. Shapiro

and

William D. Harrison

Geophysical Institute
University of Alaska
Fairbanks, Alaska 99701

March 31, 1976

I. SUMMARY

The goal of this project is to develop an understanding of the forces and mechanisms involved in the formation of pressure ridges, shear ridges and hummock fields in the near shore zone, and the environmental parameters which cause these features to occur in particular areas. When these results are available, it may prove possible to develop procedures through which average and worst possible occurrences of heavily deformed ice at various localities can be predicted.

Some preliminary conclusions based upon the work done to date are:

(1) Forces approaching the crushing strength of sea ice may be reached during the growth of grounded pressure ridges. This has obvious implications for the design of offshore structures which are to be sited in landfast ice.

(2) The approximate coincidence of the bounding shear ridge of landfast ice with the 20m depth contour may be explainable in terms of the maximum forces which pack ice approaching the coast at low-angle can exert against the landfast ice edge.

(3) In July 1975, the landfast ice sheet was driven onshore at Barrow. During the movement, the ice sheet was driven up a rubble pile at a 20° angle, then bent back to the horizontal without losing coherence. The ability of the ice sheet to bend through these angles and still maintain continuity should be considered in the design of structures such as gravel or ice islands.

II. INTRODUCTION

A. General Nature and Scope of Study

The goal of this project is to develop an understanding of the forces and mechanisms involved in the formation of pressure ridges, shear ridges and hummock fields in the near shore zone, and the environmental parameters which cause these features to occur in particular areas. When these results are available, it may prove possible to develop procedures through which average and worst possible occurrences of heavily deformed ice at various localities can be predicted.

The problem of the formation of pressure ridges in drifting pack ice has been treated by Parmerter and Coon (1972, 1973) and this provides a useful starting point for the study of grounded ridges. However, the processes by which ridging occurs in shallow water are different in many respects from those which operate in the open sea. Ridging in pack ice normally occurs at the boundary between the thin ice in refrozen leads and the thicker pack. In the nearshore zone, however, thin ice is usually absent (except for the initial stage of ridging at the edge of the landfast ice, when thin ice may be present over the flaw lead) so that the heavy ice of the pack and landfast ice sheet are directly involved in ridging. Ridging may thus occur at the pack ice-landfast ice boundary, at the shoreline, or at stress concentrations within the landfast ice sheet itself.

The problem of determining the mechanisms and forces involved in the growth of grounded ridges is difficult because of the general lack of field observations upon which to base an analysis of the process. One objective of this project is to contribute towards filling these

data gaps. However, it is important to have as many "working hypotheses" as possible in mind when doing field work, because these serve to indicate the variables which should be measured in the field. Accordingly, simple, semi-quantitative analyses of processes which may operate during ridging are being studied. The input for these is the available data so that there is constant "feedback" between theory and observation as the study progresses.

The final product of this study is partly dependent upon the results of other projects relating to the occurrence of ridges in the landfast ice off the coast of Alaska. When this information becomes available, so that the degree of repeatability of ridging in different areas can be estimated, then the knowledge of mechanisms will be applied to attempt to develop the predictive capability noted above.

B. Specific Objectives

The objectives of this project are:

(1) To develop an understanding of the environmental parameters which localize pressure ridges, shear ridges (and related shear zones) and hummock fields within the landfast ice zone of the Arctic Coast.

(2) To gather field data regarding the mechanisms by which these structures form.

(3) To prepare a semi-quantitative model of the processes involved in the formation of these features, in order to test the validity of the concepts developed in (1) and (2) above.

(4) To use these results to develop a procedure for estimating average and worst possible occurrences of heavily deformed ice

within the landfast ice zone in terms of environmental parameters (such as water depth, bottom configuration, shoreline geography), ice thickness, and prevailing and unusual meteorological events.

C. Relevance to Problems of Petroleum Development

Within the landfast ice sheet, ridges mark the sites at which stresses in the ice reach their maximum values. As discussed below, these may approach the crushing strength of the ice and thus present the maximum hazard from ice forces to offshore structures. It can reasonably be expected that early drilling offshore from the barrier islands along the Arctic coast will occur within the area seasonally covered by landfast ice. Siting of drilling platforms to avoid potential ridging sites where possible, or to compensate for the higher forces through design changes, thus depends upon a capability to predict the severity of the deformation to be expected at any point.

Given a sufficiently long period of observation, it is probable that such predictions could be made on a statistical basis. However, it is unlikely that adequate data will be available to use this procedure prior to the start of offshore development in the Beaufort Sea shelf. Therefore, it is necessary to approach the problem through the development of an understanding of the mechanisms involved in the ridging process and the parameters which cause these to operate. The results of these studies, in combination with a lesser amount of data on occurrences of ridging, may then permit reliable predictions to be made even in the absence of long-term continuous observations.

As lines of intense deformation, ridges and hummock zones act as energy sinks in that they absorb the motion imparted to the ice by the driving forces of wind and currents. Further, once firmly grounded they tend to anchor the landfast ice sheet thus retarding its motion. Both these aspects have the potential to be used to protect a properly sited offshore structure, provided again that the location and intensity of ridging is reasonably predictable.

Finally, grounded floes of any size can serve as stress concentrations around which ridges can form. It is reasonable to expect that an offshore structure, whether a drilling platform, pier, gravel island or ice island, will have the same effect. It is therefore important to understand the mechanisms and force levels associated with ridging as an aid in the design of such structures.

III. CURRENT STATE OF KNOWLEDGE

The problem of the origin and growth of pressure ridges in drifting pack ice has been treated in the model of Parmerter and Coon (1972, 1973), but no similar analysis has been done for ridging in the near shore zone. Descriptions of grounded ridges, and some possible mechanisms of origin, have been given by Kovacs (1972), Kovacs and Mellor (1974), Shapiro (1975a,b), Weeks and Kovacs (1970) and Weeks et al. (1971). In addition, Allen (1970), Bruun and Johannesson (1971) and Zubov (1943) have considered the related problem of ice piling in shallow water or against an obstruction.

At present it is possible to identify at least some of the energy sinks in the ridging process and, as shown below, this provides the

basis for preliminary estimates of the required forces. However, in order for these estimates to be refined, there is a need for much more data regarding:

(1) Cross-sections of grounded ridges and hummock fields.

(2) Size distribution of the rubble pile.

(3) Extent of gouging of the sea floor associated with the ridging process.

(4) Mechanism by which ice is added to the ridge. That is, is the advancing pack ice edge driven directly into the rubble pile, up over it, or at some angle in between?

(5) Relationship between the relative angle of approach of the ice on opposite sides of a growing ridge to the final form of the ridge.

There is also a need to develop ideas on how the energy lost in frictional work resulting from grinding and rolling between blocks in the growing rubble pile is to be determined.

Finally, there has been no analysis done of the simple kinematics of the ridging process through which the important parameters and additional energy sinks might be identified.

IV. STUDY AREA

The site of most of the field work will be the Naval Arctic Research Laboratory at Barrow, where the University of Alaska sea-ice radar system is located. This system is operated at ranges of three or six miles and provides continuous data on the drift vector of the ice in the near shore area. It is hoped that a sufficient number of ridging events will be observed in these areas over the duration of the program to fill

some of the data gaps noted above. Additional work may also be done at other locations if warranted.

V. SOURCES, METHODS AND RATIONALE OF DATA COLLECTION

Data for this project will come from field work and study of the information from the radar system. This will include mapping, profiling and sampling of typical shear and pressure ridges within the radar field-of-view to determine the geometry and internal structure of these features. The distribution of ridges, their time of formation, and the direction and velocity of the pack ice at those times will be mapped from a combination of air photos and radar data. Finally, field measurements will be made of the thickness of the ice involved in the ridges, and the size and shape of blocks, for information regarding failure mechanisms of the ice which operated during the ridging process.

VI. RESULTS

Little progress has been made in the field aspects of this study to date. This is due to the unusual ice conditions at Barrow in the summer of 1975, during which the landfast ice never went out. Instead, numerous pans of multi-year ice, which formed a significant part of the landfast ice emplaced in the fall of 1974, remained in the area throughout the summer. Shortly after freeze-up in 1975, these moved slightly forming low ridges along their margins. However, because of the presence of these, no new ice was driven into shallow water, so that no new pressure ridges were formed. Several shear ridges have developed offshore from the zone of multi-year ice plans and some profiling of these is anticipated later in the spring.

The work in this project to date has therefore been directed toward analyses based upon available data. Some preliminary results of calculations of force-height relationships of grounded ridges, using an extension of Parmerter and Coon's (1973) geometric model of a floating ridge, are given below. In addition, the results of a first attempt to examine possible processes which occur at the offshore face of a growing ridge are also presented.

Finally, in early July 1975, strong winds drove the landfast ice sheet ashore at Barrow, forming a series of piles along the beach. A short field examination of these was conducted, and some of the observations are summarized below. A more complete report is in preparation.

A. Force-Height Relationships for Grounded Ridges

The approach used here follows closely from that used by Parmerter and Coon (1972, 1973) in their study of ridging in the open sea. Those authors identified four energy sinks as: (1) gravitational potential energy, (2) friction as the moving ice sheet is driven into the growing ridge, (3) surface energy associated with the formation of new surfaces by fracture, and (4) elastic energy stored in the ice sheet and water. These sinks are also operative in the case of grounded ridges, but their relative importance is probably somewhat different than for the case of ridging in the open sea (Shapiro, 1975a,b). Finally, an additional energy sink which needs to be considered in the case of grounded ridges is the energy lost due to gouging of the sea floor during ridge building.

The calculations completed to date include only those related to gravitational potential energy. It is anticipated that this is the dominant energy sink in the process, and will in fact be greater than

the remaining sinks by at least an order of magnitude. This tentative conclusion is based upon calculations given below, which show that the forces required to build a grounded pressure ridge range up to two orders of magnitude greater than those associated with building a ridge of equal volume in drifting pack ice.

Parmerter and Coon (1973) and Rothrock (1975) have calculated the energy loss due to friction in ridging in the open sea. The assumption is that the leading edge of the ice sheet being broken to form the ridge is pushed straight ahead into the growing debris pile. The frictional forces to be accounted for are those at the top and bottom of this ice sheet which result from the vertical forces exerted by the sail and keel. For floating ridges, the resulting frictional work is shown to be up to the same order of magnitude as the gravitational potential energy. However, in the case of grounded ridges, as shown below, the gravitational potential energy is one or two orders of magnitude greater than that of a floating ridge of comparable volume. Thus, the frictional work will be at least one order of magnitude lower than the potential energy and, to a first approximation, may be neglected. An additional reason for neglecting friction is that, based upon limited observational data, it appears that in the case of grounded ridges the advancing ice sheet is driven up the offshore side of the rubble pile rather than straight ahead into the pile. This will tend to reduce the friction to a negligible amount, because the only vertical force acting across the ice sheet will be the weight of the ice sheet itself.

Finally, note that Rothrock (1975) and Shapiro (1975a,b) have pointed out that the frictional work from blocks rubbing together in the

ERRATUM

The derivation beginning at the bottom of page 127, Volume 14 (Ice), 1976 PI Annual Reports, includes an error that invalidates the results and discussion through page 136. These should therefore be ignored.

growing pile cannot as yet be estimated. As a result, it has simply not been included in any of the calculations done to date.

Energy losses due to the formation of new fracture surfaces were accounted for by Parmerter and Coon (1973) by using data from Weeks and Kovacs (1970) which indicates that for pressure ridging in the open sea, the ice breaks to block sizes of about five times the ice thickness. This was estimated from air photos, and does not include the size distribution and volume of small fragments in the ridge. Shapiro (1975a) measured the sizes of larger blocks in a grounded ridge, and found that, for that ridge, blocks 2-3 times the ice thickness were most abundant, while the blocks in the ridges which formed at Barrow in July 1975 were only 1-1.2 times the thickness (see below). Unfortunately, it was not possible to determine the quantity of small fragments in either of these cases. Based upon these data it can be calculated that the contribution of fracture energy as an energy sink is insignificant compared to the potential energy, and it has thus been ignored for the present. Note, however, that it is still necessary to determine the volume and size distribution of smaller fragments in typical ridges, because they will increase the magnitude of this energy sink by an unknown amount.

The contribution of gouging of the sea floor and storing of strain energy in the ice sheet and water have not yet been considered.

Calculations related to the gravitational potential energy of grounded ridges follow closely from those of Parmerter and Coon (1972, 1973) for free-floating ridges. The initial geometry of the ridge is assumed to be that used by these authors, simply for purposes of comparison. The general result is independent of the geometry. The keel

of the ridge is permitted to ground, and subsequently grow upwards and laterally as ice is added.

Consider a pressure ridge of sail height H_I and keel depth D_I, such that

$$D_I = \xi H_I$$

where if ρ_i is the density of sea ice ($\rho_i = .92$ g/cm^3) and ρ_w is the density of sea water ($\rho_w = 1.03$ g/cm^3) then

$$\xi = \frac{\rho_i}{\rho_w - \rho_i}$$

for the isostatic case. In actual ridges, values of ξ from 4.4-9.3 have been measured (Francois, 1972).

The geometric model chosen for the ridge is shown in Figure 1. The dimensions are considered to be constant along the strike of the ridge. Then, the volume per unit length along the ridge is given by

$$V_I = \frac{H_I^2}{\tan\theta} + \frac{D_I^2}{\tan\phi}$$

and the length ℓ is

$$\ell = \frac{D_I}{\tan\phi} - \frac{H_I}{\tan\theta} .$$

Next, let the ridge be grounded in water of depth D_I and then continue to grow from that point. Note that there is nothing in the final results which depends upon whether the ridge was initiated over the point of grounding, or developed at sea and drifted into shallow water. It is assumed that the symmetry of the ridge is maintained as the ridge grows and, in particular, that the length ℓ is constant. The geometry

of the grounded ridge is shown in Figure 2, and the volume per unit length can be shown to be

$$V_g = \frac{H_g^2}{\tan\theta} + \frac{2D_I(H_g-H_I)}{\tan\theta} + \frac{D_I^2}{\tan\phi} . \qquad (1)$$

Then, if ρ_r is the mass density of the ridge (ρ_r = 0.7 g/cm^3) and g is the acceleration of gravity (g = 980 cm/sec^2), the total vertical force exerted by the ridge is

$$W_g = \rho_r g \frac{H_g^2}{\tan\theta} + (\rho_w-\rho_i) \frac{\rho_r}{\rho_i} g \left[\frac{2D_I(H_g-H_I)}{\tan\theta} + \frac{D_I^2}{\tan\phi}\right]$$

and the gravitational potential energy is the integral of this,

$$E_{pg} = \frac{\rho_r g}{3\tan\theta} H_g^3 + (\rho_w-\rho_i) \frac{\rho_r}{\rho_i} g \left[\frac{D_I^2}{2\tan\theta} (H_g-H_I)^2 + \frac{D_I^3}{3\tan\phi}\right]. \qquad (2)$$

The work required to produce this potential energy is FU, where F is the average force required to move the advancing ice sheet a distance U. U, in turn, is determined by considering the distance through which ice of thickness t must be moved in order to supply the ice needed to build a ridge of a given volume. Thus, for an increment of movement dU, the volume of the ridge is increased by $\frac{\rho_i}{\rho_r}$ t dU. Equating this to the derivative of the expression for the volume of a grounded ridge (Equation 1), noting that D_I is constant, and solving for dH_g gives

$$dH_g = \frac{\rho_i t}{2\rho_r} \frac{\tan\theta}{(H_g+D_I)} dU \qquad (3)$$

The increment in gravitational potential energy with ridge height is the derivative of Equation (2) with respect to H_g. Performing this, and

substituting for dH_g from Equation (3) gives an expression for normal force per unit length of ridge as a function of ridge height, depth of grounding, and initial height,

$$F_g = \frac{gt}{2(H_g+D_I)} [\rho_i H_g^2 + (\rho_w-\rho_i)D_I^2(H_g-H_I)] \qquad (4)$$

where as noted above $H_g > H_I$. This equation is plotted in Figure 3, for t = .5m for several values of D_I, with the assumption that the initial ridge was in isostatic equilibrium at the time of grounding. Some results for the case when the initial ridge was not in equilibrium are shown in Figure 4 for values of the initial keel depth/sail height ratio between 5 and 8.36 (isostatic equilibrium). In these cases, the height of the ridge at any given force is increased, because some of the initial height of the floating ridge was supported by shear stresses in the ice sheet. Note that F_g is linear in t so that the curves of Figures 3 and 4 are simply translated for values of t other than 0.5m.

It is important to emphasize that the force calculated from Equation (4) is at best a lower limit to the actual force involved in building a grounded ridge. The true value must obviously account for the energy lost in the remaining energy sinks listed above.

In Figure 3 the force-sail height curve for a floating, isostatically compensated ridge of ice of thickness t is also shown. This curve was plotted from the relationship given in Parmerter and Coon (1973),

$$F = \frac{1}{2} \rho_i \, gt \, H_{sail}$$

It is apparent from Figures 3 and 4 that the force levels associated with building a grounded ridge to some height will always be greater

than the forces associated with a free-floating ridge of equal height. This seems to be an obvious comparison to make because sail height is the most readily observable feature of any pressure ridge. However, it is of greater interest to compare the forces or gravitational potential energy between floating and grounded ridges of equal volume, because this emphasizes the effects of differences in ice distribution over equal movement intervals. For this purpose, the sail height of an isostatically compensated floating ridge, $\bar{H}_f$, of volume equal to a grounded ridge of height H_g is

$$\bar{H}_f^2 = K \left[\frac{H_g^2}{\tan\theta} + \frac{2D_I(H_g - H_I)}{\tan\theta} + \frac{D_I^2}{\tan\phi} \right]$$

where $K = \left(\frac{1}{\tan\theta} + \frac{\xi^2}{\tan\phi}\right)^{-1}$ and the remaining symbols are as defined above. Then, the potential energy difference can be shown to be

$$\Delta E = E_g - E_f = \rho_r g \left[\frac{H_g^3 - H_I^3}{3\tan\theta} + \frac{D_I^2(H_g - H_I)^2}{2\tan\theta} - \frac{K^{-1}}{3}(\bar{H}_f^3 - H_I^3) \right]$$

and the difference in forces

$$\Delta F = F_g - F_f = \frac{1}{2}\rho_i g t \left[\frac{H_g^2}{2(H_g + D_I)} - \bar{H}_f + \frac{\rho_w - \rho_i}{\rho_i} \frac{D_I^2(H_g - H_I)}{2(H_g + D_I)} \right]$$

where the subscripts g and f refer to grounded and floating ridges, respectively. Calculations from these equations show that E_g and F_g are larger than E_f and F_f by an order of magnitude even for low ridges, when ridges of equal volume are considered. Differences range up to two orders of magnitude for high ridges (i.e., > 10m) in deeper water.

The force-height relationships shown in Figure 3 show that ridges in excess of 10-15m can be produced along beaches, or in very shallow

water, at force levels which, according to Parmerter and Coon's model, are typical of pressure ridge formation in the open sea. Forces of such magnitude therefore commonly develop and there is no need to infer extraordinary events such as storms, high tides, etc., to grow large ice piles along beaches although these may, of course, be a factor. The factor which limits the ultimate height of ridges in such environments would appear instead to be the duration of movement of the ice to the beach. For example, from the integral of Equation (3), it can be calculated that for an ice thickness of .5 cm, the volume of ice necessary to build a ridge 15 meters high at a depth of one meter can be supplied by movement of the ice through a distance of 830 meters and this distance is reduced proportionally for thicker ice.

From Figure 3 it can be seen that for water depths greater than about 2m, forces in excess of those usually associated with typical wind fields (i.e., say 10^7 dynes/cm) are required to form ridges of any significant height. Yet, ridges with heights of greater than 10m often occur in water depths of up to 20m along the Alaska coast. As examples, Kovacs (1971) shows the profile of a ridge 12m high grounded in 12 meters of water, while grounded ridges 8-9 meters high in 15 meters of water, and consisting of ice about .6-.8m thick, were observed at Barrow in 1974 and 1975. From Figure 3 it can be estimated that ridges of this height imply forces approaching the crushing strength of sea ice in uniaxial compression. Forces of this magnitude obviously cannot be maintained over large areas or for long distances along the edge of a growing ridge. It is to be expected, however, that the line of contact between moving ice and a growing ridge is not continuous, but consists

instead of a series of projections from the edge of the ice sheet, separated by open water, thin ice, or rubble. Thus, the forces driving the ice are opposed by reaction forces distributed over only part of the ice edge so that high force levels are reached locally as suggested by Weeks and Kovacs (1970) and pressure ridge heights tend to be variable along strike, with local highs separated by longer, lower ridges between them.

The possibility that forces as great as the crushing strength of the ice may be developed during the formation of grounded ridges is important for engineering purposes. It is therefore of interest to attempt to calculate the extent of the area under which such high forces can be expected to occur. This can be a difficult problem, in which the result will depend upon several parameters which may be impossible to estimate for any given case. These include (1) the geometric relationships between the advancing pack ice edge and the stationary ice sheet, (2) the configuration of the fast ice edge, (3) the extent and "firmness" of grounding within the fast ice near the growing ridge, and (4) the state of the fast ice, particularly with regard to the continuity (or lack of same) of the ice (that is, how closely the landfast ice approximates a floating elastic plate). A probable upper limit to the area of high stresses can be calculated by considering the solution for the stresses in a semi-infinite half-plane loaded over a segment of length 2a along its edge (Jaeger and Cook, 1969). From this solution, along a line normal to the center of the loaded length, the force can be expected to drop to 50% of the load at the growing ridge in a distance of about 2a from the edge. Thus, for an applied force of order 10^9, this still represents a minimum force of 5×10^8 dyne/cm.

The curves of Figure 3 can also be used to suggest an explanation for one of the more puzzling aspects of landfast ice distribution, that the stable boundary of the landfast ice sheet along most of the Alaska coast tends to approximately coincide with the 20 meter depth contour. The observational data upon which the discussion below is based is provided by radar observation of the emplacement of the landfast ice at Barrow on four different occasions. In all cases, the angle between the velocity vector of the pack ice and the edge of the landfast ice sheet was less than 10°, and the ridge which marked the boundary was a shear ridge. A zone of hummocked ice up to 200 meters wide was always present on the inshore side of this ridge. Field observations indicate that the first ridges formed were generally low, although they would often increase in height later in the year as thicker pack ice was driven against them.

It should be noted that in order to ground a ridge firmly it is not sufficient for the keel simply to grow to a depth equal to the water depth. Instead, it is likely that some height greater than this must be reached in order to fix the ridge in place either by driving the keel into the sea floor or by simply increasing the area of contact at the base of the ridge to increase frictional resistance to further movement. The growth of the ridge, however, probably does not occur in small increments, but rather by adding elevation in at least integral multiples of the ice thickness. That is, it is assumed that ice is added to the ridge by the mechanism of driving the leading edge of the moving pack ice either into or up over the grounded pile.

It is readily verified that for reasonable ice thicknesses (say 50 cm or greater), a height increment of one times the ice thickness is

sufficient to drive the ridge keel into the sea floor. To show this in a semi-quantitative manner, consider the interaction of the ridge keel with the sea floor to be represented by the plane-strain problem of the indentation of a rigid, lubricated wedge into the surface of a perfectly plastic half-space. The solution to this problem is (Prager and Hodge, 1951)

$$P = 4kd\ f(\beta)$$

where P is the force required to drive the wedge a distance d into a plastic half-space of shear strength k, 2β is the apex angle of the wedge, and $f(\beta)$ describes the geometry of the plastic flow field along the sides of the wedge. Using a value of 5×10^4 dyne/cm^2 for k (i.e., 100 psf), as typical of sea-floor sediments, and taking $2\beta = 90°$ then gives

$$P \approx 1.4 \times 10^5\ d\ (\text{dyne/cm})$$

as the indentation force for a wedge. Assuming that the height of the ridge is incremented by 0.5 cm with a mass density of .7 g/cm^3, then the vertical force available to drive the ice down is about 3.4×10^4 dyne/cm^2 along the ridge profile. For any reasonable spacing of "wedges" across the keel profile (say 1m minimum), the force available to drive the keel into the sea floor is of order 10^6, sufficient to penetrate to depths of tens of centimeters if it is assumed that no work is done in consolidating the keel. This indicates that the loading postulated should be adequate to stabilize the ridge as suggested above.

In Figure X 5 the curves of the force-height relationship for an ice thickness of .5m and depths of 15, 20 and 25m are replotted from Figure

3, and the forces associated with .5m increments in height are indicated. In addition, the maximum force components normal to the face of the growing ridge are shown for angles of incidence of the pack ice between 5 and 10 degrees to the landfast ice edge. These were calculated simply by assuming that the force vector at the ridge boundary is directed parallel to the velocity vector of the moving pack and that only the component of force normal to the ridge can do work to increase the height of the ridge. The magnitude of the force vector was taken as that associated with the average value of the crushing strength which, as noted above, is indicated to be reached or approached during the building of high ridges.

From Figure 5 it is apparent that the forces required to ground a ridge in 25m of water at low angles of approach of the pack ice will not be reached. Thus, it is simply not possible to develop the type of continuous, grounded shear ridge which typically bounds the landfast in water of this depth. Conversely, this should be accomplished in depths of say 15 to 20m. Neither the data nor the model are sufficiently well-defined to permit the limit to be refined any further and the calculations must be extended to a range of ice thicknesses. However, the results presented do suggest that the proposed mechanism for formation of the boundary near the 20m depth contour may be valid.

B. A Simple Model of Some Interactions of the Offshore Face of a Growing Ridge

It is possible to construct a simple model which illustrates some of the processes involved in the interaction between the incoming pack and a growing ridge. Although the model may apply to special situa-

tions, it does not seem to represent what typically happens. It seems to merit consideration nevertheless, as an instructive first-step to a more realistic picture.

We consider the behavior of a homogeneous sheet of ice incident on a ramp, as illustrated in Figure 8.

The ramp itself may be composed of broken ice blocks, but for the purposes of the model it is assumed that its surface, up which the ice slides, remains fairly well defined, and the inclination α is constant. The ramp will increase its length ℓ in response to an increase in the forces driving the ice onto it.

In addition to this simple kinematic picture, we adopt the basic physical assumption that the interaction of the ice with the ramp, and with itself along the base of the ramp, can be described by Coulomb friction:

$$F = fW \tag{1}$$

where F is the force required to slide the ice across a surface, W is the normal force across the surface and f is a coefficient of friction. f_1 will be used to describe the interaction between the ice and the surface of the ramp; f_2, the interaction along the crack at the base of the ramp. Another physical assumption is that inertial forces can be neglected.

We first consider the forces in the plane of the ramp. It is convenient to do this in terms of the weight of ice on a unit width of ramp, w, given by

$$w = \rho g \ell t \tag{2}$$

where ρ is the ice density, t its thickness, g the acceleration of gravity, and ℓ the length of the ramp. The component of the weight perpendicular to the plane of the ramp is w $\cos\alpha$; that directed down the ramp, w $\sin\alpha$. The force $\underset{\sim}{F}_U$ per unit width driving the ice up the ramp must balance the component of weight down the ramp, together with the frictional force f_1 w $\cos\alpha$, which is directed along the line of motion of the ice on the ramp. The components of the driving force are therefore

$$F_{\perp} = w \sin\alpha + f_1 w \cos\alpha \sin\gamma' \qquad (3)$$

$$F_{\parallel} = f_1 w \cos\alpha \cos\gamma' \qquad (4)$$

where $F_{\perp}$ is the component of force normal to the base of the ramp, and $F_{\parallel}$ is that parallel to it.

If the incident angle γ of the incoming ice is sufficiently large, the ice will merely move up the ramp in the same direction as it is incident; that is, $\gamma' = \gamma$. As γ decreases, γ' also decreases, so that the parallel component of the driving force $F_{\parallel}$ (equation 4), which tends to cause shearing at the base of the ramp, becomes larger and the perpendicular component $F_{\perp}$ (equation 3), which tends to prevent shearing, becomes smaller. At some critical angle γ_c the Coulomb friction preventing shearing at the base of the ridge may be overcome. This will happen when

$$F_{\parallel} = f_2 F_{\perp},$$

(see equation 1), or using equations (3) and (4),

$$f_1 \cos\alpha \cos\gamma_c = f_2(\sin\alpha + f_1 \cos\alpha \sin\gamma_c).$$

This can be solved for the critical angle γ_c, with the result

$$\gamma_c = \cos^{-1}\left\{\frac{f_2}{f_1\sqrt{1+f_2^2}}\tan\alpha\right\} - \cos^{-1}\left\{\frac{1}{\sqrt{1+f_2^2}}\right\}$$

Because this has a solution for positive γ_c only if $\tan\alpha < \frac{f_1}{f_2}$, there will be no shearing regardless of incident angle unless this inequality is satisfied (in the limit $\tan\alpha = \frac{f_1}{f_2}$, shearing just begins as the incident angle approaches 0°).

The condition for no shearing implied in the above discussion is $F_{\shortparallel} > f_2 F_{\perp}$ which is satisfied when $\gamma > \gamma_c$. It does not follow that $F_{\shortparallel} > f_2 F_{\perp}$ when $\gamma < \gamma_c$, because $F_{\shortparallel} \leq f_2 F_{\perp}$ if Coulomb friction applies. Therefore, when $\gamma < \gamma_c$, $F_{\shortparallel} = f_2 F_{\perp}$ and $\gamma' = \gamma_c$. In other words, for $\gamma < \gamma_c$ the angle in the ramp γ' followed by the ice is γ_c, independent of γ. The situation can be summarized as follows:

$\gamma > \gamma_c$ pressure ridging and $\gamma' = \gamma$,

$\gamma = \gamma_c$ shear ridging begins

$\gamma < \gamma_c$ shear ridging and $\gamma' = \gamma_c$ independent of γ.

It is worthwhile noting that γ_c depends upon the ramp inclination α, but not its length ℓ.

Another kinematic consequence of this model is that the magnitude of the velocity discontinuity across the base of the ramp can be determined. Let v and v' be the velocity magnitudes of the incident ice and of the ice on the ramp, respectively, and let the subscripts $\perp$ and $\shortparallel$

denote components up the ramp and parallel to it, respectively. Then by conservation of mass, $v_\perp$ is continuous across the base of the ramp, or

$$\begin{aligned} v_\perp &= v \sin\gamma = v' \sin\gamma' \\ &= v' \sin \gamma_c \text{ if } \gamma < \gamma_c. \end{aligned} \tag{5}$$

On the other hand, $v_\parallel$ is not continuous at the base of the ramp if $\gamma < \gamma_c$; the magnitude of the discontinuity $\Delta v_\parallel$ is given by

$$\begin{aligned} \Delta v_\parallel &= v \cos\gamma - v'\cos\gamma_c \\ &= v \frac{\sin(\gamma_c - \gamma)}{\sin\gamma_c}, \text{ if } \gamma < \gamma_c \end{aligned} \tag{6}$$

using equation (5).

Equation (6) can be used to calculate the rate of power dissipation associated with shearing; that is, the power available for grinding up ice in the shearing process. The power P dissipated in shearing per unit width of ramp is given by

$$\begin{aligned} P &= F_\parallel \Delta v_\parallel \\ &= f_1 w \cos\alpha \cos\gamma_c v \frac{\sin(\gamma_c - \gamma)}{\sin\gamma_c} \\ &= f_1 w \cos\alpha \cot\gamma_c \sin(\gamma_c - \gamma). \end{aligned}$$

This will be a maximum for $\gamma = 0$, and it will go to zero as $\gamma \to \gamma_c$.

Two components of the stress tensor are determined at the base of the ramp. The normal component is the same as $F_\perp$ and is given by equation

(2), and the shear stress is the same as $F_{\parallel}$, which is given by equation (3). In these equations

$$\gamma' = \gamma, \quad \gamma > \gamma_c$$

$$\gamma' = \gamma_c, \quad \gamma < \gamma_c .$$

It is worth noting that in this model $F_{\parallel}$ and $F_{\perp}$ depend on the incident angle γ only when γ is greater than the critical angle γ_c. If $\gamma < \gamma_c$, $F_{\parallel}$ and $F_{\perp}$ are independent of γ.

The discussion in these paragraphs illustrates the wide range of questions that can be discussed with a very simple model, and that would have to be discussed in a more complicated, but more realistic model. In fact, the discussion of even this simple model is far from complete as presented here. A problem is that the force solution assumed [equations (3) and (4)] leads to a non-vanishing moment on the ice on the ramp. This means that the ice on the ramp, and the incoming ice, will tend to rotate, as well as translate, during the motion. A generalization of the solution to account for this is certainly possible, but it has not yet been undertaken. Another obvious question, the relation between the direction of the driving force and the resultant motion is fairly easily answered within the framework of this model, although it is not discussed here. The height of the pressure ridge as a function of the angle of the driving force to the ramp could also have been discussed.

C. Field Work in July 1975

In early July 1975, winds in excess of 20 knots drove the landfast ice adjacent to the Naval Arctic Research Laboratory ashore, forming a

continuous series of grounded ridges and ice piles 5-6 km long, and up to 5m high. Most of the ice movements at that time were recorded by the University of Alaska radar system. An 8mm movie camera was mounted on the radar tower when the ice moved, and a time-lapse motion picture of a 3.5m high ridge forming along shore was also obtained. Approximately 8 man-days of effort was devoted to field examination of the ridges. Finally, weather data for the time during which the ice moved has been obtained from the NOAA air sampling station located just northeast of NARL, and from the N.W.S. station in Barrow. As a result, a reasonably complete data set is available for this event.

Unfortunately, analysis of the data has lagged because of problems with the projection equipment needed to evaluate the radar data. This difficulty has now been resolved, and the work will begin shortly. As a result, only conclusions based upon field observations can be reported here.

At the time the movement occurred, the ice was about 1-1.2m thick, and the temperature throughout was near the melting point. Melting had progressed far enough that a lead about 10m wide was present along the shore so that the ice was no longer bonded to the beach. Further, although numerous grounded blocks were present within the landfast ice, it is likely that vertical movement of the ice sheet resulting from tides and loss of surface ice by melting had at least partly separated the floating ice from the grounded blocks. Thus, the ice sheet was relatively free of restraints to its motion under the influence of an appropriate driving wind. This situation occurs almost every year during melting and is thus a time of particular hazard to near-shore installations.

From field observations and study of the 8mm time-lapse motion picture, the general process by which the near-shore ridges developed can be outlined. First, the ice sheet was driven ashore and up the beach as a coherent unit for distances ranging up to about 15m. Then, failure occurred a few meters offshore and the incoming ice was thrust up over the stationary ice ahead. The leading edge of the advancing ice sheet fractured into blocks as it was thrust above the surface of the stationary ice, thus creating a small rubble pile just inshore from the thrust line. With additional movement, the advancing ice sheet traveled up the rubble pile, and the leading edge broke into blocks with dimensions of 1-1.2 times the ice thickness when it had advanced far enough that its weight was no longer supported. These blocks obviously increased the size of the rubble pile, so that the ice sheet could then be lifted higher before breaking. In this manner, the ridges were built to their ultimate height.

Throughout the growth process, the advancing ice sheet maintained continuity as it rode up the rubble pile. It was possible to walk on the ice sheet from flat, floating ice, up the approximately 20° slope of the offshore side of the ridges, almost to the ridge crests without observing a single crack. Undoubtedly, some were present on the lower side of the ice sheet as a result of bending, but none propagated to the surface. At the crest of the ridge tension cracks were present where the ice was beginning to fail as it lost the support of the rubble pile.

These observations thus provide useful information regarding the manner in which grounded ridges are built. In addition, the recognition that an ice sheet over 1m in thickness could be bent through a 20° angle

and still maintain coherence is of some interest in the design of offshore installation if the possibility of over-riding is to be avoided.

REFERENCES CITED

Allen, J. L., 1970, Analysis of forces in a pile-up of ice, in Ice Engineering and Avalanche Forecasting and Control, Proc. Calgary Conf., 1969, Nat'l. Res. Council of Canada, Comm. on Geotech. Res., Tech. Mem. 98, p. 49-56.

Brown, P. M. and P. Johanneson, 1971, The interaction between ice and coastal structures: Proc. 1st Int. Conf. on Port and Ocean Eng. under Arctic Conditions, Trondheim, Norway, p. 683-712.

Francois, R. E., 1972, New observations of ice topography, Trans. Amer. Geophys. Union, 53, 1018.

Jaeger, J. C. and N. G. W. Cook, 1969, Fundamentals of Rock Mechanics, Methven & Co. Ltd., London, 513 p.

Kovacs, A., 1971, On pressured sea ice, in Sea Ice, Prof. of an Int'l. Conf., Reykjavik, Iceland, May 1971, p. 276-298.

Kovacs, A. and M. Mellor, 1974, Sea ice morphology and ice as a geologic agent in the southern Beaufort Sea, in The Coast and Shelf of the Beaufort Sea, ed. J. C. Reed and J. E. Sater, AINA, p. 113-161.

Parmerter, R. R. and M.D. Coon, 1972, A model of pressure ridge formation in sea ice, J. Geophys. Res., 77, 6565-6575.

Parmerter, R. R. and M. D. Coon, 1973, Mechanical models of ridging in the Arctic sea ice cover, AIDJEX Bull. 19, 59-112.

Prager, W. and P. G. Hodge Jr., 1951, Theory of Perfectly Plastic Solids, John Wiley & Sons, New York, 264 p.

Rothrock, D. A., 1975, The energetics of the plastic deformation of pack ice by ridging, J. Geophys. Res., 80, 4514-4519.

Shapiro, L. H., 1975a, A preliminary study of the formation of landfast ice at Barrow, Alaska, winter 1973-74, U. of Alaska Geo. Inst. Rpt. UAG R-235.

Shapiro, L. H., 1975b, A preliminary study of ridging in landfast ice at Barrow, Alaska, using radar data, Proc. 3rd Int'l. Conf. on Port and Ocean Eng. under Arctic Conditions, Fairbanks, Alaska, August 1975 (in press).

Weeks, W. F. and A. Kovacs, 1970, On pressure ridges, USA CRREL draft contract report to the U.S. Coast Guard, 60 pp.

Weeks, W. F., A. Kovacs and W. D. Hibler III, 1971, Pressure ridge characteristics in the Arctic coastal environment, Proc. 1st Int'l. Conf. on Port and Ocean Eng. under Arctic Conditions, Trondheim, Norway, p. 152-183.

Zubov, N. N., 1943, Arctic Ice, Izdatel'stro Glavesevmorputi, Moscow (Trans. AD426972, NTIS, Springfield, Va.) 491 p.

VII. DISCUSSION

The purpose of the theoretical work described above is to develop a framework for the understanding of the complex processes which occur in the near-shore area. This work is not complete, nor is this report a complete description of what we have done. Nevertheless, it illustrates the approach. At the beginning we are trying to apply general ideas, such as the conservation of energy, the balance of forces and kinematic constraints, so that the results are not overly dependent upon exact details of models. For example, the force-height relationship for grounded ridges is not particularly restricted to the geometrical details assumed, nor is the proposed explanation for the boundary of the fast ice at the 20m contour. The ideas arising from the simple theory are being used as aids in interpretation of radar data and in the planning of field work.

VIII. CONCLUSION

The application of simple energy considerations to the growth of grounded pressure ridges suggests the following preliminary conditions:

(1) Gravitational potential energy is the dominant energy sink in the process of ridging in shallow water as it is in the open sea.

(2) Forces approaching the crushing strength of sea ice may be reached in the growth of high ridges in the near shore zone.

(3) The approximate coincidence of the edge of landfast ice with the 20m depth contour may possibly be explained in terms of theice drift direction at the time the bounding ridge of the landfast ice is formed.

Some of the interactions between the incoming ice and a growing pressure ridge can be examined with a simple model. Some of the results that can be obtained with a simple Coulomb friction model are: a criterion for the transition from pressure to shear ridging, the magnitude of the velocity discontinuity at the base of the shear ridge, and the power dissipated there.

The observation that, in spring, the landfast ice sheet can coherently be driven up a relatively steep slope has implications for the design of gravel or ice islands.

IX. NEEDS FOR FURTHER STUDY

The need for additional field data is apparent from the discussion in Section III. In addition, the models presented in Section VI represent only a first step in a series of models and calculations which need to be completed.

A specific task which should be accomplished as soon as possible is the preparation of a detailed map of the bathymetry within the radar field-of-view. This is needed for interpretation of data regarding movements and ridging patterns. Arrangements were made to acquire the necessary data during August of 1975, but this was not possible because, as noted above, much of the landfast ice remained in place throughout the summer. Another attempt to obtain this data will be made during August or September of this year.

X. SUMMARY OF FOURTH QUARTER OPERATIONS

During the past quarter, the activities of both principal investigators were devoted to the calculations and models presented in Section VI.

FIGURE CAPTIONS

Figure 1. Geometric model of a floating ridge (after Parmerter and Coon, 1973).

Figure 2. Geometric model of a grounded ridge.

Figure 3. Force-height curves for grounded ridges calculated from Equation 4 for $\xi = 8.36$. D indicates depth of grounding in centimeters and T is ice thickness in centimeters.

Figure 4. Force-height curves for grounded ridges calculated from Equation 4 for $\xi = 8.36$ and $\xi = 5$. D and T as in Figure 3.

Figure 5. Force-height curves for grounded ridges calculated from Equation 4 for $\xi = 8.36$. D and T as in Figure 3. See text for explanation.

Figure 6. Geometry of interaction between a moving ice sheet and the offshore side of a growing ridge.

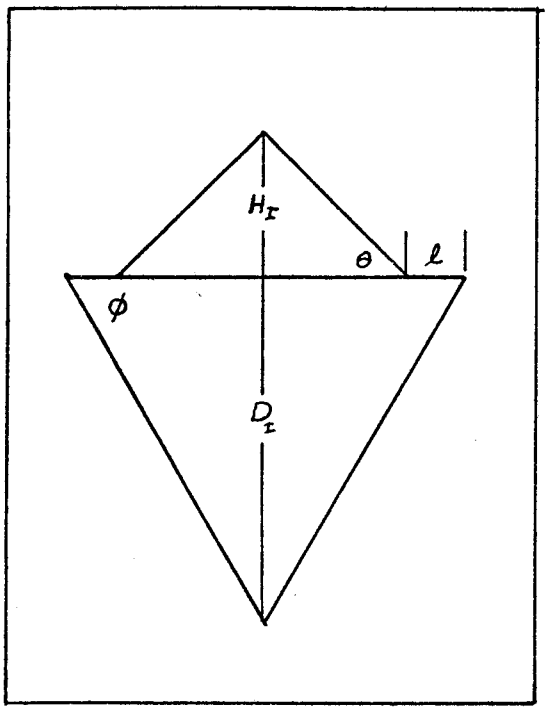

Figure 1

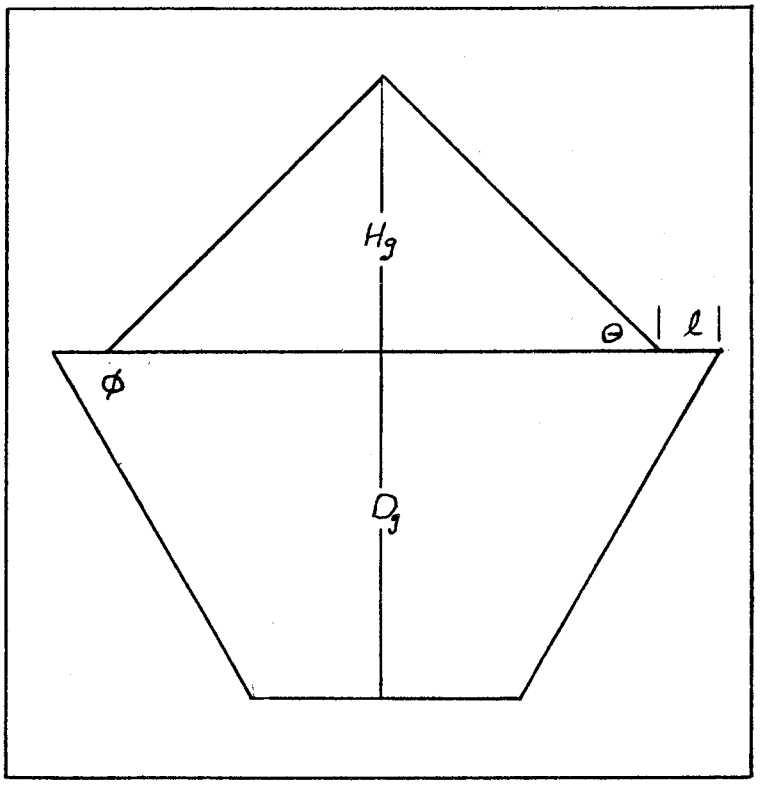

Figure 2

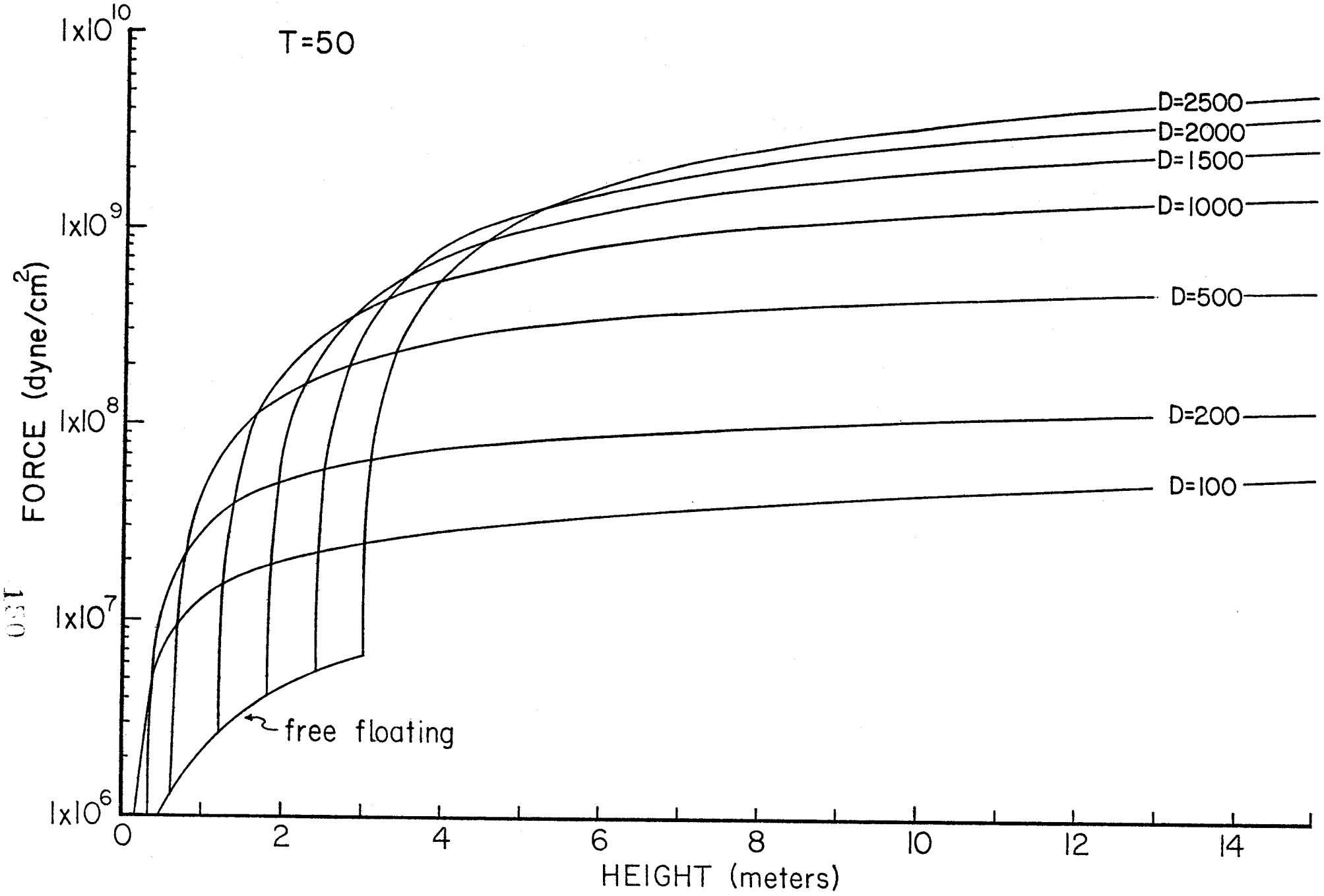
T=50
1x10^10
1x10^9
1x10^8
1x10^7
1x10^6
FORCE (dyne/cm^2)
D=2500
D=2000
D=1500
D=1000
D=500
D=200
D=100
free floating
0
2
4
6
8
10
12
14
HEIGHT (meters)

Figure 3

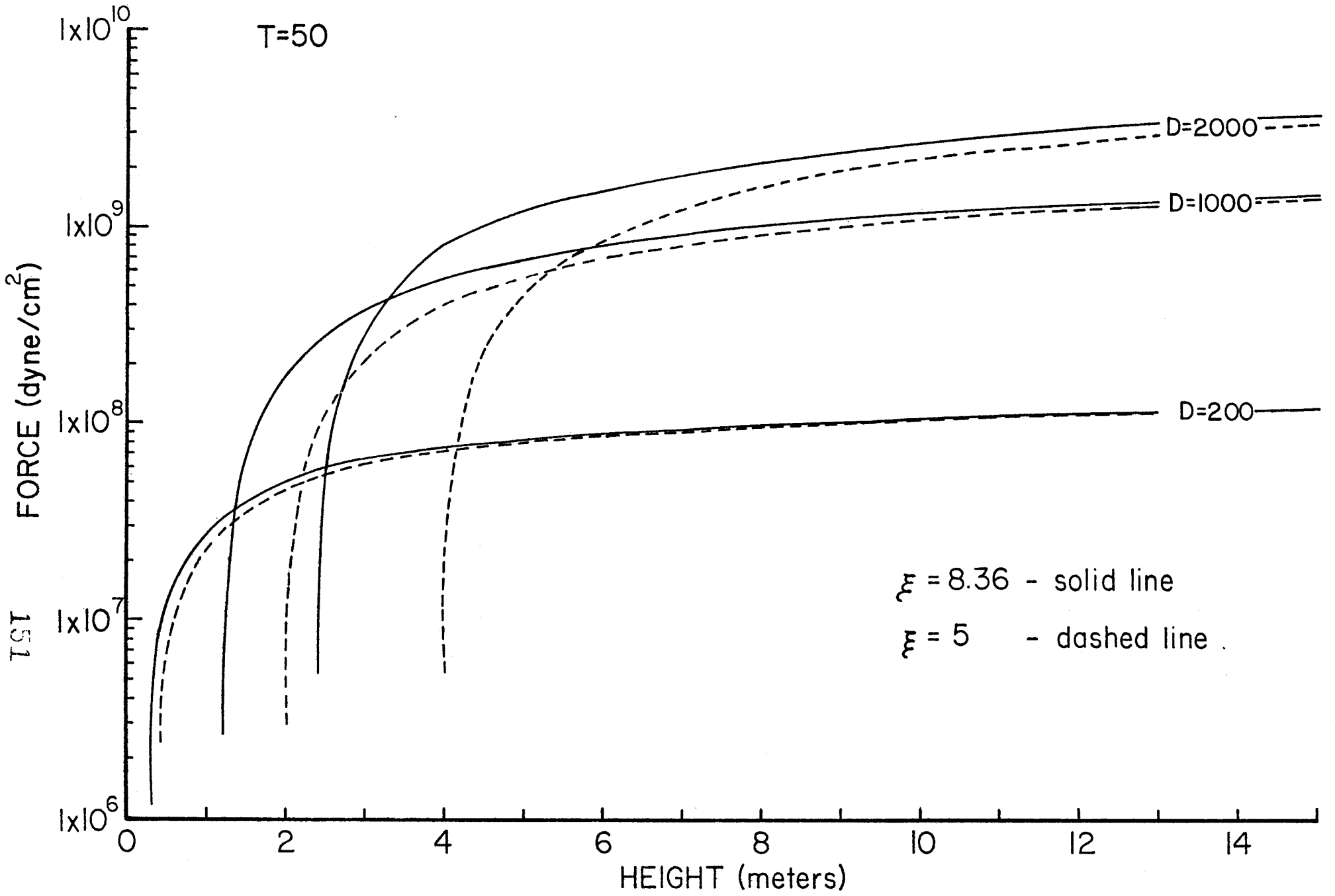
T=50
1x10^10
1x10^9
1x10^8
1x10^7
1x10^6
FORCE (dyne/cm^2)
D=2000
D=1000
D=200
ξ = 8.36 - solid line
ξ = 5 - dashed line
0
2
4
6
8
10
12
14
HEIGHT (meters)

Figure 4

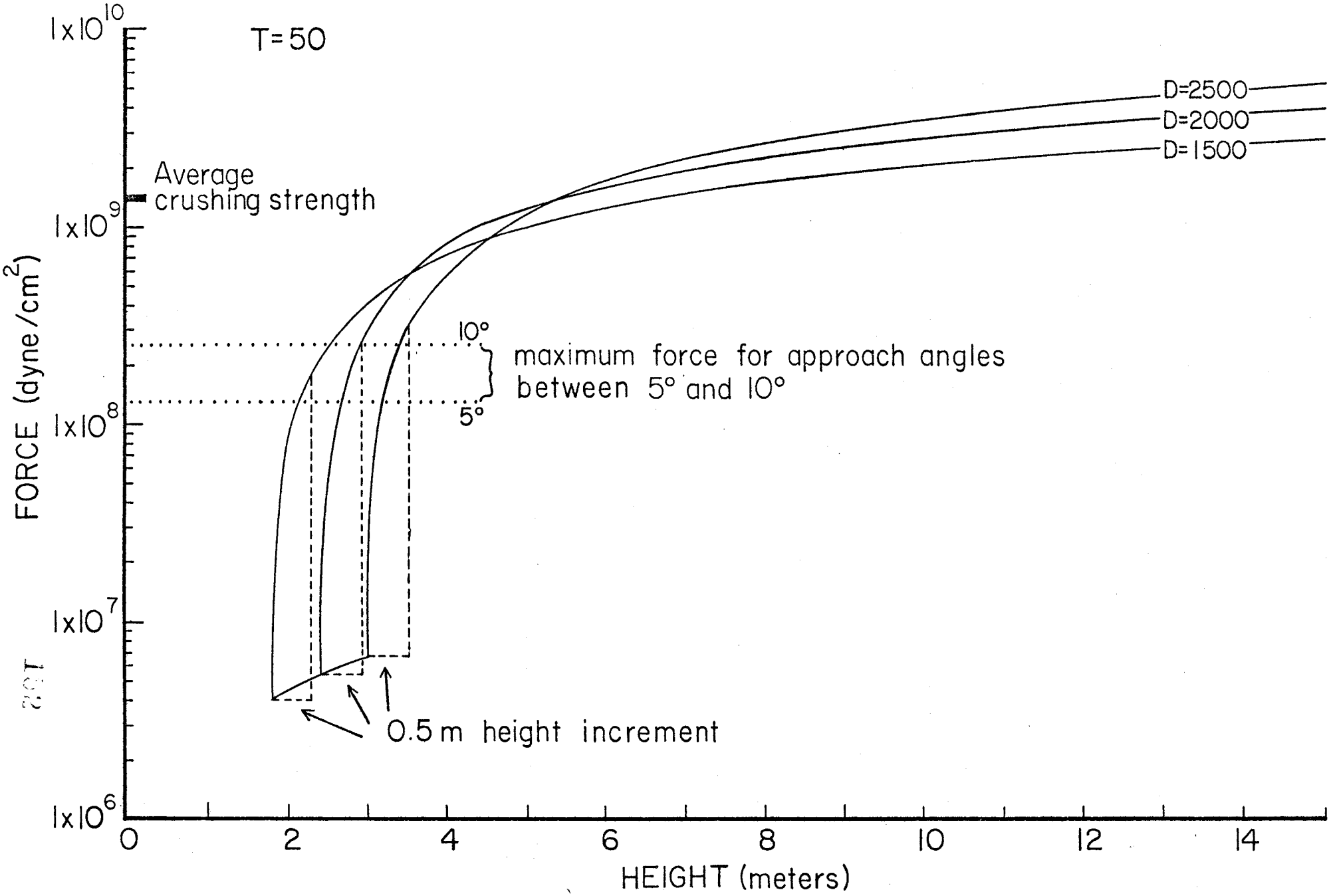
T=50
D=2500
D=2000
D=1500
Average
crushing strength
10°
5°
maximum force for approach angles
between 5° and 10°
0.5 m height increment
FORCE (dyne/cm²)
HEIGHT (meters)
1x10¹⁰
1x10⁹
1x10⁸
1x10⁷
1x10⁶
0
2
4
6
8
10
12
14

Figure 5

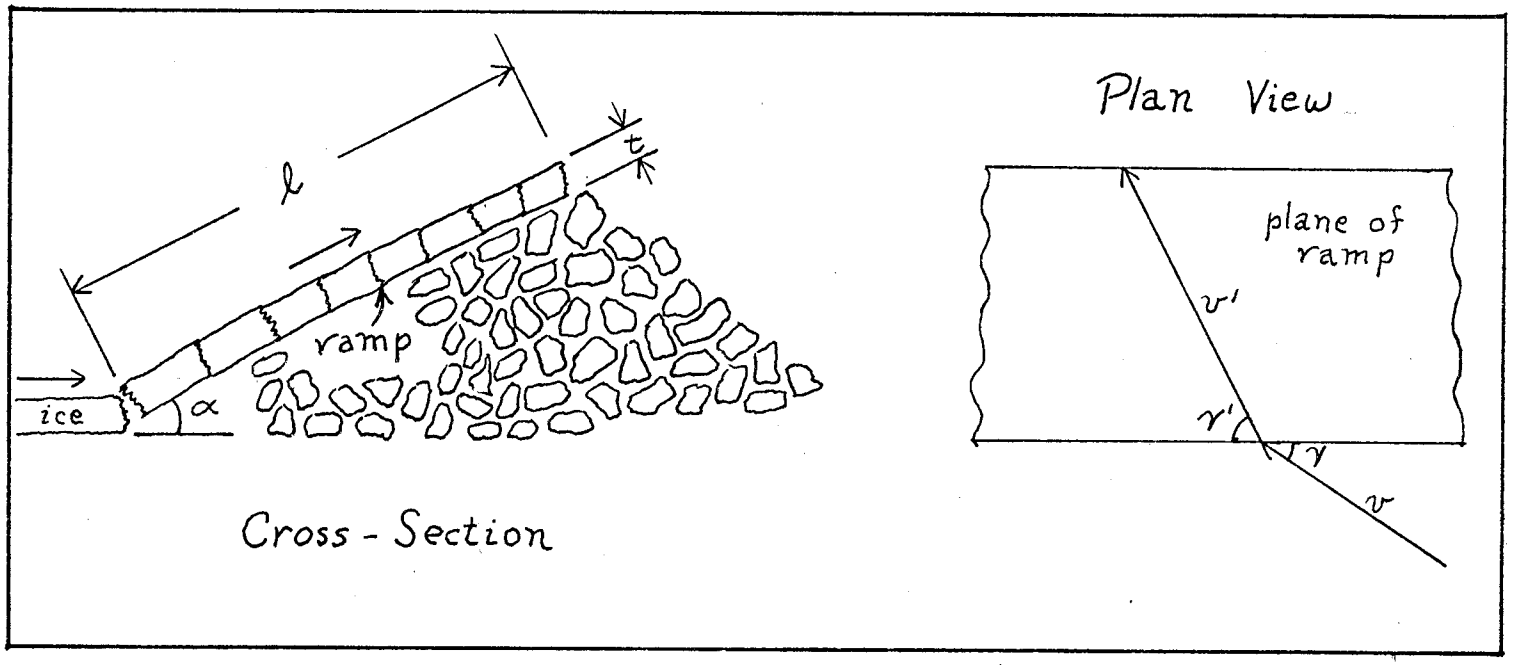

Figure 6

RU#257

OCS COORDINATION OFFICE

University of Alaska

ANNUAL REPORT

Project Title:	Morphology of Bering Near Shore Ice Conditions by Means of Satellite and Aerial Remote Sensing
Contract Number:	03-5-022-55
Task Order Number:	5
Principal Investigator:	W. J. Stringer

I. SUMMARY OF OBJECTIVES, CONCLUSIONS AND IMPLICATIONS WITH RESPECT TO OCS OIL AND GAS DEVELOPMENT

The objective of this study is to develop a comprehensive morphology of ice conditions in the near shore areas of the Bering Sea with special emphasis given to ice conditions which might be hazardous to offshore petroleum exploration and development. The preliminary conclusions are that, unlike ice conditions along the Beaufort coast, ice conditions along the Bering coast are highly variable. Dynamic ice events are possible in the near shore areas during the entire ice season except for the most highly protected bays and inlets. The nature of these events is highly dependent on location and meterological conditions. The major implication with respect to OCS oil and gas development is that except for a few highly localized areas, it is not possible to depend on a stable sheet of ice from which to conduct exploration and other petroleum-related activities. It would follow that all activities including exploration, platform construction, etc would have to be performed during the ice-free season.

II. INTRODUCTION

A. General Nature and Scope of Study

The objective of this study is to develop a comprehensive morphology of near shore ice conditions in the Bering Sea. This morphology will include a synoptic picture of the development and decay of fast ice and related features along the Bering Sea coast, and in the absence of fast ice, the nature of older ice (pack ice, hummock fields, etc.) which may occasion in the near shore areas in other seasons. Special emphasis will be given to consideration of potential hazards to offshore facilities and operations created by near shore ice dynamics. A historical perspective of near shore ice dynamics will be developed to aid in determining the statistical rate of occurrence of ice hazards.

B. Specific Objectives and Relevance to Problems of Petroleum Industry

There are two categories of results to be anticipated. The first category consists of direct data products while the second consists of indirect data products, which will be combined with studies performed by others within the study program.

a) Direct Data Products: These products would consist of a morphology of Bering Sea near shore ice and a series of maps showing persistent locations of major ice features including ice hazards within the near shore zone. These include the locations of large grounded pressure ridge systems, the location of summertime pack ice visits to the near shore areas and the drift pattern of ice islands. The morphology developed will provide a comprehensive picture of the development and decay of fast ice and the description of the sea ice cover on the Alaskan Continental Shelf.

b) Indirect Data Products: The morphology developed would yield information toward the determination of ice movement and deformation mechanism in the coastal fast ice zone. The ice type maps will indicate where to apply data relating stress-strain relationships to man-made and natural structures. The mapped pressure ridge locations and sites of ice groundings will provide data toward a predictive technique for ice-scoring processes. The assembled data will be of use to the study of the relationship of living resources to the ice environment.

III. CURRENT STATE OF KNOWLEDGE

The general description of ice in near shore areas has been investigated and reported. For instance, Zubov (1943) discusses a variety of near shore ice conditions. Most recently, Kovacs and Mellor (1973) have given a review of the state of knowledge of sea ice including near shore ice. The principal near shore ice, fast ice, has been investigated to the point that several general parameters have been accepted -- at least in terms of Beaufort Sea shore fast ice. Briefly these are:

a) Sometime around midwinter, the ice along the shoreline is no longer subject to breaking free and having open water except under the most unusual circumstances.

b) This "shorefast" ice sheet may contain many pressure ridges. Its seaward edge is defined by the most seaward grounded pressure ridge.

c) Bottom sediments appearing in the piled ice are generally taken to be evidence that a pressure ridge is grounded.

d) The most seaward grounded pressure ridge is characteristically near the 18-m contour.

e) From time to time, a floating sheet of ice can be attached to the shorefast sheet and extend many kilometers farther seaward.

f) The grounded pressure ridge system endures into summer, sometimes as late as mid-July.

It is expected that tidal effects will play a strong role in the behavior of Bering Sea near shore ice, modifying the above list.

Virtually nothing is known about the dynamic morphology of shore-fast ice; formation processes, stress-induced changes, year-to-year variations in location of its edge and locations of hummock fields, stability and other parameters related to specific weather patterns or geomorphological features.

IV. STUDY AREA

The geographic area under study by this project is the near-shore area adjacent to the ice-bound portion of the Bering Sea coast of Alaska. This coastal zone begins on the Bristol Bay shore of the Alaska Peninsula and follows the coast to the Bering Strait.

V. SOURCES, METHODS AND RATIONALE OF DATA COLLECTION

Past and historical data from all seasons will be used to compile a series of maps of the Bering Sea near shore areas denoting summer and fall pack ice behavior, fall freezing characteristics and growth and decay of the fast ice zone. Particular attention will be paid to the behavior of large free ice features, hummock fields, pressure and shear ridges, open and refrozen leads, etc. A written morphology associating ice behavior patterns with winds, storms, currents, temperature and bathymetric data will be developed. (For example see Stringer, 1974a).

1. Sampling Strategy

a) Remote Past (preERTS): Data gathered by investigators analyzing historical records will be incorporated into the morphology,

generally to confirm persistent locations of major ice features or determine patterns of extreme behavior. This investigator anticipates continuous interaction with the investigators researching historical ice records. In conjunction with them, a map of historical ice behavior can be developed. Historical information can be utilized to determine locations to give particular attention to at present. Similarly, present date may give them additional information toward interpretation of historical data.

b) Immediate Past: ERTS imagery will be combined with aerial photographic surveys performed in the past by the author and others (NASA, USGS) to perform a detailed and comprehensive study of near shore ice previous to this time. Thus maximum utilization will be made of the 2-1/2 years of ERTS data which have been collected and archived at the University of Alaska ERTS archives. It is anticipated that this data can be nearly as valuable as ERTS data taken during this study. However, the project airborne remote sensing activities are anticipated to enhance the utility of present ERTS data over past ERTS data.

c) Present: ERTS imagery combined with data from project remote sensing aircraft will be used to monitor the behavior of shore-fast and other ice within the near-shore zone. It is anticipated that interaction will take place with many other investigators studying related subjects (shear zone ice dynamics, pressure ridge modeling, sea mammal habitat, etc.) to yield additional information for incorporation into development of a coastal ice morphology.

Results

(Note: Because of our internal management requirements, no funds were expended nor was work performed until contract negotiations were final on June 30, 1975).

During the first quarter under funding Landsat coverage maps were prepared for each Landsat cycle. A near-shore ice map will be drawn for each of these data cycles. Hard copy of 1:500,000 scale prints were ordered for the earliest Landsat cycle with reasonably complete coverage for each winter season. At the end of the quarter, approximately 50% of the order arrived.

A major accomplishment during this reporting period was the preparation of the transparent map overlays to be used to transfer the Landsat data to a geographic map at 1:500,000 scale Lambert Conformal Conic Projection map prepared by the Department of Commerce. Bathymetric data from NOAA coast and Geodetic Survey Nautical Charts at varying scale around 1:500,000 was transfered to these overlays by means of pantograph. These overlays are the map base for the maps produced by this OCS project. Bathymetric data is correlated with its conditions.

During the first reporting period under funding we moved into larger quarters and took delivery of our drafting tabl-, map cases and other equipment described in the University of Alaska OCS 5 and 8 budgets.

During the second quarter under funding using Landsat band 7 hard copy produced at 1:500,000 scale, preliminary Bering Sea near shore ice maps were compiled for late winter (Feb.-March) 1973). These maps were reproduced at half scale for reporting convenience. Particular care was taken to locate the ice features relative to geographic coordinates and

bathymetric 10-fathom contours. Half-scale reproductions of these maps were reproduced with annotation discussing the features delineated as part of the quarterly report for the period ending, Dec. 31, 1975. It should be stressed that these maps are not final products, but represent an initial stage of interpretation of each year's ice conditons. For instance, even though large ridge systems can be identified, many others are shown here as boundaries between distinctive ice categories. Analysis of later Landsat images during the melt season will determine to a greater extent the complete identification of these and other features.

During the third quarter under funding, late winter near-shore Bearing Sea ice maps for 1974 and 1975 were prepared. Half scale reproductions of these maps with annotation appear here as part of Section X, Summary of 4th quarter operations.

VII. DISCUSSION OF PRELIMINARY RESULTS

Although analysis of data is not yet complete, some general results in terms of near shore ice morphology can be described. It should be emphasized that these results are general and preliminary and of a verbal descriptive nature. The final morphology will utilize annotated maps with reference to specific landsat images as examples.

This description will start on the north side of the Alaska Peninsula and proceed along the coast to the vicinity of Nome, and the Seward Peninsula.

1) North side of Alaska Peninsula: (south side of Bristol Bay). The ice in Bristol Bay has been observed to have been driven toward

this shore from the north. The result is a series of shear ridges parallel to the coast. During the events observed, the location of the ridges (apparently grounded) appears to be related to a uniform distance from shore and not to water depth. However, these observations are based on single episodes and should not be taken to represent the cumulative result of an entire season of ridge building. In the absence of these ridge-building events, ice stationary with respect to the shore is located only within well-protected areas and in some locations as a narrow apron close to the shore.

2) North Side of Bristol Bay: (Kvichak River to Cape Pierce) It appears that typically ice is pulled away from this coast and that new ice is being constantly formed between the ice edge and the coast. Ice stationary with respect to the coast is found generally in well-protected areas and shoals. At times aprons of ice extend seaward several km from moderately well protected areas but eventually these areas break up and drift off during times when the ice pack has been pulled away from the shore.

3) Kuskokwim Bay: In many respects the ice behavior here is similar to that on the north side of Bristol Bay. However, the mouth of the Kuskokwim River and extensive mudflats to the west present physiographic features so significantly dissimilar to the former area that they need separate descriptions. Often a tongue of green water extends well into the Kuskokwim River. This could well be the effect of the very large tides in this area. In addition to this feature there are often extensive ice sheets apparently stranded on the very large shoals and mudflats in this area.

4) Western Bering Coast: (Cape Avinof to North Yukon Delta) There are extensive mudflats along this coast which often have ice stranded on them. There is good evidence that the edge of this stranded ice advances and receeds frequently but at all times the ice edge is not located near the 10-fathom contour except where this contour is close to shore just opposite Nelson Island. Ice which appears to be relatively permanent is only found in well-protected bays and inlets. Considerable shearing ice motions often take place along this shore.

5) Norton Sound: (North Yukon Delta to Nome) In many respects ice behavior in Norton Sound appears similar to that in Bristol Bay: The ice appears to be more-or-less continuously moving out of the sound toward the Bering Sea. New ice is constantly being formed in the leads and polynyas caused by this motion. Along the coast of the inner sound the ice edge is located far shoreward of the 10-fathom contour. Thus, the correlation appears to be stronger between protective geomorphological shoreline structure and ice edge than bottom contour here. However, in the Nome area the sheet of stationary ice extends at times beyond the 10-fathom contour and is bounded by apparently grounded shear ridges.

VII. CONCLUSIONS FROM PRELIMINARY RESULTS

The Bering coast exhibits a variety of near shore ice condition which are influenced by two major conditons not experienced along the Beaufort coast. These are: significant tidal fluctuations and 2) open sea conditons adjacent to the ice pack. The tidal fluctuations

can cause the break-up and rafting away of grounded ice --- thus cleansing the coastal area of all but the most tenacious ice. Open sea conditons adjacent to the ice pack insure that the ice pack will be free to move away from shore under favorable wind and current conditons with the result that considerable amounts of new ice will be generated adjacent to those coastal areas. At the same time, this seaward ice movement can generate significant ice hazards in other areas in the form of massive shear ridges in the locations where this ice motion is forced along coastal areas. This latter effect has been noted in several locations --- the best example being the Bristol Bay coast of the Alaska Peninsula.

IX. NEEDS FOR FURTHER STUDY

Analysis of coastal zone ice conditions has brought attention to several areas along the Bering coast which may possess unusually severe ice conditions and others which may exhibit particularly stable qualities. There is a definite need to perform a detailed aerial photographic reconnaissance of these areas in late winter and early spring to confirm these results and allow the assignment of numerical values to height of shear ridges, etc.

X. SUMMARY OF 4th QUARTER OPERATIONS

During this Quarter

The following set of ice maps were prepared from the earliest available Landsat sequence for 1974 and 1975. Major ice features and the shore have been delineated and the 10-fathom contour shown for correlation of depth to major ice features. As little inference as possible has been made at this stage. Many features have been designated

as "boundaries" which will very likely be identified as pressure and shear ridges after examination of subsequent data. Similarly, "shore-fast" ice has not been delineated but ice contiguous with the shore has been identified. Just which of this "contiguous" ice is "shore-fast" will be determined on the basis of subsequent Landsat scenes.

These maps are reproductions of working products and are, therefore, somewhat complicated. Later maps, based on interpretation of these and later imagery, will be considerably simpler. The original maps are produced at a scale of 1:500,000 and have been reduced here to half-scale for reporting convenience.

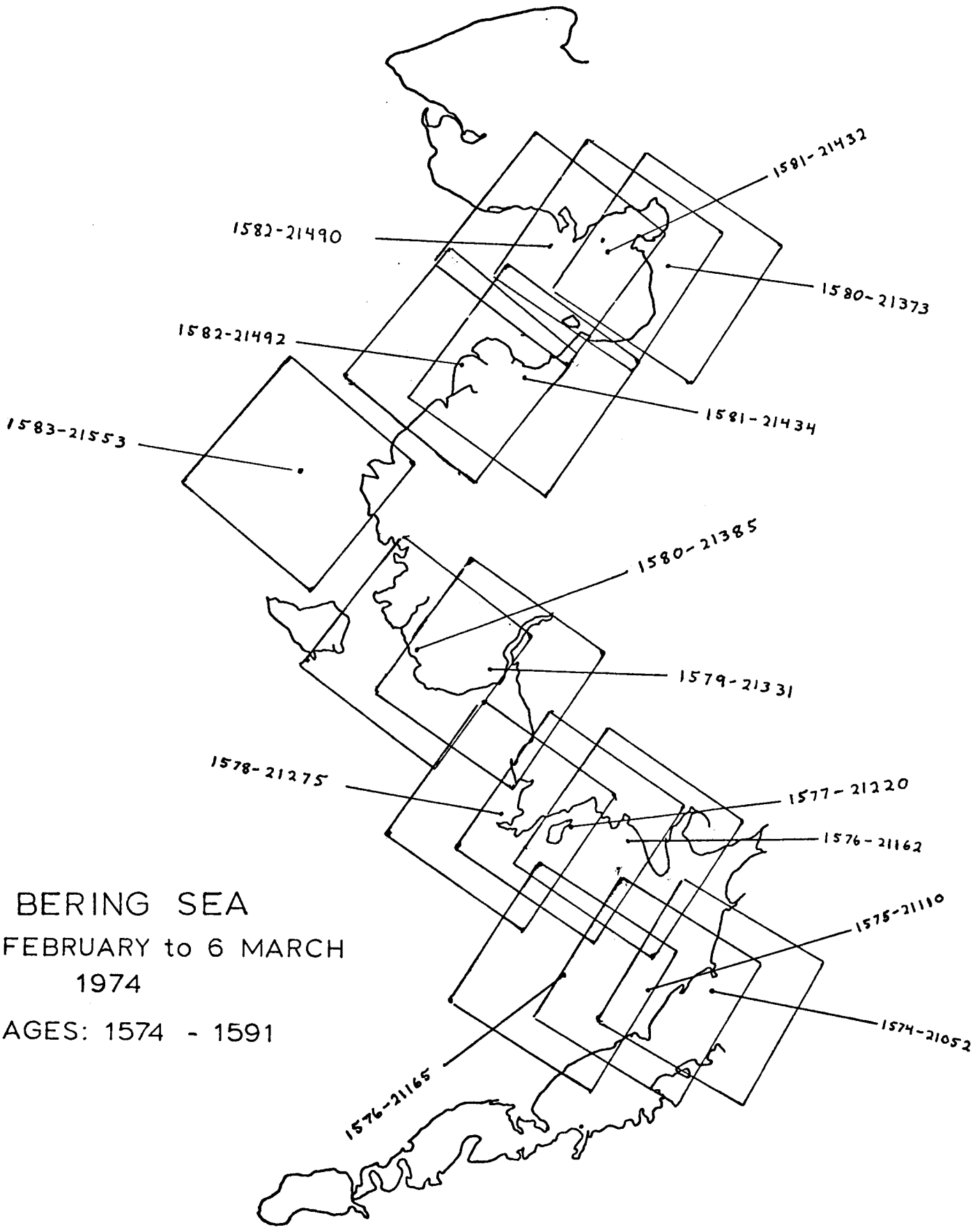

BERING SEA

17 FEBRUARY to 6 MARCH

1974

IMAGES: 1574 - 1591

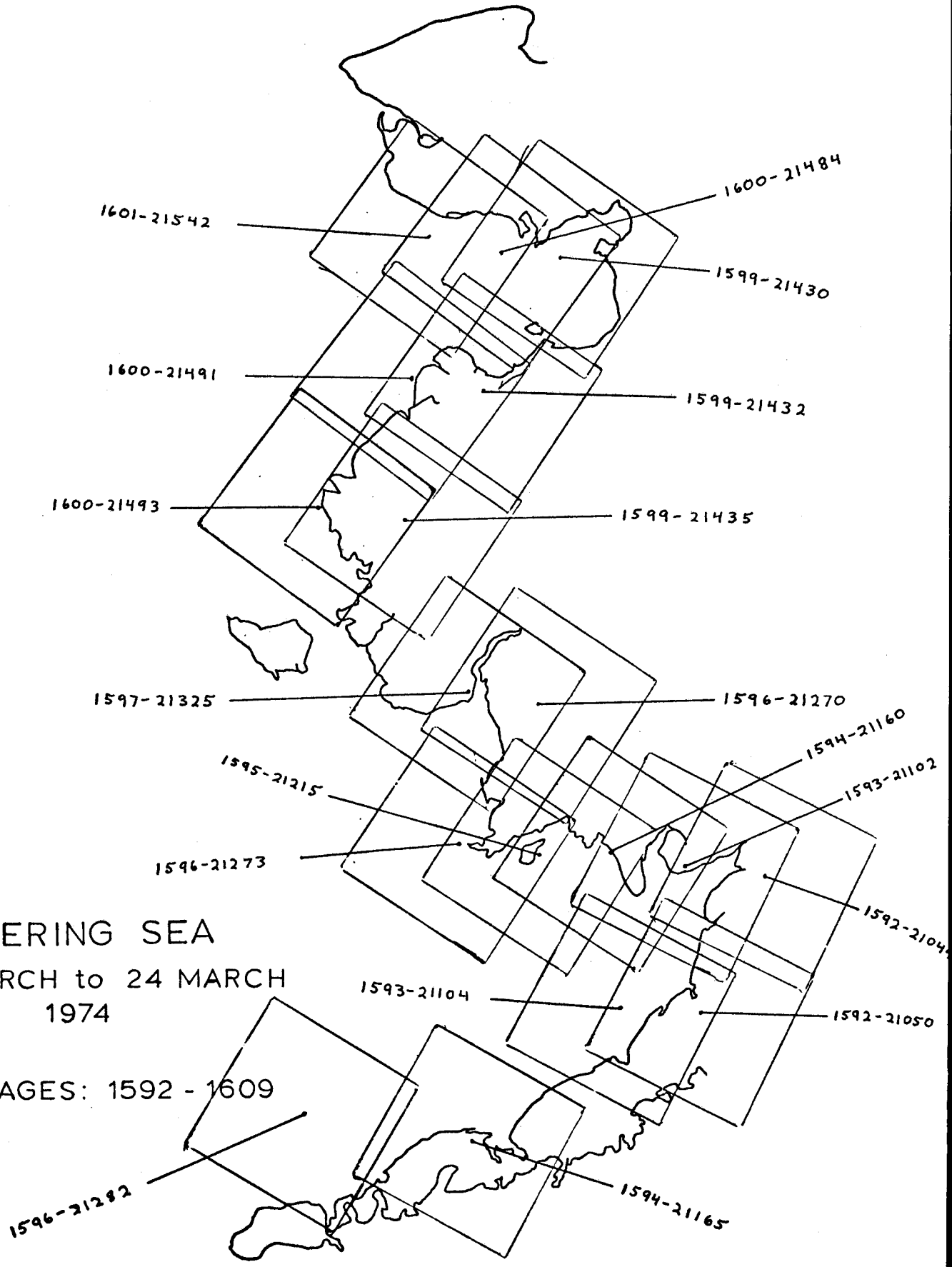

BERING SEA

7 MARCH to 24 MARCH
1974

IMAGES: 1592 - 1609

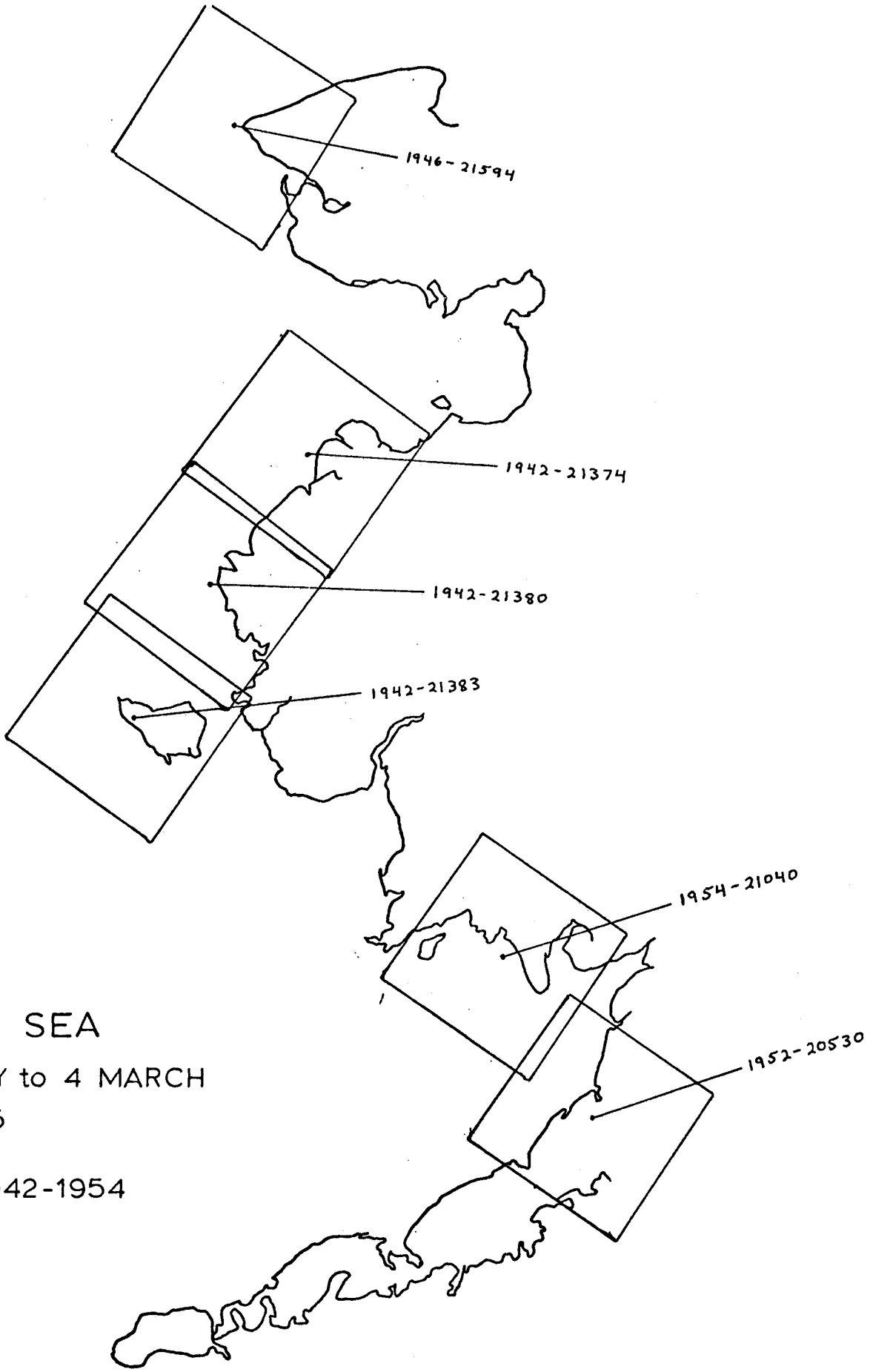

BERING SEA

20 FEBRUARY to 4 MARCH
1975

IMAGES: 1942-1954

SYMBOLS AND DEFINITIONS

B	Boundary between apparently different ice types.
BN	Broken sheet of new ice.
BPN	Pans in broken matrix of new ice.
BPY	Pans in broken matrix of young ice.
BY	Broken sheet of young ice.
C	Stationary ice - ice which is contiguous with the shore.
CF	Fragmented or broken contiguous ice.
F	Ice floe.
FY(B)	First year ice (broken or fragmented).
G.	Grounded ice floe or stranded ice.
H	Hummocked ice - sea ice piled haphazardly one piece over another to form an uneven surface.
IY	Young ice.
L	A lead, usually open, but may be too narrow to determine if it is open or not.
N	Newly refrozen lead or polyna - a lead or polyna composed of dark ice, not yet fractured and milky, or covered with snow, thin enough to allow light to pass through to the water.
O	Old refrozen lead - a lead old enough to have either turned milky with cracks or been covered by snow; thick enough to reflect most of the incident sunlight and thus appear gray to white.
P	Partially refrozen lead, usually some dark ice with open water.
PN	Pans in matrix of new ice.
PY	Pans in matrix of young ice.
R	Ridge system, may be either pressure ridge or shear ridge system.
T	Tidal or tension cracks - cracks due to tidal action in shallow waters, may be indicated by piled ice and/or snow drifts.

W	Open water.
Y	Polynya.
Z	Zone of shear.

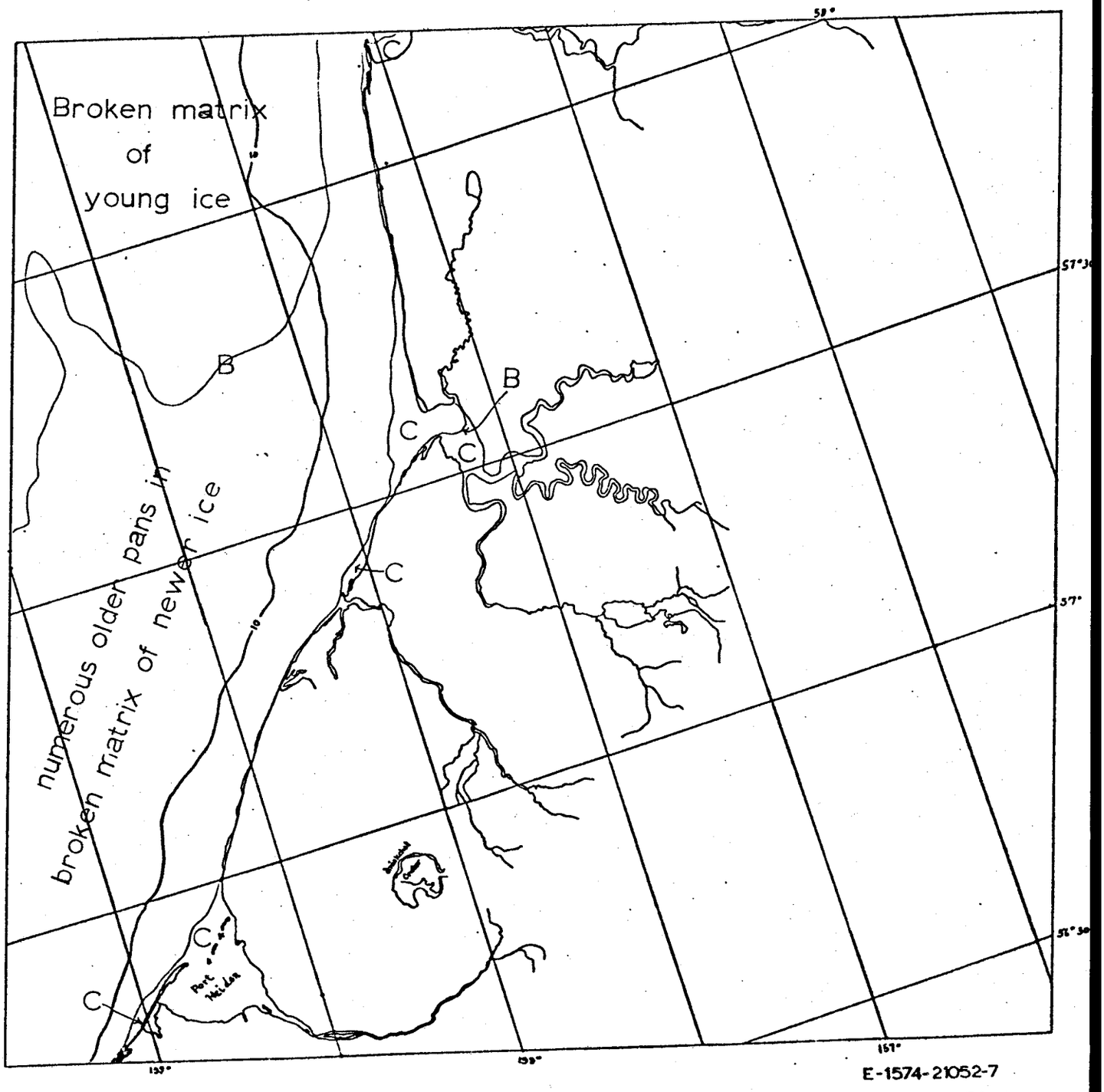

KILOMETERS
0 10 20 30 40 50
SCALE APPROX 1:1,000,000

BERING SEA

Scene 1574-21052

This scene shows the portion of the Alaska Peninsula from Ugashik Bay (top) to Seal Island (bottom, below Port Heiden). There is very little contiguous ice along this coast. Most of what there is appears to be relatively young. There is a continuous strip along the coast which is quite irregular and shows signs of having been broken repeatedly. Just offshore there are several large pieces of ice which appear to have broken off this thin shelf. The 10-fathom contour is located considerably seaward of the edge of contiguous ice. Within the major bays and inshore of Seal Island there are expanses of contiguous ice which appear to be considerably older than the rest of the contiguous ice.

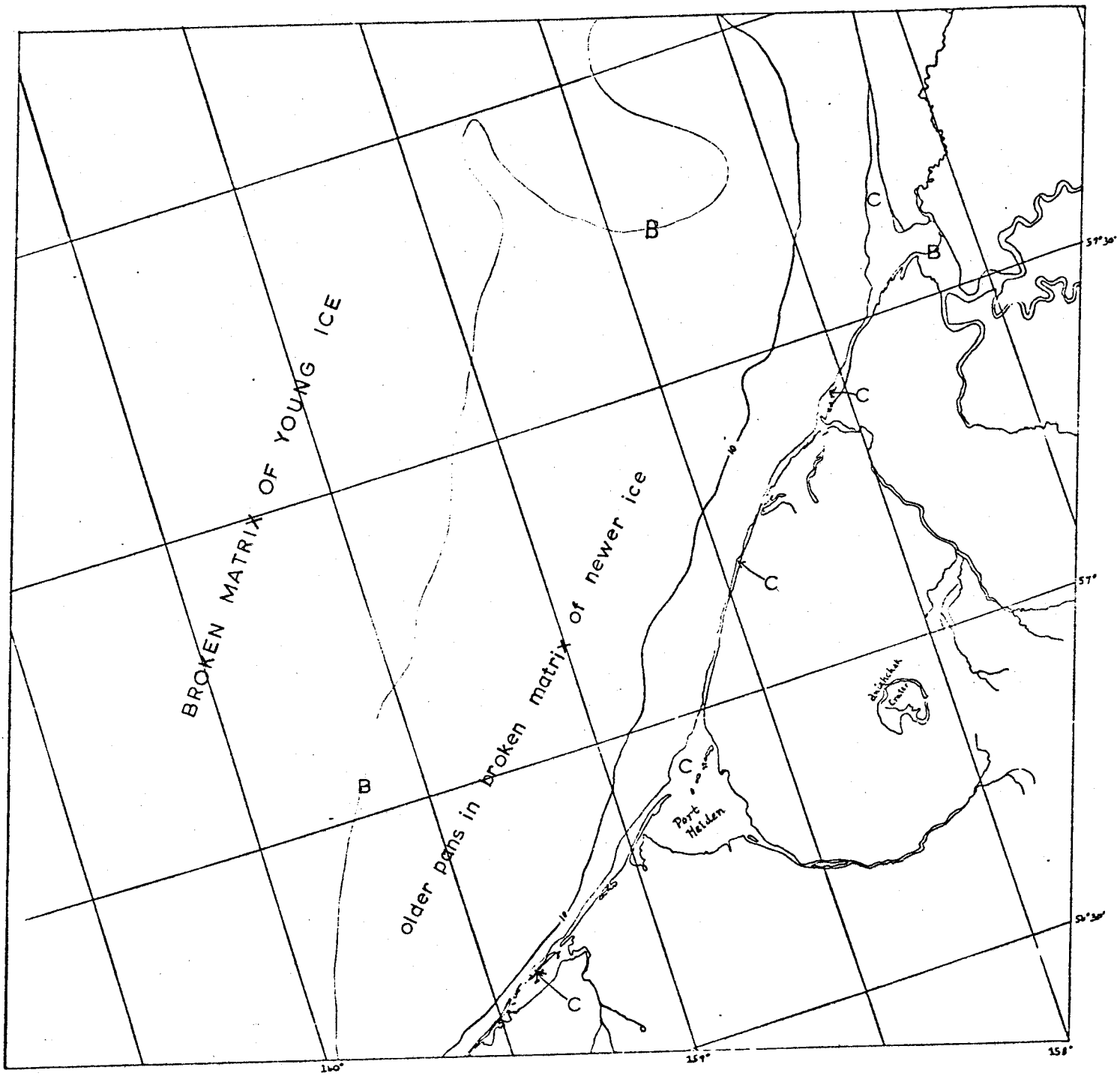

KILOMETERS
0 10 20 30 40 50
SCALE APPROX 1:1,000,000

BERING SEA

E-1575-21110-7
18 FEB. 1974

Scene 1575-21110

This scene shows the portion of the Alaska Peninsula from just north of Port Ugashik to just south of Seal Island. There is very little contiguous ice along this coast. Most of that which exists appears to be relatively young. Only within the more protected areas of bays and shoreward of islands (for instance Seal Island just south of Port Heiden) does the contiguous ice appear to be old enough to be white and not gray. North of Seal Island the 10-fathom contour is considerably seaward of the limit of contiguous ice. However, south of Seal Island this contour is quite close to shore. Along this portion of the coast there is an indication of a linear ice feature roughly coinciding with this contour. This scene should be compared with scene 1574-21052 for determination of one-day ice motions.

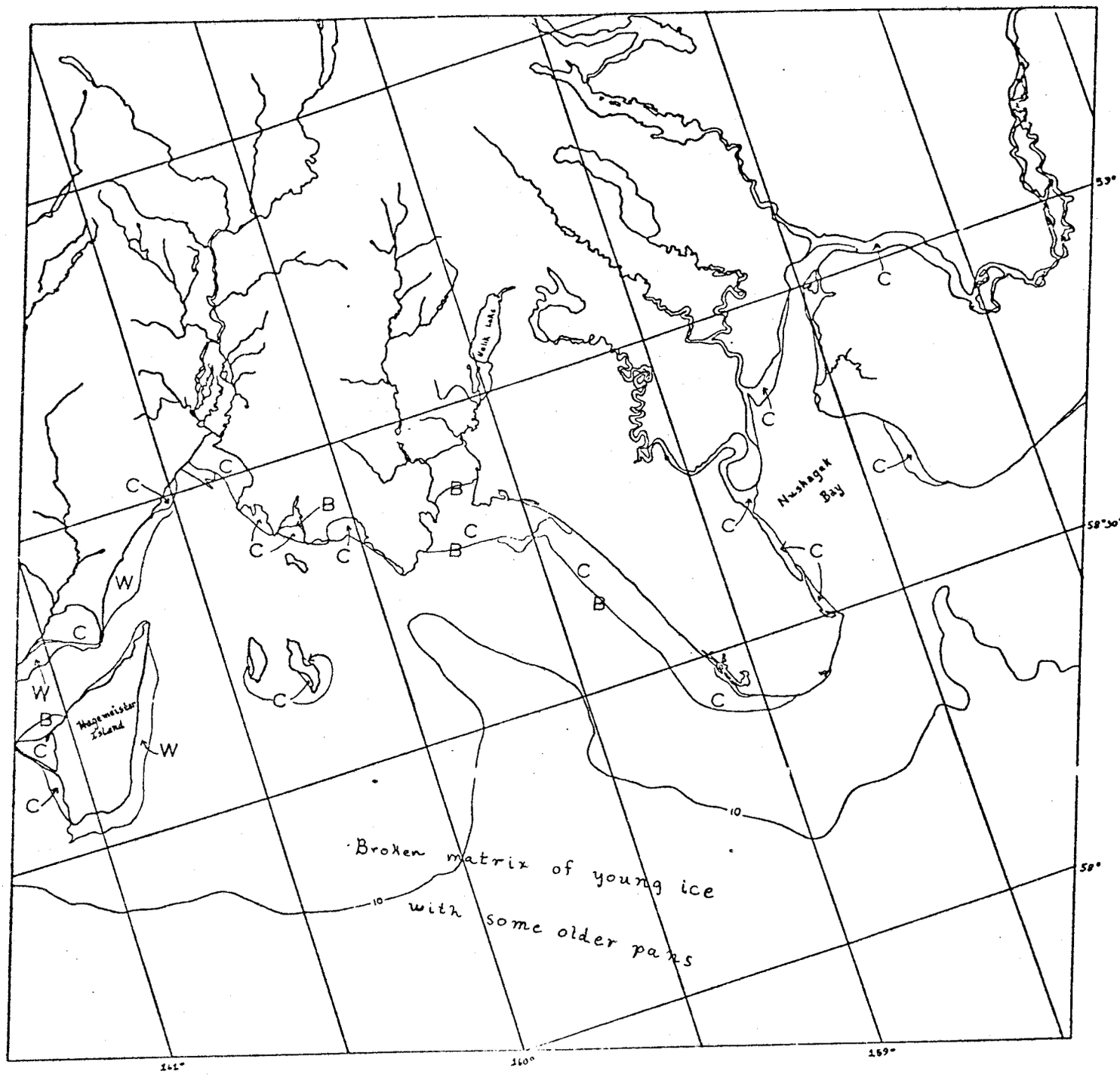

KILOMETERS
0 10 20 30 40 50
SCALE APPROX 1:1,000,000

BERING SEA

E-1576-21162-7
19 FEB. 1974

Scene 1576-21162

This scene shows the portion of coast from the eastern side of Nushagak Bay to the west side of Hagemeister Island. No correlation can be found between the edge of contiguous ice and the 10-fathom contour. Much of the contiguous ice appears to be young with the only old contiguous ice being found in well-protected areas.

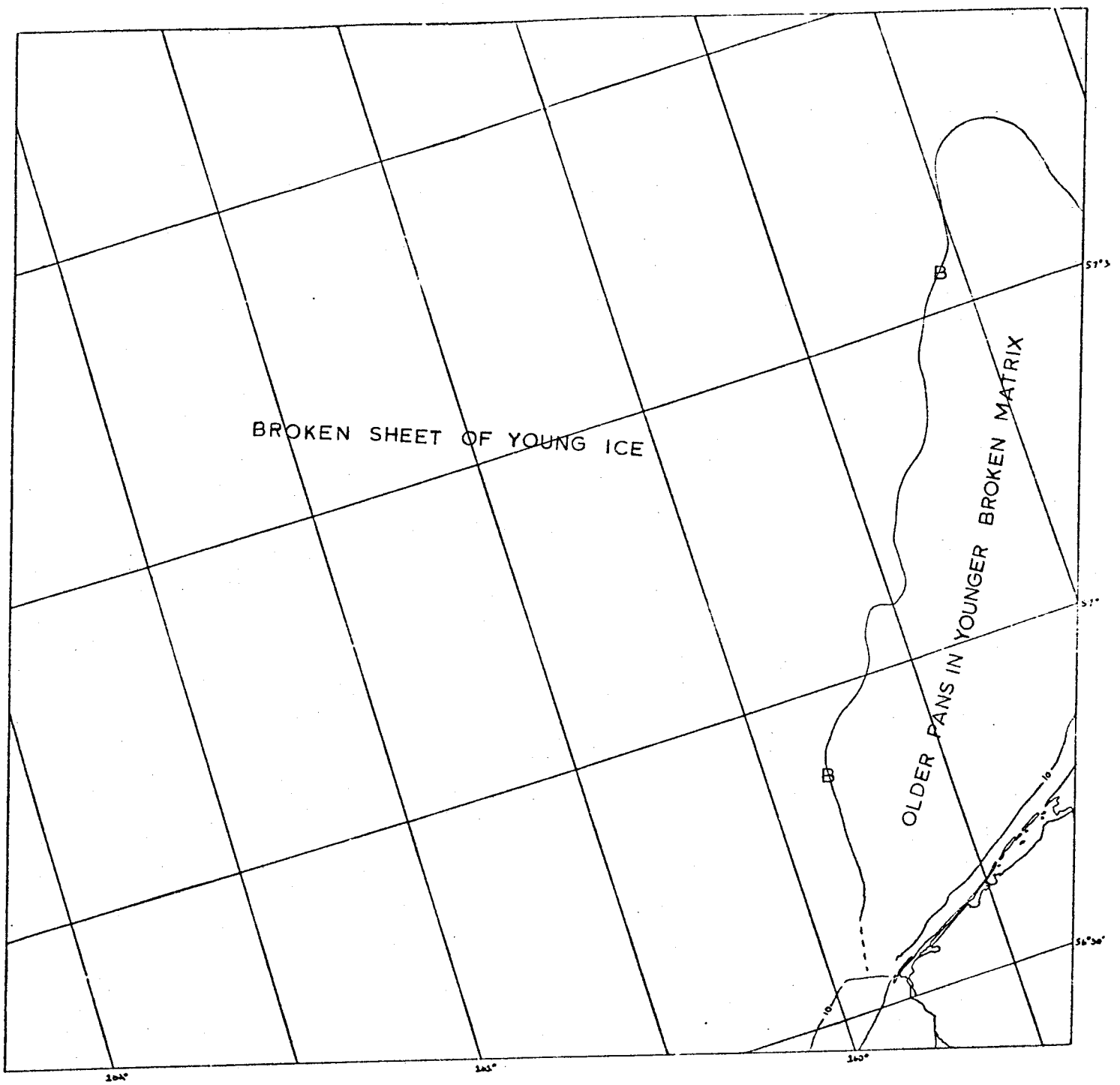

E-1576-21165-7
19 FEB. 1974

KILOMETERS
0 10 20 30 40 50
SCALE APPROX 1:1,000,000

BERING SEA

Scene 1576-21165

Only a small portion of the Alaska Peninsula coast can be seen in this image. The area shown includes Seal Island just south of Port Heiden. Along this stretch of coast, whenever the 10-fathom contour is close to the shore, there appears to be a sea ice boundary, possibly a shear ridge, associated with it.

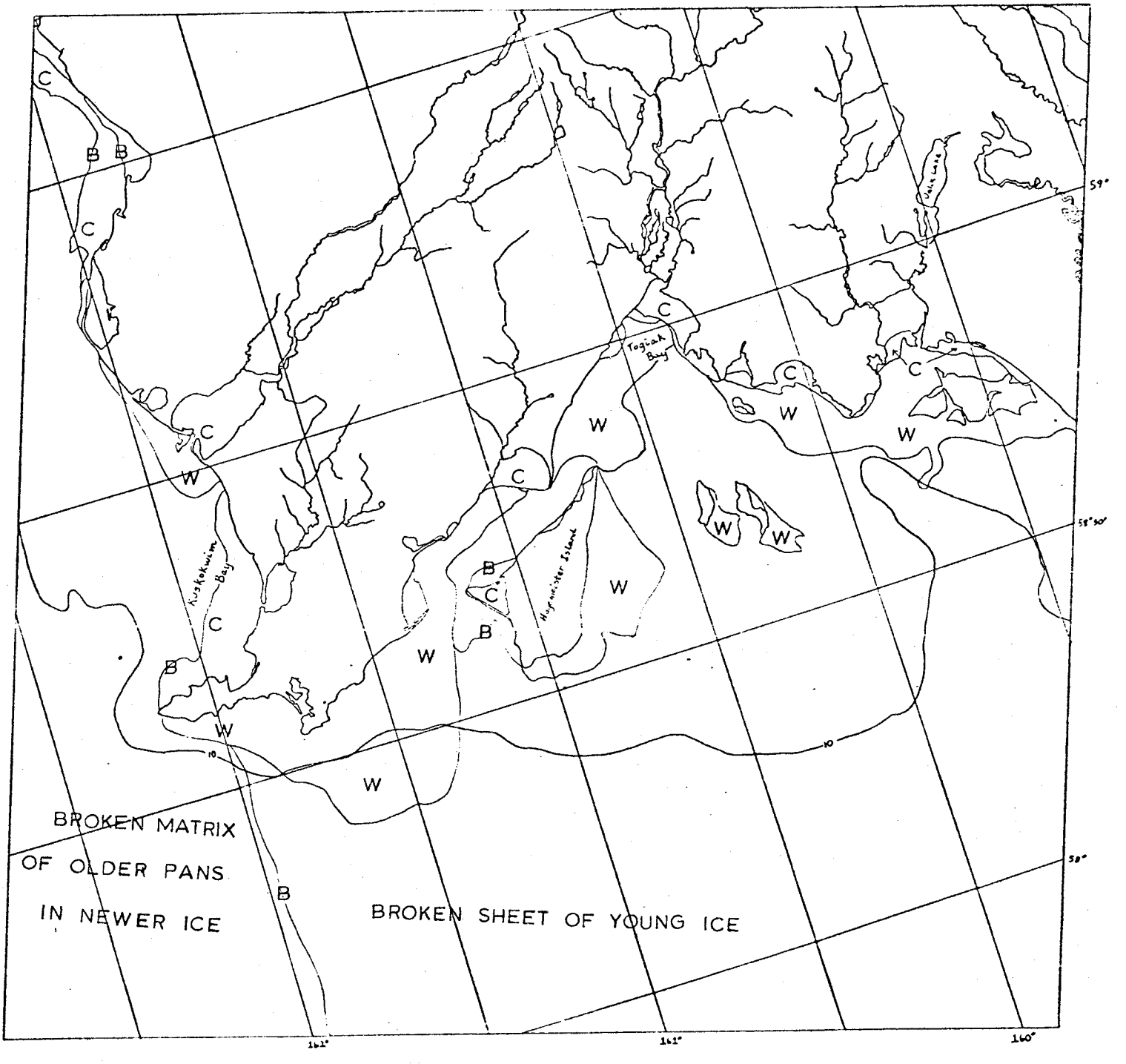

KILOMETERS
0 10 20 30 40 50
SCALE APPROX 1:1,000,000

E-1577-21220-7
20 FEB. 1974

BERING SEA

Scene 1577-21220

This scene shows the portion of coast from the west wide of the Nushagak Peninsula to Jacksmith Bay. When compared with scene 1576-21162, evidence of the strong tidal action in this area can be seen. This is particularly true in Kulukak Bay where a large sheet of contiguous ice has broken free and moved several km seaward. Contiguous ice is only found in bays and other protected areas and even in these locations there is often a boundary between older, more permanent ice and younger, temporary contiguous ice.

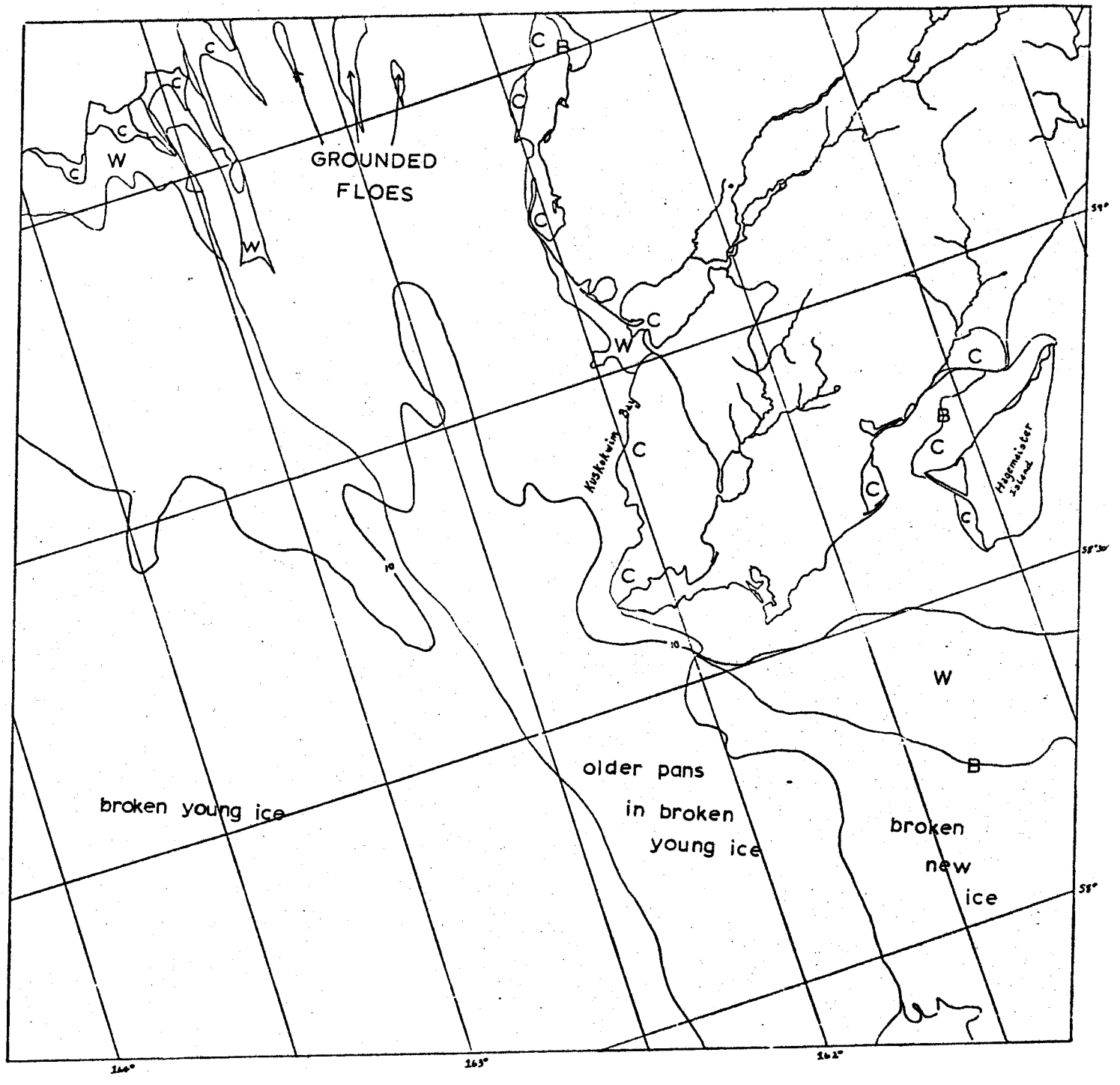

KILOMETERS
0 10 20 30 40 50
SCALE APPROX 1:1,000,000

BERING SEA

E-1578-21275-7
21 FEB. 1974

Scene 1578-21275

This scene includes the portion of coast from the east side of Kuskokwim Bay. Contiguous ice is only found in protected areas. Often, as in the large expanse of contiguous ice south of Goodnews Bay, this ice is quite young. Only in the well-protected areas has the ice become thick enough to appear white.

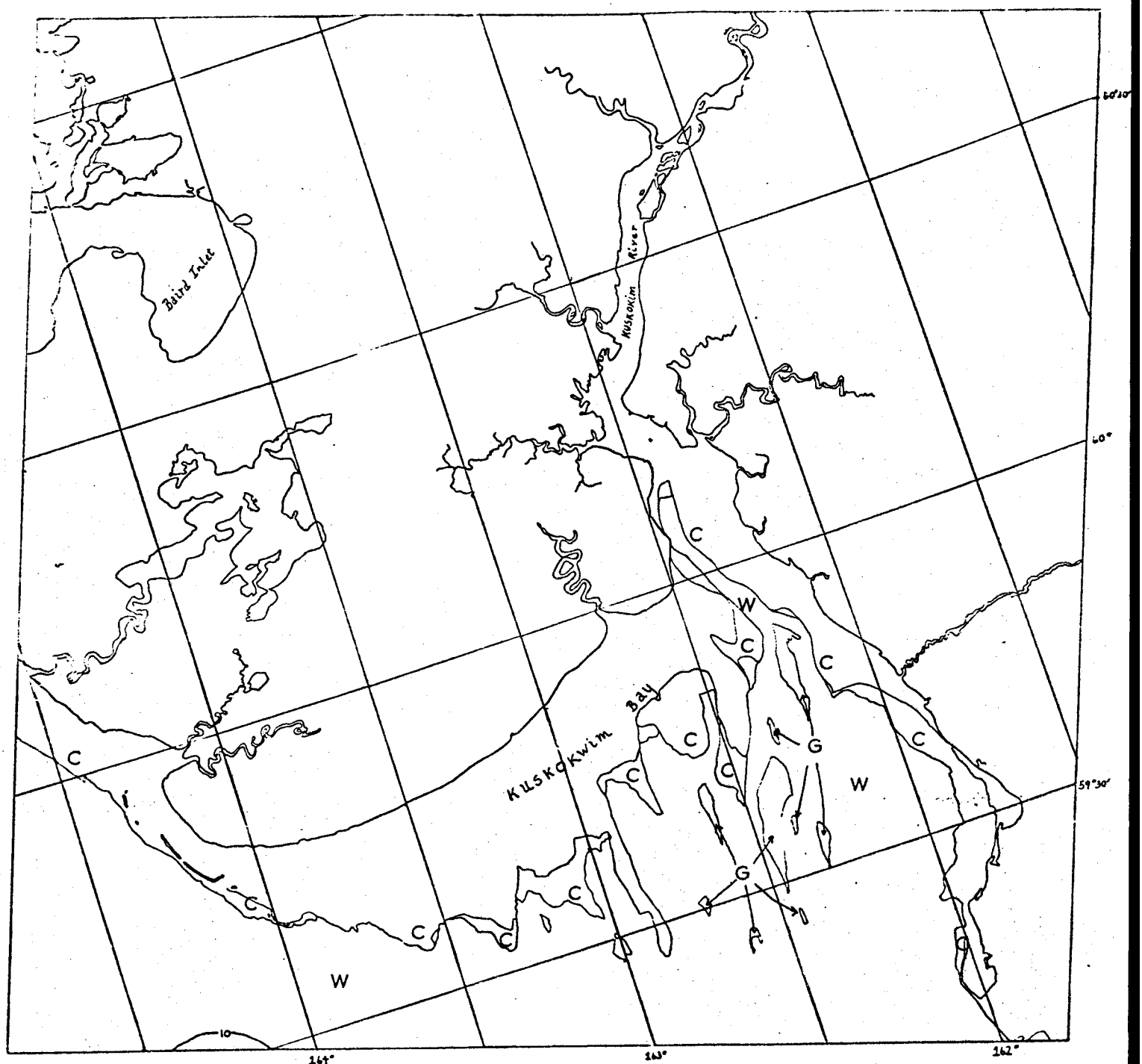

KILOMETERS
0 10 20 30 40 50
SCALE APPROX 1:1,000,000

BERING SEA

E-1579-21331-7
22 FEB. 1974

Scene 1579-21331

Kuskokwim Bay is the central feature of this scene. The finger of open water extending up the Kuskokwim River is almost certainly the result of tidal action. A very large expanse of contiguous ice can be found on the mud flats and shoal areas of Kuskokwim Bay. Isolated patches of ice can be found on shoals surrounded by deeper water. Often several ages of contiguous ice are apparent.

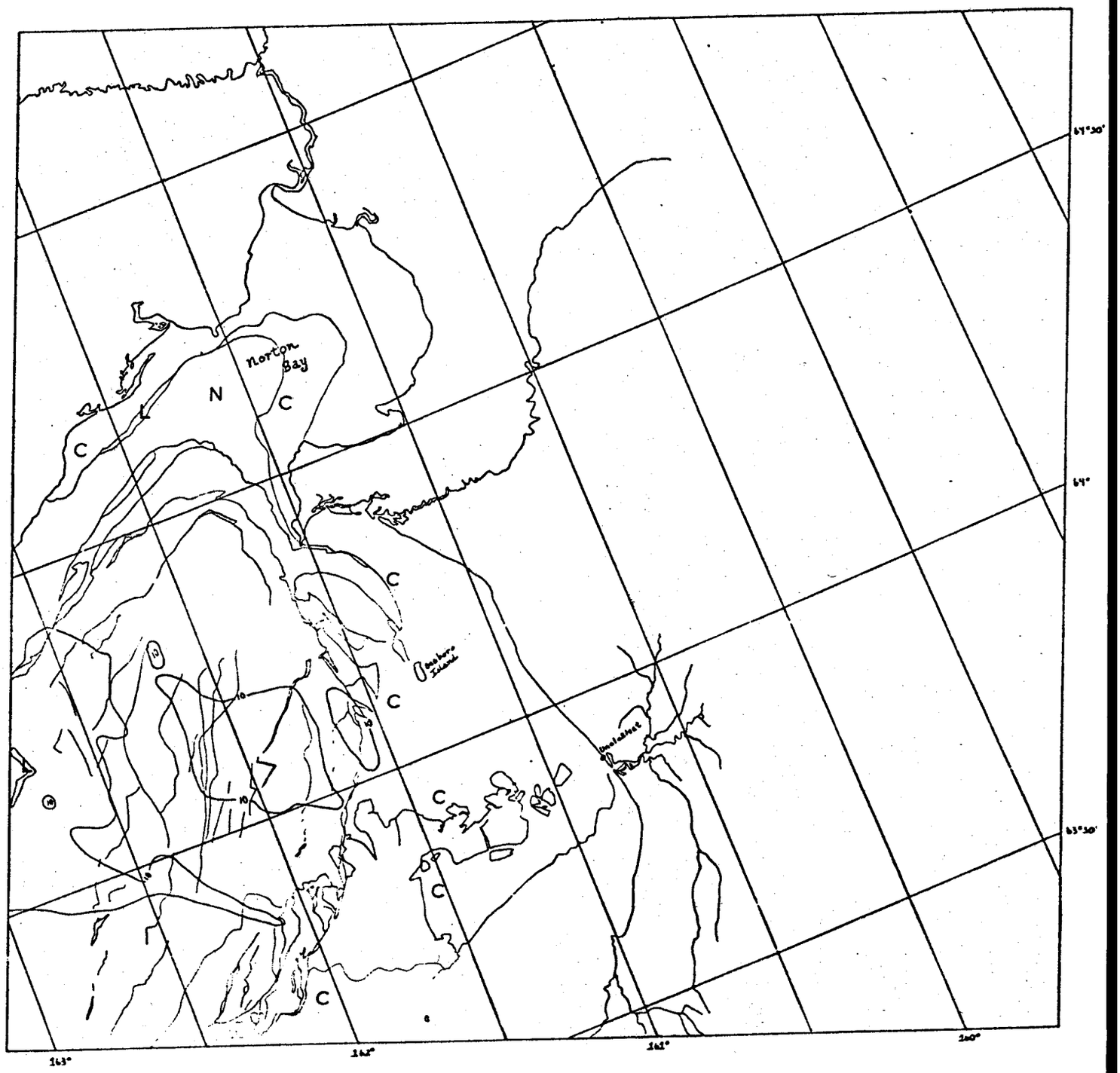

KILOMETERS
0 10 20 30 40 50
SCALE APPROX 1:1,000,000

BERING SEA

E-1580-21373-7
23 FEB. 1974

Scene 1580-21373

Norton Bay is the central feature of this scene. Several different ages of contiguous ice are apparent. There is evidence that tidal action has had a strong influence on ice motions within Norton Sound.

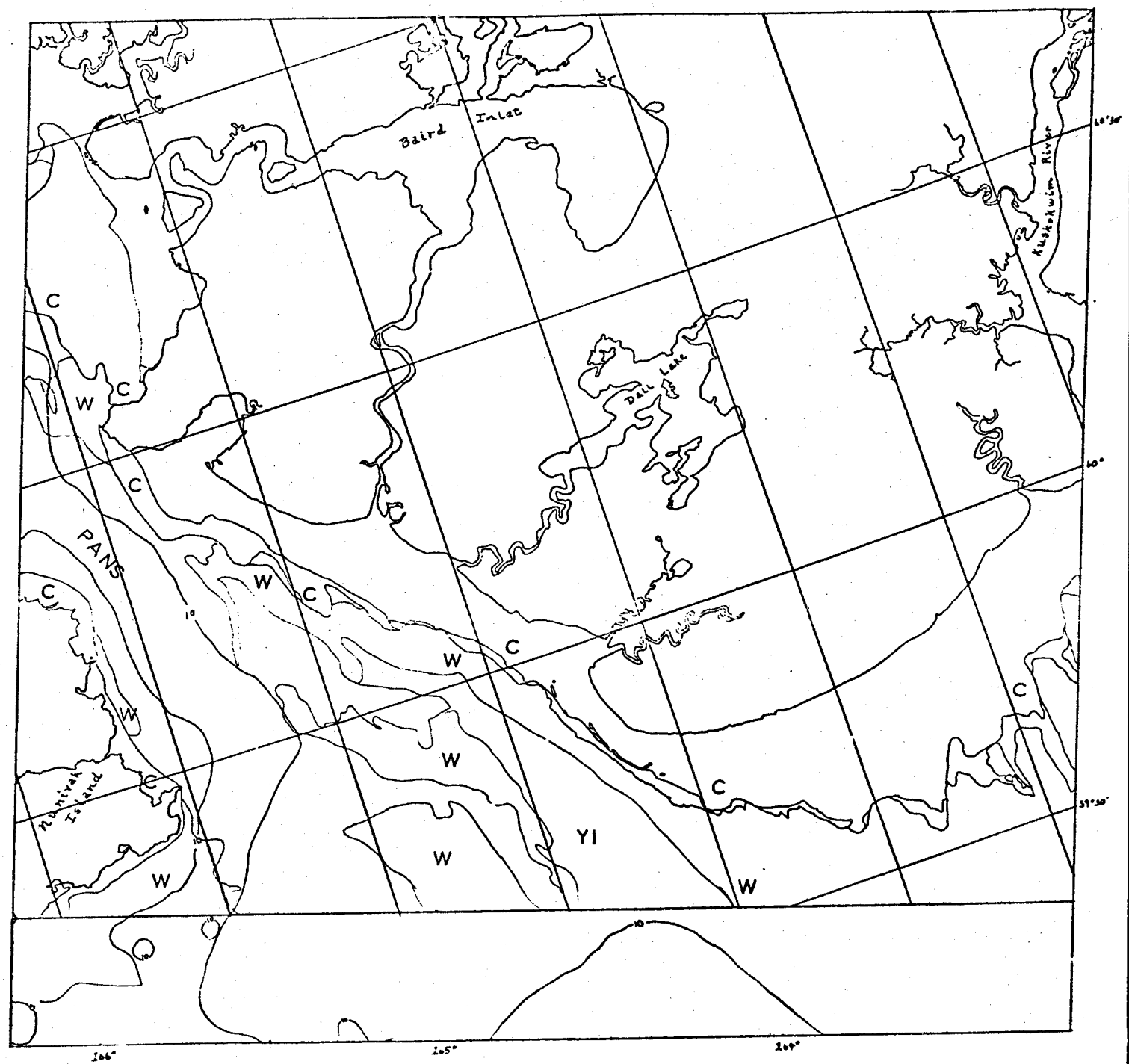

KILOMETERS
0 10 20 30 40 50
SCALE APPROX 1:1,000,000

BERING SEA

E-1580-21385-7
23 FEB. 1974

Scene 1580-21385

This scene includes western Kuskokwim Bay and Nunivak Island. Large expanses of contiguous ice are to be found on mud flats and protected areas (for instance, west of Nelson Island). Other contiguous ice can be found in well protected areas along the coast of Nunivak Island. There appears to be a great deal of ice stranded on shoals between Nunivak Island and the mainland.

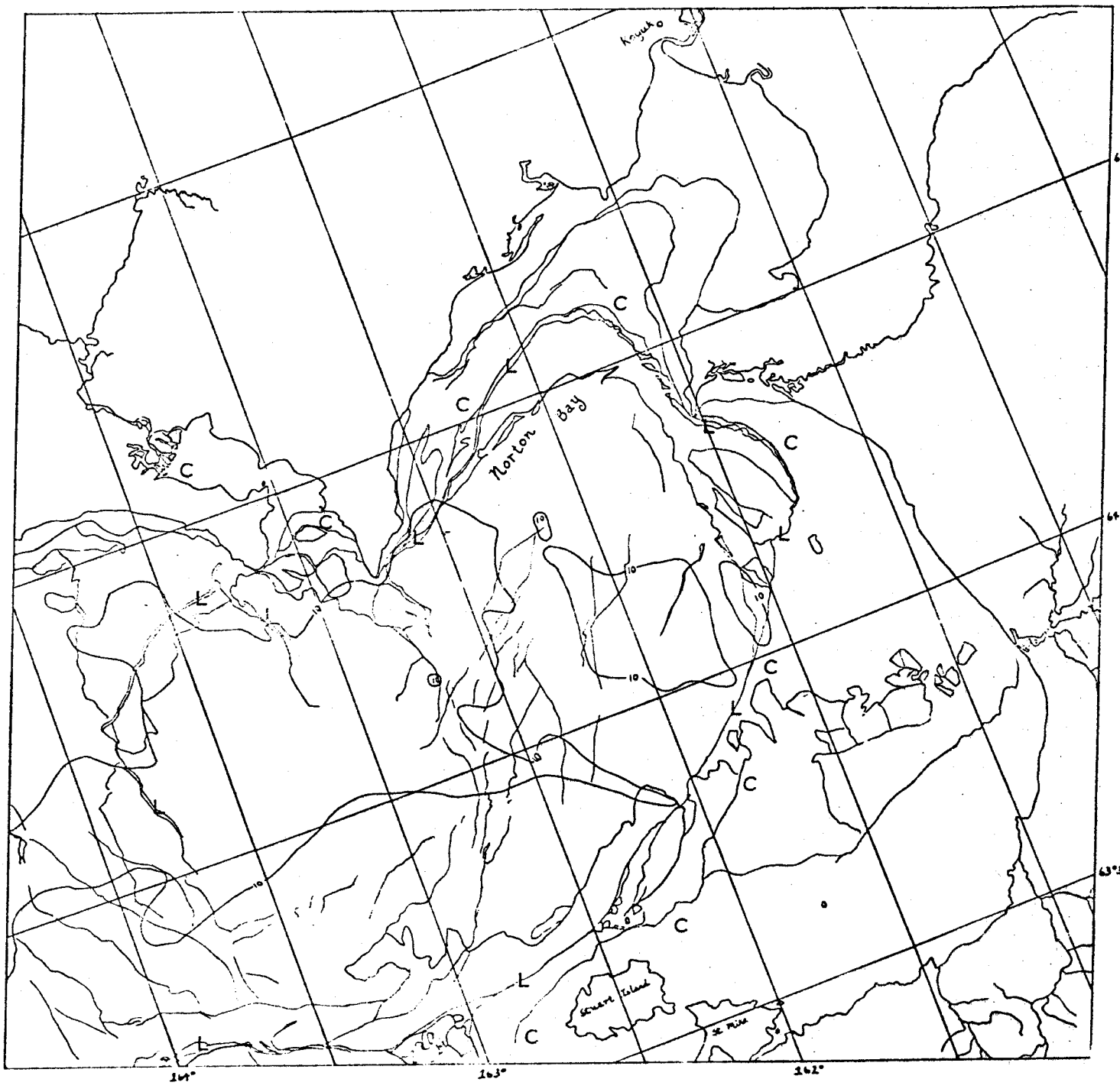

KILOMETERS
0 10 20 30 40 50
SCALE APPROX 1:1,000,000

BERING SEA

E-1581-21432-7
24 FEB. 1974

Scene 1581-21432

This scene of Norton Sound illustrates the countervailing effects of freezing conditions producing contiguous ice and wind and tides breaking it up and transporting it away. In this scene there is a lead system which can be identified all around the inside perimeter of the sound. Between this lead and the shore there is contiguous ice of various ages. In some places large blocks of ice which had broken free of the contiguous ice have now been re-frozen into it.

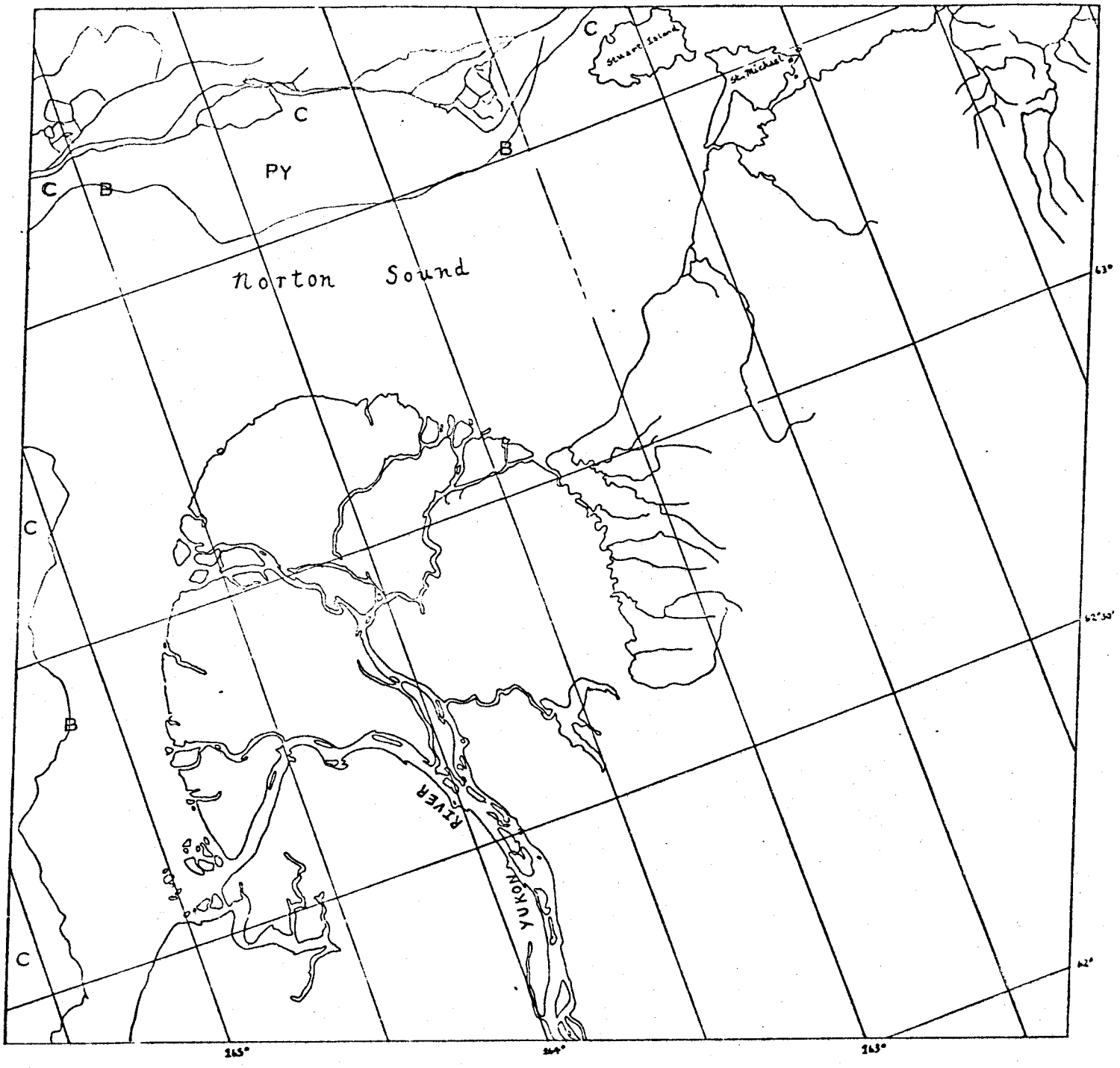

KILOMETERS
0 10 20 30 40 50
SCALE APPROX 1:1,000,000

BERING SEA

E-1581-21434-7
24 FEB. 1974

Scene 1581-21434

The control feature in this scene is the mouth of the Yukon River. Large expanses of contiguous ice can be found in all directions around the delta.

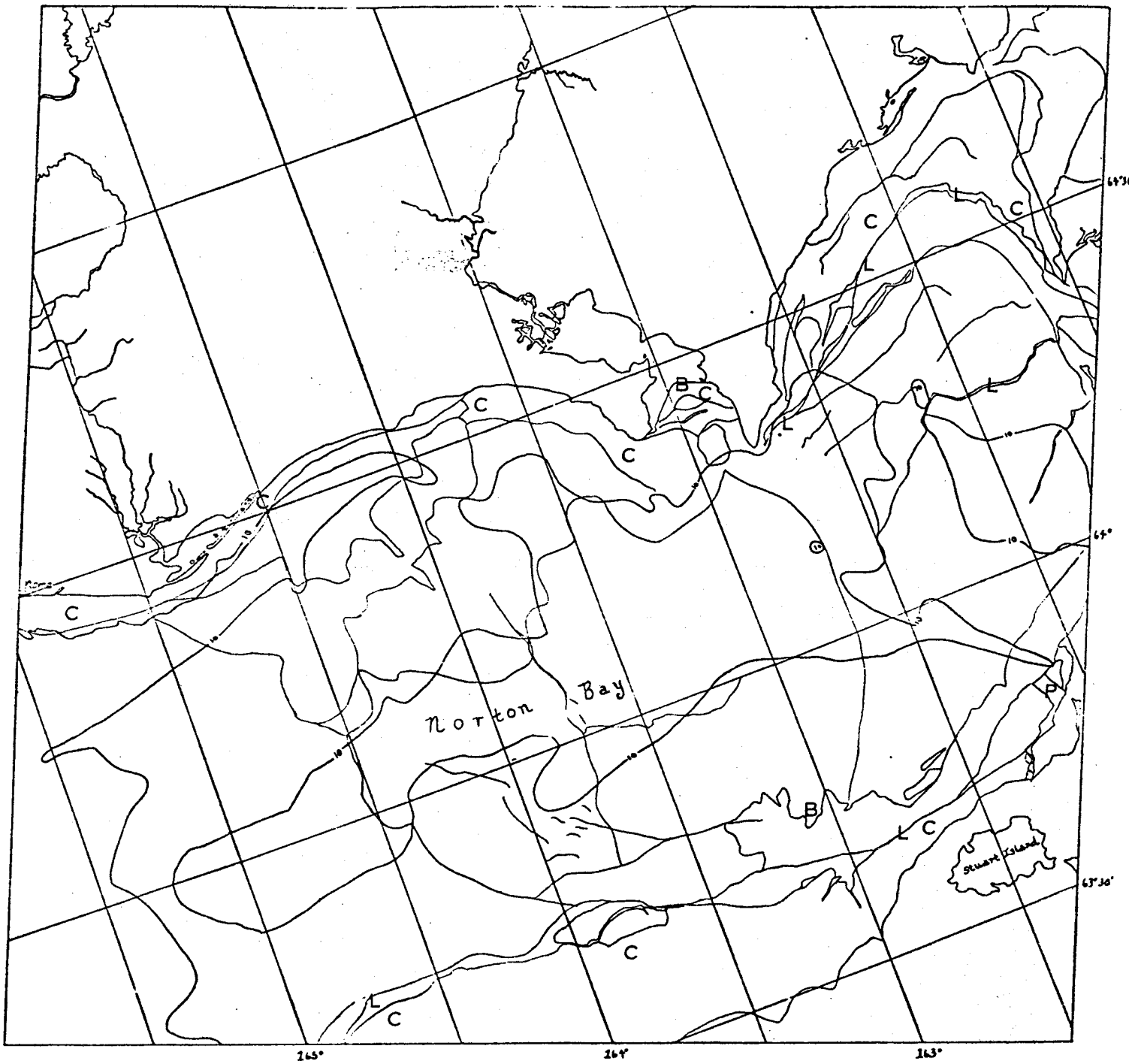

KILOMETERS
0 10 20 30 40 50
SCALE APPROX 1:1,000,000

BERING SEA

E-1582-21490-7
25 FEB. 1974

Scene 1582-21490

This complex map of ice in Norton Sound results from the many dynamic influences acting on this ice. Contiguous ice is found in protected and shallow areas and usually cannot be related to the 10-fathom contour except in the vicinity of Nome where the correlation appears significant. In most areas, including Nome, several ages of contiguous ice can be identified.

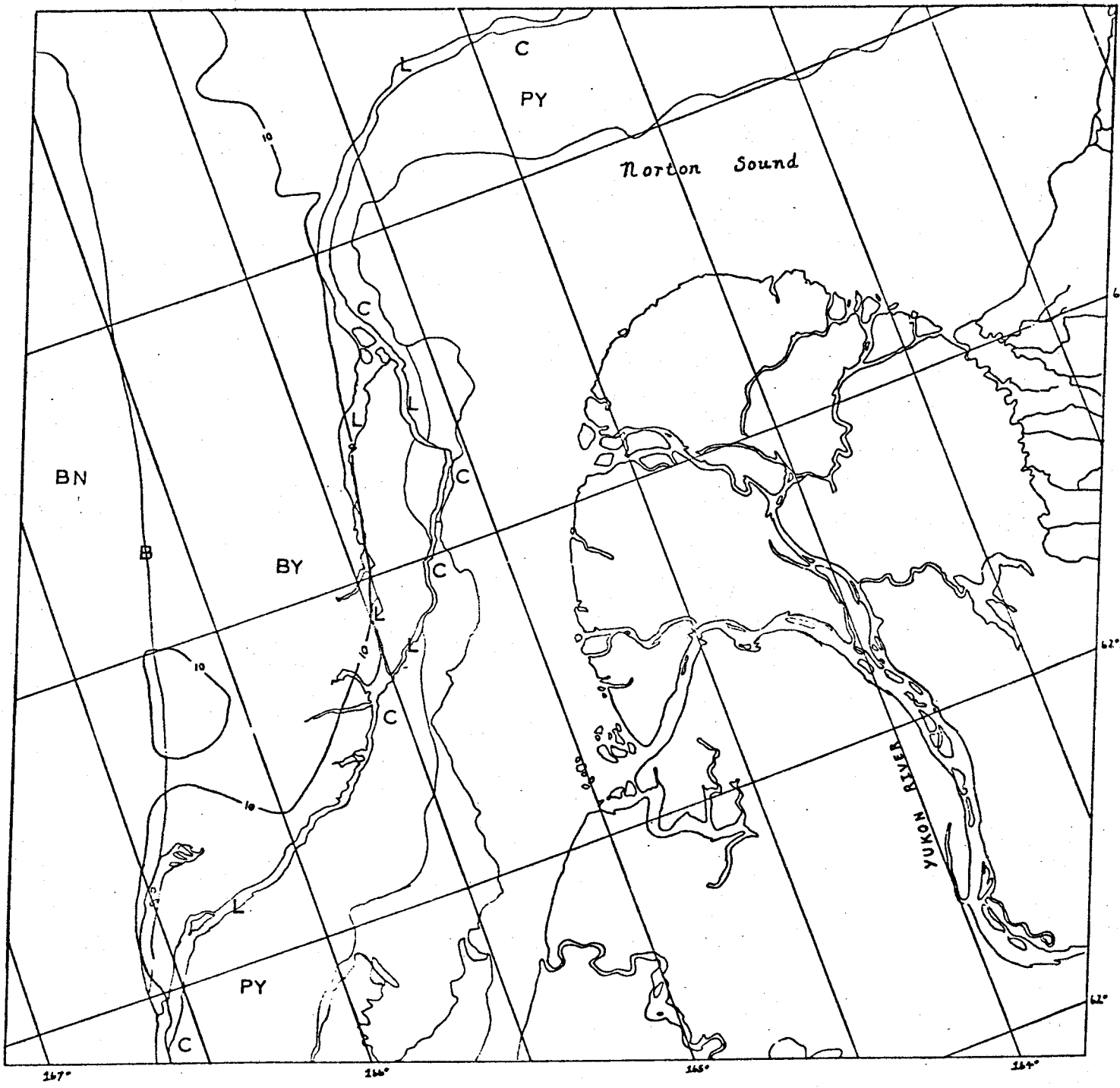

KILOMETERS
0 10 20 30 40 50
SCALE APPROX 1:1,000,000

BERING SEA

E-1582-21492-7
25 FEB. 1974

Scene 1582-21492

This scene of the Yukon Delta shows a large piece of contiguous ice being broken off. The piece being broken off was, like much of the contiguous ice, not all of the same age. It consisted of many older pans frozen into a sheet of newer ice.

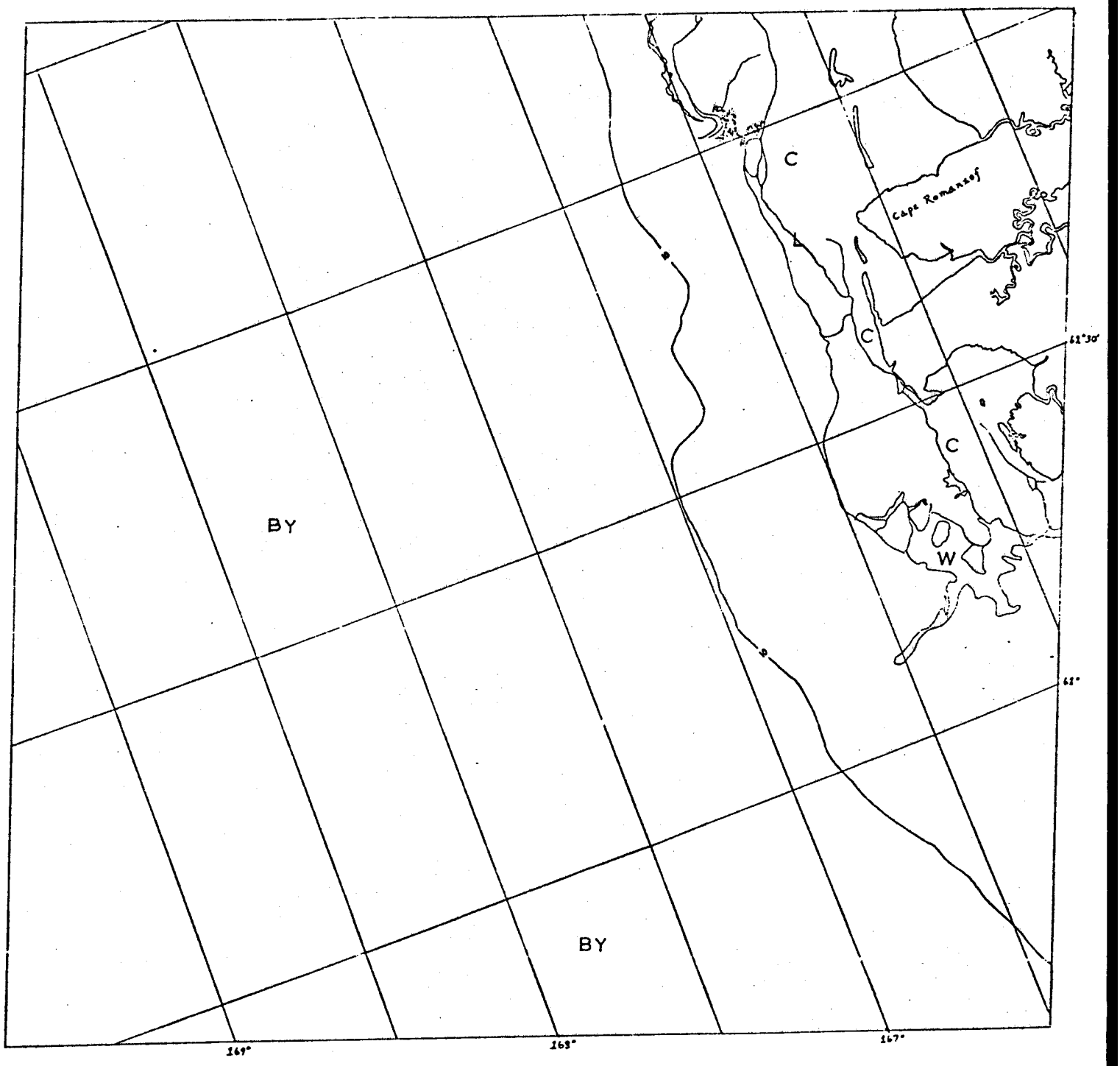

KILOMETERS
0 10 20 30 40 50
SCALE APPROX 1:1,000,000

BERING SEA

E-1583-21553-7
26 FEB. 1974

Scene 1583-21553

This scene containing Cape Romanzof shows contiguous ice quite shoreward of the 10-fathom contour.

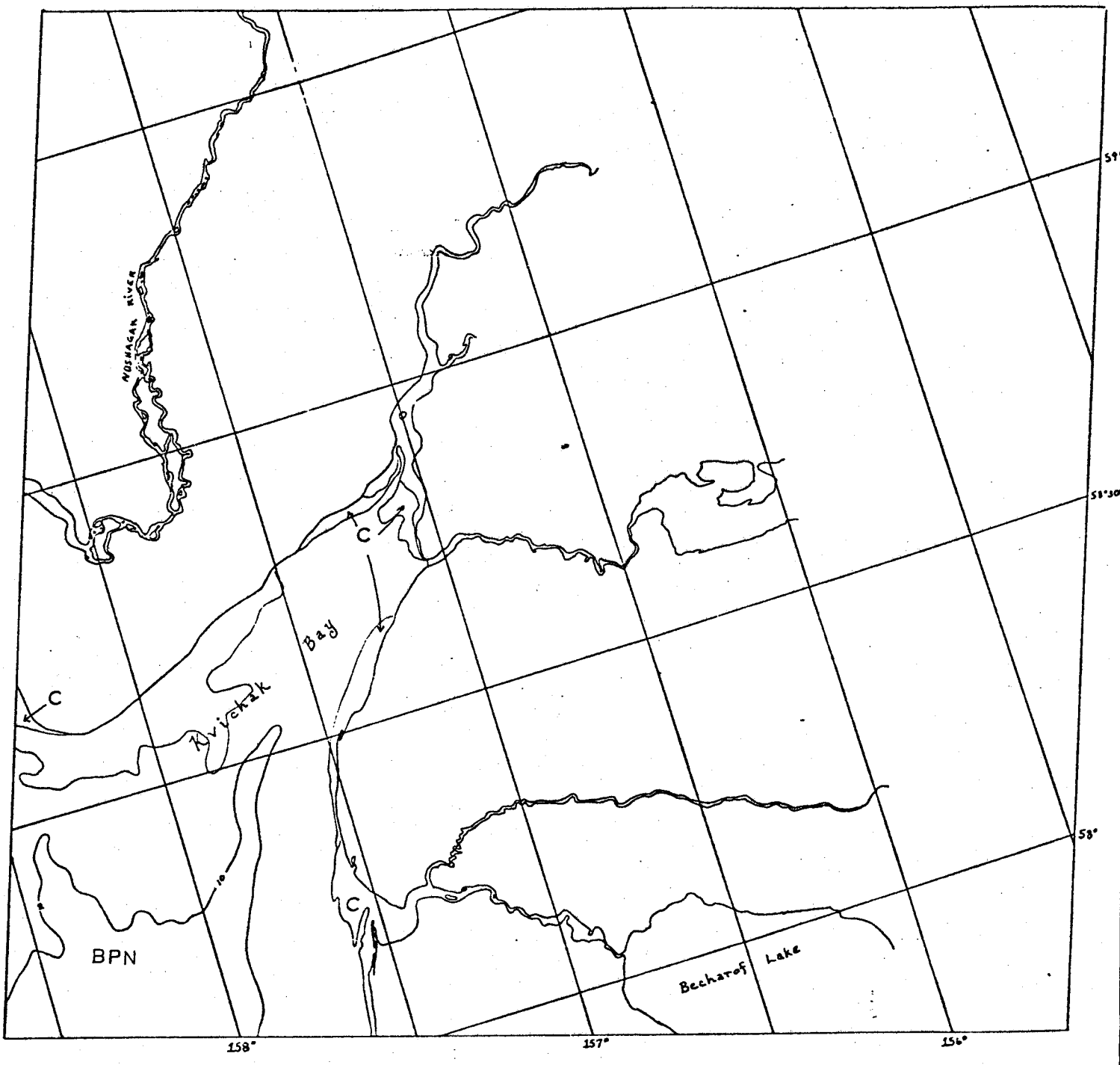

KILOMETERS
0 10 20 30 40 50
SCALE APPROX 1:1,000,000

BERING SEA

E-1592-21044-7
7 MARCH 1974

Scene 1592-20144

This scene of Kvichak Bay shows very little contiguous ice. Water appears to extend completely to the shore on the west side of the bay while on the east side the contiguous ice appears to be a temporary nature.

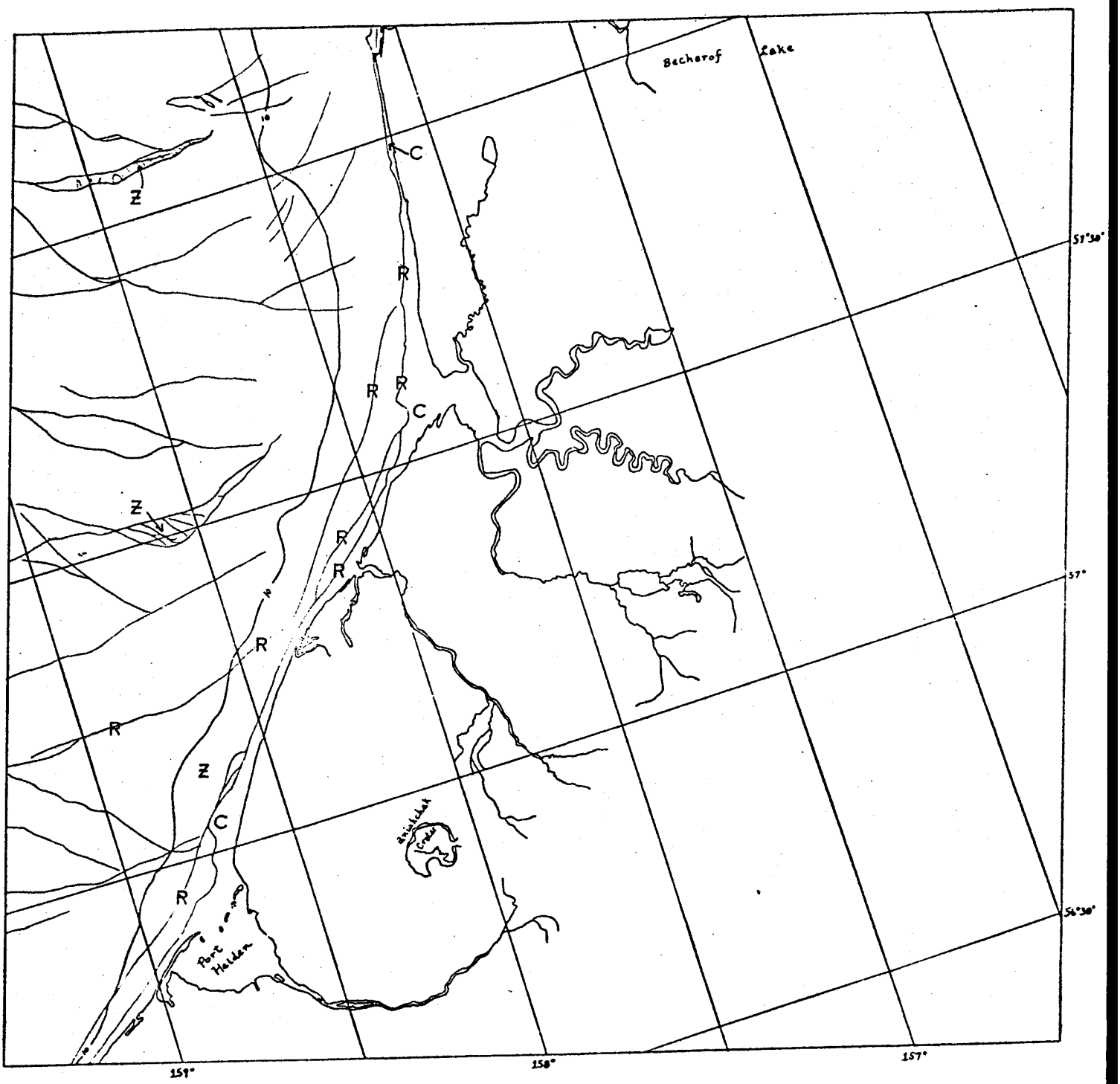

KILOMETERS
0 10 20 30 40 50
SCALE APPROX 1:1,000,000

BERING SEA

E-1592-21050-7
7 MAR. 1974

Scene 1592-21050

This scene includes the Alaskan Peninsula coast from Egegik to just south of Port Heiden. This scene should be compared with scene 1574-21052. During this interval (Feb. 17 - March 7). The nature of the ice along this coast has completely changed. The ice in Bristol Bay has grown considerably thicker and there is evidence of significant shear ridges being created parallel to the shore yet within the 10-fathom contour.

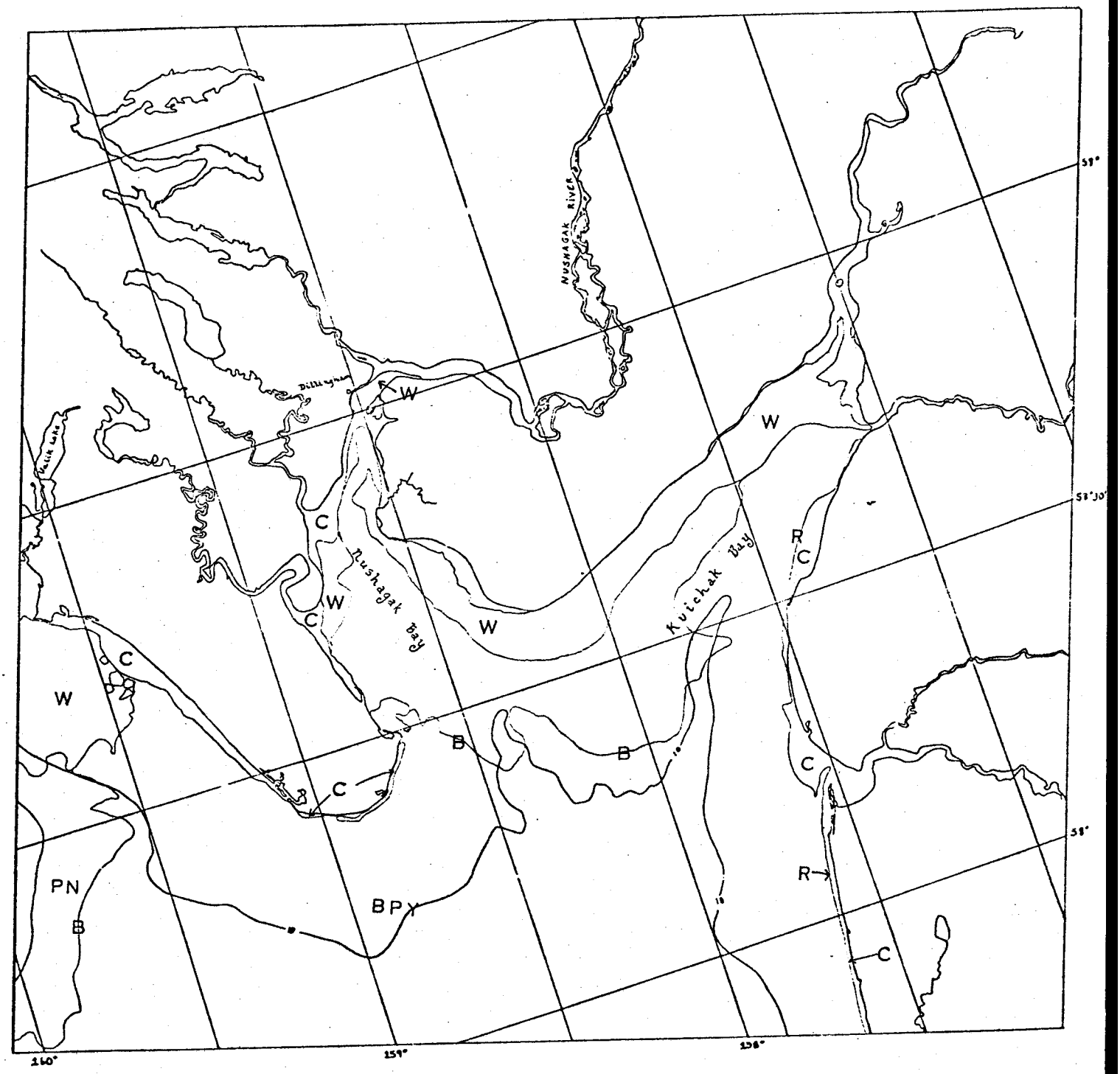

KILOMETERS
0 10 20 30 40 50

SCALE APPROX 1:1,000,000

BERING SEA

E-1593-21102-7
8 MARCH 1974

Scene 1593-21102

This scene shows Bristol Bay from Kvichak Bay to the west side of the Nushagak Peninsula. Contiguous ice can be found close to the shore and in protected areas. There is evidence of shear ridging on the boundary of contiguous ice on the eastern side of the bay.

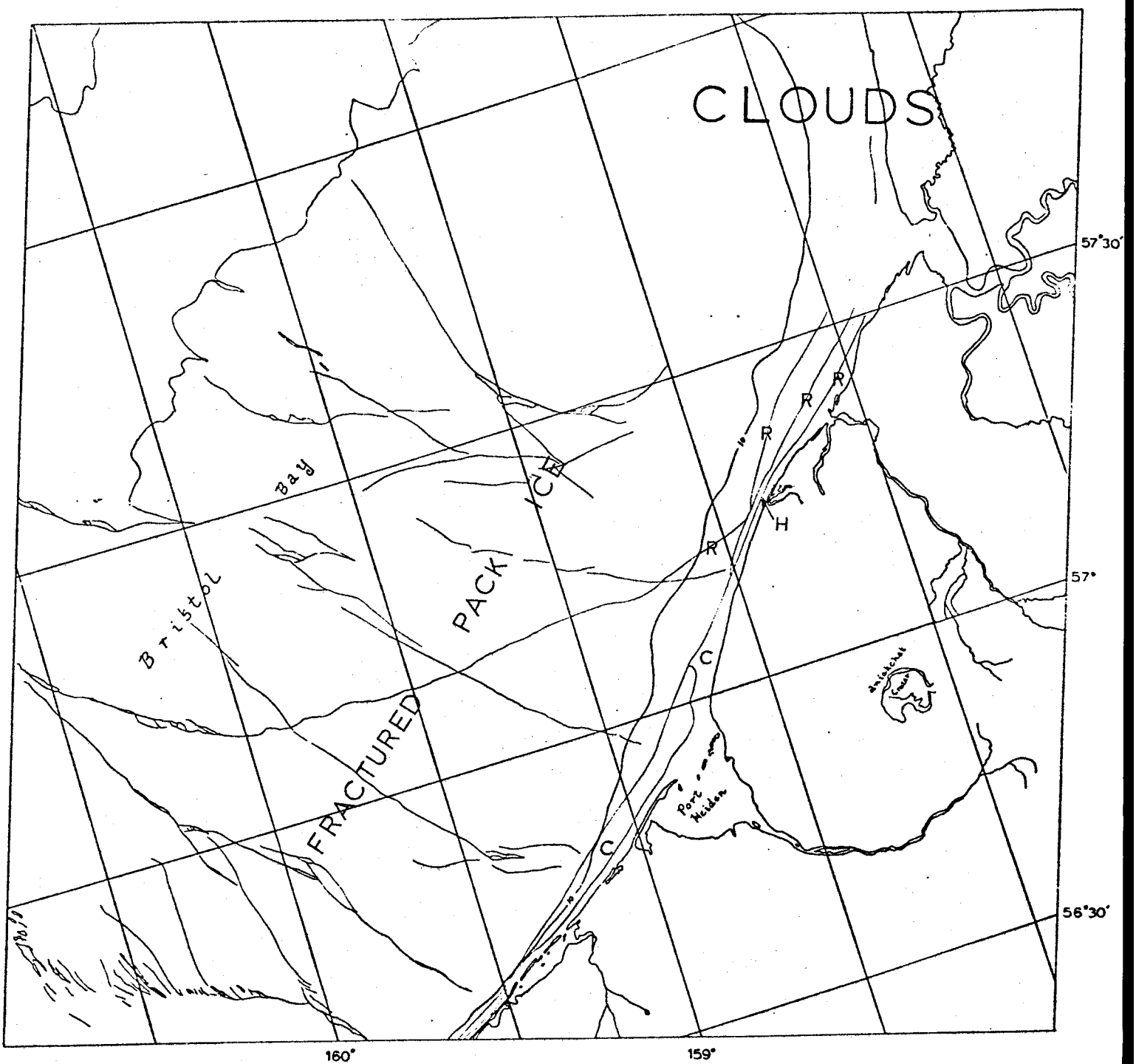

KILOMETERS
0 10 20 30 40 50
SCALE APPROX 1:1,000,000

BERING SEA

E-1593-21104-7
8 MARCH 1974

Scene 1593-21104

This scene showing the eastern shore of Bristol Bay should be compared with scene 1592-21050 for the previous day. The fractured pack ice in the bay has moved approximately 10 km southward during this period and it appears that during this time the shear ridges parallel to the coast have been significantly enhanced. At one location the field of piled ice has grown large enough to be considered a hummock field.

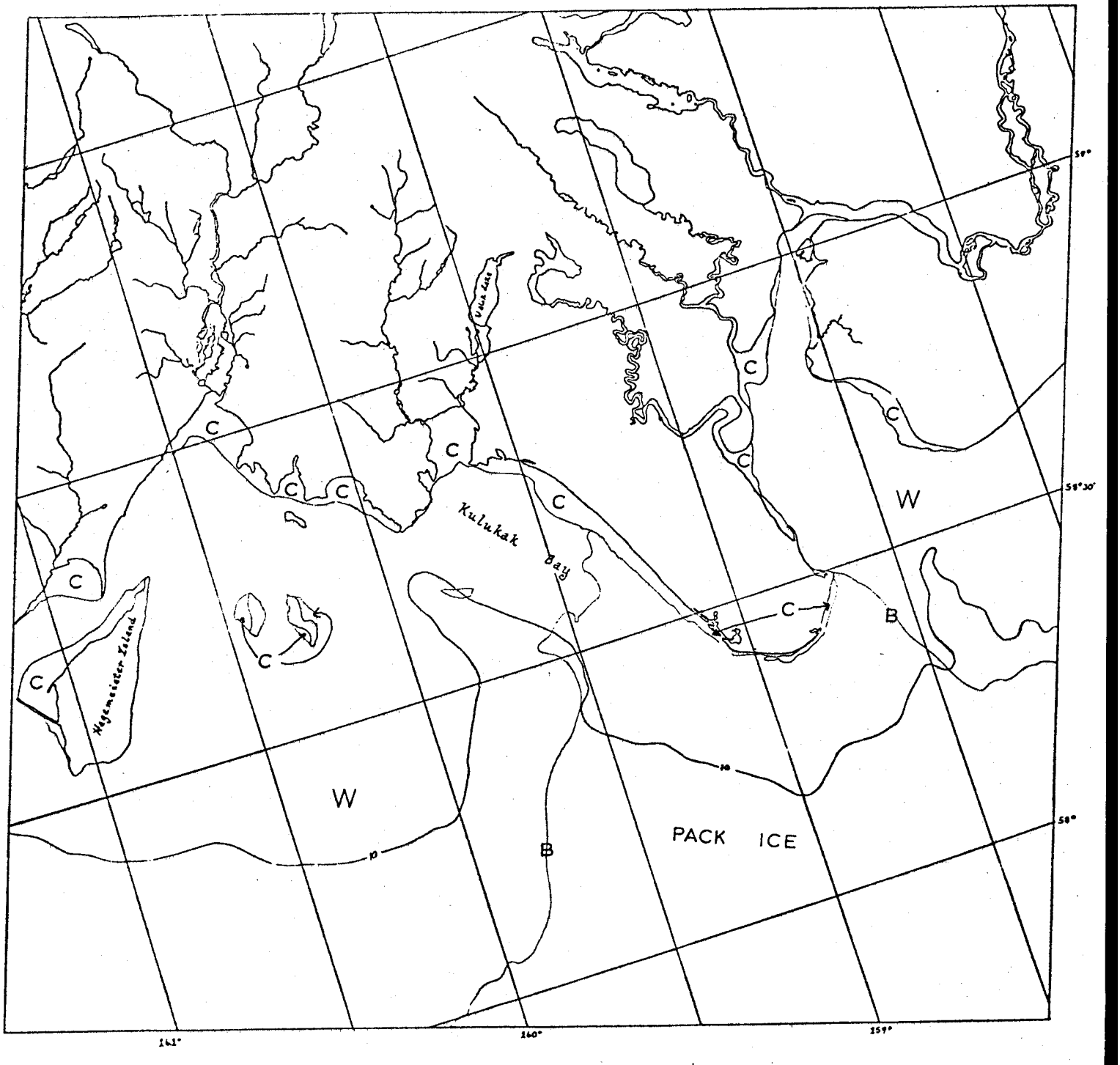

KILOMETERS
0 10 20 30 40 50
SCALE APPROX 1:1,000,000

BERING SEA

208

E-1594-21160-7
9 MARCH 1974

Scene 1594-21160

This scene shows the portion of coast from Nushagak Bay to Hagemeister Island. Apparently the wind has driven the pack ice away from this shore leaving the extent of contiguous ice well defined.

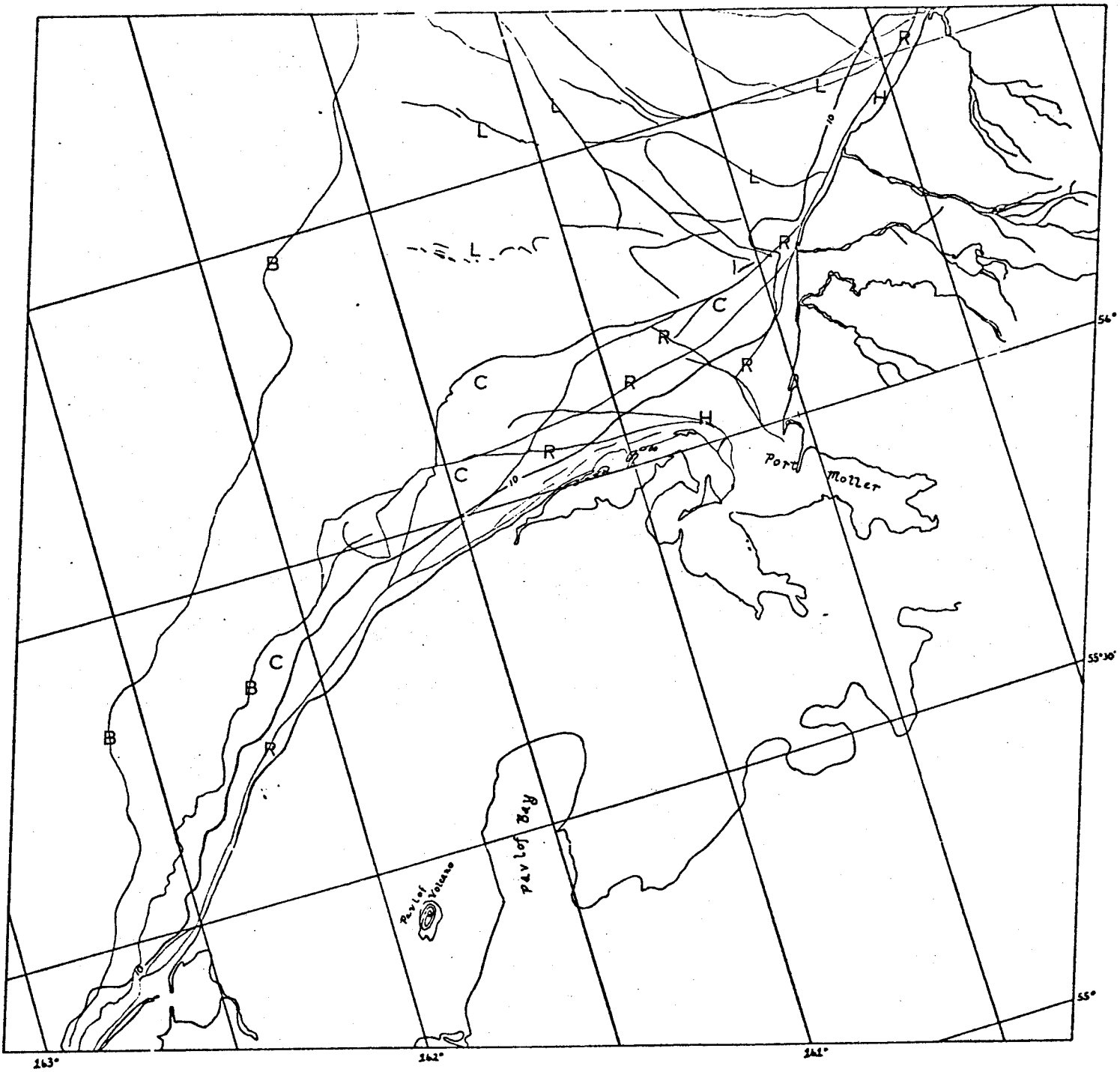

KILOMETERS
0 10 20 30 40 50
SCALE APPROX 1:1,000,000

BERING SEA

E-1594-21165-7
9 MARCH 1974

Scene 1594-21165

This scene shows the Alaska Peninsula coast in the vicinity of Port Moller. Apparently the Bristol Bay pack ice is being driven southward onto this shore with sufficient force to create many ridges and hummock fields. For the time being contiguous ice extends far seaward.

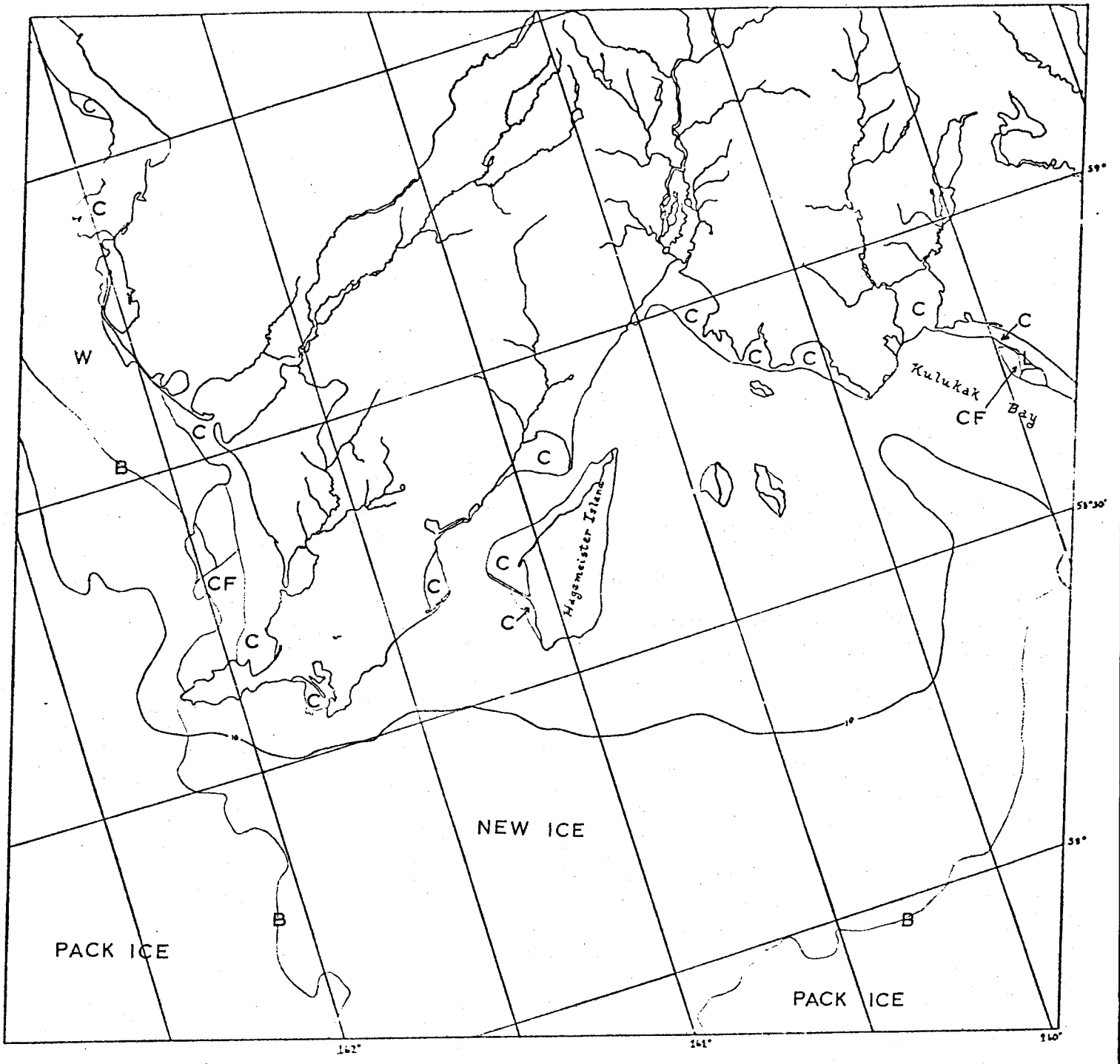

KILOMETERS
0 10 20 30 40 50
SCALE APPROX 1:1,000,000

BERING SEA

E-1595-21215-7
10 MARCH 1974

Scene 1595-21215

This scene shows the western Bristol Bay coast centered on Hagemeister Island. Apparently winds have blown the ice away from this portion of the coast leaving contiguous ice in protected and shallow areas. At two locations large fragments of contiguous ice are being broken away and are drifting seaward.

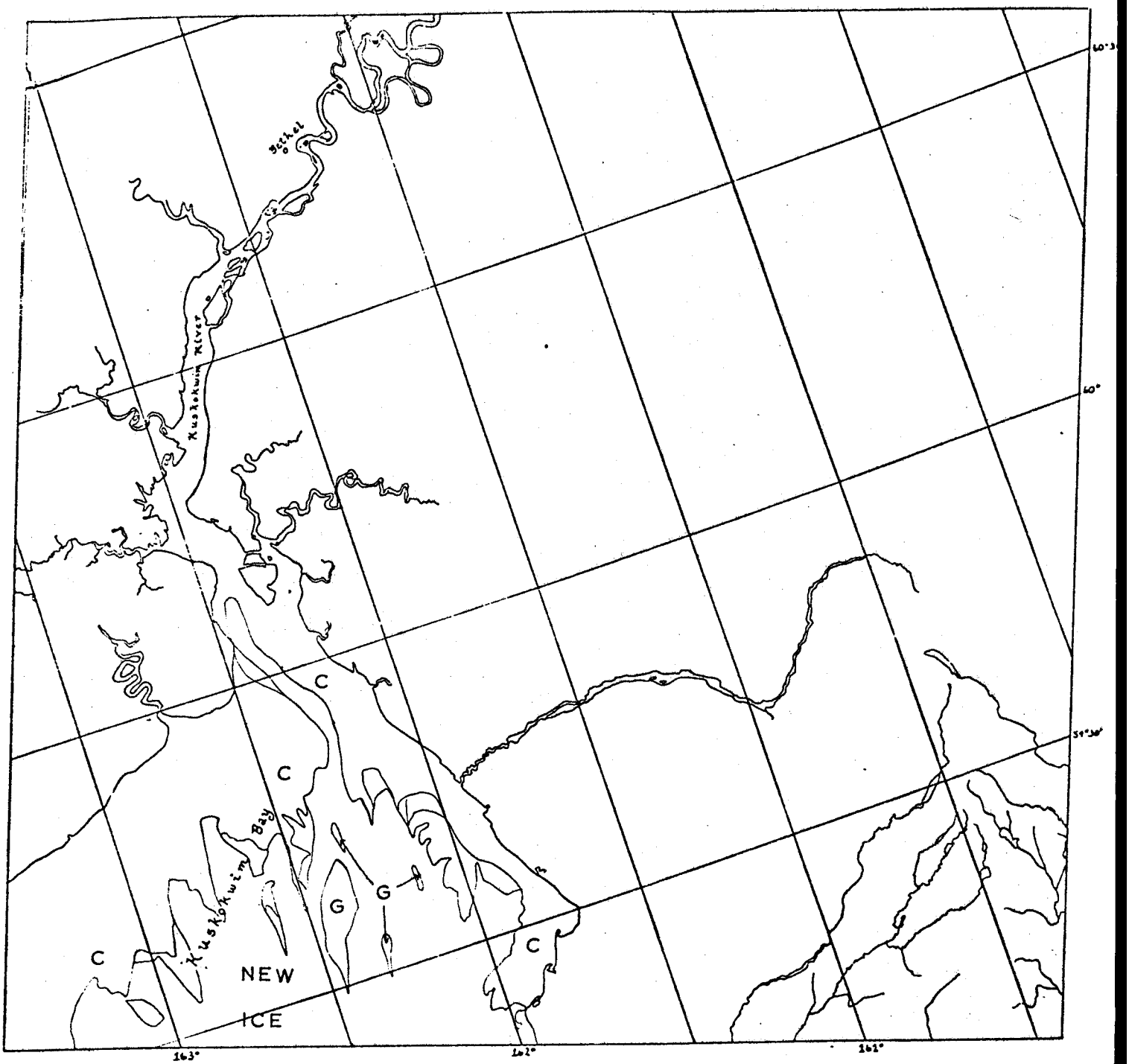

KILOMETERS
0 10 20 30 40 50
SCALE APPROX 1:1,000,000

BERING SEA

E-1596-21270-7
11 MARCH 1974

Scene 1596-21270

This scene, centered on Kuskokwim Bay shows new ice forming in the outer portion of the Bay. There is a considerable extent of contiguous ice in shallow and protected areas around the bay and new ice being formed within the open areas of the bay.

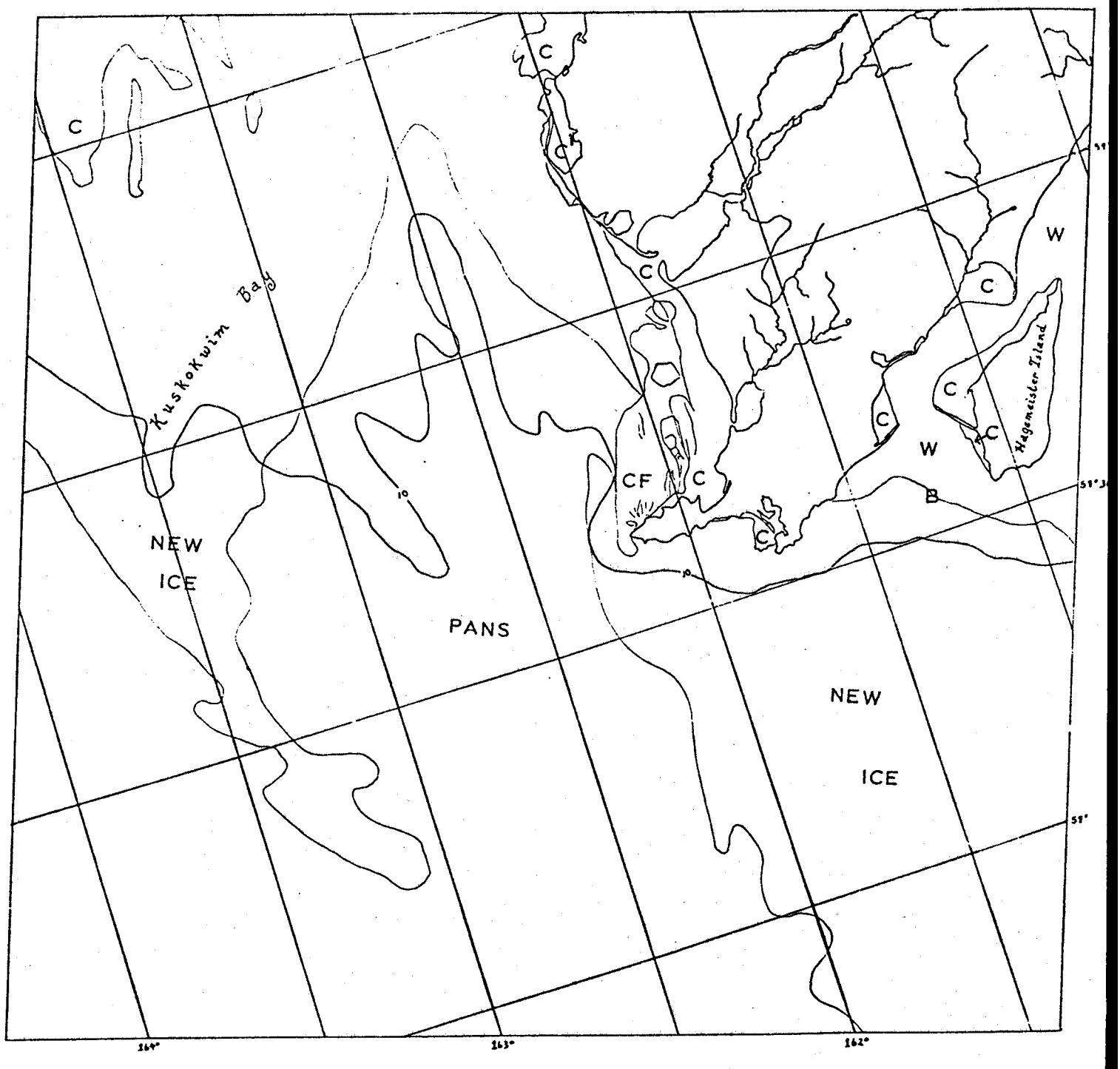

KILOMETERS
0 10 20 30 40 50
SCALE APPROX 1:1,000,000

BERING SEA

E-1596-21273-7
11 MARCH 1974

Scene 1596-21273

There is very little contiguous ice alone the shore in this image except on the north side of Cape Newenham. There, the contiguous ice is being broken off by the force of the pack ice moving south. The part of Bristol Bay that can be seen has a thin veneer of quite new ice south of Hagemeister Island whereas the areas around Hagemeister Island are almost totally ice-free. The increasing age and thickness of the ice westward from Bristol Bay indicate the ice is moving out of Bristol Bay.

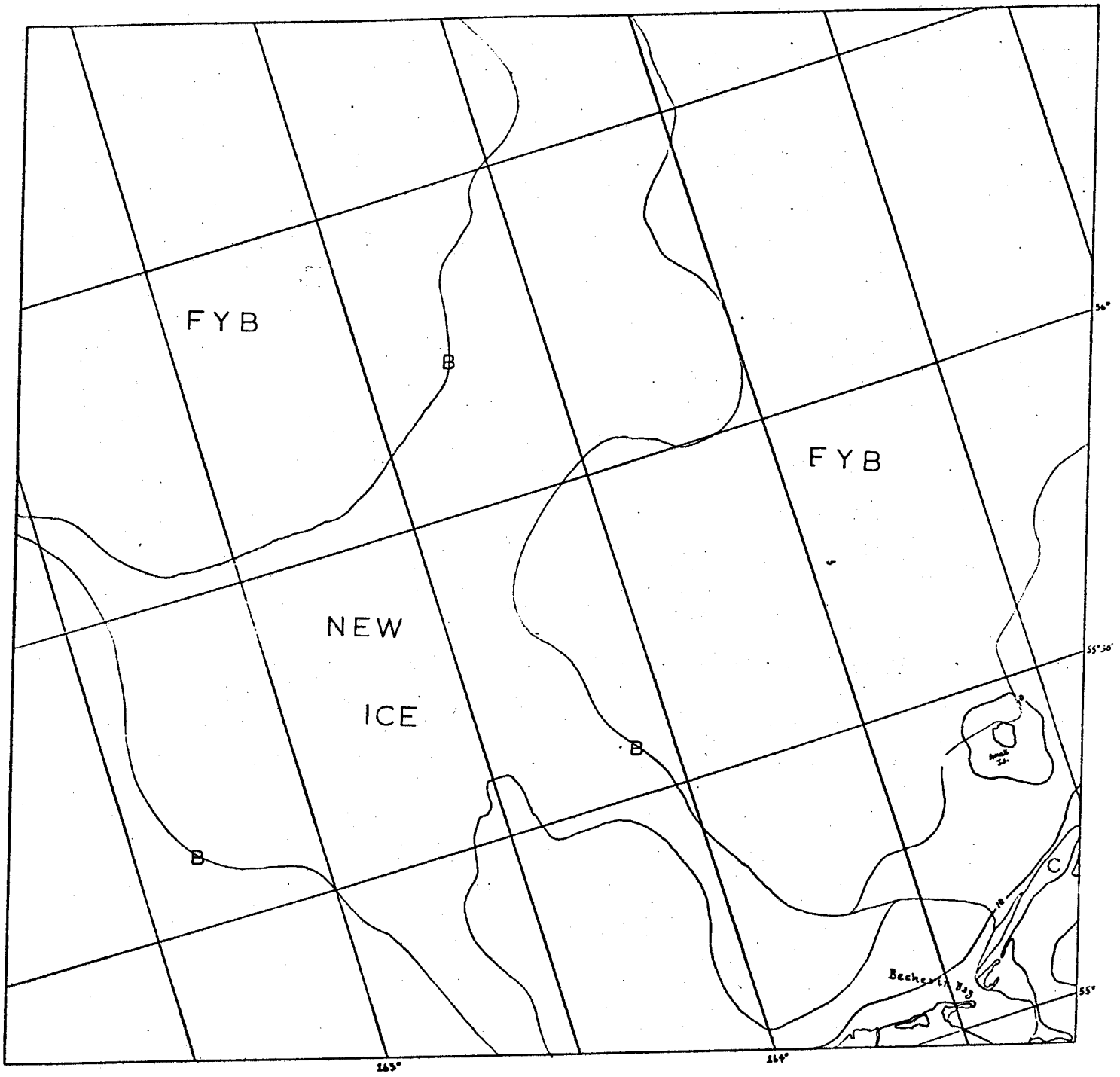

KILOMETERS
0 10 20 30 40 50
SCALE APPROX 1:1,000,000

BERING SEA

E-1596-21282-7
11 MARCH 1974

Scene 1596-21282

This scene shows Becherin Bay as the southern limit of contiguous ice along the Alaska Peninsula.

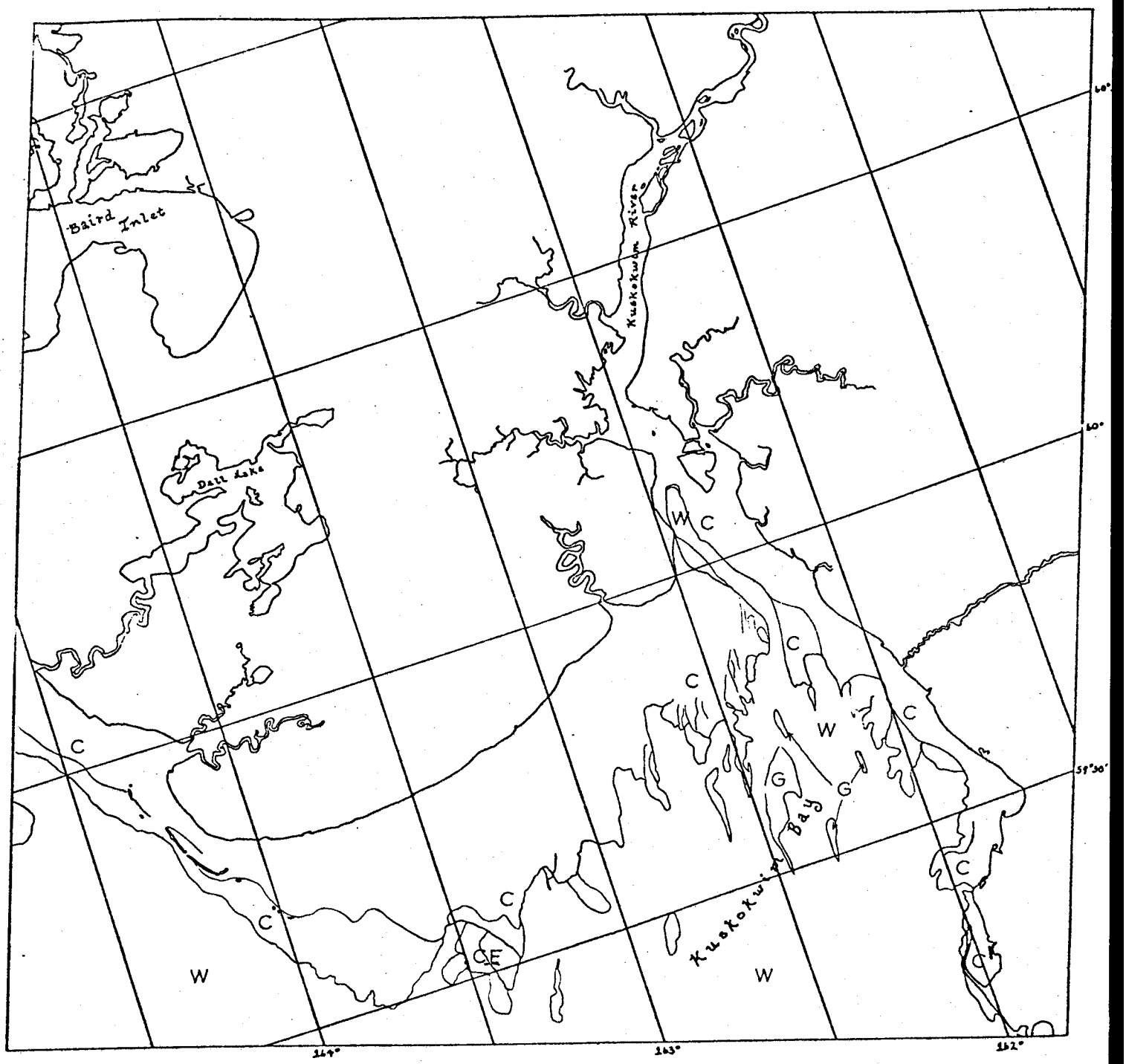

E-1597-21325-7
12 MARCH 1974

KILOMETERS
0 10 20 30 40 50
SCALE APPROX 1:1,000,000

BERING SEA

Scene 1597-21325

Kuskokwim Bay is the central feature in this scene. Contiguous ice can be found in protected and shallow areas. In several locations fragments of detached ice can be seen adjacent to the contiguous ice.

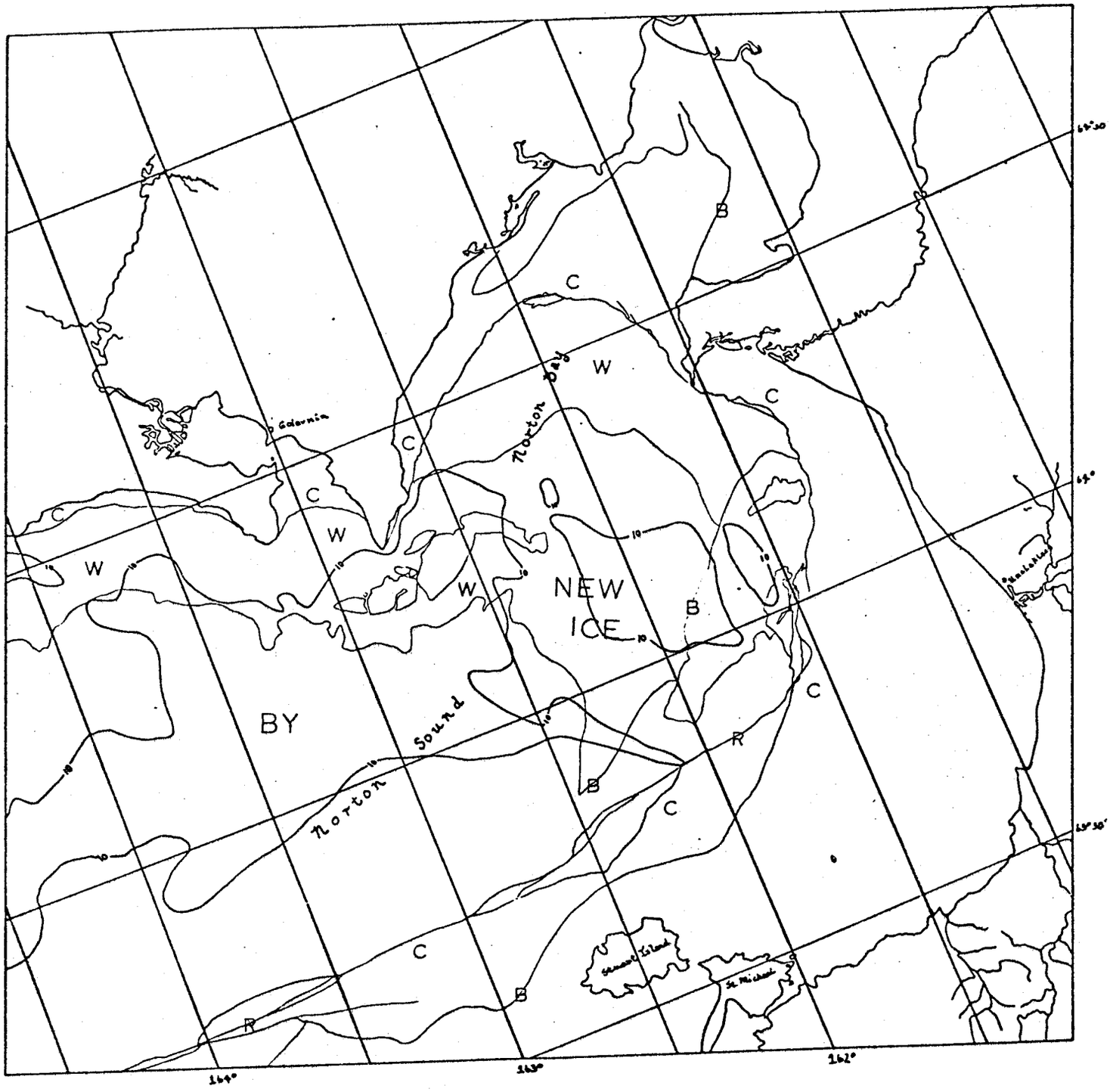

E-1599-21430-7
14 MARCH 1974

KILOMETERS
0 10 20 30 40 50
SCALE APPROX 1:1,000,000

BERING SEA

Scene 1599-21430

As usual for Norton Sound, this scene is rather complicated. The pack of broken-up first year ice has withdrawn leaving large areas of open water. In many areas the contiguous ice has become fairly old. Shear ridges appear along the southern shore of the sound.

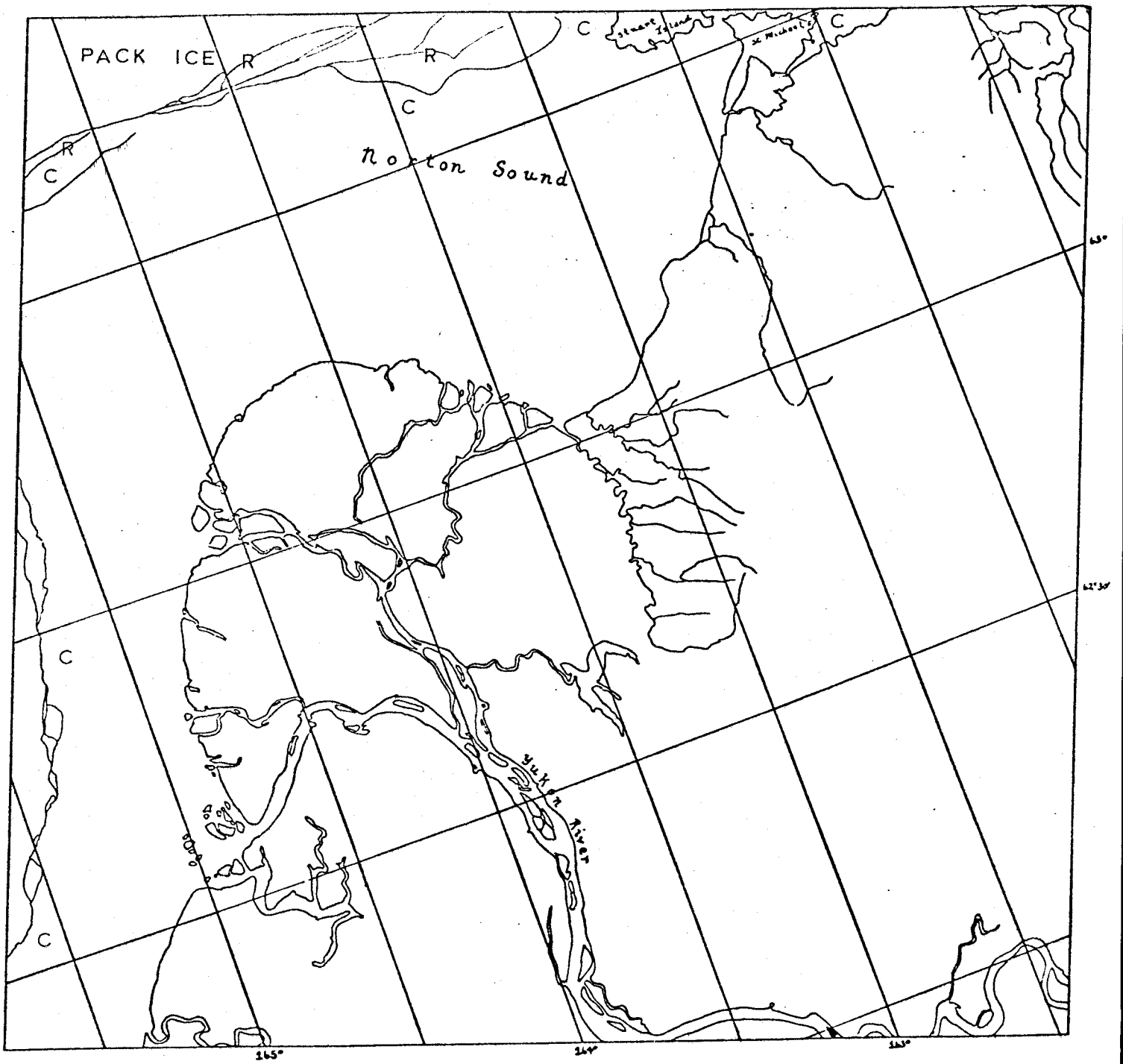

KILOMETERS
0 10 20 30 40 50
SCALE APPROX 1:1,000,000

BERING SEA

E-1599-21432-7
14 MARCH 1974

Scene 1599-21432

This scene features the Yukon Delta. Around the delta there is considerable contiguous ice on the rather shallow outwash plain. On the north side of the delta there are significant shear ridges apparently produced by ice motion in Norton Sound.

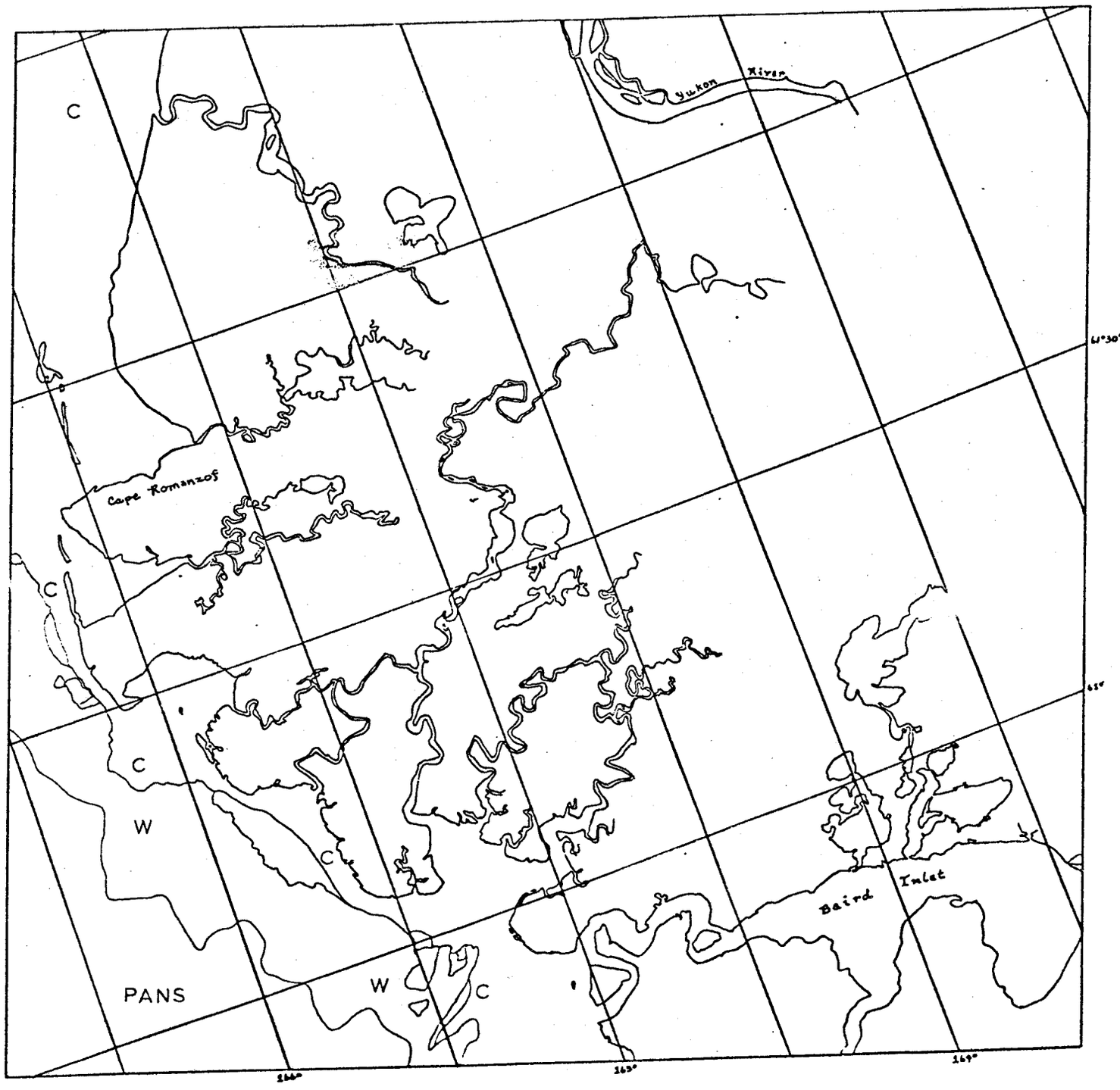

KILOMETERS
0 10 20 30 40 50
SCALE APPROX 1:1,000,000

BERING SEA

E-1599-21435-7
14 MARCH 1974

Scene 1599-21435

This scene centered on Cape Romanzof shows the contiguous ice south of the Yukon Delta as having a quite irregular seaward edge. No large ridge systems are apparent.

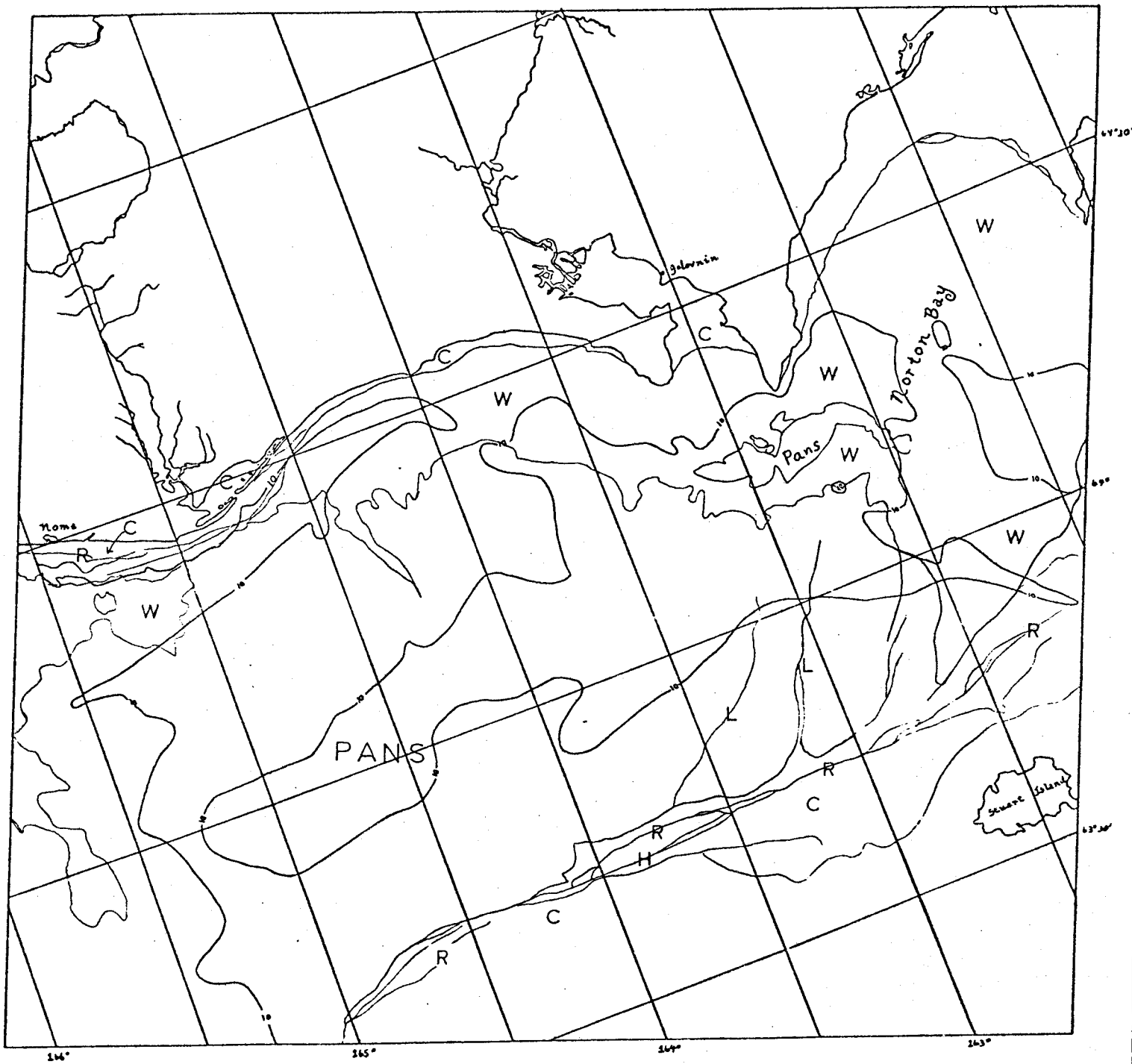

KILOMETERS
0 10 20 30 40 50
SCALE APPROX 1:1,000,000

BERING SEA

E-1600-21484-7
15 MARCH 1974

Scene 1600-21484

This Norton Sound scene shows close correlation between the 10-fathom contour and shear ridges in the Nome area but on the south side of the sound ridges are located considerably shoreward of this contour.

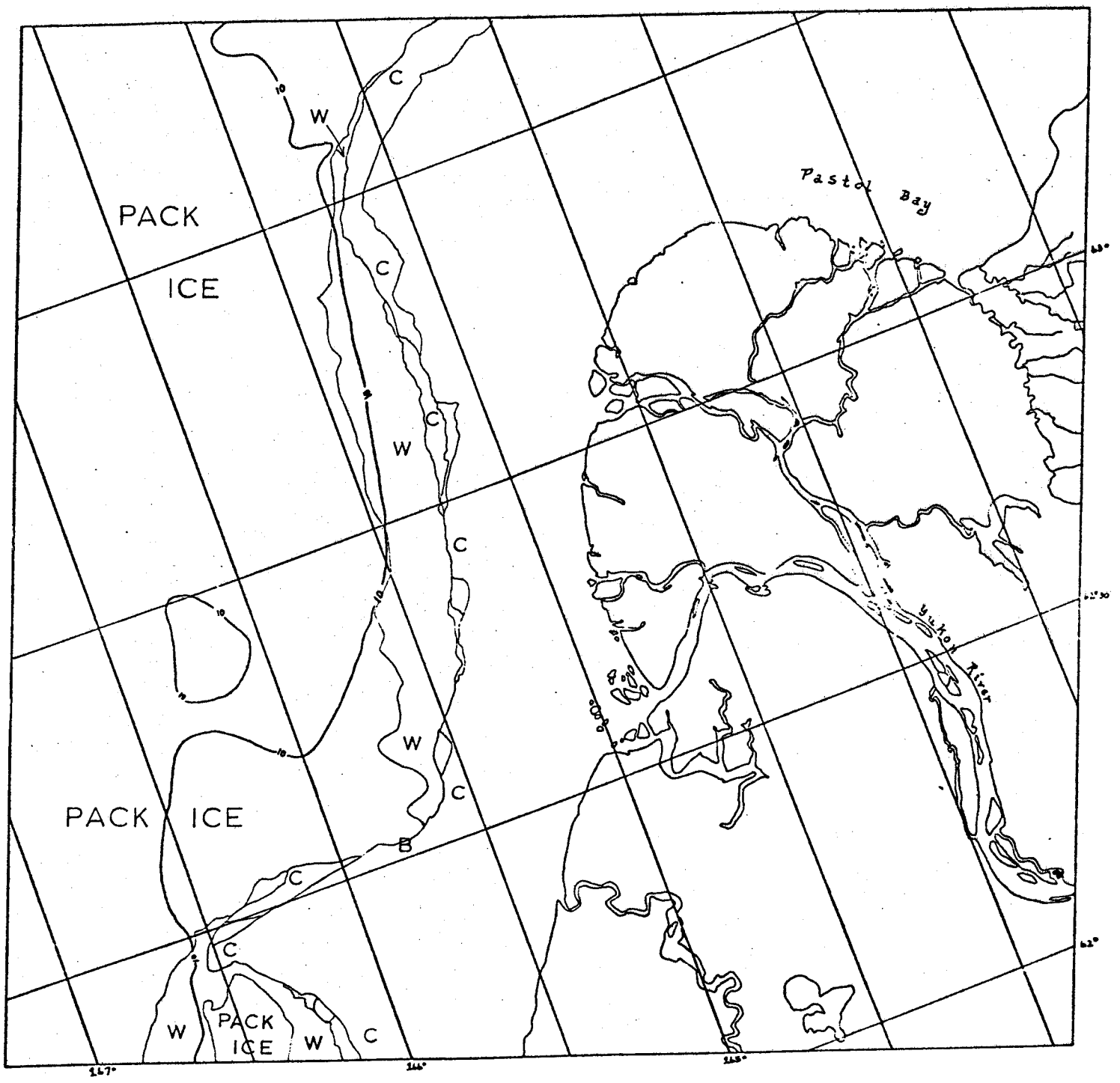

KILOMETERS
0 10 20 30 40 50
SCALE APPROX 1:1,000,000

BERING SEA

E-1600-21491-7
15 MARCH 1974

Scene 1600-21491

The major feature of note on this Yukon Delta scene is the rather large seaward extension of contiguous ice just south of the delta. It may be worthy of note that this feature almost reaches the 10-fathom contour.

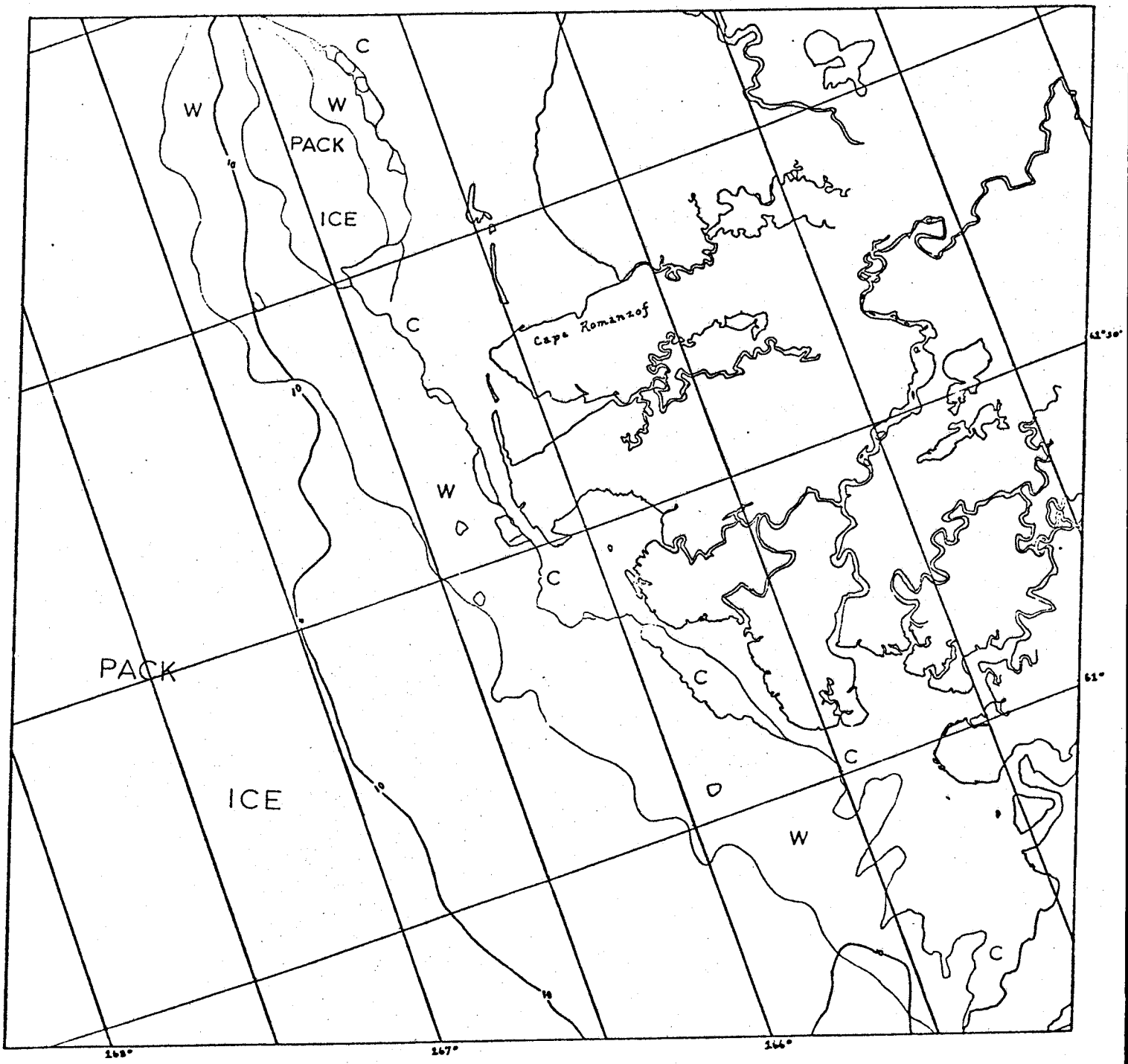

KILOMETERS
0 10 20 30 40 50
SCALE APPROX 1:1,000,000

BERING SEA

E-1600-21493-7
15 MARCH 1974

Scene 1600-21493

This scene is centered on Cape Romanzof. For most of this coastal area contiguous ice is located well inshore of the 10-fathom contour.

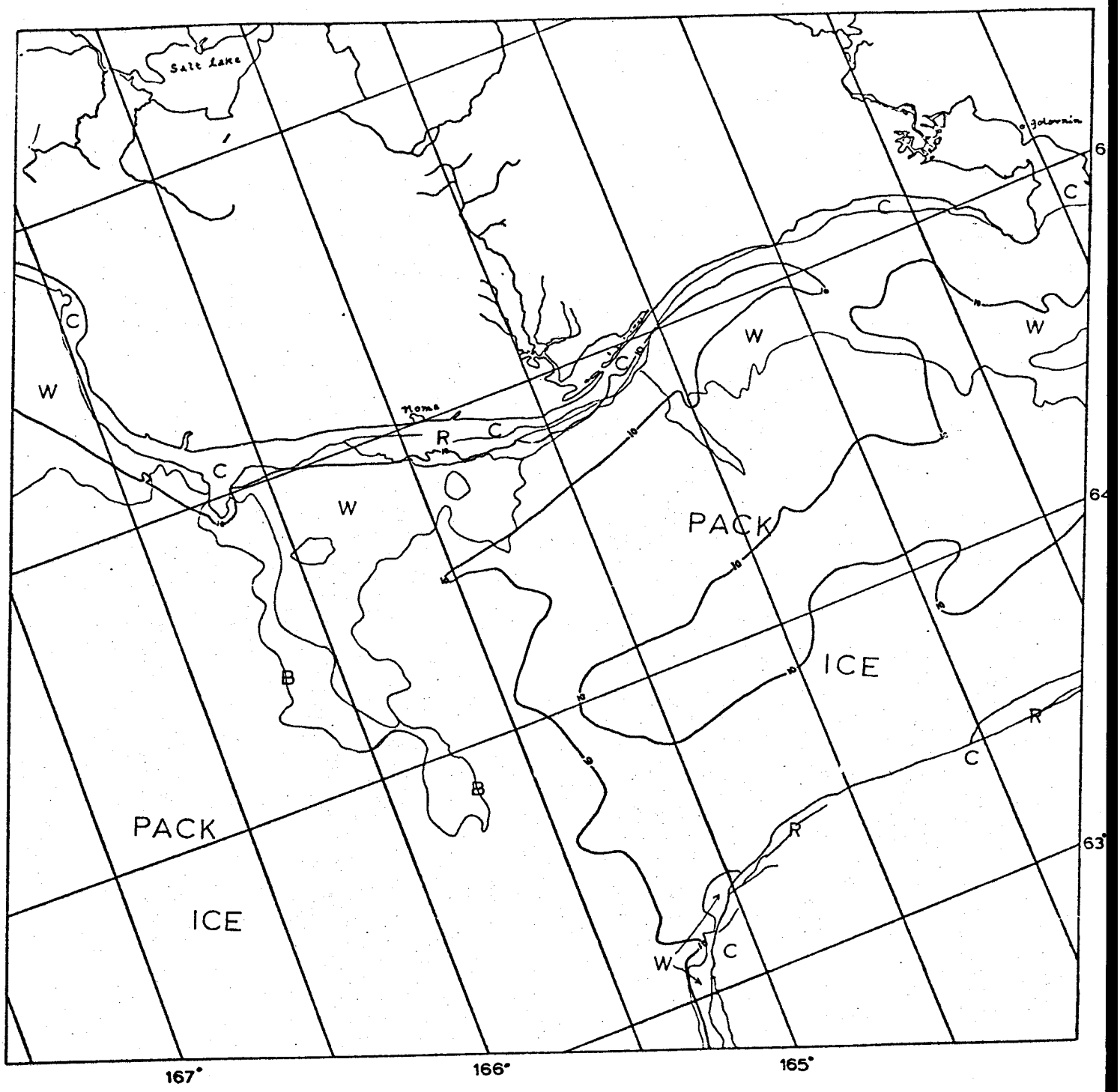

E-1601-21542-7
16 MARCH 1974

KILOMETERS
0 10 20 30 40 50
SCALE APPROX 1:1,000,000

BERING SEA

Scene 1601-21542

This scene is centered on outer Norton Sound. It is interesting to note the close correlation between the edge of contiguous ice and the 10-fathom contour in the Nome area and the absence of this correlation elsewhere. Furthermore, there are major shear ridges in the Nome area associated with the contiguous ice. There are also shear ridges at the edge of the contiguous ice on the south side of the sound but there is not always the same close correlation with the 10-fathom contour.

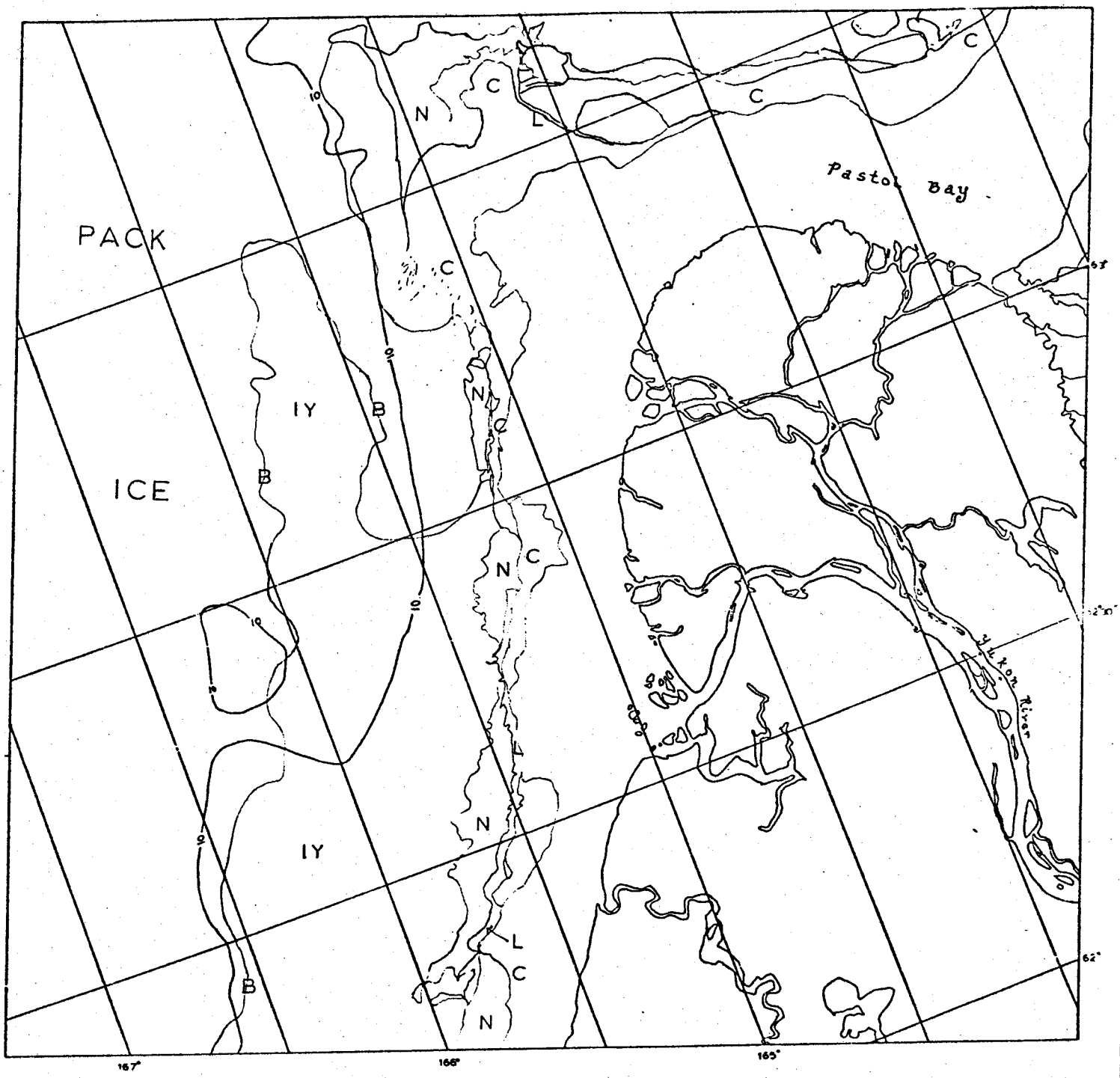

KILOMETERS
0 10 20 30 40 50
SCALE APPROX 1:1,000,000

BERING SEA

E-1942-21374-7
20 FEB. 1975

Scene 1942-21374

This scene of the Yukon Delta area shows contiguous ice confined to the relatively shallow areas near the shore. In some locations several thicknesses of contiguous ice are apparent.

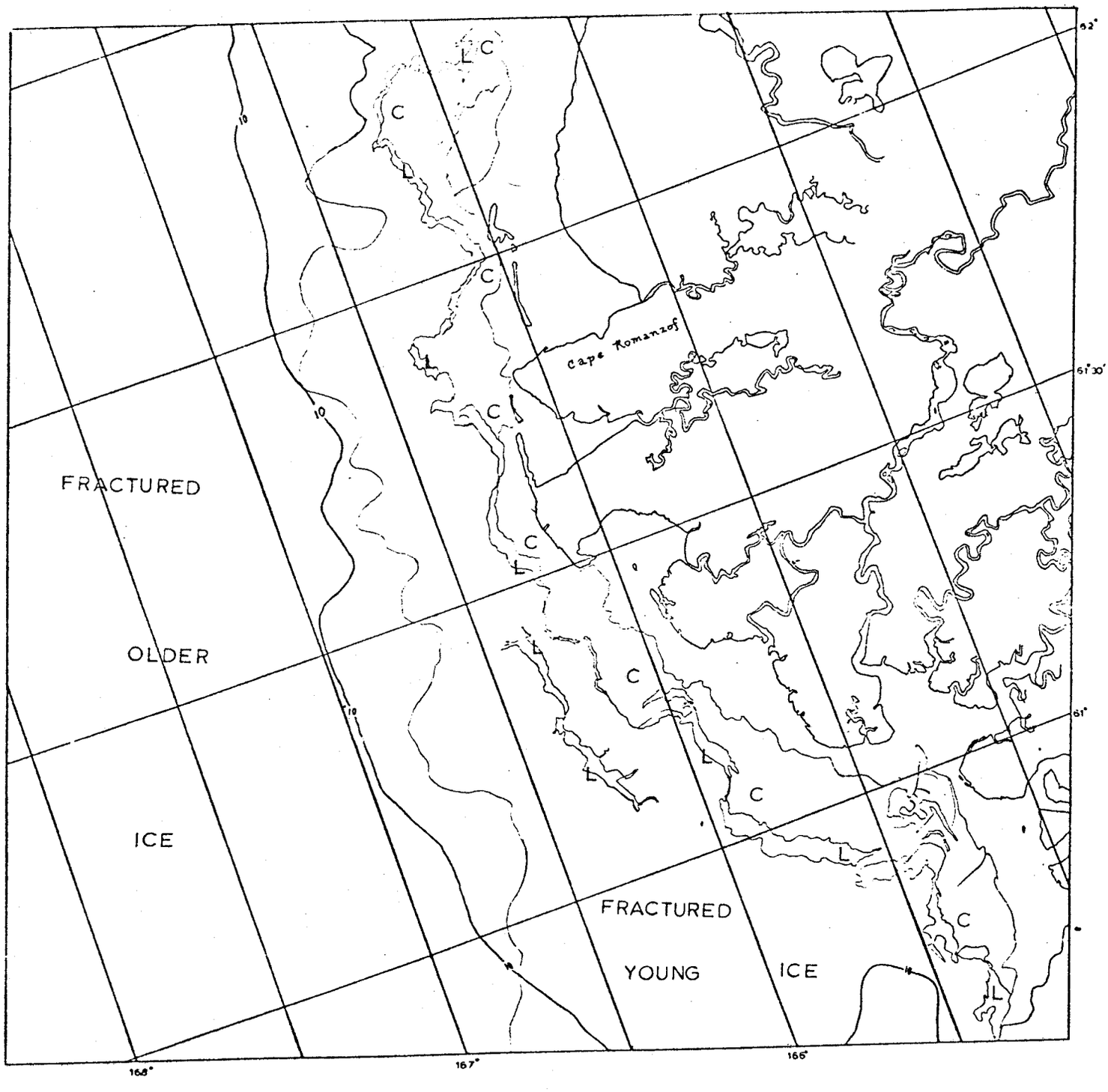

E-1942-21380-7
20 FEB. 1975

KILOMETERS
0 10 20 30 40 50
SCALE APPROX 1:1,000,000

BERING SEA

Scene 1942-21380

This scene of the Cape Romanzof area shows two main ages of contiguous ice. Near shore, in well protected areas there is relatively permanent, thick ice. Seaward of this there is in places a second belt of much younger ice. This young ice has just been formed. It extended out to the edge of older ice located approximately at the 10-fathom contour. Very recently tension has been applied and extensive lead systems have occurred defining a seaward limit of this new contiguous ice.

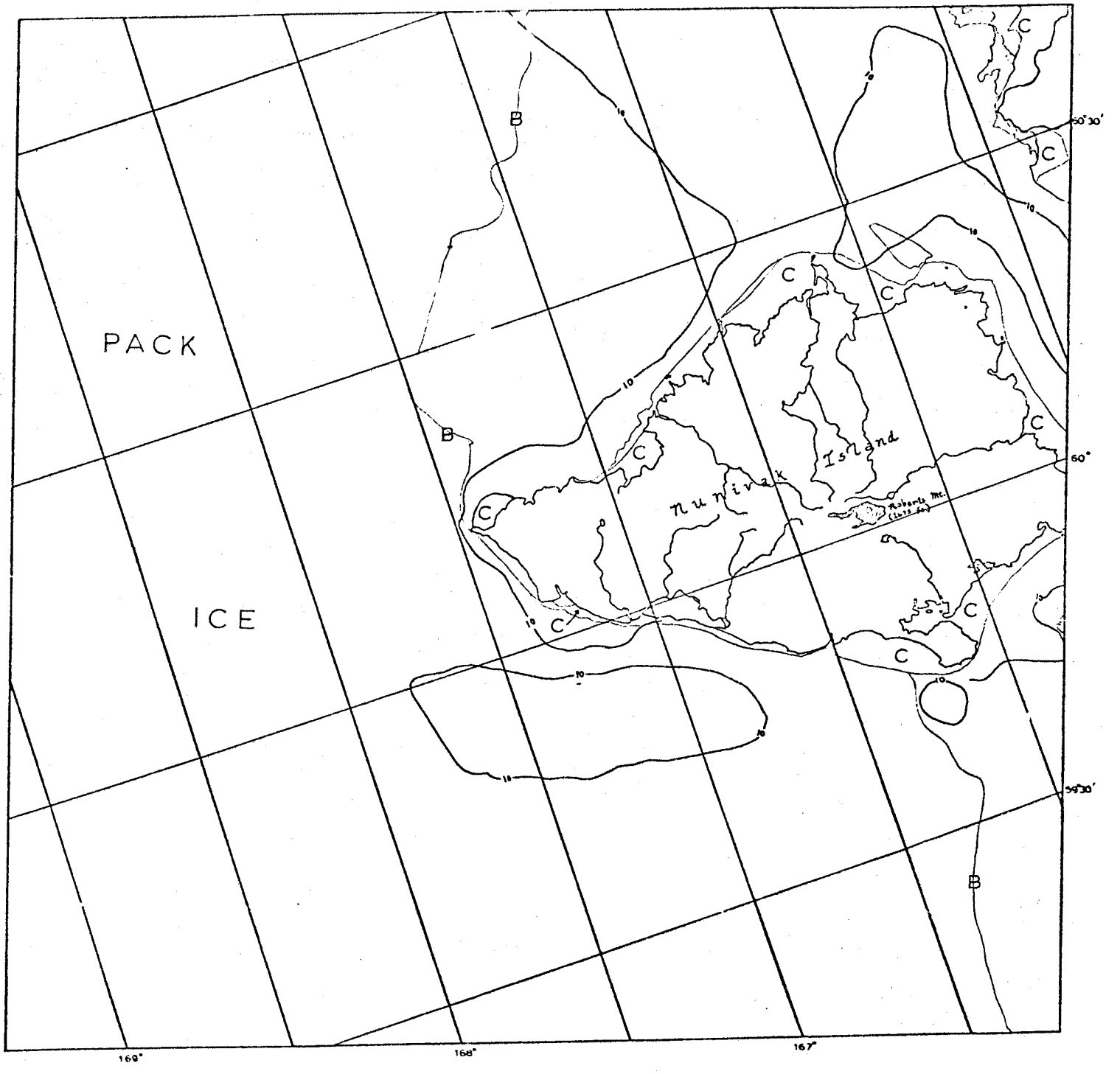

KILOMETERS
0 10 20 30 40 50
SCALE APPROX 1:1,000,000

BERING SEA

E-1942-21383-7
20 FEB. 1975

Scene 1942-21383

This scene of Nunivak Island shows contiguous ice only in shallow and well-protected areas. The large piece of contiguous ice on the south side of Nunivak Island is relatively new while on the north side of the island a large piece of contiguous ice has broken off and is being carried away.

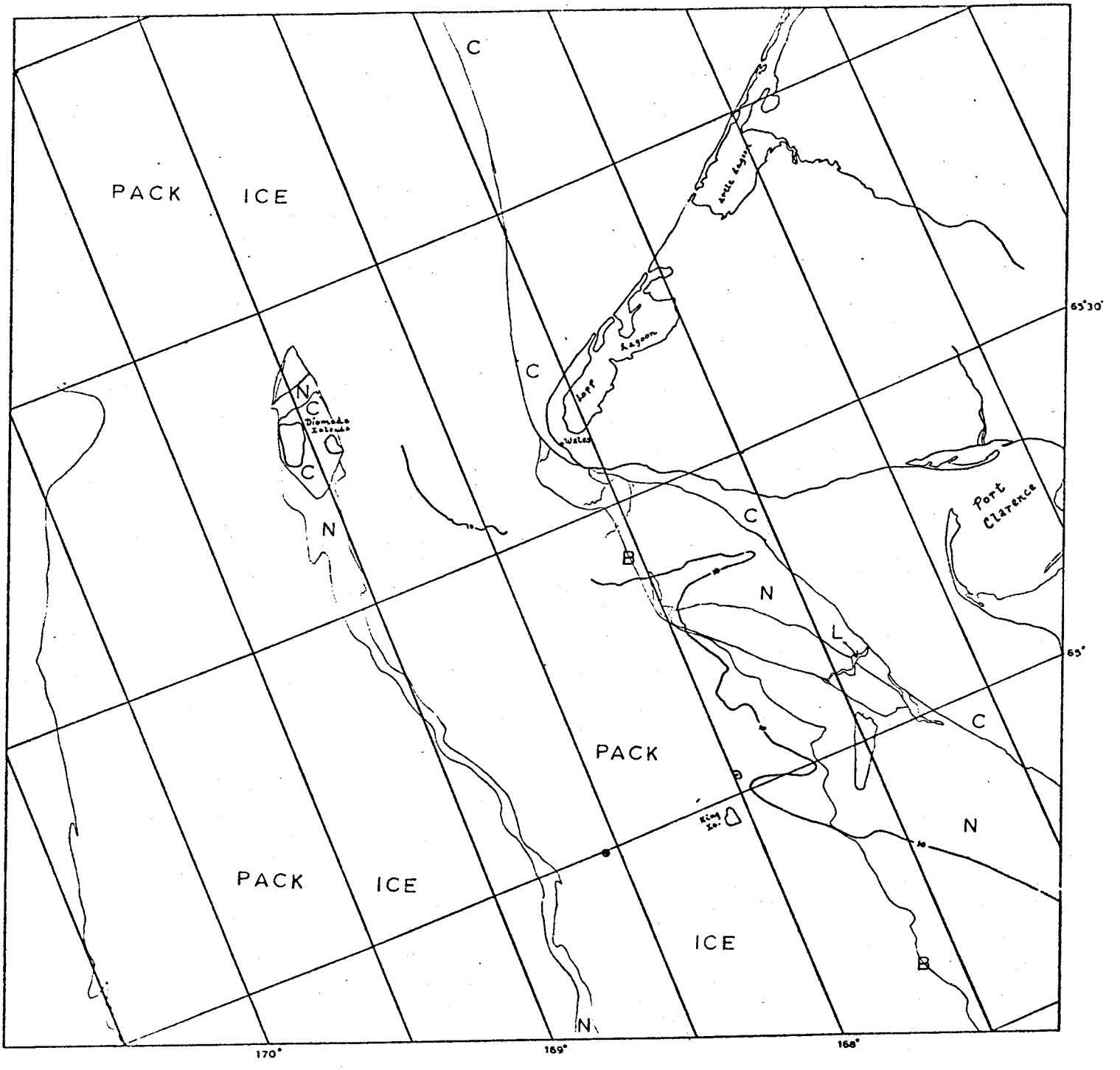

KILOMETERS
0 10 20 30 40 50
SCALE APPROX 1:1,000,000

BERING SEA

E-1946-21594-7
24 FEB. 1975

Scene 1946-21594

This Bering Strait image shows the result if ice motion through the strait. Ice contiguous to the mainland is considerably inshore of the 10-fathom contour south of the strait. On the other hand, depths around the Diomede Islands are on the order of 30 fathoms, and contiguous ice surrounds the islands and fills the gap between them.

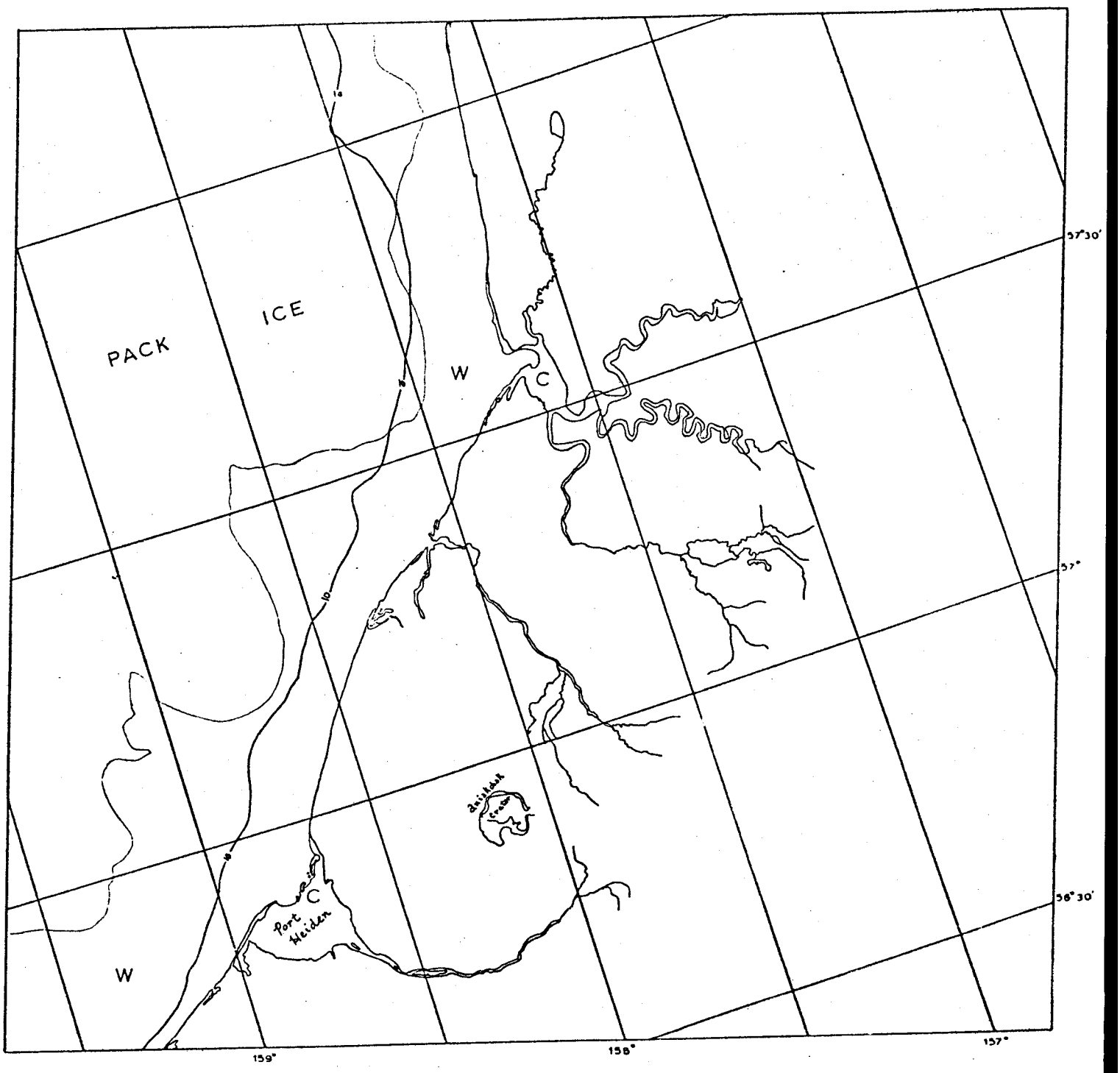

KILOMETERS
0 10 20 30 40 50
SCALE APPROX 1:1,000,000

BERING SEA

E-1952-20530-7
2 MARCH 1975

Scene 1952-20530

This scene shows the Alaska Peninsula between Ugashik Bay and Port Heiden. The only contiguous ice to be found here is in very well protected areas.

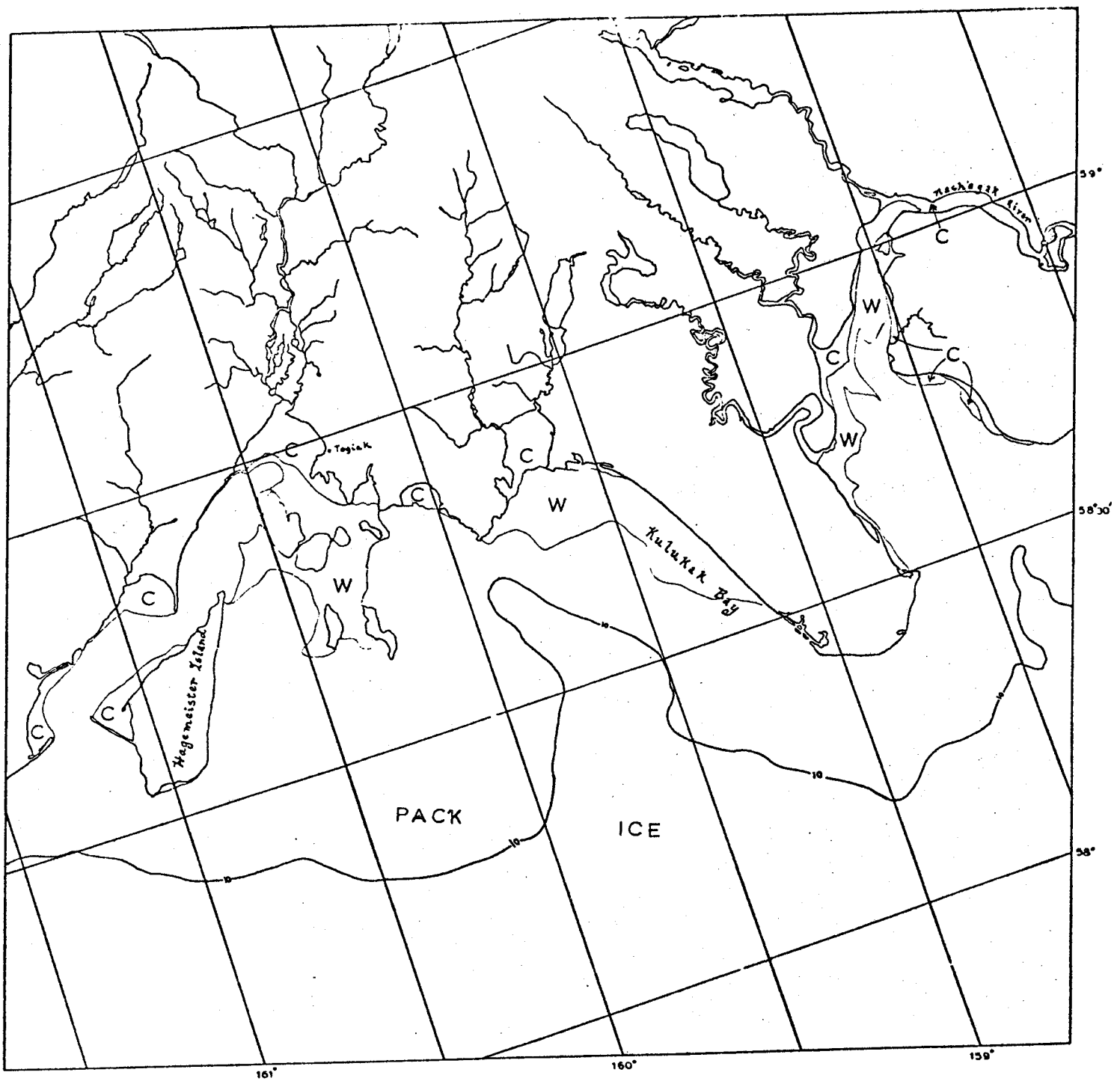

KILOMETERS
0 10 20 30 40 50
SCALE APPROX 1:1,000,000

BERING SEA

E-1954-21040-7
4 MARCH 1975

Scene 1954-21040

This scene shows the regions of Bristol Bay between Nushagak Bay and Hagemeister Island. Contiguous ice is found in protected areas and on shallow areas well away from the 10-fathom contour. Along most of the coast there is open water at this time.

XI. PLANS FOR SUBSEQUENT REPORTING PERIODS

A. 5th Quarter. During this quarter we anticipate completion of retroactive sea ice maps for 1973, 1974 and 1975. Mapping of special events noted during the preparation of retroactive maps and epoch summary maps generalizing seasonal ice conditons will be initiated.

B. 6th Quarter Special event and epoch summary maps will be completed. Based on the retroactive maps, special event and epoch summary maps and meterological data, a preliminary morphology of Bering Sea ice conditons will be prepared.

XII. REFERENCES

Colovocresses, A. P. and R. B. McEwen, 1973. Progress in cartography, EROS Program. Printed in Proceedings of NASA Sumposium on Significant Results Obtained from the Earth Resources Technology Satellite-I, Published by the National Aeronautics and Space Administration, 1973.

Kovacs, A. and M. Mellor, 1974. Sea ice morphology and ice as a geologic agent in the southern Beaufort Sea. Printed in the Proceedings of the Symposium on Beaufort Sea Coast and Shelf Research, Published by the Arctic Institute of North America, December 1974.

Stringer, W. J., 1974a. Shore-fast ice in vicinity of Harrison Bay, Printed in the Northern Engineer, Vol. 5, No. 4, Winter 1973/74.

Stringer, W. J., 1974b. The morphology of Beaufort Sea shorefast ice. Presented at the Beaufort Sea Symposium, January 1974, and published in the Proceedings of the Arctic Institute of North America, December 1974.

Zubor, N. N. 1943, Arctic Ice. U.S. Navy Oceanographic Office translation from Russian.

RU#258

OCS COORDINATION OFFICE

University of Alaska

ANNUAL REPORT

Project Title:	Morphology of Beaufort Near Shore Ice Conditions by Means of Satellite and Aerial Remote Sensing
Contract Number:	03-5-022-55
Task Order Number:	8
Principal Investigator:	W. J. Stringer

I. SUMMARY OF OBJECTIVES, CONCLUSIONS AND IMPLICATIONS WITH RESPECT TO OCS OIL AND GAS DEVELOPMENT

The objective of this study is to develop a comprehensive morphology of ice conditions in the near-shore areas of the Beaufort Sea with special emphasis given to ice conditions which might be hazardous to offshore petroleum exploration and development. The preliminary conclusions is that within a certain range of variability, ice conditions along the Beaufort coast are predictable: for several months a great deal of reliability can be placed on the existence of a stable sheet of ice extending to roughly the location of the 10-fathom contour. The precise location of the stable ice boundary will be determined from the morphology being developed. Beyond this stable ice boundary, dynamic ice events can occur at any time depending largely on meterological conditions. The implications to OCS oil and gas development are that within the stable ice boundary, for several months of the year, ice conditions are favorable to the use of the ice surface for exploration and other activities. Beyond this boundary conditions become unreliable or predictably hazardous.

II. INTRODUCTION

A. General Nature and Scope of Study

The objective of this study is to develop a comprehensive morphology of near shore ice conditions in the Beaufort Sea. This morphology will include a synoptic picture of the development and decay of fast ice and related features along the Beaufort Sea coast, and in the absence of fast ice, the nature of other ice (pack ice, ice island, hummock fields, etc.) which may occasion the near shore areas in other seasons. Special emphasis will be given to consideration of potential hazards to offshore facilities and operations created by near shore ice dynamics. A historical perspective of near shore ice dynamics will be developed to aid in determining the statistical rate of occurrence of ice hazards.

B. Specific Objectives and Relevance to Problems of the Petroleum Industry

There are two categories of results to be anticipated. The first category consists of direct data products while the second consists of indirect data products, which will be combined with studies performed by others within the study program.

Direct Data Products: These products would consist of a morphology of Beaufort Sea near shore ice and a series of maps showing persistent locations of major ice features including ice hazards within the near shore zone. These include the locations of large grounded pressure ridge systems, the location of summertime pack ice visits to the near shore areas and the drift pattern of ice islands. The morphology developed will provide a comprehensive picture of the development and decay of fast ice and the description of the sea ice cover on the Alaskan

Continental Shelf.

Indirect Data Products: The morphology developed would yield information toward the determination of ice movement and deformation mechanism in the coastal fast ice zone. The ice type maps will indicate where to apply data relating stress-strain relationships to man-made and natural structures. The mapped pressure ridge locations and sites of ice island groundings will provide data toward a predictive technique for ice-scoring processes. The assembled data will be of use to the study of the relationship of living resources to the ice environment.

III. CURRENT STATE OF KNOWLEDGE

The general description of ice in near-shore areas has been investigated and reported. For instance, Zubov (1943) discusses a variety of near-shore ice conditions. Most recently, Kovacs and Mellor (1973) have given a review of the state of knowledge of sea ice including near-shore ice. The principal near-shore ice, fast ice, has been investigated to the point that several general parameters have been accepted -- at least in terms of Beaufort Sea shore-fast ice. Briefly these are:

a) Sometime around midwinter, the ice along the shoreline is no longer subject to breaking free and exposing open water except under the most unusual circumstances.

b) This "shorefast" ice sheet may contain many pressure ridges. Its seaward edge is defined by the most seaward grounded pressure ridge.

c) Bottom sediments appearing in the piled ice are generally taken to be evidence that a pressure ridge is grounded.

d) The most seaward grounded pressure ridge is characteristically near the 18-m contour.

e) From time to time, a floating sheet of ice can be attached to the shore-fast sheet and extend many kilometers farther seaward.

f) The grounded pressure ridge system endures into summer, sometimes as late as mid-July.

Virtually nothing is known about the dynamic morphology of shore-fast ice: formation processes, stress-induced changes, year-to-year variations in location of its edge and locations of hummock fields, stability and other parameters related to specific weather patterns or geomorphological features.

IV. STUDY AREA

The geographic area under study by this project is the near-shore area of the Beaufort Sea coast of Alaska. This coastal zone is bounded on the east by the Canadian border and Point Barrow on the west. In addition, starting this next reporting period our geographic study area will be extended to the Chukchi coast of Alaska, which will include the near-shore areas from Barrow on the north to the Bering Strait on the south.

V. SOURCES, METHODS AND RATIONALE OF DATA COLLECTION

Past and historical data from all seasons will be used to compile a series of maps of the Beaufort Sea near-shore areas denoting summer and fall pack ice behavior, fall freezing characteristics and growth and decay of the fast ice zone. Particular attention will be paid to the behavior of ice islands and other large free ice features, hummock fields, pressure and shear ridges, open and refrozen leads, etc. A written morphology associating ice behavior patterns with winds,

storms, currents, temperature and bathymetric data will be developed (see, for instance, Stringer, 1974a).

1. Sampling Strategy

Remote Past (preERTS): Data gathered by investigators analyzing historical records will be incorporated into the morphology, generally to confirm persistent locations of major ice features or determine patterns of extreme behavior. This investigator anticipates continuous interaction with the investigators researching historical ice records. In conjunction with them, a map of historical ice behavior can be developed. Historical information can be utilized to determine locations to give particular attention to at present. Similarly, present data may give them additional information toward interpretation of historical data.

Immediate Past: ERTS imagery will be combined with aerial photographic surveys performed in the past by the author and others (NASA, USGS) to perform a detailed and comprehensive study of nearshore ice previous to this time. Thus maximum utilization will be made of the 2-1/2 years of ERTS data which has been collected and archived at the University of Alaska ERTS archives. It is anticipated that this data can be nearly as valuable as ERTS data taken during this study. However, the project airborne remote sensing activities are anticipated to enhance the utility of present ERTS data over past ERTS data.

Present: ERTS imagery combined with data obtained by project remote sensing aircraft will be used to monitor the behavior of shore-fast and other ice within the near-shore zone. It is anticipated that interaction will take place with many other investigators studying related subjects (shear zone ice dynamics, pressure ridge modeling, sea mammal habitate, etc.) to yield additional information for incorporation into development of a coastal ice morphology.

VI. RESULTS

(Note: Because of our internal management requirements, no funds were expended nor was work performed until contract negotiations were final on June 30, 1975.)

During the first quarter under funding Landsat coverage maps were prepared for each Landsat cycle. A near-shore ice map will be drawn for each of these data cycles. These maps will generally be produced at 1:500,000 scale by using hard copy of 1:500,000 scale Landsat prints. During this quarter, based on the Landsat coverage maps described above, hard copy at 1:500,000 scale was ordered for the earliest Landsat cycle with reasonably complete coverage for each winter season. At the end of the quarter, approximately 50% of the order had arrived.

In order to expedite the map-making process, 1:500,000 scale prints of the scenes selected for hard copy for the winter, 1974 season were ordered from the Geophysical Institute's special photo section. This process is considerably more expensive than ordering prints from the USGS Sioux Falls Photographic Laboratory. Unfortunately, although every attempt was made by us to insure proper scale, the resulting prints were produced at a scale quite far from 1:500,000. As a result, all

attempts at mapping were postponed until arrival of the Sioux Falls hard copy.

A major accomplishment during this reporting period was the preparation of the transparent map overlays to be used to transfer the Landsat data to a geographic map at 1:500,000 scale Lambert Conformal Conic Projection map prepared by the Department of Commerce. Second, bathymetric data was transferred from NOAA Coast and Geodetic Survey Nautical Charts at varying scales to 1:500,000 by means of a pantograph. These overlays became the map base for the maps produced by this project.

During this reporting period we moved into larger quarters and took delivery of our drafting table, map cases and other equipment described in the University of Alaska OCS 5 and 8 budgets.

During the second quarter under funding using Landsat band 7 hard copy produced at 1:500,000 scale, preliminary Beaufort Sea near-shore ice maps were compiled for late winter (Feb.-March) 1973, 1974 and 1975. These maps were reproduced at half scale for reporting convenience. Particular care was taken to locate the ice features relative to geographic coordinates and bathymetric 10-fathom contours. Half-scale reproductions of these maps were reproduced with annotation discussing the features delineated as part of the quarterly report for the period ending Dec. 31, 1975.

It should be stressed that these maps are not final products but represent an initial stage of interpretation of each year's ice conditions. For instance, even though large ridge systems can be identified, many others are shown here as boundaries between distinctive ice categories. Analysis of later Landsat images during the melt season will determine

to a greater extent the complete identification of these and other features.

No attempt was made here to delinate "shore-fast" ice. Indeed, at this season only "contiguous" ice (ice that is contiguous with the shore without interruption) can be identified. However active lead systems in the vicinity of the near-shore areas can be monitored for ridge-building activities.

By making these late winter maps, the relative age of major features can be established. For instance, a very extensive ridge system had been formed north and west of Cross Island (off Prudhoe Bay) well before March 10, 1974. This ridge system was located near the 10-fathom contour. Presumably, it was grounded. Analysis of melt season data should give a clue regarding this hypothesis. Another question to be answered by subsequent analysis is "Did this ridge system create a relatively stable ice shelf shoreward?"

During the third quarter under funding, spring sea ice maps for 1973 were drawn. This season yielded an extremely valuable cycle of Landsat coverage with no gaps resulting fron cloudiness. Half scale reproductions of these maps with annotation appear in this report as part of Section X, Summary of 4th Quarter Operations.

VII. DISCUSSION OF PRELIMINARY RESULTS

Although analysis of data is not yet complete a preliminary discussion of results to date can be made.

In general, ice conditions along the Beaufort coast are sufficiently uniform that ice morphology for different geographic areas need not be described separately. Here, these generalitics will be discussed without reference to specific geographic localities. However, the final

morphology developed will include a detailed map of the Beaufort coast and specific references to particular locations. The general aspects of Beaufort Sea morphology observed are:

A. By mid-February the seaward limit of ice contiguous with the shore can be well beyond the 10-fathom contour. When shearing motions do take place they are roughly along the line parallel to a segmented line drawn between prominent coastal headlands. There appears to be a tendency for this line of shear to be located seaward in mid-winter and move shoreward as the season advances. Although determination of the location of truly grounded ice delineating the boundary of shore-fast ice will depend on detailed analysis of late spring and summer imagery, it is apparent that the 10-fathom contour is roughly the location of the most seaward grounded ice and therefore during this time the seaward boundary of contiguous ice is beyond the boundary of shore-fast ice.

B. By late March, shearing is often taking place along a line extending along the seaward limits of the 10-fathom contours. Embayments of this contour are ignored by the shearing motion. Often, however, lead systems showing a stress-relief pattern do occur within these areas.

C. Ice translation during these mid-winter shearing events is often quite small --- on the order of 10 to 20 km. This results from the "locked-in" nature of Beaufort Sea ice: the Canadian Archepellago on the east essentially blocks ice motion toward that direction and ice to the west usually only moves in such a way to allow the limited motion noted here.

D. The significance of the above observations is that the grounded ridge systems responsible for shore-fast ice have been created before mid-February when (until this year) Landsat data becomes available after the mid-winter dark period.

VIII. CONCLUSIONS FROM PRELIMINARY RESULTS

The general conclusions of this study to date are that: 1) The over-all pattern of near-shore sea ice conditions repeats from year to year in the Beaufort Sea region and 2) The specific features (hummock fields, shear ridges, etc.) are somewhat predictable and are formed relatively early in the ice season. This would mean that starting with the return of light in February, a relatively stable platform from which to conduct exploration and other petroleum-related activities could be depended upon with some degree of confidence. This, in turn, could be related to a minimal probability of adverse environmental impact resulting from ice-dynamic related environmental hazards as long as the activity was located within a "safe zone".

The determinations of the "safe zone" will be made at the time of construction of the Beaufort Sea near shore morphology, but it is apparent now that it will generally follow the 10-fathom contours. Beyond this "safe zone", depending on yearly ice conditions, areas of relative safety can be defined. The significance of this conclusion is that before the Landsat data from several years had been examined it was not entirely clear that this conclusion could be made.

IX. NEEDS FOR FURTHER STUDY

1. The morphology of Beaufort sea near-shore ice conditions being developed included correlating sea ice dynamic events with meterological conditions. Thus, the morphology will only closely relate these two data sources for the four years of Landsat data availability. In order to test the relative reliability of the morphology developed it will be necessary to test the meterological data correlated with Landsat data against other years' meterological records to determine the statistical reliability of the predictive portions of the morphology. It is believed that this work can be done at least in part based on the results of Mr. William Serby's OCS project being conducted at the Arctic Environmental Information and Data Center.
2. The determination of grounded ice features will largely be based on the behavior of those features during the melt season. However, it would be most useful for predictive models to have ridge height data available for correlation purposes once the relative grounded stability of the feature has been determined. For that reason profile transects would be very useful.

X. SUMMARY OF 4th QUARTER OPERATIONS

The following sets of annotated Beaufort Sea ice maps were prepared from two very complete Landsat cycles during late winter and mid-spring, 1974. Major ice features and the shore have been delineated and the 10-fathom contour shown for correlation of depth to major ice features. As little inference as possible has been made at this stage.

Many features have been designated as "boundaries" which will very likely be identified as pressure and shear ridges after examination of subsequent data. Similarly, "shore-fast" ice has not been delineated but ice contiguous with the shore has been identified. Just which of this "contiguous" ice is "shore-fast" will be determined on the basis of subsequent Landsat scenes.

These maps are reproductions of working products and are, therefore, somewhat complicated. Later maps, based on interpretation of these and later imagery, will be considerably simpler. The original maps are produced at a scale of 1:500,000 and have been reduced here to half-scale for reporting convenience.

BEAUFORT SEA

MARCH 15 - APRIL 3, 1974

IMAGES: 1600 to 1619

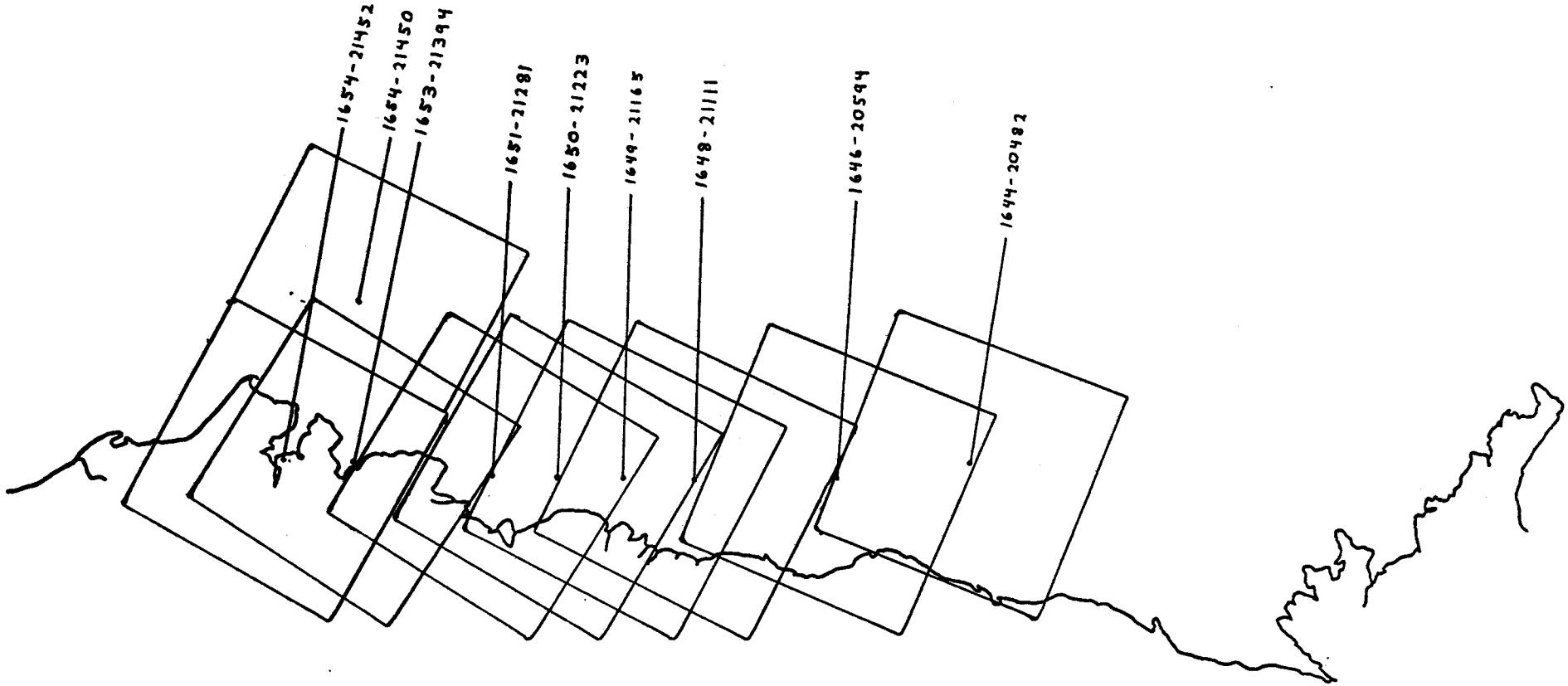

BEAUFORT SEA

APRIL 20 - MAY 8, 1974

IMAGES : 1636 to 1654

SYMBOLS AND DEFINITIONS

B	Boundary between apparently different ice types.
BN	Broken sheet of new ice.
BPN	Pans in broken matrix of new ice.
BPY	Pans in broken matrix of young ice.
BY	Broken sheet of young ice.
C	Stationary ice - ice which is contiguous with the shore.
CF	Fragmented or broken contiguous ice.
F	Ice floe.
FY(B)	First year ice (broken or fragmented).
G.	Grounded ice floe or stranded ice.
H	Hummocked ice - sea ice piled haphazardly one piece over another to form an uneven surface.
IY	Young ice.
L	A lead, usually open, but may be too narrow to determine if it is open or not.
N	Newly refrozen lead or polyna - a lead or polyna composed of dark ice, not yet fractured and milky, or covered with snow, thin enough to allow light to pass through to the water.
O	Old refrozen lead - a lead old enough to have either turned milky with cracks or been covered by snow; thick enough to reflect most of the incident sunlight and thus appear gray to white.
P	Partially refrozen lead, usually some dark ice with open water.
PN	Pans in matrix of new ice.
PY	Pans in matrix of young ice.
R	Ridge system, may be either pressure ridge or shear ridge system.
T	Tidal or tension cracks - cracks due to tidal action in shallow waters, may be indicated by piled ice and/or snow drifts.

W	Open water.
Y	Polynya.
Z	Zone of shear.

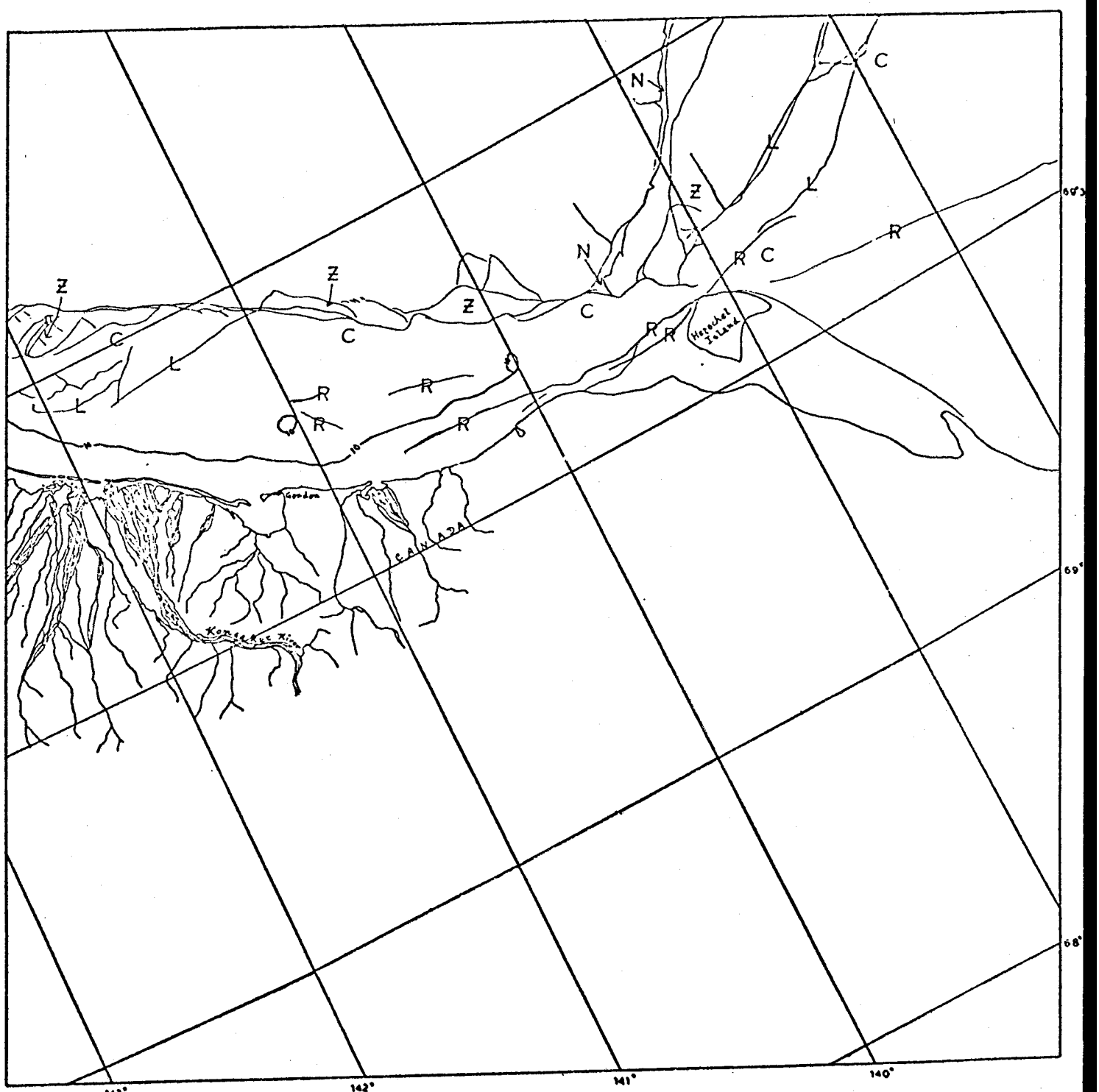

E-1606-20380-7
21 MARCH 1974

KILOMETERS
0 10 20 30 40 50

SCALE APPROX 1:1,000,000

BEAUFORT SEA

Scene 1606-20380

This scene shows the Canadian border portion of the Beaufort coast. A considerable amount of ridge-building has taken place at an earlier time with the resulting ridges and hummock fields now located well within the area of contiguous ice. Over a large part of this scene contiguous ice extends some distance (10's of km) seaward of the 10-fathom contour; at its edge there is a shear zone toward the area of the 10-fathom contour. As is often observed in MacKenzie Bay, a large, reversed "L"-shaped segment of ice has moved several km westward leaving a north-south lead system in the vicinity of Herschel Island. This westward motion created the zone of fractured ice mentioned earlier.

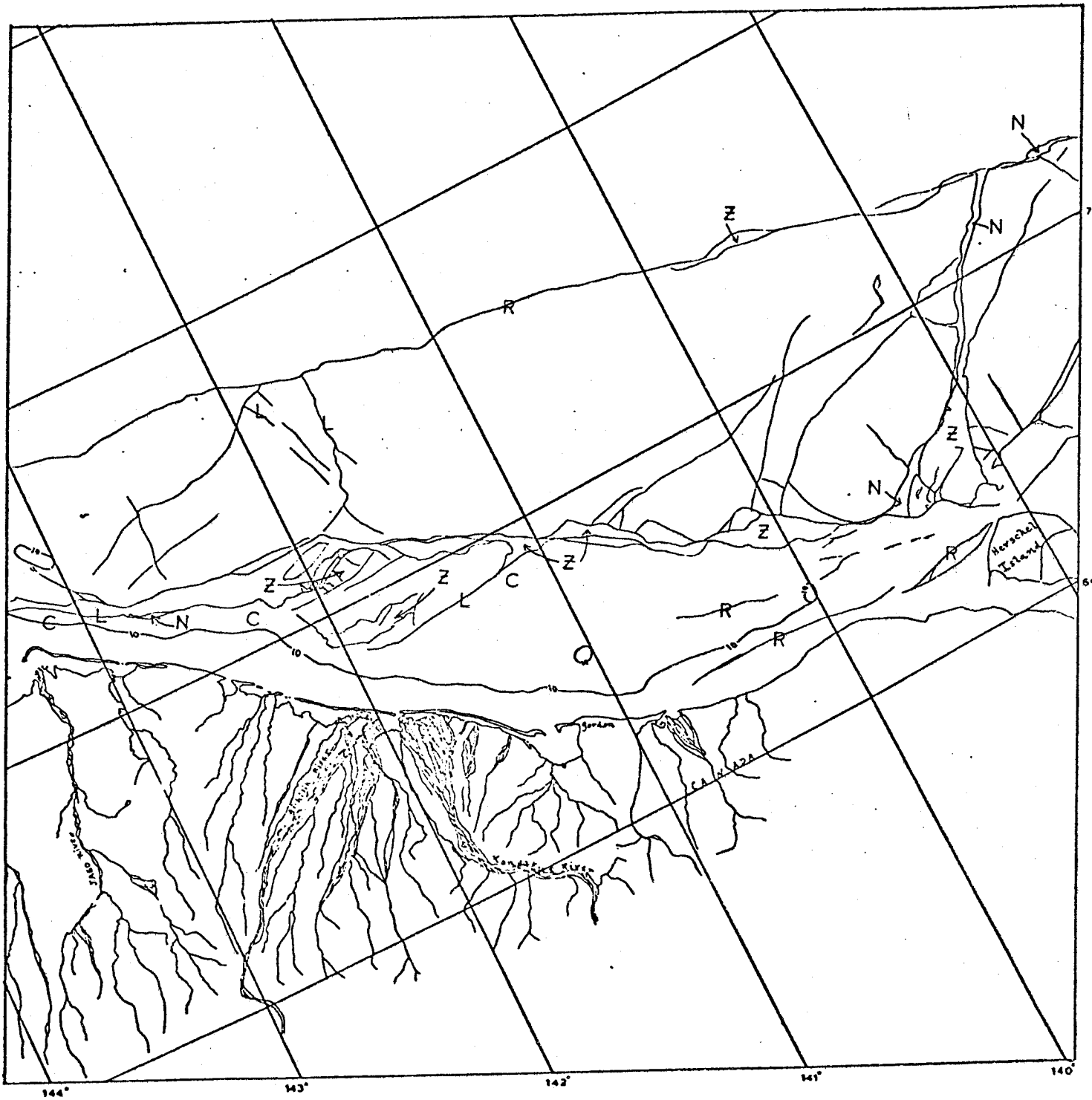

E-1607-20435-7
E-1607-20432-7
22 MARCH 1974

KILOMETERS
0 10 20 30 40 50

SCALE APPROX 1:1,000,000

BEAUFORT SEA

Scenes 1607-20432
1607-20435

These scenes cover the portion of Beaufort Sea coast from the Jago River to Herschel Island. The eastern portion of this scene was discussed for scene 1606-20380. In the western portion the zone of shear can be found just beyond the 10-fathom contour thereby limiting the edge of contiguous ice to that position.

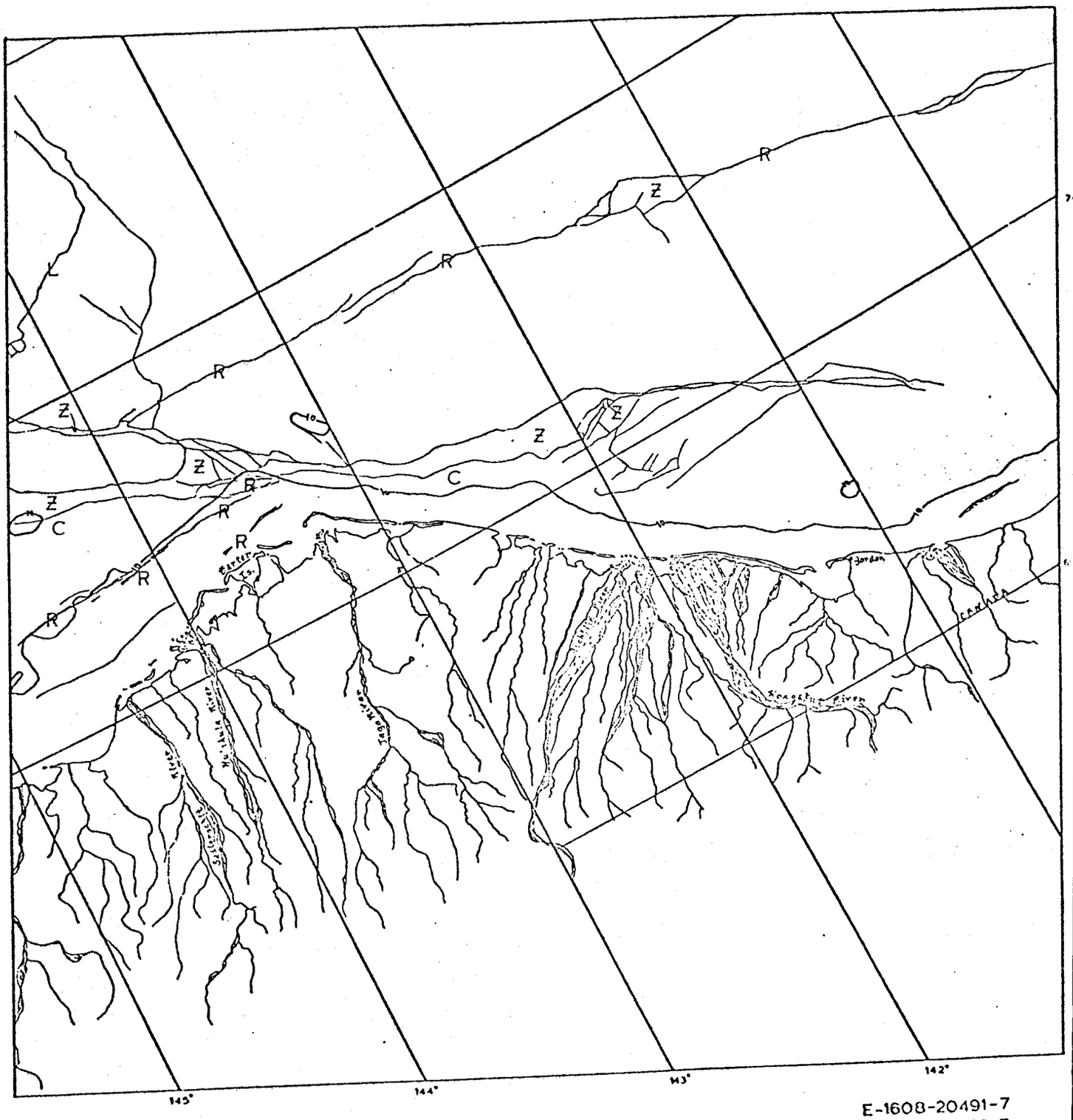

E-1608-20491-7
E-1608-20493-7

23 MARCH 1974

KILOMETERS

0 10 20 30 40 50

SCALE APPROX 1:1,000,000

BEAUFORT SEA

Scene 1608-20491
1608-20493

These scenes shows the portion of Beaufort Sea coast from the Canadian border to Barter Island. Only the western portion of this area has not been described for other scenes. In the vicinity of Barter Island the coastline and 10-fathom contour each make an 80-degree bend to cause the coastline to have a bearing along a line somewhat south of west. Near this bend are located several pressure ridges and hummock fields. However, whereas the ridge systems indicate that at one time shear may have taken place along the 10-fathom contour, at this time the zone of shear is not deflected to follow the 10-fathom contour.

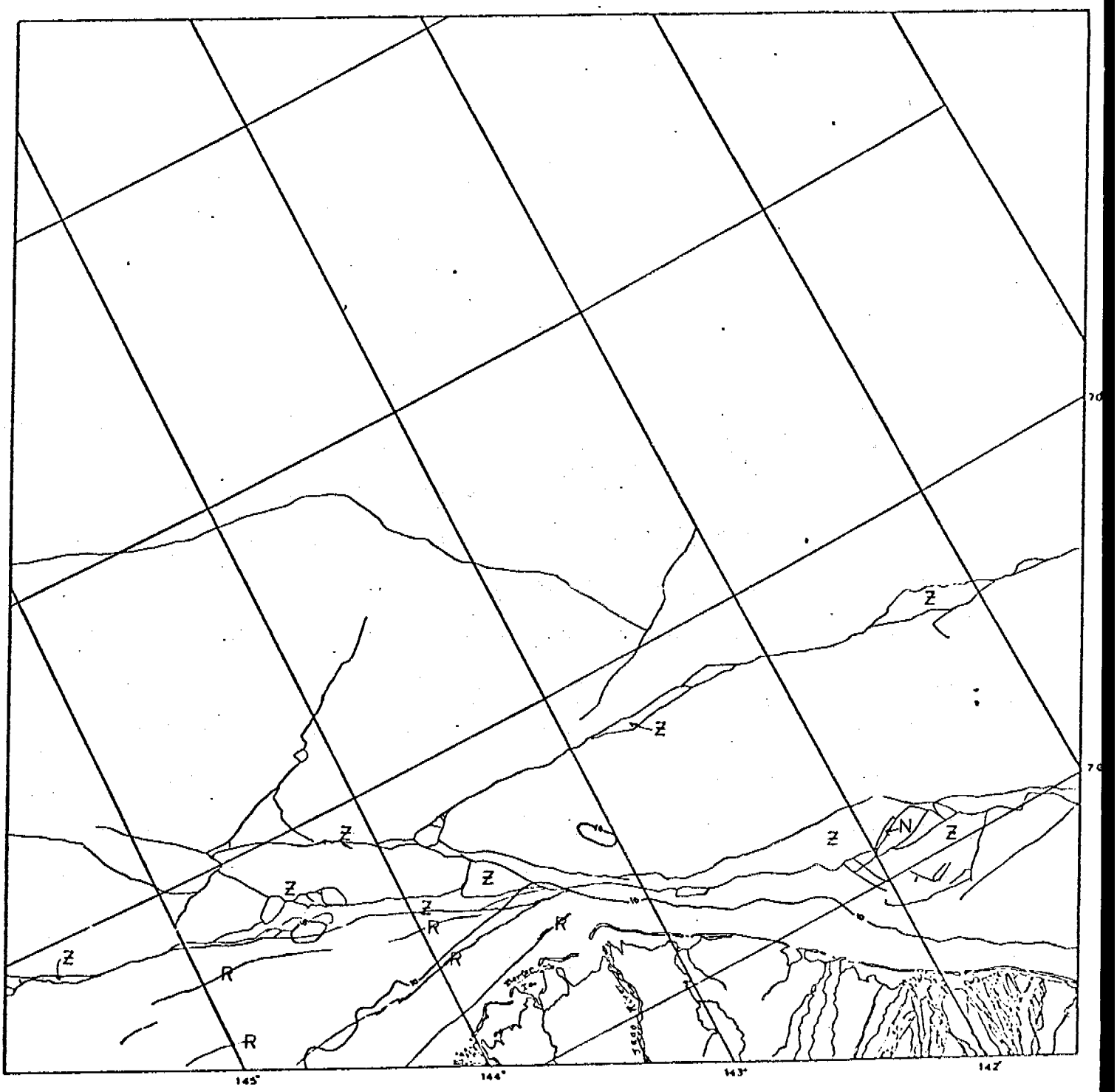

KILOMETERS

0 10 20 30 40 50

SCALE APPROX 1:1,000,000

BEAUFORT SEA

E-1609-20545-7
24 MARCH 1974

Scene 1609-20545

This scene of the Beaufort coast centered on Barter Island shows the zone of shear to the west of Barter Island not following the indented 10-fathom contour into Camden Bay. There is evidence from the several concentric ridge systems that at earlier times this boundary did indent to follow the coastline and 10-fathom contour more closely.

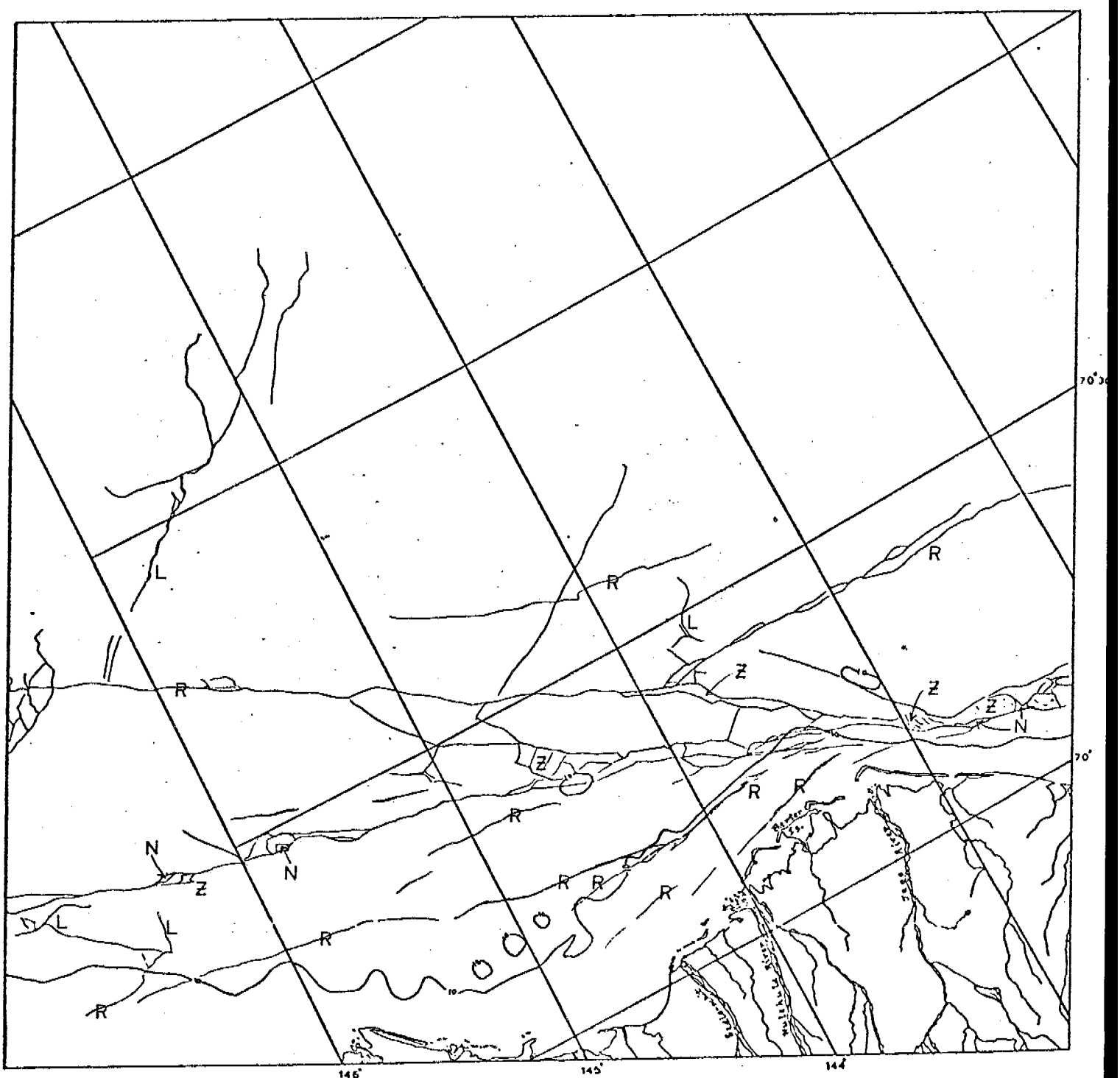

KILOMETERS

0 10 20 30 40 50

SCALE APPROX 1:1,000,000

E-1610-21003-7

25 MARCH 1974

BEAUFORT SEA

Scene 1610-21003

This scene of the Beaufort coast centered on Barter Island shows the zone of shear to the west of Barter Island not following the indented 10-fathom contour into Camden Bay. There is evidence from the several concentric ridge systems that at earlier times this boundary did indent to follow the coastline and 10-fathom contour more closely.

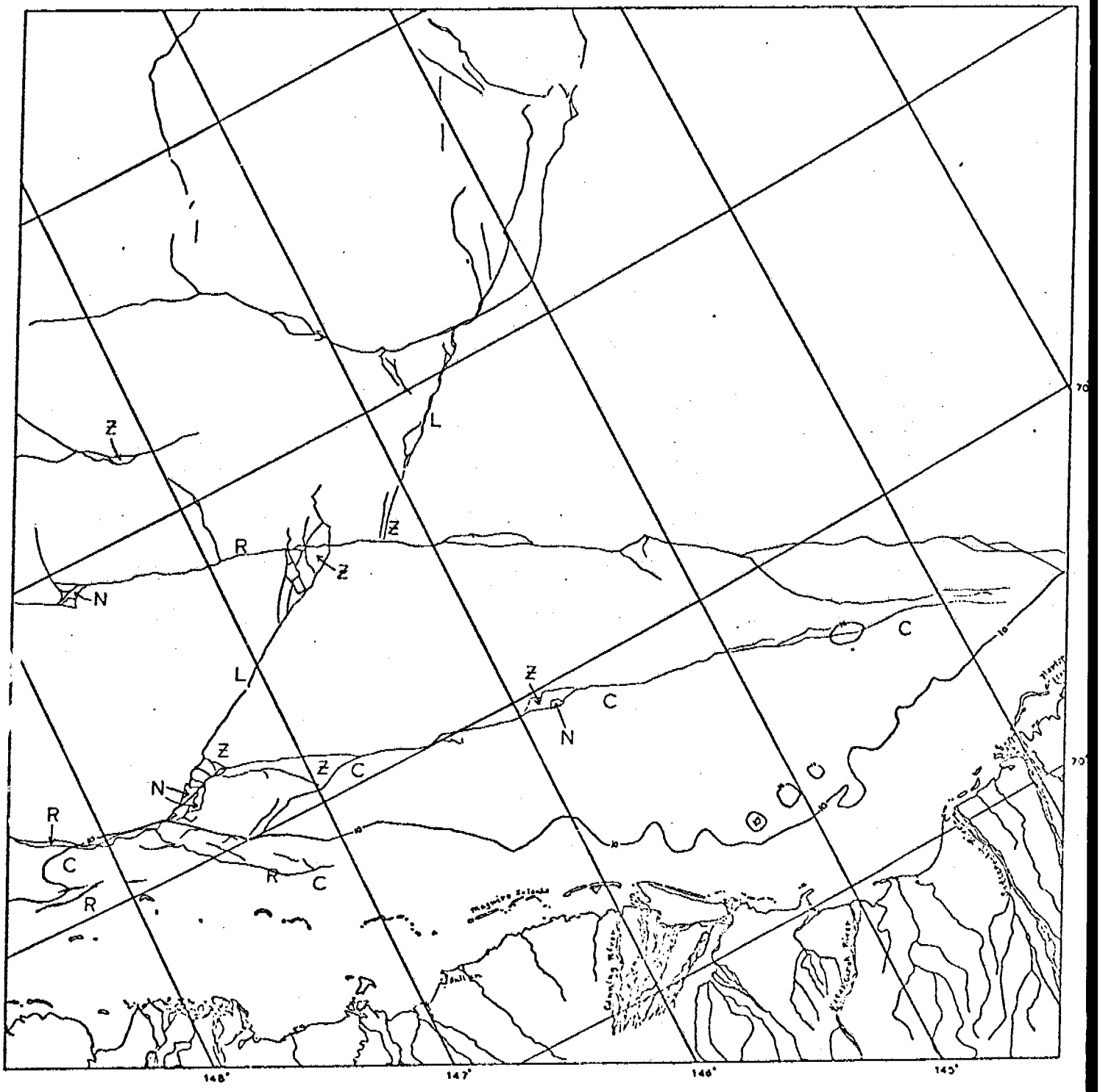

KILOMETERS

0 10 20 30 40 50

SCALE APPROX 1:1,000,000

E-1611-21061-7

26 MARCH 1974

BEAUFORT SEA

Scene 1611-21061

This scene shows the Beaufort coast from Prudhoe Bay on the west to Barter Island on the east. Only the western portion of this scene is not obscured by cloud. The areas under cloud have been mapped from previous scenes. The large lead aligned NE-SW appears to be fairly new. It extends shoreward to the vicinity of the east-west shear zone where it rejoins the 10-fathom contour.

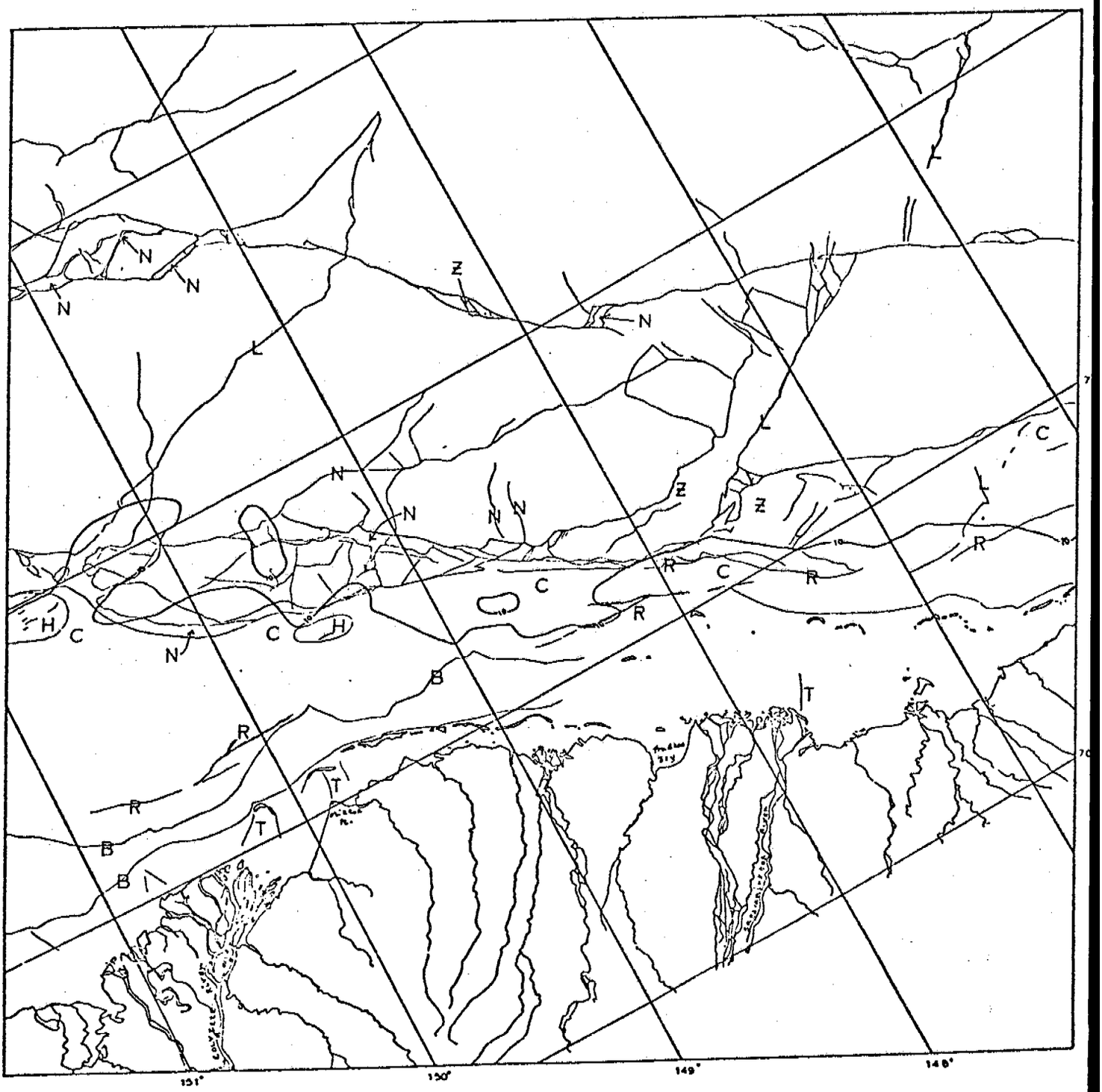

KILOMETERS

0 10 20 30 40 50

SCALE APPROX 1:1,000,000

E-1613-21174-7

28 MARCH 1974

BEAUFORT SEA

Scene 1613-21174

This Beaufort coast scene centered on the mouth of the Kuparuk River shows the eastern two thirds of Harrison Bay. Throughout most of this area the zone of shear is roughly aligned with the 10-fathom contour except in areas of local indentations. Several large ridge systems can be found shoreward of the shear zone indicating that at an earlier date shear was taking place at these locations.

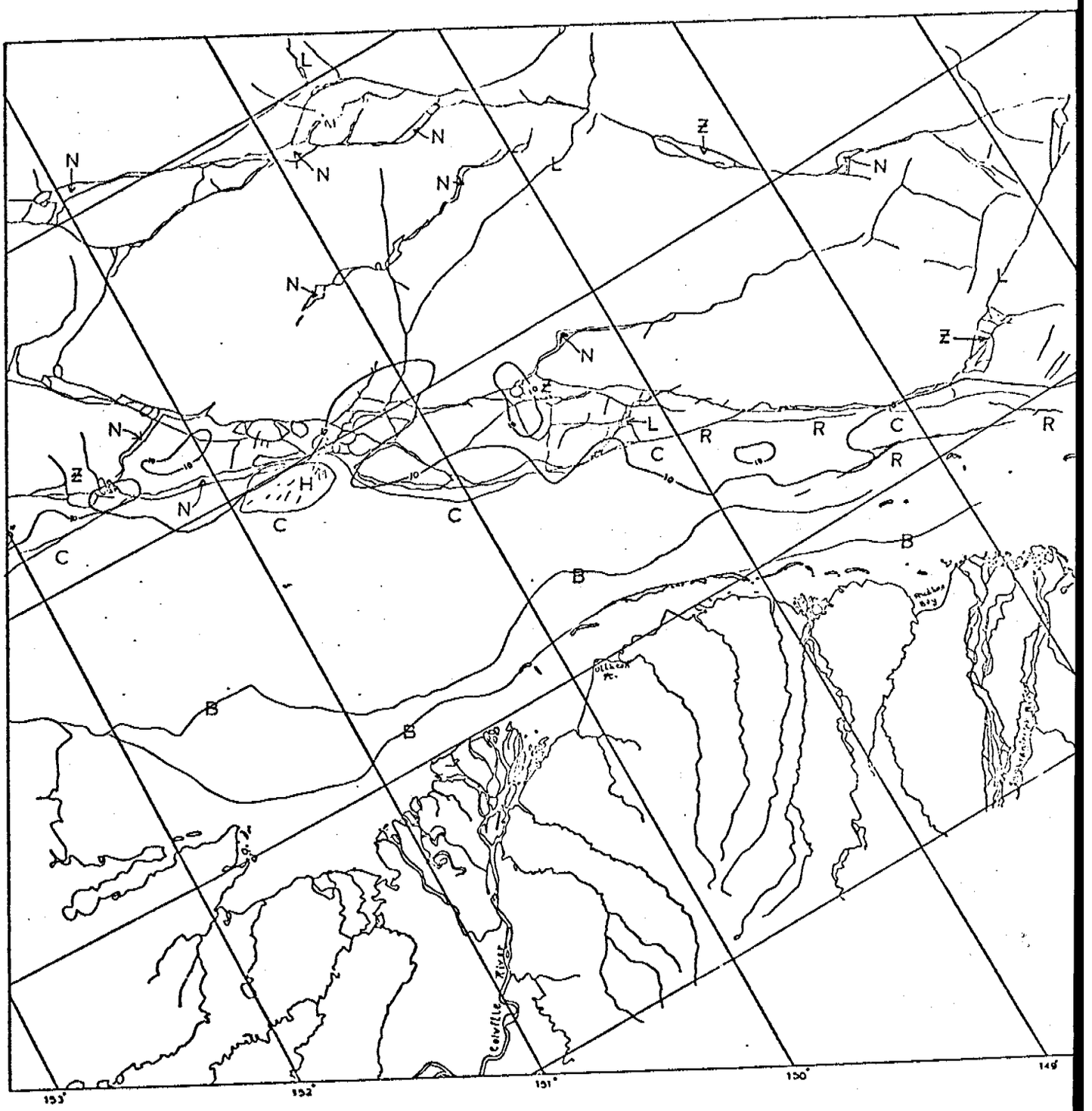

E-1614-21232-7
29 MARCH 1974

KILOMETERS
0 10 20 30 40 50

SCALE APPROX 1:1,000,000

BEAUFORT SEA

Scene 1614-21232

This scene includes the portion of coast from Cape Halkett to Pr Prudhoe Bay. The edge of contiguous ice coincides quite well with the 10-fathom contour across most of this image. The only deviation from this general rule is found where the 10-fathom contour makes a major indentation west of Cross Island.

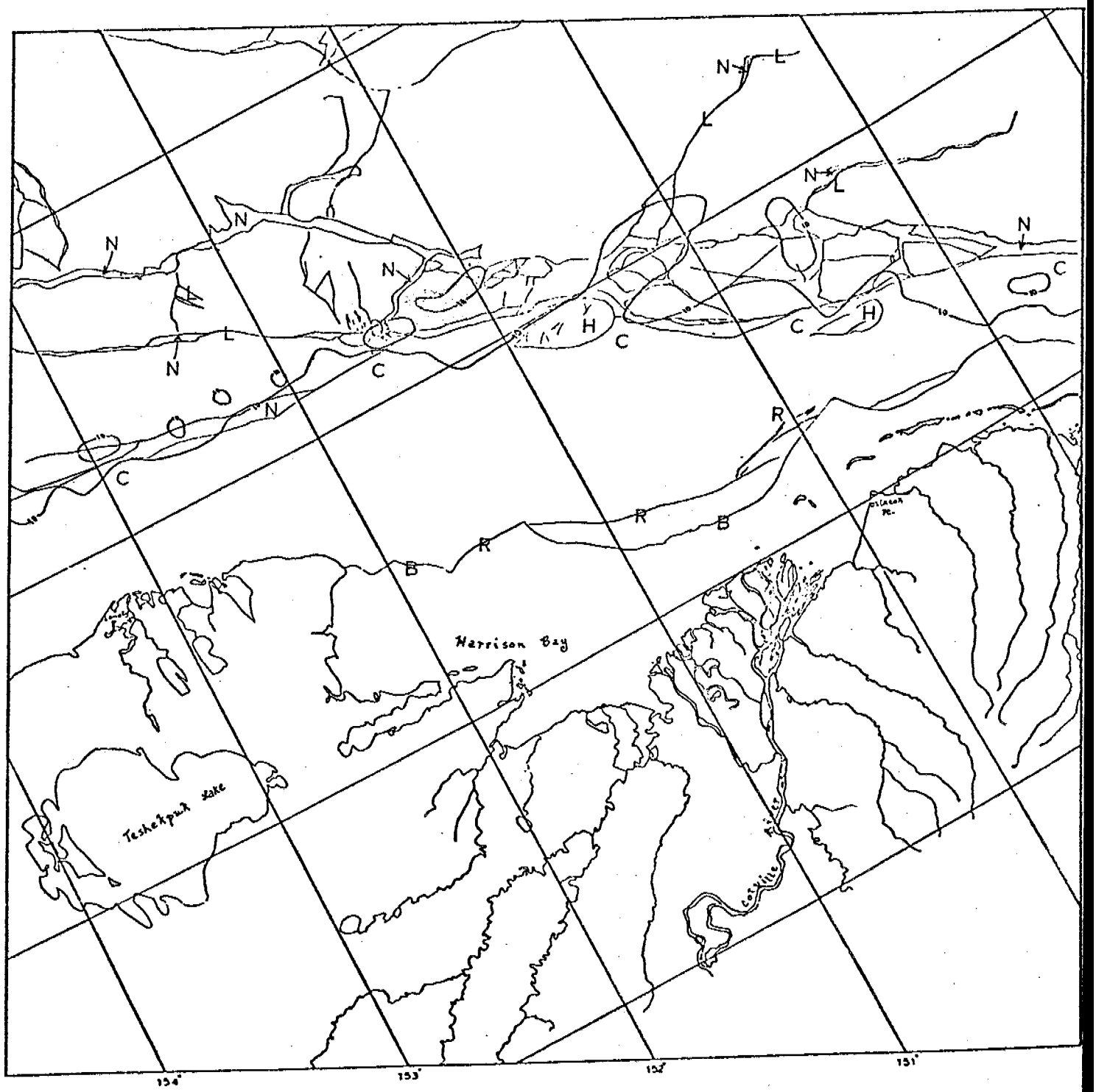

E-1615-21291-7
30 MARCH 1974

KILOMETERS
0 10 20 30 40 50
SCALE APPROX 1:1,000,000

BEAUFORT SEA

Scene 1615-21291

This scene, centered on Harrison Bay again shows a close correlation between the limit of contiguous ice and the 10-fathom contours. The ridges and boundaries within the contiguous ice appear to be quite old. Two large hummock fields can be found in outer Harrison Bay which appear to be at least partly responsible for the local configuration of lead systems.

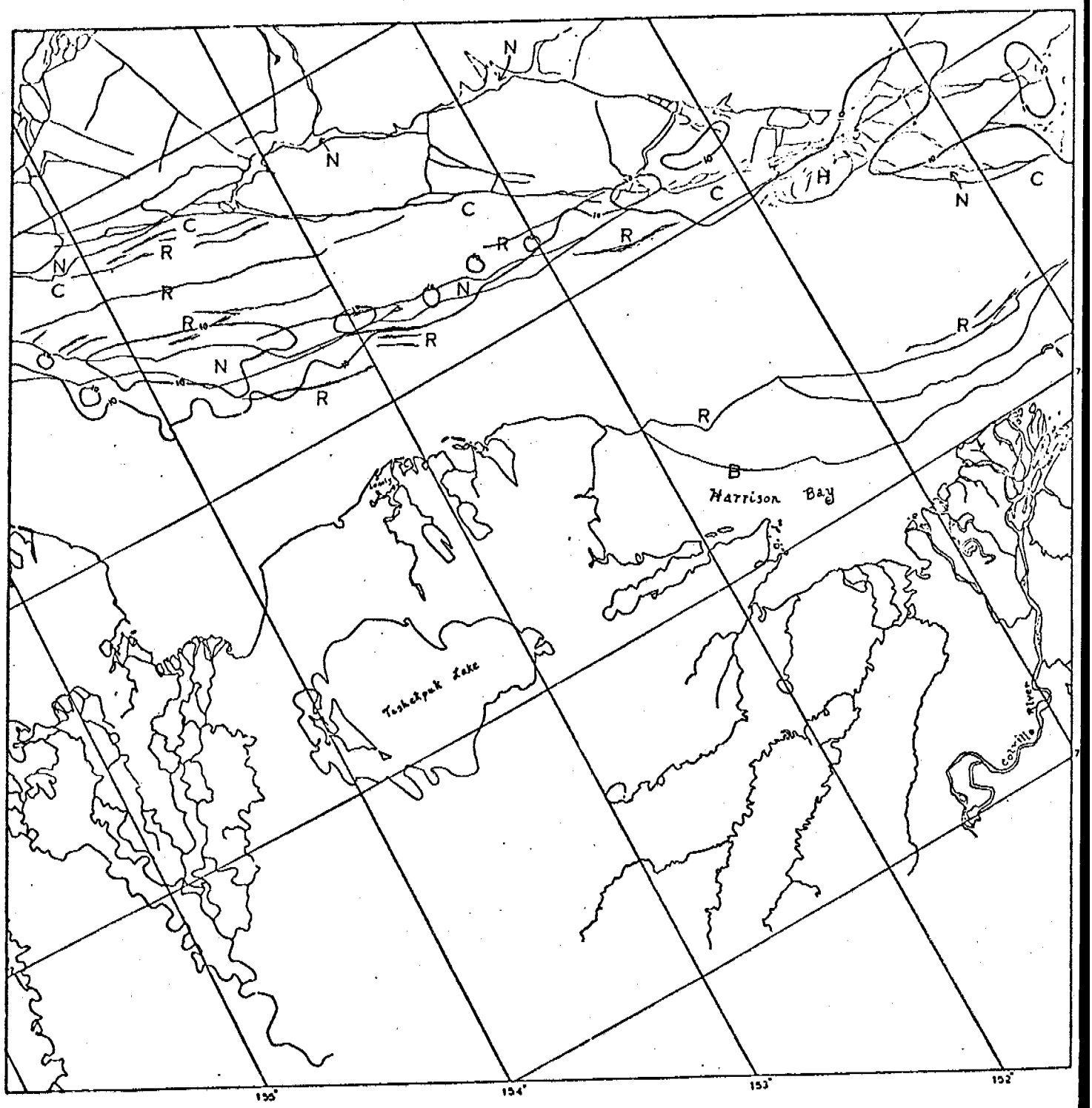

KILOMETERS

0 10 20 30 40 50

SCALE APPROX 1:1,000,000

E-1616-21345-7

31 MARCH 1974

BEAUFORT SEA

Scene 1616-21345

This scene shows the Alaska coastline from Smith Bay to the mouth of Colville. From the east the edge of the contiguous ice follows closely the 10-fathom contour until it reaches the hummock field in outer Harrison Bay. Then it continues westward while the 10-fathom contour indents toward Smith Bay. In the recent past, the contiguous ice in the Smith Bay area has broken and been displaced several km eastward in this area and, interestingly, this break was along the 10-fathom contours. Since that time the open water created by that break has frozen. Inshore of this recent break and nearly coinciding with the 10-fathom contour are several massive ridge systems which probably represent the boundary of contiguous ice at earlier times.

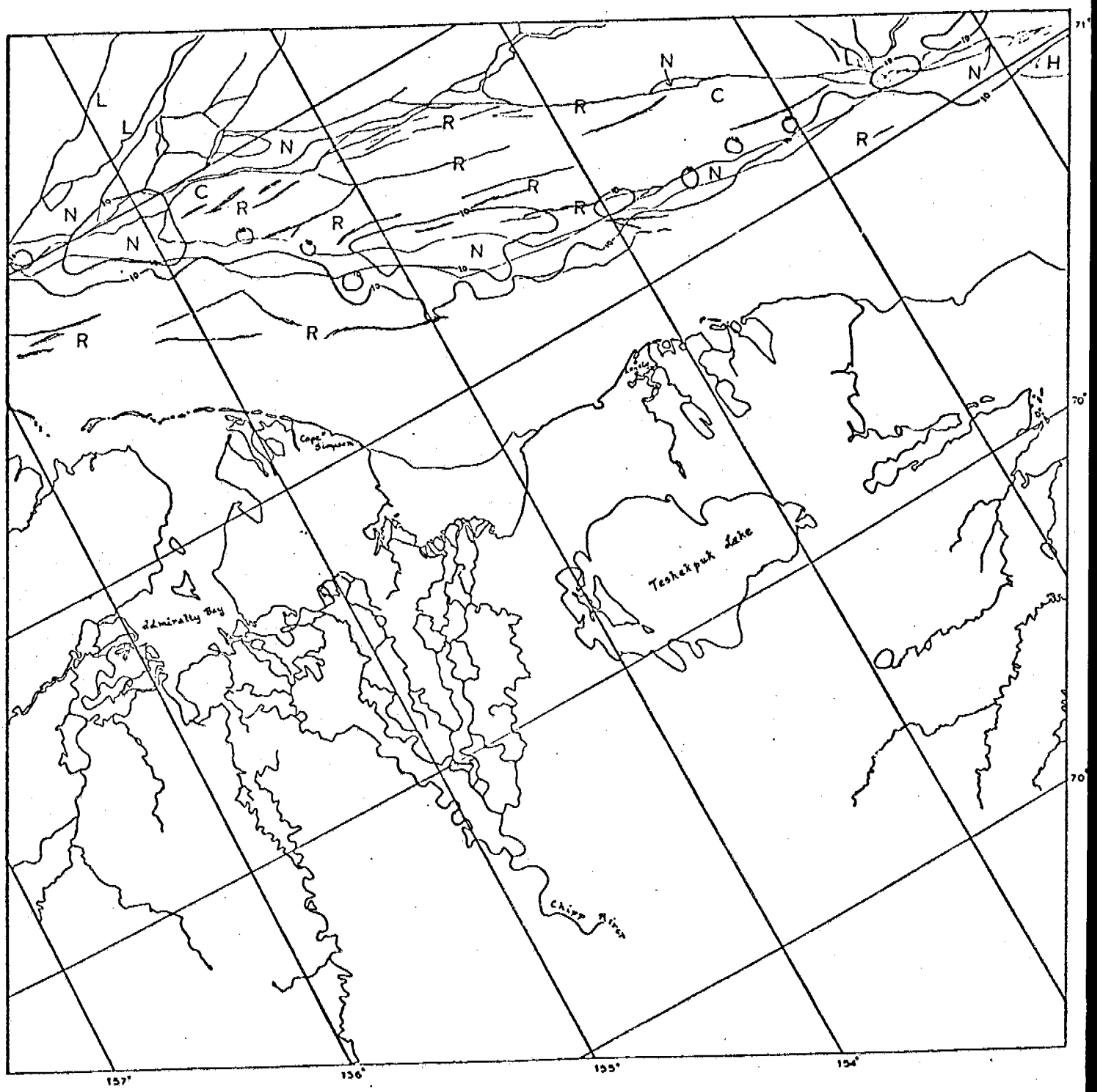

E-1617-21403-7

1 APRIL 1974

KILOMETERS

0 10 20 30 40 50

SCALE APPROX 1:1,000,000

BEAUFORT SEA

Scene 1617-21403

This scene shows the Beaufort Coast from Admiralty Bay to Harrison Bay. At this time contiguous ice extends considerably seaward of the 10-fathom contour in the Smith Bay area. In the recent past it has indented toward Smith Bay generally following the 10-fathom contour. A large block of contiguous ice had broken loose and drifted several km east causing a large lead to open. By this date the lead had frozen over so that ice was contiguous out to the more remote location described earlier. Considerably inshore of the 10-fathom contour is located a more-or-less continuous line of ridges which apparently mark the position of shear at a much earlier date.

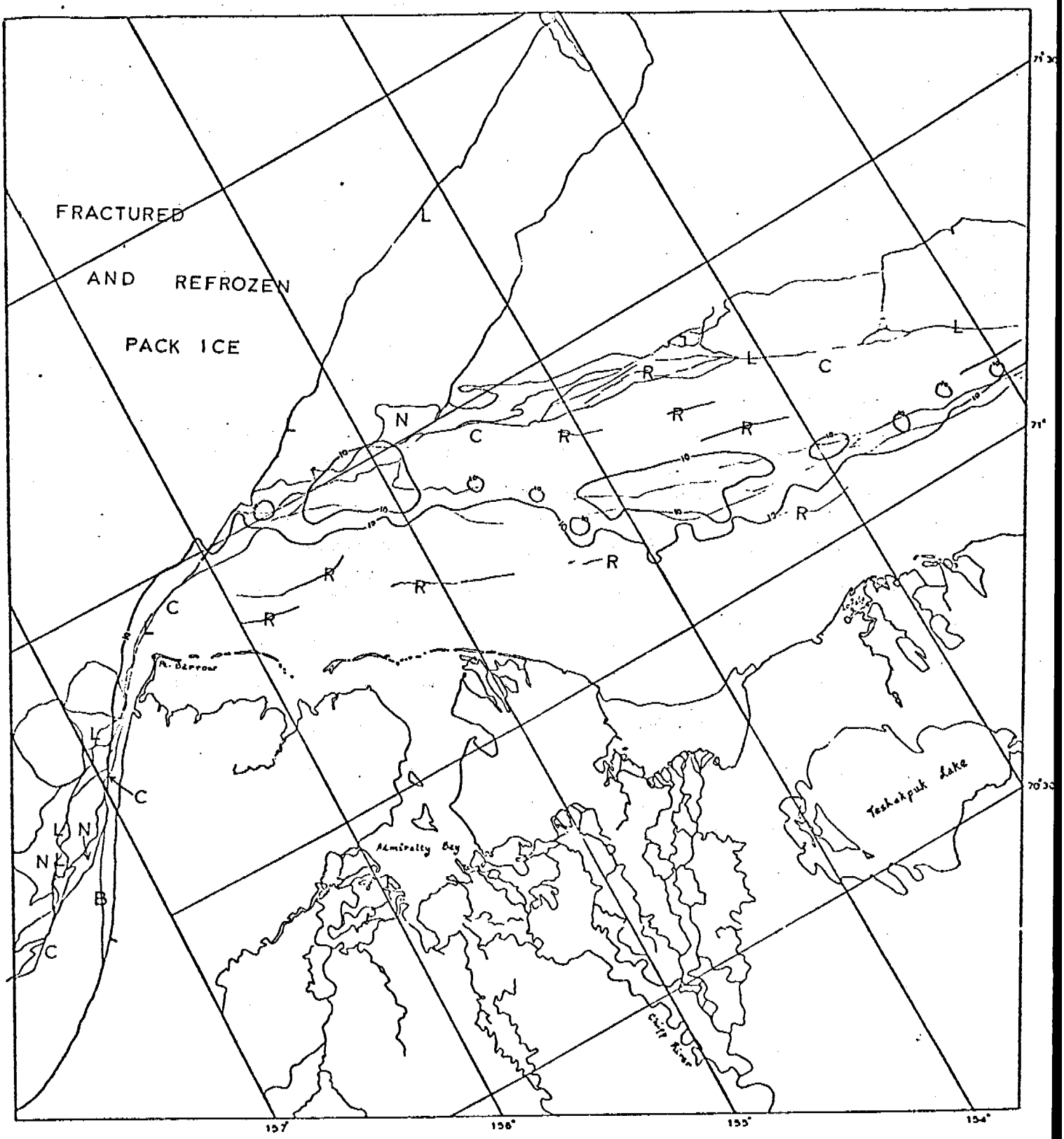

KILOMETERS

0 10 20 30 40 50

SCALE APPROX 1:1,000,000

BEAUFORT SEA

E-1618-21455-7
E-1618-21462-7
2 APRIL 1974

Scene 1618-21455
1618-21462

These scenes show the Beaufort coast from Pt. Barrow east almost to Cape Halkett. Presently shear is taking place along a line extending from north of Pt. Barrow to a hummock field located in outer Harrison Bay. This represents a chord to the arc made by the 10-fathom contour as it follows the indentation of the coastline in this area. At a recent time a large piece of contiguous ice located between the chord and arc has broken loose and moved several km to the east opening up new water which has frozen and thereby extending contiguous ice out to the present limit. It is interesting to note the line of large ridge systems located well within the 10-fathom contour. These may well represent the edge of contiguous ice at an earlier date.

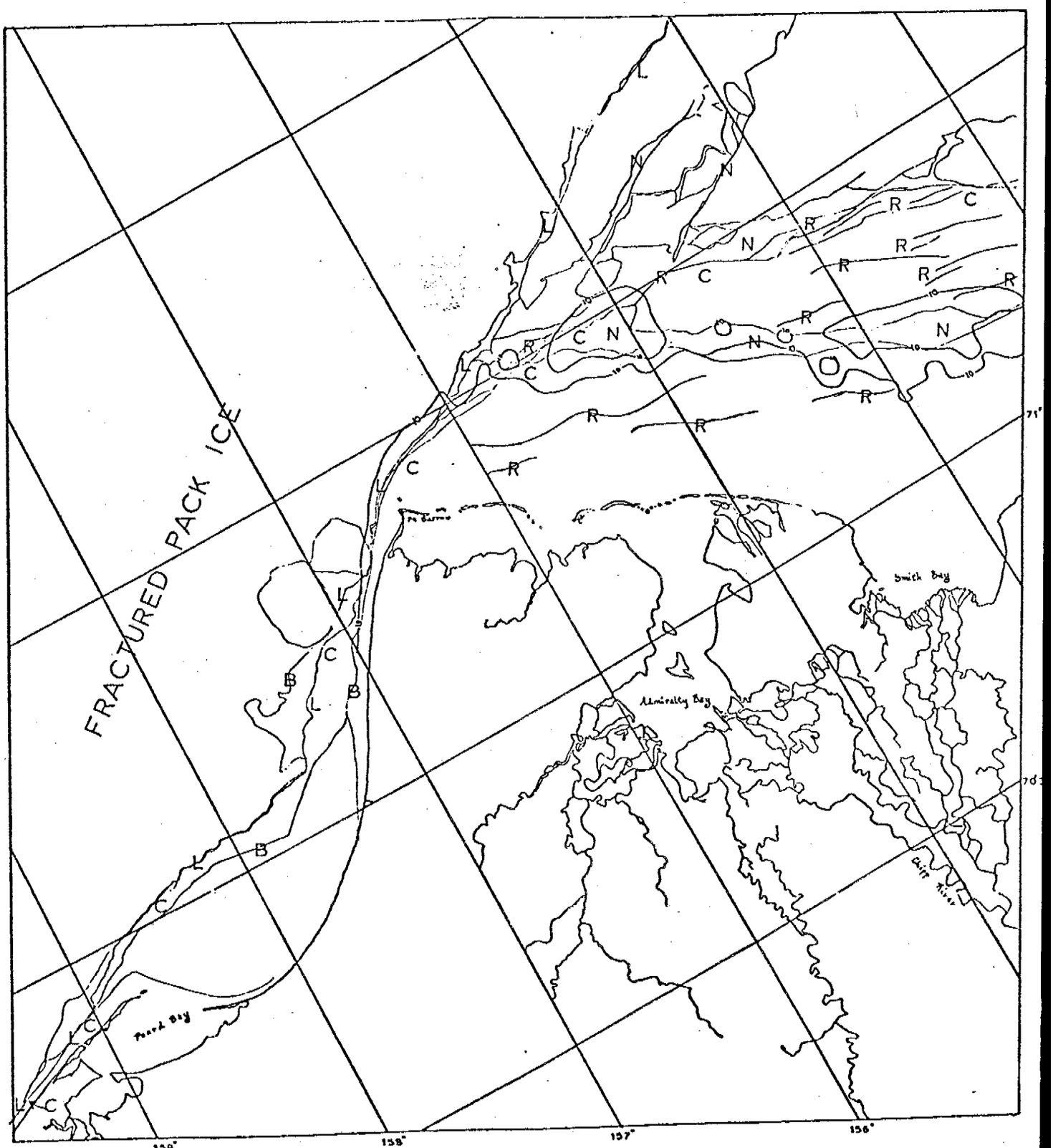

KILOMETERS

0 10 20 30 40 50

SCALE APPROX 1:1,000,000

BEAUFORT SEA

E-1619-21513-7
E-1619-21520-7
3 APRIL 1974

Scene 1619-29520

This combination of scenes is of the area from Peard Bay to Point Barrow to Smith Bay. From Peard Bay to Point Barrow and extending north-eastward, a narrow lead has opened up, separating the fractured pack ice of Chukchi and northwestern Beaufort Seas from the contiguous ice along the Chukchi coast and the more solid pack ice of the Beaufort Sea. A fairly new ridge-lead system separates the contiguous ice from the pack ice in the Beaufort Sea. Shoreward of this boundary, many large ridge systems are visible. In this area, a large lead had opened up, truncating many of the ridge systems, but has since refrozen.

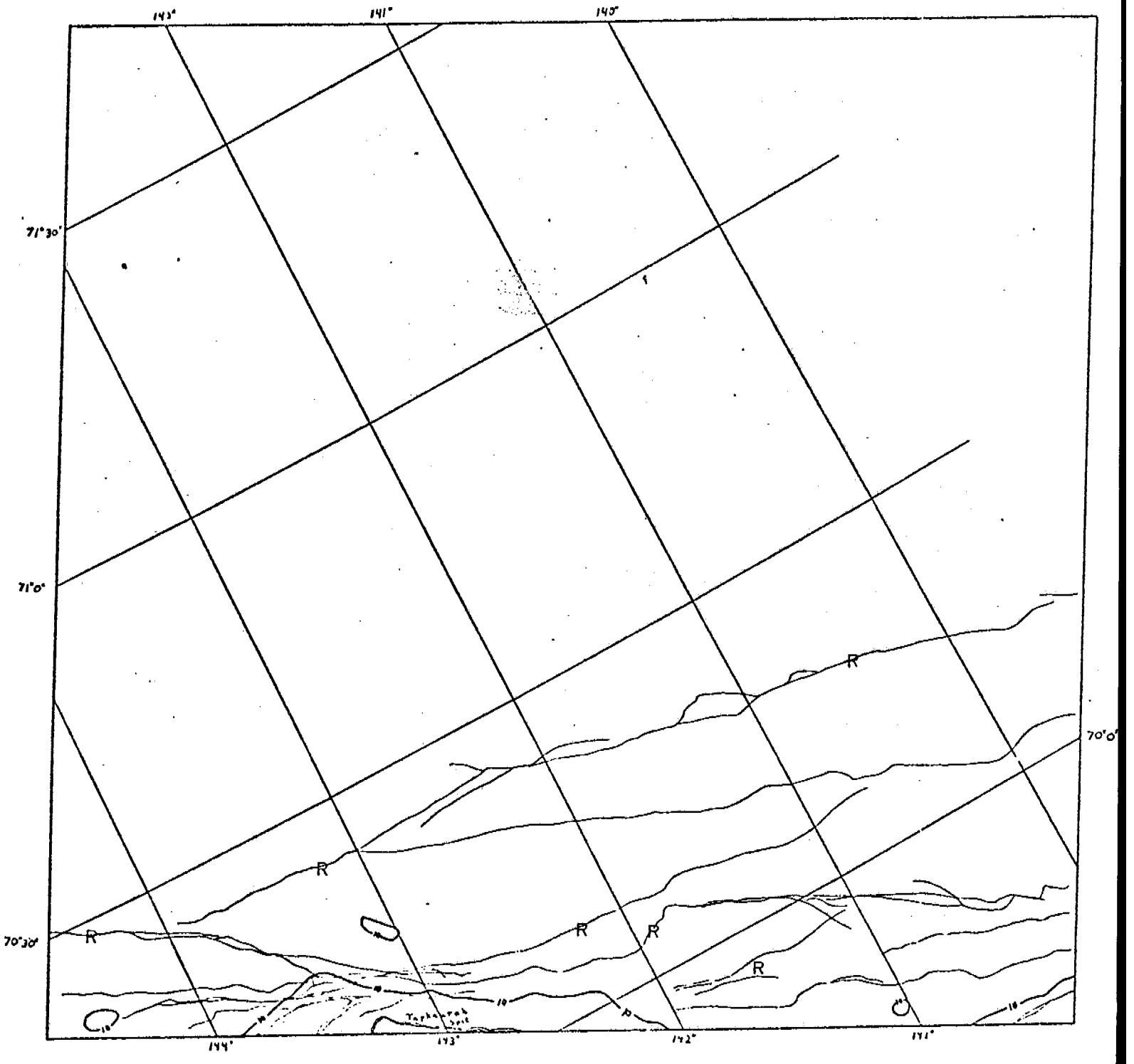

E-1644-20482
28 APRIL 1974

KILOMETERS
0 10 20 30 40 50

SCALE APPROX 1:1,000,000

BEAUFORT SEA

Scene 1644-20482

This scene shows the Beaufort coast in the vicinity of the Barter Island, NWT. Comparison should be made with scene 1608-20491 obtained a little more than a month previously. Apparently, during this time there has been little or no ice motion. Contiguous ice extends beyond the edges of the landsat scene.

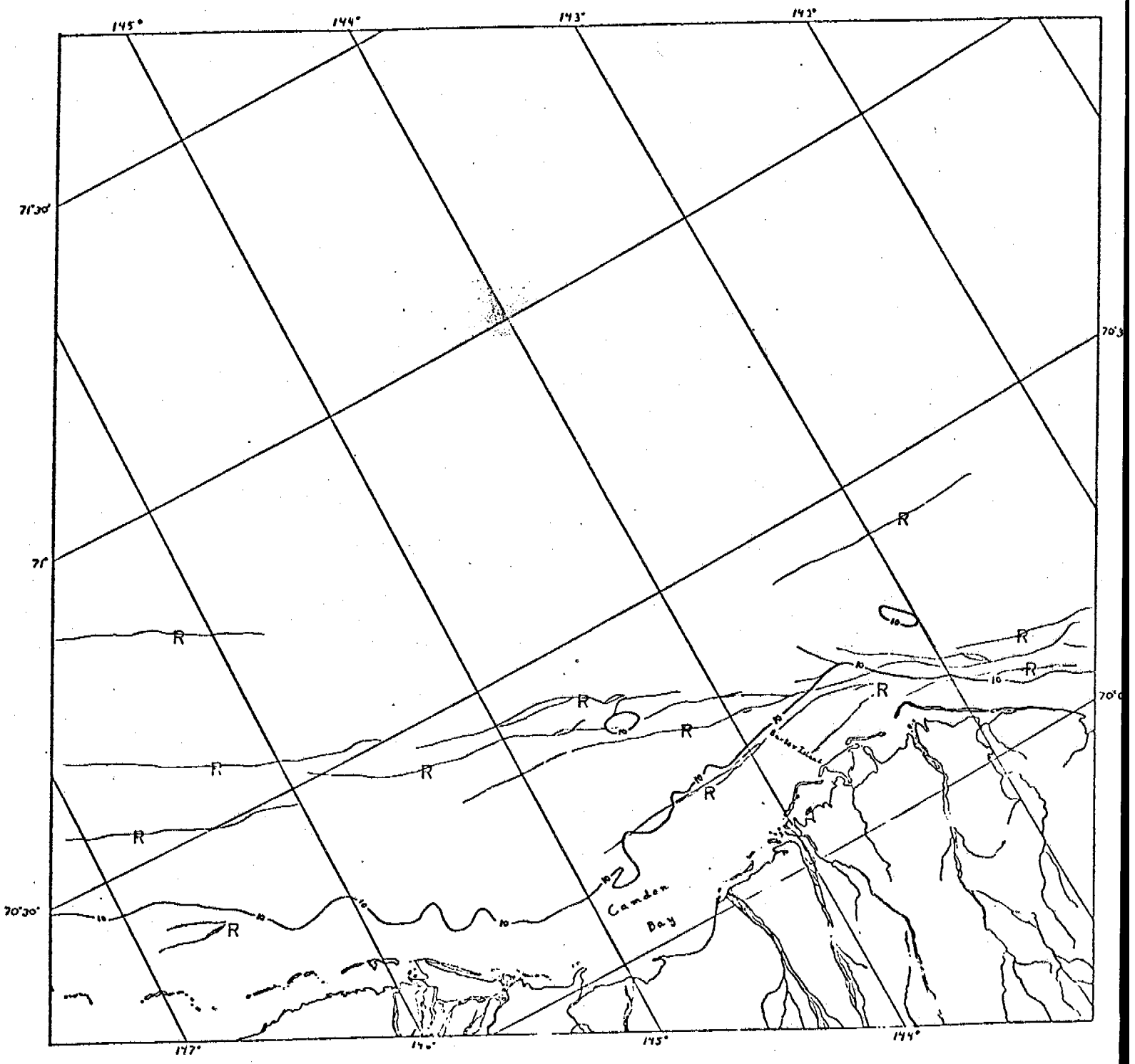

E-1646-20594
30 APRIL 1974

KILOMETERS
0 10 20 30 40 50
SCALE APPROX 1:1,000,000

BEAUFORT SEA

Scene 1646-20594

This scene shows the Beaufort coast in the vicinity of Camden Bay. Comparison should be made with scene 1610-21003 obtained 36 days previously. Apparently, during this time there has been little or no ice motion and consequently no leads formed. Ridge systems can be identified in the locations of active shear on the earlier scene. Contiguous ice extends past the limits of the landsat scene.

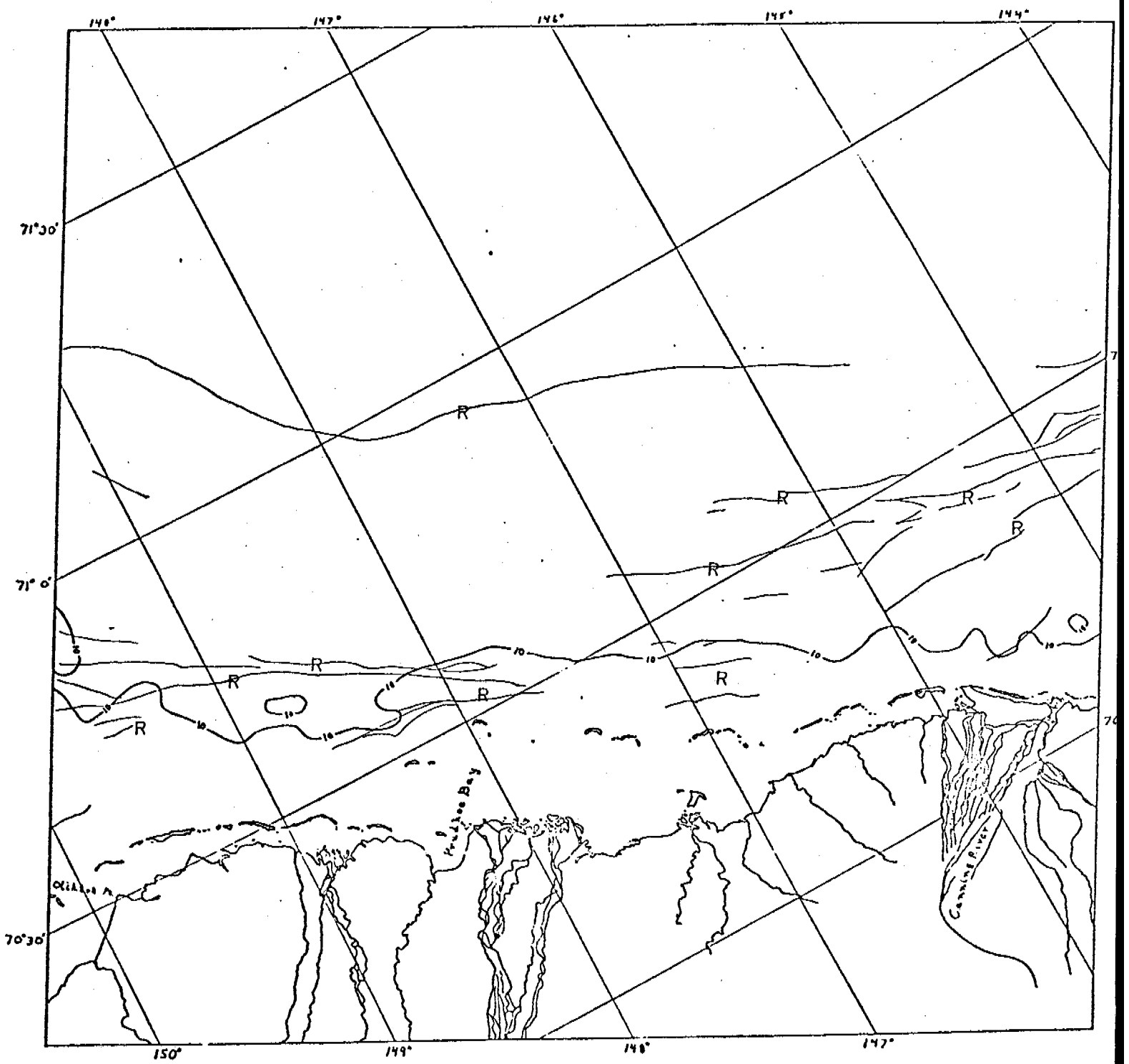

E-1649-21111
2 MAY 1974

KILOMETERS
0 10 20 30 40 50

SCALE APPROX 1:1,000,000

BEAUFORT SEA

Scene 1648-21111

This scene shows the Beaufort coast in the vicinity of Prudhoe Bay and should be contrasted with the nearly corresponding scene, 1613-21174, obtained 35 days previously. Apparently, during this time there has been little or no ice motion with the result that contiguous ice extends beyond the edge of the landsat scene.

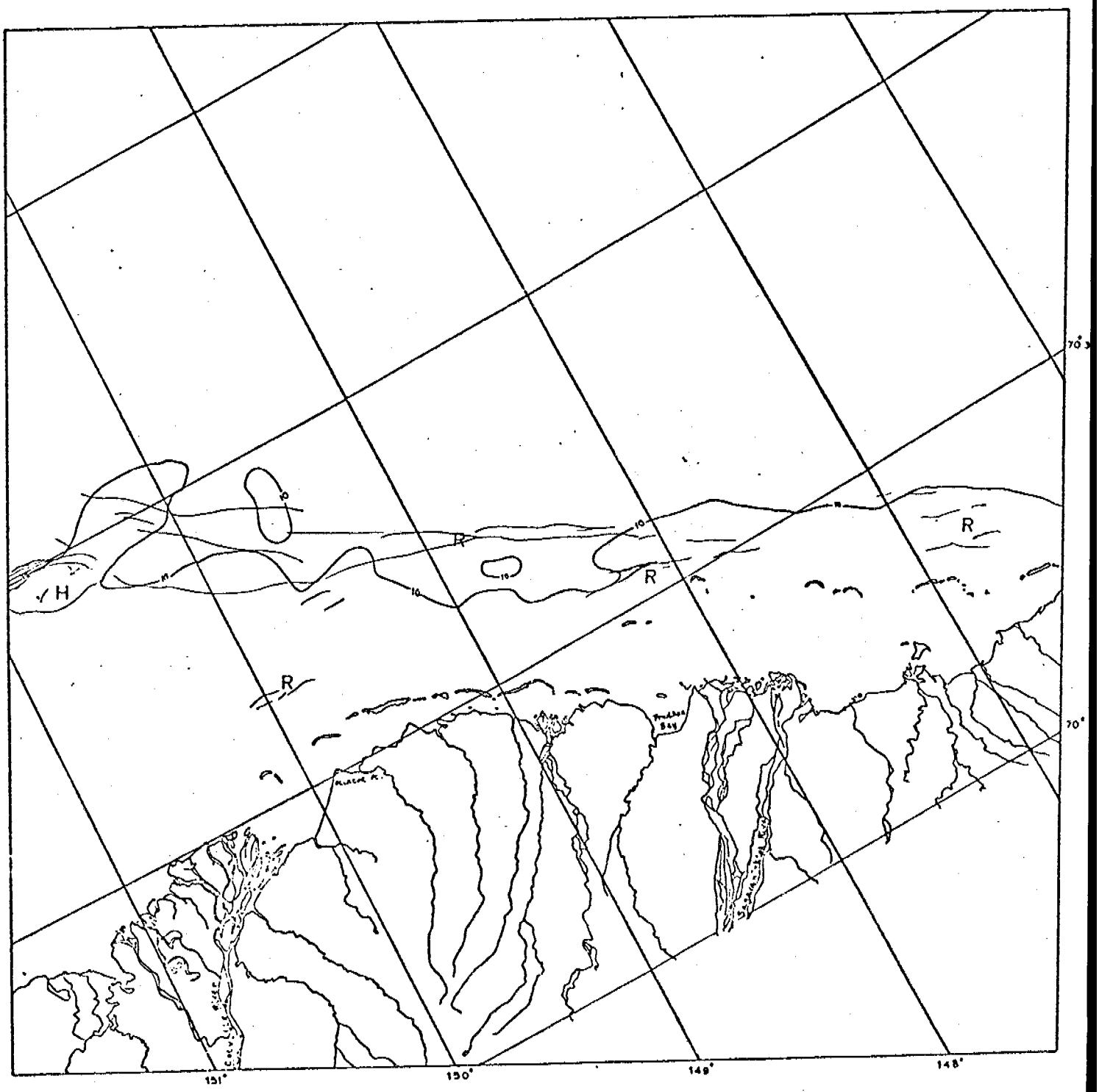

E-1649-21165-7

3 MAY 1974

KILOMETERS

0 10 20 30 40 50

SCALE APPROX 1:1,000,000

BEAUFORT SEA

Scene 1649-21165

This scene showing the Beaufort coast eastward from Harrison Bay should be contrasted with scene 1613-21174 obtained 36 days earlier. During this time there has been little or no ice motion with the result that all leads have frozen and all shear motion has ceased. The result is that contiguous ice now extends beyond the limits of the scene.

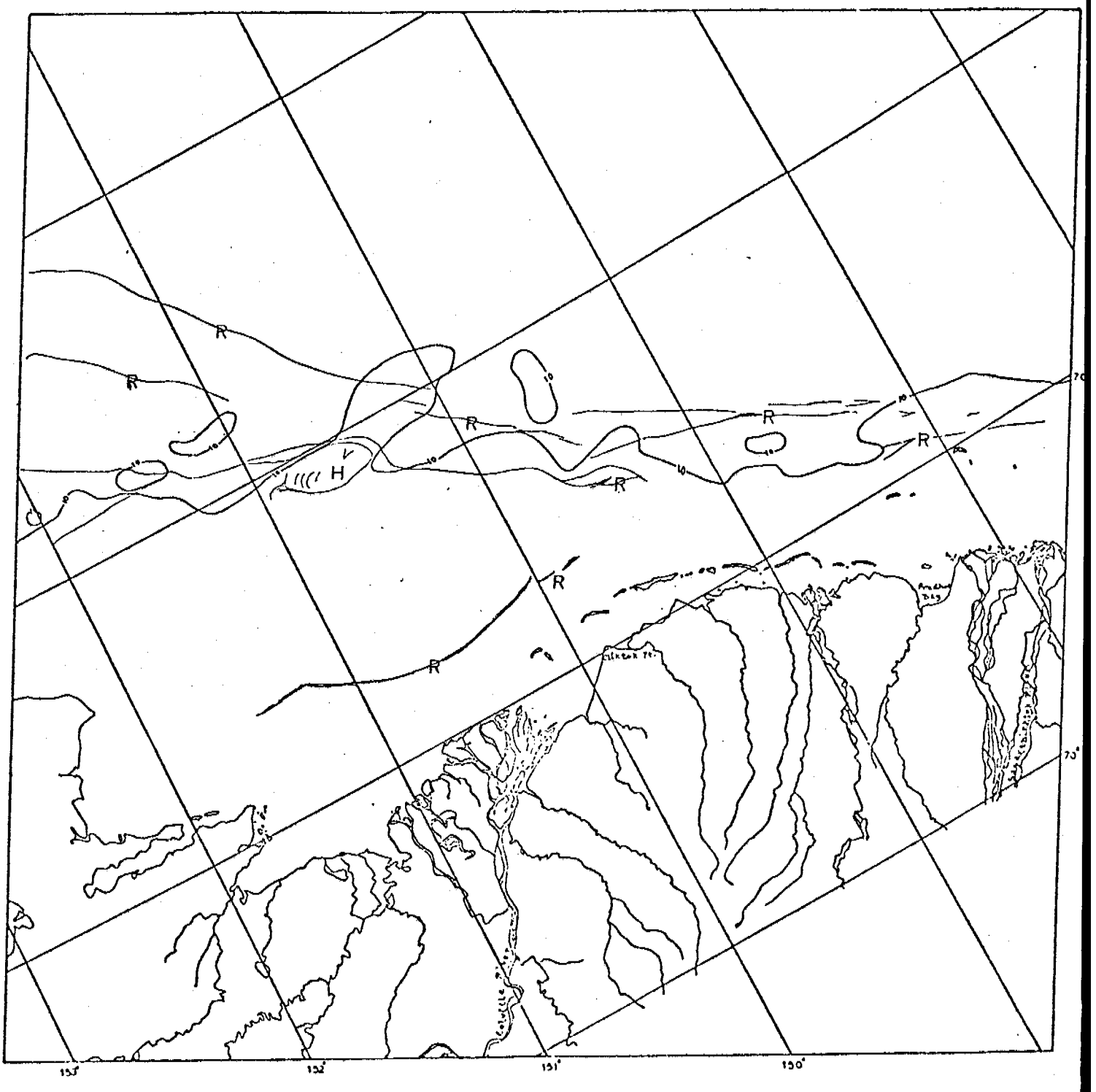

KILOMETERS

10 20 30 40 50

SCALE APPROX 1:1,000,000

E-1650-21223-7

4 MAY 1974

BEAUFORT SEA

Scene 1650-21223

This scene showing the Beaufort coast from Harrison Bay to Prudhoe Bay should be contrasted with scene 1614-21232 obtained 36 days previously when considerable shearing motion had just taken place. During the interval between these scenes there has been little or no ice motion with the result that all leads have frozen and all shearing motion has ceased. The result is that contiguous ice now extends beyond the limits of the scene.

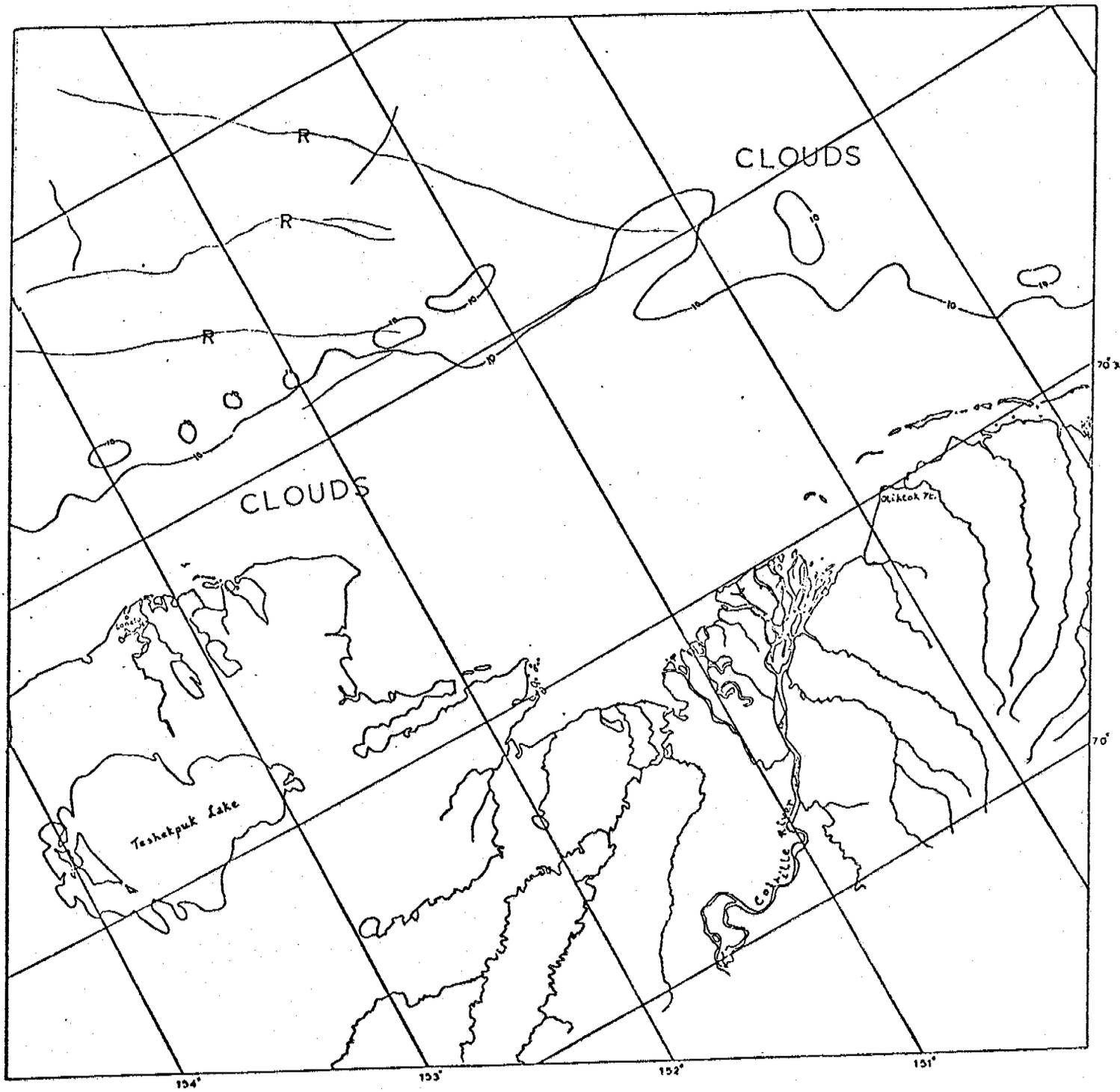

E-1651-21281-7

5 MAY 1974

KILOMETERS

10 20 30 40 50

SCALE APPROX 1:1,000,000

BEAUFORT SEA

Scene 1651-21281

This scene showing the Beaufort coast from Harrison Bay to Prudhoe Bay should be contrasted with scene 1615-21291 obtained 36 days previously when considerable shearing motion had just taken place. During the interval between these scenes there has been little or no ice motion with the result that all leads have frozen and all shearing motion had ceased. The result is that contiguous ice now extends beyond the limits of the scene.

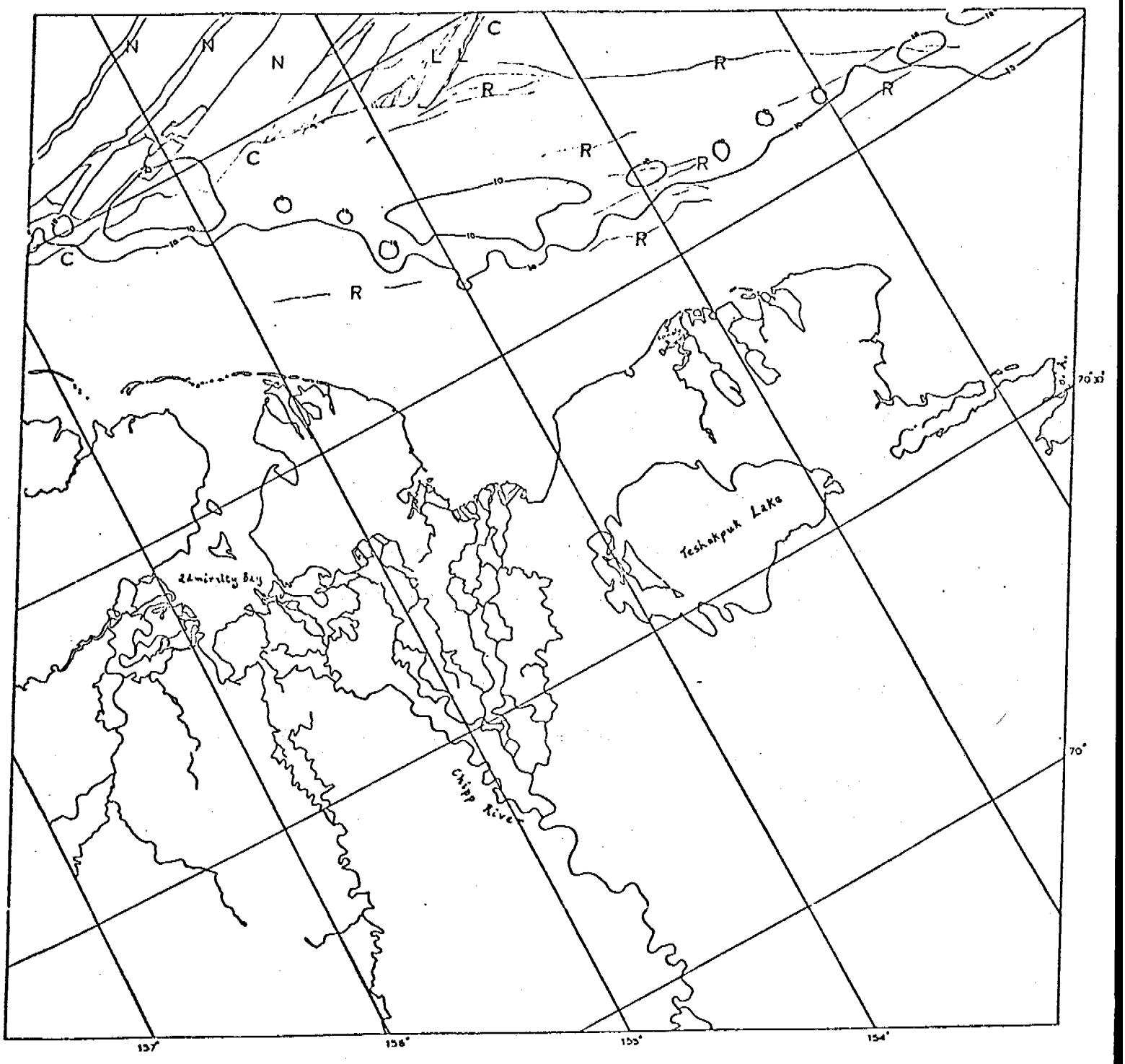

E-1653-21394-7
7 MAY 1974

KILOMETERS
10 20 30 40 50

SCALE APPROX 1:1,000,000

BEAUFORT SEA

Scene 1653-21394

This Beaufort scene centered on Smith Bay should be compared with scene 1617-21403 obtained 36 days previously. The ice to the east of the active lead system shown here has apparently not moved during this interval with the result that all leads have frozen and shearing motions ceased. However, there is an active lead system north and east of Pt. Barrow in this new scene which appears somewhat similar to the lead system seen in this location on the earlier scene.

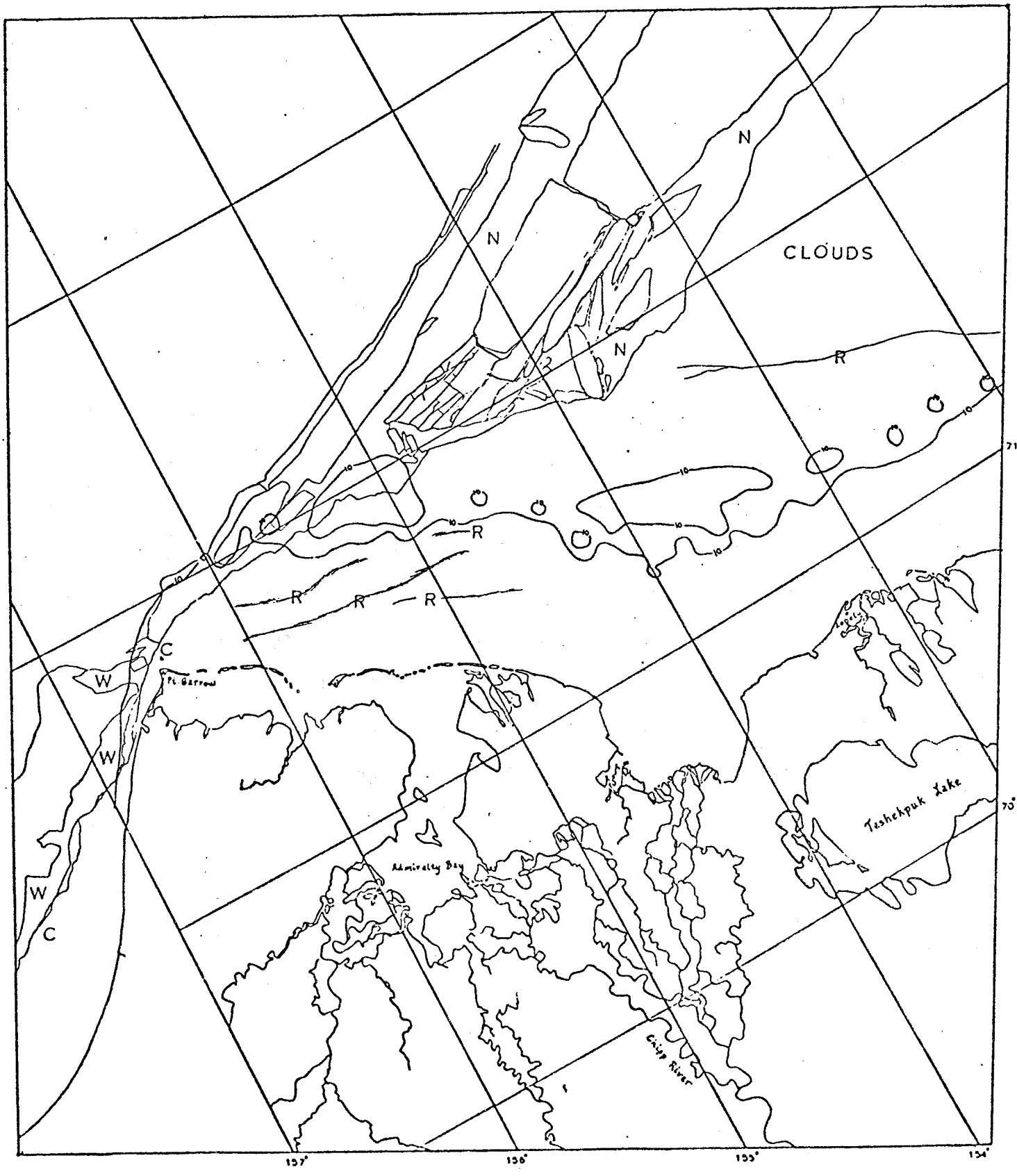

KILOMETERS

10 20 30 40 50

SCALE APPROX 1:1,000,000

BEAUFORT SEA

E-1654-21450-7
E-1654-21452-7
8 MAY 1974

Scene 1654-21450
1654-21452

This scene showing the Beaufort coast eastward from Pt. Barrow should be compared with scene 1618-21462 obtained 36 days earlier. Shearing motions are taking place in much the same location as in the earlier scene: slightly inshore of the 10-fathom contour at Barrow and far beyond that contour around the point to the east. Little or no shearing motion has taken place to the east of the active lead system shown in this image.

XI. PLANS FOR NEXT REPORTING PERIOD

A. Beaufort Sea

1. Epoch summary "maps are being prepared to summarize ice conditions at various times in each ice year.

2. Several "special events" have been identified which will be described by means of a map format.

3. "Retroactive maps" of melt season data from the several years of available Landsat data will be prepared.

B. Chukchi Sea

1. Base maps at 1:500,000 scale will be prepared with bathymetric data transferred from existing charts.

2. Chukchi Sea Landsat imagery will be examined, and the most useful data coverage cycles will be ordered in hard copy form at 1:500,000 scale.

REFERENCES

Colvocresses, A. P. and R. B. McEwen, 1973. Progress in cartography, EROS Program. Printed in Proceedings of NASA Symposium on Significant Results Obtained from the Earth Resources Technology Satellite-I, Published by the National Aeronautics and Space Administration, 1973.

Kovacs, A. and M. Mellor, 1974. Sea ice morphology and ice as a geologic agent in the southern Beaufort Sea. Printed in the Proceedings of the Symposium on Beaufort Sea Coast and Shelf Research, Published by the Arctic Institute of North America, December 1974.

Stringer, W. J., 1974a. Shore-fast ice in vicinity of Harrison Bay, Printed in the Northern Engineer, Vol. 5, No. 4, Winter 1973/74.

Sringer, W. J., 1974b. The morphology of Beaufort Sea shorefast ice. Presented at the Beaufort Sea Symposium, January 1974, and published in the Proceedings of the Arctic Institute of North America, December 1974.

Zubov, N. N., 1944, Arctic Ice. U. S. Navy Translation from Russian, 112-15.

R.U. #259

OCS COORDINATION OFFICE

University of Alaska

Annual Report for Period Ending March 31, 1976

Project Title:	Experimental Measurements of Sea Ice Failure Stresses Near Grounded Structures
Contract Number:	03-5-022-55
Task Order Number:	7
Principal Investigators:	R. D. Nelson, W. M. Sackinger

I. SUMMARY

The objectives of this study are to measure, in situ, the stresses generated in a sea ice sheet as it fails in the vicinity of a static obstacle and the rate of approach of the ice sheet during this process.

At the time of this writing, only one of three proposed field experiments had been performed and the second was in progress. The results of the first experiment support the hypothesis that stresses generated by pack ice impingement on land fast ice are low when the motion is predominantly shearing past land fast ice. This implies that at certain times land fast ice may be a safe location for oil exploration or drilling activities.

II. INTRODUCTION

Recently the mechanics of the interaction of large sea ice sheets with fixed obstacles has become of interest. This new interest has sprung up because of the need in the near future for fixed offshore structures in ice bound waters. Of major importance to the design of such structures is a knowledge of the forces which would be applied to the structure by sea ice moving past it. The magnitude of these forces depend on three general factors:

a. The mechanics of elastic and plastic deformation of the quasi-continuum of ice floes in the ice sheet.

b. The failure strength of the ice as found in nature.

c. The nature of the forces driving the ice sheet and the associated strain rates during ice-structure interaction.

Each of these factors may be examined experimentally, but it is now known that the results are affected by the size of the ice sample and the degree to which natural conditions are preserved in the experiment. Because of this, the excellent work done on sea ice in the past 20 years has served to provoke nearly as many new questions as it has answered and there is the need for full scale in-situ experiments which preserve as many natural variables as possible. Tabata's large scale beam tests (1958), the plate bending tests performed by Hobbs et. al (1962) and the Aidjex experiments are examples of this development. When it comes to ice-structure interaction, full scale tests are not so easily performed. For arctic conditions, almost any structure large enough to provide an adequate test would be quite expensive. For this reason, the present work has chosen to use natural occuring obstacles as "test structures." Four such static obstacles occur in the arctic environment:

1. Islands

2. Ice Islands

3. Grounded accumulations of ice

4. Grounded pressure ridges at the seaward edge of shore fast ice.

In order to examine the stresses when moving pack ice encounters a structure, we are performing measurements near the grounded pressure ridges at Barrow, Alaska and near a grounded ice accumulation located in the open ocean 100 miles N.W. of Barrow /2° 3.4'N., 162° 4.6 W. This accumulation of ice floes and ridges has been termed a "floeberg" by Stringer and others, but as pointed out by Kovacs is not a "floeberg" as the term has been classically used. In this report, the term floe-island will be used to indicate that is a more or less permanent

feature composed of ice floes and ice ridges. Our primary purpose is to measure the stresses present in a failing ice sheet near such an obstacle and this is being accomplished by the use of embedded load cells (stress transducers). A secondary objective is to measure ice motion and/or strain. At Barrow, this is provided by radar surveillance of the ice pack. For the experiments at the floe-island, no such instrumentation is available and ice motion will be inferred from satellite photography, on-site surveying and navigational data obtained from the helicopter used for logistics.

III. PRESENT STATE OF KNOWLEDGE

Several studies have been conducted in which instrumented pilings were used to measure forces imposed by moving ice when failure is of the crushing or "cutting" type. The study by Blenkarn (1970) is typical while that by Schwartz (1970) is the most complete in that 50 points were instrumented on the piling. Both of these studies dealt with warm, relatively thin ice. Theoretical studies have been performed on the interaction of ice with pilings and with piers whose surfaces slope in order to induce bending in the ice. No experimental data are available in the open literature for structures of an extended nature where the ice must fail by pressure ridging, although several proprietary studies have been done by Imperial Oil Limited. Artificial islands, ice islands, causeways, and docks are typical extended structures which would induce pressure ridging. In addition, multiple piling or single piling structures might have an effective radius much larger than the nominal radius if hummocked ice were to adfreeze to them, or if the cutting action were prevented by interaction with a deep or partially grounded moving pressure ridge. In this case, the structure would become an extended structure for which the ridging mechanism would apply.

IV. STUDY AREA

Near the grounded ice feature or floe-island located approximately 109 miles west of Barrow at 72° 3.4'N, 162° 4.6 W.

V. SOURCES, METHODS, AND RATIONALE OF DATA COLLECTION

In previous work, we had used self contained remote data stations to measure stresses in land fast ice. An aerial reconnaissance of the floe island was made in May, 1975 and again in September, 1975. These flights disclosed several features of its morphology which dictated important changes in the data gathering techniques to be used. We had previously envisioned laying cable from a safe location to several sites of ice activity where transducers would be emplaced. The island is several miles in extent and is composed of broken floes separated by pressure ridges estimated to be as high as 50 feet. It would take several days to walk across it, and even more to string cable through it. The size of the island and its extreme ruggedness make this impossible and require radio telemetry links for data transmission. We had also considered using chart recorders to record the data. However, if a chart recorder is to be capable of recording rapidly varying data, its paper speed must be high which requires frequent paper changes and in general a recorder with high power consumption. Very little is known about the rapidity with which stresses fluctuate in breaking ice. However, it is known that the rate of stress application seriously affects the measured strength of sea ice in laboratory tests and Schwartz's (1972) results from an instrumented bridge pier include some variations at frequencies above 10 Hertz. Therefore, we felt we must have the ability of recording data at frequencies up to 10 Hertz. A digital recording system using magnetic tape was selected as the one most likely to meet the requirements of power consumption and frequency response. In this system, which was designed and built at the University of Alaska, data acquisition is under the control of a micro-computer which makes decisions as to whether significant changes in stress have occurred within successive sampling periods. Thus, data compression can be effected on both the time axis and the stress axis during inactive periods without losing the ability to follow rapidly occuring events during fracture. A parallel recording system using low-cost chart recorders with a frequency response of 1/50 Hertz provides redundancy.

EQUIPMENT

The stress measuring technique used during the experiments has been described by Nelson (1974, 1975). While the electronics instrumentation used at the floe-island differed from that used at Barrow, the principal of stress measurement was the same in each case:

The stress transducers used in these tests are essentially load measuring devices. When embedded in a host such as ice, their output is directly proportional to whatever loading is transferred to them from the ice. If a transducer is stiff, it supports more than its share of the stress. In this case, the transducer output reflects both the magnitude of the ice stress and a stress concentration factor which depends on transducer geometry, transducer stiffness, and rheology of the ice. It has been shown (Hawkes, 1969; Nelson, 1975) that the stress concentration factor is reasonably constant for a given transducer, regardless of the effective ice stiffness (including creep), provided it is in fact stiff relative to the host. Therefore, such a load cell can be used as an embedded stress-measuring transducer. Nelson et al., (1972) have found that stiff transducers can be used to measure ice stresses close to compressive failure of the ice. In addition, stiff transducers should be capable of measuring initial stresses present at the time of transducer installation if the host material can creep. An in-situ emplacement usually involves removing a block of ice from an existing ice floe, making a small hollow in the ice to accept the transducer, and refreezing the block and the transducer into the ice sheet. Subsequent creep in the ice should readjust the local stress field until the transducer and replaced block assume their full share of the load, a process which takes place most rapidly for warm, saline ice.

The transducers used in the land-fast ice near Barrow contain four strain gages connected in a Wheatstone bridge supplied by a Zener diode-regulated DC source. The signal from the bridge is amplified by an operational amplifier. A DC to DC converter provides $\pm$ 15 V from a 12 V source. A relaxation oscillator and solid state timer feed timing pulses to a relay which shunts the bridge with 750,000 ohms once each hour to provide time marks on the recorder chart. Two-point Rustrak recorders are used at 1 point per 8 seconds and 1 inch per hour chart speed. The movement is diode protected. Since each recorder has two data channels, one channel is used at a sensitivity corresponding to approximately 0 $\pm$ 90 psi ice stress. The second channel monitors the same transducer at approximately 0 $\pm$ 1800 psi to record high stress events. Both the batteries and the electronics are housed in a rugged, insulated box which has a thin, uninsulated bottom. Snow is heaped up around the box for further insulation. Thus, the effects of severe air temperature variations on the electronics, recorder, and power supply are minimized by the insulation and the thermal mass of the ice, while the interior of the box is heated by power dissipated in the electronic package.

Because of the remoteness of the floe-island, its size, and the fact that destruction of the data gathering stations was likely, it was decided to telemeter data from the stress transducers to a safe recording location at the center of the island. For this purpose, each transducer was equipped with an internal voltage controlled oscillator (VCO) to convert the amplified output of the

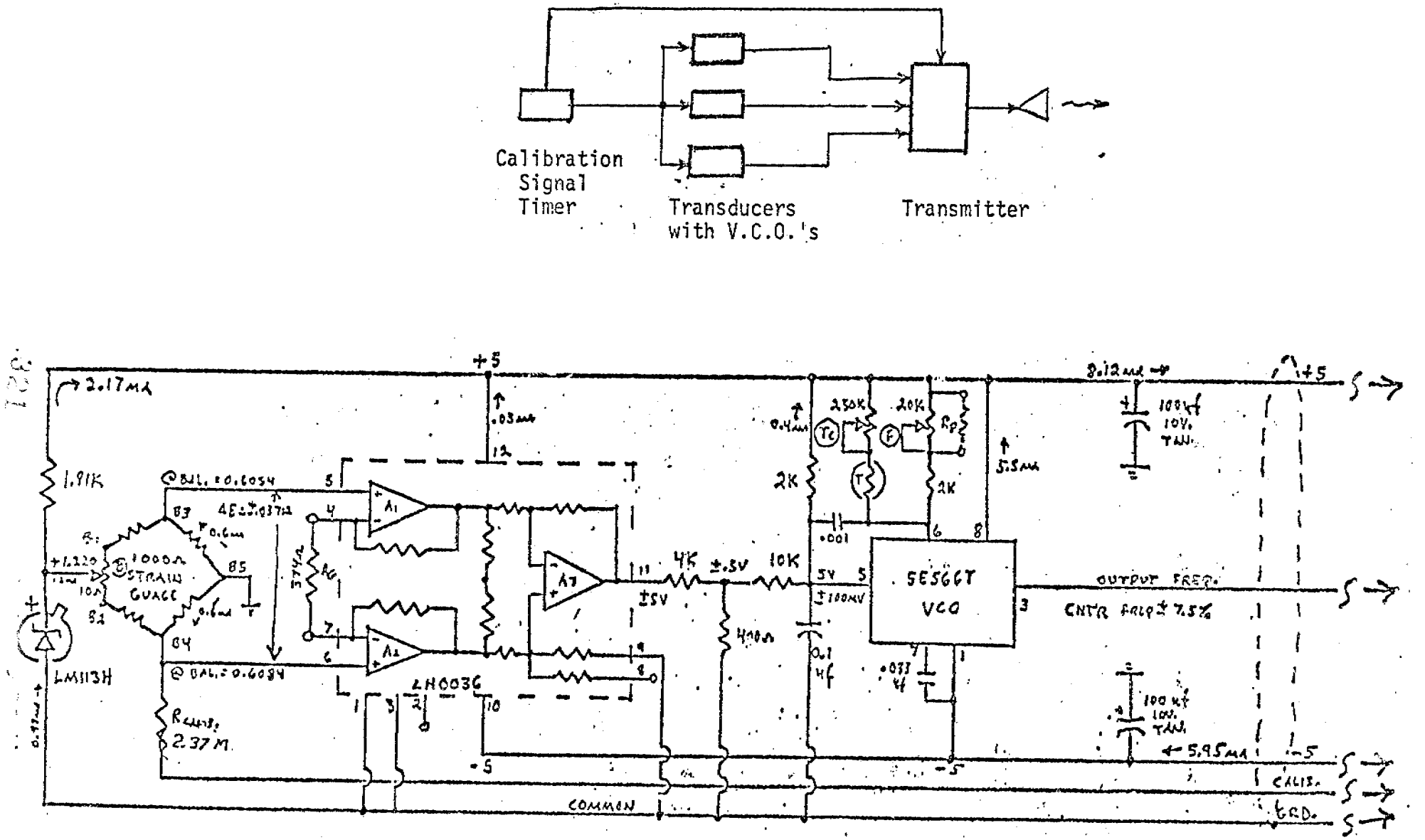

Figure 1. Strain Gage Bridge, Amplifier, and V.C.O. Built Into Transducers.

1000 ohm strain-gage bridge to a frequency modulated (FM) signal. As shown in Figure 1, four FM signals were multiplexed into one transmitter (Monitron T-15F-13) whose signal was sent to the central receiving station. Standard IRIG center frequencies were used for the VCO's with ± 7 1/2% modulation. At each transmitter three channels were used for stress transducers while the fourth was used for an auto-calibration signal. Each transducer was fitted with a 2.37 megohm resistor which could be shunted through a relay across one leg of the Wheatstone bridge to provide a known calibration signal. These relays were controlled by a central timing network which also controlled the signal level on the fourth channel. In the reduction of the data, a signal on channel four going from negative full scale to positive full scale was regarded as an indicator that the outputs of all channels during that period were to be regarded as calibration data. System sensitivity was 800 psi full scale.

Because of possible severe temperature changes during the experiments, close attention was paid to thermal compensation of the transducer systems. Since the strain bridge, amplifier, and VCO were all contained in the transducer shell a two point thermal compensation of the entire subsystem could be effected by including the thermister (T). The system was balanced to zero output at 0° C by adjusting resistors (B) and (F). The system was then cooled to -20°C and rebalanced with resistor (T_c). This provided the desired thermal compensation and reduced temperature generated signals to less than 20 psi between the two calibration points. Thermally caused variations in the transmitter were specified by its manufacture to be less than 0.005% of center frequency over the range of -40°F to +80°F. The transducers and transmitter are powered by lithium batteries placed in an insulated box on the ice.

Each transmitting channel uses a Monitron R15F-N receiver. The four signals on each channel are then separated and demodulated as shown in Figure 2. The four data channels are then sequentially sampled and converted to digital information at a rate of one channel every 0.008 seconds. This permits recording data at frequencies up to 15 Hertz when eight data channels (two transmitters) are in use. The frequency response is limited by the digital panel meter which is used to digitize the analog data. Channel sampling is under the control of the central processor (CPU) which stores the signal level of each channel and the time only if the stress level is ± 5 psi different from the previously stored reading on that channel. When the CPU memory fills up, all recorded data are dumped onto the magnetic tape in B.C.D. code and the memory is reset for further data taking. Data is put on the tape at a density of 1.66×10^4 data points per tape. During the time the data is being dumped to the tape frequency response is limited to 0.15 Hertz.

Since the equipment at the central data recorder was in a protected environment, its thermal sensitivity is less critical. The equipment was located in an insulated box inside a shelter at the center of the island. Lead/acid batteries were used to supply power.

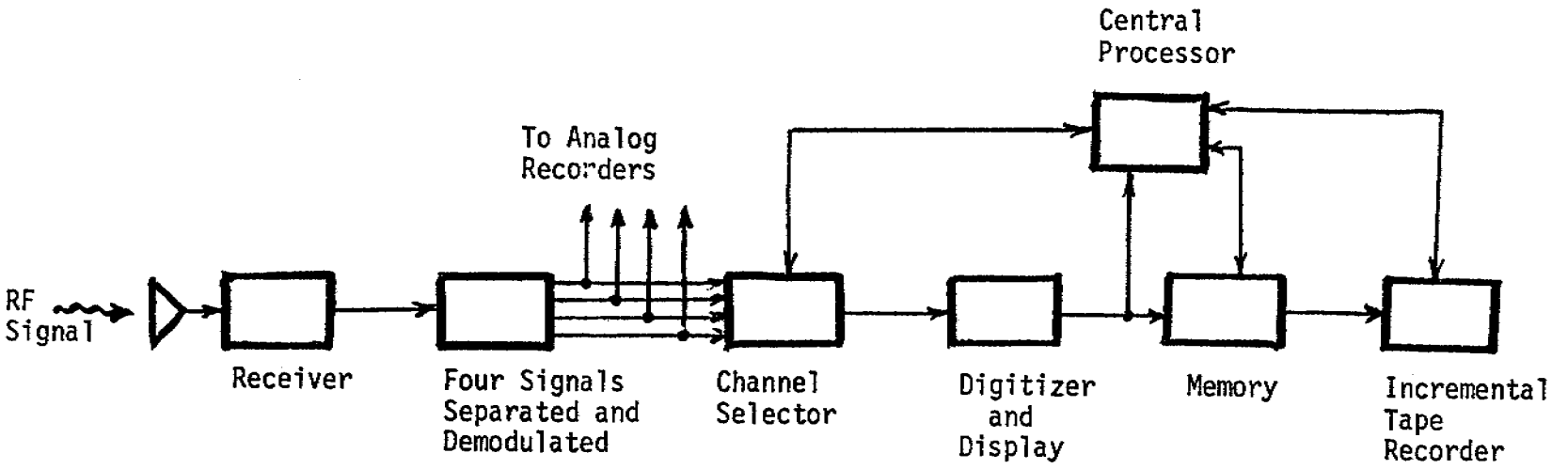

Figure 2. Block Diagram for Receiver and Data Handling Equipment. Channel Selector accepts Signals from Two Receivers.

VI. RESULTS

Experiment in Shorefast Ice at Barrow, Alaska - November, 1975:

It was originally planned to conduct a field trip to the floe-island during late October. However, because of the shortage of electronic supplies, the telemetered stress stations were not available.

At that time, it was brought to our attention that a number of grounded multi-year ice floes were present in water up to about 50 foot depth at Barrow, Alaska. If massive enough and truly grounded, one of these floes would provide a safe location for non-telemetered instruments, while forcing the surrounding annual ice to break during the approach of pack ice. An additional factor was that the ice surveillance radar system operated by the University of Alaska, at N.A.R.L., Barrow, Alaska, would be available to monitor ice motion. On a reconnaissance flight, October, 1975, a suitable grounded floe was found by Dr. Lewis Shapiro and Mr. Robert Simms. Six transducer systems were obtained on loan from the University of Alaska Sea Grant Program and prepared for service. On November 5, 1975, a second reconnaissance flight was made to find the previously selected floe. However, in the interim the pack ice had begun to move, closing the open lead near the shorefast ice, and generating a strong shearing action as it moved in a generally southwesterly direction parallel to shore. As a result the once-smooth shorefast ice was pressured into a field of broken blocks composing the early stages of the barrier ridge which would form along the coast later. The previously selected floe could not be found and was apparently either buried or broken up. An alternate floe was located near the shear ridge which was then actiye parallel to shore, but when equipment was landed on it by helicopter it became apparent that it was not safe, as the adjacent blocks were visibly moving and the floe itself was cracking. On November 7, a third floe was located approximately one and one-half miles off-shore of N.A.R.L. Six transducers were installed at this location on November 9.

By this time, the ice action had ceased and later the pack moved away. Since the ice surrounding the floe was broken and piled to about three feet, it was not possible to install the transducers in ice adjacent to the floe. Therefore, they were installed in the floe itself at a depth of 10 inches. Figure 3 shows the orientation of the shear ridge. It was reasoned that stresses in the floe would be related to forces at the border between the pack and shorefast ice masses during subsequent motion. No other measurements would have been feasible.

Although no thickness measurements were made, it is unlikely that the floe or the adjacent broken ice was grounded since the water depth at this location is estimated to be over 50 feet.

Several days after installation of the transducers, the pack ice returned. The instruments and data were retrieved on December 18, 1975.

Figure 3. Transducer Location for Experiment at Barrow, Alaska, November, 1975.

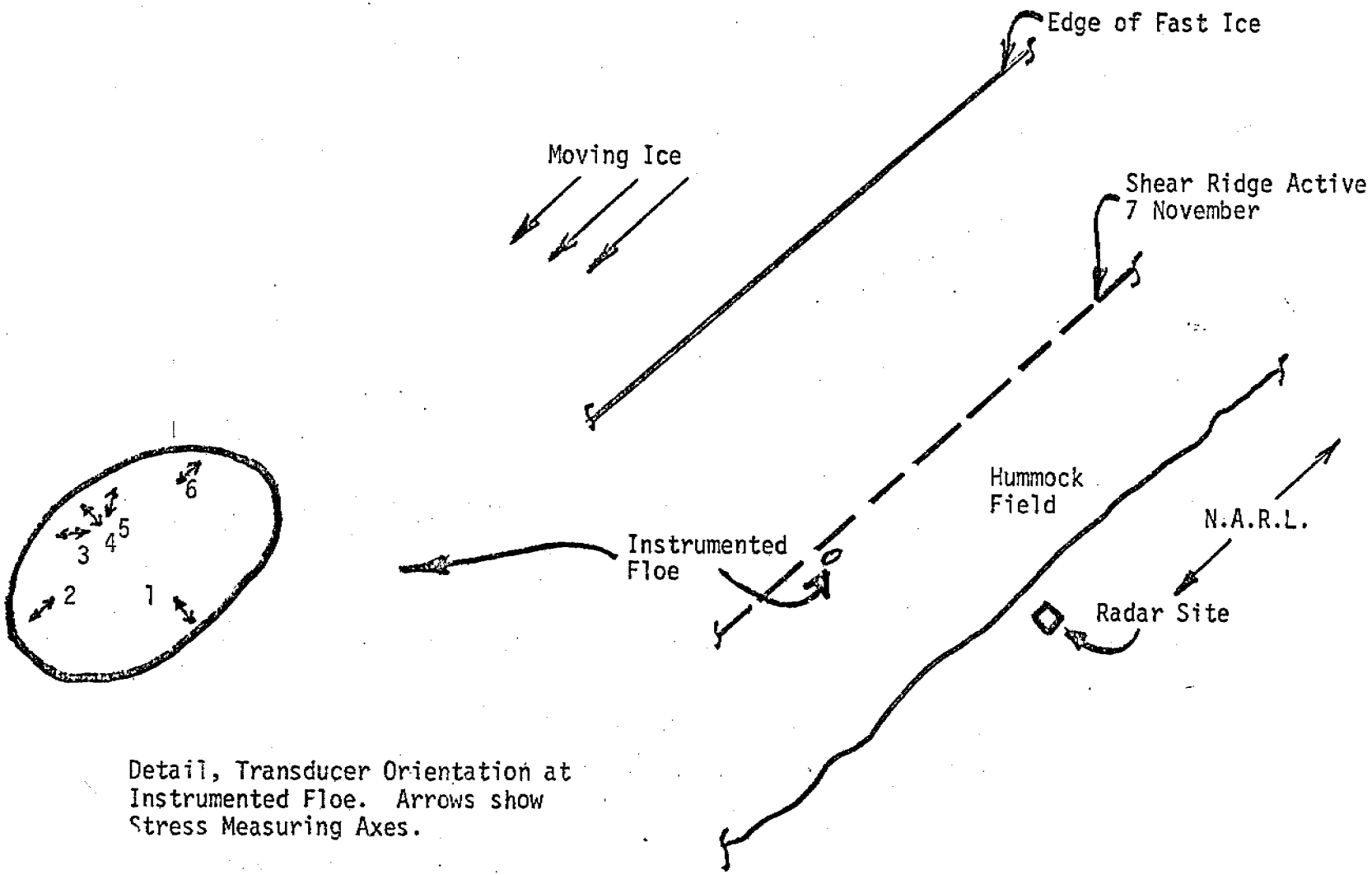

Detail, Transducer Orientation at Instrumented Floe. Arrows show Stress Measuring Axes.

Experiments, Spring, 1976, at the Floe-Island

The main experimental periods were selected to be March 15-23, 1976 and April 3-10, 1976. These periods coincide with coverage of the area by the LANDSAT II Satellite. On February 20, 1976, an attempt at a dry-run was made on the floe-island. The purpose of this dry-run was to determine whether an adequate radio link would be established by the 10 foot high antennas which we expected to place at the top of high ridges in the floe-island and the adjacent pack. A sending site consisting of a transmitter and an antenna was established near the lee end of the floe-island. The floe-island in this area consisted of floes about 100 yards in diameter and pressure ridges 10 to 20 feet high. A floe was selected which was well removed from the new ice which had formed behind the island. We then expected to move away several miles toward the head of the island and check for radio reception. However, operational problems with the helicopter forced an immediate return to Barrow without being able to retrieve the transmitting station. Further difficulties with the helicopter prevented our return for 7 days. During this time, the ice in the area reversed its motion, breaking up both the new ice and the existing floes and creating ridges as high as 50 feet. The transmitting station could not be found.

On March 17, 18 and 19, 1976, coincident with the LANDSAT II overpass, logistics items (fuel and shelter) were successfully deployed to the floe-island by helicopter. Extensive aerial photography was obtained for the three days. The change in ice configuration around the island during the changing weather conditions of the three days provided considerable insight into the dynamics of pack ice around grounded structures. Both steady-state and transient flow patterns of the ice sheet were observed. Details of the observations, together with illustrative photographs, will be included in a later report.

VII. DISCUSSION

Experiment in Shorefast Ice at Barrow, Alaska, November, 1975

Examination of the time lapse films taken of the ice surveillance radar screen shows that the ice returned with relative motion nearly parallel to the land-fast boundary, which lay about 2 1/2 miles off shore, with about 1 1/2 miles of ice extending from the main pressure ridge. No new pressure ridge formation could be detected on the radar image. This shearing motion continued with some interruptions until December 6, 1975. No ice motion with a strongly on-shore velocity component occurred during this period and there was no accumulation of ice at the boundary. The chart records from all of the stress stations have been examined to locate high stress events. All of the charts contain off-scale events with some records being highly erratic much of the time. We do not believe these events are valid occurrances of high stress. Instead, we feel that they are spurious results which are due to damage caused to the main electronics battery pack which was dropped while being unloaded from the helicopter. Previous experience has shown that the DC-to DC converters used in the electronics package have a poor tolerance for supply voltage variations and when the battery voltage runs low a specific type of off-scale event occurs. This low battery condition is characterized by failure of the relays in the timer circuit and in the coarse/fine alternation circuit to operate. The result is the loss of both timing marks and the coarse trace (low gain trace). Discounting events of this type there was no indication of high stress events in any of the recorded data. Those periods of time where one or more channels were in operation indicate only semi-diurnally varying stresses of about 10 psi peak to peak which are probably tidally generated.

On December 6, 1975, at about 2100 hours, the moving ice approached the shorefast ice at an angle of about 45° to the edge of the land fast ice. That is, it approached from nearly due north. Between 2130 hours and 2200 hours, a pressure ridge formed at the outer edge of the shore fast ice, about 2 1/2 miles offshore. The ridge grew progressively from the northeast to the southwest and was clearly discernable on the radar images. None of the stress transducers were operating during this time as their batteries had all apparently run out of power.

Because of difficulties with the electronics power supplies, the experiment produced only intermittent data and it is difficult to draw firm conclusions about the stresses in the ice during this time. Further complicating the picture is the fact that the transducers were placed within a large hummock field and over a mile from the boundary at which ice activity occurred following their placement. However, the distinct lack of either identifiable stress events or deformation in the fast ice indicates that stresses generated in the interior of land-fast ice may be low when the pack shears past it. Further experiments with telemetered data and extensive on-site visual monitoring would be required to adequately examine this mode of ice action.

VIII. CONCLUSIONS

1. High stresses were not observed to be generated during events involving shear of pack ice past land-fast ice.

2. A telemetered measuring system was developed for sea ice which is now being deployed.

IX. NEEDS FOR FURTHER STUDY

The radio telemetry system developed for the stress sensors provides a particularly convenient method of stress analysis. The study which is being performed here will only begin to answer questions about the failure of sea ice *in situ*. The limited number of transducers will not allow defining clearly either the stress profile around an obstacle or the stress profile through the depth of the ice sheet. An experiment with about 21 transducers should be performed to answer questions on stress profile. Similar experiments should be performed simultaneously with local ice strain measuring devices and/or bottom referenced motion sensors. Such experiments could be done at reasonable cost levels because the basic electronics data acquisition equipment is now available.

X. SUMMARY OF FOURTH QUARTER ACTIVITIES

1. Field Trip Schedule

   a. February 21 - NOAA Helicopter to Floe-island

   b. February 29 - NOAA Helicopter to Floe-island

   c. March 16-23 - Several trips, ERA Helicopter to Floe-island

2. Parties

   Trip (a) R. D. Nelson, University of Alaska, P.I.
   E. R. Hoskins, South Dakota School of Mines, Consultant

   (b) E. R. Hoskins

   (c) W. M. Sackinger, University of Alaska, P.I.
   Wayne Pinger, University of Alaska, Technical Assistant

3. Methods

   N/A

4. Locality - Floe-island is located at 72° 03.4' N, 162° 04.6' W.

5. Data Collected

   Trips 1-a and 1-b above were to establish possibility of radio communication in region. Results inconclusive because of loss of equipment. Trip 1-c above established logistics base at floe island and investigated ice action in vicinity.

   Analysis of data from November testing in land-fast ice continued.

XI. REFERENCES

1. Blenkarn, K. A.; "Measurement and Analysis of Ice Forces on Cook Inlet Structures." Off Shore Technology Conference Paper OTC 1261, 1970.

2. Hawkes, I., 1969. "Stress Evaluation in Low-Modulus and Viscoelastic Materials Using Photoelastic Glass Inclusions." Experimental Mechanics, pp. 58-66, February, 1969.

3. Hobbs, H.A., Cutcliffe, J. L., and Kingery, W.D.; "Effect of Creep and Temperature Gradients on Long-time Deformation of Ice Sheets," in Ice and Snow, W. D. Kingery Ed., M.I.T. Press, Cambridge, Mass., 1963.

4. Nelson, R. D., Taurianinen, M, and Borghorst, J.; 1972, "Techniques for Measuring Stress in Sea Ice," University of Alaska, Institute of Arctic Environmental Engineering.

5. Nelson, R. D., 1974. "Measurements of Tide and Temperature Generated Stresses in Shorefast Sea Ice," in The Coast and Shelf of the Beaufort Sea, J. Reed and J. Sater, Editors, Arctic Institute of North America, Arlington, Virginia.

6. Nelson, R. D., 1975. "Internal Stress Measurements in Ice Sheets Using Embedded Load Cells," Presented at Third International Conference on Port and Ocean Engineering under Arctic Conditions, University of Alaska, Fairbanks, Alaska.

7. Schwartz, J., 1970; "The Pressure of Floating Ice Fields on Piles," Proc. I.A.H.R. Symposium on Ice and Its Action on Hydraulic Structures, Reykjavik, Iceland.

8. Tabata, T.; "Studies on Visco-Elastic Properties of Sea Ice," in Arctic Sea Ice, Nat. Acad. Sci./Nat. Res. Council Pub. 598, Washington, D.C., 1958.

RU 261/262

OCS ANNUAL REPORT

Beaufort Sea, Chukchi Sea, Bering Strait Historical Baseline Ice Study

William R. Hunt
Claus-M. Naske

I. Task Objectives:

The objectives of this study are to collect data on the history of ice conditions in the Beaufort and Chukchi Seas, and Bering Strait, to synthesize this data, and to present the results in report and cartographic form.

II. Field or Laboratory Activities:

A. William R. Hunt searched records at the Scott Polar Research Institute in the summer of 1975 and the Public Archives of Canada and in the National Archives in the spring of 1975.

Claus-M. Naske worked at the National Archives November 15-25, 1975 and at the Old Dartmouth Historical Society Whaling Museum in New Bedford, Massachusetts, and at libraries of Harvard University in Boston from December 29, 1975 to January 17, 1976.

B. William R. Hunt
SS.#532-22-1162
Professor of History
University of Alaska

Claus-M. Naske
SS#574-12-5479
Associate Professor of History
University of Alaska

C. Methods:

The investigators have determined the location of resource material likely to be worthy of investigation and gathered it for analysis.

D. Not Applicable.

E. Date Collected or Analyzed:

1. Number and types.

18 whaling logs for the 19th century

5 U.S. Coast Guard cutter logs covering the period from 1927 to 1970.

One Canadian Coast Guard patrol vessel log.

One Summation of Captain C. T. Pedersen's observations over a 40 year period.

One Station logs and Meteorological Reports of the Point Barrow Refuge Station from 1891-1896.

22 Published narratives of polar explorers and other travelers

10 Collections of commercial papers and manuscript journals.

2. Number and Type of Analysis:

All data available for the Beaufort, Chukchi and Bering Seas will be summarized in map form. Each map will reflect ice conditions noted for a given month, summarized in ten year increments (i.e. all reports within the study area will be noted onto one map and then transferred to a final map reflecting condition changes during ten year periods).

Since there is no consistent formula for reporting ice conditions, the investigators have developed the following measurement standard:

1. A circle represents pack ice of unstated density or thickness.
2. A triangle represents drift ice, open leads or rotten ice at the edge of the ice pack.
3. A square represents an undesignated ice condition (Pack or drift ice observations that are not explained in vessel logs).

Each monthly map, for any given year, may reflect open water or unknown ice conditions. It is expected that the use of ten-year map units will provide the means of extrapolating and/or forecasting conditions for the unreported areas.

III. Results:

Appended Log Summaries

Appended Charts with Vessel Tracks.

Data Used:

The source materials examined thus far include the field notes of explorers - Vilhjalmur Stefansson, Ernest Leffingwell, George DeLong, Henry Kellett, W. H. Hooper, Bob Bartlett, Henry Collinson, Edward McClure, W. Beechey, and Knud Rasmussen. Also investigated have been the journels of coastal residents and traders - Charles Brower, Carl Lomen, William Van Valin, Charles Klengenberg, Ellsworth West, and Gus Maskik.

Some whaling journels have been published and those of John Cook, John Lawrence, and Herman Bodfish have been examined.

Manuscript logs examined at this point include the following:

1. E. Morgan, 10 November 1868 to 14 September 1871.
2. Revenue Steamer Corwin, 1 March 1881 to 26 August 1884.
3. Revenue Steamer Bear, 1 June 1898 to 17 September 1898.
4. Belvedere, 27 April 1897 to 27 October 1898.
5. Helen Mar, 13 May 1872 to 14 October 1878.
6. U.S.C.G. Cutter Staten Island, 1 October 1967 to 7 September 1970.
7. St. Roch, 1940-1944 (two transits of the Northwest Passage).

IV. Preliminary Interpretation of Results:

The investigators are presenting as comprehensive a report as possible of ship position, ice conditions, weather, and the vessel's track. In addition to this data, all comments in the log relative to numbers of ships, catches of whales and walrus, storms, shipwrecks, icing on the ship, and any other observations of possible interest have been recorded. The documentation of such miscellaneous data represents a task of some magnitude. Reading the original logs is a tedious, time consuming process, particularly when ships' officers wrote in a script which is difficult to decipher. This difficulty is compounded further when microfilms of logs must be utilized. Sometimes the quality of reproduction is very poor because of the condition - stained or faded - of the original material.

The data gathered from 19th century sources has not been as consistently valuable as that available for the modern era. But enough data exists to indicate a 26-year cycle of mounting severity of ice conditions. Records examined go back as early as the 1860's. It is remarkable that in 1871 heavy ice trapped and destroyed the entire whaling fleet in the Beaufort Sea. Ice conditions were equally severe in 1897, 1923, 1949, and, of course, in 1975 when the barge convoy to Prudhoe Bay encountered heavy ice which forced some vessels to return south with their cargoes.

Maritime records reveal that experienced Arctic navigators from mid-19th century customarily skirted the Siberian shore in making their passage through the Bering Strait. Ice breaks free earlier along the Siberian side of the strait than it does on the Alaskan side. It may be that the Prudhoe Bay barge fleet would have had less difficulty with the ice in 1975 if this historic knowledge of ice conditions had not been lost.

Our preliminary interpretation of results indicates the usefulness of the data gathered and synthesized. The chief value is in what the data reveals of ice patterns during the navigational season. The extent of available data on ice navigation creates the possibility of prediction of ice movement. The investigators' documentation of a probable 26-year cycle of severe ice conditions is significant.

Efforts to determine shore ice conditions have been disappointing. A search has been made of all available published and archival journels of Arctic traders, military, missionaries, and other shore based observers. Unfortunately the reporting of shore ice conditions has been spotty and inconsistent - thus of minor value. The best observations analyzed thus far have been the Station Logs and Meteorological Reports of the Point Barrow Refuge Station from 1891-1896 which have been appended.

Published narratives of explorers have proved less useful than had been anticipated. Observations reported are not comprehensive enough to provide more than random information. In an effort to find more data we investigated the original field notes of several explorers. Those of Stefansson and others failed to yield any better data than his published narrative of the Canadian Arctic Expedition (1913-1918). Stefansson was a precise investigator but saw no reason to report on ice conditions in other than general terms, and according to his particular concerns.

On the whole, the investigators are confident that the completed project will be a successful demonstration of the importance of a thorough search and analysis of the historic literature. The results of this study will be even more useful if it is extended into the Bering Sea.

V. Problems Encountered/Recommended Changes:

The determination of the location of relevant data has been one problem. But, one greater frustration has been in getting government archivists to respond in a timely manner to requests for material.

Another problem has been in the paucity of ice information in Lomen Company records and the Annual Reports of the U.S. Bureau of Indian Affairs teachers. And it was disappointing to learn that the U.S. Navy kept no ice records along the coast of Pet-4 over the period of active petroleum searches. Logs of the Foss Launch and Tug Company proved to be barren of ice observations, yet one might have expected Foss navigators to have a strong interest in recording such information for future use.

In November, one of the investigators spent two weeks in the National Archives in Washington, D.C. and at the Federal Records Center in Suitland, Maryland. The National Archives yielded logs of the U.S. Coast Guard Cutter Northland from 1928 to 1938. No problems were encountered here. At Suitland, Maryland, where the more recent Coast Guard logs are kept, considerable difficulties were encountered. The staff of the Federal Records Center knew that it held these records, but had no idea where they were because no inventory numbers had been assigned as yet. Phoning the Coast Guard, the investigator was asked which logs he wanted to work with. No list of cutter names with their areas of operation existed. The investigator secured a copy of all Coast Guard ships, and then guessed which ones might have worked in the Arctic. The names of likely vessels were phoned to the Coast Guard which, in return, supplied the Records Center with the necessary accession numbers.

Huge truckloads of dusty cases with logbooks arrived. All had to be checked to determine which vessels had worked in the Arctic. Those who had,

the investigator held back to extract the raw data, i.e., xerox or film appropriate pages.

Some 711 pages or pertinent raw data were xeroxed from the Staten Island, Storis and Northwind covering the years 1967 through 1970. Additionally, some 821 frames of film were ordered covering pertinent data from the Northwind and Storis covering the 1950's through 1966. That material, although ordered in November of 1975, has not yet been received. Repeated inquiries have been sent. The investigators were told that the camera broke down and that we could expect delivery sometime in the spring of 1976.

One of the investigators spent three weeks in December and January in New Bedford, Massachusetts, at the Whaling Museum. A wealth of material is available and good data was secured. Much more is available, but most of the microfilm copies we ordered are extremely difficult to read, some impossible. Another trip to New Bedford is planned to scan and extract data from the original logs both at the Whaling Museum and the New Bedford Free Public Library.

One week again was spent in Washington, D.C. at the National Archives on the heels of the New Bedford stay, in order to discover the location of the logs of the BIA supply ships Boxer (1922-1938), and North Star (1932-1955). Nobody knew the whereabouts of the logs. Many phone calls to various Federal Records Centers finally yielded the suspicion that the logs might be stored in St. Louis, Missouri. In March 1976, the investigators learned that the logs are located at the BIA offices in Seattle, Washington. We plan to extract data from these logs.

It is clearly apparent that the search and collection of the data so far has been exceedingly tedious and time consuming. Much time is needed, both for collection and analysis.

We recommend that the project be extended into the next fiscal year so that the Bering Sea may be included within this study. It would seem that a knowledge of historic ice conditions in the Bering Sea will be even more essential than for Bering Strait, Chukchi Sea, and Beaufort Sea because of the high interest in petroleum development and the competing commercial interest of the rich fisheries. Bering Sea shipping traffic has been more extensive than the total of that in the Chukchi Sea, Beaufort Sea, and Bering Strait so that a vast amount of ice data exists. Analysis of this considerable body of historical material will complement and complete the original project.

APPENDIX A

U.S. Revenue Cutter Service

Alaska File of the Revenue Cutter Service, 1867-1914

Point Barrow Station, 1891-1896

(Shore Observations)

U.S. Revenue Cutter Service - Alaska File of the Revenue Cutter Service, 1867-1914. Point Barrow Station, 1891-1896 (Shore Observations)

Aug. 16, 1891

Moderate winds and cloudy all day. Ice breaking up and leads off shore opening. Still ice on the bar remains piled up high - prospect for ships arriving this season looks slim.

Aug. 17, 1891

Ice seems opening a little. Everybody having business with the ships have either gone down or are going to meet them. Apparently ships are at Pt. Belcher.

Aug. 21, 1891

Ice opening - a good deal of open water in sight.

Aug. 22, 1891

A number of steamers anchored off station. At 2 p.m. all three ships got underway to go round the Point for shelter from ice.

Aug. 24, 1891

Ice setting in upon the shore - One sail well to the S.W. in sight, underweigh.

Aug. 25, 1891

Plenty of ice in every direction but rather loose.

Aug. 27, 1891

All 5 steamers still at anchor in sight of the Station - Ice closing in - but little water in sight - In the p.m. Narwhale got so jammed in by

the ice that the Balena came to her assistance. After considerable labor the N. was got out of her precarious situation when she went about a mile further N. and anchored.

Aug. 29, 1891

Ice closing in on the shores.

Aug. 30, 1891

Ice holds quite compact with but little open water, but ice moving north rapidly.

Sept. 1, 1891

Ice closing in from the shores.

Sept. 2, 1891

Heavy ice closing in upon the shores and heavy as seen in every direction- but little open water to be seen and only inside the ridge of ice lying along on the bar where the Orca and Narwhale are now lying. Everywhere else seaward, compact broken ice.

Sept. 3, 1891

Ice very compact - no open water to be seen except a little along inside the bar where the two steamers are now lying.

Sept. 4, 1891

This morning report from the Point says 2 steamers lying there direct from Mckenzie Bay with 21 whales, bound to S.F. direct as soon as ice opens. Ice still heavy and compact off this station - no chance for the ships to get out.

Sept. 5, 1891

In the night heavy showers of rain, 43 in. fell. Wind changing suddenly from S.E. to S.W. in heavy squalls. Ice leaving the shores.

Sept. 6, 1891

Word came from down the coast this noon that 4 schooners, Rosario, Nicoline, Alton and Silver Wave were jammed in by ice in Pearl Bay, and were in a critical position. As far as can be seen all the steamers are around the Point at anchor in clear water.

Sept. 9, 1891

A storm threatening - water outside ridge ice, opening, from appearances ships might get out.

Sept. 11, 1891

Clear water to the S & W - Ice remains on the bar but open water inside.

Sept. 12, 1891

Ice still remains on the bar, open water outside with floating ice.

Sept. 13, 1891

Moderate gale with fog from E, NE. Ice rapidly disappearing.

Sept. 17, 1891

Weather thick and foggy, with a fresh breeze and heavy swells setting in from the S.

Sept. 19, 1891

Sea quite clear of ice.

Sept. 21, 1891

Little or no ice in sight - but little change during the day.

Sept. 22, 1891

Strong breeze and misty weather. No ice.

Sept. 23, 1891

No ice in sight - ships reported cruising off the Point.

Sept. 24, 1891

Little snow in the morning with mist all day - no ice in sight.

Sept. 25, 1891

Moderate winds and foggy weather - no ice nor vessel in sight. Continues the same through the day.

Sept. 27, 1891

Much calm weather during the day.

Sept. 28, 1891

Cold, raw wind with veins of fog - no ice in sight.

Sept. 30, 1891

No ice nor sail in sight.

Oct. 1, 1891

No sail nor ice in sight.

Oct. 2, 1891

No ice nor sail in sight.

Oct. 3, 1891

No ice nor sail in sight. Heavy swell setting in on the shore - a blizzard prevailing.

Oct. 4, 1891

Blizzard continues with an increased swell setting on shore - wind backing to the N.

Oct. 5, 1891

In the morning clearing weather but still cloudy. Plenty of heavy pack ice drifting down.

Oct. 7, 1891

No ice but a few drifting pieces in sight.

Oct. 8, 1891

No ice in sight but a few drifting pieces.

Oct. 9, 1891

Pack ice in sight - drifting in toward the shore.

Oct. 10, 1891

Pack ice setting in on shore. At night a heavy swell setting on shore.

Oct. 11, 1891

Strong winds and a heavy swell setting on shore - no ice, except a few floating pieces in sight.

Oct. 13, 1891

Light winds - some floating ice in sight.

Oct. 14, 1891

Fresh winds and clearing weather- floating ice coming down rapidly from N. In the p.m. young ice making fast.

Oct. 15, 1891

In the morning light winds and clearing weather - ice making at sea quite fast. In the p.m. the sea covered with ice.

Oct. 16, 1891

Sea frozen over.

Oct. 17, 1891

Ice in the sea broken up. Pack in sight six miles off shore.

Oct. 18, 1891

Ice in the sea broken up.

Oct. 21, 1891

No open water in sight. Ice piling up in the open sea.

Oct. 23, 1891

A.M. - sea all frozen over.

P.M. - some open water in sight, ice broken up and rough.

Oct. 26, 1891

Ice broken up outside the bar - plenty of open water.

Oct. 27, 1891

In a.m. fair weather with wind W. having shifted in the night from S.E. Much open water and the winds from it quite warm.

Oct. 29, 1891

In the a.m. light winds and fair weather - but little open water in sight. No open water in sight at sundown.

Oct. 30, 1891

Some open water in sight - many Bears have been seen lately prowling about on the ice. Two seen yesterday - one shot and wounded.

Nov. 1, 1891

In a.m. overcast with light variable winds - plenty of open water.

Nov. 2, 1891

In a.m. some open water in sight. In p.m. and at night clear. No open water in sight.

Nov. 13, 1891

No open water in sight.

Nov. 16, 1891

No open water in sight.

Nov. 23, 1891

Considerable open water in sight. At 10 clear except a bank of mist at the N.W. hanging over the open water.

Nov. 24, 1891

In the morning light winds and clear weather. A bank of mist lying over the open water at the N.W.

Nov. 25, 1891

In the a.m. fresh winds and clear weather with the exception of a heavy bank of mist over the open water in the N.W.

Nov. 26, 1891

In the a.m. fresh winds and clear weather with the exception of a bank of mist lying over the open water in the N.W.

Nov. 29, 1891

In the p.m. and evening clear excepting a bank of mist over the open water in the N.W.

Nov. 30, 1891

Ditto.

Dec. 1, 1891

In the a.m. clear and cool. A bank of mist lying over the water in the N.W. otherwise not a sign of a cloud to be seen.

Dec. 2, 1891

Bank of mist over the water in the N.W.

Dec. 3. 1891

A bank of mist in the N.W. . In the a.m. thick mist - frozen - driving in from the open water making a perceptible deposit similar to frost or snow.

Dec. 4, 1891

Same mist from open water.

Dec. 6, 1891

No water and but little mist to be seen.

Dec. 14, 1891

No. open water in sight - no mist.

Dec. 24, 1891

No open water in sight but the ice can be heard grinding and crushing together.

Jan. 3, 1892

Ice grinding in the offing with open water beyond.

Jan. 8, 1892

In p.m. plenty of open water.

Jan. 9, 1892

Plenty of open water in sight.

Jan 13, 1892

A low bank of mist lying over the open water offshore.

Jan. 14, 1892

A low bank of mist extending half way round the horizon from N.E. to S.W. over the open water, indicating a large amount of open water in those directions.

Jan. 15, 1892

Mist bank over the open water extending from S.W. to N.E.

Jan. 17, 1892

Bank of mist lying steadily over the open water extending from S.W. round W to the N.E.

Jan. 19, 1892

At 9 a.m. a light mist came in from the open water and continued until about 2 p.m. when it cleared up.

Jan. 21, 1892

Much open water with a bank of mist lying over it in the W.

Jan. 27, 1892

In the a.m. frozen mist continues falling. This mist undoubtedly arises from the open water in the sea as the bank of mist is always seen in clear weather having the appearance of a low fog bank.

Feb. 4, 1892

Plenty of open water with a bank of mist lying over it.

Feb. 5, 1892

No open water in sight - the pack ice having closed in.

Feb. 6, 1892

No water in sight.

Feb. 8, 1892

Some sight of open water in the W.

Feb. 10, 1892

No open water in sight.

Feb. 11, 1892

Ditto.

Feb. 18, 1892

Plenty of open water in sight.

Feb. 14, 1892

The ice floe seems to be breaking off and floating away (a.m.). At 12 mist had lifted and ice pack had closed in - no open water in sight.

Feb. 15, 1892

Ice grinding and piling up in ridges - no open water.

Feb. 17, 1892

No open water in sight but the ice in the offing moving crunching and grinding fearfully.

Feb. 18, 1892

A bank of mist lying over the open water in the W and N.W.

Feb. 19, 1802

Some open water in sight.

Feb. 24, 1892

No open water to be seen - ice pack closed in.

Feb. 25, 1892

No open water in sight.

Feb. 27, 1892

No open water in sight.

Feb. 28, 1892

Ditto.

March 1, 1892

Ditto.

March 4, 1892

Ditto.

March 5, 1892

Ditto.

March 7, 1892

Ditto.

M[illegible] 9, 1892

Ditto.

March 10, 1892

Ditto.

March 11, 1892

Ditto.

March 13, 1892

In the a.m. light winds and clear weather - heavy mirage over the ice no open water.

March 15, 1892

No open water in sight. Natives can catch no seal. All the women and children obliged to go out on the ice to obtain tomcod for a precarious living.

March 17, 1892

No open water in sight.

March 23, 1892

Ditto, but natives report open water 6 miles out.

March 25, 1892

Some mist lying over the water to the W and N.W. indicating open water in that direction.

March 29, 1892

Mist hanging over the ice to the N.W. indicating open water in that direction.

March 30, 1892

No open water in sight.

March 31, 1892

No open water in sight.

April 2, 1892

Lead of open water in the N.W.

April 3, 1892

Ditto.

April 4, 1892

Weather warmer - open water in sight some four miles out.

April 8, 1892

In a.m. fresh winds and clear weather except a light mist near the horizon. Indications of much open water.

April 9, 1892

Mist bank lying over the open water in the W and N.W.

April 10, 1892

Ditto.

April 12, 1892

In the a.m. - open water about three miles out.

April 16, 1892

Open lead of water some three miles out.

March 17, 1892

No water in sight.

April 20, 1892

Open lead of water all along the shore about five miles out.

April 22, 1892

No open water in sight, the pack ice having set in and filled the lead.

April 24, 1892

No open water in sight.

April 29, 1892

No open water in sight.

April 30, 1892

No open water in sight, report from whalemen on the ice read that the pack ice has closed the lead.

May 1, 1892

Ditto.

May 2, 1892

Ditto.

May 3, 1892

Ditto.

May 4, 1892

Ditto.

May 6, 1892

Ditto.

May 7, 1892

No open water in sight - lead closed - most of the natives out on the ice - no whales but plenty of ducks coming along in large flocks.

May 10, 1892

No open water in sight.

May 11, 1892

Ditto.

May 13, 1892

Ditto.

May 14, 1892

Ditto.

May 16, 1892

Open water in sight from top of thy house. In the p.m. overcast, no changes in the ice.

May 17, 1892

Natives report another large whale, making four taken by them this season.

May 18, 1892

No open water in sight. Natives report two more whales taken.

May 20, 1892

Natives report two more whales killed today and two yesterday (19th).

May 23, 1892

Ice floe broke off about one mile from shore leaving all the boats of the village out on the ice, but near night three or four boats came across the ice, then crossed the open lead and landed on the shore floe.

May 26, 1892

Lead filling with ice - no whales - plenty of ducks.

June 2, 1892

Much open water.

June 3, 1892

Much open water - ice moving off shore with the winds - current setting strong to the N.E.

June 4, 1892

Ice closing in and filling the lead.

June 5, 1892

Ditto.

June 7, 1892

Ice closed up the lead - no movement in the ice.

June 8, 1892

Lead of open water making something like a mile off shore.

June 9, 1892

Lead of open water about one mile out.

June 10, 1892

Wide lead of open water about one mile from shore.

June 11, 1892

Lead well open off shore - no ice in sight beyond the lead.

June 12, 1892

Plenty of open water.

June 13, 1892

Ice from the floe constantly breaking off in small parcels and drifting away. Plenty of open water off shore.

June 15, 1892

Floe ice breaking off and drifting away constantly.

June 19, 1892

No ice in sight except along on the bars, and between the bars and shore.

June 23, 1892

No ice except along the shores in sight.

June 26, 1892

8 a.m.: Wind E steady, 18 miles an hour.

Noon: Wind E steady, 24 miles an hour.

No ice in sight except along shore.

June 28, 1892

8 a.m.: Wind N.W. variable, 3 miles an hour.

Noon: Wind N.W. steady, 4 miles an hour.

8 p.m.: Wind N variable, 4 miles an hour.

In the a.m. light winds and part cloudy with warm weather - ice pack in sight gradually working inshore.

June 29, 1892

8 a.m.: Wind N steady, 3 miles an hour.

Noon: Wind N steady, 5 miles an hour.

8 p.m.: Wind E variable, 9 miles an hour.

Ice pack remains the same as yesterday in the a.m.

In the p.m. baffling winds and mostly overcast - but little ice excepting along the shores in sight.

July 1, 1892

8 a.m.: Wind E steady, 14 miles an hour.

Noon: Wind E steady, 19 miles an hour.

8 p.m.: Wind E steady, 15 miles an hour.

In the a.m. moderate winds and partly cloudy. But little ice in sight. In the p.m. clearing, warmer.

July 5, 1892

8 a.m.: Wind N.W. steady, 25 miles an hour.

Noon: Wind N.W. steady, 23 miles an hour.

8 p.m.: Wind N.W. steady, 16 miles an hour.

At 10 a.m. snowing occasionally in light flurries - and continues through the day. Ice pack closing in.

July 6, 1892

8 a.m.: Wind N.W. steady, 5 miles an hour.

Noon: Wind N variable, 4 miles an hour.

8 p.m.: Wind E variable, 19 miles an hour.

Ice pack in and the beach closed, the first time since it opened on the 22nd of May. In the p.m. wind changed to the E with warmer weather. Ceased snowing and threat of rain.

July 7, 1892

8 a.m.: Wind S.E. variable, 23 miles an hour.

Noon: Wind S.W. variable, 6 miles an hour.

8 p.m.: Wind W variable, 19 miles an hour.

In the a.m. fresh winds from S.E. and overcast with drizzling rain, .023 of an inch fell during the night. No ice in sight except shore ice and a few floating pieces drifting to the N.E.

July 8, 1892

8 a.m.: Wind W steady, 5 miles an hour.

Noon: Wind S.W. variable, 7 miles an hour.

8 p.m.: Wind S.W. steady, 12 miles an hour.

In the a.m. light winds and cloudy threatening rain. Floating ice setting N.E. P.M. - clearing, lead filled with floating ice setting rapidly to the N.E.

July 9, 1892

8 a.m.: Wind S.W. steady, 18 miles an hour.

Noon: Wind S.W. steady, 25 miles an hour.

8 p.m.: Wind S.W. steady, 11 miles an hour.

In the p.m. clear weather except a few S clouds - no open water in sight.

July 10, 1892

8 a.m.: Wind E variable, 4 miles an hour.

Noon: Wind E steady, 19 miles an hour.

8 p.m.: Wind E steady, 9 miles an hour.

In the a.m. light winds and cloudy. Ice scattering and drifting N Considerable open water off shore, weather warm.

July 12, 1892

8 a.m.: Wind W steady, 15 miles an hour.

Noon: Wind W steady, 13 miles an hour.

8 p.m.: Wind S.W. variable, 7 miles an hour.

In the a.m. moderate winds and overcast with fog - no open water in sight.

July 13, 1892

8 a.m.: Wind N.E. variable, 4 miles an hour.

Noon: Wind N.E. steady, 11 miles an hour.

8 p.m.: Wind E variable, 8 miles an hour.

No open water in sight - ice drifting to N.E. with plenty of walrus on it.

July 14, 1892

8 a.m.: Wind E steady, 4 miles an hour.

Noon: Wind E steady, 8 miles an hour.

8 p.m.: Wind E steady, 8 miles an hour.

Ice leaving the shore - floating ice in every direction as far as the eye can reach.

July 15, 1892

8 a.m.: Wind S variable, 18 miles an hour.

Noon: Wind W variable, 5 miles an hour.

8 p.m.: Wind E variable, 9 miles an hour.

Ice scattering and drifting rapidly to the N.

At 11-1/2 p.m. St. Balena Norwood, S.F., four days from Port Clarence, came to anchor off the Station. First vessel of the season.

July 19, 1892

8 a.m.: Wind W variable, 24 miles an hour.

Noon: Wind W variable, 25 miles an hour.

8 p.m.: Wind S variable, 15 miles an hour.

In the a.m. fresh winds and cloudy with fog. Ice pack closing in.

July 20, 1892

8 a.m.: Wind W variable, 32 miles an hour.

Noon: Wind W steady, 32 miles an hour.

8 p.m.: Wind S.W. variable, 16 miles an hour.

In the a.m. fresh breeze from W with cloudy weather. At 9 last night wind changed suddenly to S.W. blowing a gale. Heavy ice piled up along the shores. This a.m. one sail in sight to the S.W. in clear water. In the p.m. ice closed in - no movement in the ships, except one bound to the E.

July 21, 1892

8 a.m.: Wind N.W. variable, 10 miles an hour.

Noon: Wind W variable, 17 miles an hour.

8 p.m.: Wind W steady, 30 miles an hour.

All day cloudy with fresh winds. Ice quite compact as far as eye can reach.

July 22, 1892

8 a.m.: Wind W steady, 30 miles an hour.

Noon: Wind W steady, 25 miles an hour.

8 p.m.: Wind N.W. variable, 25 miles an hour.

In the a.m. fresh winds and cloudy. Ice pack in heavy resting upon the shore. No open water in sight. No change in the p.m., ice compact.

July 23, 1892

8 a.m.: Wind N.W. steady, 21 miles an hour.

Noon: Wind N.W. steady, 19 miles an hour.

8 p.m.: Wind N.W. steady, 7 miles an hour.

In the a.m. fresh winds and cloudy, flitting snow occasionally. Ice compact - no open water in sight - same in p.m.

July 24, 1892

8 a.m.: Wind E variable, 6 miles an hour.

Noon: Wind N.E. variable, 18 miles an hour.

8 p.m.: Wind N.E. steady, 22 miles an hour.

a.m. - ice still compact, no opportunity for ships to arrive. In the p.m. ice beginning to open.

July 30, 1892

8 a.m.: Wind W steady, 19 miles an hour.

Noon: Wind W steady, 19 miles an hour.

8 p.m.: Wind W steady, 18 miles an hour.

In the a.m. fresh winds and fog and clouds with occasional showers of rain - ice setting in from off shore. In the p.m. rain.

July 31, 1892

8 a.m.: Wind calm

Noon: Wind E steady, 9 miles an hour.

8 p.m.: Wind E steady, 18 miles an hour.

In the a.m. ice closed in upon the shores. In the p.m. drizzling rain - ice opening.

Aug. 1, 1892

8 a.m.: Wind S.E. variable, 10 miles an hour.

Noon: Wind N.E. variable, 12 miles an hour.

8 p.m.: Wind N.E. steady, 12 miles an hour.

In the a.m. moderate winds and thick fog. Ice leaving the shores.

Aug. 20, 1893 (Record keepers changed Aug. 1)

Strong N.N.E. wind with heavy rain. Plenty of ice in sight in the a.m. moving south.

Aug. 23, 1893

A.M. wind S.E. light with some fog until nearly noon, then clearing with wind S. P.M. fine, light air from S. No ships and but very little ice in sight. This is the first southerly wind there has been for 60 days and the clearest since I have been here - E. Akin, Keeper.

Aug. 24, 1893

Have part fine, clear and warm light air. The Doctor and I went up to the duck station. Shooting started 2 a.m. Quite a number of whales went south this morning.

Aug. 25, 1893

A.M. strong breeze N.E. with some rain and fog. The Doctor and I got back from shooting at noon with 61 ducks.

Aug. 31, 1893

A.M. strong breeze N.E. with fog. P.M. strong breeze with some snow and fog. No ice in sight.

Sept. 2, 1893

The Schooner Jane Grey anchored off the station and sent in a boat with a letter for me to send down. Reported the ice all gone along the East shore. Steamers all gone East. She had been as far as Harrisons Bay.

Sept. 5, 1893

A.M. wind N.N.W. quite strong. P.M. good weather, wind N.N.W. Could see the ice pack today at 3 p.m. The Steamer Jeanie came to anchor off the station from Herschel Island with 130 heads of bone from the fleet at the Island, reports 140 whales taken this season off the Island.

Sept. 6, 1893

A.M. wind N light with some flurries of snow. Some scattering ice to be seen.

Sept. 8, 1893

A.M. light wind N.E., some scattering ice to be seen.

Sept. 10, 1893

A.M. wind N quite strong with fine snow.

P.M. snowing, quite fast wind N, heavy scattering ice two miles off shore as far as can be seen.

Sept. 13, 1893

Fine weather, light breeze N. At 2:30 p.m. the steamer Belvedere came to anchor off the station with 17 whales all told, from Herschel Island.

Sept. 15, 1893

At 8 a.m. steamer Beluga came to anchor off the station. She had taken 18 whales, 17 at Herschel Island.

Sept. 18, 1893

A.M. blowing a gale from S hauling by noon to the S.W. P.M. still blowing heavily from S.W. to W with a heavy surf on the shore.

Sept. 26, 1893

P.M. nearly calm airs from N.E. Some ice in sight in the N.W.

Oct. 22, 1893

A.M. moderate wind S.W. with snow. P.M. light air from S.E., no snow. A few pieces of heavy ice.

Oct. 30, 1893

A.M. light breeze N.E., clear and cold. P.M. nearly calm, airs from E, all of the young ice started off from shore this afternoon.

Nov. 1, 1893

A.M. light breeze N, quite a pack of young ice on the shore extending off to the ridge.

Nov. 4, 1893

A.M. light wind S.E., good weather, quite a pack of young ice in shore moving N.

Nov. 5, 1893

A.M. wind light S.W. with young ice so the Natives are out sealing for the first time. P.M. wind W quite strong and more ice.

Nov. 12, 1893

A.M. wind N.E., all clear water outside the ridge.

Nov. 19, 1893

A.M. airs from N.E., P.M. airs from E, some of the ice has broken off from the ridge and gone, all open water outside the ridge (or bank).

Nov. 23, 1893

A.M. calm, fine weather. P.M. airs from N.E., the ice from shore extends off a mile with open water beyond.

Dec. 16, 1893

Last night the ice broken off from the ridge, and clear water from the ridge as far as I can see.

Dec. 30, 1893

A.M. airs from N.W., cloudy, P.M. nearly calm, airs from N.W., quite a number of seals taken by the Natives today.

Jan. 5, 1894

A.M. wind W quite strong, clear. P.M. wind W.S.W., cloudy. Today the ice has come in so there is but little water to be seen. Seals quite plentiful and quite a number taken today.

Jan. 6, 1894

A.M. wind N.W., clear. P.M. strong breeze W, clear, no water to be seen.

Jan. 22, 1894

A.M. blowing a gale N.E., P.M. strong breeze N.E., clear water beyond the ridge.

Jan. 28, 1894

A.M. strong breeze W.N.W., cloudy. P.M. same, no water to be seen.

Jan. 31, 1894

A.M. wind light N.E. P.M. wind light N.W. Thick weather, foggy or frozen fog. The ice is all gone from the ridge.

Feb. 3, 1894

Weather fine, clear and calm. I think the coldest we have had it yet. P.M. same, no water to be seen.

Feb. 7, 1894

A.M. calm, clear and cold. P.M. light air from N.N.E., no water to be seen.

Feb. 17, 1894

A.M. strong breeze N.E., clear. P.M. strong breeze E.S.E., clear, plenty of water in sight from 3 to 4 miles off shore.

Feb. 18, 1894

Last night the ice crushed in and formed a ridge about two hundred yards from the shore. Plenty of water there off shore.

Feb. 19, 1894

A.M. blowing strong S.S.W., ice a packing up, but not coming any closer to the shore. P.M. blowing a gale S.W., some snow, and drifting badly. No water to be seen.

April 10, 1894

Getting ready for whaling. No lead yet or water to be seen.

April 12, 1894

A.M. strong breeze N.E., overcast. P.M. blowing strong N.E., snow drifting, a disagreeable day. Four more canoes went off today from Mr. Kelly's whaling, quite a lead open today from 3 to 5 miles offshore.

April 15, 1894

A.M. light wind N.E., clear. P.M. light airs from N. Clear, fine weather. Three canoes went out from Mr. Kelly's today whaling.

April 16, 1894

A.M. fine weather, wind light N.E. P.M. same. The first whale reported seen this morning going North.

April 20, 1894

A.M. wind W.N.W. quite strong, P.M. strong breeze N.W., clear. The lead is closed, has been for two days, no whales seen for the past two days. Five seen all told so far.

April 21, 1894

A.M. fine weather, air from S and W mostly, clear. P.M. calm or nearly so, clear. Reports from the lead say a few whales seen today in holes.

April 30, 1894

A.M. fine weather, nearly calm, air from N, clear. P.M. the same. Mr. Kelly came in from the ice and reports no water, young ice as far as can be seen from four miles out (to the edge of the flow ice). The first ducks were seen today going North.

The average temperature for April was 11-1/4 degrees below zero.

May 2, 1894

A.M. light wind from N.W., cloudy with fine, light snow. P.m. air from N.W. to N.E., partly cloudy, no sign of water.

May 3, 1894

Reports from the flow no whales. No water.

May 7, 1894

A.M. airs from N.E. to N.W., clear, fine weather. P.M. light airs from N, clear. No lead, and no whales seen for the last week.

May 17, 1894

A.M. blowing strong N.E., overcast, snow drifting badly. P.M. same. The first whale reported killed today but the Cape Smythe Trading and Whaling Co., quite a large one 10 ft. 6 inches bone.

May 18, 1894

A.M. blowing strong N.E., partly cloudy, snow drifting, same in P.M. The CST&W Co. captured another whale today (small one).

May 19, 1894

A.M. Blowing a gale N.E., clear, snow drifting badly, same P.M. The CST&W Co. station captured 3 whales today.

May 20, 1894

A.M. still blowing a gale N.E., clear, snow drifting badly, same in P.M. Another whale taken by the CST&W Co.

May 21, 1894

A.M. blowing still N.E. strong, clear. P.M. fine, light wind N.E., clear. More whales. One for the SWCo. and two for the CST&W Co. and two reported taken from Point Barrow, and two taken from the village.

May 22, 1894

A.M. blowing again strong N.E., clear, P.M. the same. SWCo. one whale.

May 23, 1894

A.M. blowing a gale N.E., clear, P.M. still blowing N.E., partly overcast. Three more whales taken yesterday by the SWCo. Village one. Latter one SWCo.

May 25, 1894

A.M. blowing strong N.E., cloudy, P.M. wind N.E. quite strong, cloudy. Quite a flight of ducks yesterday. Two whales for the CST&W Co. today, three for the SWCo., two for the village. 28 all told.

May 26, 1894

A.M. wind N.N.E. quite strong, clear, fine weather, same in P.M. Three more whales for SWCo.

May 28, 1894

A.M. strong Breeze N.E., clear. P.M. Strong breeze N.E., partly cloudy. The lead is closed but a few whales seen in the last two days.

June 5, 1894

A.M. fine weather, wind N.N.E. light, clear. P.M. wind N, cloudy. Last night the ice broke off within three miles of the shore with all the whalemen on it, but all ogt in safe with the loss of some dogs and sleds and one or more canoes.

June 17, 1894

A.M. wind N.E. with some snow, P.M. same. All the whalers came from the ice today.

July 20, 1894

A.M. blowing a gale N.E., clear, P.M. blowing strong N.E., cloudy. Today the ice has broken off about one mile from the shore and is going off for the first time in a month.

July 21, 1894

A.M. strong breeze N.E. with rain. This morning the steamers came in sight, eight of them. All made fast to the ice, but the wind going the pack ice came in so they all steamed North. P.M. nearly calm with thick fog, air from S.W.

July 22, 1894

A.M. calm, clear, fine weather. P.M. light breeze from N to N.E., clear most of the time. See all the steamers laying off the shooting station. The man, woman, and boy that was suppose to be lost on the ice May 24th got ashore at Point Lay after being on the ice 61 days. They came up on one of the steamers yesterday.

July 26, 1894

A.M. light wind N, partly cloudy, fine weather, the same in p.m. Several sailing vessels have passed going N, some have come to anchor off the duck station. No steamers in sight, suppose they have all gone Eastward.

July 31, 1894

A.M. strong breeze S.W., some fog, p.m. light wind W with fog. Lots of ice came in along shore and as far as can be seen off shore.

Aug. 1, 1894

A.M. wind light N.W., some frozen fog but clear overhead. P.m. light air N.W., partly cloudy, no water to be seen off shore.

Aug. 2, 1894

A.M. light breeze N.E., partly cloudy. P.M. strong breeze, N.E., party. cloudly. The ice is leaving fast.

Aug. 3, 1894

A.M. wind N.E., strong, cloudy. P.M. the same. The ice all out of sight but part of the ridge.

Aug. 5, 1894

A.M. strong breeze S.W. to W with some fog. P.M. strong breeze W with some fog. At noon the Revenue Cutter Bear came in off the Station and made fast to the ice.

Aug. 8, 1894

A.M. airs from N.E., clear of fog. P.M. light wind N.E., partly cloudy. The ice came in last night quite heavy, but afternoon was off all clear of the shore.

Aug. 10, 1894

A.M. strong breeze N.E. with rain. P.M. wind S.E. with rain and fog. This morning 12:30 a.m. a part of the crew of the Bark Reindeer came to the station, two boats with 16 men. Reported the loss of the Reindeer on or

near Return Reef on the 4th of August 1894. The vessel full of water and mast cut away. Was laying at anchor in 4 fathoms of water when the ice came in and pushed her ashore in 10 feet of water.

Aug. 19, 1894

A.M. light breeze N.W. with some fog. Quite a lot of ice in sight. Current running south strong. P.M. the same.

Aug. 24, 1894

A.M. wind south, cloudy with some rain. P.M. wind S.W. with some heavy rain, until 6 p.m. then fine weather. Some scattering ice came in.

Aug. 25, 1894

A.M. nearly calm airs from N to N.E., clear fine weather. P.M. fine weather, light wind N.E. partly cloudy. Six vessels in sight off the Point.

Sept. 16, 1894

A.M. wind N.E. with snow. P.M. strong breeze N with snow. The steamer Belvedere came to anchor off the Station. Capt. Slocum gave us a call. She had taken two whales.

Oct. 8, 1894

A.M. fine weather, light wind N to N.N.E., partly cloudy. P.M. the same. A few pieces of ice in sight, the lagoon froze all over last night.

Oct. 15, 1894

A.M. light wind N.E., cloudy. P.M. the same. Some quite heavy ice (scattering) in sight today.

Oct. 16, 1894

A.M. fine weather, light airs from N.E., overcast. P.M. the same. One whale seen from the Station and several was [sic] heard last evening from the other Station.

Oct. 18, 1894

A.M. light breeze N.E. cloudy, P.M. the same. No ice in sight.

Oct. 19, 1894

A.M. light wind N.N.E., cloudy, P.M. strong breeze N.N.E. with some snow. Quite a pack of heavy ice in sight.

Oct. 20, 1894

A.M. wind N.N.E. with snow squalls. P.M. wind light N, no snow but cloudy. Plenty of heavy ice in sight to the N & W.

Oct. 21, 1894

A.M. light wind N, partly cloudy. P.M. the same. Young ice made last night a mile from shore, and quite a pack off two miles.

Oct. 27, 1894

A.M. blowing strong N.E., cloudy. P.M. the same. The young ice broke off from the shore last night. All clear water.

Average temperature for month of October 14-1/5 above zero.

Nov. 3, 1894

A.M. fine weather, clear and cold. P.M. air from S.E., clear and cold. Quite a number of seal killed today.

Nov. 5, 1894

A.M. clear, calm, fine weather. P.M. the same. Young ice formed two miles off shore so they [natives] are out sealing.

Nov. 9, 1894

A.M. strong breeze N partly cloudy. P.M. wind N.W. quite strong. Quite a number of seals taken.

November average temperature 6-5/6 degrees below zero.

December average temperature 11-2/7 degrees below zero.

January average temperature 17-1/5 degrees below zero.

February average temperature 23-1/4 degrees below zero.
Coldest 43 below, warmest 0 degrees.

March average temperature 15-1/7 degrees below zero.
Lowest 32 below, highest 0 degrees.

April 8, 1895

A.M. strong breeze N.E., clear. P.M. light wind E, clear.
Mr. Kelly sent out another canoe today. About 2 p.m. the ice broke off about a mile from the shore.

April 9, 1895

A.M. fine weather, calm, clear. The same in the p.m. No. water in sight.

April 18, 1895

A.M. calm, cloudy, fine weather. P.M. airs from N.E., partly overcast. Whales were reporeted the 16th and more today.

April 23, 1895

A.M. wind S to S.E., quite strong, snowing, p.m. blowing strong S, some snow. The ice broke about one mile off shore then came in.

April 27, 1895

A.M. fine weather, light wind S.W. P.M. fine, airs from S.W., clear. Quite a number of flocks of ducks reported today bound North. The first of the season, spring is coming.

April 28, 1895

A.M. wind light N.W., partly cloudy. P.M. airs from N, clear. No water to be seen.

April 30, 1895

A.M. fine, airs from S to S.E., clear. P.M. the same. No water to be seen since the blow. Whalemen all ashore.

April average temperature 6° below. Lowest 20° below, highest 17° above.

May 3, 1895

A.M. strong breeze N.E., clear. P.M. the same. The ice is cracked but don't go off, about a mile from shore. P.M. the ice is going and the canoes are all going out tonight.

May 7, 1895

A.M. light wind N, clear. P.M. airs from N, clear. The first whale of the season was killed today by the P.S.W. Co. up off the Point (Barrow) 4 seen up there.

May 10, 1895

A.M. light wind N.E., overcast. P.M. wind N.E., cloudy with some snow. Quite a number of whales were seen last night but none taken. Nearly all of the canoes are off Point Barrow as the ice is in better shape there for whaling.

May 11, 1895

A.M. strong breeze N.E., cloudy. The same in P.M. One small whale taken by the C.S.W.& T Co. today.

May 14, 1895

A.M. airs from S.E., overcast. P.M. calm, cloudy, with light snow. The C.S.W. & T Co. captured a whale today.

May 15, 1895

A.M. airs from S.E. to S, overcast. P.M. nearly calm, airs from S.E. The PSCo. got a small whale today, a few seen

May 19, 1895

A.M. fine weather, light breeze from N.E. to E, clear P.M. fine, wind E, cloudy. Two whales taken today, one by the C.S. Co. and one by the Natives. P.M. one more [whale] taken at Point Barrow by the Natives.

May 20, 1895

A.M. blowing strong, N.E. to E, cloudy. P.M. strong breeze E, cloudy. No ice to be seen outside the ridge. One whale taken by the P.S.W.CO.

May 21, 1895

A.M. fine and warm wind E, clear. P.M. airs from N.N.E, clear. The thermometer went up to 36° above, quite a flight of ducks today, the first of the season. The P.S.W. Co. got another whale today, all small so far.

May 22, 1895

A.M. light wind E, cloudy. P.M. airs from S.E. to S.W., foggy. PSCo. got another whale today.

May 23, 1895

A.M. calm with thick fog until 8 a.m., then clear and warm. P.M. airs from N, clear, nice weather. Quite a flight of ducks today. I got 22, the first this season.

May 24, 1895

A.M. fine weather, wind light E. P.M. light breeze from E to N.E, clear and warm. Quite a flight of ducks this afternoon. All water and no whale.

May 25, 1895

A.M. light wind N.E., clear, warm. P.M. the same. Plenty of ducks over the water.

May 26, 1895

A.M. light airs from N to N.W., partly cloudy, fine weather. P.M. light wind N.W., thick fog. Killed 22 ducks on the ice this morning.

May average temperatures 17° above. Coldest 8° below, warmest 40° above at 8 a.m.

June 1, 1895

A.M. fine, clear and warm. Airs from N.E. to S.E. P.M. fine, light breeze from E. A large flight of ducks today mostly over the lead.

June 3, 1895

A.M. strong breeze S.W., with some snow. P.M. the same. Ice coming in fast.

June 4, 1895

A.M. light wind E, partly cloudy. P.M. wind S.E., quite strong. The ice closed in last night. Very little water to be seen today.

June 5, 1895

A.M. strong breeze S.W., clear. P.M. the same. No water, the village canoes all hauled in this morning from the ice. I think given up whaling for this season.

June 6, 1895

A.M. fine weather, airs from E to S, clear and warm. P.M. airs from S.W., warm. No water in sight.

June 27, 1895

A.M. strong breeze E.S.E. with fog. P.M. wind E.S.E. strong with fog. The pack ice started off last night and this morning there was quite a lead of water. In the afternoon whales were sighted and all the canoes that could go out went.

June 28, 1895

A.M. wind light from S.E. to S, fog. The same in P.M. The canoes all came in today. See quite a number of whales but the pack ice came in and closed up the lead.

July 9, 1895

A.M. light breeze, N.W., cloudy. P.M. airs from N.E., cloudy. The ice inside the ridge is rotting away fast. The Lagoon back of Mr. Kelly's is clear of ice, fully a month sooner than last year.

July 10, 1895

A.M. light wind S to S.W., cloudy. P.M. light breeze S.W., clear. Quite a number of Ogourooks and two walrus and lots of seals in the few days killed by the Natives.

July 12, 1895

A.M. light wind S.W., cloudy. The same in P.M. No water to be seen outside the ridges.

July 14, 1895

A.M. wind W.S.W., clear, fine weather. P.M. wind W.S.W. quite strong with light fog. Most of the flat ice inside of the ridge has broken up and moved North. The pack still is closed in on the ridge outside. Quite a lot of eider ducks going South.

On July 25, 1895 at noon the thermometer stood at 68° above.

Aug. 3, 1895

A.M. wind N.W. with some fine snow. The same in P.M. No water in sight inside - outside the ridge.

Aug. 14, 1895

Report that the cutter Bear and the whaling all at Icy Cape.

Aug. 15, 1895

A.M. wind N.E. quite strong with some fog. The same in P,M. The pack of ice has left the shore and some holes has [sic] broken through the ridge.

Aug. 15, 1895

A.M. light breeze N.E. with some fog. P.M. light airs from N.W. to N.E., again clear but high fog. This afternoon the pack ice came in again and closed up tight.

Aug. 20, 1895

A.M. air from N with thick fog until 10 a.m., then clear. P.M. airs from the N, clear, fine weather. Two steamers were reported seen 40 miles down the coast yesterday and several canoes have gone down to meet them. P.M. - 8 p.m. four steamers have gone past to the North two miles off shore through the ice, I think trying to get around the end of the ridge.

Aug. 28, 1895

A.M. wind N.E., quite strong, cloudy. P.M. strong breeze N.E., clear. The ice is most all out of sight.

Sept. 9, 1895

A.M. wind S to S.W., strong, some rain. P.M. wind S.W. strong, ice coming in. The steamers will have to leave.

Sept. 18, 1895

A.M. wind S.W. quite strong with snow. P.M. wind W partly cloudy, clearing. Mr. Smith, first mate of Schooner Rosario from Herschel Island bound home but is now ice bound at Point Barrow. The pack ice has been in for a week or more.

Sept. 20, 1895

A.M. airs from S to S.E., partly cloudy. P.M. light breeze S.E., overcast. Ice moving N fast but not off.

Sept. 22, 1895

A.M. wind E.N.E. with fog in squalls. P.M. wind E.N.E., some fog, some snow. The ice broke off at the ridge and opened quite a lead. The Rosario got underway this morning and stood out but it came in thick [fog] and we could not see whether she got out or not. Later reported going south.

Sept. 27, 1895

A.M. light breeze E.N.E., clear and cool. P.M. airs from S.E. with fog. The lagoon froze over last night and remained frozen all day. Quite a heavy strip of ice came from the south.

Oct. 1, 1895

A.M. airs from S.E. to E, cloudy. P.M. wind E.N.E., with thick fog. The ice has nearly all gone, only a few cakes of ground ice to be seen, ducks still flying quite plentiful at the duck station.

Oct. 4, 1895

A.M. wind N with snow. P.M. wind N.W., snow in squalls. No ice in sight.

Oct. 10, 1895

A.M. light breeze N.E., cloudy. P.M. the same. Quite a lot of young ice today and current running south strong.

Oct. 16, 1895

A.M. light breeze N.E., partly cloudy. Same in the P.M. Quite a number of bears killed at the Point in the last 4 days, 17 all told.

Oct. 20, 1895

A.M. strong breeze N.E., cloudy. P.M. light breeze N.E., cloudly. No ice to be seen now from the station but two or three pieces of old ice off shore.

Oct. 28, 1895

A.M. calm, airs from all quarters. P.M. light breeze N.W., clear and fine. The shore ice is out as far as the ridge, and looks as though it had come to stay.

Average temperature October 9-1/2 degrees above.

Nov. 5, 1895

A.M. airs from S & S.E., overcast. P.M. calm, fine weather, partly cloudly. The shore ice has made off. A mile clear water beyond. 44 bears have been killed, mostly at the Point and Eastward.

Nov. 12, 1895

A.M. wind N.W., clear, fine weather. P.M. strong breeze W, clear. About noon the ice began crashing in on the shore, it came within 60 yards of the Station piling up 20 ft high it commenced 100 yards, south of the house and how far North I can't tell, at the C.S.W. & T Co. station they packed up to move inland. The ice coming nearly up to the houses. The ice is 12 to 15 inches thick.

Nov. 21, 1895

A.M. blowing strong N.E., overcast. P.M. blowing a gale N.E., partly cloudy. The ice broke off at the ridge and went off with one village Native.

Nov. 23, 1895

A.M. strong breeze S.W. to W, cloudy. P.M. light breeze W, cloudy. The ice came today and with it the Native that went off on it.

Nov. 30, 1895

A.M. light breeze N.E., cloudy. P.M. blowing strong E, cloudy, snow drifting badly. The ice makes off about a mile from shore. Not much of an outer ridge formed yet.

Average November temperature 6-1/15 degrees below.

Dec. 16, 1895

A.M. strong breeze N.E., snow drifting. P.M. blowing strong N.E., snow drifting badly. Quite a number of seals taken last night. One Native caught 33, about 60 taken.

Average December temperature 24-1/2 degrees below.

Jan. 24, 1896

A.M. blowing strong N.E., snow drifting. P.M. blowing a gale N.E., overcast. Ice broke off and gone outside the ridge.

Average January temperature 32 degrees below.

ANNUAL REPORT

Contract Number: 03-5-022-55

Research Unit Number: 265

Reporting Period: June 1975 to March 31, 1976

Number of Pages: 20

DEVELOPMENT OF HARDWARE AND PROCEDURES FOR IN-SITU MEASUREMENT OF CREEP IN SEA ICE

Lewis H. Shapiro
Richard D. Nelson
William M. Sackinger

Geophysical Institute
University of Alaska
Fairbanks, Alaska 99701

Contributing Scientist:

Earl R. Hoskins

Department of Mining Engineering
South Dakota School of Mines & Technology
Rapid City, South Dakota

March 31, 1976

I. SUMMARY

The objectives of this program are to develop and test the hardware and techniques needed to conduct in-situ measurements of the mechanical properties of sea ice. These will provide the tools through which a new series of measurements of several of these properties can be made with minimal disturbance to the test sample. The project was initially directed towards determination of the creep behavior of sea ice, but the relative ease with which these techniques can be used to measure the strength of ice in certain failure modes suggested that this be investigated also.

At the time of writing, the project has been in the field for approximately one month. During this time the system being used for loading the ice, flatjacks expanded with bottled nitrogen gas, has functioned properly. The problems associated with the use of small strain gauges to measure strain in coarse, crystalline ice have apparently been solved by freezing the gauges into small cylinders of fine-grained NaCl ice which acts as a strain cell. Bonding of the gauge the ice appears to be very satisfactory. Testing of stress transducers for use in this study is just starting, and no results are available at this time. A series of in-situ ice strength tests have been conducted, including three direct shear tests, one uniaxial compression test, and one modified indirect tension test (Brazil test). The direct shear test worked satisfactorily, but further work is needed to perfect the techniques of the other tests. Finally, several creep and relaxation tests have been run, but the data have not yet been analyzed.

The results to date do not yield conclusions which have immediate implications for OCS development. Instead, they represent steps in the

development of techniques which will ultimately provide data needed for the design and evaluation of offshore structures for use in the Arctic.

II. INTRODUCTION

A. General Nature and Scope of Study

The problem of translating results from laboratory tests to field conditions is well known in many branches of science, and it likely to be an important aspect of studies of the mechanical properties of sea ice. It is difficult in the laboratory to simulate the effects of temperature and salinity gradients, continuous variations in grain size and ice fabric, and the presence of inhomogeneities on scales larger than laboratory samples. Further, mechanical properties of the ice can change during the processes of removal, transport and storage. A program of determining the mechanical properties of sea ice *in situ*, and with minimal disturbance to the ice, is thus needed to supplement and verify laboratory results.

As initially proposed, this project included only an examination of techniques for the *in situ* measurement of the creep properties of sea ice. However, due to late arrival of some of the equipment required for this work, time was available to attempt several *in situ* tests of ice strength in different modes of failure. These were satisfactory, and the results are presented in this report although they do expand the scope of the project. It should also be noted that static elastic properties can also be determined from some of these tests.

Studies of creep in fresh ice have been conducted for many years, often with the objective of examining the long term flow of glaciers. In this case stresses remain relatively constant and the secondary creep stage is of prime interest. For sea ice in its natural setting, however,

stresses are seldom constant for more than short periods of time, but instead, change rapidly with variations in wind directions, currents, or internal stresses induced by motion of the pack under forces applied at a distance. Thus, the entire creep curve, including both primary and secondary creep, is of interest, as well as the transition from creep to failure. A final objective of this program is to generate the data necessary for establishing the creep properties of sea ice through *in situ* testing. The objective of this phase is to conduct the necessary hardware and techniques development for these measurements to be made.

B. Specific Objectives

The specific objective of this project is to develop hardware and procedures for the *in situ* measurement of the creep behavior of sea ice. Also, as noted above, the study has been expanded to include fracture strengths as well.

C. Relevance to Problems of Petroleum Development

Any permanent or semi-permanent structures off the Arctic Coast of Alaska must contend with the hazard that sea ice presents to its stability. In order to properly design such installations it is necessary that reliable values of the mechanical properties of the ice be available both for establishing the design of the structure, and for the evaluation of that design by public agencies. In addition, significant savings in cost of construction can be realized if less conservative safety factors can be utilized.

III. CURRENT STATE OF KNOWLEDGE

Previous work on the determination of creep properties of sea ice was reviewed by Weeks and Assur (1967). The work of most direct interest

is that of Tabata (1958) who performed a series of in situ tests using cantilever and fixed end beams. In these tests, a constant load was applied to the beam and the deflection at that point was measured as a function of time. The resulting curve of deflection vs. time has the form of a creep curve, and the constants for a 4-parameter, linear viscoelastic model were derived from it.

Peyton (1966) conducted a laboratory study in which cylinders of natural sea ice were subjected to constant tensile or compressive loads of different magnitudes to generate creep curves. Loads were removed after the creep curves were esablished, and the elastic components of the deformation were recovered. Unfortunately, for all but a very few of the tests, no information was given regarding the temperature, salinity, or crystal orientation of the test specimens. These parameters obviously influence the mechanical properties of the specimens and interpretation of the results, for the purpose of determining the parameters of a stress-strain law, is not possible without them. Note that Peyton did not include any analysis of the results of these tests in his final report. However, the unpublished notes and laboratory records of these tests, which include the necessary data, are archived at the University of Alaska, and with Dr. Peyton's permission we are using these in an analysis of the test data.

Creep curves for fresh ice show a pronounced increase in strain rate following the initial decrease leading to the secondary creep stage, for the case of loads above some threshold value (about 4 kg/cm^2). For sea ice, Peyton's (1966) data show a similar effect, but in some tests the increase in strain rate is restricted to a short time period,

after which the rate decreases again. This introduces an obvous 'kink' into the curve. Karlsson (1972) interpreted this effect as an example of strain rate dependent yield, and developed a three-dimensional visco-elastic-plastic stress-strain law from which good approximations to some of Peyton's one-dimensional, experimental curves have been calculated. Note, however, that the effects of salinity, temperature and mechanical anisotropy is not included in the law.

Finally, a detailed laboratory investigation of the viscoelastic properties of sea ice has been outlined by Katona and Vaudry (1973), but there is no indication as yet that the work is being carried out.

No experimental program comparable to this project has been attempted to date. However, instrumentation for measuring stress in ice has been developed (Nelson, 1974, 1975; Nelson et al., 1972), and the problems of the measurement of strain by gauges embedded in sea ice has been discussed by Vaudrey (1973). Both these techniques are applicable to this project.

V. SOURCES, METHODS AND RATIONALE OF DATA COLLECTION

In order to meet the objectives of this program, three types of instrumentation are required. These are: (1) a loading device, (2) stress sensors and (3) strain sensors.

The loading device must have the capability of generating stress fields approaching the magnitude of the crushing strength of the ice over reasonably large volumes. Further, the device must be capable of maintaining these stresses for times on the order of 2-3 days at low stress and correspondingly shorter times at high stress levels. Flat-jacks are admirably suited to these purposes.

The use of these instruments for measuring stresses or mechanical properties of rocks in situ is well established (Jaeger and Cook, 1969; Hoskins, 1966). Briefly, flatjacks consist of two plates of any suitable material fastened together along their edges to form an envelope of any desired size or shape. They are loaded by pumping a fluid between the plates which cause an expansion of the envelope, thus imparting a stress to the medium in which they are embedded. The geometry of the expanding plates is such that a uniform stress field is achieved over about 90% of the jack face. Naturally, the magnitudes of the stresses decrease with increasing distance from the flatjack, but significant stress levels are probably still present at distances of up to twice the flatjack width (i.e., approximately 30% of the jack pressure at that distance).

The flatjacks are installed in the ice simply by freezing them into a vertical slit cut with a chain saw. Loading for creep tests is done with nitrogen gas, with the pressure maintained at any desired constant value through a pressure regulator. For the strength tests loading has been done using JP-5 pumped into the flatjacks with a hydraulic hand pump.

Two types of stress sensors are being evaluated for possible use in the project. The first are the stress transducers designed by R. D. Nelson and referred to above. These are brass load cells which are sensitive only to axial loads, and thus measure the component of the stress tensor along their axis. The second type of stress sensor consists of a small, thick, brass plate, with a strain gauge rosette in a flat cavity at its center. This configuration should permit measure-

ments to be made of the maximum and minimum principal stresses in the plane of the transducer.

Some difficulties were anticipated in the preparation of strain sensors, but these simply have not materialized to date. The procedures which have been adopted for the preparation of these devices are described below.

The objective of the present program is to integrate these three elements into a system for measuring the mechanical properties of sea ice in situ. The basic scheme envisioned for actually performing the creep measurements is to install the flatjacks into the ice, either singly or in arrays, depending upon the loading conditions desired, and then, using the symmetry properties of the resulting stress field, install stress and strain transducers at corresponding points within that stress field. In this manner, stress and strain can be monitored simultaneously and the results, when plotted, yield curves from which a stress-strain law can be determined.

VI. RESULTS

A. Equipment and Instrumentation

1. Flatjacks

As noted above, flatjacks have long been used in rock mechanics studies, and techniques for fabrication are well-known. Approximately 50 flatjacks have been prepared for this project. These range in size from 230 cm^2 to 3,700 cm^2, and are constructed of steel or aluminum in square, rectangular and triangular shapes. Approximately 12 have been used and all have functioned properly. The only problem encountered to date occurred during a preliminary series of tests conducted at Barrow

in May 1975 (Shapiro and Hoskins, 1975). At that time, one 30 cm x 30 cm flatjack was loaded too long and allowed to over-expand. Further, because of the presence of a strong temperature gradient near the surface of the ice, the gradient of mechanical properties of the ice was such that the jack expanded irregularly, with the top reaching a width about 2 cm greater than the bottom. This obviously tends to distort the stress field around the jack, and the results from tests in which the flatjack does not expand uniformly are probably not valid. Note that other flatjacks with dimensions of 46 x 46 cm were subjected to similar loading histories in the same series of tests, and these expanded uniformly.

It is not necessary to risk over-expansion of a flatjack in order to maintain creep in the ice over a relatively long time period in weak ice. This problem can be avoided simply by installing two or more flatjacks in the ice instead of a single jack. These can be loaded simultaneously, and the travel before over-expansion thus increased.

Loading of the flatjacks has been done by the use of bottled nitrogen gas, with the load controlled by a pressure regulator, and by JP-5 through a hydraulic hand pump. The former system is clearly perferred for long-term tests in which constant pressure is desired. The hand pump can be used for this purpose, but with a notable decrease in efficiency of the system at maintaining constant pressure. However, the hand pump is adequate for rapidly loading a sample to fracture.

2. Strain Gauges

As noted above, some difficulty was expected in preparing strain gauges for emplacement in the ice, but this did not materialize. All of the gauges used to date have functioned properly.

The gauges are cast into small strain cells by a simple procedure. A waterproof, single element, foil, strain gauge (1/4" Micro Measurement EA-06-250BG-120) on its polyimide carrier, is waterproofed with liquid vinyl (B.L.H. Barrier B) and a thin (about .1-.2 cm) layer of RTV silastic. Special care is taken at this stage to assure that the lead wires and connections are also waterproofed. Note that a gauge prepared in this manner was suspended in a beaker of sea water in the laboratory for one week. Monitoring of the gauge condition with a Beam Model 201 strain indicator showed no evidence of salt water leakage during this time.

The waterproofed strain gauge is then frozen into a small cylinder of ice prepared from water with a salinity of about 5%. The cylinder is prepared by putting about 1-2 cm of water into a small cup about 4 cm in diameter and allowing it to freeze. Some attempt has been made to seed the water with snow in order to cause the ice to freeze as small crystals, but it is not yet certain how successful this procedure has been. When the ice in the cup is solid, the strain gauge is moistened and frozen to the ice surface. Additional water is then added to cover the gauge, and allowed to freeze. This completes the preparation of the cell. Naturally, it is removed from the cup before being placed in the ice.

Emplacement is simply a matter of drilling the smallest possible hole which will accommodate the strain cell and still leave space for the fresh water, which is used to freeze the cell in, to flow to the bottom of the hole so that no voids are left below the cell. Care must also be taken when lowering the cell into the hole so that the strain gauge remains as close to horizontal as possible. After insertion of the gauge, the hole is filled with a mixture of fresh water and ice cuttings and allowed to freeze.

There are three apparent sources of error associated with using strain gauges in sea ice. First, the ice is a coarse-grained, polycrystalline solid, each crystal of which can deform differently, depending upon its orientation (see Maser, 1972). When using small strain gauges the possibility thus arises that the gauge may be fixed to only one or two grains, so that the measured strains are not representative of the deformation of the larger ice mass. However, this difficulty should be avoided by the use of the strain cell described above. The cell is large enough to be in contact with a sufficient number of grains so that compatibility requires that it deform in a manner which is representative of the entire ice mass. The gauge itself only senses the strain in the fine-grained ice to which it is bonded. Note that for measurements deep in the ice sheet, where crystal size is large, it may be necessary to use larger stress cells (and possibly longer strain gauges as well). However, it seems desirable to use the smallest possible cells in order to minimize the disturbance to the ice.

The second source of error arises from the question of whether the bonding between the strain gauge and the ice is sufficiently tight to insure that there is no slippage during deformation. If this should occur, then naturally the strain gauge readings will be in error.

To date, approximately 12 strain cells, prepared as described above, have been installed in the ice and deformed. In all cases, the gauges have responded instantly to rapid changes in the load in the flatjacks, both increasing and decreasing. This indicates that the bonding is adequate. In addition, one gauge embedded approximately 10 cm into the ice was tested against a strain gauge extensometer which,

through the use of a small frame of aluminum rods, monitored the average strain in the top 8 cm of ice adjacent to the buried strain gauge. The test lasted about 2 hours and involved creep at two different loads followed by relaxation. The maximum strain reached during the test was 1.8×10^{-4} During loading, the strain gauge responded faster than the extensometer, which seems reasonable because the extensometer was monitoring the strain of the fine-grained surface ice which was at lower temperatures than the coarser ice at the depth of the strain gauge. With this exception, however, the strain readings were within 5% of each other. This indicates again that the strain gauge was responding accurately to the load, and further, that it was sensing the average strain in the ice. This tends to support the conclusions above regarding the use of the strain cells for averaging the deformation of several grains. However, further tests of type are planned, both to test the strain gauges at larger strain, and to test the strain cells in coarse ice. The latter test will probably involve quarrying a block of coarse ice from deep in the ice sheet and loading it in a large loading frame with the strain cell and extensometer installed as outlined above.

The third possible source of error in the strain measurements arises from temperature effects in the gauge performance. However, calculations based on the manufacturer's specifications for the gauges show that these effects are negligible as long as the temperature remains relatively constant during the test. Note that ice temperatures are measured continuously so that necessary corrections can be made if required.

3. Stress Transducers

As noted above, the one-dimensional stress transducers designed by R. D. Nelson will be used to measure stresses around the flatjacks for comparison with strain gauge readings from equivalent points in the stress field. The first of these was recently installed for this purpose, and the stresses measured appear to be lower than anticipated for the distance between the flatjack and the transducer. There has not been sufficient time to determine the reason for this (if indeed the readings are too low). However, it seems possible that the problem may simply be that these transducers are too large for the intended use. As rigid load cells, stress transducers act as stress concentrators in the ice, and the effect of this is included in their calibration. This stress concentration is reflected by a unique geometry of the stress field around the transducer. Any interference with the form of this stress field, such as the proximity of another rigid body, will tend to change the value of the stress concentration factor of the transducer, thus producing a measured stress which is different from the true value. Further, the size of the stress field around the transducer is directly related to the size of the transducer. Thus, if the distance between the flatjack and the stress transducer is not sufficiently large for the proper stress field to develop, then the measured stresses will be too low. Should this prove to be the case, then smaller transducers of similar design will be fabricated and tested.

The two-dimensional stress transducers discussed above are in the process of testing in the ice, and no results are available yet as to their performance. As noted, these consist of a thick brass plate (5 cm diameter x 2.5 cm thick) with a strain gauge rosette fixed in the mid-

plane of the transducer in a small, flat cavity. Key slots have been cut around the edges of the plates to facilitate bonding between the ice and the transducer.

The calculation of principal stress directions from a transducer of this type appears to be straightforward as outlined by Jaeger and Cook (1969). This is because, assuming that there is no slip at the ice-transducer boundary, the strain in the transducer can be calculated using the solution to the problem of a circular inclusion in an infinite region. The resultant strains are homogeneous, so that the principal strains in the transducer can be calculated from the values measured by the strain gauge rosettes. Assuming homogeneity of the brass, and with values for its elastic parameters known, the magnitudes of the principal stresses in the transducers can be determined, and these in turn permit an approximate value of the stress outside the inclusion to be made. The validity of the calculations will be checked by calibration against flatjacks in the field and by laboratory tests.

B. Temperature Effects

Because the mechanical properties of ice are strongly temperature-dependent, it is important to know what effect the introduction of a flatjack has on the temperature profile in the surrounding ice. An experiment was performed at Barrow in April 1975 to examine this. The details of the experiment and the results have been reported in Shapiro and Hoskins (1975).

The experiment consisted simply of freezing a steel plate and a plexiglass plate, each with dimensions similar to a typical flatjack (46 x 46 x .6 cm), into the ice. A series of thermocouple strings were

placed in the ice to measure temperature profiles at various distances from the plates, and a reference thermocouple string was installed out of the area of possible disturbance. Measurements were made over a five-day period following installation of the plates. The results showed that at a distance of 30 cm from the plates, the temperature profiles never varied by more than 1°C from those of the reference string. Further, by the fifth day, all of the thermocouple strings, including those almost in contact with the plates, were within 1°C at each depth.

Based upon these results, it can probably be assumed that at distances greater than .6-.7 times the flatjack width, the temperature effect of the flatjack is negligible. Further, experiments to verify and refine this result are planned.

C. Preliminary Field Tests

A short series of tests was conducted at Barrow in May 1975, to examine the suitability of flatjacks for the purposes of this project. The results have been reported in Shapiro and Hoskins (1975). Briefly, the purpose of the tests was to determine whether the basic steel flatjack could expand sufficiently to meet the requirements of long-term creep tests in sea ice, or whether jacks fabricated of other, more flexible materials would be required. The results indicated that steel was satisfactory. Incidental to these tests some crude values of Young's modulus and the coefficient of Newtonian viscosity were determined. The average values of these were 4.0×10^9 dynes/cm^2 for the former, and 2×10^{11} dyne-min/cm^2 for the latter.

For the present field season, tests have been in progress Barrow since mid-February. These have included creep tests to evaluate the performance of the strain cells (results were reported above) and to determine the appropriate working distances between the jacks and the strain cells. These tests produced good creep curves, but the data have not yet been analyzed. Also, as noted, tests of the two stress transducers are in progress, but results are not yet available.

Three types of tests designed to measure the fracture strength of the ice in different loading configurations have also been done. These include direct shear tests, a modified indirect tension test (Brazil test), and uniaxial compression tests.

Three direct shear tests have been conducted to date using flatjacks of different dimensions. In each case, the procedure was the same. Chain saw cuts were made in the ice in the shape of a square with dimensions equal to the length of the flatjack to be used in the test. The depth of the cut corresponded to the flatjack width. After the cuts were made, the flatjack was frozen in along one side of the square, and then loaded. In all three cases, fracture occurred along a rough plane which originated at the base of the jack, and intersected each chain saw cut at or close to the bottom. The flatjack sizes used in the three tests were 15 x 15 cm, 15 x 46 cm and 61 x 61 cm. Assuming an ice density of .91 g/cm^3 the normal stress on the fracture planes can be evaluated as .014 kg/cm^2, .014 kg/cm^2 and .054 kg/cm^2, respectively. The calculated shear stresses on the failure plane were 4.5 kg/cm^2, 8.7 kg/cm^2 and 5.3 kg/cm^2.

One test was performed which simulates an indirect tension test (Brazil test). A circle 59 cm in diameter was cut in the ice surface to

a depth of 60 cm. Two 15 x 60 cm flatjacks were then installed at opposite ends of a diameter of the circle, giving a cylinder with line loads along opposite sides, as is done for the Brazil test. Note that ring-tension tests could be done in the same configuration simply by drilling a hole in the center of the cylinder. When loaded, the cylinder failed in the expected manner at a tensile stress of 5.5 kg/cm^2, with a compressive stress of 16.5 kg/cm^2 along the loaded diameter.

The question of the validity of the test arises from the fact that the cylinder is still attached to the ice sheet at its base. Thus, it is certain that plane-strain conditions are not met over the entire length of the cylinder. However, there is no doubt that these conditions do exist near the top surface where the fracture originated. Thus, further investigation (both field tests and calculations) are needed to determine what percentage of the volume of the cylinder is in plane-strain, and establish the meaning of the test results.

A single uniaxial compression test has been run to date. In this test, two triangular flatjacks 38 x 38 x 38 cm were frozen into the ice with one edge at the surface and facing each other about 76 cm apart. Two saw cuts were then made connecting the ends of the flatjacks. These were inclined at 60°, parallel to the sides of the jacks, and met under the block. This forms a triangular prism with the dimensions given above, which is entirely free from the ice sheet except for its connection through the flatjacks.

When loaded, the specimen failed in extension, at a pressure of 33 kg/cm^2, so that compressive failure was not achieved. The test will be repeated shortly, but the cross-sectional area of part of the prism will

be reduced (i.e., 'dog boned') to give a higher stress concentration in that area. It is expected that this will permit the compressive strength to be reached.

D. Other Work

Some preliminary work was done in a cold room on problems relating to bonding strain gauges to ice, and temperature compensation of strain gauges for long-term tests where constant temperature conditions may not prevail.

Work is progressing on the study of Peyton's (1966) tests results. At present, plots of the strain-time data for most of his approximately 200 creep tests in compression have been prepared, and the appropriate temperature, salinity and orientation data extracted from Dr. Peyton's archived notes. This work is being delayed during installation of a new computer, but should resume shortly. When organization of the data is complete, an attempt will be made to formulate a viscoelastic stress-strain from it for use in comparison with the *in situ* measurements.

REFERENCES CITED

Hoskins, E. R., 1966, An investigation of the flatjack method of measuring rock stress; Int. J. Rock. Mech. Min. Sci., Vol. 3, p. 249-64.

Jaeger, J. C. and N. G. W. Cook, 1969, Fundamentals of Rock Mechanics: Methuen & Co. Ltd., London, 513 p.

Karlsson, T., 1972, A viscoelastic-plastic material model for drifting sea ice, in Sea Ice, Proc. Conf., Reykjavik, Iceland, May 10-13, 1971, p. 188-195.

Katona, M. G. and K. D. Vaudrey, 1973, Ice engineering -- summary of elastic properties research and introduction to viscoelastic and non-linear analysis of saline ice, Tech. Rept. R797, Naval Civ. Eng. Lab., Port Hueneme, Calif., 67 p.

Maser, K. R., 1972, An analysis of the small-scale strength testing of ice, Rept. MITSG 72-6, Mass. Inst. Tech. Sea Grant Office, 138 p.

Nelson, R. D., 1974, Measurements of tide and temperature generated stresses in shorefast sea ice, in The Coast and Shelf of the Beaufort Sea, ed. J. Reed and J. Sater, AINA, p. 195-204.

Nelson, R. D., 1975, Internal stress measurements in ice sheets using embedded load cells, P.O.A.C. 1975 Conf. U. of Alaska, Aug. 11-15, 1975 (in press).

Nelson, R. D., M. Taurianen and J. Borghorst, 1972, Techniques for measuring stress in sea ice, Inst. of Arctic Environ. Eng. Rept., U. of Alaska.

Peyton, H. R., 1966, Sea ice strength, Geophysical Inst., U. of Alaska, Rept. UAG R-182, 273 p.

Shapiro, L. H. and E. R. Hoskins, 1975, The use of flatjacks for the in-situ determination of the mechanical properties of sea ice, P.O.A.C., 1975 Conf., U. of Alaska, Aug. 11-15, 1975 (in press).

Tabata, T., 1958, Studies on visco-elastic properties of sea ice, in Arctic Sea Ice, U.S. NAS-NRC pub. 598, p. 39-147.

Vaudrey, K. D., 1973, Development of a sea ice strain transducer, Tech. Note N-1310, U.S.N. Civil Eng. Lab., Port Hueneme, Calif., 24 p.

Weeks, W. F. and A. Assur, 1967, The mechanical properties of sea ice, CRREL Monograph II-C3, 94 p.

VII., VIII. DISCUSSION AND CONCLUSIONS

In general, progress has been made on all aspects of this study. The use of steel flatjacks, expanded with nitrogen gas, for loading devices has proved successful in all the tests to date. Similarly, no serious problems have been encountered in the preparation of strain cells although more work is needed, particularly in coarse crystalline ice where the size of the grains may be large enough to distort the strain field in the cell. In addition, there is still a question as to whether small strain gauges will be adequate for testing later in the spring when higher temperatures will permit the strain to become much greater than those encountered to date. These, however, are operational problems to be solved if the need arises. The basic questions regarding the design of a suitable strain cell appears to have been resolved.

The testing of the stress transducers is still in the preliminary stage, and no evaluation of their utility for the program can be made as yet.

The in situ strength tests completed to date suggest that these will be useful techniques for determining these values. However, additional tests and calculations are needed to define the appropriate geometry for the indirect tension and uniaxial compression tests. In addition, several additional tests of each type need to be conducted under as nearly identical conditions as possible, in order to establish that the measured values are repeatable. Given these results, and the fact that the tests are simple to run, it should be possible to devise a test series to determine these strength parameters under a variety of conditions.

Finally, several creep tests have been conducted involving cycling of stress over several days, and maintenance of constant stress for up to 14 hours. Those curves that have been plotted show that the data are of good quality. However, no analyses of the test results have been made to date.

IX. NEEDS FOR FURTHER STUDY

Needs for further study have been indicated in Sections VI, VII and VIII. These generally include further evaluation of the test instrumentation and procedures, and completion of organization (followed by interpretation) of the data from Peyton (1966). These, of course, are short-term objectives which much be met before the long-term study of mechanical properties can begin.

X. SUMMARY OF 4th QUARTER OPERATIONS

At the start of the 4th quarter cold room tests were in progress as described above.

The field program began at Barrow in early February and Drs. E. Hoskins, R. D. Nelson and L. H. Shapiro have participated in this work to date. Mr. R. Metzer has been on site since the start of the program and will remain there until its completion.

The results of the work to date were given above.

ANNUAL REPORT

Contract # 03-5-022-55
Research Unit #267
Reporting Period: June 12, 1975 to
March 31, 1976
Number of pages: 47

OPERATION OF AN ALASKAN FACILITY FOR APPLICATIONS OF REMOTE-SENSING DATA TO OCS STUDIES

Albert E. Belon
Geophysical Institute
University of Alaska

April 1, 1976

I - SUMMARY

The primary objective of the project is to assemble available remote-sensing data of the Alaskan outer continental shelf and to assist OCS investigators in the analysis and interpretation of these data to provide a comprehensive assessment of the development and decay of fast ice, sediment plumes and offshore suspended sediment patterns along the Alaskan coast from Yakutat to Demarcation Bay.

Four complementary approaches are used to achieve this objective. They are 1) the operation of a remote-sensing data library which acquires, catalogs and disseminates satellite and aircraft remote-sensing data; 2) the operation and maintenance of remote-sensing data processing facilities; 3) the development of photographic and computer techniques for processing remote sensing data; and 4) consultation and assistance to OCS investigators in data processing and interpretation.

Thus, the project has primarily a support role for other OCS projects, and in itself does not usually generate disciplinary conclusions and implications with respect to OCS oil and gas development. Such results will be generated by the various disciplinary OCS projects, some of which are frequest users of remote-sensing data and services provided by our project. At this time at least a dozen OCS projects are utilizing remote-sensing data routinely, four of them (RU #89, 99, 257, 258) almost exclusively. In addition, the availability of near-real-time remote-sensing data (NOAA satellite) and delayed repetitive data (Landsat and aircraft) provides a continuous monitoring of environmental conditions along the Alaskan continental shelf for research and logistic support of the OCSEAP Program.

II - INTRODUCTION

A. General Nature and Scope of Study.

The outer continental shelf of Alaska is so vast and so varied that conventional techniques, by themselves, are unlikely to provide the detailed and comprehensive assessment of its environmental characteristics which is required before the development of its resources is allowed to proceed during the next three years. The utilization of remote-sensing techniques, in conjunction with conventional techniques, provides a solution to this dilemna for many disciplinary investigations. Basically the approach involves the combined analysis of ground-based (or sea-based), aircraft and satellite data by a technique known as multistage sampling. In this technique, detailed data acquired over relatively small areas by ground surveys or sea cruises are correlated with aerial and space photographs of the same areas. Then the satellite data, which extend over a much larger area and provide repetitive coverage, are used to extrapolate and update the results of the three-way correlations to the entire satellite photograph. Thus, maximum advantage is taken of the synoptic and repetitive view of the satellite to minimize the coverage and frequency of data which have to be obtained by conventional means.

B. Specific Objectives.

The principal objective of the project is to make remote-sensing data, processing facilities and interpretation techniques available to the OCS investigators so that the promising applications and cost effectiveness of remote-sensing techniques can be incorporated in their disciplinary investigations. The specific objectives of the project are: 1) the acquisition, cataloging and dissemination of existing remote-sensing data obtained by aircraft and satellites over the Alaskan outer continental shelf, 2) the operation and maintenance of University of Alaska facilities for the photographic, optical and digital processing of remote-sensing data, 3) the development of photographic, optical and computer techniques for processing remote-sensing data for OCS purposes and 4) the active interaction of the project with OCS users of remote-sensing data, including consultation and assistance in disciplinary applications, data processing and data interpretation.

C. Relevance to problems of petroleum development.

The acquisition of remote-sensing data, specially satellite data, has proved to be a cost-effective method of monitoring the environment on a synoptic scale. Meteorological satellites have been used for over a decade to study weather patterns and as an aid to weather forecasting. The earth resources satellite program, initiated in 1972, offers a similar promise to provide, at a higher ground resolution, synoptic information and eventually forecasts of environmental conditions which are vital to petroleum development on the continental shelf. For instance the morphology and dynamics of sea-ice which are relevant to navigation and construction of offshore structures, the patterns of sediment transport and sea-surface circulation which will aid to forecast trajectories of potential oil spills and impact on fisheries, the nature of ecosystems in the near-shore regions which can be changed by human activity, are among the critical development-related environmental parameters which can be studied, in conjunction with appropriate field measurements, and eventually routinely monitored by remote-sensing.

III - CURRENT STATE OF KNOWLEDGE

The utilization of remote-sensing techniques in environmental surveys and resource inventories has made great strides during the last few years with the development of advanced instruments carried by aircraft and satellites. The early meteorological satellites had a ground resolution of a few miles and a broad-band spectral response which made them well-suited to meteorological studies and forecasting but inadequate for environmental surveys. The ground resolution of the sensors has been gradually much improved over the years and thermal sensors were added for cloud and sea temperature measurements, but generally the relatively low ground and spectral resolution of the meteorological satellites is a limitation for environmental surveys.

The initiation of a series of Earth Resources Technology Satellites (now renamed Landsat) in July 1972 was intended to fill the need for synoptic and repetitive surveys of environmental conditions on the land and the near-shore sea. With a ground resolution of about 80 meters and sensitivity in four visible spectral bands, Landsat-1 and 2, have fulfilled

that promise beyond all expectations. Landsat-3, scheduled to be launched in spring 1977 will have a higher ground resolution (40 meters for the RBV system) and a thermal spectral band which will improve its capabilities enormously. The Seasat satellite, to be launched in 1978, will have all weather capabilities through the use of imaging radars and, as the name implies, has been specially designed for environmental surveys of the sea.

The development of techniques for analyzing and interpreting Landsat have proceeded at an even more rapid pace than the satellite hardware. While in 1972 much of the Landsat data interpretation was done by visual photointerpretation, the last four years have seen major developments in photographic, optical and, in particular, digital techniques for processing and interpreting the Landsat data. Some of these techniques, applicable to OCS studies, will be discussed in section V and VI of this report.

Through the impetus provided by the national commitment to satellite observations of the earth, the aircraft remote-sensing program has also made great strides in the last few years. While in the early 1960's airborne platforms were mostly used for aerial photography, the late 1960's saw the development of advanced multispectral scanners, thermal scanners, side-looking radars and microwave radiometers, partly for the testing of future satellite hardware and partly because the airborne observations serve for middle-altitude observations between ground and satellite measurements as part of the multistage sampling technique. Two philosophies are apparent in the airborne remote-sensing program: the first, exemplified by the NASA program as well as several universities and industrial agencies, involves relatively large aircraft and sophisticated instrumentation which produce vast quantities of data usually processed by computer techniques. The costs of data acquisition and data processing are quite high and for this reason this approach is usually applied to intensive, non-repetitive surveys of relatively small areas. The second approach uses airborne remote-sensing in a truly supporting role for ground-based or satellite measurements. The aircraft are smaller and the instrumentation usually consists of proven, simpler instruments such as aerial cameras, single-band thermal scanners, and single wavelength side-looking radars which usually generate data only in photographic format. The costs of data acquisition and data processing, while they are not small, are sufficiently low that the approach is often used for repetitive surveys of relatively large areas. In our opinion the second approach fulfills best the needs of the NOAA/OCSEAP program and we have been working very closely with the NOAA Arctic Project Office toward the implementation of such a remote-sensing program.

IV STUDY AREA

The study area for the project includes the entire continental shelf of Alaska, except for the southeastern Alaska panhandle. This area includes the Beaufort, Chukchi and Bering Sea and the Gulf of Alaska shelves and coastal zone. Temporal coverage is year-around, although the data coverage from November 1 to February 15 is limited owing to the very low solar illumination prevailing at high latitudes during winter.

V - SOURCES, METHODS AND RATIONALE OF DATA COLLECTION

A remote-sensing data library and processing facility was established in 1972 on the Fairbanks campus of the University of Alaska as a result of a NASA-funded program entitled "An interdisciplinary feasibility study of the applications of ERTS-1 data to a survey of the Alaskan environment". This experimental program, which covered ten environmental disciplines and involved eight research institutes and academic departments of the University, terminated in 1974, but the facility which it established proved to be so useful to the statewide university and government agencies that it has continued to operate on a minimal basis with partial funding from a NASA grant and a USGS/EROS contract. In view of the large potential demand of the OCS program on these facilities, a proposal was submitted to NOAA in March 1975 for partial funding of the facility for OCS purposes. This proposal resulted in a contract from NOAA on June 12, 1975, and the work performed since that time is the basis for the present report.

As a result of the NASA-funded program, the remote-sensing data library had total cloud-free and repetitive coverage of Alaska by the ERTS-now renamed Landsat-satellite from the date of launch (JUly 29, 1972) to May 1974 (about 30,000 data products), 60 rolls of imagery acquired by NASA aircraft (NP3 and U-2) some of which includes coverage of the Beaufort Sea, Cook Inlet and Prince William Sound, and substantial facilities for photographic, optical and digital processing of these data. Through a NOAA-funded pilot project, which studied applications of NOAA satellite data in meteorology, hydrology, and oceanography, the remote-sensing data library also had nearly complete coverage of Alaska by the NOAA satellites since February 1974.

A. Remote-Sensing Data Acquired for the OCS Program.

1) Landsat data

At the initiation of the project we performed searches of the EROS Data Center (EDC) data bank for Landsat and aircraft remote-sensing data obtained over the four areas of interest to the OCSEAP program. From the several thousand scenes so identified, we selected the scenes which we did not have in our files and which had satisfactory quality and 30% or less cloud cover. As a result of this search 566 Landsat scenes (2830 data products) were ordered from the EROS Data Center in the following data formats

- -70mm positive transparencies of multispectral scanner (MSS) spectral bands 4, 5 and 7
- -70mm negative transparency of MSS spectral band 5
- -9½ inch print of MSS spectral band 6

Throughout the reporting period we continued to search the EDC data bank weekly for cloud-free Landsat scenes of the OCS areas acquired in the intervening periods. 265 additional Landsat scenes (1325 data products) were ordered from EDC as of 31 March 1976.

2) NOAA satellite data

With the termination of the NOAA pilot project, sponsored by

NOAA/NESS in October 1975, the flow of NOAA satellite images stopped after having accumulated 1230 scenes since February 1974.

From November to February, we arranged with the Fairbanks station of the National Weather Service to examine their facsimile copies of the data from which we could select scenes suitable for OCS purposes and order high quality copies from the NOAA Satellite Data Acquisition Facility near Fairbanks, before the original photographs were shipped to NOAA/NESS in Suitland, Maryland. Sixty scenes were ordered in this manner, as positive transparencies of both the visible and thermal infrared spectral bands.

The arrangement with the National Weather Service was not satisfactory for reasons described in Quarterly Report No. 3. Therefore, after consultation with the NOAA/OCS Arctic Project Office, we submitted a proposal to NOAA/OCSEAP for a supplemental appropriation to cover the costs of purchasing NOAA satellite data on a routine basis. This proposal was accepted and a purchase order was issued to NOAA/NESS. Under this purchase order we are receiving since February 1, 1976, 2 NOAA scenes daily from the Bering Sea pass (covering the Beaufort and Bering Sea, respectively) and one scene daily from the interior Alaska pass (covering the Gulf of Alaska) in both the visible and infrared spectral bands (6 images daily). In addition we have made arrangement with the NOAA/NESS facility to save digital tapes of the thermal infrared data, upon request and for the cost of tape replacement, for scenes which are specially cloud-free or of high interest to OCS investigators. These tapes will allow the mapping of sea-surface temperature at locations and at times of special interest to OCS investigators.

3) USGS/OCS aircraft remote-sensing data

In November 1975, we started receiving the remote-sensing data acquired by USGS aircraft under a NOAA/OCS contract, along the Alaskan arctic coast since July 1975. These data consist of six 250 ft rolls of black and white aerial photography and 42 strips of side-looking radar imagery.

4) NASA aircraft remote-sensing data

Over the last few years the NASA Earth Resources Aircraft Program has flown several missions over preselected test sites within Alaska. The program is directed primarily at testing a variety of remote-sensing instruments and techniques and to support NASA-sponsored investigations. However, black and white and color-infrared aerial photography were obtained on most missions and in particular during the May 1967, July 1972 and June 1974 missions which include flights over portions of the Alaskan coast and coastal waters. We have acquired copies of these data from NASA.

The U-2 imagery of the Beaufort Sea obtained in June 1974 should be of particular interest to OCS investigators because it was obtained during the sea-ice break-up period, it covers a large area (20x20 mi.) in a single frame with good ground resolution (~10 ft), and nearly concurrent Landsat data are available.

We have a request pending with NASA for the U-2 aircraft to acquire aerial photography of the entire Alaskan coastal zone (except the Seward Peninsula) during June 1976.

5) Preparation and distribution of remote-sensing data catalogs

All the remote-sensing data available in our files for the Alaskan continental shelf have been indexed and plotted on maps. Two catalogs summarizing the availability of these data were prepared and distributed to all OCS investigators and interested parties as appendices to Arctic Project Bulletins No. 6 (August 15, 1975) and 9 (February 11, 1976). The catalogs also contained instructions for selecting and ordering the available remote-sensing data.

B. Remote-Sensing Data Processing Facilities and Techniques

The facilities and equipment commonly used for remote-sensing data processing are listed in Figure 1. Most of this equipment is not devoted exclusively to remote-sensing data processing but arrangements have been made to support the needs of the OCS investigators on a shore-time and work order basis, and to take into account the needs of the OCS program in any planned modifications or expansions.

The optical and photographic processing techniques developed for the remote-sensing program are described in the flow diagram of figure 2.

Photographic processing probably needs no further explanation. The full range photographic laboratory of the Geophysical Institute is well adapted to the generation of custom, as distinct from production run, photographic products. However the available equipment limits photographic enlargements to 16x20" maximum size from 4x5" maximum size originals. Electronically dodged prints or transparencies are produced by contact printing only.

Optical processing revolves around the use of specialized equipment such as the multiformat photo-interpretation station, the zoom transfer scope, the color additive viewer and the VP-8 image analyzer in addition to conventional light tables, stereoscopes and a binocular zoom magnifier.

Multiformat Photo Interpretation Station - Analysis of aerial imagery in roll form is a cumbersome task and is likely to damage the original material even with careful handling if one uses ordinary reel holders and a light table. With stereo coverage, it is impossible to achieve stereo viewing with the frames appearing on the roll format unless one uses the photo interpretation machine. It can accommodate either 5-inch or 9-inch film formats and the film transport adjusts to permit stereo viewing with varying amounts of forward lap between frames. The viewing turret includes zoom binoculars with up to 5X magnification.

Zoom Transfer Scope - The time-consuming process of transferring information from images to maps is made considerably easier by the use of the zoom transfer scope. This table-top instrument allows the operator to view simultaneously both an image and a map of the same area. Simple controls allow the matching of differences in scales (up to 14X) and provide other optical corrections so that the image and the map appear superimposed. In particular a unique one-directional stretch capability (up to 2X) allow the matching of computer print-out "images" to a map or photograph.

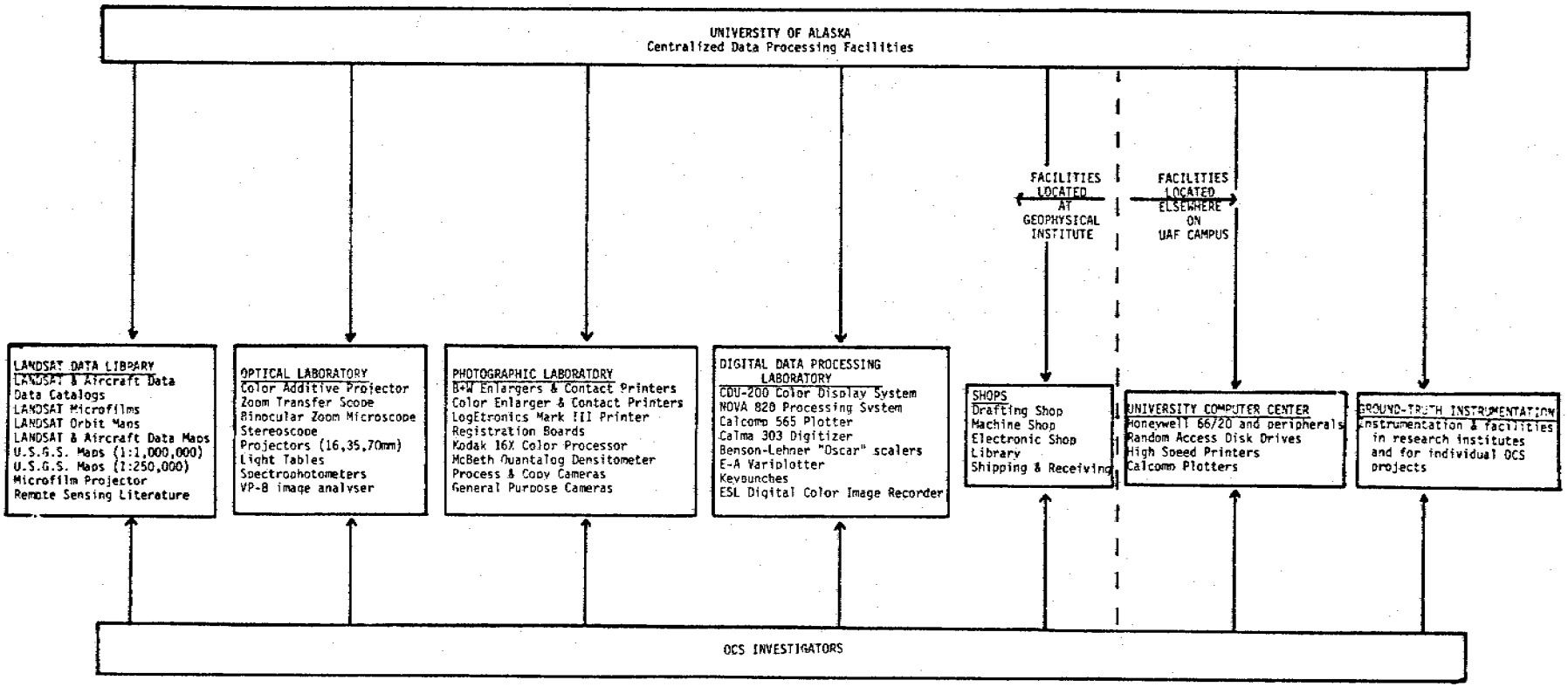

Centralized Data Processing Facilities

Figure 1

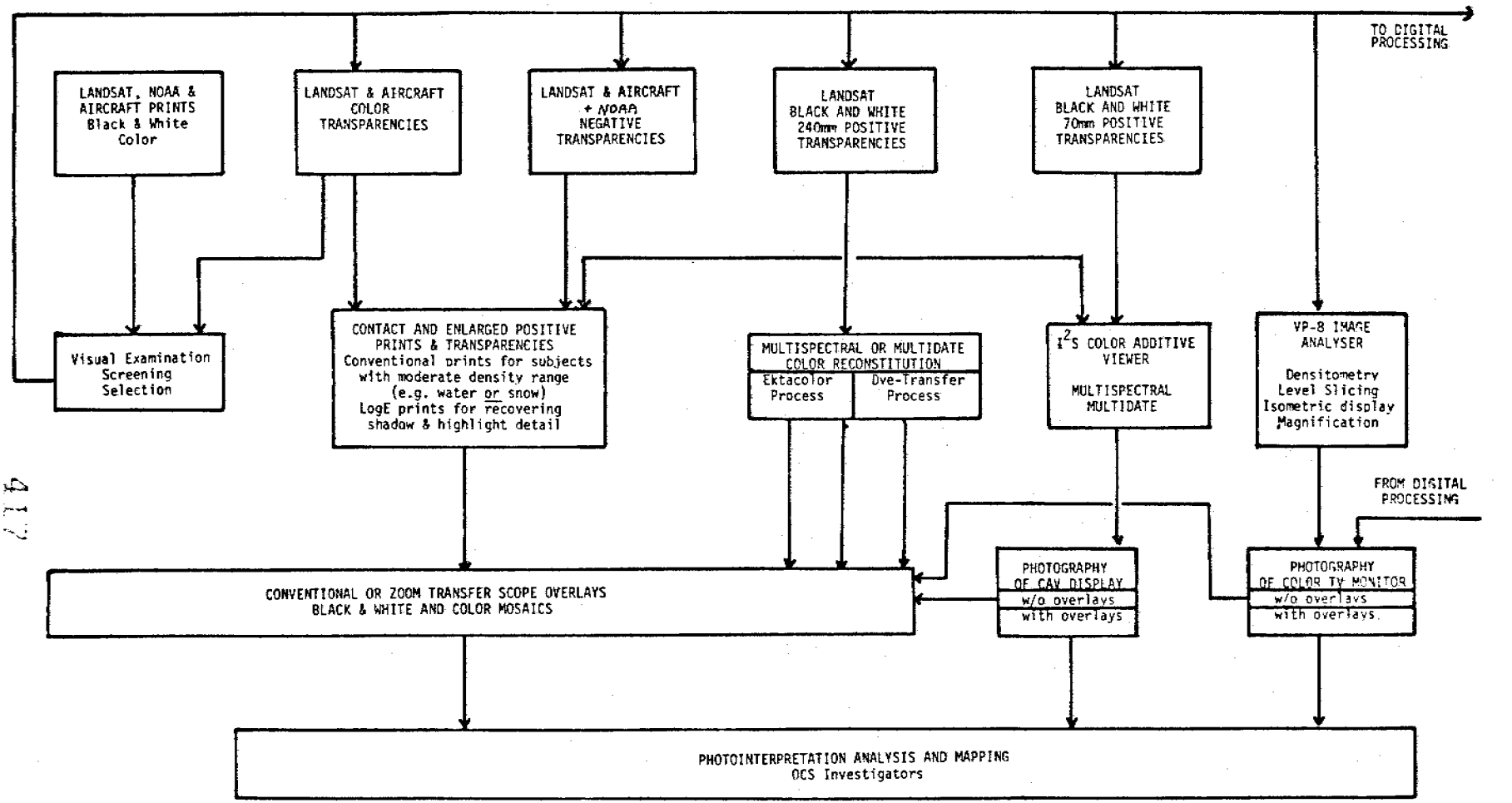

Optical and Photographic Processing

Figure 2

Color Additive Viewer/projector/tracer - This instrument is primarily intended for the false-color recomposition of Landsat images from 70mm black and white transparencies and tracing information contained on these images at scales of 1:1,000,000 and 1:500,000. However it has proved to be very useful also for superimposing and color-coding Landsat images acquired on different dates and looking for change or movement and for viewing any other enlarged image on 70mm film format.

VP-8 Image Analysis System - The VP-8 image analysis system provides an electronic means of quantizing information contained in a photograph when the sought information can be expressed in terms of density ranges. It consists of:

- a light table having uniform brightness and a working surface of 15x22 inches
- a vidicon camera which transforms the photographic (transmittance) data to electrical signals
- an electronic image analyser which quantizes and formats the vidicon signals
- a CRT oscilloscope
- a color television monitor as an output device

The capabilities of the VP-8 image analysis system include:

- density level slicing. This feature allows lines of uniform density on the input image to be displayed as contours. These contours form the boundaries of density bands which are displayed as up to 8 color bands on the color television monitor. The base density levels and the density range of the bands are individually as well as collectively variable. An example and illustration of the density slicing technique applied to coastal sedimentation studies are provided in of this report.
- single scan line display. Any single horizontal scan line of the vidicon camera can be selected for display on the CRT oscilloscope by positioning a horizontal cross-hair on the image. This display of a single scan line is effectively a microdensitometer trace.
- digital read-out of point densities, selected by adjustable cursors or of total area of the image having a given (color-coded) density range. For instance the VP-8 image analysis system is well adapted to the area measurement of sea-ice, newly refrozen ice, and open water in any area of the Beaufort sea imaged by Landsat.
- 3-D display. This mode of operation allows a three-dimensional presentation where the X and Y coordinates of the original image are displayed in isometric projection and intensity information is shown as a vertical deflection. Subtle features of the image, which are often lost on level-sliced displays, become obvious in 3-D displays.
- 5X magnification. This feature allows the expansion of a small part of the image to full screen size.

The digital data processing equipment available to the OCS investigators include the main University computer, a Honeywell model 66/20 with 1M bytes of core memory, which will soon have a remote time-share terminal at the Geophysical Institute, a NOAA 820 data preprocessing computer as well as conventional typewriter printers, plotters and digitizers. Most remotely-sensed imagery in digital format is reformatted, classified or otherwise processed on off-line computing systems and displayed on two specialized systems available at the Geophysical Institute.

The CDU-200 digital color display system is described by the simplified block diagram of figure 3. The CDU-200 performs three primary functions:

1) it provides a capability, similar to the VP-8 image analysis system for density slicing up to 3 bands of Landsat data in digital format. The accuracy of digital density-slicing is greater and more reproducible than with the VP-8 system because digital Landsat data have a more accurate radiometric calibration than photographic data and because up to 127 levels of intensity can be sliced (in groups of 16). Furthermore three digital images can be stored at once on the disc of the CDU-200 system and displayed sequentially for multispectral or multidate signature determination.

2) it provides a capability, similar to the color-additive viewer, for registering and combining three black and white digital images into a false-color image (displayed on the color television monitor) which has a larger scale, spatial and intensity resolution than the images displayed on the color-additive viewer.

3) it provides a capability to generate color-coded thematic displays from the output of classification processing techniques performed by off-line computer systems (see appendix A of this report).

Digital Color Image Recorder - It often is necessary to reconstitute an image from the processed digital data in order to convey information in the most suitable form to the human mind. Also, if one deals with multispectral data it is impossible to convey the density of information required without the use of color. A digital image recorder with the capability of reconstituting color products should be available for use starting in April. Basically it is a rotating-drum film recorder which will produce four simultaneous standard images on film up to 8"x10" in size. Density resolution is 64 levels of gray, and spatial resolution is 500 lines per inch and 500 samples per inch. Recording rate is 3 lines per second. Any combination of the four negatives so produced can be registered and printed with suitable filters to produce a reconstituted color negatives which can be processed and enlarged photographically using standard techniques.

Remote-Sensing Data Interpretation Techniques - Visual photointerpretation, density-slicing and automatic classification techniques using the facilities described in this bulletin are illustrated in greater detail in Appendix A of this report. Variations of these and other techniques offer considerable promise of effective application to OCS studies, but are too numerous and varied to be discussed in detail here. Instead, we refer to other OCS investigators, with whom we have worked very closely, who have applied these techniques to their disciplinary investigations.

C. Consultation and Assistance to OCS Investigators

In order to familiarize OCS investigators with the available remote-sensing data, processing equipment, and interpretation techniques, we prepared three substantial reports which were included as appendices to Arctic Project Bulletins No. 6, 7 and 9, and distributed to all OCS investigators active in studies of the Beaufort, Chukchi and Bering Seas and the Gulf of Alaska.

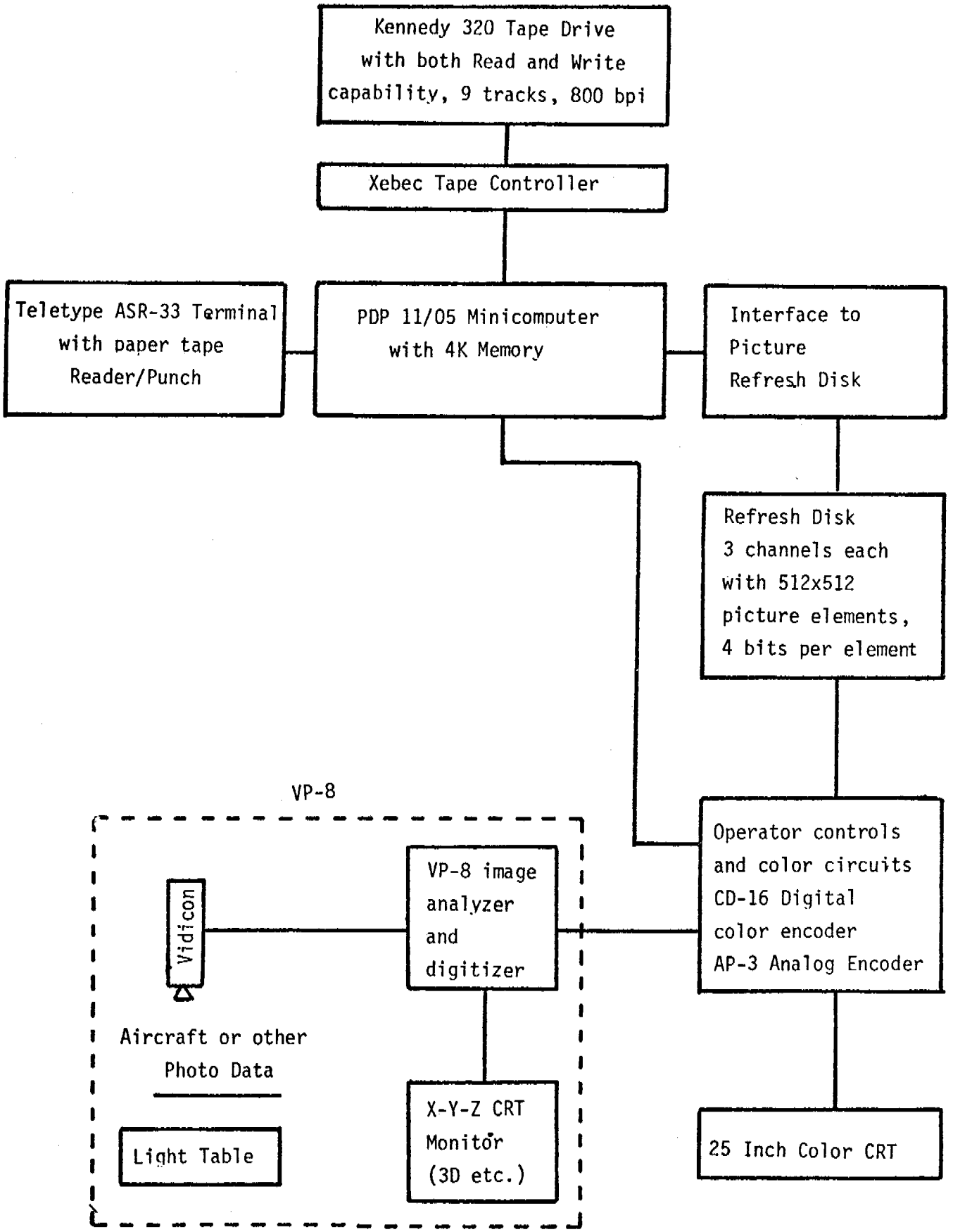
Kennedy 320 Tape Drive with both Read and Write capability, 9 tracks, 800 bpi
Xebec Tape Controller
Teletype ASR-33 Terminal with paper tape Reader/Punch
PDP 11/05 Minicomputer with 4K Memory
Interface to Picture Refresh Disk
Refresh Disk 3 channels each with 512x512 picture elements, 4 bits per element
VP-8
Vidicon
VP-8 image analyzer and digitizer
Operator controls and color circuits CD-16 Digital color encoder AP-3 Analog Encoder
Aircraft or other Photo Data
Light Table
X-Y-Z CRT Monitor (3D etc.)
25 Inch Color CRT

Figure 3

The appendix to Arctic Project Bulletin No. 6 described the operation of the remote-sensing data library, provided catalogs of Landsat and aircraft data available in our files and provided instructions to OCS investigators on the selection and ordering of these data.

The appendix to Arctic Project Bulletin No. 7 described the facilities and techniques available for analysing remote-sensing data and included a scientific report in which these facilities and techniques were used to analyse and interpret remote-sensing data in three representative investigations of the Alaskan continental shelf: sea-surface circulation and sediment transport in Alaskan coastal waters, studies of sea-ice morphology and dynamics in the near-shore Beaufort Sea, and mapping of terrestrial ecosystems along the Alaskan coastal zone. This scientific report is reproduced in Appendix A of this annual report.

The appendix to Arctic Project Bulletin No. 9 provided a cumulative catalog of all available OCS remote-sensing data including Landsat and NOAA satellite data, USGS/OCS aircraft data and NASA aircraft data.

Although the existing remote-sensing data base is very useful in supporting OCS disciplinary projects, there is also a vital need for an airborne remote-sensing data acquisition program dedicated to OCS purposes. To this end we have worked very closely with the NOAA Arctic Project Office in attempting to implement such a program. We participated in several meetings at the Geophysical Institute and one at Pt. Barrow in an attempt to set the USGS/OCS airborne remote-sensing data acquisition program on the right course, and took over responsibility for cataloguing, reproducing and disseminating these data. When this program failed and was terminated in January 1976, we studied alternatives and recommended several options to NOAA, one of which is now being negotiated. In parallel with these activities we have negotiated with NASA for the acquisition of high altitude (U-2, 65,000 ft) aerial photography of the entire Alaskan coastal zone. This program was approved by NASA. The first attempt to acquire the requested data in June 1975 failed because of prevailing heavy cloud cover during the 3 weeks the U-2 aircraft was in Alaska. A second attempt has been approved by NASA and will occur in mid-June 1976.

In addition to this general assistance we interacted continuously with at least 15 OCS investigators and sporadically with many more on the applicability of remote-sensing data to their studies and assisted them in data selection, data interpretation and the use of data processing equipment. This individual assistance has gradually increased in number and scope over the last year, and we expect that it will continue to increase. At this time over a dozen OCS projects are utilizing remote-sensing data routinely, four of them (RU#89, 99, 257, 258) almost exclusively.

At a meeting in Boulder, Colorado on November 12-13, 1975, Roger Barry (INSTAAR-OCS/RU244), William Stringer (UofA-OCS RU's 257 and 258) and Tom George (UofA - representing our project OCS RU267) formulated a cooperative program involving Landsat and U-2 mapping of the coastal fast ice zone from multidate data obtained in 1973, 1974 and 1975, digital classification of Landsat scene 1702-21093 (for which concurrent aerial photography exists) in an attempt to identify sea-ice types and their areal distribution from remote-sensing data, and future field measurements of meteorological and sea-ice conditions to optimize the ground-truth data necessary to the interpretation of satellite and aircraft imagery. Our

project's contribution to this cooperative program would be to select and and reproduce the imagery for the mapping project and perform the digital Landsat classifications in which we have considerable experience. Six other OCS projects have expressed their interest in participating in this study.

Through our participation in the USDI/EROS Program, EROS has agreed to provide us free of charge two Data Collection Platforms (DCP) for testing their operation in the arctic environment. Each DCP automatically collects data from up to eight sensors, transmits them to either the Landsat or GOES satellite which relays them to a satellite data acquisition station where they are listed on a computer printout. We have made arrangedments with Dr. William Sackinger (UofA-OCS RU259) to utilize one of the DCP to measure sea-ice stresses in the Beaufort Sea. The DCP will be installed in the Beaufort Sea when received from the manufacturer (April or May).

We are also negotiating with NASA for the establishment of a Landsat "Quick-Look" facility at the Geophysical Institute. This facility would provide real-time, good quality photographic images of the Landsat data as they are being acquired. In our opinion it would have great value for both research and logistic support of the OCSEAP Program.

Finally, we have recently received several requests from the NOAA/OCSEAP Headquarters, in Boulder, Colorado for Landsat and NOAA images which document certain environmental conditions in the Gulf of Alaska and Beaufort Sea and which will be used in the impact statement. Prompt responses to these requests would not have been possible without the availability of copies of the data and support services provided by our project.

VI - RESULTS

The results of the project so far can be separated into two categories: the operational results (establishment of a remote-sensing data facility) and the research results (disciplinary applications of remote-sensing data to OCS studies).

A. Establishment of a Remote-sensing Facility for OCS STudies

The principal result of the project, as specified in the work statement of the contract, is that there now exists at the University of Alaska an operational facility for applications of remote-sensing data to OCS studies. This facility and its functions have been described in detail in the previous section of the reports. Briefly it consists of:

1) A remote-sensing data library which routinesly acquires, catalogs and disseminates information on Landsat and NOAA satellite imagery and aircraft imagery of the Alaskan continental shelf.

2) A remote-sensing data processing laboratory which provides specialized instrumentation for the photographic reproduction and optical or digital analysis of remote-sensing data of various types and formats.

3) A team of specialists that generates and develops techniques of remote sensing data analysis and interpretation which appear to be particularly well suited for OCS studies (see the next section of this report).

4) A staff that is continually available to OCS investigators for consultation and assistance in searching for, processing and interpreting remote-sensing data for their disciplinary investigations.

As a result of the establishment of the remote-sensing facility established by our project, over a dozen OCS projects are routinely using remote-sensing data, four of them almost exclusively, and many more OCS investigators are occasional users of remote-sensing data.

B. Disciplinary Results of the Applications of Remote-Sensing Data to OCS Studies

In general, the results of applications of remote-sensing data to OCS studies will be contained in the annual reports of the individual projects and need not be repeated here. However as part of our function to develop techniques of remote-sensing data analysis and interpretation, we did prepare a scientific report entitled "Environmental Assessment of Resource Development in the Alaskan Coastal Zone based on Landsat Imagery" which illustrates the applications of Landsat data to three important aspects of the OCSEAP program: studies of sea-surface circulation and sediment transport in Alaskan coastal waters, studies of sea-ice morphology and dynamics in the near-shore Beaufort Sea, and mapping of terrestrial ecosystems in the Alaskan coastal zone. This report was presented at the NASA Earth Resources Symposium, Houston, Texas, June 1975 where it was acclaimed as one of the best presentations. It was also distributed to OCS investigators as part of Arctic Project Bulletin No. 7 and is now out of print due to heavy demand in spite of the fact that 250 copies were made. It is also reproduced as Appendix A of this annual report although, to our regret, the black and white facsimile reproductions of the original color illustrations are very inadequate.

VII,VIII + IX - DISCUSSION, CONCLUSIONS, AND NEEDS FOR FURTHER STUDY

The principal objective of the contract, as specified in its work statement, has been achieved: a facility for applications of remote-sensing data to outer continental shelf studies has been established at the University of Alaska and is now fully operational.

The remote-sensing data library has acquired all available cloud-free remote-sensing imagery of the Alaskan continental shelf, catalogued it and provided information on its availability to all OCS investigators through the series of Arctic Project Bulletins.

Existing instrumentation for analysing remote-sensing data has been consolidated into a data processing laboratory and techniques for its use have been developed with particular emphasis on the needs of the OCSEAP program. New instrumentation is being acquired and new analytical techniques are continually being developed from this contract and other funding sources.

The staff of the project is interacting with a gradually increasing number of OCS investigators, providing consultation and assistance in all aspects of remote-sensing applications from data searches and ordering to advanced analyses of the data in photographic and digital format. We have also worked very closely with the NOAA Arctic Project Office in designing an effective remote-sensing data acquisition program using contract and NASA aircraft.

At this time over a dozen OCS projects are using remote-sensing data and processing facilities routinely, some of them almost exclusively of other research activities, and many more OCS investigators are occasional users of remote-sensing data. The number of user projects has gradually increased over the last year. We expect that this trend will continue, specially as OCS investigators extend their localized intensive field studies to a synoptic scale where the benefits and cost effectiveness of remote-sensing attain their greatest impact.

It is clear from the foregoing discussions and from consultations with OCS investigators, regarding their study plans for the next year. that there will be a continuing need for the research support that our project provides. We intend to submit a continuation proposal to NOAA for this purpose.

X - SUMMARY OF FOURTH QUARTER OPERATIONS

This quarterly report covers the period January 1 to March 31, 1976.

A. Laboratory Activities During the Reporting Period

1) Operation of the remote-sensing data library.

We continued to search periodically for new Landsat imagery of the Alaskan coastal zone entered in the EROS Data Center (EDC) data base. As a result, 80 cloud-free Landsat scenes (400 data products) were selected and ordered from EDC at a total cost of $967.

Until January 31, we examined facsimile NOAA images borrowed from the Fairbanks National Weather Service and, on this basis, ordered 18 partially cloud free images from the NOAA/NESS Satellite Data Acquisition Facility near Fairbanks, at a total cost of $81.00. After February 1, our request for a supplemental appropriation having been accepted by NOAA/OCSEAP, we placed a purchase order to the NOAA Satellite Data Acquisition Facility for 3 daily images in both the visible and infrared spectral bands until September 30, 1976. This order involved 1458 NOAA scenes for a total cost of $6561. In addition we made arrangements with the manager of the facility to save the digital tapes of some specially cloud free images, upon requests and for the cost of tape replacement. These tapes will be used to map sea-surface temperatures at times and locations of special interest to OCS investigators.

OCS investigators placed several orders totalling $514.00 for remote-sensing data and requested several computer searches of the EDC data bank.

2) Operation of data processing facilities

Most of the data processing equipment was kept operational during the reporting period and was utilized by several OCS investigators. The exception was the CDU-200 Digital Color Display System which continued to have problems in its disk memory and interface. We expect that the CDU-200 will be returned to operational status in April. Fortunately very few OCS investigators have utilized the CDU-200 so far and its unavailability has caused no problems for the OCS program.

Several months ago we ordered a digital image recorder from non-OCS funds. The manufacturer has advised us that this equipment will be shipped in early April, and the rest of the month will be needed to develop computer programs for it and to test its operation. This instrument was custom-built to our specifications and will have capabilities for producing black and white or color negative images from digital imagery data.

A Variscan 9½" film projector has been acquired from federal surplus property. After minor repairs, it will be used to project 9½" aerial photography in roll format at various scales on a tracing screen.

3) Development of data analysis and interpretation techniques.

No fundamentally new techniques were developed during the fourth quarter of the contract. However, existing techniques continue to be improved as time allows.

The return to operational status of the CDU-200 and the availability of the digital image recorder will call for the development of new data processing techniques during the next reporting period, particularly for the UofA - INSTAAR cooperative OCS investigation described in the third quarter report. We will also develop a computer program for extracting sea-surface temperature data from the NOAA satellite digital tapes.

4) Assistance to OCS investigators.

Twenty OCS investigators outside the Geophysical Institute and at least that many more affiliated with the Institute, requested our assistance in searching for or analysing remote-sensing data. In particular prints of all the SLAR data acquired by USGS/OCS aircraft were prepared and sent to Dr. Weeks and Dr. Campbell (RU #89), and selected prints of the USGS/OCS aerial photography were sent to Dr. Barnes (RU #204). Imperial Oil, Ltd. and Exxon Co. have also contacted us regarding these data. In addition several investigators requested prints of NOAA and Landsat imagery.

Jerry Galt (RU #140, 146, 149) and John Robinson (OCSEAP program) requested imagery of the Gulf of Alaska, west of Kayak Island, to provide experimental evidence for sea-surface circulation models in an area tentatively scheduled for leasing. We understand that a report of the results of this study was presented to BLM in March, and on this basis, it was decided to withdraw 16 tracts from the lease sale.

Although several OCS investigators expressed strong interest in it, the UofA - INSTAAR cooperative OCS investigation described in quarterly report No. 3, has not yet reached the implementation stage, primarily because of a lack of input from the principals involved. However, we have ordered the Landsat data to be used in this investigation and have prepared a detailed flow diagram of the analysis procedure.

We continued to work very closely with the Arctic Project Office in developing options for a remote-sensing data acquisition program to replace the now-terminated USGS/OCS program. Aerial photography will be obtained in April over the Beaufort and Chukchi Sea by NARL aircraft in conjunction with Dr. Week's laser profilometer measurements. Arrangements have been made with NASA/Ames Research Center for acquiring U-2 aerial photography of the entire Alaskan coastal zone in mid-June, 1976, weather permitting. We are also hopeful that negotiations with the U.S. Army will result in remote-sensing data acquisition over the Beaufort and Chukchi Sea during July 1976, using an aerial camera, a thermal infrared scanner and a side looking radar.

B. Problems Encountered/Recommended Changes

No significant problems were encountered and there are no recommended changes. However, we wish to point out the importance of field measurements of sea-ice conditions in the Beaufort and Chukchi Seas during June and July when concurrent aircraft and satellite imagery will be obtained. Concurrent ground-based measurements are also vitally needed, as part of the multistage sampling technique.

C. Estimate of Funds Expended

As of February 29, 1976 (the last available financial report), $62,723.66 remained available in the contract except for several outstanding obligations which were not yet entered in the books.

ENVIRONMENTAL ASSESSMENT OF RESOURCE DEVELOPMENT IN THE ALASKAN COASTAL ZONE BASED ON LANDSAT IMAGERY*

By A. E. Belon, J. M. Miller and W. J. Stringer, Geophysical Institute, University of Alaska, Fairbanks, Alaska

ABSTRACT

The United States' search for domestic sources of energy has focused much of its activities in Alaska where geological data suggest a strong potential for vast deposits of petroleum along most of the coastal zone, both onshore and offshore. The exploration and eventual development of these potential deposits presents major problems for industry, government and the inhabitants of the coastal zone. Owing to the very large areas involved, remotely-sensed data from satellites and aircraft, in conjunction with strategically located field activities, plays a major role to provide the necessary environmental information within the limited time available.

Three representative projects are presented to demonstrate the application of LANDSAT imagery to an environmental assessment of the Alaskan coastal zone. Density-slicing of LANDSAT images in photographic format, along with existing field data, is used to develop models of sea-surface circulation and sediment transport in Alaskan coastal waters. Visual photointerpretation of LANDSAT and aircraft images is used to study the morphology and dynamics of shore-fast ice along the Alaskan coast of the Beaufort Sea. An unsupervised classification technique applied to LANDSAT imagery in digital format has been used to map ecosystems along the Alaskan coastal zone and offers promise in the study of near-shore sea-ice conditions.

INTRODUCTION

The development of additional domestic sources of energy is a prime objective of the United States in the mid-1970's. At the present time the development of energy sources in Alaska means primarily petroleum exploration and production. The Cook Inlet field has been producing for a decade, and the major oil and gas field near Prudhoe Bay is being prepared for production in 1977. Geological data strongly suggest that other vast petroleum and gas potential exists offshore along the northern, western and southern coasts of Alaska. An assessment of these potential new reserves and the development of known deposits requires new knowledge of their environmental setting to serve the sometimes conflicting objectives of carefully exploiting resources while preserving most of the environmental values.

Remotely-sensed data play an important role in Alaskan efforts to ease the nation's energy shortage. Data from both aircraft and satellites are heavily used by organizations engaged in activities related to both resource development and environmental conservation; however, the vast expanses involved tend to emphasize the benefits of satellite data. The University of Alaska, in cooperation with state and federal agencies, has applied current remote-sensing techniques to many aspects of resource development in the State. Results of three representative projects are presented.

---

* Report presented at the NASA Earth Resources Symposium, Houston, Texas, June 1975.

SEA-SURFACE CIRCULATION AND SEDIMENT TRANSPORT IN ALASKAN COASTAL WATERS*

The Alaskan coastal environment provides a particularly feasible situation for the application of remote-sensing techniques to the study of sediment transport and deposition. The very large quantities of suspended sediment discharged into Alaskan coastal waters are clearly visible on LANDSAT images which facilitate tracing the sources and movement of the surface suspended sediments and assist studies of the dynamic relationship between sediment input, transport and deposition. Such studies are important not only in terms of the marine geology and physical oceanography of the region, but particularly so at this time because a knowledge of the transport path of surface suspended sediments is applicable to the prediction of the movement of oil spills in areas which are currently subject to intensive petroleum exploration and development.

Cook Inlet

Figure 1 is a mosaic of two LANDSAT images of Cook Inlet acquired on 24 September 1973. Even in the red spectral region (MSS band 6) the suspended sediment load ranging from 20 to 1000 milligrams per liter (mg/l) is clearly seen. The use of images acquired at shorter wavelengths (MSS bands 4 and 5) permits the suspended sediments to be visible at concentrations of one mg/l or even less when atmospheric haze is totally absent.

In order to quantify the relative variations in the suspended sediment load observed by LANDSAT, the gray shades present in LANDSAT negative transparencies were density-sliced and color-coded so that boundaries between ranges of gray shades (representing different ranges of suspended load concentration) can be positively differentiated. This was accomplished using an analog image analyzer consisting of a light table, vidicon camera, control equipment and a color television receiver. After placing a negative transparency of the LANDSAT image on the light table, the vidicon camera transmits the image to the control equipment where the image is density-sliced and color-coded into as many as 8 different colors. The color-coded image is then displayed on the color television screen.

The range of gray shades coded as any particular color and the total range of gray shades contained in the entire color spectrum of the display are all continuously variable such that the normally small range of gray shades found in coastal waters can be density-sliced into the full 8 colors, each color representing a different range of reflectance value or suspended load concentration. The color-coded image displayed on the television screen was photographed using the high speed 35 mm direct-positive color film (Figure 2). The 35 mm color slides thus obtained were then projected, using a photographic enlarger, onto base maps

*Much of this section has been summarized from the M.S. dissertation of David C. Burbank and the ERTS-1 final report of G. D. Sharma, F. F. Wright, J. J. Burns and D. C. Burbank, Institute of Marine Science, University of Alaska.

of the Alaskan coast. The projection of the color slide was aligned such that the color image and the base map coastlines conformed, and the color boundaries were traced onto the base map to produce the relative suspended load concentrations as shown in the black and white drafted map illustrated in Figure 3.

The analyzer control settings used in density-slicing the various images are, for the most part, arbitrary. The base level and the bandwidth of the total color-code spectrum were normally adjusted such that the entire range of gray shades contained in the coastal waters of the specific image being analyzed equaled the range of the color spectrum displayed by the analyzer. Individual color bandwidths were normally kept equal to each other (linear slicing), however, for some images the relative bandwidths were varied to bring out specific details, such as eddies. In one instance, an acetate transparency showing the suspended load distribution for a scene for which near-synchronous sea-truth data had been obtained was overlain on the analyzer TV screen. After enlarging and orienting the TV screen image to conform with the overlay, the image was density-sliced to conform with the suspended load contours of the sea-truth data. This procedure gives good results where at least a limited amount of sea-truth data is available.

A series of LANDSAT images acquired over Cook Inlet during 1972 and 1973 were density-sliced in the manner described above. The resulting maps of relative suspended sediment concentration on different dates were then used to develop the net sea-surface circulation model of Cook Inlet illustrated in Figure 4.

The major water movement in Cook Inlet is a to and fro pulsation in the lengthwise direction of the inlet caused by the flood and ebb of the tide. However, Coriolis force, basin morphology and probably winds modify the pulsations to produce a net circulation pattern within the inlet. The major sediment sources are the Susitna River and Knik Arm at the head of the inlet.

Tidal and Coriolis forces produce a net counterclockwise circulation in lower Cook Inlet such that clear seawater intrudes up the east side of the lower inlet, carried in by the westward flowing Alaska current, and turbid, relatively fresh water is carried out of the inlet along its western shore. Due to the configuration of the Forelands region, the intrusion of clear seawater is apparently deflected to the west side of the upper inlet to form a net clockwise gyre in the region bounded by the East, West and North Forelands. However, this deviation from the normally expected counterclockwise circulation may be a temporary result of the prevailing southerly summer winds (no winter LANDSAT images are available), in addition to possible variations in circulation due to the tidal amplitude (lunar cycle - coincidentally, most cloud-free LANDSAT images of Cook Inlet were obtained near flood tide at the mouth of the inlet). Available evidence indicates a highly complex and variable circulation system throughout the region north of Kalgin Island, with extreme mixing of outflowing turbid water and intruding clear seawater. Ship navigation in this area is notoriously difficult.

Tidal current velocities are sufficient to prevent deposition of muds in the central Cook Inlet basin. Substantial deposition of the fine sediments occurs in southwestern Kamishak Bay (south of Iliamna Bay); however, a considerable amount of the Cook Inlet suspended load is carried out of the inlet and into Shelikof Strait (left bottom corner of Figure 4).

The analysis of sea-surface circulation and sediment transport performed for Cook Inlet were repeated for most of the Alaskan coast from Yakutat in the southeast to Barrow at the northernmost point. No attempt was made to study southeast Alaska and too few cloud-free and ice-free LANDSAT images existed for the coast east of Barrow to allow a meaningful analysis of that region. The results of these analyses are summarized in Figure 5 which shows, in a highly simplified form, the major pathways of suspended sediment transport in the Alaskan coastal and shelf environment. This model, developed by Burbank (1974), is based on LANDSAT imagery, limited field data on sea temperature, salinity, suspended load and bottom sediment distributions and on various previous reports, particularly for the Bering and Chukchi seas. Detailed descriptions of the individual coastal areas are given in Burbank's dissertation and in Sharma et al. (1974).

Gulf of Alaska

Glacially derived sediments introduced into the coastal waters are transported predominantly westward in the Alaska Current. Part of the nearshore suspended load is typically deflected into the various embayments lining the coast. The amount of offshore transport is variable, but in some areas it reaches significant proportions.

In the northeastern Gulf of Alaska, between Kayak Island and Yakutat Bay, the major sources of suspended sediment are Dry Bay, Yakutat Bay, Malaspina Glacier, Icy Bay (Guyot Glacier) and the Bering Glacier. In the Dry Bay region, offshore shunting of the near-bottom suspended load by Alsek Canyon, coupled with a minimal sediment input from farther east, has left relict glacial sediments exposed on the shelf between Alsek Canyon and Yakutat Sea Valley. Yakutat Sea Valley also provides an effective offshore shunt for the near-bottom suspended load derived from Yakutat Bay and the coast immediately to the east, leaving some relict glacial sediments exposed on the shelf immediately west of Yakutat Sea Valley; however, the considerably increased suspended sediment input from the coastal glaciers west of Yakutat Bay produces a cumulative increase (in a westward direction) in total sediment transport and spreads a progressively wider (in a westward direction of transport) blanket of modern mud over the shelf.

Although some offshore transport of suspended sediments occurs along the entire coast, it is particularly significant where the westward moving suspended load encounters Kayak Island; the suspended load has been observed to be deflected offshore over 60 km (toward the southwest) in this region. This offshore deflection of fine sediments has greatly enhanced the deposition of mud on the outer shelf southwest of Kayak Island.

A large, apparently permanent clockwise gyre consistently encircles Kayak Island and sediments are transported north up the west side of Kayak Island to rejoin the nearshore suspended load transport system.

The Copper River discharge greatly increases the coastal suspended sediment load in the north-central Gulf of Alaska. The westward moving Copper River plume, upon confronting Hinchinbrook Island, splits into several components. A minor amount of the suspended load enters Prince William Sound through channels northeast of Hinchinbrook Island, while a major proportion of the suspended load enters Prince William Sound through Hinchinbrook Entrance, intruding north almost to the Columbia Glacier, and providing the major source for the fine sediments deposited within Prince William Sound.

The remainder of the Copper River plume is carried southwestward along the southeast coast of Montague Island, beyond which the sediments rapidly disperse and settle. As a result, there is an increasing frequency of exposure of relict and palimpsest glacial sediments westward and southwestward of Montague Island.

Aleutian Shelf

Cook Inlet suspended sediments enter Shelikof Strait as a well-defined nearshore plume flowing southwestward along the northern shore of the strait. With passage through the strait, the plume diffuses across the strait until, near the southwest entrance to the strait, the plume normally has diffused across the entire strait. Bulges in the plume are often observed along the southeastern boundary of the plume, apparently due to transient reversals of the net southwestward movement of the plume during flood tides. With farther southwestward movement, beyond the southwest entrance to the strait, the plume rapidly disperses and settles from surface suspension.

Bottom sediments within Shelikof Strait reflect the cumulative settling and deposition of the fine sediments as they pass through the strait. Beyond the southwest entrance to the strait, the near-bottom suspended sediments are shunted offshore by the sea valley extending from Shelikof Strait to the shelf edge.

The surface temperature and salinity distributions indicate Cook Inlet waters, and therefore probably some suspended sediments, are carried several hundred kilometers westward of Shelikof Strait along the Alaska Peninsula coast, however, there is no evidence of deposition of fine bottom sediments in this region. The shelf seaward of Kodiak Island likewise appears to have little or no input of suspended sediments; the shelf is covered predominantly by relict or palimpsest glacial sediments, with mud filling only the deeper depressions.

Bering Sea

Suspended sediment transport in the Bering Sea is in a general northward direction. In the Bristol Bay region, the Kvichak and Nushagak rivers supply most of the suspended load. Offshore transport is minimal

and, coupled with the high energy of the Bristol Bay environment, the bottom sediments within Bristol Bay have evolved into a well-graded (predominantly sand) shelf in near equilibrium with the energy of the environment.

Transport of the Bristol Bay suspended load is confined mostly to the nearshore zone until the Kuskokwim Bay region is reached. Some of the nearshore transport is deflected north up the eastern coast of Kuskokwim Bay, although entry is slight. The combined Bristol Bay-Kuskokwim Bay suspended loads are normally transported towards the northeast; however, during winter and early spring some Kuskokwim Bay suspended sediments are carried southwest into Bristol Bay. The northwestward moving suspended load, upon confronting Nunivak Island, bifurcates, part passing north through Etolin Strait to join the Yukon River plume, and part passing west of Nunivak Island to be dispersed offshore into the region south of St. Lawrence Island. Although some of the Kuskokwim suspended load is deposited south of St. Lawrence Island, a significant proportion is redirected to the northeast, producing relatively high subsurface suspended load concentrations in the region between St. Lawrence Island and the Yukon delta.

The Yukon River discharge, comprising 9/10 of the total (river) suspended sediment input to the eastern Bering Sea, is the predominant influence in the northeastern Bering Sea and Norton Sound. Most of the Yukon River suspended load is observed moving north and northwest towards the Bering Strait. However, a significant amount of the Yukon River suspended load has been observed moving over 100 km directly south in the nearshore zone, while experiencing considerable offshore dispersion towards St. Lawrence Island.

A second offshoot of the major northwestward moving plume moves into Norton Sound along its southern and southeastern shore, forming an incomplete counterclockwise gyre within Norton Sound. Most of these sediments are deposited in southern and southeastern Norton Sound; however, some of these sediments are transported out of Norton Sound in subsurface waters in central and northern Norton Sound. Most of the Yukon River suspended load is transported into the Chukchi Sea in near-bottom suspension near the eastern coasts of the northeastern Bering Sea and the Bering Strait.

The observed suspended load transport and the bottom sediment distribution correlate well in the northeastern Bering Sea. The major pathways of suspended load transport are generally underlain by relatively high concentrations of silt in the bottom sediments.

Chukchi Sea

The Yukon River provides the major input of suspended sediments to the Chukchi Sea. After passage north through the Bering Strait, the mainstream of Yukon River sediments is carried directly north into the northeastern Chukchi Sea, primarily as a near-bottom turbid layer. Some Yukon River sediments, however, move eastward into the southeastern Chukchi Sea; a minor amount of these sediments enters Kotzebue Sound

around Cape Espenberg, while some Noatak River sediments are discharged from Kotzebue Sound around Cape Krusenstern and join the general northward transport in the southeastern Chukchi Sea.

An additional small percentage of Yukon River sediments, after passing through the Bering Strait, are carried northwestward up the Chukotsk Peninsula coast. Upon confronting the southeastward moving coastal current, these suspended sediments are transported directly offshore in a (initially) northeastward direction and are reincorporated in the general northward transport of Yukon River sediments.

Coastal suspended sediments between Points Hope and Barrow are primarily locally derived from coastal runoff and erosion; however, the input of suspended sediments into this region appears relatively small. The generally northeastward flowing coastal current produces clockwise eddies within the coastal indentations. In the vicinity of Barrow, where the northwestward flowing Chukchi Sea coastal current meets the westward drift of the Arctic Ocean, considerable offshore transport of suspended sediments occurs.

Circulation within Kotzebue Sound is a general counterclockwise gyre. Most of the Noatak River suspended load is transported directly south into central Kotzebue Sound, whereas smaller amounts are carried east into Hotham Inlet and west into the southeastern Chukchi Sea. The bottom sediment distribution conforms well with the surface suspended load distribution within Kotzebue Sound, showing markedly greater concentrations of fine sediments underlying the higher surface suspended load concentrations. The counterclockwise gyre in southern Kotzebue Sound allows deposition of very fine suspended sediments. Most Kobuk River sediments are deposited within Hotham Inlet.

Conclusion

LANDSAT imagery has proven itself quite valuable for the study of sea-surface circulation and suspended sediment transport in Alaskan coastal waters. The synoptic overview of large areas provided by the LANDSAT satellite has added a new dimension to the study of dynamic processes and, although remote sensing cannot supplant the need for basic sea-truth data, the combination of limited sea-truth data and comprehensive remote sensing data can provide far more information than either method by itself.

LANDSAT imagery can be especially beneficial in the planning of oceanographic research and environmental surveys. Through the delineation of water mass boundaries and regions having particularly dynamic and variable circulation regimes, both of which are readily apparent in the LANDSAT imagery of most Alaskan coastal regions, it is possible to design sea-truth sampling grids which can obtain considerably more information for the available ship time and funding. Because of the generally close correlation between the surface suspended sediments and the bottom sediment distribution, LANDSAT imagery can also be beneficial in the advance planning of bottom sediment and benthos investigations.

The tentative circulation and sediment transport models described in this study will hopefully provide background information to better direct future research in the Alaskan coastal and shelf environment. Future work in remote sensing should be directed toward the acquisition of more comprehensive satellite and simultaneous sea-truth data for various tidal phases and seasons; and toward the development of more quantitative and standardized data analysis techniques. With these two major improvements over the current situation, the present investigation strongly suggests that the use of satellite imagery can contribute significantly to the cost-effective preparation of a comprehensive atlas of sea-surface circulation and sediment transport in the Alaskan coastal zone.

MORPHOLOGY OF SHORE-FAST ICE ALONG THE ALASKAN COAST OF THE BEAUFORT SEA

Geologic studies suggest a potential of very large petroleum deposits under an offshore area of arctic Alaska between Prudhoe Bay and the Colville River Delta. The State of Alaska is planning a lease sale of these near-shore submerged lands in the near future and the federal government will be preparing an impact assessment for the possibility of a similar lease sale farther offshore. The oil industry has expressed a great interest in bidding for leases of these offshore areas, but recognizes that the seasonal presence of sea-ice presents unusual problems for petroleum exploration and development. Certainly, in shallow areas it will be possible to build and maintain artificial islands in suitable locations on which structures and drilling rigs can be built. However, sooner or later the question will arise as to whether structures can be safely erected in the deeper waters within the zone of shore-fast ice. Furthermore, the existence of large masses of grounded ice along the borders of the shore-fast ice indicates that underwater cables, pipelines and other structures must be buried sufficiently deep in the ocean floor to avoid being disrupted by moving ice ridges or piles. The amount of bottom plowing caused by grounded ice is determined by the manner in which the grounded ice pile is created and there are indications that this effect is more pronounced in some places than others. It is clear that a detailed study of the morphology and dynamics of sea-ice must be made before governmental and industrial activities can proceed in this area. The study reported in this section is an initial step in this direction.

General Behavior of Shore-Fast Ice

During the arctic winter, a relatively stable sheet of ice develops along the northern Alaska coastline, extending distances ranging up to several kilometers seaward. The general characteristics of this shore-fast ice have been reported by Nelson (1969), Reimnitz and Barnes (1973), and Zubov (1943) as follows:

(1) Sometime around midwinter, the ice along the shoreline is no longer subject to breaking free and leaving open water except under the most unusual circumstances.

(2) This shorefast ice sheet may contain many pressure ridges. Its seaward edge is defined by the most seaward grounded pressure ridge.

(3) Bottom sediments appearing in the piled ice are generally taken to be evidence that a pressure ridge is grounded.

(4) The most seaward grounded pressure ridge is characteristically near the 18 meter depth contour.

(5) From time to time, a floating sheet of ice can be attached to the shorefast sheet and extend many kilometers farther seaward.

(6) The grounded pressure ridge system endures into summer, sometimes as late as mid-July.

Ultimately, offshore engineering in northern Alaska will have to consider the behavioral characteristics and physical properties of this yearly recurring ice sheet. The recent acquisition of LANDSAT imagery is making possible surveillance of shorefast ice leading to a descriptive morphology.

Reimnitz and Barnes (1973) generalized that the seaward edge of shorefast ice along the north Alaskan coastline follows the 18 m contour. While the results of this study largely confirm this, pronounced deviations of the boundary of shorefast ice from the 18 m contour are also apparent. At one location, shorefast ice appears to extend beyond the 18 m contour, and at another its boundary may be well inside the 18 m contour. The overall sea bottom configuration is similar in both cases.

Interpretation of Spring 1973 LANDSAT Data

The relationship between the orbital frequency of LANDSAT and the areal extent of the acquired images is such that because of the convergence of meridians at the earth's poles, given points in the Beaufort Sea region are imaged up to 4 days in succession. This overlapping of images, coupled with the fortuitous occurrence of much clear weather in the spring of 1973, made data from that period extremely valuable.

Figures 6 and 7 were prepared by visual photointerpretation of data collected from many successive LANDSAT images of the Harrison Bay region between early March and July 1973. In order to illustrate adequately the major sequential ice features during this period and their relationship to one another, the information has been drawn on two separate maps of the same area.

Figure 6 shows the most prominent newly formed leads imaged during a series of LANDSAT passes in early March. This figure also shows a rather pronounced unfrozen shear line imaged at that time and, near the shore, the location of the 18 m contour and the seaward limits of extensive hummock fields. Figure 7 shows the features in Figure 6 and also successive locations of shear lines during April through July, as well as the locations of systems of cracks which developed during this time. The interpreted limit of grounded shorefast ice is shown as a series of dots wherever it is different from the shear line of July 2. The 18 m depth contour is indicated for comparison with the boundary of shore fast ice.

In early March 1973, when the earliest 1973 data were acquired, there was an extensive shelf of ice attached to the seaward side of the shorefast ice off Harrison Bay. At that time, part of the large fissure at the right of center in Figure 6 was new, while another part of it and the north-south cracks in the center of this figure were somewhat older. Based on Barter Island wind data, we place the date of the new part of this crack at March 7 when 3-hour average winds of 12.1 m per second from 280° were measured. The older cracks probably date to February 10 or earlier (February 10 was the last date on which winds on the order of 11 m per second were recorded at Barter Island).

LANDSAT images of March 19 and 20 illustrate the growth of the lead system shown on the left-hand side of Figure 6. On March 21, the ice fractured along a path which followed the refrozen shear line running across the map to a point north of the western side of Harrison Bay and then turned seaward roughly along a line parallel to the lead shown for March 19.. Even after this event, a considerable expanse of attached ice remained off Harrison Bay.

Early April data show the extent of the attached ice shelf even further reduced, with the shear line running parallel to the older refrozen shear line mentioned earlier.

Late May data show shearing motions with average velocities of 0.5 km per hour along a line parallel to the coast and tangent to what was later identified as a seaward bulge in the boundary of shorefast ice off Harrison Bay. The series of small cracks shown along the 18 m contour to the east of Harrison Bay and just west of Cross Island were new at this time. They are related to stress within the area defined by this shear zone, indicating some structural failure before shearing took place at a more seaward location. Note that a refrozen lead was identified in this area on the mid-March data. These failures were probably located seaward of well-grounded ice.

Later, data for early July show an even more diminished zone of stationary ice, including little attached ice. Note that there is a portion of the stationary ice at this date seaward of the May 27 shear line. The reason for this appears to be a large block of ice grounded in 31 meters deep water at the tip of the extension of stationary ice. An examination of the June 14 LANDSAT image shows no sign of this feature. At that time shearing was taking place along the probable boundary of shorefast ice (the dotted line).

The boundary of shorefast ice shown here extends seaward in a bulge off Harrison Bay. Burns and Harbo (1972) indicate a similar bulge based on mid-June data. At the vicinity of this bulge the 18 m contour indents toward shore. The depths along the western part of the bulge are very close to 18 m, while those along the eastern edge are up to 27 m.

These departures of the boundary of grounded sea-ice from the 18 m depth contour could possibly result from a coastline-averaging process; however, just to the east near Cross Island the boundary of shore fast ice appears to follow the 18 m contour much more closely.

Figure 8, an enlarged portion of LANDSAT image 1345-21342, shows the central portion of the shorefast bulge in outer Harrison Bay. Although somewhat broken up by this date, July 3, a substantial portion of the ring of grounded ice remains. At the top of the figure the ring consists largely of a slender curved band of ice. This feature has been observed by aircraft during spring 1973 and 1974 and appears to consist of hummocked ice. The relative stability of the ring of shorefast ice has posed a problem for some time. It is generally presumed that the boundary of shorefast ice is formed mainly by grounded shear and pressure ridges. This ring of ice appears to be quite stable -- demanding some explanation beyond ordinary grounded pressure ridges. The large expanse of hummocked ice may be the explanation.

Although the morphology and dynamics of shorefast ice is complex and dependent on sporadic meteorological and oceanic conditions, the results of this remote-sensing analysis reveals that the major morphological features are consistent from one year to the next and with previous reports. This recurrent tendency of sea-ice morphology should help in the planning of petroleum activities and structures in an area of Alaska which presents unusual problems for the oil industry.

Floeberg in the Arctic Ocean

Another related area of sea-ice study where satellite remote-sensing has proved beneficial is the location of observation platforms in the Arctic Ocean. Some of these are the relatively rare ice islands (massive tabular icebergs) and ice floes (multi-year ice), but they slowly move carried by the Arctic Ocean circulation. For some applications, stable fixed platforms are preferred. For the past two years, LANDSAT images have revealed what appears to be a grounded floeberg located at N72°, W162° (a strategic location approximately 160 km northwest of Barrow, Alaska). A floeberg is a large piece of multi-year ice --- usually consisting of old pressure ridges. This feature is grounded on a seamount in water approximately 30 meters deep. Figure 9 shows a portion of LANDSAT image 1282-22261 obtained May 1, 1973. In this image, the feature has dimensions approximately 5 by 16 km and appears to be in the process of acquiring new ice as the arctic ice pack is driven around it. Figure 10 (LANDSAT image 1606-22203) shows the same feature nearly a year later, March 21, 1974. Here the floeberg is nearly as wide as the previous year but only about half as long. These data would seem to indicate that the floeberg is relatively stable. We recently acquired LANDSAT image 1406-22131 obtained September 2, 1973 containing the coordinates of the floeberg. At first we thought that some mistake had been made because the usually obvious feature did not appear to be within the scene. Finally, using the coordinates on the image, the floeberg was located. At that time, its size was approximately 1 km by 2 km.

The September 1973 LANDSAT image has greatly changed our perspective of that feature. Apparently, very little, if any, of the feature is a true floeberg --- most of it is a recurring hummock field perhaps initiated by a grounded ice feature but reduced in size by disintegration

during summer. Nevertheless, there are many interesting aspects of this ice feature. One of these relates to shorefast ice discussed earlier. How similar is this feature to the fields of hummocked ice comprising the ring of shorefast ice in Harrison Bay? Perhaps this type of structure is more stable than grounded pressure ridges.

The feature at 72°N, 162°W offers an opportunity to study many aspects of ice dynamics and is, at this time, the object of possibly two surface expeditions next year --- if it is still there.

MAPPING OF ECOSYSTEMS ALONG THE ALASKAN COASTAL ZONE

Petroleum exploration and development offshore and onshore has a profound effect upon the adjacent land and its people. This is currently exemplified in Alaska by the sometimes conflicting activities of extractive industries and the small socio-economic structure of native villages in the sparsely inhabited areas faced with imminent development of massive scale. The challenge of these fast-paced events for governing bodies is to become capable of managing and controlling the development in a constructive and timely manner, so that divergent interests can accommodate reasonably well those values which best serve the indigenous people, the state, the nation, the land and sea environment, and the total resources of the region impacted by the development.

One method which is actively considered to meet this challenge is to establish a system of land classification in the coastal regions based upon the natural ecosystems which dominate an area. Specific species of vegetation or types of wildlife habitat which seem to prevail in a given area need not necessarily receive priority in planning; however, at the minimum there is a basic need to have detailed knowledge of what is present before one can sort through priorities and determine what should be permitted to alter or replace the naturally occurring ecosystems. On a region-wide basis there are sites which are more suited to development than others. These need to be identified and agreed upon in any land-use regulating system. There are other areas which are particularly deserving of protection under current and anticipated values, and these critical areas should be recognized and receive the appropriate regulation.

With half of Alaska's coastline potentially or actually impacted by petroleum exploration and development, the regulation of coastal zone activities is an enormous endeavor, especially when one contemplates that Alaska has more than half of the total United States coastline. A systematic survey on this scale would stretch over several years and with conventional techniques alone would be incapable of addressing the urgent need of the present era.

General Approach

The University of Alaska, with support from NASA and the Alaska Department of Environmental Conservation, is analyzing LANDSAT data by computer-aided techniques to map ecosystem units and coastal processes in four representative regions of the Alaskan coastal zone. Included

are Prudhoe Bay and Beechey Point on the Arctic Coast which consist chiefly of arctic tundra, thaw lakes and coastal wetlands; the Seward Peninsula, which has a mix of upland and lowland tundra, barrier islands, and some mountain terrain; Kotzebue Sound which contains uplands, a major river delta, and lowland tundra; and a portion of the eastern shore of Cook Inlet which is dominated by wetlands, forests, and glacier-fed rivers. The latter region has already been impacted by oil and gas development for the past decade.

These four regions were selected to refine the techniques which can prove most useful in land-use planning of the coastal zones. Computer-aided analysis was chosen to minimize the time necessary to extend the ecosystem mapping efforts to the entire coastal area of the mainland of Alaska. In view of the lack of ground-truth information and the random-mosaic patterns in wildland areas, we decided not to use the supervised approach which depends heavily upon the quantity of identified training-sites and the uniformity of the information which can describe them.

The unsupervised classification method of computer processing lends itself well to mapping the multitude of units of ground cover that occur naturally in wildlands, provided that the many spectral differences which are inherent in the data can be found to have informational value to resource managers. Care must be exercised to maintain control of the automatic classification algorithms so that meaningful outputs are obtained that can be related reliably to the real world. Indeed, multi-spectral systems tend to reveal more feature classes than we at present know how to use profitably, although this by no means need be a disadvantage. The key is to be able to economically select those features which have informational value, and to (temporarily) discard or merge those which appear to have unknown or superfluous meaning.

The Unsupervised Classification Technique

The classification technique used to generate Alaskan ecosystem maps is illustrated by the flow diagram of Figure 11. The method first defines a number of spectrally distinct categories from the iterative cluster analysis of small samples from the area to be mapped. This is followed by the classification of the entire area by a maximum likelihood program into the number of classes previously defined by the cluster analysis. Geometrically corrected output formats can be made at any scale and include both line printer maps, color-coded classification maps, or a series of colored thematic maps.

While the classification is basically unsupervised, there is adequate provision to ensure that the computer is producing useful results before the output products are generated. A review of the number of classes and their spectral characteristics and statistics can determine whether or not problems are inherent in the definition of the categories during the cluster analysis step. The number of discrete categories, which are generated from varying types of terrain in the area to be mapped, can be regulated by manipulation of the sample selection and limit definition criteria. Once well-behaved statistics have been

produced by the cluster analysis on the representative sample of the raw data, the entire data set is economically classified by a maximum likelihood program or other appropriate classification scheme.

The output of the classification program is in digital tape form which can drive a color image recorder after specific colors have been assigned to each class. Typically, there are more discrete categories identified than are desired or useful for a given application; it is necessary to tentatively identify each class as to landform or type of vegetation by correlation with ground truth and the study of the spectral signature of each class. This can be relatively straightforward or quite an extensive effort, depending upon the orderliness of the original data and the amount and type of ground truth available.

In one important operating mode, the unsupervised classification technique can be used as a tool whose chief purpose is to identify those areas in the region to be mapped for which detailed ground truth need be acquired. It is not at all necessary to acquire ground truth prior to performing the classification, and in fact, one usually obtains the right kinds of ground truth data of better quality at lower cost once the automatic classification processing has indicated where it is and is not needed.

Once appropriate colors are assigned to each class, the output products are generated in the form of color coded classification maps or a series of colored thematic maps for those classes of interest. Any or all of the recognizable classes can be used in the final color product, which can be generated at any desired scale. The classified digital tape forms a permanent data record from which different themes and color products may be produced in the future for application to other disciplines.

Results

The unsupervised classification technique has been applied successfully to several areas of Alaska in the coastal zone as well as in the interior. As an example for the coastal zone, it was applied to the Prudhoe Bay and Beechey Point areas on Alaska's North Slope which are both contained in LANDSAT scene 1344-21833 acquired on July 2, 1973 (Figure 12). For the 5000 km^2 region mapped near Prudhoe Bay, the unsupervised classification of the land area resulted in 15 ecosystem categories, excluding snow and ice. These categories were identified by correlation with independently available ground-truth and are listed in Table 1. Six of these categories represent various types of tundra vegetation, four represent bare ground and five represent water with varying degrees of siltation or depth. In addition to the fifteen land categories, the computer analysis recognized 35 spectrally different categories of snow and ice. Six of those represent snow and ice found on some of the lakes in the area, with one apparently associated with anchor ice which forms on the bottom of shallow lakes, remains submerged during spring and melts more slowly than surface ice. The other snow and ice categories occur offshore and are believed to be relatable to sea-ice morphology and conditions, based on the spatial pattern of their

distribution and their spectral signatures which suggest varying degrees of wetness. Unfortunately, the purpose of this project being the mapping of land ecosystems, the ground-truth data on sea-ice and lake ice conditions during early July 1973 are not available for detailed identification and verification of the snow and ice categories. Nevertheless, the ability of the unsupervised classification technique to differentiate between various types of snow and ice, as well as between varying degrees of water siltation, is promising and of considerable interest to scientists and engineers studying the near-shore and outer continental shelf in preparation for petroleum leasing.

Color-coded classification maps resulting from this analysis are illustrated in Figure 13 for the Prudhoe Bay area and Figure 14 for the Beechey Point area. The color code for these maps is listed in Table I. In these examples we selected colors to provide good contrast between classes within the main categories of water, barren, and vegetated cover. The colors in the blue and violet end of the spectrum are assigned to water classes, and the remaining colors are assigned to the non-water classes in a manner which emphasizes contrasts between the tundra types. The snow and ice categories, while not of primary interest in this study, have been assigned the pastel shades, with white and tan representing the dry pressure ridges and the green and reddish-brown tones represent wet or slushy ice. The aqua and magenta colors represent intermediate states of "wetness" of the ice. Much of the green, aqua and magenta colors on some inland lakes are thought to be bottom-fast ice with water up to 3 feet deep standing on top of the ice.

For the coastal zone management application, the first question to be addressed is to define the boundary of the coastal zone. It may extend from one to hundreds of kilometers inland. This first order application of the computer-processed LANDSAT data is at a scale of 1:250,000 which is usually adequate for the appraisal of the extent of the coastal zone, based on ecosystem indicators of areas dominated by the influence of the sea, sea-storms for example. For this application, the preliminary conclusion reached from an examination of Figures 13 and 14 is that, for the most part, the analysis of the LANDSAT scenes was not carried far enough inland to define the coastal zone boundary. It only appears distinctly at the bottom of Figure 14 for the Beechey Point area where the coastal tundra starts to break into well-drained tundra with vigorous shrubs, forbs and grasses.

This vegetation-cover analysis also reveals another anomalous area which may be impacted by prevailing storm patterns. The northwest-southeast trending aligned lake patterns which are a general characteristic of North Slope geomorphology are caused by prevailing northeasterly winds. Southwest from Prudhoe Bay (the central feature in Figure 13) the vegetation has a more marked tendency toward the wet tundra (characterized by the brighter orange tones) than the regions to the east or west. This region of more prominent orange tones lies roughly between the Kuparuk and Putuligayuk rivers and happens also to be directly downwind from the prevailing winds coming off Prudhoe Bay.

Management decisions, of course, must be made upon more detailed knowledge of landforms and ecosystems than the definition of coastal zone boundaries. The same computer outputs as those listed in Table I and illustrated in Figures 13 and 14, when they are reproduced at larger scales such as 1:63,360 or 1:24,000, can also be used during the second order application of processed satellite data. At these scales the extent and variety of surface features and ecosystems classes are accurately mapped in the detail needed for the decision-making process of land use management.

CONCLUSION

The demonstration projects described in this paper are expected to contribute significantly to two programs related to the nation's search for additional energy sources in Alaska: the environmental assessment of the Alaskan outer continental shelf undertaken by NOAA and BLM in preparation for the leasing of offshore tracts with petroleum potential and the formulation of a coastal zone management plan by the State of Alaska. In particular, the demonstration projects have shown that LANDSAT data can be used effectively for developing models of suspended sediment transport and therefore for preparing contingency plans based on the movement of oil spills in Alaskan coastal waters, for planning navigation routes and offshore drilling structures in coastal areas where sea-ice is prevalent, and for assessing the potential physical and biological impact of developmental activities on the coastal zone.

ACKNOWLEDGMENTS

The investigations described in this report were supported by grant NGL-02-001-092 from the NASA Office of University Affairs, by contracts NAS5-21833 and NAS5-20959 from the NASA Goddard Space Flight Center and by the Alaska Department of Environmental Conservation, and by contract 03-5-022-55, Task 10, by the NOAA OCSEAP Program.

REFERENCES

Burbank, D. C., Suspended sediment transport and deposition in Alaskan coastal waters with special emphasis on remote-sensing by the ERTS-1 satellite, M.D. Dissertation, Institute of Marine Science, University of Alaska, December 1974.

Burns, J. J. and S. J. Harbo Jr., An aerial census of ringed seals, northern coast of Alaska, Arctic, 25, 279-290, 1972.

Nelson, R. K., Hunters of the northern ice, University of Chicago Press, 1969.

Reimnitz, E. and P. W. Barnes, Studies of the inner shelf and coastal sedimentation environment of the Beaufort Sea from ERTS-1, NASA Report No. NASA-CR-132240, p. 3, 1973.

Sharma, G. D., F. F. Wright, J. J. Burns and D. C. Burbank, Sea-surface circulation, sediment transport, and marine mammals distribution, Alaska continental shelf, NASA Report No. NASA-CR-139544, 1974.

Zubov, N. N., Arctic ice, U. S. Navy Oceanographic Office, translation from Russian, 112-115, 1943.

TABLE I. - LAND ECOSYSTEM CLASSES FOR TWO AREAS OF ALASKA'S ARCTIC COAST NEAR PRUDHOE BAY AND BEECHEY POINT

Color Code (Fig. 13 and 14)	Feature
Water Categories (5)	
Dark Blue-Gray	Clear, deep water
Gray	Clear, moderately shallow water
Blue	Shallow or slightly turbid water
Cyan	Very shallow or turbid water
Violet	Silty water
Barren Ground Categories (5)	
Dark Green	Wet sand or mud
Olive	Wet outwash sand and gravel
Light Green	Dry outwash sand and gravel
Light Olive	Gravel pads, camps and runways
Light Brown	Mineral soil with very sparse or stressed vegetation such as forbs, grass, and dwarf shrubs
Vegetation Categories (6)	
Brown	Wetland bog
Medium Green	Wet tundra with good cover of sedges, aquatic grasses and mosses
Orange	Wet tundra, with moderate cover of cotton grass sedges, and aquatic moss (frequently drained lake bottoms)
Green	Poorly drained tundra marsh, frequently low-centered polygons with sedges and dwarf shrubs
Light Orange	Moderately drained coastal tundra, frequently high-centered polygons with willows, dwarf shrubs and lichens
Yellow	Well-drained upland tundra with vigorous shrubs, forbs and grasses

FIGURE CAPTIONS

FIGURE 1. Mosaic of two LANDSAT images of Cook Inlet, Alaska, acquired on 24 September 1973. Note that the pattern of suspended sediments in the inlet is clearly visible even in this MSS band 6 image.

FIGURE 2. Color-coded, density-sliced image of the Cook Inlet sedimentation pattern illustrated in Figure 1. The color bar at the left shows the color code, blue to brown, for increasing concentration of suspended sediments.

FIGURE 3. Schematic diagram of relative suspended sediment concentration in Cook Inlet, drawn from the density-sliced image illustrated in Figure 2.

FIGURE 4. Surface water circulation in Cook Inlet when the tidal stage is near low at Anchorage and high at Seldovia. This model is based on interpretation of sedimentation patterns observed on several LANDSAT images such as those illustrated on Figures 1, 2 and 3.

FIGURE 5. Major pathways of suspended sediment transport in Alaskan coastal waters as interpreted from LANDSAT imagery, field data on suspended load, temperature, salinity and bottom sediment distribution, as well as published reports.

FIGURE 6. Sea-ice conditions near Harrison Bay, Alaska, observed on March 1973 LANDSAT images.

FIGURE 7. Development of sea-ice conditions near Harrison Bay, Alaska, during spring 1973 as interpreted from sequential LANDSAT images acquired from March to July 1973.

FIGURE 8. Enlarged portion of LANDSAT image 1345-21342 showing the central part of the shore-fast ice bulge in Harrison Bay on July 3, 1973.

FIGURE 9. A floeberg (grounded multi-year ice) located approximately 160 km northwest of Barrow and first noticed on LANDSAT image 1282-22261 acquired on May 1, 1973. The floeberg is located at the right-center of the illustration and has dimensions of 5 x 16 km.

FIGURE 10. The same floeberg as in Figure 9, observed almost a year later on March 21, 1974, has dimensions of 6 x 8 km.

FIGURE 11. Flow chart of the unsupervised classification algorithms used for generating ecosystem maps of the Alaskan coastal zone from LANDSAT digital imagery.

FIGURE 12. LANDSAT image 1344-21283 acquired on July 2, 1973 over Prudhoe Bay (right center) and Beechey Point (left center), Alaska.

FIGURE 13. Color-coded ecosystem map of a 5000 km^2 area about Prudhoe Bay, Alaska, based on an unsupervised classification of the LANDSAT image illustrated in Figure 12. The color code for the land ecosystem classes is provided in Table I.

FIGURE 14. Color-coded ecosystem map of the Beechey Point, Alaska, area, based on an unsupervised classification of the LANDSAT image illustrated in Figure 12. The color-code for the land ecosystem classes is provided in Table I. Note, by comparison with Figure 12, that the classification has enhanced the barrier island chain, and has separated the sea-ice types in an apparently meaningful way.

FIGURE 1. Mosaic of two LANDSAT images of Cook Inlet, Alaska, acquired on 24 September 1973. Note that the pattern of suspended sediments in the inlet is clearly visible even in this MSS band 6 image.

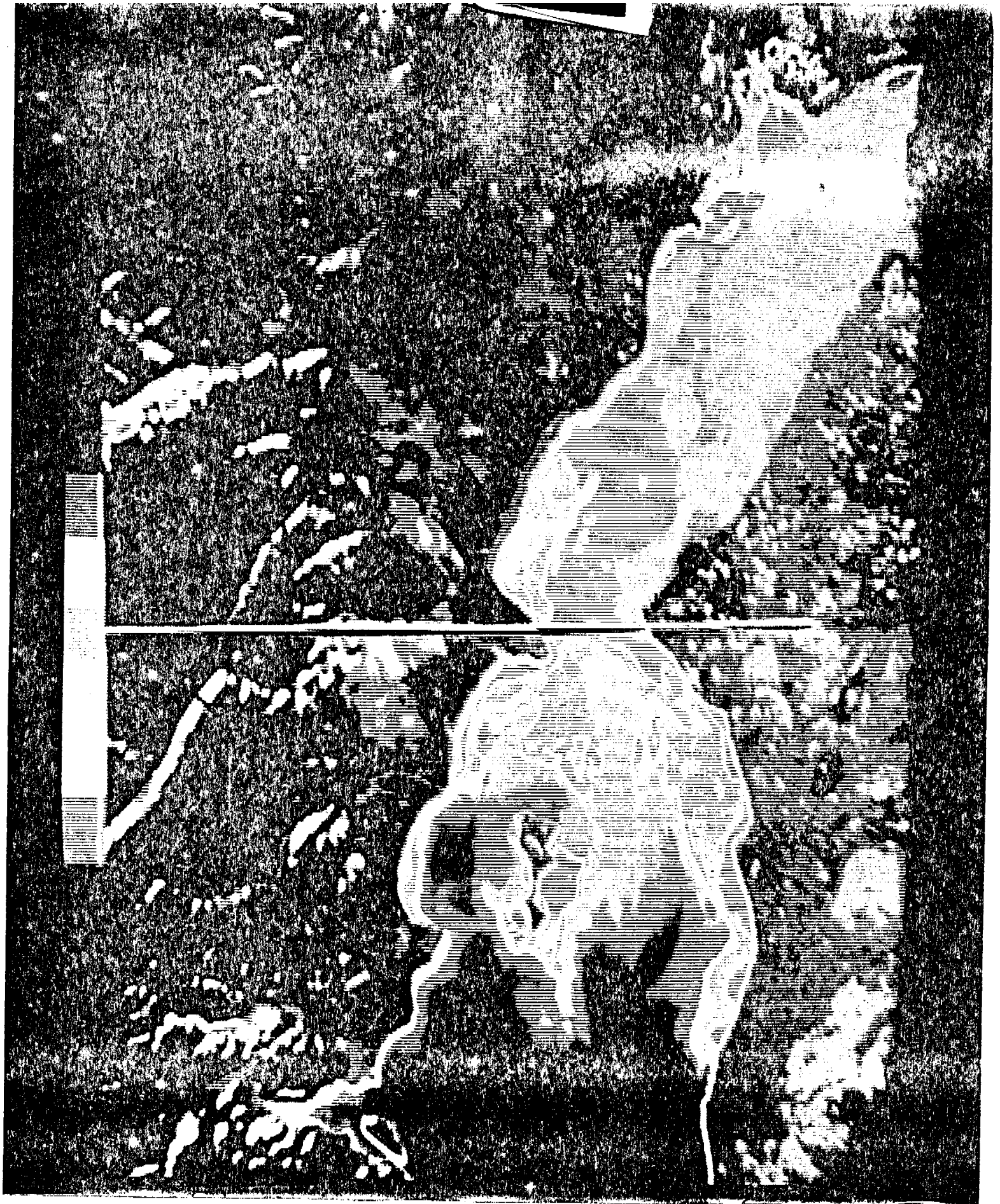

FIGURE 2. Color-coded, density-sliced image of the Cook Inlet sedimentation pattern illustrated in Figure 1. The color bar at the left shows the color code, blue to brown, for increasing concentration of suspended sediments.

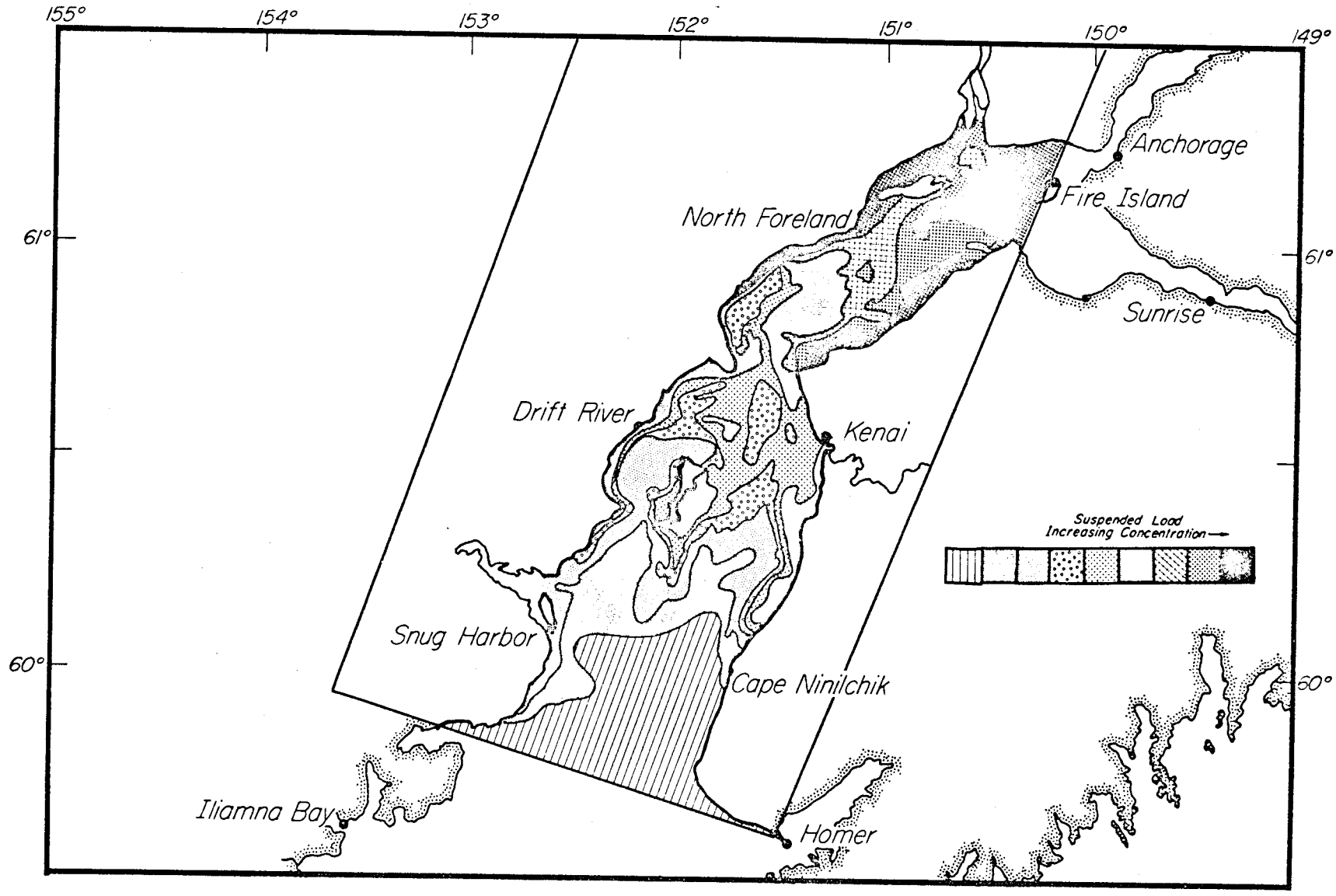

FIGURE 3. Schematic diagram of relative suspended sediment concentration in Cook Inlet, drawn from the density-sliced image illustrated in Figure 2.

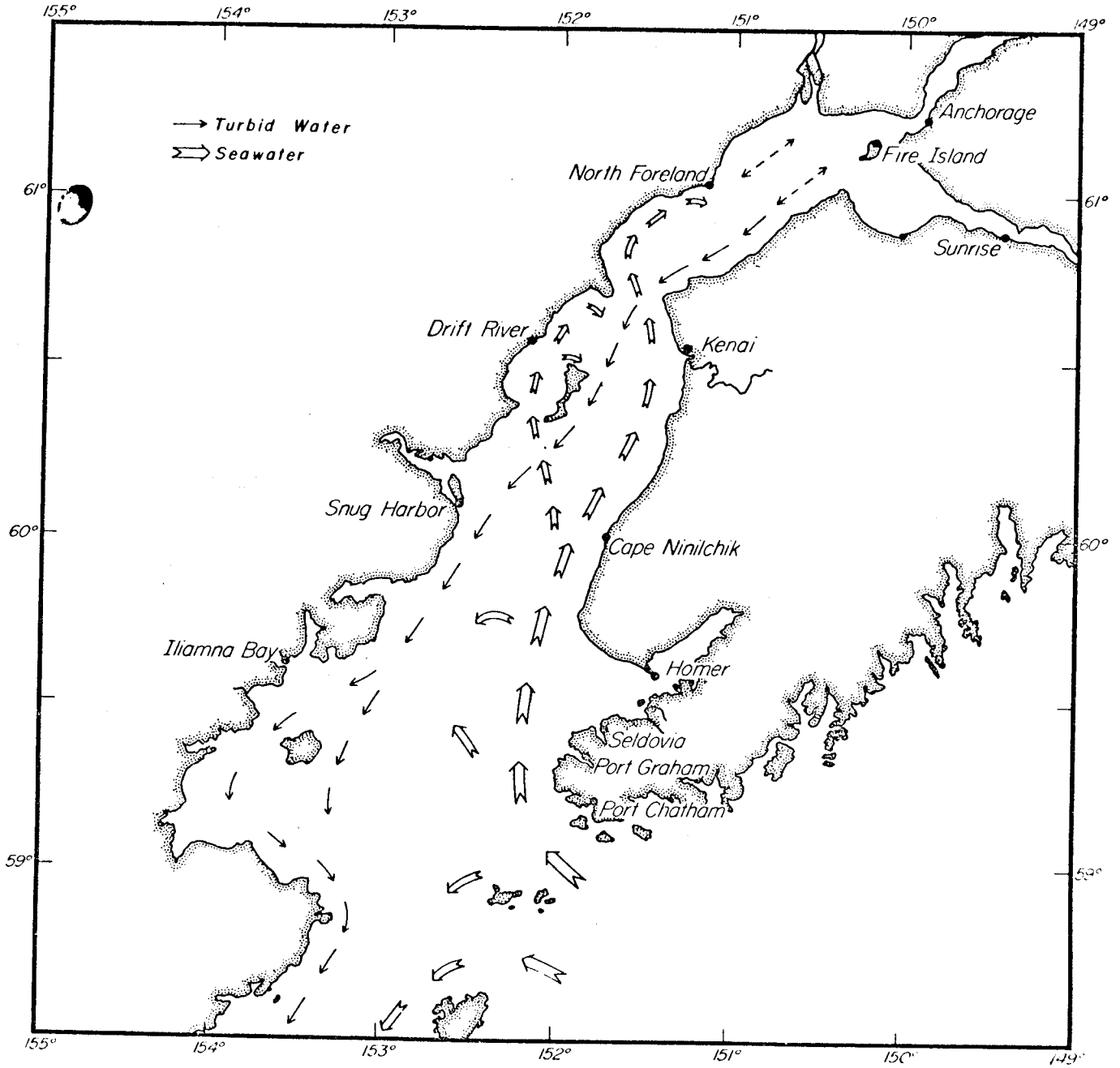

FIGURE 4. Surface water circulation in Cook Inlet when the tidal stage is near low at Anchorage and high at Seldovia. This model is based on interpretation of sedimentation patterns observed on several LANDSAT images such as those illustrated on Figures 1, 2 and 3.

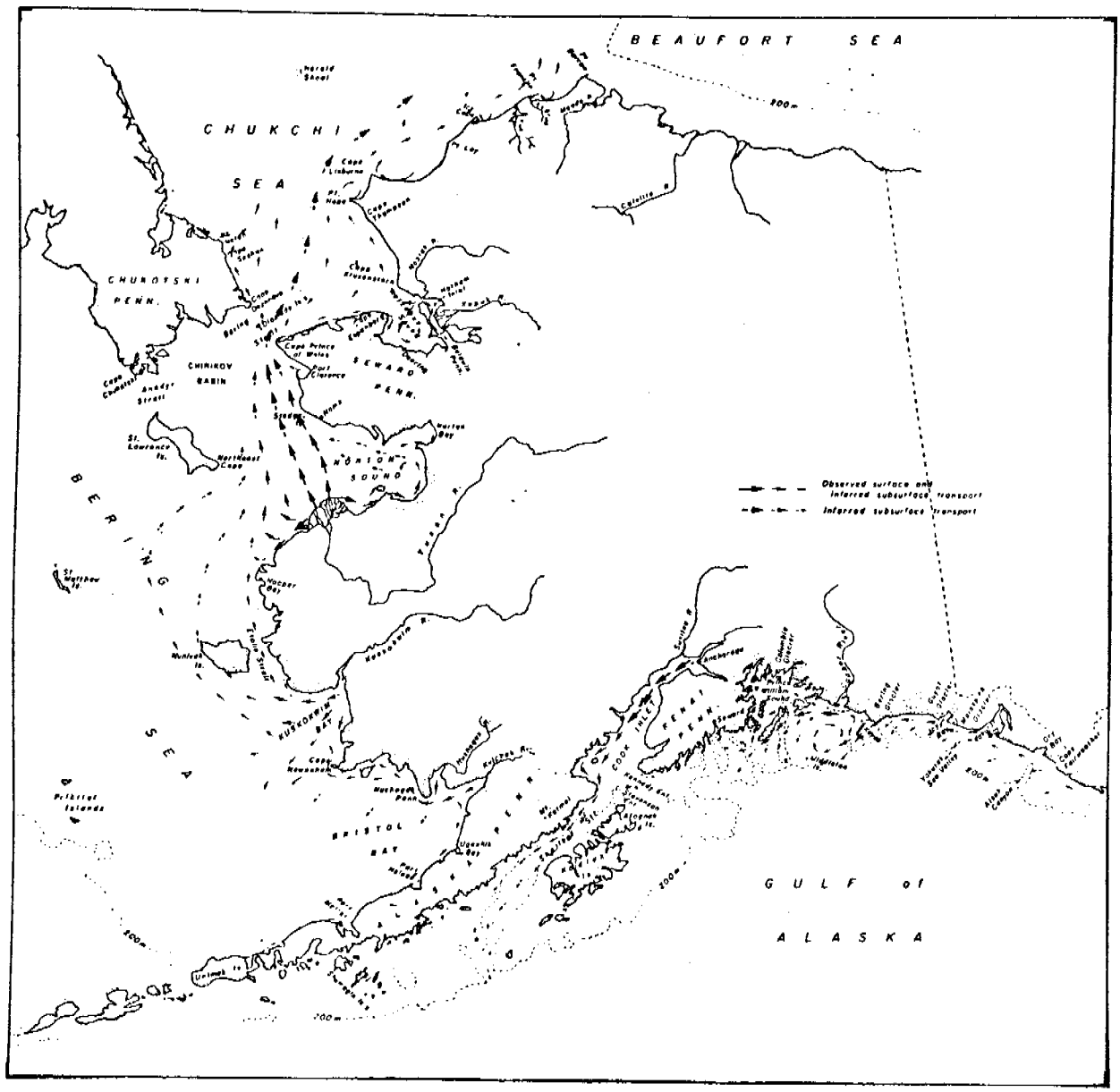

FIGURE 5. Major pathways of suspended sediment transport in Alaskan coastal waters as interpreted from LANDSAT imagery, field data on suspended load, temperature, salinity and bottom sediment distribution, as well as published reports.

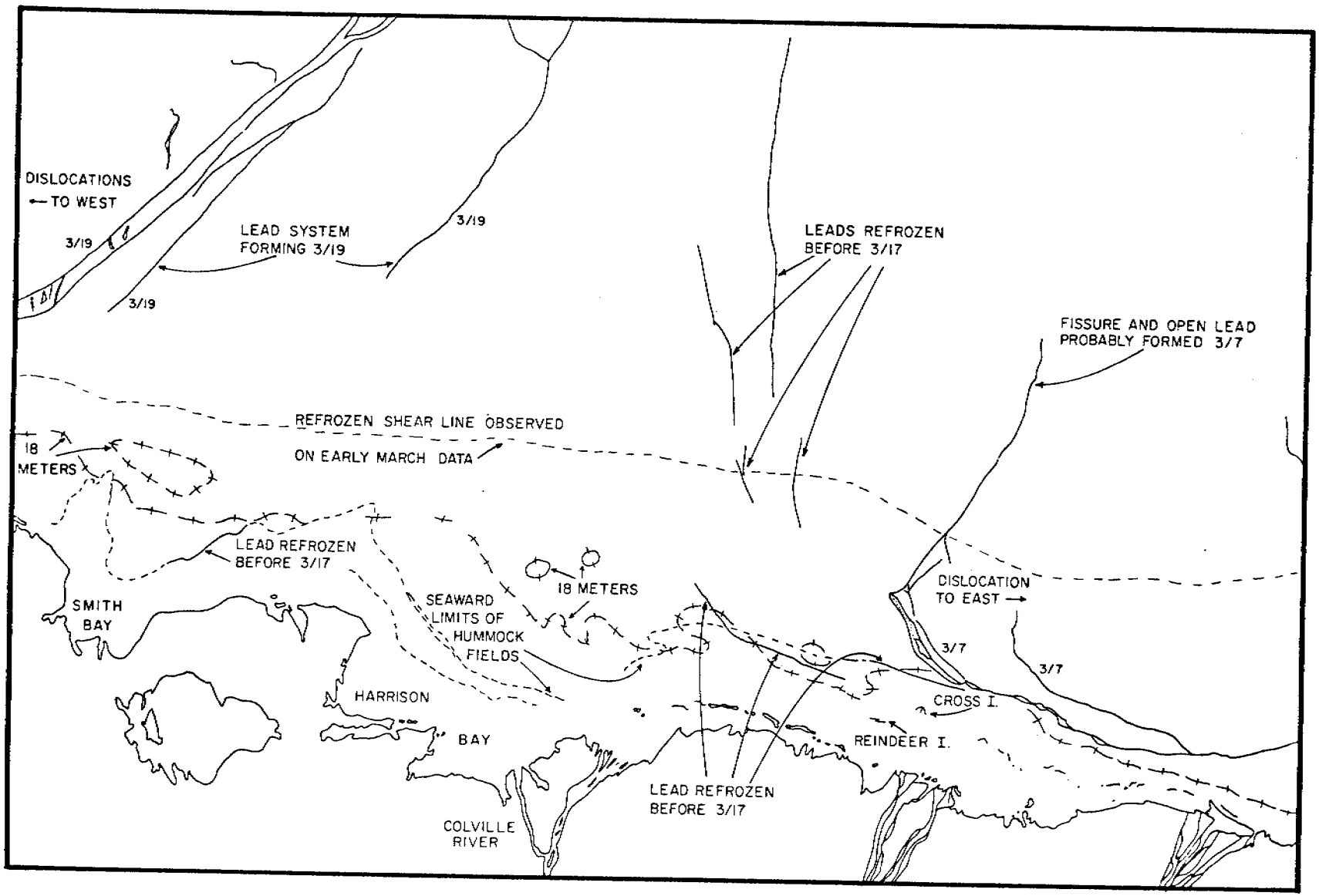

FIGURE 6. Sea-ice conditions near Harrison Bay, Alaska, observed on March 1973 LANDSAT images.

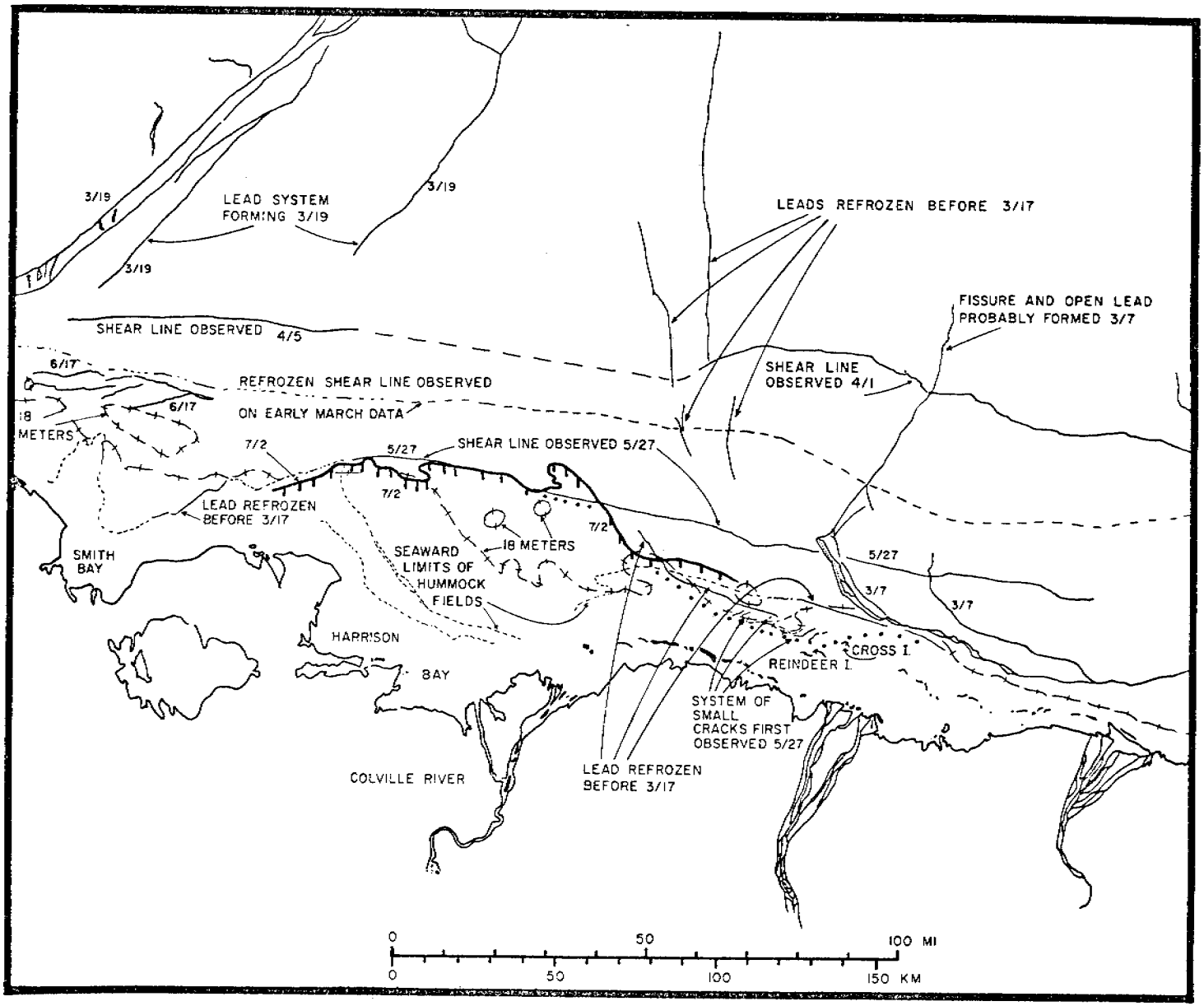

FIGURE 7. Development of sea-ice conditions near Harrison Bay, Alaska, during spring 1973 as interpreted from sequential LANDSAT images acquired from March to July 1973.

FIGURE 8. ENLARGED PORTION OF LANDSAT IMAGE 1345-21342 SHOWING THE CENTRAL PART OF THE SHOREFAST ICE BULGE IN HARRISON BAY ON JULY 3, 1973.

FIGURE 9. A FLOEBERG (GROUNDED MULTI-YEAR ICE) LOCATED APPROXIMATELY 160 KM NORTHWEST OF BARROW AND FIRST NOTICED ON LANDSAT IMAGE 1282-22261 ACQUIRED ON MAY 1, 1973. THE FLOEBERG IS LOCATED AT THE RIGHT-CENTER OF THE ILLUSTRATION AND HAS DIMENSIONS OF 5 X 16 KM.

FIGURE 10. THE SAME FLOEBERG AS IN FIGURE 9, OBSERVED ALMOST A YEAR LATER ON MARCH 21, 1974, HAS DIMENSIONS OF 6 X 8 KM.

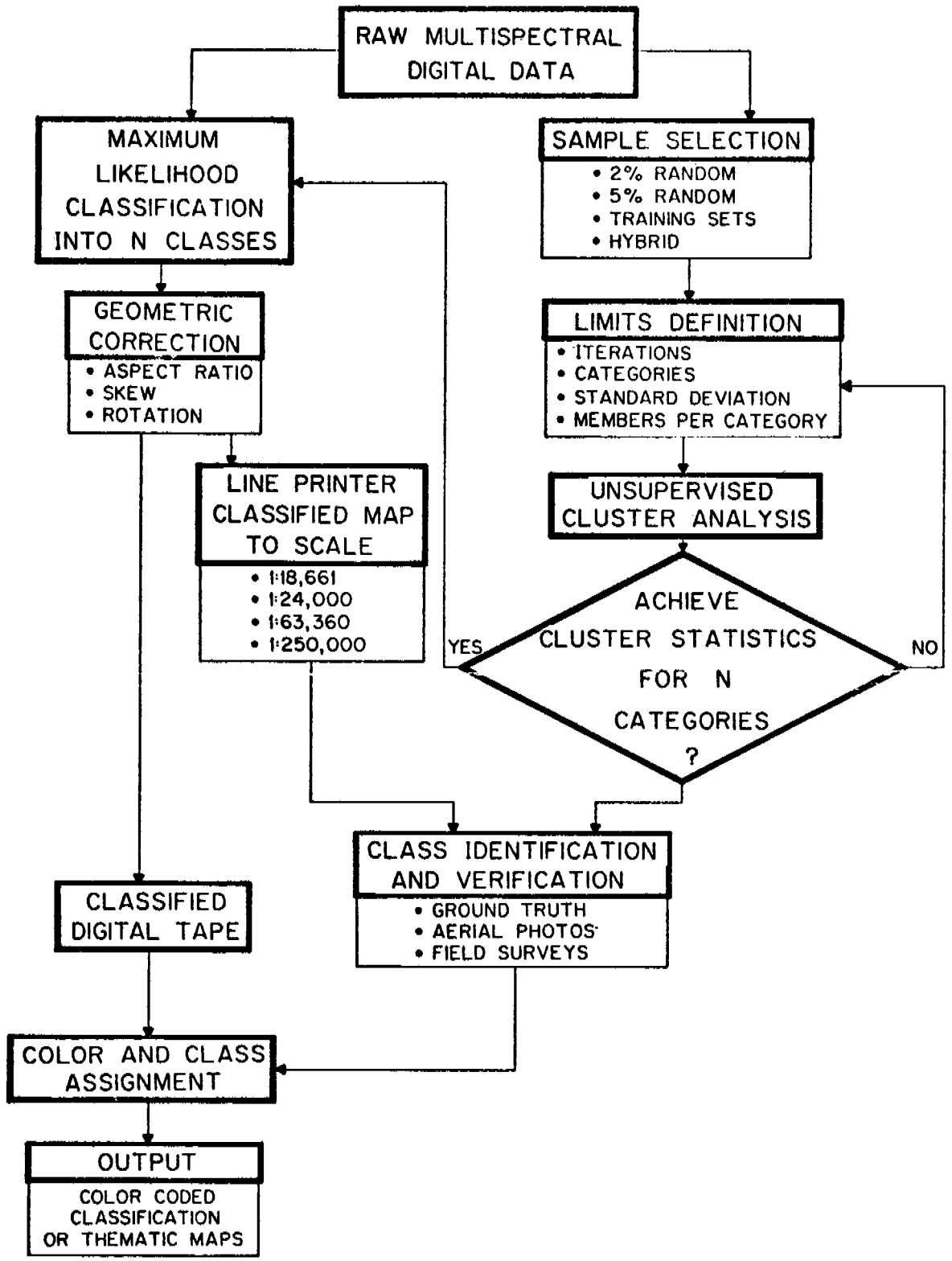

FLOW CHART FOR GENERATING ECOSYSTEM MAPS

FIGURE 11. Flow chart of the unsupervised classification algorithms used for generating ecosystem maps of the Alaskan coastal zone from LANDSAT digital imagery.

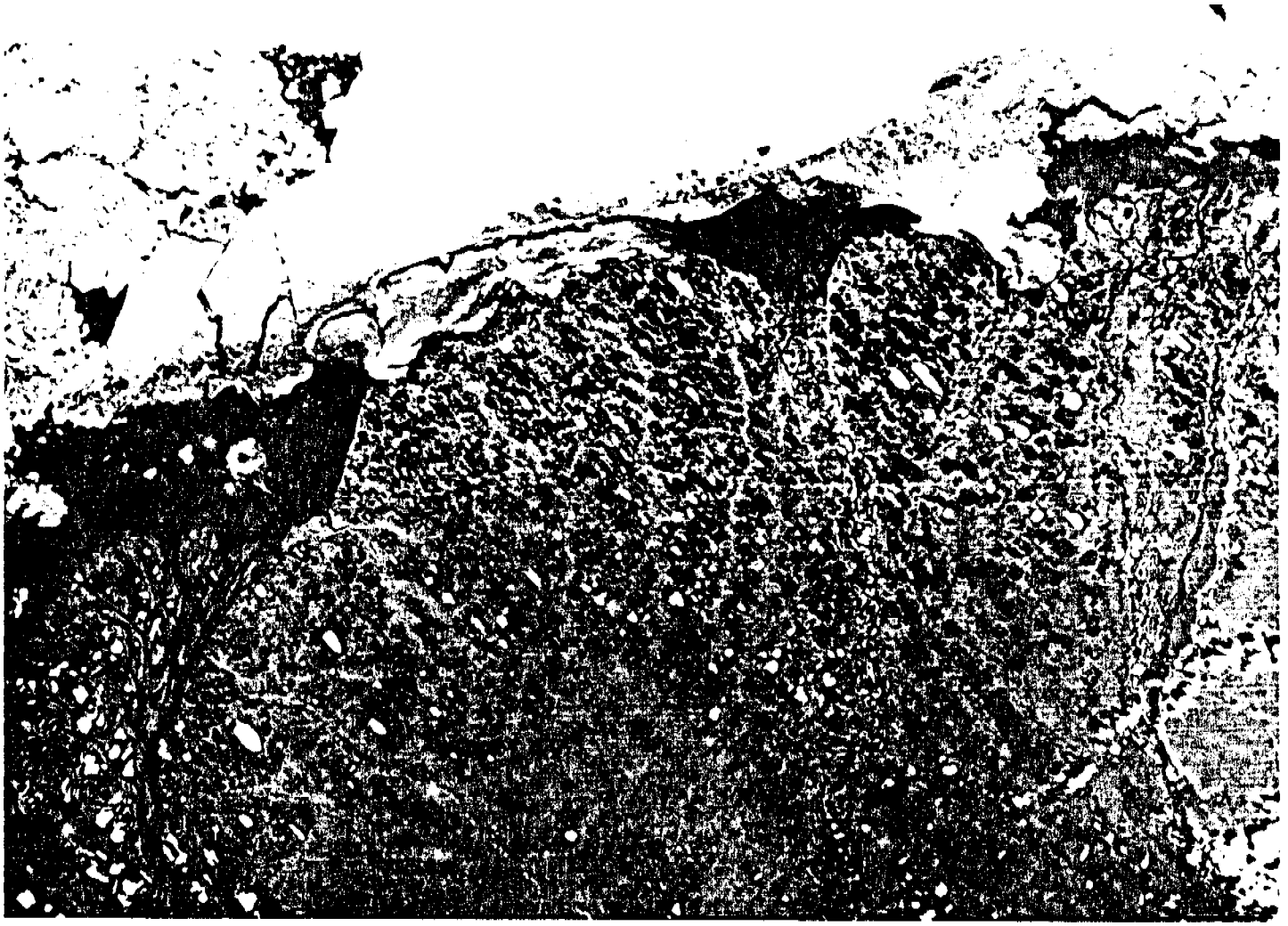

FIGURE 12. LANDSAT IMAGE 1344-21283 OF PRUDHOE BAY AND BEECHEY POINT.

FIGURE 14. COLOR-CODED ECOSYSTEM MAP OF BEECHEY POINT

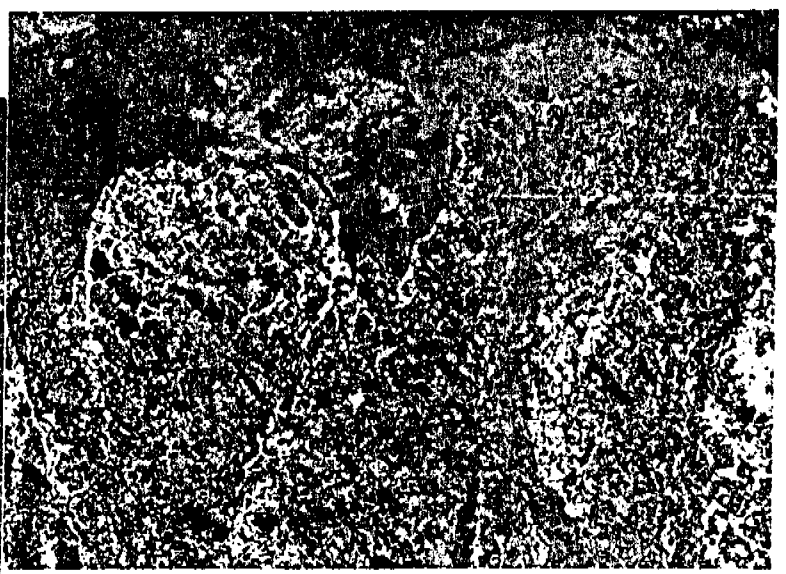

FIGURE 13. COLOR-CODED ECOSYSTEM MAP OF PRUDHOE BAY

☆ U.S. Government Printing Office: 1976-679-582/464 Region 8